



A University of Sussex PhD thesis

Available online via Sussex Research Online:

<http://sro.sussex.ac.uk/>

This thesis is protected by copyright which belongs to the author.

This thesis cannot be reproduced or quoted extensively from without first obtaining permission in writing from the Author

The content must not be changed in any way or sold commercially in any format or medium without the formal permission of the Author

When referring to this work, full bibliographic details including the author, title, awarding institution and date of the thesis must be given

Please visit Sussex Research Online for more information and further details

Design, Synthesis and Characterisation of Tool Inhibitors Targeting BLM Helicase

Yusuf I Ali

Co-Supervisors: Prof Simon E Ward and Dr Frances MG Pearl

A thesis submitted to the University of Sussex for the degree of Doctor of Philosophy (DPhil),
August 2018

I. Declaration

I hereby declare that this thesis has not been and will not be, submitted in whole or in part to another University for the award of any other degree.

Signed

Yusuf Ali

All work presented in this thesis was conducted by me except for the cases outlined below:

- Small molecules synthesised in this work were tested for biological activity and aqueous solubility at the Sussex Drug Discovery Centre, University of Sussex
- X-Ray crystallography efforts were led by Xiangrong Chen at the Oliver group (GDSC), University of Sussex
- Workflow used to remove PAINs and other non-preferred compounds was devised by Dr Ben Wahab, Sussex Drug Discovery Centre, University of Sussex.

II. Acknowledgements

I would like to thank my co-supervisors; Prof Simon Ward and Dr Frances Pearl for their academic guidance and encouragement throughout my PhD. Prof Ward's success in leading drug discovery projects and Centres is inspiring and Dr Pearl's research, which integrates informatics and drug discovery, has encouraged me to pursue this sub-discipline in the coming years. Therefore, I must thank them for giving me the opportunity to tackle an exciting project that provided much enjoyment and satisfaction despite the odd tough moment.

I would like to thank the School of Life Sciences funding at the University of Sussex for allowing my PhD to be possible.

I want to thank my mentor Dr Tristan Reuillon whose advice and guidance was significantly helpful during my PhD. Thanks to Xiangrong Chen, Dr Marco Derudas, Dr Alessandro Mazzacani, Dr Darren Le Grand, Dr Ben Wahab, Will Pearce, Dr Sarah Walker, Dr Antony Oliver and Dr Marcus Hanley for their work on the project and to Dr Catherine Tighe and Dr Penny Turner for proof-reading.

I am grateful to have a new close friend in Dr Chloe Koulouris and thankful for the support with proof-reading, brainstorming, and motivation, for the conversations and for the TV binging. A big thank you to my colleagues from the SDDC, past and present, for their help and encouragement. In particular, thanks to the chemistry team for great advice, the oncology team and the students of the PhD office. I'd also like to thank the Pearl bioinformatics group and the individuals from Life Sciences with whom I have made acquaintances over the years.

Finally, I'd like to thank family and friends outside work. Firstly, a massive thank you to my wife Farahnaaz who has supported me hugely during the past four years. Secondly, to my parents who have always taken care of me and to my siblings for their support. Lastly, I'd like to thank all my friends with whom I have enjoyed many good times over the past four years.

III. Abstract

Helicases, described as ‘guardians of the genome’, are enzymes that unwind DNA or RNA. Certain helicases, such as Bloom syndrome protein (BLM), are highly implicated in the DNA damage response (DDR). For example, BLM has various roles in homologous recombination (HR), a key pathway in the repair of DNA double strand breaks. Targeting proteins involved in DDR has recently garnered potential as a selective chemotherapeutic strategy. In this work, a tool inhibitor targeting BLM helicase was sought to increase understanding of its role and relevance in DNA damage repair.

The only characterised BLM helicase inhibitor, ML216, was developed from the results of a quantitative high-throughput screen (qHTS) screen on BLM helicase.¹ This reported inhibitor presented as a good candidate for a starting point in a hit optimisation campaign that ultimately was not successful due to poor physicochemical properties of this compound series.

In order to identify a more suitable hit optimisation candidate, 672 actives from the MLSMR qHTS screen [AID2528]² were analysed and 7 series were selected for in-house synthesis and biological evaluation. This led to the discovery of a single series that is a relatively potent inhibitor of BLM helicase. Hit optimisation primarily focused on the design and synthesis of a highly potent compound with a good solubility profile. Subsequently, co-crystallisation of BLM with this novel series led to the application of rational structure-based methods in the design of tool BLM inhibitors.

IV. Contents

I. Declaration	i
II. Acknowledgements	ii
III. Abstract.....	iii
IV. Contents.....	iv
V. Abbreviations	viii
1. Introduction.....	1
1.1. Introduction to cancer	1
1.1.1. Approaches to cancer therapy	3
1.2. The drug discovery process	4
1.3. Chemical probes.....	7
1.4. Targeting DNA damage response (DDR) in cancer	11
1.4.1. What is the DNA damage response?	11
1.4.2. Targeting DDR in cancer.....	16
1.5. Helicases in DNA repair.....	21
1.5.1. Structure and classification of helicases	21
1.5.2. Helicases in DDR.....	23
1.5.3. DDR helicases as cancer targets.....	25
1.5.4. DDR Helicases and synthetic lethality	26
1.5.5. Inhibiting DNA helicases.....	27
1.6. BLM helicase.....	31
1.6.1. Structure	31
1.6.2. Bloom syndrome (BS)	33
1.6.3. Function.....	34
1.6.4. Non-specific inhibitors of BLM helicase.....	38
1.6.5. ML216.....	40
1.7. Project aims.....	43
2. Development BLM helicase inhibitors based on ML216	45
2.1. Introduction	45
2.1.2. Aqueous solubility.....	46
2.2. Validation of ML216 as a starting point for the development of BLM inhibitors	47
2.2.1. Rationale	47
2.2.2. Synthesis of ureas from aromatic amines.....	48
2.2.3. Synthesis of ML216 and its reported analogues.....	50
2.3. Design of more soluble ML216 analogues	54
2.4. Synthesis of more soluble ML216 analogues.....	58
2.4.1. Exploration of phenyl ring	58
2.4.2. Addition of solubilising groups at 4-phenyl	60
2.4.3. Guanidine replacement of the urea core	64
2.4.4. Methyl urea replacement of the urea core	67
2.4.4. Amide replacement of the urea core	69
2.4.5. Replacement of 1,3,4-thiadiazole moiety with 2-pyridyl moiety	70
2.4.6. Synthesis of related BLM HTS hit MLS00000767020	70

2.5. Biological evaluation of ML216 and its analogues	71
2.5.1. Determination of BLM DNA unwinding inhibition by ML216 and its analogues	71
2.5.2. Assessment of thermodynamic solubility of selected compounds	77
2.5.3. Summary of biological results	79
2.6. Summary and conclusion.....	80
3. Hit identification of novel BLM helicase inhibitors from high-throughput screening (HTS) data	82
3.1. Introduction	82
3.2. HTS analysis and triage.....	87
3.2.1. Computational filtering	87
3.2.2. Manual assessment of remaining compounds	90
3.2.3. Results of screening: biological assessment of commercially prepared compounds	93
3.3. Series B hit validation	93
3.3.1. Rationale	93
3.3.2. Synthesis.....	94
3.3.3. Biological assessment.....	95
3.4. Series C hit validation	98
3.4.1. Rationale	98
3.4.2. Synthesis.....	98
3.4.3. Biological assessment.....	99
3.5. Series A hit confirmation	99
3.5.1. Rationale	99
3.5.2. Synthesis.....	101
3.5.3. Biological assessment.....	104
3.6. Series G hit confirmation	105
3.6.1. Rationale	105
3.6.2. Synthesis.....	106
3.6.3. Biological assessment.....	109
3.7. Discussion	110
3.7.1. Hit identification.....	110
3.7.2. Cheminformatic analysis	112
3.7.3. Manual triage	114
3.7.4. In-house biological data	115
3.8. Conclusion	120
4. Series G Part One.....	122
4.1. Introduction	122
4.1.1. Microscale thermophoresis (MST)	123
4.1.2. Aims	124
4.2. SAR studies of the aniline ring.....	125
4.2.1. Rationale	125
4.2.2. Synthesis and SAR at the 2-position.....	126
4.2.2. Synthesis and SAR at the 3, 4, 5 and 6-position.....	128
4.2.3. Third substituent effect – synthesis and SAR.....	131
4.2.4. Solubility	133
4.2.5. Summary	134

4.3. Amide library at the 5-position	135
4.3.1. Rationale	135
4.3.2. Synthesis.....	135
4.3.3. SAR.....	136
4.3.4. Summary	137
4.4. Heterocyclic replacement of the aniline ring.....	137
4.4.1. Rationale	137
4.4.2. Synthesis and SAR of pyridyl analogues.....	138
4.4.3. Diverse heterocycles	140
4.4.4. Summary	141
4.5. Discussion	142
4.6. Conclusion	143
5. Series G Part Two	145
5.1. Introduction	145
5.1.1. Aims	146
5.2. SAR exploration of the amide bond	146
5.2.1. Rationale	146
5.2.2. Synthesis and SAR	147
5.2.3. Summary	148
5.3. Introduction of <i>ortho</i> methyl substitution and pyridyl replacement of the core phenyl ring.....	148
5.3.1. Rationale	148
5.3.2. Synthesis and SAR	149
5.3.3. SAR.....	153
5.4. Synthesis of thiazole replacements utilising Suzuki-Miyaura cross-coupling	154
5.4.1. Rationale	154
5.4.2. Synthesis.....	155
5.4.3. SAR.....	157
5.4.4. Summary	158
5.5. Discussion	158
5.6. Conclusion	161
6. Series G Part Three	162
6.1. Introduction	162
6.1.1. Employing a miniaturised BLM assay to assess BLM inhibition	162
6.1.2. Aims	163
6.2. SAR investigations of thiazole motif with closely related analogues	164
6.2.1. Rationale	164
6.2.2. Exploration of the potential use of CH activation chemistry on the 4-position of 1,3-thiazoles	164
6.2.3. Extension of the methyl substituent.....	166
6.2.4. Extension of the methyl substituent with <i>N</i> -alkylation	167
6.2.5. Extension of the methyl substituent with <i>O</i> -alkylation	168
6.2.6. Replacement with thiazole regioisomers and assessment of methyl substituents	169
6.2.7. Replacement with classical thiazole isomers	170
6.2.8. SAR.....	171
6.2.9. Synthesis of selected thiazole analogues with a more soluble scaffold	174
6.2.10. SAR of thiazole motif.....	177

6.2.11. Summary	178
6.3. Design, synthesis and evaluation of analogues comprised of favoured motifs	178
6.3.1. Rationale	178
6.3.2. Synthesis.....	179
6.3.3. SAR.....	180
6.3.4. Summary	181
6.4. Discussion	181
6.5. Conclusion	185
7. Analysis of the BLM helicase co-crystal structure.....	186
7.1. Introduction	186
7.2. Methods	186
7.2.1. Binding site analysis	186
7.2.2. Druggability analysis.....	187
7.2.3. Sequence alignment	187
7.3 Results	187
7.3.1 Analysis of the inhibitor binding site.....	187
7.3.2 Structural Analysis of the allosteric binding site.....	191
7.3.3 Druggability analysis of the allosteric binding pocket	193
7.3.4 Selectivity analysis of the allosteric binding pocket.....	194
7.4. Conclusion	194
8. Computer-aided drug design.....	196
8.1. Introduction	196
8.1.1. Structure Based Drug Design (SBDD)	196
8.1.2. Utilising structure-based drug discovery to develop potent tools of BLM helicase.....	198
8.1.3. Aims	198
8.2 Methods and Results	199
8.2.1. Compound selection	200
8.2.2. Molecular docking	201
8.2.3. Synthesis.....	207
8.2.4. Biological activity of the novel compounds	209
8.3. Discussion	210
8.4. Conclusion	212
9. Conclusions and Future Work.....	213
10. References	218
11. Experimental Information	228

V. Abbreviations

μM	Micromolar
1-10-PHEN	1,10-Phenanthroline, $\text{C}_{12}\text{H}_8\text{N}_2$
ABL	Abelson murine leukaemia viral oncogene homolog 1
ALT	Alternative lengthening of telomere
AMBER	Assisted model building with energy refinement
aNHEJ	Alternative NHEJ
APE1	Apurinic/apyrimidinic endonuclease 1
Aq.	Aqueous
ATA	Aurintricarboxylic acid, $\text{C}_{22}\text{H}_{14}\text{O}_9$
ATM	Ataxia-telangiectasia mutated
ATP	Adenosine 5'-triphosphate
ATR	ATM- and Rad3-related
ATRIP	ATR interacting protein
B₂pin₂	Bis(pinacolato)diboron, $((\text{CH}_3)_4\text{C}_2\text{O}_2\text{B})_2$
BCR	Breakpoint cluster region protein
BER	Base Excision Repair
BET	Bromodomain and extra terminal domain family
BGS	Baller–Gerold syndrom
Bipy	2,2'-Bipyridine
BLM	Bloom syndrome protein
BMIM	1-Butyl-3-methylimidazolium hexafluorophosphate
Boc	<i>tert</i> -butyloxycarbonyl
BRCA1	Breast cancer type 1 susceptibility protein
BRCA2	Breast cancer type 2 susceptibility protein
BRIP1	Fanconi anaemia group J protein / BRCA1-interacting protein 1
BRR2	Pre-mRNA-splicing helicase BRR2
brs	broad singlet
BS	Bloom syndrome
<i>C. elegans</i>	<i>Caenorhabditis elegans</i>
cat.	Catalytic
CDI	1,1-carbonyldiimidazole
CDK2	Cyclin-dependent kinase 2
CHD3	Chromodomain-helicase-DNA-binding protein 3
CHD4	Chromodomain-helicase-DNA-binding protein 4
CHD5	Chromodomain-helicase-DNA-binding protein 5
chEMBL	European Molecular Biology Laboratory chemical database
CHK1	Serine/threonine-protein kinase Chk1
CHK2	Serine/threonine-protein kinase Chk2
clogD	Calculated logD
clogP	Calculated logP
CO₂	Carbon dioxide
Cpd	Compound
CSD	Cambridge structural database
CtIP	DNA endonuclease RBBP8
CYP	Cytochrome P450
D loop	Dissociation loop
Da	Daltons
DBU	1,8-Diazabicyclo(5.4.0)undec-7-ene, $\text{C}_9\text{H}_{16}\text{N}_2$
DCC	<i>N,N'</i> -dicyclohexylcarbodiimide, $\text{C}_{13}\text{H}_{22}\text{N}_2$
DCM	Dichloromethane, CH_2Cl_2
DDR	DNA damage response
DDX	DEAD box
DDX1	DEAD box protein 1
DDX11	DEAD box protein 11
DDX3	DEAD box protein 3
DDX36	DEAD box protein 36
DDX3X	DEAD box protein 3X
DDX3Y	DEAD box protein 3Y
DDX4	DEAD box protein 4
DHX	DEAH box
DIPEA	<i>N,N</i> -diisopropylethylamine, $\text{C}_8\text{H}_{19}\text{N}$
DMAc	Dimethylacetamide, $\text{C}_4\text{H}_9\text{NO}$
DMAP	4-Dimethylaminopyridine, $\text{C}_7\text{H}_{10}\text{N}_2$

DME	Dimethyl ether, C ₂ H ₆ O
DMF	Dimethylformamide, C ₃ H ₇ NO
DMSO	Dimethyl sulfoxide, C ₂ H ₆ OS
DNA	Deoxyribonucleic Acid
DNA2	DNA replication ATP-dependent helicase/nuclease DNA2
DNAB	Replicative DNA helicase
DNA-PKcs	DNA-dependent protein kinase, catalytic subunit
DSB	DNA double-strand break
DSBR	DNA double-strand break repair
dsDNA	Double strand DNA
EDCI	1-Ethyl-3-(3-dimethylaminopropyl)carbodiimide, C ₈ H ₁₇ N ₃
EIF4A2	Eukaryotic initiation factor 4A2
EIF4A3	Eukaryotic initiation factor 4A3
Eq.	Equivalents
ERCC1	DNA excision repair protein ERCC-1
EU-OPENSREEN	European Infrastructure of Open Screening Platforms for Chemical Biology
EXO1	Exonuclease 1
FA	Fanconi anaemia
FANCD	Fanconi anaemia group D protein
FANCI	Fanconi anaemia group J protein
FANCM	Fanconi anaemia group m protein
FBH1	F-box DNA helicase 1
FDA	US food and drug administration
FEN1	Flap endonuclease 1,
Fe-S	Iron-Sulphur
FID	Fluorescent intercalator displacement
G4-DNA	G-quadruplex DNA
GGNER	Global genome NER
H₂O	Water
HATU	1-(Bis(dimethylamino)methylene)-1H-1,2,3-triazolo(4,5-b)pyridinium 3-oxidhexafluorophosphate, C ₁₀ H ₁₅ F ₆ N ₆ OP
HBA	Hydrogen bond acceptor
HBD	Hydrogen bond donor
HBTU	2-(1H-benzotriazol-1-yl)-1,1,3,3-tetramethyluronium hexafluorophosphate, C ₁₁ H ₁₆ F ₆ N ₅ OP
HCV	Hepatitis C virus
HELQ	Helicase POLQ-like
HER2	Helicase POLQ-like
hERG	Human ether-à-go-go-related gene
him-6	Bloom syndrome protein homolog
HIV-1	Human immunodeficiency virus 1
HJ	Holliday junctions
HOBt	Hydroxybenzotriazole
HR	homologous recombination
HRDC	helicase-and-ribonuclease D/C-terminal
HTS	high throughput screening
IC₅₀	half maximal inhibitory concentration
ICL	Interstrand crosslink
ICR	Interstrand crosslink repair
INO80	Chromatin-remodelling ATPase INO80
IPA	Isopropyl alcohol, C ₃ H ₈ O
ITC	Isothermal titration calorimetry
K_d	Dissociation constant
KOAc	Potassium acetate, C ₂ H ₃ KO ₂
Ku	Ku70 and Ku80
LBDD	ligand based drug design
LC-MS	Liquid chromatography–mass spectrometry
LCMS-LCQ	LCMS-Liquid Chromatography Quadrupole
LiHMDS	Lithium bis(trimethylsilyl)amide C ₆ H ₁₈ N ₂
LogD	Partition-coefficient
MCM	Minichromosome maintenance protein complex
MD	Molecular dynamics
MDM2	Mouse double minute 2 homolog
MeCN	Acetonitrile, C ₂ H ₃ N
MeI	Iodomethane, CH ₃ I
MgADP	Magnesium - Adenosine diphosphate complex
MgATP	Magnesium - Adenosine triphosphate complex
MK2	MAP kinase-activated protein kinase 2

MLI	Molecular Libraries and Imaging
MLP	Molecular Libraries Program
MLSCN	Molecular Libraries Screening Centres Network
MLSMR	Molecular Libraries Small Molecule Repository
mM	Millimolar
MMFF94	Merck molecular force field 94
MMR	Mismatch mediated repair
MRE11	Double-strand break repair protein MRE11
MRN	Mrotein complex consisting of Mre11, Rad50 and Nbs1
mRNA	Microsomal RNA
MSH2	MutS protein homolog 2
MSH3	MutS protein homolog 3
MSH6	MutS protein homolog 6
MST	Microscale thermophoresis
MW	Molecular weight
NBS	<i>n</i> -bromosuccinimide, C ₄ H ₄ BrNO ₂
<i>n</i>-buli	<i>n</i> -butyl lithium, C ₄ H ₉ Li
<i>nd</i>	Not determined
NER	Nucleotide excision repair
NHEJ	Non-homologous end joining
NIH	National Institute of Health
nm	Nanomolar
NMD	Nonsense-mediated RNA decay
NMP	<i>N</i> -methylpyrrolidone, C ₅ H ₉ NO
NMR	Nuclear magnetic resonance
NS3	Nonstructural protein 3
OB	Oligonucleotide-binding
OGG1	Oxoguanine glycosylase
PABL2	Partner and localizer of BRCA2
PAINS	Pan-assay interference compound
PARP1	Poly(ADP-Ribose) polymerase 1
PARP2	Poly(ADP-Ribose) polymerase 2
PARPi	PARP inhibitor
PCNA	Proliferating cell nuclear antigen
Pd	palladium
Pd(dppf)₂Cl₂	(1,1'-Bis(diphenylphosphino)ferrocene)dichloropalladium(II), (C ₁₇ H ₁₄ P) ₂ Fe · PdCl ₂
Pd(OAc)₂	Palladium(II) acetate, Pd(CH ₃ COO) ₂
Pd(PhCN)₂Cl₂	Bis(benzonitrile)palladium(II) chloride, (C ₆ H ₅ CN) ₂ PdCl ₂
Pd(PPh₃)₄	Tetrakis(triphenylphosphine)palladium(0), C ₇₂ H ₆₀ P ₄ Pd
PDB	Protein data bank
PEPPSITM-<i>i</i>Pr	(1,3-Bis(2,6-diisopropylphenyl)imidazol-2-ylidene)(3-chloropyridyl)palladium(II) dichloride, C ₃₂ H ₄₀ Cl ₃ N ₃ Pd
PFI	Property forecast index
PIF1	ATP-dependent DNA helicase PIF1
PIKK	Phosphatidylinositol-3 kinase related kinase
PML-NB	Promyelocytic leukaemia protein nuclear bodies
Pol β	DNA polymerase β
Pol δ	DNA polymerase δ
POLH	DNA polymerase H
POLI	DNA polymerase I
POLK	DNA polymerase K
POLQ-like	Helicase POLQ-like
poly(Di-dC)	Poly(deoxyinosinic-deoxy tydyllic) acid
POT1	Protection of telomeres protein 1
ppm	Parts per million
PSA	Polar surface area
pTsOH	<i>p</i> -toluenesulfonic acid
QSAR	Quantitative structure–activity relationship
R&D	Research and development
r.t.	Room temperature
Rt	Retention time
RAD18	E3 ubiquitin-protein ligase RAD18
RAD51	RAD51 recombinase
RAD51C	RAD51 paralog C
rcq-5	<i>C. elegans</i> rcq-5 protein
RECQ1	ATP-dependent DNA helicase Q1
RECQ2	ATP-dependent DNA helicase Q2

RECQ5	ATP-dependent DNA helicase Q5
REOS	rapid elimination of swill
RMI1	RecQ mediated genome instability 1
RMI2	RecQ mediated genome instability 2
RNA	Ribonucleic acid
RNAi	RNA interference
Ro5	Rule of five
RPA	Replication protein A
RQC	RecQ C-terminal
RTel1	Regulator of telomere elongation helicase 1
Rtel-1	Regulator of telomere elongation helicase 1 homolog
SAR	Structure-activity relationships
SBDD	Structure-based drug design
SBVS	Structure-based virtual screening
SCE	Sister chromatid exchanges
SDDC	Sussex drug discovery centre
SDSA	Synthesis-dependent strand annealing
SF	Superfamily
Sgs1	BLM homolog
SiRNA	Small interfering RNA
SMARCA2	Probable global transcription activator SNF2L2
SMARCA4	Transcription activator BRG1
SMILES	Simplified molecular-input line-entry system
S_NAR	Nucleophilic aromatic substitution
SP	Standard precision
SSB	Single strand break
SUPV3L1	ATP-dependent RNA helicase SUPV3L
T3P	Propylphosphonic anhydride, C ₉ H ₂₁ O ₆ P ₃
TBABr₃	Tetrabutylammonium tribromide, C ₁₆ H ₃₆ NBr ₃
TBAF	Tetrabutylammonium fluoride, C ₁₆ H ₃₆ NF
TBS	Trimethylsilyl
TC-NER	Transcription-coupled NER
TEMPO	(2,2,6,6-Tetramethylpiperidin-1-yl)oxyl, C ₉ H ₁₈ NO
TFA	Trifluoroacetic acid, C ₂ HF ₃ O ₂
TFIIH	Transcription factor II human
THF	Tetrahydrofuran, C ₄ H ₈ O
TLC	Thin layer chromatography
TMSCl	Trimethylsilyl chloride, C ₃ H ₉ SiCl
TopBP1	DNA topoisomerase 2-binding protein 1
TopoIIa	Topoisomerase IIIa
tPSA	Topological polar surface area
TRF1	Telomeric repeat binding factor 1
TRF2	Telomeric repeat binding factor 2
Tris.HCl	Tris(hydroxymethyl)aminomethane hydrochloric acid
T-SCE	Telomere sister chromatid exchange
TTBT	<i>N,N'</i> -bidentate-10,11,12,13-tetrahydro-4,5,9,14-tetraazabenzotriphenylene
UFB	Ultrafine anaphase DNA bridge
UV	Ultraviolet
WH	Winged-helix
WRN	Werner syndrome ATP-dependent helicase
XLF	Non-homologous end-joining factor 1.
XPA	DNA repair protein complementing XP-A cells
XPB	General transcription and DNA repair factor IIH helicase subunit XPB
XPC	DNA repair protein complementing XP-C cells
XPB	General transcription and DNA repair factor IIH helicase subunit XPB
XRCC4	DNA repair protein XRCC4
XRCC1	DNA repair protein XRCC1

1. Introduction

1.1. Introduction to cancer

Cancer is a major public health problem and is the leading cause of morbidity and mortality worldwide, with its incidence expected to rise as global population and life expectancy increases. The incidence of cancer worldwide was estimated to be over 14 million new cases in 2012, with deaths related to cancer estimated to be over 8 million.³ In the UK, if all cancers were grouped together, it is the leading cause of death with 165,000 deaths from cancer in 2016 alone.⁴ Moreover, as life expectancy increases, the incidence of cancer cases worldwide is predicted to rise by 75% to reach 25 million in 20 years.³ Despite people living ten times longer with cancer than 40 years ago, the mean survival rate for 10 years does not exceed 50%, emphasising the continual need for novel therapeutics targeting the disease.

Cancer is a disease in which cellular control over growth and replication has been lost. Such changes result from the accumulation of genetic and epigenetic alterations that drive the transformation of a normal cell towards a malignant derivative.⁵ Tumourigenesis can be considered a Darwinian process in which a build-up of mutations result in cells that have a growth advantage over normal cells. The result of this growth deregulation is the formation of tumour cells in a multi-step process that ultimately spread across the body in a process known as metastasis; the cause of most deaths in cancer. Each tumour is unique and contains tens to hundreds of thousands of mutations. Mutations conferring growth advantages are known as drivers whilst those that confer little phenotypic advantage are termed passengers.⁶



Figure 1.1. The hallmarks of cancer. Illustration of the 8 proposed hallmarks capabilities of cancer cells and 2 enabling characteristics of cancer.^{7,8}

Both genetic and environmental factors can play a role in an individual's cancer susceptibility. To depict the genetic origin of cancer, Hanahan and Weinberg described eight hallmarks of cancer cells that allow normal cells to acquire characteristics that guide their tumourigenic and malignant phenotype; six well established and two recently emerging.^{7,8} These capabilities are traits of cancer cells and its tumour microenvironment and are gained by genetic and epigenetic mechanisms.⁵ They are: sustaining proliferative signalling, evading growth suppressors, avoiding immune destruction, enabling replicative immortality, activating invasion and metastasis, inducing angiogenesis, resisting cell death and deregulating cellular energetics (Figure 1.1). Additionally, two enabling characteristics have also been proposed: genomic instability and tumour promoting inflammation. The nature by which genomic instability can enable the acquisition of these hallmarks is of high relevance to the purpose of this thesis and is described in more detail in Section 1.4.

1.1.1. Approaches to cancer therapy

Most cancers are treated with a combination of surgery, radiation therapy and/or chemotherapy. The development of molecular chemotherapeutic agents emerged after the observation that rapidly proliferating cancer cells can be killed.⁹ DNA integrity is critical to ensure cellular function and proliferation. Usually, DNA damage is detected and appropriately repaired to ensure cell cycle progression. Cancer cells have reduced DNA damaging detection/repair capabilities and the ability to ignore cell cycle checkpoints that allow them to achieve high proliferation rates, and consequently they are highly susceptible to DNA damage and associated cell death. In order to profit from this susceptibility, numerous anticancer compounds were developed that targeted DNA, such as cisplatin and doxorubicin. DNA damaging agents such as these, administered in combination, have been the mainstay of treatment up to the end of the 20th century before the arrival of molecular targeted therapy. Use of such cytotoxic treatments has been limited by their high toxicity as they harm normal cells even when not rapidly proliferating. In particular, those cells that have higher replication rates, such as those of the digestive tract and hair follicles, are particularly susceptible to damage resulting in a wide cytotoxicity profile for chemotherapeutic agents. In addition to drug toxicity, resistance to these agents by tumours has also limited their effectiveness.¹⁰ Therefore, it is vital that molecular agents with chemotherapeutic activity are selectively killing cancer cells over normal cells.

In the past two decades a transition from cytotoxic chemotherapy to the development of molecular targeted anti-cancer agents has resulted in a number of successful therapies.¹¹ These mechanism-based targeted therapies aim in some form to target the one or more hallmarks and enabling characteristics of cancer.⁷ These therapies target individual gene products after rigorous assessment of their contribution to tumourigenesis. Targeted agents are composed of small molecule agents and monoclonal antibodies. For example, imatinib is a small molecule inhibitor of specific tyrosine kinase enzymes that primarily target the BCR-ABL pathway and is an effective treatment for chronic myeloid leukaemia patients carrying a BCR-ABL mutation.¹² The clinical success of imatinib has established a paradigm for cancer targeted therapies.

Another early successful example is trastuzumab, a monoclonal antibody that is beneficial for patients with breast cancers overexpressing HER2.¹³

Most conventional chemotherapeutic agents are designed to kill cells by inducing DNA damage. DNA damaging agents can induce various types of DNA damage including intrastrand and interstrand crosslinks, DNA double strand breaks (DSBs), and single-strand breaks (SSBs). A co-ordinated network of proteins and signalling cascades, termed the DNA damage response (DDR), functions to maintain genome integrity and has recently become the source for novel targets for targeted cancer therapy.¹⁴ The rationale and implications for targeting such a network is discussed in Section 1.4.

1.2. The drug discovery process

The discovery of new drugs is an expensive and labour-intensive process. It is estimated that a single drug can take 12–15 years to develop and costs approximately \$2.9 billion (Figure 1.2).^{15,16} As promising compounds advance through the drug discovery process, many inevitably face problems relating to their poor pharmacokinetic, efficacy, and safety profiles. The high cost of drug development is due to this high attrition rate as well as a poor clinical success rate, with less than 12% of clinical candidates gaining regulatory approval.¹⁶

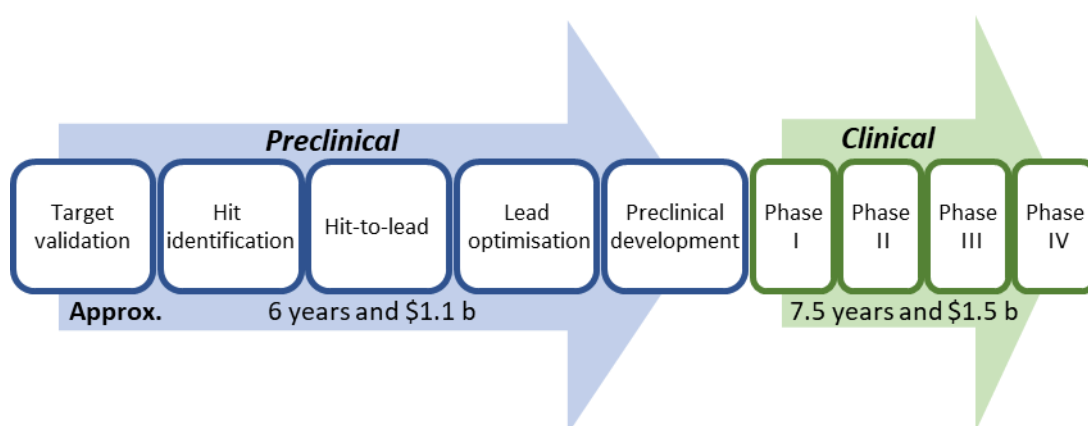


Figure 1.2. The drug discovery pipeline. Preclinical research identifies how to target disease using a drug candidate. Clinical trials assess the efficacy and safety of the drug candidate in humans both before and after approval. b: billion.

Drug discovery begins with target identification during which hypotheses are generated regarding the potential therapeutic effect of regulation of a specific protein on a

particular disease state. In addition to evoking the desired biological response, a good drug target should also be considered 'druggable'. Introduced in 2002, the concept of the 'druggable genome' relates to genes that code for proteins that can be modulated by small drug-like molecules.¹⁷ The druggability of a protein refers to the ability of therapeutic protein targets to bind small molecules due to the presence of protein folds that favour interactions with small drug-like molecules. Finally, determining the target's downstream processes, associated biological pathways and protein partners, natural substrate(s), isoforms, and phylogenetic family are also important to assess the safety of the protein as a therapeutic target.

This identified target protein is then assessed as a potential drug target in a process termed target validation. The use of multiple techniques is generally preferred as an approach to target validation. Popular approaches utilise antisense RNA technology, small interfering RNA (siRNA), transgenic animal models, monoclonal antibodies and chemical tool compounds.¹⁵

Following target validation, the next step in the drug discovery process is hit identification. A hit is a compound which produces the desired activity against a target in a compound screen (high-throughput compound, fragment, virtual, etc), and confirmed on retesting, *in vitro* and/or *in vivo*. High-throughput screening (HTS) of large libraries is the most widely applicable technology for the identification of hits.¹⁸ In addition to screening large diverse libraries based on no assumed knowledge of the preferred chemotype for the target, more focused libraries are useful when prior knowledge about preferred chemotypes exists for the target. All screens are usually followed by careful post-triage to ensure improved success. Alternative strategies, such as fragment-based approaches, de novo design, virtual screening, natural product extraction and data-mining also exist and all have various benefits and limitations.¹⁵

In the hit-to-lead phase, structure-activity relationship (SAR) studies of initial hits are carried out to identify the most potent and selective hits. Also established are pharmacokinetic parameters (plasma protein binding, microsomal stability, permeability) and off-target pharmacology properties (hERG inhibition, CYP inhibition).¹⁵ SAR analysis is an iterative process to enable development of more

analogues if an individual property is not desirable. When a lead compound or series is identified, the best candidates are then optimised for progression into clinical trials, usually via a multiparameter method that aims to optimise lead entities according to potency, selectivity, toxicity, pharmacokinetic and pharmacodynamic parameters.¹⁹

Despite advances in scientific, technological and managerial factors in drug research and development activities, attrition rates for small-molecule drug candidates in the clinic have remained high, leading to the perception that the pharmaceutical industry has low productivity.^{20,21} The reason for such failures have been attributed to rising costs and falling income.¹⁶

A major factor contributing to rising costs is the high rate of project attrition during clinical trials. This is usually due to insufficient target validation and 'proof-of-concept' trials or the result of drug candidates possessing high molecular weight and lipophilicity, which possess limited potential for optimisation.^{19,20,22} In addition, authorities such as the FDA have become increasingly wary of drug safety and this lower tolerance of risk increases expenditure of R&D and clinical trials.¹⁶ The number of new FDA-approved drugs per billion US dollars spent has halved every nine years since 1950. The industry is failing to deliver enough 'blockbuster' drugs (more than \$1 billion in annual sales) to cover such costs. 'Me too' drugs, which are structurally similar analogues but available at lower costs due to the reduced R&D required, present further competition that can reduce potential profits of such blockbuster drugs. Presently, novel drugs are more likely to treat orphan diseases as therapeutics for easy-to-treat disease targets have already been identified. Costs for the treatment of such rare diseases are more difficult to recoup due to the smaller population requiring treatment.¹⁶ In order to combat such issues, disciplined approaches to identify drug targets and lead compounds are required.²³ Drug targets should be rigorously selected and well validated while defining physicochemical properties that predict long-term viability of drug candidates should be instilled during the drug discovery program with particular focus on safety and toxicology.²²

1.3. Chemical probes

Increasingly, researchers use chemical probes as an integral part of target validation.^{24–26} The demand for high quality chemical probes against a range of targets sets the context of this thesis.

To understand the function of proteins, their mRNA expression can be modulated directly by RNAi or antisense technology, or genetically in transgenic and knockout models. In general, these methods cause complete elimination of the target protein from the cell. More recently, chemical biology is playing an integral role in elucidating the role and function of novel targets in human biology and in the treatment of disease through the use of chemical probes as they inactivate proteins without causing major removal of it. Therefore, such probes serve as useful adjuncts in a multi-validation approach of a target. Additionally, these tools can also serve as a starting point for hit to lead development programs.

A chemical probe is a small molecule modulator of a protein function that inactivates a protein without eliminating it, and allows the user to ask mechanistic and phenotypic questions about the molecular target in biochemical, cell based and animal studies.²⁶ Only high-quality probes generate meaningful biological data. The ideal properties of a defined probe are context given, with properties such as potency, solubility, permeability and selectivity important. Whilst such properties resemble those for a drug-like compound, it is important to note that chemical probes, which are primarily intended to explore protein function *in-vitro* and *in-vivo*, are not necessarily intended to become drugs. Therefore, probes can often have less than ideal pharmacokinetic and toxicological profiles. However, they must be highly selective as any off-target effects can prevent reliable interpretation of protein validation data.^{24,27} Chemical probes serve as useful adjuncts in a multi-validation approach of a target, and can also serve as a starting point for hit-to-lead development programs.

Numerous breakthroughs in biology have been enabled by chemical biology. For example, a recent growth of bromodomain biology research has been sparked by the discovery of selective chemical probes such as JQ1²⁸ and I-BET.²⁹ Such research in this field can potentially pave the way for new cancer therapeutics. Academic and open-

source initiatives have contributed to these efforts through their involvement in early drug discovery and screening. For example, the NIH (National Institute of Health) Molecular Libraries And Imaging (MLI) initiative aimed to produce small-molecule tools to aid target validation and downstream drug development.³⁰ The program ran between 2005 to 2013 and in the pilot phase itself (2005–2008), 64 chemical probes were identified through the work of multiple centres running HTS of a 355,000 compound library and subsequent probe development.³¹ Unfortunately, despite the positive contribution of many small molecule inhibitors to target validation, there are many other widely published chemical probes that fail to function as such and therefore are not fit-for-purpose in target validation processes.

As a result, various commentaries in chemical biology have attempted to outline the ideal attributes of chemical probes required to answer important biological questions.^{25,26,32,33} Bunnage *et al.* proposed four ‘pillars’ of cell-based target validation that would then facilitate successful drug programs in the clinic. By retrospectively analysing successful and failed drug programs that progressed to phase 2 clinical trials, the authors proposed this framework to ensure appropriate use of small molecule probes during the target validation phase and thereby reduce attrition rates. The first pillar states that a probe should have sufficient exposure at the site of action. Probes therefore require sufficient cell permeability and such properties should be validated appropriately. For example, permeability can be assessed through *in vitro* permeability assays, which can also determine whether active efflux or active uptake and accumulation occurs. In some cases, it may be necessary to precisely determine the concentration of the probe inside cells by techniques such as liquid chromatography-mass spectrometry (LC-MS) analysis of cell extracts. The second pillar is proof of target engagement and selectivity. This is the most technically challenging as it requires a complete understanding of the performance of the probe in a whole-cell or an *in vivo* context in order to discern the ‘true’ on- and off- target effects. Obtaining selectivity profiles, using inactive analogues as negative controls and the use of proteomic tools also facilitate understanding of target engagement. The third pillar states the probe should affect the biochemical function of the target and therefore express functional pharmacology in appropriate biochemical assays. The fourth pillar is proof of phenotype

perturbation, which emphasises the importance of identifying the link between disease-related biomarkers and the inhibition of the protein, as sometimes probes may reverse a particular phenotype but have no impact on rectifying the disease. The use of mammalian or more primitive models (such as zebrafish) can be employed at this stage. Overall, if these criteria are adhered to during the target validation, the risk of attrition in drug discovery projects can be reduced. Therefore, developing high-quality chemical probes will increase opportunities for these criteria to be met during biological experiments.

Whilst these pillars provide guidance in a biological context, further parameters have been provided on the physical and chemical properties of the probe itself. In advocating probes fit-for-purpose, Workman and Collins³² outlined fitness factors to aid authentication of high-quality chemical probes. These factors are classified into four categories and are described in Figure 1.3. The first category, chemistry, relates to chemical probes possessing sufficient solubility, permeability and stability. In addition, the probe should be well characterised and have the capacity to be prepared with reproducible methods. These factors can be controlled during drug design by the medicinal chemist. In particular, aqueous solubility and membrane permeability, which are of significant importance to ensure sufficient exposure at the site of action, can be regulated by ensuring physicochemical parameters are within known guidelines such as Lipinkisi's rule of five.³⁴ The second category is biological potency that encompasses both biochemical and cellular potency. It is also important to ensure the probe has suitable pharmacokinetic properties to achieve relevant concentrations in cellular studies. As defined in the second pillar by Bunnage *et al.*, the third category of fitness factors is selectivity. The probe should have defined selectivity with related targets and its chemical activities should be well understood. When investigating target engagement, it is also recommended that inactive analogues exist. The final category of fitness factors relates to the context of use of the probe. It is suggested a multivalication approach is taken, for example, the use of RNAi or mouse models for complementary experiments to validate the effect of the probe. Additionally, the cellular context of the target and any linked activities should be taken into consideration whilst it should also be asked whether the probe itself is suitable for a particular investigation.

Chemistry		Potency	
Structure	Discrete chemical species; Characterised spectroscopically; Defined structure with reproducible synthetic method	Biochemical	Typically <0.1 μM for <i>in vitro</i> assay; sufficient to confidently associate with cellular activity
Stability	Defined purity; Defined stability; No non-specific chemical reactivity	Cellular	Typically <1-10 μM in mechanistic cell-based assay; sufficient to confidently address hypothesis in cellular context; concentration-dependent effect on target
Solubility	Sufficient aqueous solubility e.g. >100 μM ; No aggregation effects in biochemical assay	Analogs	Defined SAR; correlation of biochemical and cellular target activity.
Permeability	Proven passive membrane permeability or defined active transport	In vivo	Pharmacokinetic properties sufficient to achieve levels in target tissue
Context		Selectivity	
Genetic methods	RNAi and/or mutants of target available for complementary experiments	Profile	Defined selectivity against related targets (>10-100 fold)
Target	Cellular context of the target and potential linked activities considered	Inactive analog	Analog with no biochemical activity shows no activity in cells
Application	Fitness of probe to assess specific hypothesis is considered suitable for application	Other chemotypes	Probes from a different chemical class with similar activity available
Availability	Available for use without restriction; Accessible in sufficient quantities (>20mg); Origin, identity and properties disclosed	Chemo-informatics	Awareness of other bioactivities of chemical class

Figure 1.3. Fitness factors for chemical probes described by Workman and Collins.³² The fitness factors are split into four categories of criteria that a probe should be evaluated to determine its overall suitability for use. Whilst not all probes can reach the thresholds for each criterion, consideration of the criteria can allow for a robust assessment of whether the probe is fit-for-purpose.

The field of chemical biology has grown considerably and resulted in an increasing output of chemical probes in the literature that have served as powerful tools to assess potential targets. A major concern is that there is some inappropriate use and promulgation of low quality chemical probes. For example, of 64 probes produced by the NIH program described above, only 50% were considered to have a high confidence rating.³¹ On the other hand, high quality probes provide enormous potential and promise to test therapeutic hypotheses during target validation. Chemistry probes should therefore be designed with this in mind and adhering to proposed guidelines set out by Bunnage et al.,²⁵ Workmen and Collins,²⁴ and more recently by Blagg and Workmen,³³ can aid progress.

1.4. Targeting DNA damage response (DDR) in cancer

DNA repair plays a prominent role in tumour progression and tumour response to therapy.³⁵ Whilst DDR defects cause and escalate disease, they can provide a weakness that can be exploited therapeutically.^{36–38} As a result, continuing biological and medicinal chemistry research in the DNA damage response (DDR) network has resulted in better targets and candidate drugs in the field of oncology.²⁰

1.4.1. What is the DNA damage response?

Human cells are estimated to typically undergo more than 20,000 DNA damaging events and more than 10,000 replications errors a day. As described in Section 1.1, genomic instability is a major factor underlying the hallmarks that drive cancer.³⁹ Genomic instability, caused by damage to DNA by a variety of agents and processes such as ultraviolet (UV) light, ionising radiation, industrial chemicals and endogenous processes that generate reactive oxidative species,⁴⁰ is counteracted by coordinated signal transduction pathways which are collectively known as the DNA damage response (DDR) (Table 1). The processes generally start off by detection of DNA lesions, followed by signalling of repair factors and finally the physical repair of lesions.⁴¹

Table 1.1. Pathways and key components of the DNA damage response (DDR). BER, MMR, NER, HR and NHEJ are 5 major DNA repair pathways.

DDR pathway	Function	Key pathway sensors, mediators and effectors	Helicase components involved
Base Excision Repair (BER)	Repairs most of the subtle lesions to DNA such as single strand breaks (SSBs) and oxidative damage	PARP1, PARP2, OGG1, APE1, Ligase I, Pol β , XRCC1, FEN1	DNA2, WRN
Mismatch Mediated Repair (MMR)	MMR repairs DNA mismatches and insertion/deletions that arise from replication	MSH2/3/6, EXO1, Ligase I, Pol δ	-
Nucleotide Excision Repair (NER)	Removes bulkier single strand lesions, in particular those caused by UV damage	XPA, XPC, TPS, ERCC1, Pol δ , Ligase I/III	XPB, XPD
Homologous Recombination (HR)	Error free process to repair DSBs utilising DNA sequence on a homologous sister chromatid as a template for the synthesis of new DNA.	MRN, EXO1, ATM, ATR, MK2, BRCA1/2, PALB2, RPA, RAD51, Pol θ , TOPOIII	BLM, WRN, RECQ1, RECQ2, RECQ5, DNA2, BRIP1 (FANCI), RTEL1
Non-Homologous End Joining (NHEJ)	Repairs DSBs by directly ligating the ends of DSBs together	DNAPK, PARP1, CtIP, XRCC4, Ligase IV, XLF, FEN1, Ligase III	KU70, KU80, WRN, RECQ1
Fanconi Anaemia (FA)	Repairs inter-strand DNA crosslinks (ICLs)	FA complex, FANCD, PALB2, RAD51C	BRIP1 (FANCI), FANCD, BLM, XPB, XPD
Translesion synthesis	Acts on base damage that blocks replication-fork progression. Specialised DNA polymerases synthesize DNA using a template strand encompassing a DNA lesion	PCNA, RAD6/18, POLH/I/K	--

1.4.1.1. DNA damage detection and signalling

DDR signal transduction pathways are activated by the detection of aberrant DNA structures caused by DNA damage or replication stress. Sensor proteins directly recognise these aberrant DNA structures and activate the most upstream DDR kinases; ATM (ataxia-telangiectasia mutated), ATR (ATM- and Rad3-related) and DNA-PKcs (DNA-dependent protein kinase catalytic subunit) (Figure 1.4).⁴² These DDR transducers are large serine/threonine kinases and members of the phosphatidylinositol-3 kinase-related kinase (PIKK) family. PIKKs phosphorylate hundreds of proteins that maintain

genome integrity through vital cellular processes.⁴³ All three kinases sense damage through protein-protein interactions that initiate their recruitment to the damage sites, then post-translational modifications and additional protein-protein interactions induce a cascade of phosphorylation events that lead to DNA repair.⁴³

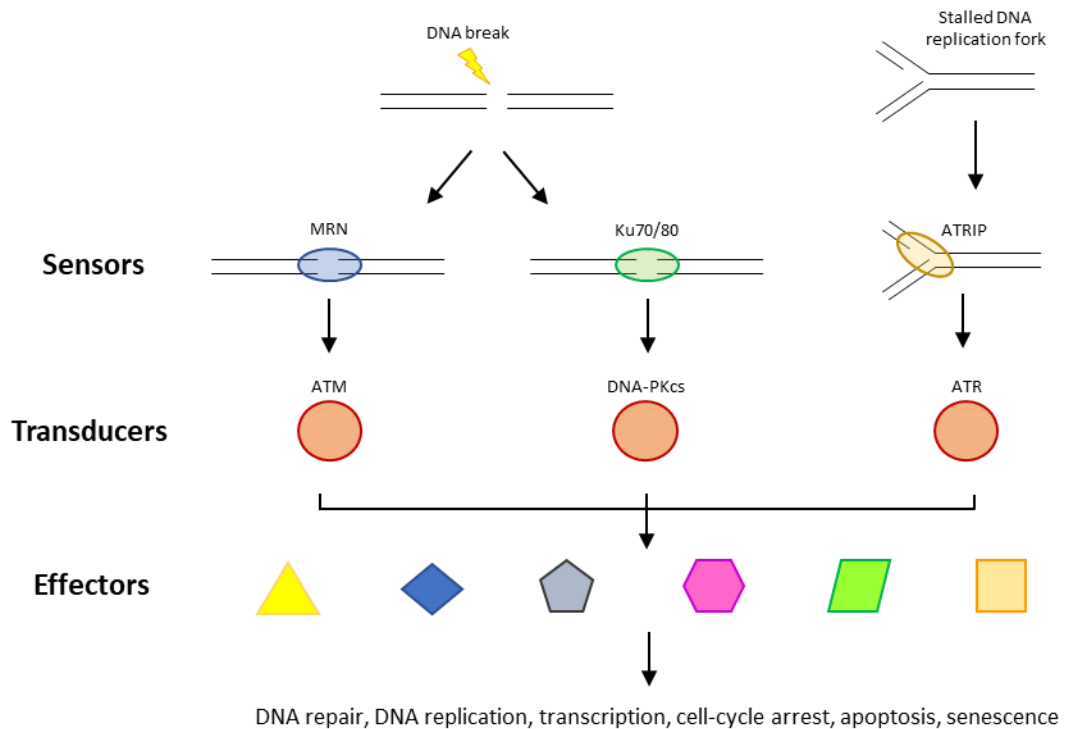


Figure 1.4. The framework of the DDR signalling pathway which consists of signal sensors, transducers and effectors. Sensors recognise DNA structures, transducers such as ATM, ATR and DNA-PKcs relay and amplify the signal to effector substrates that are involved in a broad spectrum of cellular processes such as DNA repair, cell-cycle arrest and apoptosis.

One type of lesion, double strand breaks (DSBs), are particularly deleterious. In cells, the MRN complex (comprising Mre11-Rad50-Nbs1) is one of the first factors recruited to DSBs.⁴⁴ The MRN complex acts as a sensor of DNA ends and recruits and activates ATM. Similarly, DNA-PKcs is recruited to DSBs and activated by Ku70/80 heterodimer (Ku).⁴⁵ ATR is recruited to DNA damage sites through the binding of ATRIP and is activated through the binding of topoisomerase binding protein 1 (TopBP1). These PIKKs regulate many hundreds of downstream repair proteins that function to induce DNA damage repair proteins.^{42,43} They directly regulate the replication associated DNA repair machinery, regulate local chromatin structure and create optimal cellular environments to facilitate and promote DNA repair.⁴⁶

1.4.1.2. DNA damage repair

In humans there are five major repair pathways (Table 5.1). A process termed base excision repair (BER) can repair most of the subtle lesions to DNA such as single strand breaks (SSBs) and oxidative damage. Poly(ADP-ribose) polymerase 1 (PARP1) and PARP2 are examples of key sensors involved in this process.⁴⁷ Bulkier single strand lesions, in particular those caused by UV damage, are repaired by nucleotide excision repair (NER).⁴⁸ NER is split into two pathways: global genome NER (GGNER) which probes and repairs distortions throughout the genome, and transcription-coupled NER (TC-NER) which preferentially repairs transcribed strands.⁴⁹ These processes detect lesions in different ways but repair them by the same mechanism.⁴⁰ Defects in NER are linked to diseases that cause predisposition to cancer and accelerated ageing.⁵⁰

A single DSB can cause cell death and this is exploited in traditional cancer therapy by drugs that induce DSBs. For example, the DNA crosslinking agent cisplatin causes DSBs resulting from DNA intrastrand crosslinks (ICLs).⁵¹ However, these drugs lack selectivity and cause particularly severe side effects.

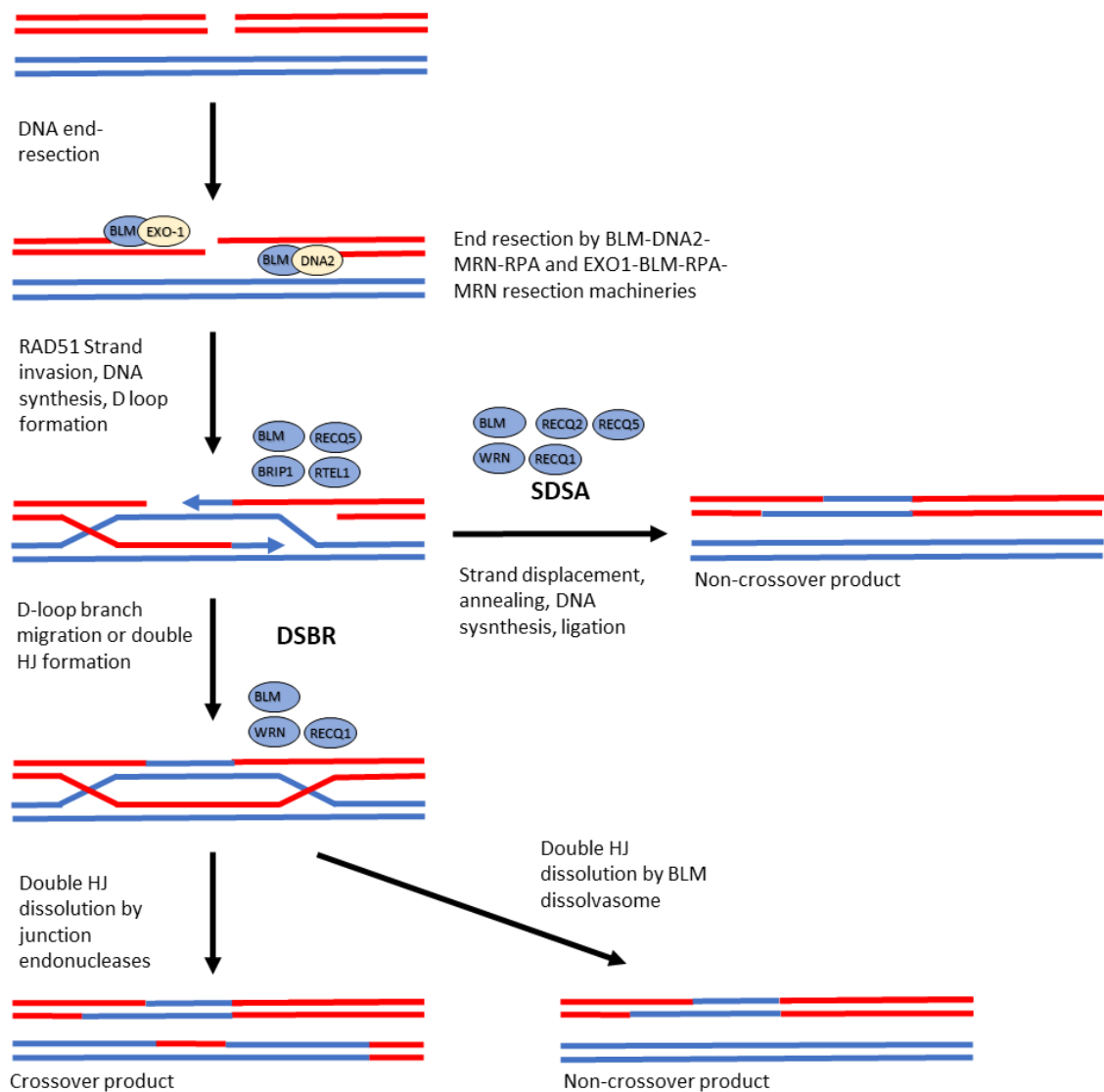


Figure 1.5. Outline of the double strand break (DSB) repair in homologous recombination (HR) mediated DNA repair. Helicases participate in various steps of the DSB repair pathway. The role of helicases in each step of the pathway is shown in blue ovals. DNA is represented by red/blue duplexes. The BLM 'dissolvosome' refers to complex formed with BLM-Topoisomerase α - RMI1-RMI2. DSBR- DNA double-strand break repair; SDSA, synthesis-dependent strand annealing.

The most important mechanisms in the repair of DSBs are nonhomologous end joining (NHEJ) and homologous recombination (HR)^{52,53} (Figure 1.5). Two other pathways, of less importance, have also been identified; alternative-NHEJ and single-strand annealing. NHEJ, the primary mechanism of DSB repair, directly re-joins broken DNA ends without the use of a template.⁵⁴ On the other hand, utilising homologous templates from sister chromatids, HR is the only accurate process available to repair DSBs. HR dominates in S and G2 phase of the cell cycle. HR can also restart stalled replication forks

and repair interstrand DNA crosslinks along with the Fanconi anaemia (FA) protein complex. Deficiency in HR will cause repair to occur through more error-prone pathways such as NHEJ resulting in genomic instability.⁵² Therefore, proteins crucial in HR are vital in suppressing genomic instability and are tumour suppressors. The first key step in HR is DNA end resection. The process occurs through the action of EXO1, a 5' to 3' exonuclease, or through the action of DNA2 with the BLM dissolvasome.⁵⁵⁻⁵⁷ Resection by degradation of DNA ends in the 5' to 3' direction produces DNA containing single-strand tails with 3'-ends, which are then used for strand invasion by RAD51 in the next step of HR. One of the defining steps in HR is DNA strand exchange. RAD51 recombinase, a DNA-dependent ATPase, plays a key role in this process by promoting homologous pairing and strand transfer.⁵⁸ RAD51 forms helical nucleoprotein filaments with ssDNA.⁵⁹ The RAD51/ssDNA complex then invades a homologous sister chromatid and, by displacing the homologous strand, produces a D-loop structure (Figure 1.5). Alternative HR pathways for the newly synthesised strand begin from the D-loop intermediate. In synthesis-dependent strand annealing (SDSA), the D-loop is displaced and the strand anneals with the other DNA end to give a non-crossover product. In DNA strand break repair (DSBR), a second DSB end is captured to form a double Holliday junction (HJ) that is resolved to give a crossover or non-crossover product.

1.4.2. Targeting DDR in cancer

There has been an increased interest in targeting proteins within the DDR,³⁶ and accordingly there are many drugs in clinical or preclinical testing targeting the DDR.⁶⁰ Recent analyses suggest that there are at least 450 proteins integral to DDR and many of these proteins can be manipulated by small molecule inhibitors to produce potential chemotherapeutic treatments.³⁶ The DDR represents a high potential source of anticancer targets as inhibiting the DNA damage response in cancer can offer a greater therapeutic window and a more selective treatment to patients with tumours lacking specific DDR functions. The reason for this is that there are at least three key aspects of DDR in cancer cells that are different to normal cells, creating several avenues that can be exploited for novel cancer therapies.

1.4.2.1. Synthetic lethality

High levels of genomic instability in cancer cells could mutate DDR protein genes and cause cells to favour alternative repair pathways. This compromised ability to repair DNA damage can be therapeutically exploited using synthetic lethality. Synthetic lethality as a chemotherapeutic strategy is based on the premise that inhibition of a DNA repair pathway in a tumour inherently deficient of a compensatory repair pathway will lead to cell death.⁶¹ That is to say that removal of two proteins in combination will lead to cell death, whereas removal of just either one will allow for cell survival.

Synthetic lethality was first demonstrated clinically through the development of small molecule inhibitors of poly(ADP-ribose) polymerase 1 (PARP1). Inhibition of PARP1, a single-strand break repair (SSBR) enzyme, increases sensitivity of cell death to cells deficient in HR proteins BRCA1 and BRCA2.^{62,63} PARP1 inhibition leads to persistence of SSBs that stall and collapse replication forks potentially creating DSBs, and in the absence of HR the accumulation of DSBs lead to cell death.⁴⁰ Non-cancerous cells will survive treatment with the inhibitor as they would have functional HR. Olaparib (AZD-2281),⁶⁴ the most progressed clinical PARP1 inhibitor, has been approved by the US Food and Drug Administration (FDA) as monotherapy in BRCA-mutated advanced ovarian cancer resistant to prior chemotherapy. PARP1 inhibitors serve as a 'proof of concept' in using synthetic lethality as a strategy in targeted cancer therapy.

1.4.2.2. Exploiting replication stress

DNA replication stress is a major component of cancer because cancer cells are characterised by a loss of control mechanism for DNA replication.⁶⁵ Obstacles to DNA replication can originate from various intracellular and extracellular sources. On a molecular level, the causes of replication stress all cause uncoupling of DNA polymerase from the replisome helicase activity. Replication stress is when an aberrant replication fork structure results in the generation of an extended ssDNA at the replication fork. This is followed by binding of RPA and a DNA repair response led primarily by ATR kinase.⁶⁶ ATR prevents replication fork collapse through multiple mechanisms using its effector CHK1. In addition to the ATR-CHK1 pathways, the WEE1-CDK1/2 pathways are also core pathways involved in coordination of DNA replication and maintenance of

stalled replication forks.⁶⁷ Due to the increasing evidence for the role of these pathways in the repair of replication forks, inhibitors of ATR, CHK, WEE1, CHK1 and CHK2 are currently being investigated in clinical trials (Table 1.2).¹⁴ It is thought that the replication stress caused by cancer chemotherapy will be greater in cancer cells than normal cells as cancers are associated with cell-cycle checkpoint loss, oncogenic drivers, and higher levels of reactive oxidative species, therefore providing a greater therapeutic window when combined with inhibitors of vital replication repair proteins.¹⁴

1.4.2.3. Combining DNA-damaging agents with DDR inhibitors

The anti-cancer efficacy of radiation therapy, a mainstay of cancer treatment, is due to an ionisation effect that generates DNA-damaging oxygen free radicals that induce SSBs and DSBs. The effect of radiotherapy can be enhanced by combination with DDR inhibitors¹⁴ and a number of DDR-targeted agents combined with radiation therapy have demonstrated preclinical efficacy,^{68,69} but knowledge of how to effectively use such agents in this combination is limited. In addition, DDR inhibitors may also be combined with DNA-damage-inducing agents such as alkylating agents, topoisomerase inhibitors and platinum salts (e.g. cisplatin) to achieve improved therapeutic windows. However, due to the fact that chemotherapies are delivered systematically, and they have overlapping toxicities with DDR inhibitors, this may not necessarily be the case. Despite some clinical trials being terminated due to adverse effects, some clinical data has shown that chemo-resistant cancers can be re-sensitised by the combination of DNA damaging agents with DDR inhibitors.⁷⁰ The use of novel approaches to therapy, such as gapping the schedules between the chemotherapy and DDR targeted therapy can aid to maximise the potential of this combination strategy.⁷¹

1.4.2.4. Current inhibitors and future targets

Table 1.2. Small molecules inhibitors of DNA repair in clinic. For complete review, see Prakesh *et al.*⁷²

Protein	Roles	Inhibitor	Mechanism	Potency	Clinical status	Ref
DNA-PK	DNA damage signalling protein in NHEJ	VX-984	ATP-competitive inhibitor	IC ₅₀ : 88 nM	Phase I	⁷³
		NU7026	ATP-competitive inhibitor	IC ₅₀ : 230 nM	Pre-clinical development	⁷⁴
CDK2	Cell cycle (G1/S transition)	Milciclib	ATP-competitive inhibitor	IC ₅₀ : 45 nM	Phase II	⁷⁵
PARP1/2	Multiple DDR pathways	Olaparib	Binds in the ADP-ribosyl transferase catalytic site	IC ₅₀ : 1–30 nM	FDA approved	⁷⁶
		Veliparib	Binds in the ADP-ribosyl transferase catalytic site	IC ₅₀ : 3–5 nM	FDA approved	⁷⁶
ATM	DSB and cell cycle	AZD0156	Binds to the ATP binding pocket	IC ₅₀ : 20 μ M	Phase I	⁷⁷
		KU-59403	Binds to the ATP binding pocket	IC ₅₀ : 3 nM	Pre-clinical development	⁷⁸
ATR	SSB and cell cycle	AZD6738	Inhibits ATR kinase activity	IC ₅₀ : 1 nM	Phase I	¹⁴
		VE-822	Inhibits ATR kinase activity	IC ₅₀ : 19 nM	Phase I	⁷⁹
MRE11	MRN complex	PFM39	Inhibits exonuclease activity	IC ₅₀ : 260 nM	Pre-clinical development	⁷⁸
CHK1	Checkpoint protein	MK-8776	Binds to the ATP binding pocket	IC ₅₀ : 3 nM	Phase II	⁸⁰
CHK1/2	Checkpoint protein	LY2606368	Binds to the ATP binding pocket	IC ₅₀ : 1 nM	Phase II	⁸¹
WEE1	Checkpoint protein	AZD1775	Binds to the ATP binding pocket	IC ₅₀ : 5 nM	Phase II	⁷⁷

The clinical success of highly potent PARP1/2 inhibitors is expected to be followed by more approved agents targeting DDR proteins. Currently, a new wave of research is under way targeting various major actors in the DDR such as DDR kinases (ATM, ATR and DNA-PK), CHK1/2 and WEE1. (Table 1.2). For a complete review of current DDR inhibitors, see Prakash *et al* 2018 and Gavande *et al* 2016.^{72,82} There have been large chemical biology research efforts by centres such as the Molecular Libraries Screening Centers Network (MLSCN) and European Infrastructure of Open Screening Platforms for Chemical Biology (EU-OPENSREEN) that have aided identification of probes be used in basic research of biological systems. In the ChEMBL database, over 50 DDR targets have small molecule modulators with activity below 1 μ M and many of these targets possess

more than a hundred inhibitors.³⁶ In addition to these, there still remain many other therapeutic opportunities within the DDR that lack inhibitory chemical matter (Figure 1.6). One family, helicases, are significantly involved in DDR, but chemical biology is less progressed in this field than for other DDR protein classes. No approved drugs for human helicases exist, and analysis of ChEMBL database shows only a few of the 98 human helicases possess some small molecule modulators. The databases demonstrate that most DDR helicases lack chemical matter and given their role in DDR, represent novel potential targets in DDR (Figure 1.6).

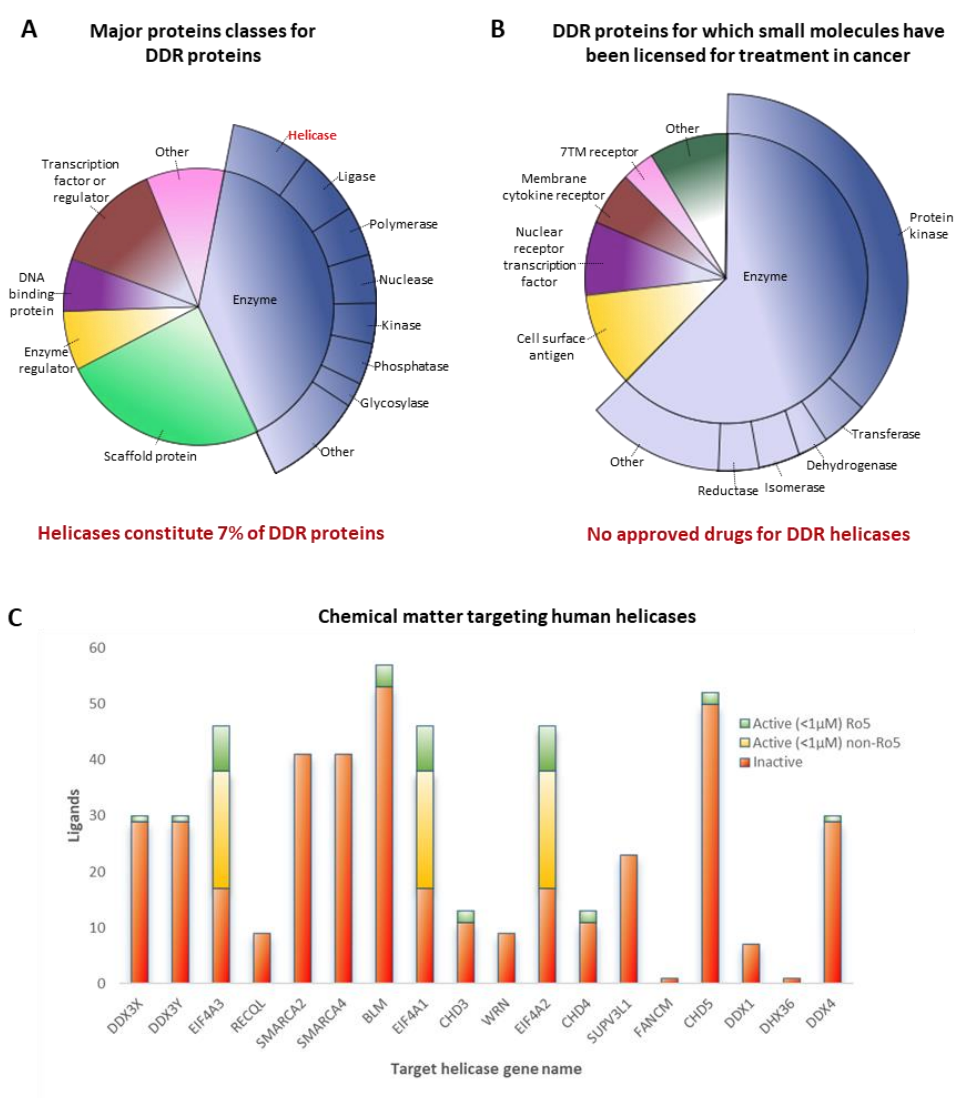


Figure 1.6. (A) Pie chart showing the distribution of the major protein functional classes to which each of the 450 DNA damage response (DDR) proteins have been assigned (B) Pie chart showing the 122 DDR proteins for which a small-molecule drug had been licensed (as of September 2014). Data of (A) and (B) were collected by Pearl *et al* and figure adapted from Pearl *et al*.³⁶ (C) Histograms of small-molecule modulators that have been reported as tested *in vitro* or *in vivo* for efficacy against DNA damage response

(DDR) proteins are indicated. Each bar shows the number of small molecules tested; Red indicates compounds that are inactive at 1 μ M, green indicates active compounds that are compliant with Lipinski's 'rule of five (Ro5)' and orange indicates compounds showing activity that are non Ro5 compliant. Only helicases for which at least one active compound is recorded in the ChEMBL database have been included.

1.5. Helicases in DNA repair

Helicases are enzymes that unwind DNA or RNA in an ATP dependent manner. Generally, helicases exhibit specific polarity depending upon the strand on which they move, either in 3'–5' or 5'–3' direction. Unwinding is not based on sequence specificity but rather on the type and structure of its nucleic acid substrate. Helicases play a significant role in DNA replication, RNA transcription, translation, DNA repair and DNA recombination.⁸³

The role of various helicases in DNA repair has sparked particular interest in the design of novel anti-cancer targeted therapies.⁸⁴ DNA helicases such as BLM, WRN and RTEL1 amongst others have been identified as key proteins involved in many of the DNA damage response (DDR) pathways in cells. Increasingly, proteins involved in DDR have been targeted⁶⁰ with small molecule inhibitors as a strategy to inhibit proliferation of cancer cells directly or through synthetic lethality.⁶¹

1.5.1. Structure and classification of helicases

Using protein alignment studies based on conserved helicase motifs, Umate et al⁸⁵ demonstrated the human genome coded for 95 human helicases. Helicases can be divided into six superfamilies (SF),⁸⁶ and comprise of those that form ring structures and those that do not. Sequence analysis has revealed that non-ring forming helicases can be classified into SF1 and SF2; the largest superfamilies. The other superfamilies are much smaller and consists of ring forming helicases divided into SF3–6.

All helicases contain the Walker A and B motifs that are required for binding of ATP and for DNA strand separation. The Walker A motifs contain end residues consisting of glycine, lysine and serine/threonine. The lysine interacts with the phosphates of the MgATP/MgADP. The Walker B motifs contain an important aspartic acid residue that can co-ordinate with the Mg²⁺ ion.

Superfamilies 1 and 2 (SF1 and SF2) are the largest group and comprise of most of the helicases.⁸⁶ The catalytic core of these two families are highly conserved and consist of 12 characteristic motifs located at conserved positions, suggesting members of these families evolved from a common ancestor.^{87,88} The presence of these motifs are highly predictive of helicase activity.⁸⁶ However, not all these motifs are always present in both families. The conservation of structure within each superfamily is even higher. However, different helicases in each superfamily show a wide diversity in function and even binding and unwinding mechanisms differ considerably. All members of the SF1 and SF2 consists of two core domains known as domains 1 (D1) and 2 (D2). Most enzymes also contain characteristic N- and C-terminal domains (Figure 1.7).

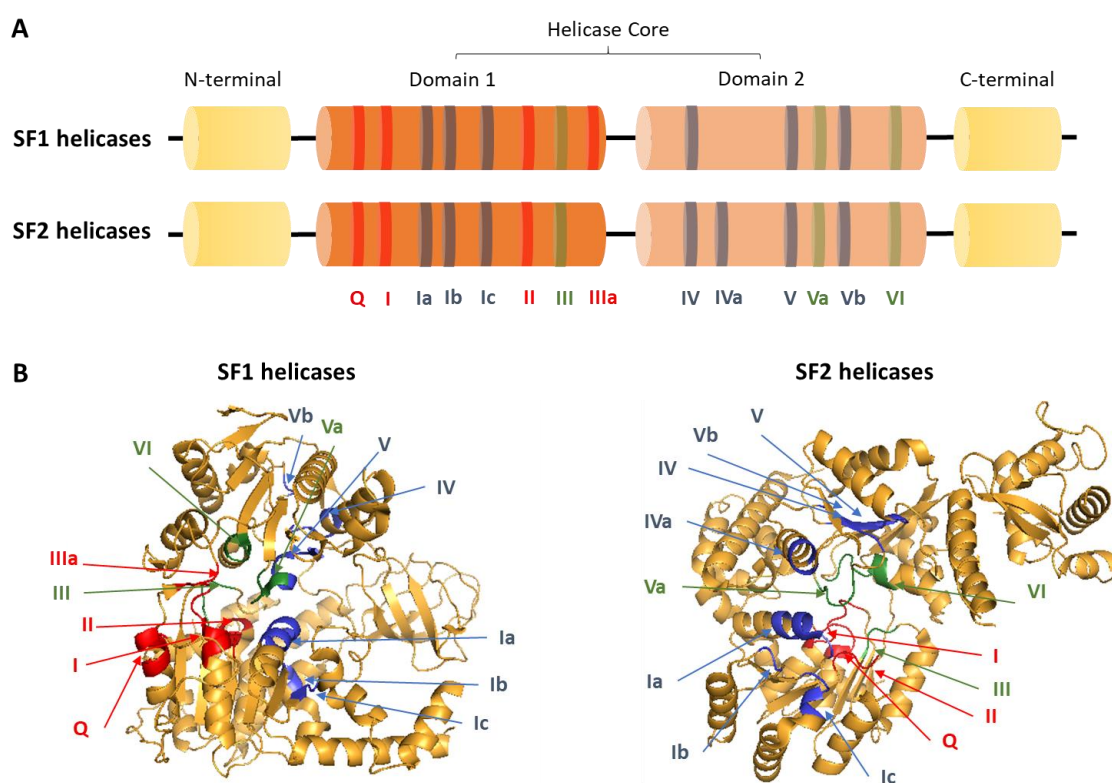


Figure 1.7. Structure of SF1 and SF2 helicases. (A) Characteristic motifs of members of the SF1 and SF2 superfamily. Motifs are coloured with respect to their predominant function: Red, ATP hydrolysis; Blue, Nucleic acid binding; Green, co-ordination between nucleic acid and ATP binding sites (B) Position of characteristic motifs in three-dimensional structures of proteins from each family. SF1 helicases are represented by the human Upf1 helicase core [PDB: 2GJK]. SF2 helicases are represented by human BLM helicase (642-1290) [PDB: 4O3M] See Fairman-Williams for review.⁸⁸

Motifs involved in ATP-binding and hydrolysis are highly conserved in SF1 and SF2 (Figure 1.7). The level of conservation within a superfamily is even higher. The conserved

residues are situated in the cleft between the two core domains. Motifs III and Va (Figure 1.7), are primarily involved in coordination between the ATP binding site and nucleic acid binding site. These motifs are highly conserved within each superfamily and mutations of residues here impair unwinding.⁸⁹ Nucleic acid binding sites are located on the surface of the core domains opposite the ATP binding site. The nucleic acid binding site is less conserved among helicases and while they include certain motifs of the core domain, they may also include non-core domains present in the helicase. These motifs are well conserved within a family, but less so across the superfamily. It is this variation in these families in nucleic acid binding that gives helicases much diversity of function.

The SF3 superfamily consists of small helicase domains and only has three conserved motifs⁹⁰. The SF4 superfamily consists of helicases that have five motifs and are related to *E.coli* DnaB protein, usually forming hexameric ring structures. The SF5 superfamily is related to the transcription factor Rho.

Some helicases that do not catalyse nucleic acid separation still fall under the umbrella of helicases because they contain a helicase domain. For example, members of the SNF2 family, such as RAD54, have been shown to promote separation of duplex DNA in cells.⁹¹ In many instances, these 'helicases' may have a role in structure remodelling, as seen with chromodomains and their unwinding activity.⁹⁰ Further, certain helicases require accessory proteins to enable helicase activity, for example MCM and EIF4A.⁹⁰

The large family of helicase proteins guard access to DNA and RNA and can thus be seen as 'guardians of the genome'. They are involved in varied and numerous processes, but from a chemotherapeutic point of view, it is the role of helicases in DNA damage repair pathways that are of most interest.

1.5.2. Helicases in DDR

Due to the prominent role of helicases in DNA and cell proliferation, there has been a concerted effort to investigate their molecular and cellular functions. These efforts have revealed a link between helicases and their role in DNA damage response and genomic stability (Table 1.1), suggesting this class of enzymes may be a viable target for chemotherapeutic strategies.

The Ku dimer, comprising of Ku70 and 80, contains ATP and helicase domains. The Ku protein recognises DSBs and leads to binding and activation of DNA-PKcs, a protein kinase which can signal repair enzymes.⁹² It should be noted that helicase activity of Ku is not needed for DSB repair. RECQ1, the most abundant helicase, promotes strand exchange on stalled DNA fork structures by unwinding the leading DNA strand, an activity modulated by RPA. This strand separating activity is necessary for an RPA-mediated response to replication stress.⁹³

Double strand breaks can potentially be lethal and all five RecQ helicases are implicated in the repair pathways involved; non-homologous end joining (NHEJ) and HR⁹⁴. All RecQ helicases are known to interact with RAD51 and RPA while 4 of the 5 RecQ proteins interact with PARP1; these protein partners all have important roles in DDR. Both WRN and RECQ1 are involved in NHEJ. For instance, WRN interacts with Ku70 and DNA-dependent protein kinase (DNA-PK), both vital in NHEJ.^{95–97} In HR, DNA end resection by DNA2 is stimulated by BLM,⁵⁷ and BLM, WRN and RECQ1 stimulate end resection by EXO-1.^{98,99} BLM, WRN and RECQ1 also interact with important HR intermediates such as D-loops and double HJs.^{100–103} All five RECQ helicases are found to have strand annealing activities and have been shown to have a role in SDSA in HR.¹⁰⁴

Along with BLM, DNA helicases FANCM and RTEL1 also dissociate D-loops.¹⁰⁵ FANCM also promotes branch migration of HJs.¹⁰⁶ RTEL1 has been shown to negatively regulate HR and therefore its dysregulation causes loss of HR control.¹⁰⁷ BRIP1, a DNA helicase also known as FANCD1 and BACH1, interacts with BRCA1 in HR. Depletion of BRIP1 results in defective HR and increased genomic instability.¹⁰⁸ Along with DNA repair proteins BRCA1 and BRCA2, mutations in the BRIP1 gene increase risk of ovarian cancer and the protein is thought to act as a tumour suppressor.¹⁰⁹ BRIP1 may enact some control on HR through inhibiting RAD51 strand exchange.¹¹⁰ In the process of NER, the TFIIH complex (consisting of DNA helicases XPD and XPB) is recruited to the site of DNA damage and is responsible for the unwinding of the duplex DNA around the lesion.¹¹¹

1.5.3. DDR helicases as cancer targets

Although our knowledge of the roles of certain proteins in DDR pathways has increased in recent years, the biochemical and genetic interactions between the various pathways are still not fully understood. The use of small molecule inhibitors of proteins could greatly facilitate understanding of these pathways. A number of enzyme classes have been identified with a role in DDR pathways, such as nucleases, ligases and polymerases.³⁶ Helicases are an important class of enzymes in DDR whose inhibition could facilitate greater understanding of DDR and advance the search for synthetically lethal interactions. A recent computational analysis identified helicases as a large class of enzymes in DDR and that many helicases lacked any chemical matter.³⁶ These included POLQ-like (HELQ), HFM1, PIF1, INO80, SMARCA2 and SMARCA4. In addition to DNA helicases, many of the DEAD/H RNA helicases have also been implicated in cancer and the therapeutic potential of targeting these helicases has been reviewed.¹¹²

The most promising helicase targets in cancer therapy are those of the RECQ family. As mentioned, defects in three of the family members are linked to diseases that predispose to cancer of a wide range of tumour types: BLM to Bloom syndrome, WRN to Werner syndrome and RECQL4 to Rothmund–Thomson syndrome (RTS), Rapadilino syndrome and Baller–Gerold syndrome (BGS).¹¹³ Further, RECQ1 and RECQ5 have also been linked to cancer. Expression of RECQ1 is upregulated in various cancer types^{114,115} and its depletion leads to increased chromosomal instability¹¹⁶ and reduced tumour progression.¹¹⁷ Inhibition of RECQ1 in cancer reduces cell proliferation and renders cells more sensitive to DNA-damaging drugs that inhibit fork progression. Depletion of RECQ5 also slows cell proliferation.¹¹⁸

Members of the human iron-sulphur (Fe-S) DNA helicases include XPD, BRIP1, RTEL1 and DDX11 and are implicated in various diseases associated with genome instability and cancer.¹¹⁹ Another DNA helicase, PIF1, has been found to suppress apoptosis,¹²⁰ and mutations in the protein causes predisposition to certain types of breast cancer.¹²¹

Anticancer agents such as topoisomerase inhibitors, mitomycin C and cisplatin introduce DSBs and this effect can be enhanced by inhibitors of DSB repair. Therefore, helicases involved in NHEJ or HR may be useful to target for use as combination therapy with these

traditional chemotherapeutic agents. RECQ helicases are implicated in the repair of interstrand crosslinks via the Fanconi Anaemia (FA) pathway, so inhibition of these helicases could enhance chemotherapeutic effectiveness by preventing DSB repair. For example, inhibition of WRN helicase enhances the tumour suppressing ability of the DNA damaging agent selenium.¹²² Helicases that are involved in BRCA1/2-mediated DSB repair and FA interstrand cross-link repair can also be potentially good targets as certain helicases such as the MCM helicase complex are implicated in cell cycle regulation.

As mentioned above, and reviewed by Gupta,⁸⁴ there is an increasing amount of evidence gathering that depletion of certain helicases causes genomic instability and the predisposition to cancer. Inhibiting DNA repair by targeting DNA helicases in rapidly proliferating cancer cells can propagate genomic instability that leads to cell death. In particular, a synthetic lethality chemotherapeutic strategy can lead to a highly selective therapy.

1.5.4. DDR Helicases and synthetic lethality

It has been hypothesised that inhibitors of helicases may cause synthetic lethality if there are mutations in key proteins in DNA repair networks that are also dependent on helicases. For example, 15% of all cancers have defects in the FA pathway, suggesting a potential avenue for synthetically lethal helicase inhibition. This was demonstrated when deficiencies in both FBH1 and BLM resulted in an increase in sensitivity to a DNA damaging agent and the number of spontaneous sister chromatid exchanges (SCEs). SCEs are a characteristic feature of Bloom syndrome (BS) patients who lack BLM¹²³.

A synthetic lethality screen against the *C. elegans* protein him-6 identified rtel-1 as a synthetically lethal partner.¹⁰⁷ Both proteins are human homologs of BLM and RTEL1, respectively. The same study also found a synthetically lethal relationship between *C. elegans* rtel-1 and rcq-5, the human homolog of RECQ5. The link suggests RTEL1 could play a role as an antagonist of HR as both BLM and RECQ5 are also known to control HR through certain antagonist activities.⁹⁴ Further screening is required to understand synthetically lethal relations with helicases and other DNA damage repair proteins.

Whilst DNA repair inhibitors may enhance the action of certain chemotherapeutic drugs thereby reducing their required dosage and associated toxicity, it is synthetic lethality that has more appeal as a chemotherapeutic option because it reduces the need for toxic drugs. Helicases play an integral role in DNA damage and so synthetic lethality with compensatory pathways of DNA repair are of huge interest. The design of tool compounds that inhibit helicases specifically can help to increase understanding of the role of helicases in DNA damage, aid synthetic lethality screens, and also provide a starting point for future inhibitors should helicase targets be validated as viable cancer targets.

1.5.5. Inhibiting DNA helicases

Most DNA repair helicases unwind dsDNA in the presence of ATP and require, or their activity is greatly enhanced by, formation of dimers or higher oligomers.¹²⁴ By targeting the ATP-binding site of helicase, a competitive inhibitor can prevent DNA unwinding (Figure 1.8). A helicase inhibitor can also disrupt helicase oligomerisation and helicase binding to DNA. Certain helicases also require other structural interactions with proteins to undertake DNA unwinding and inhibiting protein-helicase binding can be a viable mechanism to helicase inhibition. Alternatively, inhibition of an allosteric pocket can potentially prevent DNA unwinding should inhibition of this site cause detrimental conformational change. Compound inhibiting helicases can also trap DNA on BLM leading to a toxic complex.

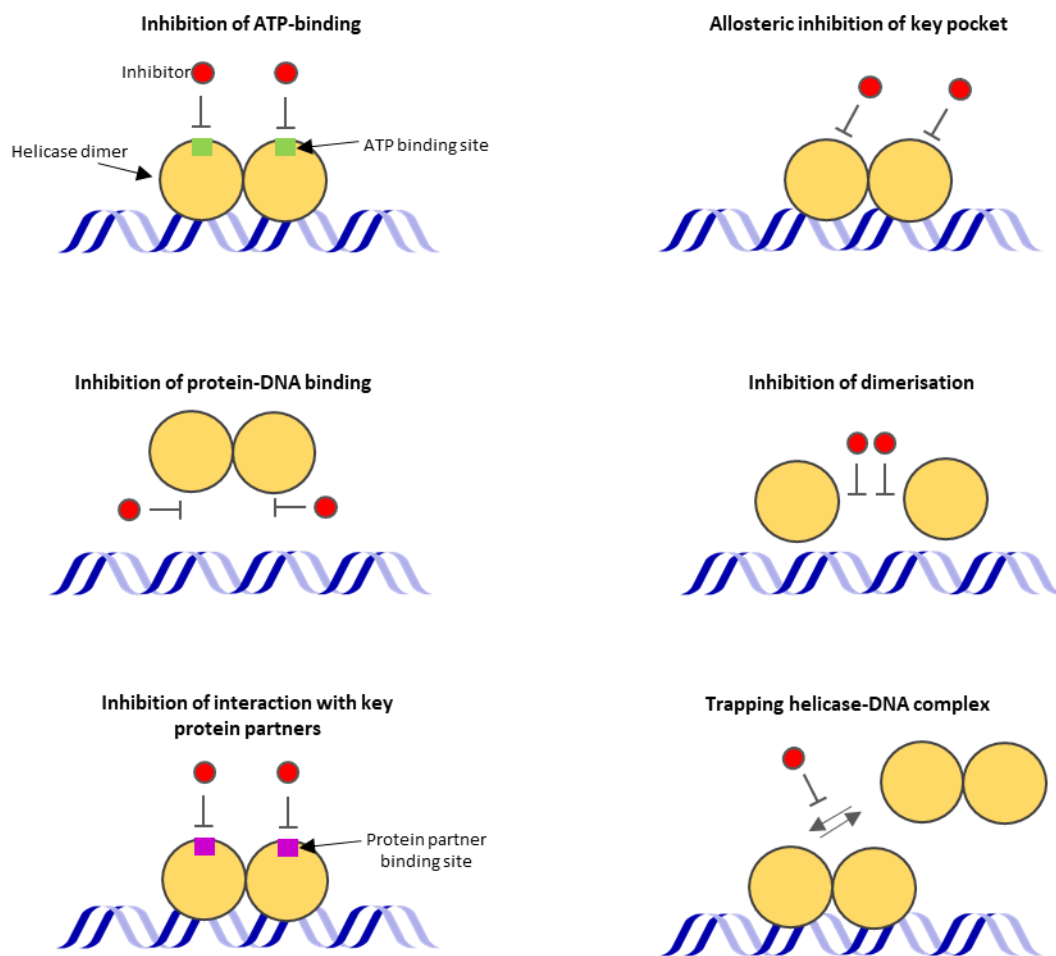
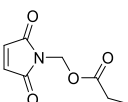
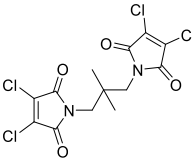
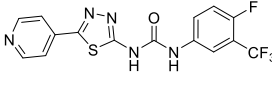
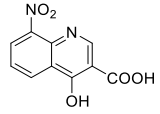
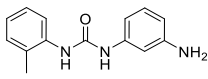
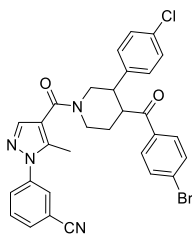
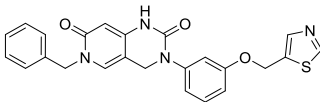


Figure 1.8. Mechanisms of DNA helicase inhibition.

1.5.5.1. DNA helicase inhibitors

The prominent role of helicases in DNA repair make them prospective targets for anti-cancer drugs. Although there has been progress in recent years, drug discovery of all helicase inhibitors has historically faced many challenges. The reasons for this are that, firstly, most hits in high-throughput screens are those that bind the nucleic acid rather than the helicase, and secondly, monitoring nucleic acid duplex separation in a high throughput format often yields few hits.¹²⁵ Efforts to counteract these effects, for example by using extensive counter screening or structure-based design, have yielded better results. Inhibitors of viral helicases, in particular the herpes simplex virus (HSV) helicase complex, have existed for many years.^{126,127} These potent viral inhibitors have inspired much of the research into helicase inhibitors over the last decade.

Table 1.3. Reported small molecule inhibitors of DNA helicases.

Helicase	Inhibitor	Screen	IC ₅₀ (μM)	Properties	Ref
WRN	 NSC19630	HTS helicase screen of NCI diversity set	20	WRN selective; inhibits cell proliferation; induces DNA damage; enhanced lethality with PARPi	128
WRN	 NSC617145	HTS helicase screen of NCI diversity set	230	WRN selective; inhibits cell proliferation; induces DNA damage; enhanced lethality with mitomycin C in FA mutant	129
BLM	 ML216	HTS helicase screen of MLSMR	3	Inhibits WRN helicase; inhibits cell proliferation; Elevates SCE: enhanced lethality with mitomycin C;	1
DNA2	 C5	Virtual screen	20	Helicase selectivity not assessed; inhibits cell proliferation; inhibits fork resection and recombination; enhanced lethality with PARPi	130
DDX3	 1-(3-Aminophenyl)-3-o-tolylurea	Virtual screen	5	Inhibits ATPase and helicase activity; suppresses HIV-1 replication	131
EIF4A3		HTS helicase screen	0.26	Selective against EIF4A1/2; inhibits nonsense-mediated RNA decay (NMD)	132
BRR2		HTS helicase screen	1.3	Inhibitor co-crystallised with protein; selective against helicases;	133

Recently, increased efforts have been undertaken to discovery inhibitors for human helicases. No human helicase inhibitor has entered clinical trials. Many known early non-human helicase inhibitors, normally consisting of nucleotide, nucleobase or polyphenols with two or three linked phenyl ring pharmacophores, inhibit the ATP binding site.¹²⁵ However, as previously mentioned, the helicase ATP domain is highly conserved and this creates challenges when attempting to design selective inhibitors.

The nucleic acid binding sites are relatively less conserved and inhibitors targeting this site would, in theory, be more selective. However, small molecules targeting this site

have been hard to discover. By designing assays to measure DNA unwinding, many small molecules inhibiting the nucleic acid itself are detected. Most groups rely on fluorescent intercalator displacement (FID) assays to detect small molecule-DNA interactions. However, these FID assays do not detect all compounds that interact with DNA and are susceptible of generating false positives, as was shown by Li¹³⁴ when developing inhibitors of HCV NS3 helicase. Many nucleic acid type inhibitors, such as the bacterial helicase Dna2 inhibitor CID1296013, tend to incorporate multiple phenyl ring systems with electron withdrawing substituents and few rotatable bonds.¹³⁵

The RNA helicase, DDX3, is implicated in HIV-1 replication and a virtual screen campaign led to the development of 1-(3-aminophenyl)-3-*o*-tolylurea that bound to residues implicated in the coordination between the ATP binding site and nucleic acid binding site (Table 1.3).¹³⁶

Most reports of human helicase inhibitors are of DNA repair proteins. In humans, the WRN inhibitor NSC19630 (Table 1.3), discovered through a screen of an NCI diversity set, was found to disrupt DNA binding in a potent and selective manner.¹²⁸ The inhibitor impaired growth and proliferation, induced apoptosis, induced DNA double strand breaks and caused accumulation of stalled replication forks. Administration of the topoisomerase inhibitor topotecan increased its antiproliferative effects in cell lines.

HTS of over 355,000 compounds led to the development of NIH molecular probe against BLM helicase termed ML216 (Table 1.3).¹ ML216, not selective against WRN, was also found to be anti-proliferative in cellular studies. Along with WRN and BLM, an extensive screen has also been performed for RECQ1. Many of the potent hits from the high-throughput screens against BLM, WRN and RECQ1 show similar pharmacophores to nucleic acid binding site helicase inhibitors described earlier.

Researchers at Takeda recently developed EIF4A3 inhibitors that were selective ATP-competitive for use as tool compounds (Table 1.3).¹³⁷ The same group have also discovered multiple series of selective tool EIF4A3 inhibitors with favourable pharmacokinetic properties that have demonstrated *in vivo* antitumour efficacy.^{132,138} Furthermore, the group's focus on another RNA helicase, BRR2, has yielded selective inhibitors that have been co-crystallised and chemically optimised.¹³³ These inhibitors

bind at a novel allosteric site between the core D1 domain and the Ig domain from the N-terminal.

Discovery of ML216, the first potent inhibitor of BLM, is of interest in this project because of its key role in certain aspects of DNA repair. The potent inhibitor, already in the public domain, could make BLM a tractable helicase target by providing a starting point to develop more potent, selective inhibitors of the helicase family using a structure-based design strategy.

1.6. BLM helicase

BLM helicase is a member of the RECQ family of helicases. The other members are RECQ1, RECQ4, RECQ5 and WRN and are part of helicase SF2. These proteins are well conserved and all share a core helicase domain where ATP binding and hydrolysis takes place to allow DNA strand separation.¹³⁹ It has roles in base excision repair and telomere maintenance, but its most important role is in DSB repair, specifically via the HR repair pathway. The role of BLM in DNA repair and its complex interactions with key proteins in these networks suggest it may be a viable chemotherapeutic target.

1.6.1. Structure

Two crystal structures have been recently reported of BLM helicase in the presence of ADP and DNA (Swan et al.⁸¹ PDB[4O3M]; Newman et al.¹⁴¹ PDB [4CDG]). Newman's structure of BLM in the presence of a nanobody shows BLM locked in an open conformation.

The overall structure of BLM can be divided into three highly conserved elements characteristic of the RecQ family of helicases: the helicase core, the RecQ C-terminal (RQC) domain, and the helicase-and-ribonuclease D/C-terminal (HRDC) domain⁸⁶ (Figure 1.9). While WRN and BLM contain the HRDC domain like their bacterial and yeast homologues (RecQ and Sgs1, respectively), the HRDC domain is not present in RECQ1, RECQ4 and RECQ5 helicases.

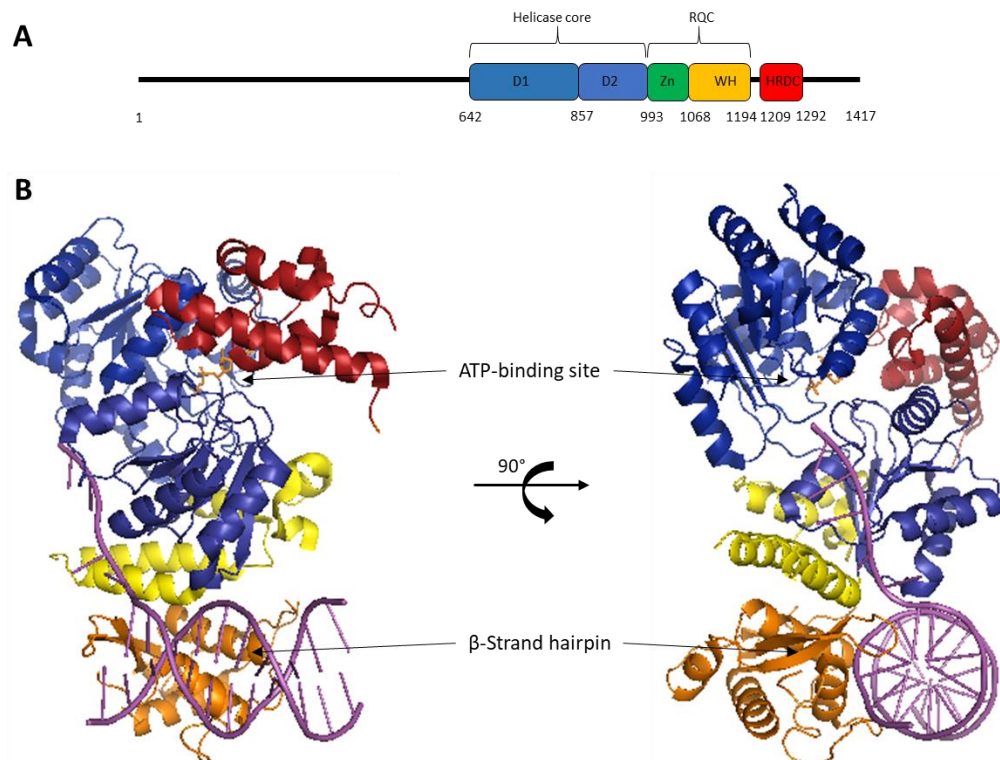


Figure 1.9. Sequence and structural organisation of BLM helicase. (A) Sequence representation of BLM organisation consisting of the helicase core, RQC and HRDC domains. The RQC domain consists of the Zn and WH subdomains. **(B)** Representation of the ternary 3D crystal structure of BLM in complex with ADP and 3'-overhang duplex DNA using PDB 403M. The protein is shown in cartoon form and the coloured domain are analogous to those in (A). ADP is shown in stick form and is coloured orange. DNA is shown in cartoon form and is coloured purple. Zn, zinc-binding subdomain; WH, winged helix; HRDC, helicase and RNaseD C-terminal.

The BLM helicase core is composed of two subdomains. The first subdomain (642-857) consists of seven parallel β -strands between five α -helices on the solvent-exposed side and four α -helices on the ATP-binding face (Figure 1.9B).¹⁴⁰ The first subdomain is most closely associated with the ATPase domain. The active site contains the highly conserved glutamine residue (Gln672), which along with Asn667 make important hydrogen bonds with ATP. The ATPase domain associates closely with the Zn subdomain of the RQC. The second subdomain is composed of six β -strands with two α -helices inserted on either side. This core helicase domain is highly conserved within the RECQ family and also in the helicase SF1 and SF2,⁸⁸ particularly for motifs that coordinate binding and hydrolysis of ATP.

The RQC domain (994-1032) is composed of a zinc-binding subdomain and a winged-helix (WH) containing subdomain. The RQC domain is involved in the binding of various DNA structures and proteins.¹⁴² The winged-helix consists of a short anti-parallel β -strand followed by four α -helices. The winged-helix motif is a subset of the helix-turn-helix superfamily which are found in many nuclear proteins, but the RecQ RQC domains do not form hydrogen bonds with bases or induce bends in DNA.¹⁴³ The loop linking the α 2- α 3 helices plays a major role in DNA interaction and Ser1121 is a vital residue that forms a hydrogen bond with the phosphate backbone of DNA.¹⁴⁴ The β -hairpin consists of two residues, Ala1163 and Asn1164 and is polar in nature. Asn1164 has been shown by mutagenesis studies to be a critical residue for DNA strand separation by BLM.¹⁴⁰ In the closely related WRN helicase, the residues of the β -hairpin are aromatic.

The HRDC domain (1209-1292) is connected to the WH subdomain by an extended linker and sits above the ATP-binding site making extensive contact with parts of the helicase core. It has been shown that the presence of the HRDC domain improves enzyme helicase activity.¹⁴⁰ The ATPase activity of BLM is reduced in the presence of the HRDC domain, however this effect is insignificant because ATP is at saturating concentrations. Due to its effects on both ATPase and helicase activity, it has been suggested the HRDC domain plays a role in coupling ATP and helicase activities in human BLM. The HRDC domain is positioned away from the DNA-binding region¹⁴⁰ and does not interact with DNA.¹⁴⁵ However, the presence of the HRDC domain is necessary to catalyse dissolution of double Holliday junctions with Lys1270, positioned at the interface of the HRDC and D1 helicase core subdomain, found to be important for efficient dissolution.¹⁴⁶

The majority of interactions with BLM and the DNA duplex occur with the bound 3'-overhang DNA and the single-strand region of BLM.¹⁴⁰ There are also key interactions between the β -hairpin of the WH subdomain and the DNA duplex where separation of the two bases occurs.

1.6.2. Bloom syndrome (BS)

The BLM gene is located at chromosome 15 at 15q26.1 and encodes a protein with a MW of 159,000 Da and 1417 amino acids in length. Mutations in the BLM protein lead

to a rare autosomal recessive disorder known as Bloom syndrome (BS).^{147–149} Clinically, BS is characterised by growth retardation, facial sun sensitivity, telangiectatic erythema, severe immunodeficiency, and a predisposition to many different types of cancers, especially acute leukaemia and lymphoma.^{147,150} In contrast to many other cancer predisposing syndromes, BS predisposes to a wide variety of cancer types and cancer is the leading cause of death in patients.

Bloom syndrome is most commonly caused by nonsense mutations that result in a truncated BLM protein, but in roughly 15% of BS patients these truncations are caused by missense mutations that occur in highly conserved regions of BLM helicase.¹⁵¹ The cells of individuals with BS show high genomic instability which enormously predisposes these individuals to cancers. BS cells are characterised by an elevated frequency of chromosome breaks and exchanges, and in particular sister chromatid exchanges (SCE) are characteristic of BS.^{123,152} Observations have shown that these hypermutated chromosomes can manifest as lesions to any part of the chromosome.

1.6.3. Function

Recently, the role of BLM and its RecQ family members in DNA repair has been extensively reviewed.^{94,119,139,153,154} BLM is an ATP-dependent DNA helicase that unwinds DNA in a 3'-5' direction.¹⁵⁵ While BLM can unwind duplex DNA, it also preferentially unwinds a variety of secondary DNA structures such as three- and four-way Holliday junctions, D-loops and G-quadruplexes.^{103,156–158} BLM's preference for these substrates, combined with the chromosomal abnormalities observed in BS, is highly indicative of its role in disrupting and resolving secondary DNA structures that arise in DNA repair processes such as HR.¹⁵⁷

Full length BLM exists as a hexameric helicase in cells.¹⁵⁹ These hexameric ring structures form as a result of association of residues from the N-termini.¹⁶⁰ The closely related RecQ family member WRN can also exist in a hexameric form in cells by association with the N-termini exonuclease domain.¹⁶¹ However, it has been shown that BLM's catalytic core (642-1290) can unwind DNA with the same substrate specificity as the full length enzyme and so BLM functions as a monomer during DNA unwinding.¹⁶² Further, more

recent kinetic studies have revealed that DNA binding of BLM is more favoured with the enzyme in its monomeric form¹⁶³ and dynamic light scattering revealed that ATP hydrolysis triggered disassociation of oligomeric BLM to the monomeric form.¹⁶⁴ However, it may still be possible that oligomerisation is needed for binding and unwinding of more complex secondary structures of DNA. For example, it has been modelled that the BLM dimer may be necessary for branch migration of a double HJ.¹⁴³ Further research is required to understand the role of higher order oligomeric forms of BLM in DNA unwinding of all types of substrates.

BLM functions in DNA repair, replication and recombination. Rapid recruitment of BLM occurs during the DNA damage response^{165,166} and expression of BLM increases in late S and G2 phase^{165,167} giving further credence to its role in DNA repair.

1.6.3.1. BLM helicase and double strand break repair

HR is a major repair pathway of DSBs that occurs in S and G2 phases of the cell cycle when a closely associated sister chromatid is used as a template. DNA end resection is one of the earliest steps in DSB repair. BLM's helicase activity is an essential component of the DNA2 repair pathway where the BLM-DNA2-MRN-RPA complex resect DNA in an ATP-dependent manner.⁵⁷ Here, BLM physically interacts with DNA2 and is recruited by MRN to the DNA end. The same study found that BLM also acts a stimulatory component of the EXO-1 dependent repair pathway, indicating a role for BLM in DNA end resection in HR.

DNA topoisomerases are molecular machines that regulate the topological state of DNA in cells by passing one strand or both strands through a break in the opposing single or double strand of DNA, respectively.¹⁶⁸ Interaction of many of the RECQ helicases with a type I topoisomerase has been shown to be vital in genome maintenance.¹³⁹ BLM interacts with Topoisomerase IIIa with the first 133 amino acids of BLM being vital to enable binding of Topoisomerase IIIa. The BLM-Topoisomerase IIIa complex can correct a high number of SCEs in BS cells, suggesting this interaction is involved in maintaining genomic stability.¹⁶⁹ In the presence of RPA, BLM recruits Topoisomerase IIIa to the promyelocytic leukaemia protein nuclear bodies (PML-NB). BLM stimulates activity of Topoisomerase IIIa on negatively supercoiled DNA through the formation of a stable

complex between BLM and Topoisomerase IIIa.¹⁷⁰ When analysed *in vitro*, the BLM-Topoisomerase IIIa complex catalyses the dissolution of double Holliday junctions (HJs) ensuring non-crossover products in HR.¹⁷¹

Along with BLM and Topoisomerase IIIa, two other proteins, RMI1 and RMI2 have an essential role in stabilising this complex. The BLM-Topoisomerase IIIa-RMI1-RMI2 complex is known as the BLM dissolvasome.¹⁵⁴ RMI1 is thought to influence stability of Topoisomerase IIIa since its depletion leads to increased levels of SCEs.¹⁷² It binds to and stimulates Topoisomerase IIIa via its N-terminus domain which catalyses dissolution of double HJs.¹⁷³ RMI2 associates with RMI1 via its oligonucleotide-binding (OB)-fold domain to form a stable subcomplex termed RMI, which is essential for stabilising this BLM complex.¹⁷⁴ Under physiological conditions, RMI is required for double HJ dissolution.¹⁷⁵ The BLM dissolvasome processes HR intermediates to ensure non-crossover products.

When BLM catalyses branch migration of Holliday junctions, two duplex DNAs interlinked via catenated single strands are formed¹⁷¹. The RMI complex and BLM both stimulate the decatenase activity of Topoisomerase IIIa in the dissolution of these double HJs.¹⁷⁶

The BLM dissolvasome works in many parts of the HR-dependent DSB repair pathway (Figure 1.5) including end resection, D-loop formation and double HJ dissolution. For example, BLM interacts with RAD51 to unwind D-loops.^{103,177} RAD51 plays a central role in DNA strand exchange in HR where it searches for homologous double-stranded DNA (dsDNA) sequences and promotes subsequent DNA strand exchange between ssDNA and homologous dsDNA sequences.¹⁷⁸ The product of this strand exchange, D-loops, can be unwound by BLM. BLM stimulates DNA strand exchange activity of the active ATP-bound RAD51-ssDNA filament,¹⁷⁹ and disrupts the inactive ADP-bound RAD51-ssDNA filament crucial in strand exchange possibly to prevent premature initiation of recombination events and thus further control HR.¹⁸⁰

1.6.3.2. BLM and other DNA transactions

As evidenced by the hypersensitivity of BS cells to replication inhibitors and the observation that cells with BS exhibit slower progression of replication forks, BLM is crucial during replication stress and thought to stabilise and process stalled forks.^{181,182} Following phosphorylation by ATR and ATM, BLM is recruited to stalled replications forks where it can accumulate in focal concentrations.^{182–184} Recruitment of RAD51 to stalled forks and subsequent HR are required for the restart of stalled replication forks and repair of collapsed forks.¹⁸⁵ A potential function of BLM could be to aid fork regression during RAD51-mediated fork remodelling.¹⁸⁶ Additionally, it may promote branch migration of the subsequent regressed fork to restore a functional replication fork.¹⁸⁷ Further approaches are required to resolve the role of BLM during fork regression.

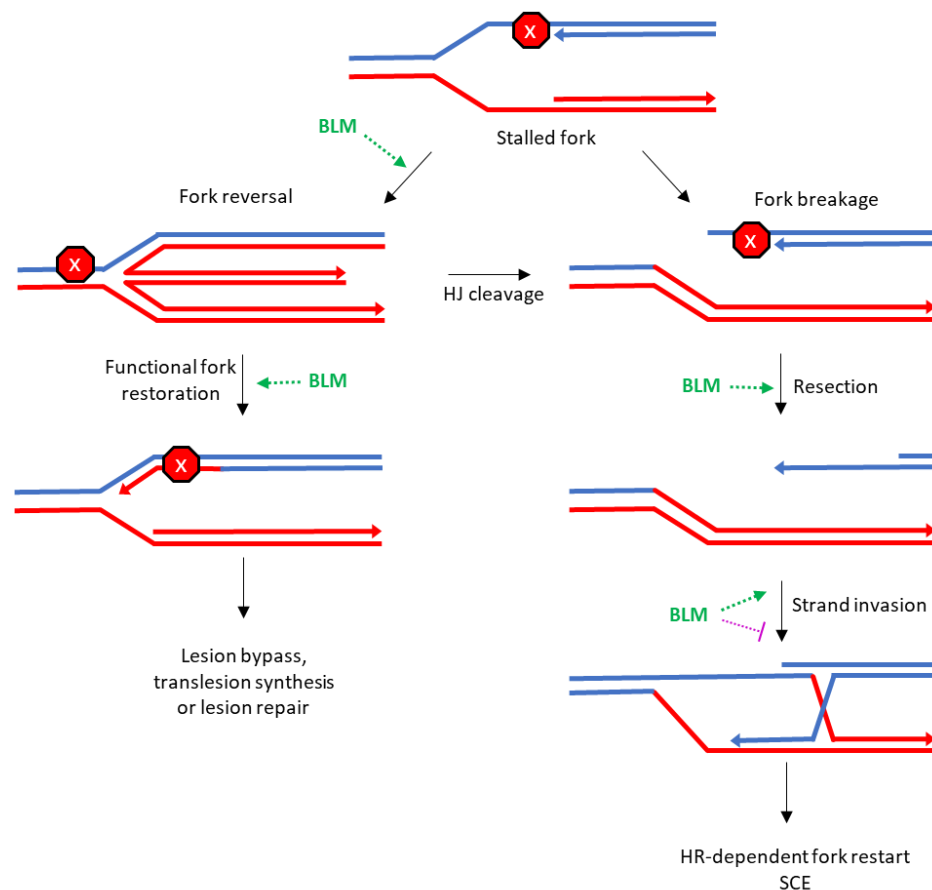


Figure 1.10. Model of BLM role in replication fork restart. When replication fork stalls, new DNA can anneal to produce a Holliday junction (HJ) or reversed fork which can be converted back to a functional fork which allows lesion bypass, repair or translesion synthesis to occur. Alternatively, it can be cleaved that leads to the formation of one-ended DSB. By using the sister chromatid as a template to restart the

fork, HR can lead to crossover products that are visualised as sister chromatid exchanges. Figure adapted from Renty and Elli, 2017.¹⁸⁸

BLM is also implicated in resolution of ultrafine anaphase DNA bridges (UFBs) which are unresolved replication intermediates that manifest in mitosis from the linking of two daughter nuclei.¹⁸⁹ BLM facilitates sister chromatid segregation as part of a complex with TopoIIIa in cooperation with the FANC pathway by resolving these structures that would otherwise result in DNA breakage. BLM deficient cells exhibit an increased frequency of UFBs and micronuclei.^{190,191}

BLM helicase is also involved in alternative lengthening of telomeres (ALT), in particular the HR-mediated telomere maintenance mechanism used in this process to evade telomere attrition.¹⁹² Depletion of BLM-induced telomere shortening in ALT cells and telomeric-sister chromatid exchanges (T-SCEs). BLM interacts with shelterin proteins TRF1, TRF2 and POT1 which stimulate the unwinding of telomeric D-loops and forks by RECQ helicases.^{193–195}

1.6.4. Non-specific inhibitors of BLM helicase

Doxorubicin (Figure 1.11), an anthracycline anti-tumour drug, treats a wide variety of cancers via intercalation of DNA.¹⁹⁶ A widely described activity of doxorubicin is its ability to act as a topoisomerase II poison. The drug is also known to potently block helicases.¹⁹⁷ It has also been suggested that blockade of DNA helicases such as BLM may be central to the mechanism of anthracycline anti-cancer activity.¹⁹⁸ A closely related analogue, 2-pyrrolinodoxorubicin (Figure 1.11), was found to have a much higher antiproliferative activity than doxorubicin which could be explained in part by its greater inhibitory effect on BLM compared to doxorubicin. Another explanation could be its effect on other helicases as anthracyclines are known to hit various helicases, the activities of which were not measured in this study.¹⁹⁹ This further highlights how targeting helicases can be a mechanism to enhance anti-tumour effects of existing drugs and the need to develop tool compounds selectively targeting vital DNA repair helicases to elucidate their mechanisms in cancer.

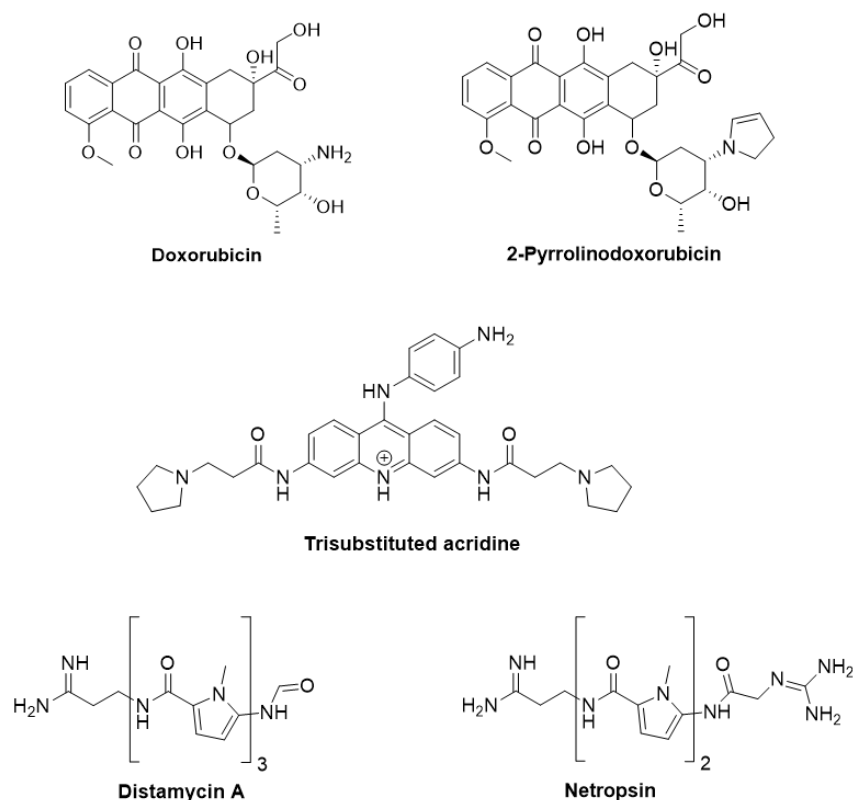


Figure 1.11. Structure of non-specific helicase inhibitors.

Brosh examined the effect of DNA intercalators, minor groove binders and topoisomerase inhibitors on BLM and WRN helicase and found that the minor groove binders distamycin A and netropsin (Figure 1.11) potently inhibited ($IC_{50} = 1 \mu M$) the unwinding activity of these two helicases without disrupting the activity of the related RecQ helicase UvrD.²⁰⁰ The results suggest that the specific modifications made to the minor groove of DNA by these inhibitors directly affect the helicase activity of BLM and WRN helicase, and that the inhibitors display some specificity.

Other specific activities of BLM have also been targeted by non-selective probes. Di- and trisubstituted acridine derivatives (Figure 1.11), known to be potent inhibitors of G4-DNA, were shown to inhibit the helicase activity of BLM and WRN.²⁰¹ This inhibition was not limited to G4-DNA unwinding but also applied to duplex DNA unwinding, and also was selective to these RecQ helicases possessing G4 unwinding activity.

Nonspecific inhibitors are likely to hit multiple proteins in a cell, increasing the toxicity risk to non-cancerous cells. Therefore, an ideal chemical probe or lead compound targeting BLM helicase would be a selective inhibitor of BLM helicase which exerts its

activity through specific binding to the BLM protein rather than an interacting partner such as DNA which would be expected to be highly promiscuous *in vivo*. The compound should also have an acceptable physiochemical profile to allow for cellular and *in vivo* assays.

1.6.5. ML216

The attempts to develop a potent and selective BLM helicase inhibitor from a HTS campaign resulted in the reports of ML216 (**1**) (Figure 1.12).^{1,202,203} As part of the National Institute of Health's (NIH) Molecular Libraries Program (MLP), which aimed to provide early stage chemical probes to aid validation of new drug targets,²⁰⁴ a HTS of 350,000 small molecules from the Molecular Libraries Small Molecule Repository (MLSMR) was performed for BLM helicase. The results of this screen have been deposited for public access in PubChem Bioassay.²⁰⁵ The primary assay used during hit identification measured helicase DNA unwinding with fluorescently labelled DNA [AID720555] (Figure 1.13).

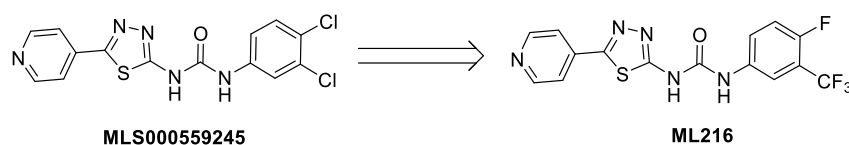


Figure 1.12. Development of ML216 from HTS hit MLS000559245.

From this screen, MLS000559245 (Figure 1.12), was chosen as the starting point for a medicinal chemistry optimisation effort aimed at producing compounds with improved physiochemical properties such as solubility and cell permeability. A small hit optimisation process led to the development of ML216 from MLS000559245.²⁰³

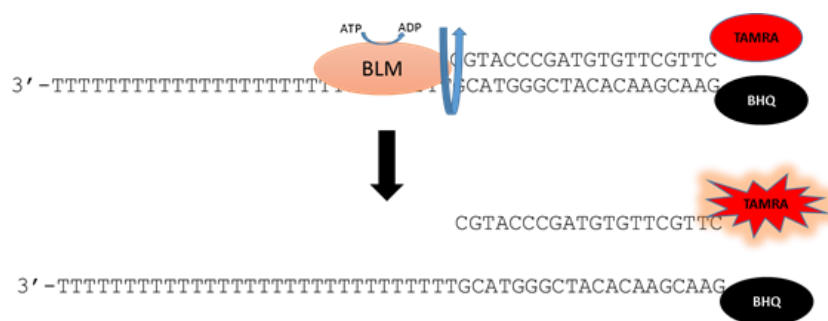


Figure 1.13. Principles of fluorescence DNA unwinding helicase assay. A dual-labelled, partial dsDNA substrate will produce fluorescence upon unwinding by BLM helicase in the presence of ATP. Fluorescence of a TAMRA is normally suppressed by BHQ present on the opposite strand and quenching is lost following ATP-dependent BLM unwinding of DNA.

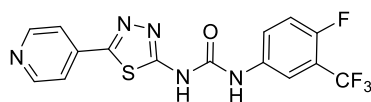
During optimisation of MLS000559245, biological analyses were performed on a truncated variant of BLM (BLM₆₃₆₋₁₂₉₈). This form is fully functional as a helicase and ML216 inhibited BLM₆₃₆₋₁₂₉₈ with an activity of 0.97 μ M as determined by the gel-based unwinding assay. Furthermore, ML216 was found to inhibit potently with full length BLM helicase at an IC₅₀ value of 3.0 μ M. The compound was shown to displace single stranded DNA (ssDNA) and forked duplex DNA from BLM helicase in a dose-dependent manner by competing with DNA for binding with BLM. ML216 also inhibited the disruption of other DNA substrates of BLM such as D-loops, G4 DNA and three/four-way Holliday junctions. However, this was only observed at high concentrations suggesting that ML216 inhibits BLM's ability to unwind duplex DNA much more potently than its ability to resolve the DNA secondary structures mentioned. Mechanism of action studies indicated the compound did not inhibit ATPase activity. A fluorescence polarisation unwinding assay demonstrated the compound had the ability to prevent the BLM/DNA complex forming, suggesting the compound competed with DNA for binding at the nucleic acid binding site.

ML216 was found to have selectivity against related helicases, however it was only 1.5 times more selective for WRN helicase. The series of analogues also showed weak inhibition against RecQ at 50 μ M. But, it was found that the compound did not interfere with WRN function in cellular studies. Cellular studies demonstrated that ML216 can inhibit proliferation and induce SCEs in cells with BLM expressed, but has no effect in BLM-negative cell lines demonstrating phenotypic effects selective with BLM inhibition. Another observation was that the inhibitor increased effectiveness of the DNA

crosslinker mitomycin C suggesting potential enhanced lethality with other anti-cancer agents.

DMPK studies on ML216 showed a favourable microsomal and plasma stability (Table 1.4). However, the aqueous solubility, Caco-2 permeability and efflux ratio of these compounds were poor, suggesting that the physiochemical properties of these compounds could cause difficulties in assay conditions and for later cell-based studies.

Table 1.4. *In vitro* ADME^a properties for ML216 (**1**).



ML216 (**1**)

Aq. solubility (pH 7.4)	MLM stability (T _½)	Plasma stability (5h)	Caco-2 permeability	Efflux ratio
1 µM	> 80 min	100%	1 × 10 ⁻⁶ cm/s	2

^a All values reported by Rosenthal *et al*²⁰²; Solubility refers to kinetic solubility; MLM stability refers to mouse liver microsome stability in the presence of NADPH; Plasma stability was performed using mouse plasma and the proportion remaining after 5 h was determined. The Caco-2 permeability value represents the P_{app} from A to B; Efflux ratio is B to A divided by A to B.

1.6.5.1. SAR summary of ML216

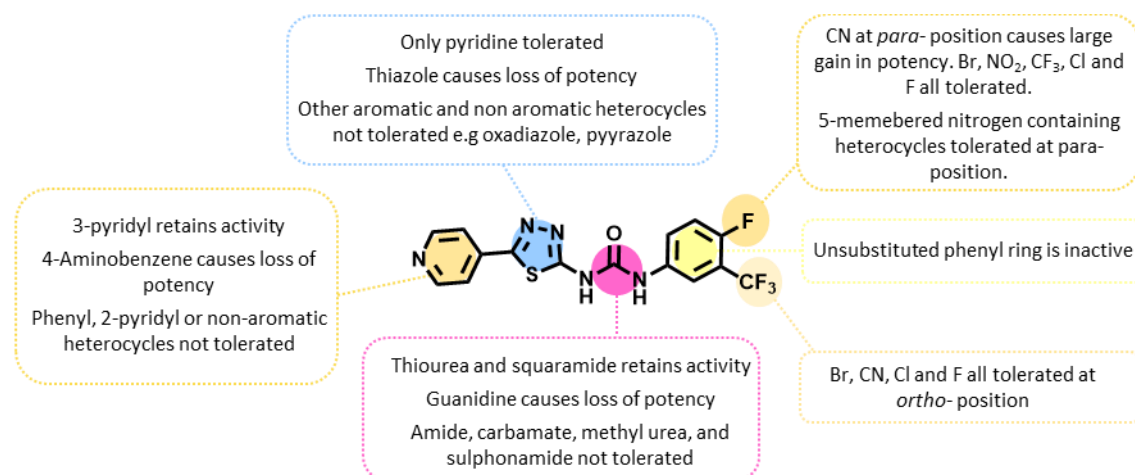


Figure 1.14. SAR summary of ML216 (**1**) conducted by Rosenthal *et al*.²⁰²

SAR exploration of ML216 focused on the four parts of the high throughput hit; the pyridine moiety, thiadiazole moiety, urea linker and the right hand side phenyl ring (Figure 1.14).²⁰³ Minor modifications to the left hand side pyridine moiety revealed that loss of aromaticity or changing to a non-substituted phenyl group resulted in inactivity. Movement of the pyridine nitrogen to the 3- position retained activity but the 2-pyridyl

was not tolerated. Inactivity also occurred when the thiadiazole moiety was replaced with a small number of nitrogen 5- and 6- membered aromatic heterocyclic structures such as oxadiazole and thiophene scaffolds. One exception was a pyridine moiety which showed similar potency. Of the 7 urea isosteres synthesized, only guanidine, squarimide and thiourea derivatives showed limited improvement.

However, exploration of the phenyl moiety did reveal improvements in potency. The exploration consisted of modifications at the *ortho* and *para* positions of the phenyl ring with electron withdrawing groups such as nitrile, nitro and trifluoro groups causing increased potency. For example, compounds **6** and **8** (Table 2.1) with a nitrile at the meta position had an IC₅₀ in the 0.1 µM range. However, the nitrile and nitro resulted in more poorly soluble compounds and were therefore deprioritised. Further, many of these compounds showed poor reproducibility in orthogonal bioassays. Finally, the linkage of 5-membered nitrogen containing heterocycles at the para position resulted in the loss of some potency but was better than having no substituent. These compounds improved solubility 10-fold, but this was still relatively poor.

Despite ML216 not showing significant advancement in structure, potency and ADME properties from the original hit (Figure 1.12), and the overall SAR campaign of 144 analogues demonstrating a narrow SAR for most regions, the series demonstrated many probe-like properties such as good potency, target engagement and some selectivity. As some analogues in this series had shown greater than 10-fold selectivity of WRN, it was expected that BLM selectivity could be achieved. Furthermore, by addressing issues of solubility and permeability during medicinal chemistry optimisation, the series could fulfil the criteria of a probe-like compound.

1.7. Project aims

The prominent role of BLM helicase in HR and DNA DSB repair is supported by a body of evidence suggesting this protein can be a potential target for cancer therapy. The aim of this project is the design, synthesis and characterisation of tool inhibitors targeting BLM helicase. It is expected such molecular probes can be used for detailed mechanistic biochemical studies of BLM, especially to elucidate its roles in DNA damage, and contain

the potential be optimised through medicinal chemistry efforts to result in a lead-like compound for drug discovery and development.

2. Development BLM helicase inhibitors based on ML216

2.1. Introduction

The search for molecular probes for DNA damage repair helicases yielded BLM helicase as a tractable target, in part due to the availability of a series of BLM inhibitors that demonstrated moderate potency and selectivity.¹ As described in Section 1.6.5, when the probe development of the reported BLM inhibitor ML216 by Rosenthal *et al*²⁰³ had ceased, the inhibition data of 148 analogues were subsequently made available.²⁰⁶ These analogues allowed an initial SAR picture to be visualised that could guide further design. At the time of writing, no other series of inhibitors that selectively inhibit BLM had been identified.

For the development of BLM inhibitors in this study, the ML216 series appeared to be a viable starting point. The availability of this BLM inhibitor possessing various desired properties bypassed the need for a hit identification campaign and permitted a hit optimisation process as the primary strategy. As discussed in Section 1.6.5, ML216 does not meet the criteria as a useful chemical probe, in particular demonstrating low solubility and permeability.²⁰³ Furthermore, ML216 failed to display selectivity over WRN helicase, a closely related RECQ family member of BLM.²⁰³ To begin with, the aim of this work was the design of a potent, soluble, permeable and selective chemical probe of BLM helicase based on ML216 preceded by replication of the reported data.

This chapter describes a failure to reproduce published data around the ML216 series that appeared to be caused by their poor solubility. It was imperative to attempt to resolve deficiencies in solubility, and accordingly the existing SAR was utilised to design and synthesise potential structural modifications that might achieve this aim. This improvement would then facilitate development of a reliable biochemical screening assay and co-crystallisation of BLM helicase with a bound ligand. Furthermore, it was desirable to retain potency similar to that of the best ML216 analogue ($IC_{50} \approx 0.1 \mu M$).

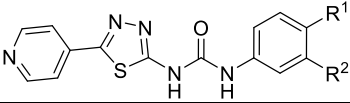
2.1.2. Aqueous solubility

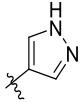
A key shortcoming of ML216 (**1**) was its low aqueous solubility and a large focus of the medicinal chemistry optimisation performed on **1** focussed on improving this parameter. In general, the aqueous solubility of small molecules depends on their hydrophobicity in solution which can be calculated as the distribution coefficient (logD). LogD is the ratio of the sum of the concentrations of all forms of the compound (ionised plus un-ionised at pH 7.4) in the aqueous and organic phases. The calculated logD (clogD) of **1** is 2.5 and is therefore not significant contributor to the compounds poor solubility. A high aromatic ring count also has a large negative impact on compound solubility. The detrimental effect of aromatic ring count on solubility, in addition to causing increased hydrophobicity, had led to the development of the 'Physical Forecast Index' (PFI), which provides a guide to predicting solubility, relative to clogD values alone, that is calculated as: $PFI = clogD + \text{number of aryl rings}$.²⁰⁷ A PFI value <5 is preferred in lead compound design to ensure high probability of good solubility. A PFI of 5.4 was calculated for **1**, which should suggest the compound should be close to acceptable solubility. Therefore, some of other factors governing solubility could likely be responsible for the poor solubility profile of **1**. For example, disruption of crystal packing could be an alternative strategy to reducing solubility, in addition to reduced clogD and the number of aryl rings. Furthermore, solubility depends on the ability of the solute to interact with water and therefore, an improvement in solubility can be achieved by introducing polar elements. The topological polar surface area (tPSA) is the surface sum of polar atoms and therefore relates to the polarity of the molecule. Generally, for bioavailable oral drugs, a tPSA <140 Å² is preferred. The tPSA of **1** is 80 Å² and well within this range indicating this parameter can be further raised. Additionally, molecular planarity is known to influence crystal packing, and disruption of molecular planarity and intermolecular bonding can reduce crystal packing.²⁰⁸ Therefore, factors such as reducing PFI and improving tPSA will be considered when optimising for the solubility of this series in addition to attempting to resolve solubility issues associated with the ML216 (**1**) scaffold itself by reducing molecular planarity and internal hydrogen bonding.

2.2. Validation of ML216 as a starting point for the development of BLM inhibitors

2.2.1. Rationale

Prior to the design of novel analogues based on ML216, attempts were made to replicate the biological data published by Nguyen *et al*¹ in-house. Assay development and protein crystallographic screening studies were performed concurrently to synthetic chemistry efforts by Ms Xiangrong Chen, a student working in the lab on a parallel PhD project. The initial project aims, from a biochemistry perspective, were to optimise a robust biochemical assay and to attempt to produce a crystal structure of BLM helicase bound to a ligand to permit structure-based design. To determine whether ML216 (**1**) was a viable starting point for the hit optimisation procedure, a group of urea analogues were synthesised that have previously been shown to be potent BLM inhibitors by Rosenthal *et al* (Table 2.1).²⁰³ It was proposed that the inhibitory activity of these compounds would provide the information required to validate this series as genuine hits, and theoretically allow these inhibitors to operate as positive controls to aid assay development. The analogues chosen for ML216 validation were based on SAR modifications to the phenyl ring, where the 100-fold difference in activity between the least and most potent compounds could further validate SAR.²⁰³

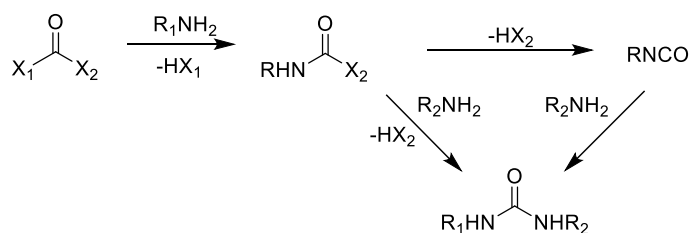
Table 2.1. Reported inhibitors of BLM for in-house synthesis.


Compound	R ¹	R ²	PFI	tPSA (Å ²)	Reported IC ₅₀ (μM) ^a
1 (ML216)	F	CF ₃	2.5	80	1.8
2	Br	Br	6.1	80	2.1
3	F	CN	4.5	103	0.3
4	CN	Cl	5.0	104	1.6
5	Br	H	5.3	80	12.6
6	Br	CN	5.1	103	0.11
7	Cl	Cl	5.7	80	1.4
8	Cl	CN	5.0	104	0.10
9		CN	ND	ND	1.1

^a Determined by gel-based BLM DNA unwinding assay by Rosenthal *et al*

2.2.2. Synthesis of ureas from aromatic amines

The simplest and most direct synthesis of substituted ureas usually involves the use of two amines in a two-step process (Scheme 2.1). First, displacement of leaving group X₁ with a selected amine to form an intermediate still possessing another leaving group; and second, reaction with a second amine through the initial intermediate or the more reactive isocyanate. For the synthesis of ML216 and its analogues (**1–9**), this approach presented as the most synthetically appropriate because the aromatic amines required for this approach were all commercially available.

**Scheme 2.1.** Typical route to urea from amine starting materials.

Typically, the formation of *N,N'*-unsymmetrical substituted ureas proceeds through the addition of amines to isocyanates.²⁰⁹ Unfortunately, these electrophilic isocyanates are generally toxic, relatively unstable, have limited commercial availability, and their synthesis usually requires the use of toxic phosgene (Figure 2.1). Rosenthal *et al*²⁰³ used phosgene (20% solution in toluene) to form aniline-derived isocyanates in their synthesis of ML216 and its analogues (**1–9**). Phosgene, infamous for its use as a chemical weapon in World War I, is difficult to handle because it is gaseous and thus poses a greater risk than diphosgene, a liquid, and triphosgene, a solid, which require fewer handling precautions.²¹⁰ However, both diphosgene and triphosgene still produce phosgene gas, which due to greater lab and environmental toxicity risks make them unsuitable for library synthesis.

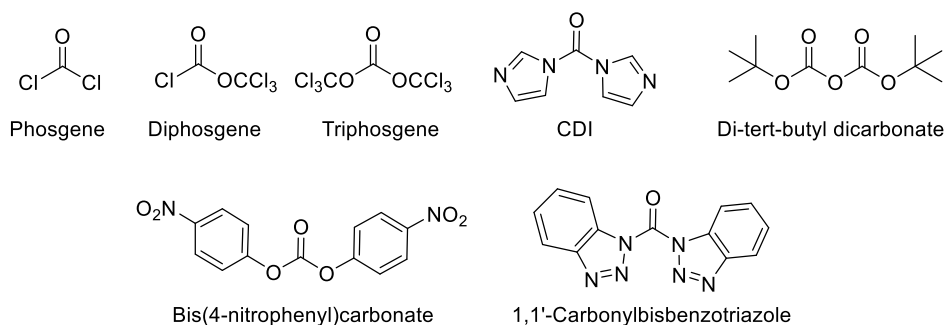


Figure 2.1. Common building blocks used in urea formation.

The traditional alternative to phosgene-based reagents is the use of other transfer reagents that do not generate chlorine or chlorinated by-products, therefore allowing a less hazardous route to the desired ureas. The most common of these building blocks are 1,1-carbonyldiimidazole (CDI), 1,1-carbonylbisbenzotriazole²¹¹ and bis(4-nitrophenyl)carbonate²¹² (Figure 2.1). These urea building blocks are safer to handle than phosgene but only some are commercially available. For example, CDI is a crystalline solid that is comparatively mild and reacts with amines to give *N*-substituted 1*H*-imidazole-1-carbonyl(carbonylimidazolides) which are generally stable.²¹³ Carbonyl imidazoles display low reactivity with amines and can be activated by *N*-alkylation of the imidazole moiety with iodomethane, which reacts more rapidly to produce the desired urea. Various other transfer reagents, such as bis(4-nitrophenyl)carbonate, allow preparation of ureas by carbamate intermediates.²¹² Again, these intermediates are

generally stable and easy to isolate. However, carbamates usually suffer from poor reactivity and there are limited reports in the use of these methodologies for rapid library generation.^{214,215} Alternative methodologies to transfer reagents, such as metal-catalysed oxidative carbonylation of amines have been reported.²¹⁶ However, these processes that employ CO₂ require harsh conditions and are considered less suitable for library generation.

2.2.3. Synthesis of ML216 and its reported analogues

Hit optimisation studies by Rosenthal *et al*²⁰³ explored changes to the phenyl ring of the initial hit to achieve considerable gains in potency. Whereas various substituent modifications were tolerated on the phenyl ring, exploration of the pyridine, thiadiazole and urea motifs displayed tight SAR (Section 1.5.6). Given that the ML216 analogues selected for synthesis were modified in the phenyl portion of the compound, an efficient synthesis would allow late diversification at the phenyl ring. Furthermore, it was anticipated that initial medicinal chemistry optimisation would focus on structure modifications of this phenyl motif due to Rosenthal's work demonstrating a wider scope to explore the SAR in this region. While the use of phosgene or its equivalents are still regarded as a traditional route to *N,N'*-unsymmetrical substituted ureas,²¹⁴ it was decided to pursue a synthesis that utilised less toxic alternative transfer reagents such as carbonyl imidazole or carbonate reagents.

It has been observed that 1,3,4-thiadiazol-2-yl isocyanate derivatives are unstable and therefore have to be freshly made during urea synthesis.²¹⁷ For late stage diversification, synthesis of a stable transfer reagent intermediate of the amine 2-amino-5-(4-pyridinyl)-1,3,4-thiadiazole (**10**) would be ideal (Table 2.2). However, it would be acceptable if urea synthesis proceeded *via* the isocyanate with sufficient yield. Attempts to make either the urea intermediate, which could be isolated, or the isocyanate with CDI in various solvents such as *tert*-butanol and DCM, with and without base, were unsuccessful. In all cases, the unreacted starting amine **10** was isolated. Further, it was observed that the starting amine **10** suffered from poor solubility in the reaction solvents, which likely contributed to the reaction failure. When assessed visually, at a concentration of 1 mg/mL, **10** was found to be soluble in DMSO and DMF (on heating) but not in a range

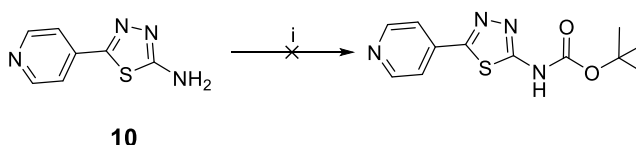
of other solvents including toluene, chloroform, DCM, ether, THF, ethyl acetate, acetone, acetonitrile, *tert*-butanol, IPA, ethanol, methanol and water.

Table 2.2. Attempts to produce a urea precursor from amine **10**.

10

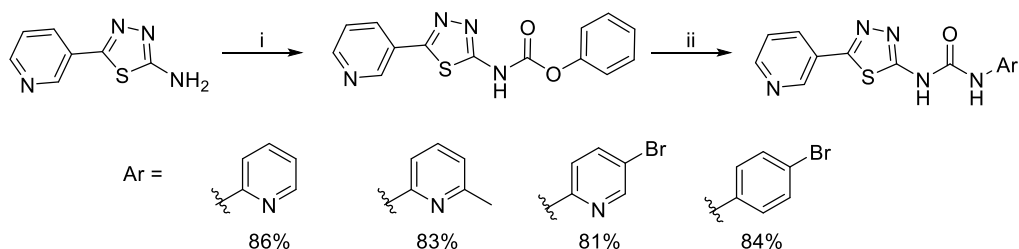
#	(i)	Reaction outcome
1	CDI(2.4 eq), 2-butanol, r.t., 7 d	No reaction. Starting material not consumed.
2	CDI(1.2 eq), <i>tert</i> -butanol, r.t., 6 d	No reaction. Starting material not consumed.
3	CDI(1.2 eq), DBU (0.2 eq), DCM, r.t., 6 d	No reaction. Starting material not consumed.
4	CDI(1.2 eq), Et ₃ N (1.5 eq), DCM, reflux, 3 h	No reaction. Starting material not consumed.

There are limited reports regarding the formation of stable carbamate intermediates from 2-amino 1,3,4-thiadiazoles that could act as precursors to ureas. Most commonly, synthesis of such intermediates occurs through precursor phenyl formates. Other approaches utilised the carbonate di-*tert*-butyl dicarbonate to form the Boc-protected intermediate.²¹⁸ There is only one reported instance for such a transformation on a heterocycle linked to a 2-amino 1,3,4-thiadiazoles.²¹⁹ However, these conditions were not successful when applied to amine **10** where no reaction occurred (Scheme 2.2).



Scheme 2.2. Reagents and conditions: (i) Boc₂O, DMAP, MeCN, reflux, 3 d, 0%.

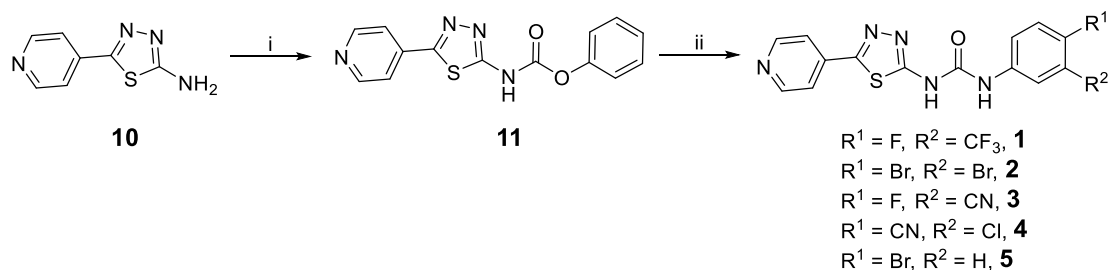
There is only one other report on the formation of a stable intermediate for a heterocycle linked to a 2-amino 1,3,4-thiadiazole, wherein Li and Chen optimised reaction conditions to produce a phenyl-5-(substituted)-1,3,4-thiadiazol-2-ylcarbamate to aid convenient synthesis of 1,3,4-thiadiazol-2-yl urea derivatives (Scheme 2.3).²¹⁷



Scheme 2.3. Li's synthesis of 1,3,4-thiadiazol-2-yl derivatives from stable carbamate intermediate.²¹⁷

Reagents and conditions: (i) NaH, THF, 0 °C, 30 min, then diphenyl carbonate, r.t., 2 d, 71%; (ii) amino compound (2 eq), THF or toluene, MW, 150 °C, 30 min.

Based on the findings of Li,²¹⁷ synthesis of a stable carbamate intermediate was performed by treating the commercially available 2-amino-5-(4-pyridinyl)-1,3,4-thiadiazole (**10**) with diphenyl carbonate and sodium hydride in anhydrous THF to yield intermediate **11** (Scheme 2.3). This reaction proceeded in high yield to form the carbamate intermediate and was carried out successfully on a 2 g scale. It is possible this reaction was successful because sodium hydride deprotonation of the amine of **10** increased its solubility in the reaction mixture. Additionally, the amine is more nucleophilic upon deprotonation, which increases its ability for a nucleophilic attack on the carbonate.

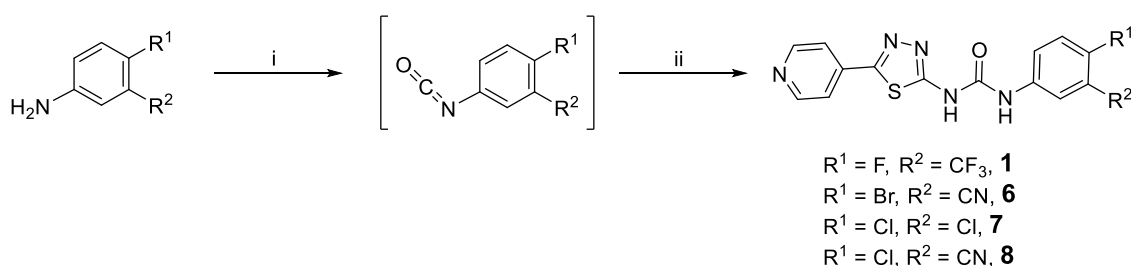


Scheme 2.4. *Reagents and conditions:* (i) THF, NaH, 0 °C, 3 h then diphenyl carbonate, r.t., 72 h, 93%; (ii) appropriate aniline, toluene, 150 °C (microwave), 30 min: (**1**, 46%; **2**, 70%; **3**, 46%; **4**, 44%; **5**, 50%).

The carbamate intermediate was then heated at 150 °C in a microwave synthetic reactor with aniline compounds to produce urea derivatives **1–5** (Scheme 2.4).²¹⁷ The harsh conditions were required to eliminate the poor leaving group phenol. LCMS-LCQ analysis showed the reactions went approximately 80% to completion, but overall yields were lower because isolation of the pure compound was challenging due to poor solubility. Only compounds **1** and **2** showed a sufficient solubility profile to allow separation using flash column chromatography with silica columns. All other ureas synthesised by this route were purified by trituration methods. One of the main difficulties in isolation arose

from a similar, or possibly even poorer solubility profile of amine **10**, which was ultimately difficult to remove.

ML216 analogues **6–8** were synthesised to aid assay development. On this occasion, the more traditional synthesis of isocyanates using triphosgene was utilised as it afforded a more robust method to produce pure urea derivatives in this series. The isocyanate derivatives from their respective anilines were formed *in situ* followed by the addition of amine **10** in DMF at 90 °C (Scheme 2.5). High temperatures in DMF allowed amine **10** to go into solution, thus aiding the reaction to completion. The ureas were crystallised in DMF/ethyl acetate or DMF/methanol. Attempts to make the isocyanate of amine **10** to aid library synthesis were unsuccessful, again likely due to solubility issues of **10** in DCM and THF.

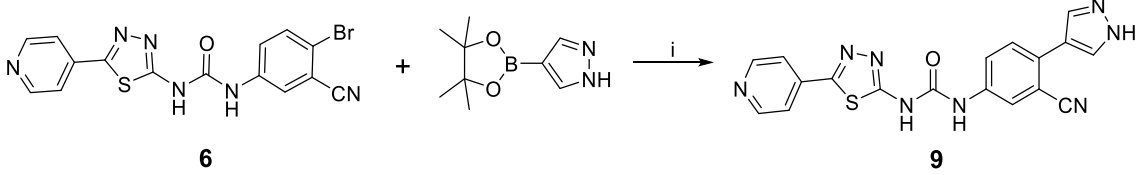


Scheme 2.5. *Reagents and conditions:* (i) appropriate aniline, triphosgene, NEt₃, DCM, r.t., 1 h; (ii) **10**, DMF, 90 °C, 2 h: (**1**, 21%; **6**, 27%; **7**, 7%; **8**, 22% [over 2 steps]).

During the medicinal chemistry development of ML216, addition of a pyrazole at the 4 position of the phenyl ring retained potency but improved solubility 10-fold.²⁰³ Synthesis of this compound was attempted in the present study using the 4-Br derivative **6** via Suzuki coupling conditions described by Rosenthal *et al* (Table 2.3).²⁰³ These conditions resulted in a thick suspension and the failure of the reaction could be attributed to solubility issues with the starting material. LCMS-LCQ revealed that increasing DMSO concentration in this reaction resulted in complete removal of starting substrate. However, due to the high polarity, it was difficult to ascertain on LCMS-LCQ how much product had formed as all components eluted very early. Isolation of the desired compound was not possible as the reaction mixture contained many components, many of which were poorly soluble. Attempting the Suzuki coupling in the microwave on a larger scale (10 mL solvent) resulted in complete destruction of the MW vial, possibly due to incomplete solubilisation of the substrates into the solvents, which caused a large

amount of heat spots to form on the vial surface. Attempts to synthesise urea **9** were abandoned, as it was decided to pursue other strategies to improve solubility that are described in the next section.

Table 2.3. Exploration of conditions for Suzuki coupling of **6**.



#	(i)	LCMS observations	Isolated yield (%)
1	K ₃ PO ₄ (2.5 eq), PEPPSITM- <i>i</i> Pr (10 mol%), DMSO/H ₂ O (2:1), 100 °C, 48 h.	Approximately 10% conversion to desired product.	0
2	K ₃ PO ₄ (2.5 eq), PEPPSITM- <i>i</i> Pr (10 mol%), DMSO/ H ₂ O (4:1), 150 °C (MW), 30 min.	No sign of starting material.	0
3	K ₃ PO ₄ (2.5 eq), PEPPSITM- <i>i</i> Pr (10 mol%), DMSO/ H ₂ O (4:1), 100 °C, 48 h.	No sign of starting material.	0

2.3. Design of more soluble ML216 analogues

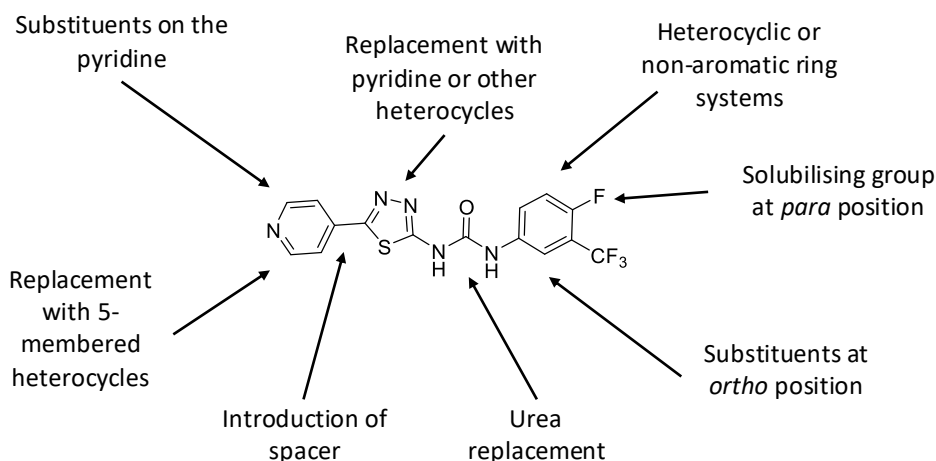


Figure 2.2. Proposed strategies to improve solubility of ML216 (**1**).

While optimising the purification of ML216 (**1**) and its analogues **2–8**, the poor solubility of these compounds in organic solvents became apparent. The compounds were only soluble in high boiling polar solvents such as DMF at high temperatures (above 80 °C). Furthermore, these compounds could only be prepared as a clear solution in DMSO at a maximum concentration of 2 mM. Poor solubility resulting in precipitation during the

assay could produce misleading data because the experimental compound concentration would not accurately reflect the target concentration. Based on the medicinal chemistry efforts conducted by Rosenthal *et al*,²⁰³ various strategies were proposed to improve solubility whilst not impacting activity (Figure 2.2). A tight SAR profile had been clearly constructed during the development of ML216 (**1**), from which it was proposed that introducing minor modifications to all the structural motifs would cumulatively improve the solubility of this series.

Reported SAR of the phenyl ring described a variety of substituted anilines, therefore it was proposed that the phenyl motif could be replaced by heterocyclic aromatics such as a pyridine as carboaromatics contribute more to poor solubility than heteroaromatics.²²⁰ Additionally, the phenyl ring could also be replaced with non-aromatic rings to substantially improve solubility as aromatic rings contribute to poor solubility.²²⁰ However, it is unlikely this modification would retain activity because reported SAR demonstrated that alkyl functionalised ureas were inactive. As discussed in Section 1.5.6., ML216 (**1**) purportedly competes with DNA for binding at the ssDNA binding pocket in BLM helicase. Therefore, alkyl derivatives may lose potency due to the ensuing loss of planarity that would affect binding at a polar ssDNA binding pocket, which often resembles a narrow groove rather than a traditional drug-like pocket. The same challenges may also apply when introducing substituents at the *ortho* position; while the twist gained from such a substituent may increase solubility due to reduced planarity, this may cause loss of binding. However, it is a common medicinal chemistry strategy to improve solubility by creating twists in the molecule in order to disrupt crystal packing. These strategies were initially probed using substrates available in-house in order to be followed up more intensively once a greater understanding of the solubility and SAR issues concerning the series was obtained. This particular strategy was implemented because there was limited SAR knowledge, and the delay between synthesis of analogues and biological evaluation could have resulted in a less rational approach to design thereby preventing focus on potentially more successful strategies.

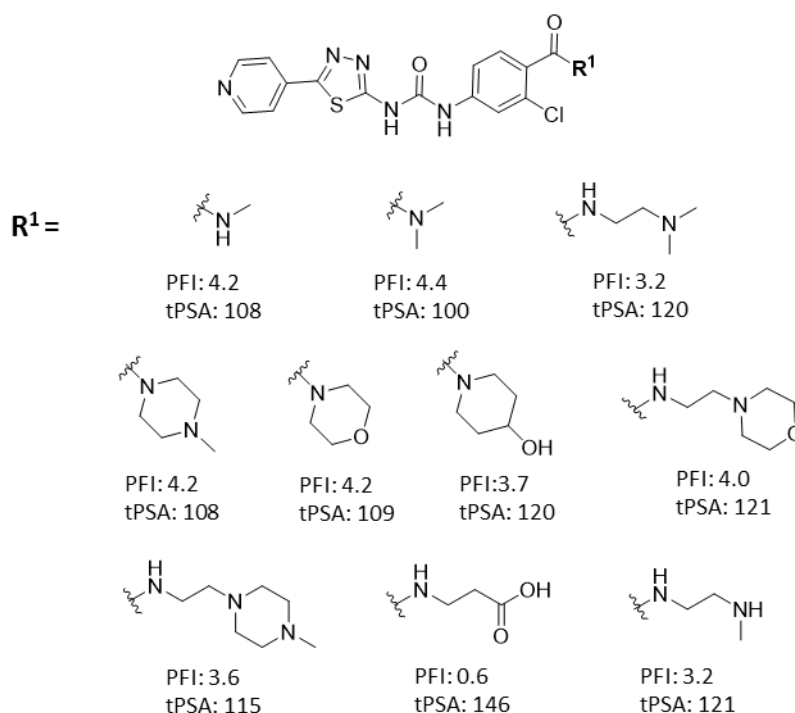


Figure 2.3. Proposed solubilising groups for *N*-acylation at the 4-position. All compounds have an increase of PFI and increase in tPSA when compared to **8**. For reference, **8** has a PFI of 5.4 and tPSA of 80.

Incorporating polar groups that can ionise or have the ability to form hydrogen bonds with water generally increases water solubility. A small set of derivatives containing amines, carboxylic acids and ethers (in the form of morpholine) with these properties were selected (Figure 2.3). There are various methods of introducing these groups and the strategy utilised here comprised of *N*-acylation with and without an ethyl linker to the proposed moiety (Figure 2.3).

SAR of ML216 at the phenyl ring showed that it was possible to extend at the 4-position with 5-membered heterocycles with only a moderate loss in activity.²⁰³ It was also noted that these types of modifications were not tolerated at the 3-position. Therefore, it was proposed that introduction of water-solubilising groups at the 4-position could be tolerated and improve the solubility profile of this series.

Amine **10** also presented with inherently poor solubility, suggesting the 4-pyridyl-1,2,3-thiadiazole portion was a large cause of solubility issues. However, the urea group also adds to the unfavourable solubility profile of this series by promoting stacking of the compound due to its planarity and strong hydrogen bonding.²²¹ Compared to the urea

moiety, SAR of this series demonstrated that a thiourea maintains similar activity and a guanidine reduces activity 10-fold.²⁰³ While the thiourea moiety is likely to display a similar physicochemical profile to a urea moiety, the more hydrophilic guanidine may improve aqueous solubility. One synthetic route to guanidines is *via* thioureas and thus both analogues were synthesised (Figure 2.4). The reported data suggested that guanidine derivatives would reduce potency by 10-fold but micromolar potencies would be achieved if appropriate motifs were utilised. Furthermore, the guanidine moiety provided another handle for the introduction of solubilising groups (Figure 2.4).

Reported SAR on the urea moiety also showed that an amide derived from the amino thiadiazole with a methyl linker to the phenyl ring was not tolerated, but no aniline-derived amide was assessed, i.e. the reverse amide.²⁰³ As a result, the reverse strategy was attempted (Figure 2.4) as amides with a linker could improve the aqueous solubility of this series by removal of the rigid amide urea with the flexible carbon linked amide. Finally, as with the amide, the *N*-methyl urea substituted to the thiadiazole was not tolerated while the *N*-methyl urea substituted to the phenyl ring was not assessed. As methylation of the urea can disrupt crystal packing and intermolecular H-bonding, this can improve aqueous solubility.²²² As mentioned previously, this disruption in planarity could diminish binding.

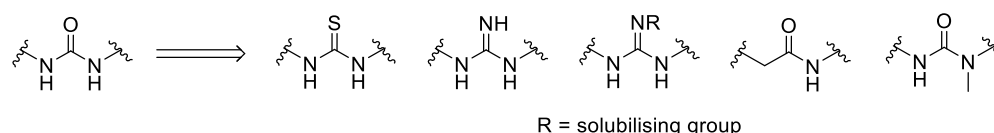


Figure 2.4. Proposed changes to urea moiety.

During handling of amine **10**, insight was gained regarding the inherent solubility issues of the 4-pyridyl-1,2,3-thiadiazole core. Therefore, changes to this structure were deemed vital. Unfortunately, reported SAR on ML216 demonstrated poor tolerance to changes of the pyridyl and thiadiazole moieties with aromatic isosteres and non-aromatic rings of similar size. It was therefore proposed to introduce changes to both structures by replacement with other heterocycles not yet evaluated (Figure 2.5). Of particular interest was a variety of small 5-membered heterocycle replacements of the 4-pyridyl, as previously only pyridine and phenyl ring systems had been assessed.

Furthermore, the addition of an *ortho* substituent on the pyridine ring would introduce a twist that could break the planarity of the molecule. Replacement of the thiadiazole with pyridine was shown to maintain potency and a pyridyl-pyridyl core may be less prone to solubility issues than the current scaffold. Finally, a C-, O- or N- linker between the thiadiazole and pyridine motifs would also disrupt planarity by the introduction of a rotatable bond between aromatic rings (Figure 2.5).

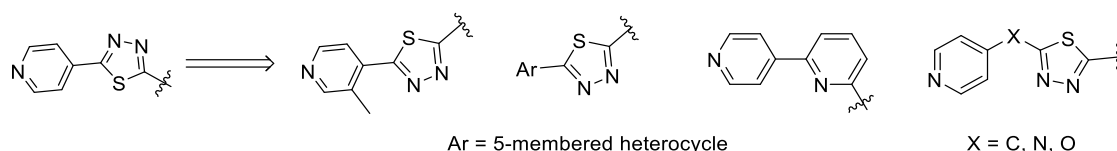


Figure 2.5. Proposed changes to 4-pyridyl-1,2,3-thiadiazole scaffold.

Due to the tight SAR of the scaffold, strategies with a higher chance of success were prioritised. This is because a more soluble BLM inhibitor would aid assay development and provide a more soluble positive control, especially as no other selective BLM inhibitors are known.

2.4. Synthesis of more soluble ML216 analogues

2.4.1. Exploration of phenyl ring

One early avenue of exploration was to replace the phenyl ring with various readily available amines and anilines to assess what could be tolerated. This synthetic route was relatively simple because a large amount of intermediate **11** had already been prepared. Accordingly, microwave reactions were carried out with a small library of amines and anilines to produce ureas (Table 2.4). Five ureas were successfully synthesised, and their improved yields may be attributed to their improved solubility in organic solvents compared to previously synthesised ML216 analogues, resulting in more efficient isolation of these compounds. The amines and anilines were chosen because they represented replacement of the phenyl ring by a non-aromatic ring, a heterocyclic ring and substitution at an *ortho* position.

Table 2.4. *Reagents and Conditions:* (i) appropriate aniline, toluene, MW, 150 °C, 30 min.

11		
Compound	R ¹	Yield (%)
12		49
13		42
14		39
15		46
16		43

One major issue observed with the aforementioned urea synthesis protocol was the significant decomposition of carbamate **11** to the amine **10**, which proved difficult to remove. Also described by Li,²¹⁷ the use of conventional heating in THF at reflux overnight as an alternative to microwave synthesis was not successful when applied to the synthesis of ML216 (**1**). Moreover, temperatures below 150 °C in the microwave were not successful in promoting urea formation from carbamate **11**. Synthesis of the five-membered heterocycles **17** and **18** was also performed (Table 2.5), but they were not isolated with sufficient purity for assay purposes despite employing numerous purification techniques including chromatography, trituration and crystallisation. Whilst compounds **17** and **18** separated from the impurity **10** on TLC, it was not possible to isolate the pure desired urea on column chromatography as **10** was often found to elute simultaneously. The synthesis of ureas with larger halogens *ortho* to the urea, as with compounds **19** and **20**, did not produce any desired product even when heated to 200 °C. It is likely this was due to the already poorly nucleophilic aniline being sterically hindered.

Table 2.5. Unsuccessful attempts to form ureas from Li's urea synthesis.

11

Compound	R ¹	Conditions ^a	Reaction outcome
17		Toluene, 150 °C, 30 min	Impurities of 10 present after purification
18		Toluene, 150 °C, 30 min	Impurities of 10 present after purification
19		Toluene, 150 °C, 1 h or toluene (drop of NMP), 200 °C, 1 h	No reaction. Starting material present. Some decomposition to 10
20		Toluene, 150 °C, 1 h or toluene (drop of NMP), 200 °C, 1 h	No reaction. Starting material present. Some decomposition to 10

^a appropriate amine (1 eq)

2.4.2. Addition of solubilising groups at 4-phenyl

SAR by Rosenthal *et al.* clearly shows that a nitrile group at the 3-position of the phenyl ring contributes roughly 10-fold more activity than trifluoro, chloro and bromo substituents.²⁰³ While ML216 (**1**) contains a trifluoro at the 3-position, the starting material containing a chloro at the 3-position was readily available. It was therefore used for the synthesis of analogues containing water solubilising groups attached at the 4-phenyl.

Acid **24** was a key intermediate in the synthesis of analogues containing solubilising groups linked to the core scaffold via *N*-acylation (Scheme 2.6). Synthesis of its methyl ester derivative was therefore attempted *via* displacement by methyl 4-amino-2-chlorobenzoate of carbamate **11**. Previously successful conditions for this synthesis (#1, Table 2.6) were not effective and the reaction conditions were optimised for solvent, temperature and length of reaction (Table 2.6) under microwave conditions. Increasing the temperature to 200 °C resulted in a greater conversion to urea **23**, however the reaction did not go to completion. Attempts to increase conversion by increasing the equivalents of aniline were not successful. The desired urea proved difficult to purify by

chromatography and crystallisation methods. Finally, saponification of the impure ester **23** resulted in the isolation of significantly impure acid **24** from an acid/base workup.

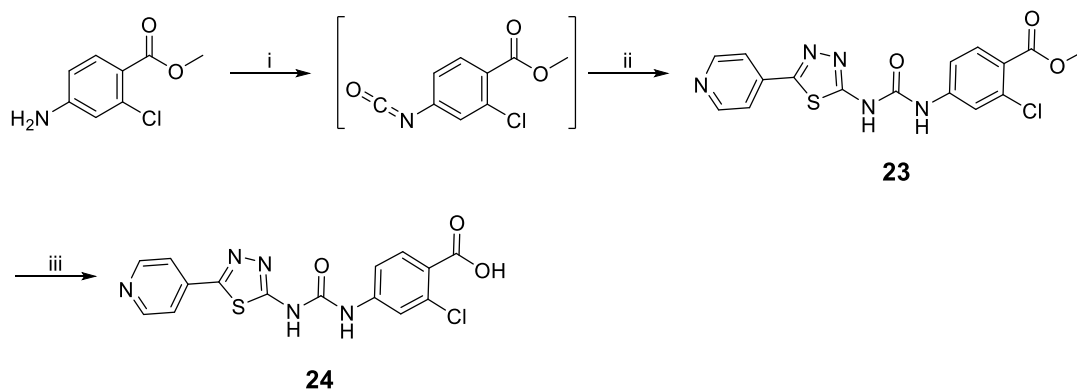
Table 2.6. Reaction optimisation for the formation of **22** from carbamate **11**.

	11		21		23
#	Eq. of 21	Solvent	Temp (°C)	Time (min)	Reaction outcome
1	1	Toluene	150	30	No consumption of starting material ^a
2	1	Toluene	150	90	No consumption of starting material ^a
3	1	THF	150	30	No consumption of starting material ^a
4	1	THF	100	30	No consumption of starting material ^a
5	1	Toluene (drop of NMP)	200	30	20% isolated yield (70% purity ^b)
6	2	Toluene (drop of NMP)	200	30	4% isolated yield (90% purity ^b)

^a As judged by LCMS-LCQ; ^b As judged by ¹H-NMR

Synthesis of ureas from carbamate **11** was discontinued as it had ultimately not shown efficacy at generating a library of 4-pyridyl-1,2,3-thiadiazole-urea derivatives. The carbamate intermediate **11** initially showed promise to allow late stage diversification of the 4-pyridyl-1,2,3-thiadiazole-urea core. Various other routes to a stable intermediate, which could be displaced with an amine to produce a urea, were either not successful (Section 2.2.3) or not reported. The formation of the urea derivative from carbamate **11** required elevated temperatures that often resulted in impurities that could not be removed, whilst for less nucleophilic amine derivatives there was no formation of the desired product. Phenol is a poor leaving group and this displacement reaction would be more successful in the presence of more appropriate leaving groups, for example, a transfer reagent such as bis(4-nitrophenyl)carbonate (Figure 2.1). However, at this stage, it was decided that the use of a more robust protocol with precedent was necessary.

Ultimately, synthesis was carried out using 3-chloro-4-isocyanato-aniline, which was formed *in situ* from the commercially available methyl 4-amino-2-chlorobenzoate (Scheme 2.6). Addition of **10** followed by heating at 90 °C in DMF resulted in acceptable yields of the urea derivative **23**. Basic hydrolysis of the ester functionality of **23** resulted in key carboxylic acid derivative **24** in good yield.



Scheme 2.6. Reagents and conditions: (i) triphosgene, NEt₃, DCM, r.t., 1.5 h; (ii) **10**, DMF, 90 °C, 1 h, 47% (over 2 steps); (iii) NaOH, H₂O/MeOH, 65 °C, 16 h, 91%.

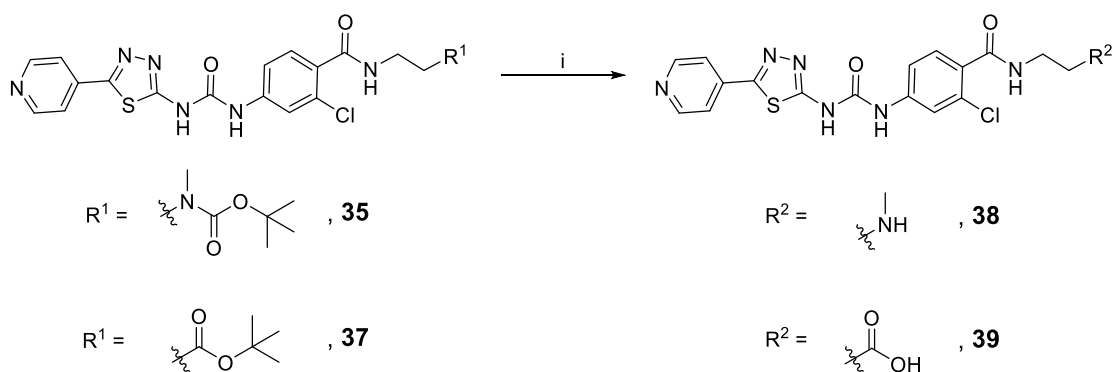
Acid **24** was then coupled to various amines using HATU to give a library of amide derived water solubilising groups (Table 2.7). In almost all cases, purification by column chromatography yielded pure compounds revealing improved handling of these amides in common lab solvents. Initial synthesis of **30** and **33** resulted in the acetate salts **31** and **34**. Further investigation revealed the celite used to dry load the crude material for column chromatography was contaminated with acetic acid resulting in their corresponding acetate salts after purification by column chromatography. The salts **31** and **34** were not neutralised and instead submitted for biological testing, as it was possible the salts would improve aqueous solubility.

Table 2.7. Reagents and conditions: (i) Appropriate amine, HATU, DIPEA, DMF, r.t., 16 h.

Reaction scheme: **24** + R^1 (amine) $\xrightarrow{\text{i}}$ Product

Compound	R ¹	Yield (%)	Compound	R ¹	Yield (%)
25		23	32		58
26		66	33		75
27		58	34		67
28		40	35		38
29		41	36		28
30		79	37		40
31		54			

Acid-mediated Boc deprotection of **35** formed **38** (Scheme 2.7). **39** was to be formed from the methyl ester. Initially, synthesis of methyl ester **36** was completed on a small scale. Isolation of the compound was challenging and a final trituration after column chromatography gave the pure isolate. However, repeating this purification on a larger scale was not successful. Hydrolysis of the impure intermediate did not produce the pure acid **39**. As an alternative, the *tert*-butyl ester **37** was synthesised with improved yields and purity, and TFA hydrolysis gave the desired acid **39**.



Scheme 2.7. Reagents and conditions: (i) TFA, DCM, r.t., 4–16 h: (**38**, 73%; **39**, 40%).

2.4.3. Guanidine replacement of the urea core

With amine **10** readily available, the most convenient synthesis to produce a library of guanidine derivatives consisted of reacting an appropriate isothiocyanate analogue with amine **10**. 1,2-dichloro-4-isothiocyanatobenzene was inexpensive and available in large quantities so was chosen as the representative phenyl ring. SAR by Rosenthal *et al*²⁰³ on these structures was also performed on the dichloro derivative, thus enabling direct comparison and relatable potency against BLM. The di-substituted guanidine analogue (**44**) of ML216 was also synthesised.

Various conditions were assessed to find optimal reaction conditions for the formation of thioureas. The reaction of amine **10** with phenylisothiocyanate (**40**) was used for reaction optimisation (Table 2.8). It was expected that isothiocyanates would be sufficiently reactive with amines in solvent to form a thiourea without the need for base. However, several literature precedents utilised bases such as triethylamine²²³ or catalysts such as DMAP²²⁴ for these types of reaction.

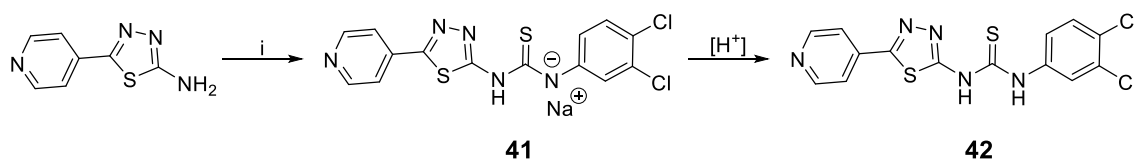
Table 2.8. Optimisation of thiourea formation using phenylisothiocyanate **40** as a model system.

#	Eq. of 34	Base	Solvent	Temp (°C)	Time (hr)	Conversion (%) ^a	Comment
1	1	Et ₃ N	THF	66	24	0	Amine insoluble in solvent
2	1	NaH	THF	50	24	80	
3	1.2	-	EtOH	80	24	0	Amine insoluble in solvent
4	1.2	-	MeCN	80	24	0	Amine insoluble in solvent
5	1.2	-	DMSO	80	24	50	Many impurities visible ^b
6	1.2	-	DMF	80	24	50	
7	1.5	-	DMSO	90	72	50	Many impurities visible ^b
8	1.5	-	DMF	90	3 d	80	

^a As judged by LCMS-LCQ; ^b As judge by ¹H-NMR

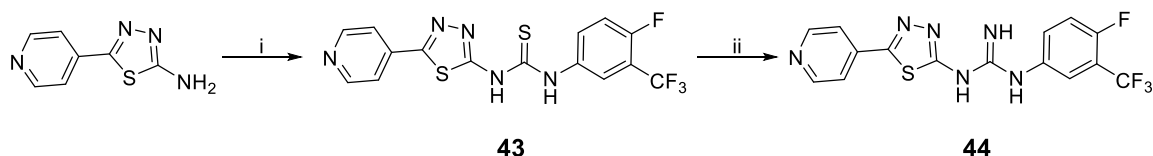
Table 2.8 outlines the conditions assessed for thiourea synthesis. It is likely that the solubility of amine **10** played a role in the formation of the desired product. It is likely that for this reason, product was only seen in solvents in which the amine was soluble such as DMF and DMSO. Entry 8 (Table 2.8) shows that no base is necessary for the reaction to proceed. Entry 2 (Table 2.8) conditions were trialled based on previous experiences when forming carbamate **11** with the same starting amine. There was no literature precedent on using such a strong base to react isothiocyanates with amines. Here, there was 80% conversion as judged by LCMS-LCQ but isolation proved difficult because many impurities had formed, perhaps due to the presence of such a strong base. Again, it seemed likely that the use of sodium hydride was only effective as it deprotonated amine **10** (which has a predicted pK_a of 15), to produce a salt that was solubilised in the reaction solvent — which would not be the case when using weaker bases such as triethylamine. As a result, 1,2-dichloro-4-isothiocyanatobenzene was reacted with sodium hydride in THF to produce the sodium salt of the thiourea **41**, which precipitated out of THF (Scheme 2.8). Some of this salt was isolated for biological

analysis. Treatment with 1 M hydrochloric acid resulted in the formation of intermediate **42**.



Scheme 2.8. *Reagents and conditions:* (i) NaH, THF, 0 °C, 30 min, then 1,2-dichloro-4-isothiocyanatobenzene, 50 °C, 24 h, 68%.

The same conditions were applied to 2-fluoro-4-isothiocyanato-1-(trifluoromethyl)benzene and the reaction achieved similar success when assessed by LCMS-LCQ. However, isolation of the pure thiourea intermediate **43** was not possible because various impurities could not be removed during purification. Because this thiourea was more soluble than **41** in the reaction solvent, it did not precipitate out to the same extent and so could not be directly isolated from the reaction mixture. To minimise the formation of impurities by removing the strong base, conditions from entry 8 (Table 2.8) were subsequently employed and resulted in the isolation of intermediate **43** (Scheme 2.9).



Scheme 2.9. *Reagents and conditions:* (i) 2-fluoro-4-isothiocyanato-1-(trifluoromethyl)benzene, DMF, 90 °C, 16 h, 36%; (ii) NaIO₄, DMF, 60 °C, 2 h, 25%.

Conversion to the guanidine can then proceed *via* many routes, with the most common being the use of coupling reagents (such as DCC and EDCI), sulphur scavenging metals (such as mercury and lead) or oxidising agents.^{225,226} It was preferable to avoid use of poisonous metals such as mercury and lead. In this instance, the thiourea intermediates were converted to *N',N'*-disubstituted and *N',N',N'*-trisubstituted guanidines through the use of sodium metaperiodate as an oxidising agent followed by displacement with ammonia.²²⁷ While no mechanistic studies have been conducted, it has been postulated that periodate oxidises the thiourea which is easily displaced by the amine.²²⁸ This route facilitated synthesis of a library of guanidines containing water solubilising groups (Table 2.9) and the *N',N'*-disubstituted guanidines **44** (Scheme 2.9) and **45** (Table 2.9).

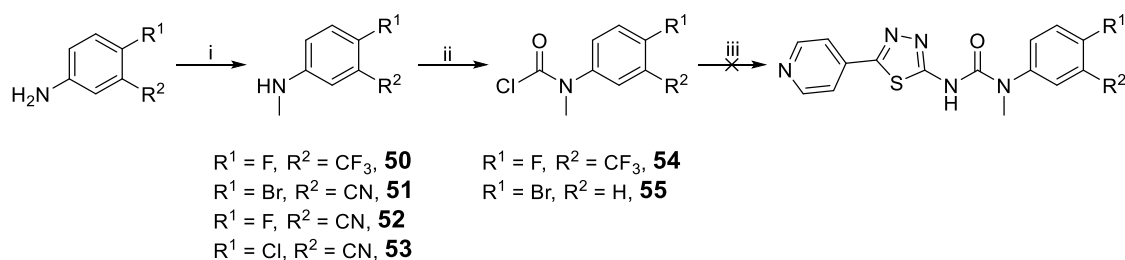
Table 2.9. Reagents and conditions: (i) NaIO₄, H₂O/DMF or DMF, 60 °C, 2 h.

42

Compound	R ¹	Yield (%)
45	H	49
46		24
47		23
48		45
49		60

2.4.4. Methyl urea replacement of the urea core

The methylation of the urea nitrogen linked to the aniline moiety was sought in an attempt to disrupt crystal packing of the molecule. Methylation of the urea nitrogen linked to the thiadiazole had previously been attempted by Rosenthal *et al.*²⁰³ Initial efforts to synthesise analogues of the desired methyl urea proceeded *via* synthesis of an intermediate carbamoyl chloride of substituted *N*-methyl anilines (Scheme 2.10). 5-Amino-2-fluorobenzotrifluoride was *N*-methylated using iodomethane while 4-bromo-*N*-methylaniline was commercially available. The carbamoyl chlorides of both analogues were then synthesised using triphosgene.²²⁹ Attempts at a one-pot synthesis of carbamoyl chloride followed by addition of amine **10** to produce the desired *N*-methyl urea derivative were not successful. Thereafter, several conditions were attempted to react the isolated carbamoyl chlorides **54** and **55** with amine **10** but were unsuccessful and resulted only in starting material (Scheme 2.10). Conditions with sodium hydride and THF, which had proved successful in several procedures discussed above (Section 2.2.3 and 2.4.3), did not succeed on this occasion.



Scheme 2.10. Reagents and conditions: (i) MeI, MeCN, 80 °C, 16 h: (**50**, $R^1 = \text{F}$, $R^2 = \text{CF}_3$, 18%; **51**, $R^1 = \text{Br}$, $R^2 = \text{CN}$, 26%; **52**, $R^1 = \text{F}$, $R^2 = \text{CN}$, 27%; **53**, $R^1 = \text{Cl}$, $R^2 = \text{CN}$, 18%); (ii) triphosgene, DCM, pyridine, -78 °C, then r.t., 16 h: (**54**, $R^1 = \text{F}$, $R^2 = \text{CF}_3$, 36%; **55**, $R^1 = \text{Br}$, $R^2 = \text{H}$, 38%); (iii) **10**, (a) pyridine, 50 °C, 1 week, or (b) K_2CO_3 , DMF, 90 °C, 16 h, or (c) NaH, THF, 50 °C, 16 h.

As an alternative approach, the same synthesis used for ureas in Section 2.2.3. was implemented with intermediate **11**, which underwent microwave reactions with various *N*-methyl aniline substrates (Table 2.10). The route failed for three compounds, but the reaction proceeded sufficiently for 4-bromo-*N*-methylaniline and **53** to produce **55** and **56**, respectively. However, only **56** was isolated after work-up in low yield, again due to its poor solubility. As mentioned in Section 2.4.1, the secondary amines may have been hindered by the methyl preventing sufficient nucleophilic displacement of the poor phenol leaving group. At this point, one representative example was considered sufficient and optimisation of the synthesis of these analogues would only be sought if biological results were positive.

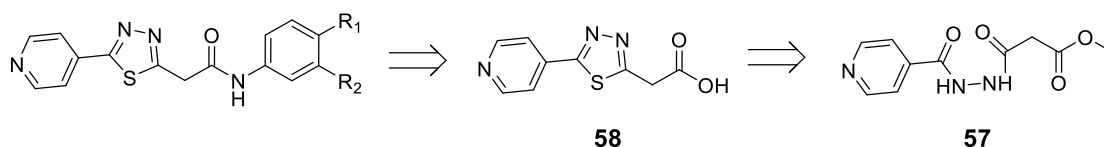
Table 2.10. Attempted synthesis of *N*-methyl urea derivatives.

Compound	R^1	R^2	Solvent	MW temp. (°C)	Time (min)	Comments	Isolated yield (%)
-	Br	H	THF	150	30	Only starting material	0
-	Br	H	Toluene	150	30	Only starting material	0
-	Br	H	Toluene	200	30	40% conversion. ^a Unable to isolate	0
-	F	CF ₃	Toluene	200	30	Only starting material	0
-	Br	CN	Toluene	200	30	Consumption of starting material. Formation of unknown product	0
56	Cl	CN	Toluene	200	30	40% conversion. ^a	3

^a As judged by LCMS-LCQ

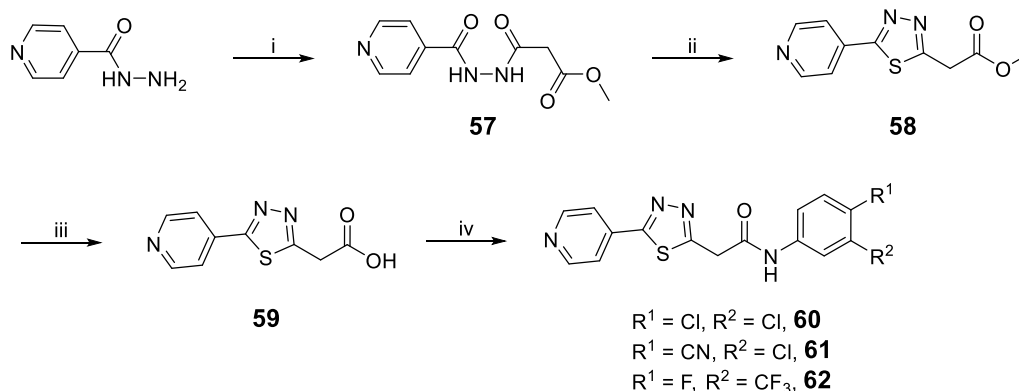
2.4.4. Amide replacement of the urea core

In an attempt to replace the urea core with one that would not promote excessive crystal packing, a synthetic route for the methyl-linked amide was sought. Synthesis of amide derivatives of ML216 and its urea analogues required the key intermediate **58** (Scheme 2.11). This would require synthesis of the pyridyl-thiadiazole core from the methyl ester compound of 1,4-diketone Paal-Knorr type substrate (Scheme 2.11). Consequently, Scheme 2.12 was devised.



Scheme 2.11. Retrosynthetic analysis of amide derivatives.

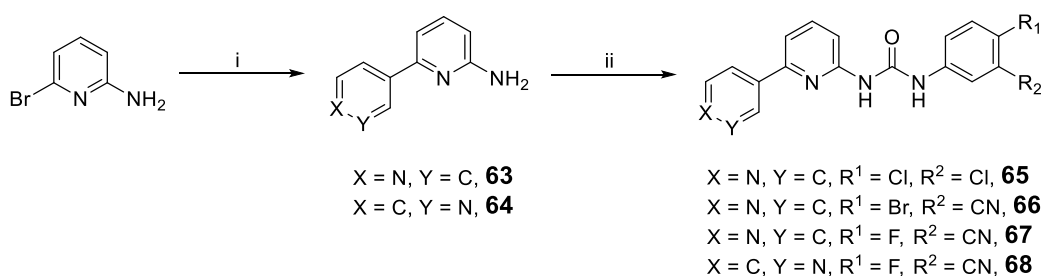
Commercially available isoniazid was coupled with methyl malonyl chloride to yield the 1,4-diketo intermediate **57** that underwent cyclisation with Lawesson's reagent at reflux in 1,4-dioxane. Isolation of the polar **57** and **58** was complicated by solubility issues. Hydrolysis of the ester **58** at reflux with sodium hydroxide in methanol/water resulted in decarboxylation. The hydrolysis performed better at room temperature with lithium hydroxide, however, low yields were observed due to difficulty extracting the highly polar **59** from the aqueous phase during purification. Finally, the carboxylic acid **59** was amide coupled using T3P to various anilines to produce the desired amides in a fairly low yield. Low yields resulted from the reaction not going to completion and loss of product during purification. Coupling using HATU conditions also showed formation of the desired product **60** which was not possible to isolate in high purity. The anilines selected for coupling were those that were of most interest due to their better potency and/or solubility. It was also not possible to isolate compound **62** with sufficient purity for assay purposes as separation by column chromatography proved difficult. The low-yielding amide coupling step was not repeated on a larger scale to produce **62** as it would require further synthesis of intermediate **59**, which was established to be highly time consuming and inefficient. The isolation of two representative examples in this amide series was deemed sufficient.



Scheme 2.12. Reagents and conditions: (i) methyl malonyl chloride, DMF, 0 °C, 3 h, 29%; (ii) Lawesson's reagent, 1,4-dioxane, 50 °C, 16 h, 42%; (iii) LiOH, THF/H₂O, r.t., 22%; (iv) appropriate aniline, T3P, Et₃N, DMF, r.t., 16 h: (**60**, R¹ = Cl, R² = Cl, 6%; **61**, R¹ = CN, R² = Cl, 7%; **62**, R¹ = F, R² = CF₃, 0%) .

2.4.5. Replacement of 1,3,4-thiadiazole moiety with 2-pyridyl moiety

With previous SAR indicating both the 3- and 4-pyridyl rings had similar activity, analogues of both these rings were made when replacing the thiadiazole moiety. Synthesis began with Suzuki-Miyaura cross-coupling of 6-bromopyridin-2-amine and the appropriate pyridine boronic acid using literature conditions²³⁰ to yield two intermediate amines **63** and **64** (Scheme 2.13). The final urea compounds were synthesised as previously using triphosgene to give three examples of 4-pyridyl derivatives and one example of a 3-pyridyl derivative. The low yields of the urea formation were attributed to the reaction of amines **65** and **66** with the isocyanates not going to completion, and difficulty in isolation of the final analogues.

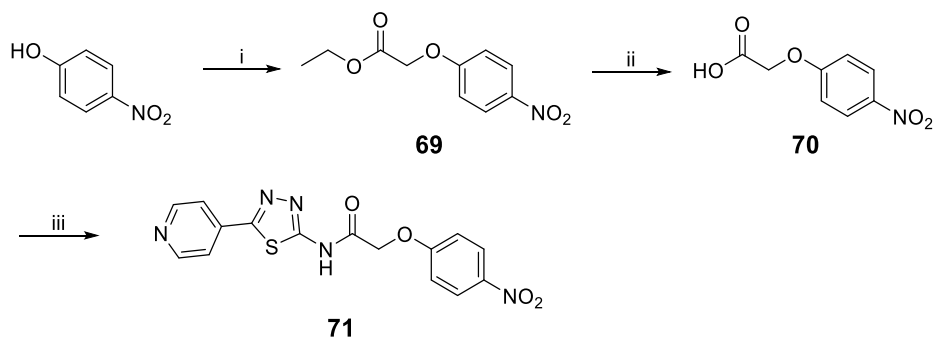


Scheme 2.13. Reagents and conditions : (i) pyridine-4-boronic acid or pyridine-3-boronic acid, Cs₂CO₃, Pd(dppf)Cl₂, 1,4-dioxane/H₂O, 120 °C, 3 h: (**63**, X=N, Y = C, 32%; **64**, X = C, Y = N, 64%); (ii) (a) triphosgene, Et₃N, DCM, r.t., then (b) DMF, 90 °C: (**65**, X = N, Y = C, R¹ = Cl, R² = Cl, 3%; **66**, X = N, Y = C, R¹ = Br, R² = CN, 4%; **67**, X = N, Y = C, R¹ = F, R² = CN, 2%; **68**, X = C, Y = N, R¹ = F, R² = CN, 3% [over 2 steps]).

2.4.6. Synthesis of related BLM HTS hit MLS00000767020

MLS00000767020, known as 2-(4-nitrophenoxy)-N-(5-(4-pyridyl)-1,3,4-thiadiazol-2-yl)acetamide (**71**) is a compound of MW 357 that was found to inhibit BLM helicase in a

qHTS screen[AID2528] deposited in PubChem with a reported activity of 16 μM . This compound was of interest because its 4-pyridyl-1,3,4-thiadiazole core showed it to be an amide analogue of ML216 which would improve solubility.



Scheme 2.14. Reagents and conditions: (i) Ethyl chloroacetate, K_2CO_3 , MeCN, 80 °C, 3 h, 62%; (ii) NaOH, $\text{H}_2\text{O}/\text{MeOH}$, 65 °C, 16 h, 12%; (iii) **10**, HATU, DIPEA, DMF, r.t., 16 h, 13%.

The strategy employed for the synthesis of **71** began with the commercially available 4-nitrophenol which was coupled with ethyl chloroacetate in the presence of potassium carbonate providing methyl ester **69** in 62% yield (Scheme 2.14). Basic hydrolysis with sodium hydroxide was undertaken at refluxing conditions in methanol overnight which proved to be quite harsh resulting in mostly the decarboxylated product; 1-methoxy-4-nitrobenzene. As a result, the desired carboxylic acid **70** was isolated in low yields. The synthesis was completed with an amide coupling of **70** with amine **10** with HATU coupling conditions in a low yielding reaction. Analysis of the crude by LCMS-LCQ showed complete consumption of the carboxylic acid and the low yields can therefore be attributed to isolation of the pure compound. As experienced previously with compounds described in this chapter, difficulty arose with separating the poorly soluble amine **10** from the final compound.

2.5. Biological evaluation of ML216 and its analogues

2.5.1. Determination of BLM DNA unwinding inhibition by ML216 and its analogues

In parallel to the synthesis of reported BLM inhibitors based on ML216 and its more soluble analogues, a BLM helicase primary screening assay was optimised by Ms Xiangrong Chen. As described in Section 1.6.5, this fluorescence-quenching assay enabled IC_{50} determination of compounds based on their ability to inhibit the unwinding

of duplex DNA by BLM helicase. Because targeting BLM is a novel strategy with consequently limited tool inhibitors (aside from the poorly soluble ML216 and its analogues), there were no available compounds to use as a specific positive control in the assay. Aurintricarboxylic acid (ATA), a general inhibitor of nucleases, was therefore used as a positive control.

Table 2.11. Primary assay screening data of ML216 (**1**) and its reported analogues.

Compound	R ¹	R ²	Reported IC ₅₀ (μM) ^{a,b}	In-house BLM IC ₅₀ (μM) ^{c,d}
1 (ML216)	F	CF ₃	1.8	5 ± 8
2	Br	Br	2.1	>100
3	F	CN	0.3	24 ± 8
4	CN	Cl	1.6	20 ± 11
5	Br	H	12.6	44 ± 10
6	Br	CN	0.11	26 ± 7
7	Cl	Cl	1.4	16 ± 5
8	Cl	CN	0.10	17 ± 5

^aReported by Rosenthal *et al.*²⁰³; ^bdetermined by gel-based assay; ^cin-house fluorescent quenching assay;

^ddeterminations ± standard deviation (n = 4).

When tested in the fluorescence-quenching biochemical assay, reported BLM inhibitors **1–8** exhibited a large variation between their literature IC₅₀ values and those determined in-house (Table 2.11).²⁰³ The in-house biochemical assay largely resembles that developed by Nguyen *et al* used in the qHTS for BLM inhibitors.¹ An important consideration when comparing the results from Tables 2.11-2.14 is the difference in assay formats used; the reported values are based on a gel based assay conducted by Rosenthal *et al.*²⁰³ It is highly unlikely the disparity between reported and in-house IC₅₀ values observed here could be in part due to the difference in assay formats. This is because both formats use the same procedure but the determination of the extent of DNA unwinding is assessed through different methods (fluorescence value shifts versus gel shifts).

Only the original hit **7** was tested in the fluorescence-quenching assay format on two occasions during the qHTS screen, and the IC₅₀ values were as follows: (1) 4 μM, from

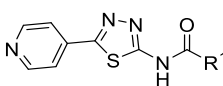
initial qHTS screen [AID2528]; (2) 3 μM , from confirmatory HTS screen [AID2585]. The in-house assay determined the IC_{50} of **7** to be 16 μM , a shift of approximately 4-fold. As shown in Table 2.11, the results for the literature BLM inhibitory activity of **7** are consistent between the fluorescence-quenching assay and the gel-based assay.²⁰³

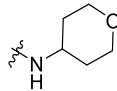
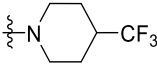
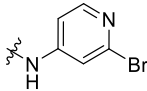
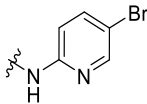
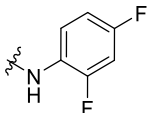
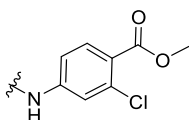
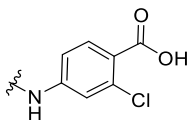
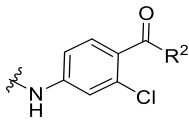
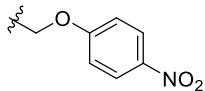
The reported BLM inhibitor ML216 (**1**) displayed an activity of 5 μM in the in-house fluorescence-quenching assay. However, on some test occasions, ML216 was inactive in the assay which demonstrated the inconsistency in data within this series. Furthermore, compounds **3–8** all show a large IC_{50} shift ranging from 4–200-fold difference from the reported value. It is unclear why this discrepancy occurred between compounds exists, but it is likely that poor aqueous solubility of the compounds was a factor. Compounds **1–8** were tested from freshly prepared 2 mM stock solutions in DMSO because they were often observed to precipitate out of DMSO over prolonged periods. Regular analysis by LCMS-LCQ and $^1\text{H-NMR}$ of the compounds showed no degradation issues of solid samples over the course of 1.5 years, therefore it was unlikely compound degradation played any significant role in the disparate results observed here.

Compound **71**, a non-urea analogue of this series, which displayed inhibitory activity in fluorescence-quenching assay format on during the BLM qHTS screen [AID2528] at 16 μM did not confirm as a BLM inhibitor when tested in-house (Table 2.12).

Removing the aromaticity of the phenyl ring resulted in loss of activity, while the 2,4-difluoro substitution **16** also showed no BLM inhibition (Table 2.12). Replacement of the phenyl with a 4-pyridyl functionality **14** resulted in the most potent compound obtained in the design of this series. While no obvious qualitative gain in solubility was achieved, it would be reasonable to assume the pyridyl **14** would have a better solubility profile than the phenyl analogue **5**. The 2-pyridyl analogue **15** was not active against BLM helicase, possibly due to the importance of having a substituent at the *ortho* and *para* positions, even if only a hydrogen at one of these positions.²⁰³

Table 2.12. Primary assay screening data for exploration of R^1 .

		
Compound	R^1	BLM IC_{50} (μM) ^{a,b}

12		>100
13		>100
14		6.8 ± 4^c
15		>100
16		>100
17		96
18		>100
19–33	 R ² = water solubilising group (See Table 2.7)	>100
71		>100

^aIn-house fluorescent quenching assay; ^bdeterminations \pm standard deviation (n = 2)

^cn = 4

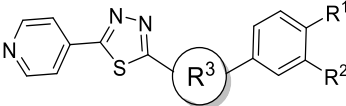
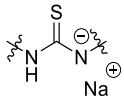
Derivatives of the *N*-acylated solubilising groups, methyl ester **17** and carboxylic acid **18** were also tested for BLM inhibition (Table 2.12). **17** demonstrated negligible activity with an IC₅₀ of 96 μ M, while **18** was inactive. The reported SAR of these compounds highlight the importance of electron withdrawing groups at the 3- and 4- position of the phenyl ring, which could explain why an IC₅₀ value for **17** was able to be determined.²⁰³ While it was possible the difference in BLM inhibition between **17** and **18** was minimal, the assay cut-off at 100 μ M limited comprehensive exploration.

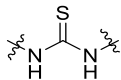
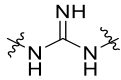
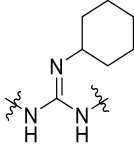
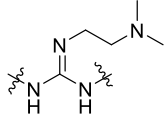
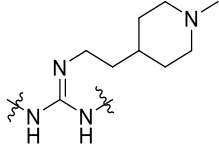
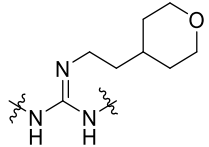
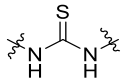
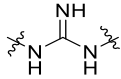
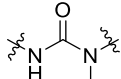
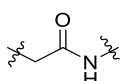
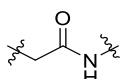
The addition of *N*-acylated water solubilising groups at the 4- position of the phenyl ring (**19–33**) completely abolished activity of the compound (Table 2.12). With regard to

compound handling, specifically for analogues **24–33** (Table 2.7), there was a clear improvement to the solubility profile, as expected. However, it was apparent that larger substituents on the 4- position of the phenyl ring were not well tolerated. Table 2.11 indicates that in our assay, a chloro group at the 3- position of the phenyl ring performs as well as any substituent. Based on the reported SAR,²⁰³ the nitrile group was expected to be an optimal substitution and compounds **7** and **8** show the chloro and nitrile substituents perform similarly. It is unlikely that there is space in the protein pocket for growth from the *para* position of the phenyl ring. Because only a 5-fold drop from the most potent substitutions would result in the compounds appearing inactive, improvements to the solubility would not be feasible without reducing the potency to impractical levels.

Compounds in Table 2.13 were synthesised to improve the solubility of ML216 through modifications to the urea core. Handling of thioureas **41** and **43** did not show a clear improvement in solubility as expected. Whilst **41**, the sodium salt of **42**, was sufficiently soluble in DMSO, it was prone to partial precipitation caused by protonation when tested under assay conditions. Thioureas **41** and **43** showed no BLM inhibition, which did not correspond with previously reported literature data.²⁰³ **41** is the thiourea analogue of **7**, and as such was expected to demonstrate a similar activity profile. Similarly, the guanidine analogue of ML216, **43**, showed no BLM inhibition.

Table 2.13. Primary assay screening data for urea replacement.

				
Compound	R ¹	R ²	R ₃	BLM IC ₅₀ (μM) ^{a,b}
41	Cl	Cl		Inactive

42	Cl	Cl		Inactive
45	Cl	Cl		Inactive
46	Cl	Cl		Inactive
47	Cl	Cl		Inactive
48	Cl	Cl		Inactive
49	Cl	Cl		Inactive
43	F	CF ₃		<i>nd</i>
44	F	CF ₃		Inactive
56	CN	Cl		Inactive
60	CN	Cl		Inactive
61	Cl	Cl		Inactive

^aIn-house fluorescent quenching assay; ^bdeterminations \pm standard deviation ($n = 2$). *nd* = not determined.

Analysis of the novel methyl urea **56** and amides **60** and **61** also showed a loss of activity from their urea counterparts. The methyl urea **56** did not indicate any obvious improvement in solubility on handling in DMSO, although the amides **60** and **61** did show improvement.

Finally, analogues were synthesised where the thiadiazole of ML216 was replaced by a 2-pyridyl moiety. The observation that the 4-pyridyl-1,3,4-thiadiazole core played a

significant role in the poor solubility of ML216 was given further credence during the synthesis of compounds **57–60**. It was apparent on handling that ring replacement with a pyridine ring resulted in a more soluble urea analogue. Again, these compounds showed no activity when tested using the in-house assay (Table 2.14), in contrast to reported data.²⁰³

Table 2.14. Primary assay screening data for urea replacement.

Compound	X	Y	R ¹	R ²	BLM IC ₅₀ (μM) ^{a,b}
65	N	C	Cl	Cl	>100
66	N	C	Br	CN	>100
67	N	C	F	CN	>100
68	C	N	F	CN	>100

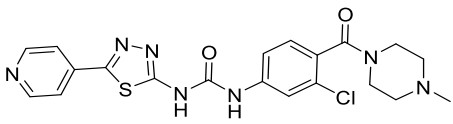
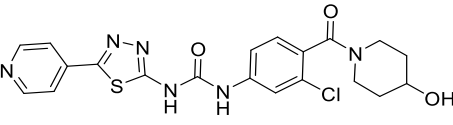
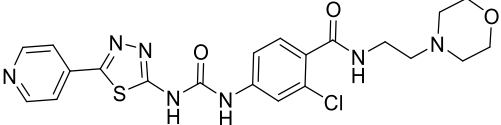
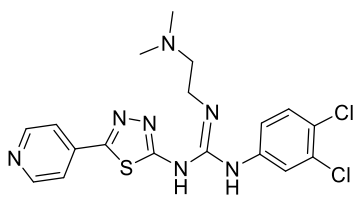
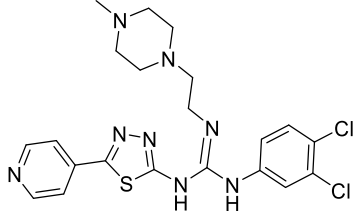
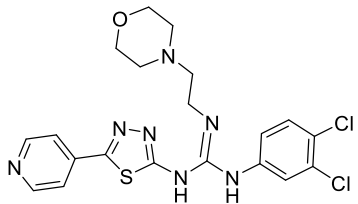
^aIn-house fluorescence-quenching assay; ^b determinations ± standard deviation (n = 2).

2.5.2. Assessment of thermodynamic solubility of selected compounds

The synthesis of more soluble ML216 analogues was successful in that many of the compounds synthesised were easier to handle in relevant solvents. Following the synthesis of various strategies utilising solubilising groups, selected compounds were assessed for thermodynamic solubility. No value for solubility was determined for ML216 (**1**) because no sample peaks were obtained, suggesting no compound was in solution in assay buffer across all dilutions. This strongly contradicted the kinetic solubility determination of ML216 reported at 1 μM.²⁰³

Table 2.15. Solubility determination of selected compounds.

Compound	Structure	Solubility (μM)	Comment
1 (ML216)		0	Standard curve attained; no sample peaks
18		28	

27		<0.1	No sample peaks
29		7	
32		<0.1	No sample peaks
47		43	
48		11	
49		0	Standard curve unattainable

The carboxylic acid **18** displayed good solubility relative to the other compounds tested because in the assay the carboxylic acid group would be ionised at pH 7.4, whereas none of the other compounds tested would become ionised at this pH. Solubility determination of compounds containing solubilising groups gave varied results. The urea **29** and guanidines **47** and **48** displayed a marked improvement over ML216 (**1**). Compounds **27** and **32** only produced standard peaks up to 0.1 μM and no sample peaks, meaning these compounds had a solubility below 0.1 μM , whilst the failure of compound **49** to produce a standard curve suggested these compounds did not yield any significant improvement over ML216 (**1**). Regardless of any quantitative gains in solubility over ML216 (**1**), all compounds with solubilising groups failed to display any biological activity against BLM helicase.

Numerous strategies were employed to improve the solubility of this series but were not supported by activity data in the biological assay. Therefore, it was decided to discontinue efforts to quantitatively determine the solubility of compounds in this series. It was unfortunate that these changes, many of which were reported in the literature, did not prove successful in inhibiting BLM helicase under in-house assay conditions.²⁰³

2.5.3. Summary of biological results

ML216 (**1**) and various reported analogues²⁰³ were assessed for their activity using a fluorescence-quenching DNA unwinding assay. The in-house IC₅₀ determinations of various reported ML216 analogues demonstrated large IC₅₀ shifts in BLM inhibition from literature data.

Analysis of the ML216 analogues synthesised to improve solubility revealed there was no BLM inhibition for both reported and novel compounds. The inconsistent behaviour observed within this series, as seen across multiple assays, raised concerns regarding the viability of the series going forward. Precipitation occurred with many analogues while performing the assays, which made the data obtained unreliable. This observation is consistent with the reported aqueous solubility profile of this series but is in direct contradiction to findings by Rosenthal *et al.*: “Of note, the compounds show improved solubility in the assay buffer system, which suggests that the biochemical data for these analogues were not compromised by this liability”.²⁰³ The report continues by stating, “Typically, the improved solubility in the assay buffer is a result of having non-ionic detergent (Tween-20) present which aids in solubilizing the more lipophilic compounds.” The same detergent, when used for the in-house assay, did not aid such solubilisation. As discussed throughout this chapter, it was very difficult to mitigate the inherently poor solubility of the ML216 core without drastically changing the structure, which would risk diminished potency in a series that had demonstrated tight SAR.

Considering the SAR determined herein displayed huge inconsistencies with reported data, no further strategies to improve aqueous solubility of this series were planned until additional biological data had been collected. Attempts to obtain a crystal structure

of BLM in complex with inhibitors from this series were also unsuccessful. Finally, through the use of DNA intercalation and dye displacement assays it was determined that the compounds in this series likely bind to DNA. Ideally, such claims would be supported by biophysical data. To date, this has not been possible to determine likely due to the solubility of these compounds in such assays. However, such evidence reveals this series would be very risky to further pursue. The data revealed that many of the claims made by Nguyen *et al.*¹ could not be confirmed and remain unsupported by in-house biological studies. Specifically, ML216 does not selectively inhibit BLM over other helicases, and that the compound does not compete with ssDNA at the nucleic acid binding site, but more likely binds to the DNA causing inhibition of the BLM-DNA complex. Therefore, ML216 is not a useful probe for BLM helicase.

2.6. Summary and conclusion

In 2013, Nguyen *et al.* described the biological evaluation of a first-in-class probe molecule of BLM helicase, ML216 (**1**), which displayed low micromolar potency, selectivity over some related helicases and on-target activity in a cellular context.¹ Subsequently, Rosenthal *et al.* reported their medicinal chemistry optimisation efforts from the hit molecule **7** that had led to the optimisation to ML216 (**1**).²⁰³ This compound series naturally presented as a suitable starting point in the design and synthesis of a potent, selective and soluble chemical probe targeting BLM helicase.

ML216 (**1**) displayed a very poor aqueous solubility profile by kinetic solubility determinations reported by Rosenthal *et al.*²⁰³ In the current study, initial medicinal chemistry optimisation on this series focussed on improving the aqueous solubility profile to allow reliable biological evaluation in the primary in-house helicase-unwinding assay. In addition, a more soluble scaffold would have aided determination of an X-ray crystal structure of BLM helicase in complex with a ligand in order to assist with structure-based design.

Various strategies were employed to produce ML216 analogues with an improved aqueous solubility profile. Some of these strategies were based on existing SAR studies in literature surrounding ML216.²⁰³ Synthesis of many of these compounds presented

challenges because their associated solubility issues diminished reactivity in most solvents and increased complexity for isolating final compounds.

Using the optimised in-house assay, it was ultimately shown that a selection of reported ML216 analogues did inhibit BLM helicase but with a 4–200-fold shift in activity. Furthermore, the SAR picture obtained in the present study was not consistent with the findings of Rosenthal *et al.*²⁰³, wherein the most potent BLM inhibitor (**8**) was described as having an IC₅₀ of 0.1 µM, whereas the best inhibitor tested in-house (**7**) had an IC₅₀ of 16 µM. Reassuringly, the DNA unwinding assay used to test these compounds was found to be consistent with other series of inhibitors described in the NIH BLM qHTS screen (Chapter 3).

The implementation of various design strategies failed to produce significant improvements in solubility or display potency. Overall, this series displayed very tight SAR whilst implementation of active scaffolds was associated with inherently poor aqueous solubility. Therefore, it was decided the ML216 series was not a tractable starting point in the development of inhibitors of BLM helicase. Chemistry on this series was discontinued while further biological work sought to assess the mechanism of binding and BLM inhibition by ML216 (**1**). Such biological investigations conducted by Miss Chen revealed ML216 inhibited ATPase activity of RECQ5 to a similar extent to that of BLM. Furthermore, these investigations also revealed that ML216 was likely binding to DNA which suggests that results of Nguyen *et al.*²⁰³ could not be confirmed and remain unsupported by in-house biological data.

The failure of the ML216 series illustrated the need for a reliable chemical probe for BLM helicase for future DDR investigations. This series was therefore not suitable for hit optimisation. Therefore, it was necessary that future medicinal chemistry efforts would focus on finding more ideal candidates for hit optimisation from the published BLM qHTS screen for the development of probe-like and drug-like inhibitors of BLM helicase.

3. Hit identification of novel BLM helicase inhibitors from high-throughput screening (HTS) data

3.1. Introduction

This chapter describes an HTS approach — data-mining through publicly available BLM HTS data to identify new inhibitors of BLM helicase. ML216 itself was developed from a hit from this screen. By examination of the screening data, it was the ambition of the work described in this chapter to discover improved drug-like tractable chemical compounds.

3.1.1. High-throughput screening (HTS)

HTS is currently the most widely used technique to identify early entry starting points for chemistry drug discovery programs, when there is no existing ligand data disclosed.^{15,231} HTS is a powerful strategy that enables researchers to test hundreds of thousands to millions of samples and has proven efficacy not only at generating hit molecules, but also producing drugs that have reached the market. This is true for many of the first molecularly targeted cancer drugs such as Sorafenib, an orally active multikinase inhibitor approved for the treatment of hepatocellular carcinoma.²³² The main caveat of HTS is that it is cost- and resource-intensive which prevents this strategy being widely implemented outside organisations with major funding or infrastructure.

The PubChem BioAssay database sought to bridge the gap between HTS data generation and data sharing and is the largest public repository for chemical structures and biological data.²⁰⁵ The database was initially established to archive HTS data from the National Institute of Health's (NIH) Molecular Libraries Program (MLP) which aimed to provide early stage chemical tools to researchers for validation of new drug targets to facilitate the development of new drugs.³⁰ One such biochemical assay screen of a library of 350,000 chemically diverse small molecules, known as the Molecular Libraries Small Molecule Repository (MLSMR), was developed for BLM helicase and led to the development of ML216 (Section 1.5.6).²⁰² As described in Chapter 2, ML216 was shown not be a suitable early stage chemical tool, in stark contradiction to the medicinal

chemistry optimisation and biological characterisation described in the literature.^{1,203} However, the availability of BLM HTS data on PubChem Bioassay²⁰⁶ [AID2528] created an opportunity to revisit hit selection for the purpose of this study.

Screening large libraries can generate false positives, which are inactive compounds that show positive activity in the assay due to aggregation or assay interference.²³³ When selecting hits or leads, it is important to avoid attrition later in the project and therefore a comprehensive assessment of initial actives is vital. A profile of the physicochemical properties, chemical integrity, promiscuity and synthetic accessibility should be assessed to aid in finding a series least likely to result in failure at a later stage.²³⁴ This should then be followed by SAR exploration and comprehensive screening, such as confirmatory screens, assay-specific counter-screens, orthogonal assays, selectivity counter-screens, preliminary mechanistic studies and cell based screens.²³¹ However, the design of such screening trees is influenced by the nature of the target, project resources and project timeline.

HTS takes a relatively unbiased approach to screening and can be utilised to find distinct chemical classes of inhibitors, potentially with novel binding modes against a particular molecular target (depending on the configuration of the screen). Using the publicly available biological data generated from the BLM HTS screen [AID2528], new chemical entities targeting BLM were identified through common triage processes and were subsequently screened in-house. This strategy enabled immediate identification of new hits from the BLM HTS data to facilitate synthetic and medicinal chemistry efforts, as opposed to pursuing other strategies from scratch (as with in-house fragment-based screening, for example).

3.1.2. qHTS assay for inhibitors of BLM [AID2528]

The PubChem database contains various bioassay data pertinent to the BLM triaging process implemented herein. A fluorescence-quenching assay that monitors DNA strand separation (Figure 1.5.6) was used in the qHTS [AID2528] to identify inhibitors of BLM (Figure 3.1). qHTS generates concentration-response curves so IC_{50} values can be determined simultaneously. The compound selection that was screened came from the NIH Molecular Libraries Small Molecule Repository (MLSMR), which has facilitated the

development of many chemical probes through its extensive implementation in HTS strategies. As a result, a large amount of screening information is available in PubChem Bioassay for the compounds in the library.

ML216, the published inhibitor of BLM helicase, was developed from the qHTS hit MLS000559245 or PubChem compound identification number (CID) 1075698.²⁰³ The results of the qHTS screen [AID2528], which were published in PubChem, include data from the original 355,000-compound qHTS as well as a confirmatory assay to reassess 222 hits triaged by the project team [AID2528] (Figure 3.1). Additionally, a selection of the MLSMR underwent spectroscopic profiling to identify false positives that interfere with the fluorescence read-out. The MLSMR has been used in a large amount of qHTS campaigns, including screening of WRN [AID651768] and RECQ1 [AID2549] in similar formats to the BLM qHTS, which allows inferences to be made regarding the promiscuity and selectivity of the library (Figure 3.1).

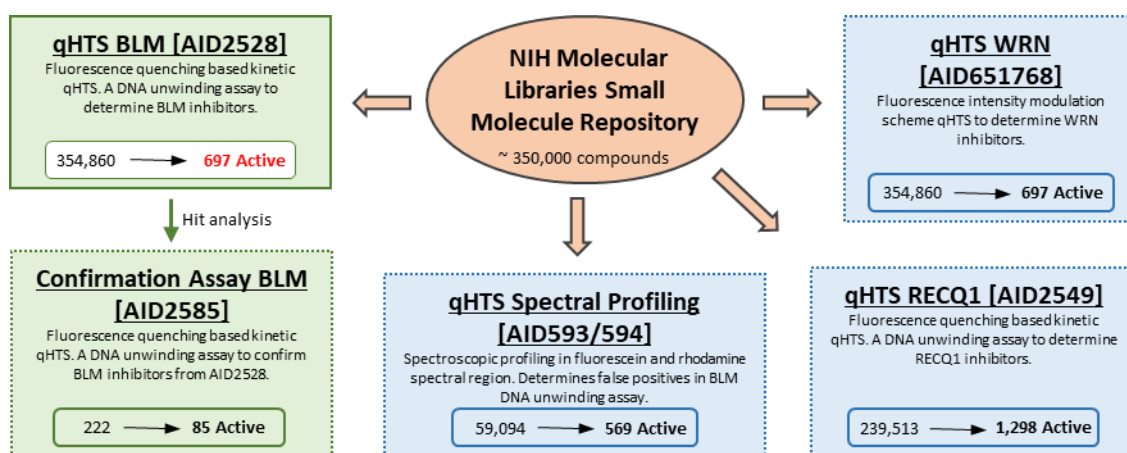


Figure 3.1. Available data in PubChem Bioassay pertaining to the identification of BLM hits.²³⁵

3.1.3. In-house screening

A fluorescence-quenching assay (described in Section 1.5.6), highly similar to that applied in the BLM qHTS [AID2528], enabled IC₅₀ determination of triaged hits based on their ability to inhibit the unwinding of duplex DNA by BLM helicase. Orthogonal confirmation would be the ideal progression in hit confirmation, but development of such biophysical assays (thermal shift, MST, ITC) or cell-based assays had not proved successful at the time of biological testing. Therefore, counter-screen measures and demonstrable SAR were used to validate the authenticity of hits.

High-throughput screens that monitor helicase-catalysed separation of nucleic acids have been shown to yield few hits, as has also been illustrated by the BLM screen (hit rate of 0.2%).¹²⁵ Furthermore, many of these appear active in the assay because they bind the nucleic acid substrate with the most potent hits usually being false positives. The main approach to avoid inadvertent pursuit of false hits is to implement counter-screening measures, although innovative cellular helicase assays and structure-based design can also eliminate these false leads.¹²⁵ A counter-screen is an assay in which compounds are tested for undesired attributes. In the case of a BLM helicase hit arising from a DNA unwinding assay, a key attribute would be to test the ability of the hit to bind DNA or to promote protein aggregation which would result in positive readouts (Figure 3.2). Furthermore, it was desirable to test the ability of such inhibitors to compete with ATP at its binding site, as this is a non-selective inhibition mechanism that is likely to target other DNA helicases.

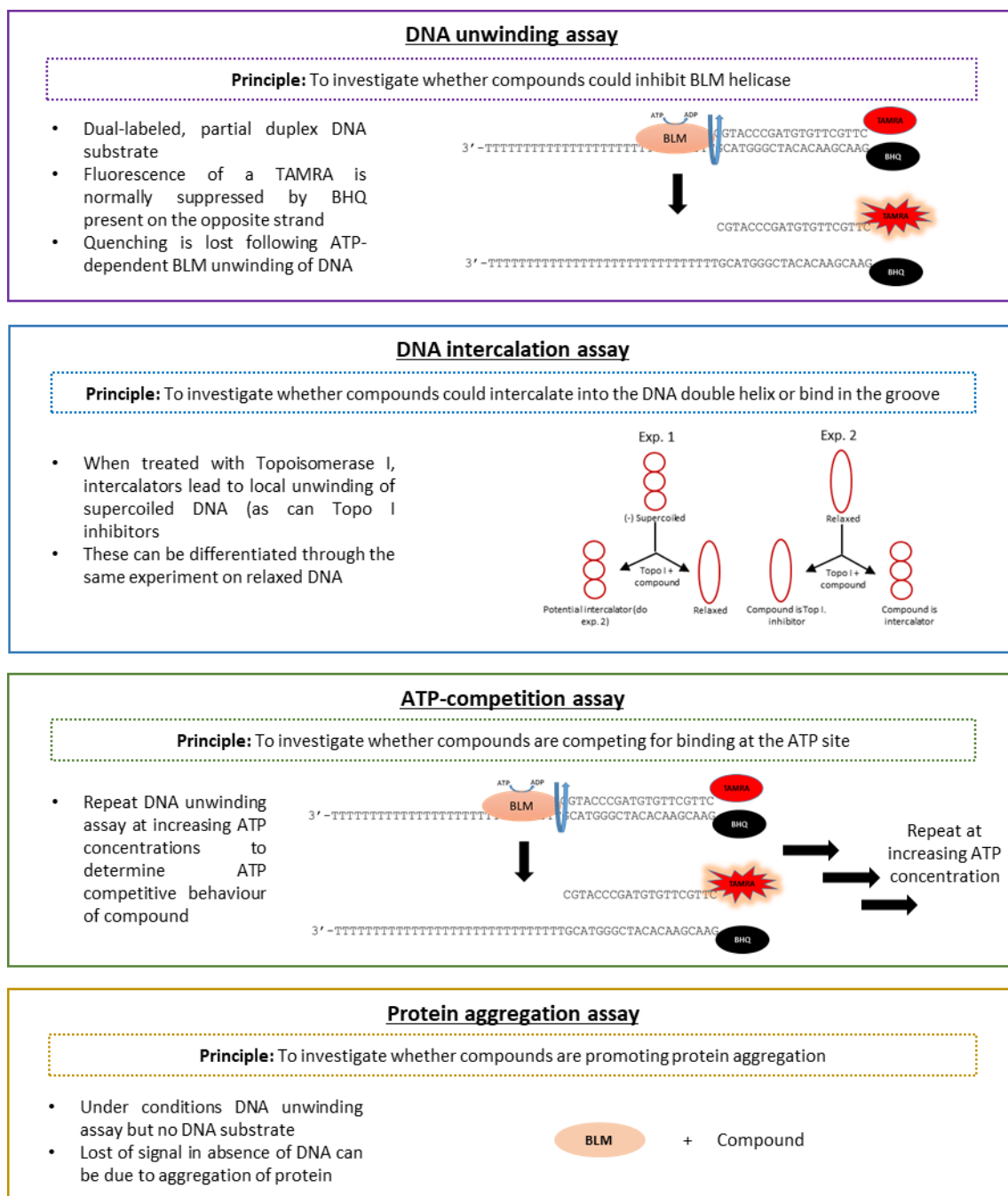


Figure 3.2. Description of the in-house BLM inhibition assay and counter-screen performed by Ms Xiangrong Chen.

3.1.4. Aim

The aim of this chapter was to assess the HTS data pertaining to BLM helicase on PubChem Bioassay in order to identify chemical starting points suitable for medicinal chemistry optimisation, with the view to ultimately develop a novel chemical probe. Therefore, to identify new lead series that inhibit BLM helicase, a cheminformatic and

medicinal chemistry analysis of the 672 actives reported in the BLM qHTS assay [AID2528] was performed prior to medicinal chemistry efforts.

The steps undertaken to achieve this aim were as follows:

1. Triage of the 672 active BLM hits using bioactivity data from PubChem Bioassay, as well as consideration of factors such as chemical integrity, promiscuity, synthetic accessibility, SAR and physiochemical properties. The objective was to identify no more than 10 series for in-house testing so as not to overextend the capabilities of a single synthetic chemist.
2. Assess the results of commercially prepared and/or synthesised compounds on the primary biochemical DNA unwinding assay for BLM inhibitory determination in conjunction with other assays performed in-house to decide which series to pursue with further medicinal chemistry efforts.
3. Demonstration of SAR for promising series in the absence of orthogonal biological confirmation of BLM inhibition.

3.2. HTS analysis and triage

The screening tree designed to triage 672 actives resulted in the follow up of one hit series (Figure 3.3).

3.2.1. Computational filtering

Active hits from the PubChem Bioassay 'qHTS Assay For Inhibitors Of Bloom's Syndrome Helicase (BLM)' [AID2528] were accessed from the PubChem Bioassay web portal (<https://pubchem.ncbi.nlm.nih.gov/bioassay>) and their PubChem compound identification (CID) number was used to export the 672 actives from the PubChem Download Service² in sdf format. These hits were initially grouped into 30 clusters using the Clustering of Ligands tool of Maestro 11.1. This enabled quick identification of closely related compounds that were filtered out for any hits taken forward.

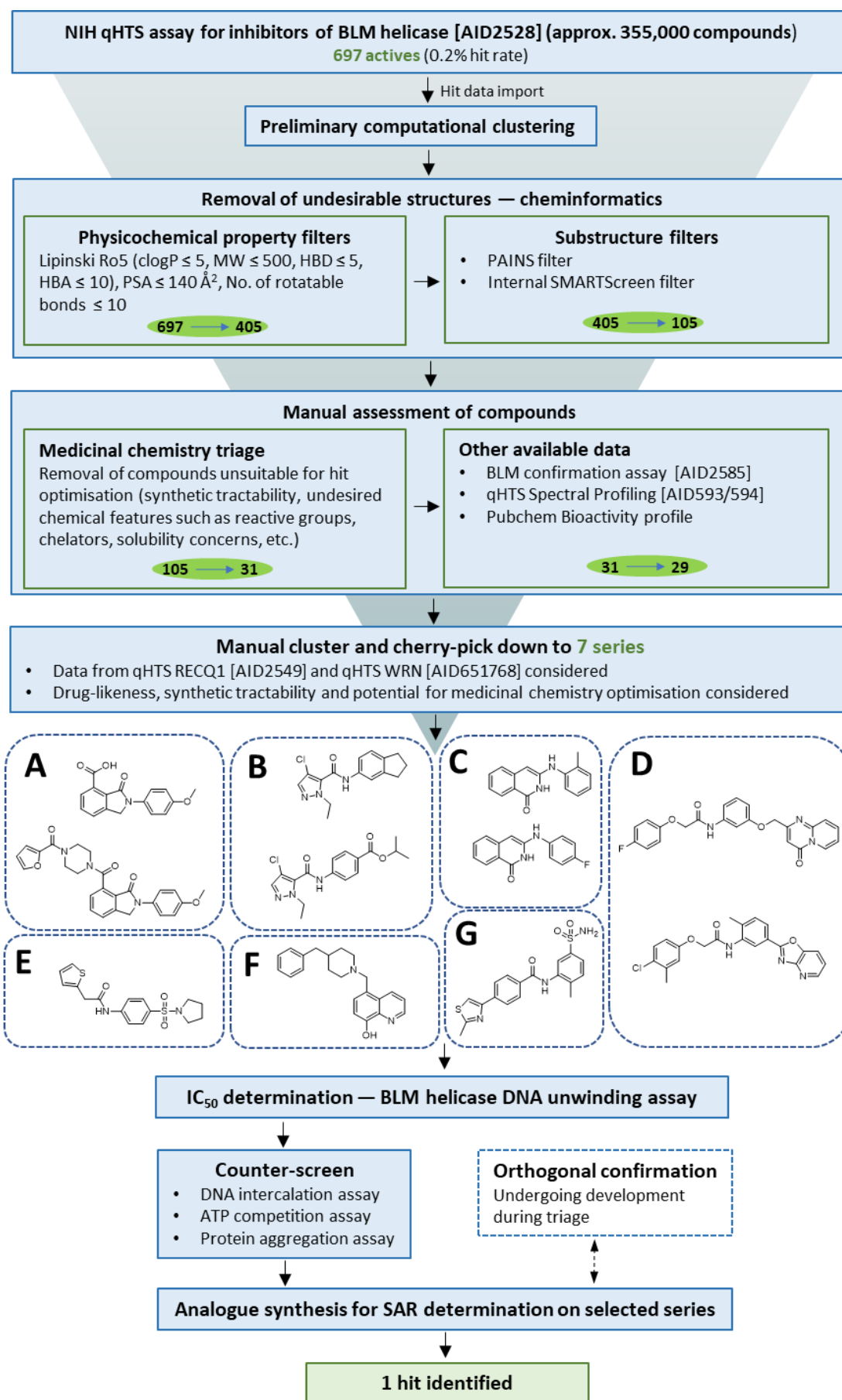


Figure 3.3. Pathway of hit identification described in this chapter.

3.2.1.1. Compound filtering – physicochemical property filters

The initial selection process involved manual assessment of the 672 actives from the qHTS of BLM helicase and removal of all compounds that were not in agreement with Lipinski rules³⁴ ($\text{clogP} \leq 5$, $\text{MW} \leq 500$, $\text{HBD} \leq 5$, $\text{HBA} \leq 10$), and Veber rules²³⁶ ($\text{PSA} \leq 140 \text{ \AA}^2$, No. of rotatable bonds ≤ 10). The sdf file containing the qHTS BLM actives was imported into the Canvas module of Schrödinger software where the physicochemical parameters for this dataset was generated. 267 compounds that did not satisfy the physicochemical parameters listed above were eliminated, with 405 compounds proceeding to the next level of filters.

3.2.1.2. Compound filtering – substructure filters

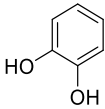
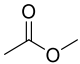
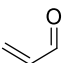
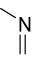
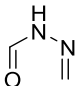
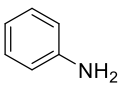
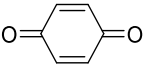
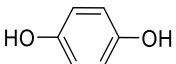
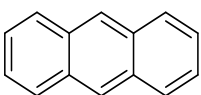
Substructure filters can be used to remove compounds with specific functional groups that have been found to interfere with screening assays. Various substructural features have been identified that appear in promiscuous compounds known as Pan-Assay Interference Compounds (PAINS),²³⁷ which have then been incorporated into substructure feature filter lists so such features can be flagged. SMiles ARbitrary Target Specification (SMARTS) is a language used for describing molecular substructure and properties and is an extension of the commonly used SMILES.²³⁸ Input of the SMARTS of each compound into such filters can allow removal of compounds containing PAINS features.

Furthermore, there are compounds that can cause problems in later stages of drug development because of their ADMET or toxicity risk. An internal substructural filter has been devised within the Sussex Drug Discovery Centre, termed SMARTScreen, which flags compounds with substructures not suitable for drug development (unpublished).

A workflow formulated in-house by Dr Ben Wahab enabled conversion of sdf structures into SMARTS format followed by input into the PAINS filters and SMARTScreen filters. The output of this process is two files. The first contains the 'good' structures that have passed both filters while the second contains the structures that were flagged by the PAINS or SMARTScreen filters along with the reason(s) for failure. Overall, 305

compounds failed to pass PAINS or SMARTScreen filters. The most common reasons for removal of compounds are presented in Table 3.1.

Table 3.1. Most common reasons for removal of compounds during PAINS and SMARTScreen substructure filter.

PAINS or SMARTScreen category	Substructure	No. of compounds
Catechol-like		71
Ester		36
Michael acceptor		34
Imine		20
Acyl hydrazide		14
Aniline		14
Quinone		14
Hydroquinone		12
Polycyclic aromatic hydrocarbon		12

3.2.2. Manual assessment of remaining compounds

3.2.2.1. Medicinal chemistry triage

The remaining 105 structures underwent further triage and manual assessment using medicinal chemistry principles and experience. Structures were categorised into 3 groups: (a) prioritised targets, (b) deprioritised targets and (c) removed structures. Compounds containing obvious undesirable features were deprioritised or removed. For example, many compounds were deprioritised when they contained thioesters (12 compounds), furans (18 compounds) and polycyclic structures (20 compounds). Various compounds also contained urea functionalities (3 compounds) and DNA base-

like cores (10 compounds), particularly related to thymine and guanine. Some structures were also removed or deprioritised if they contained cores that would require complex synthesis, as this would be limited by the resources and time available. Furthermore, some compounds were not appraised to be suited for medicinal chemistry optimisation due to their limited scope for SAR. Following triage, 31 compounds remained in the priority list.

3.2.2.2. PubChem data available

The 31 remaining compounds were cross-checked with those of the qHTS BLM confirmatory assay [AID2585] to confirm that information for all compounds (including IC₅₀ values) was present in the dataset. Additionally, PubChem Bioassay can display a single compound's performance from all previous HTS campaigns (known as the bioactivity profile of the compound). The selected compounds have an extensive bioactivity profile, having been tested in over 700 assays, therefore inferences can be made regarding their selectivity and reactivity. For instance, compounds that are frequently identified as hits are more likely to be false positives and result in wasted resources during follow-up (although a high hit rate does not always indicate reactivity or a PAINS compound). Accordingly, it was decided that compounds identified as hits in at least 10% of all assays would be deprioritised, leading to the removal of 2 compounds from the priority list. A published counter-assay also assessed which compounds interfered with rhodamine fluorescence [AID594]. None of the remaining compounds were found to exhibit off-target activity via interfering with fluorescence.

3.2.2.3. Clustering and cherry picking of series to follow up

The remaining 29 compounds were manually clustered into 14 final series. Of these, seven were cherry-picked for in-house biological study (Figure 3.3) based on factors such as drug-likeness, synthetic tractability and potential for medicinal chemistry optimisation. The properties of the inhibitors from these seven series (referred to as Series A–G) are described in Table 3.2.

Table 3.2. Properties of final 7 series from post-HTS triage including physicochemical properties and reported and in-house bioassay data.

Series	No. of hits	Lead compound PubChem CID	MW	ClogP	NIH assays IC ₅₀ (μM)				Pubchem Bioassay (No. of assays)		Commercial supplier	In house BLM IC ₅₀ (μM)	In-house synthesis?	Counter-screen		
					BLM qHTS 2528	BLM qHTS 2585	WRN qHTS 651768	RecQ1 qHTS 2549	Tested	Active				DNA binder	ATP competitive	Protein aggregation
A	2	5309875	282	2.2	16	16	50	15	810	34	ChemDiv	40	Y	N	N	N
B	2	1223798	290	3.4	25	18	nd	nd	442	6	Not available	-	Y	-	-	-
C	2	2142222	254	3.0	28	33	Inactive	Inactive	833	78	Not available	-	Y	-	-	-
D	2	46355890	433	3.2	14	6	nd	nd	85	5	ChemDiv	Inactive	N	nd	nd	nd
E	1	1077847	350	2.4	18	20	Inactive	Inactive	726	20	Vitas	Inactive	N	nd	nd	nd
F	1	698133	332	4.5	9	18	Inactive	Inactive	514	54	Vitas	33	N	nd	nd	nd
G	1	5299021	388	3.0	7	6	Inactive	nd	544	7	Vitas	5	Y	N	N	N

3.2.3. Results of screening: biological assessment of commercially prepared compounds

All commercially-available compounds from the 7 series were purchased from reputable suppliers (Table 3.2) for in-house assessment of BLM inhibition using a fluorescent quenching assay and active compounds underwent counter-screening. Compounds from Series B and C were not commercially available so required in-house synthesis (described Section 3.5 and 3.6).

The results of the BLM inhibitory screen of commercial compounds are presented in Table 3.2. Series A, G and F were confirmed hits while Series D and E were not active below the 100 μ M cut-off in this assay. Series F was eliminated due to a chemical liability discovered in its structure. Series A and G were assessed in counter-screening assays to identify potential false positives, and it was found both series did not operate via off-target mechanisms such as DNA intercalation and protein aggregation. Furthermore, these inhibitors did not compete with ATP-binding which was also a necessary criterion for continuation to ensure compounds were not binding in the highly conserved ATP-binding site. To further confirm their activity, Series A and G were resynthesised in-house.

3.3. Series B hit validation

3.3.1. Rationale

CID1223798, or 4-chloro-2-ethyl-*N*-indan-5-yl-pyrazole-3-carboxamide (**72**), is a small fragment-like compound that inhibited BLM helicase in the qHTS [AID2528] with an IC_{50} of 25 μ M (Table 3.3). This series also contained the active compound CID1316580 (**73**), a 2-ethylpyrazole-3-carboxamide analogue of **72**. **73** was originally filtered during hit triage because its ester group was considered a metabolic liability, so it was not scheduled for hit optimisation. There are no PubChem bioactivity data for **72** against WRN and RECQ1, however **73** has been shown to have no activity against either protein. Interestingly, the PubChem Bioassay data indicate Series B demonstrate very little promiscuity (Table 3.3).

Both compounds were not commercially available, therefore to confirm BLM inhibition they were synthesised in-house. The compounds are diaryl amides so it was thought synthetic efforts would be relatively straightforward using amide coupling conditions.

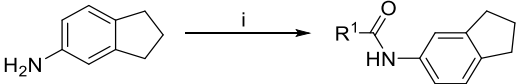
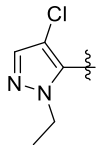
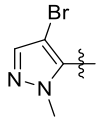
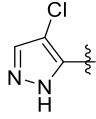
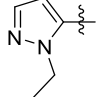
Table 3.3. Calculated physicochemical properties and reported biological data of Series B.

#	PubChem CID	Physicochemical properties				Pubchem Bioassay			
		MW	clogP	HBD	HBA	BLM qHTS 2528	WRN qHTS 651768	RECQ1 qHTS 2549	Bioactivity profile (active/tested)
72	1223798	290	3.4	1	4	25	nd	nd	4/ 442
73	1316580	335	3.2	1	6	4	Inactive	Inactive	6/769

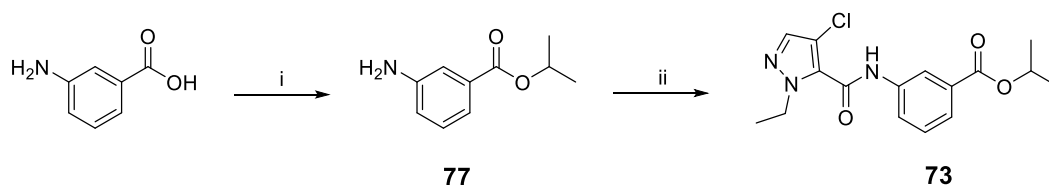
3.3.2. Synthesis

Amide **72** was synthesised from the commercially available 4-chloro-1-ethyl-1H-pyrazole-5-carboxylic acid by HATU amide coupling with 5-indanamine (Table 3.4). This was followed by synthesis of derivatives **74–76** from the same coupling conditions because **72** demonstrated BLM inhibitory activity in the DNA unwinding assay. As orthogonal confirmation was not yet available, initial medicinal chemistry efforts were directed to SAR studies of this series. Accordingly, point changes were introduced to observe effects on activity.

Table 3.4. Reagents and conditions: (i) appropriate carboxylic acid, HATU, DIPEA, DMF, r.t., 16 h.

		
Compound	R ¹	Yield (%)
72		39
74		52
75		38
76		91

Synthesis of **73** began with esterification of 3-aminobenzoic acid isopropyl alcohol in the presence of thionyl chloride at reflux (Scheme 3.1). The isolated crude then underwent amide coupling with 4-chloro-1-ethyl-1H-pyrazole-5-carboxylic acid by the conditions described above for synthesis of **72**.



Scheme 3.1. Reagents and conditions: (i) SOCl₂, IPA, 90 °C, 16 h, 40%; (ii) 4-chloro-1-ethyl-1H-pyrazole-5-carboxylic acid, HATU, DIPEA, DMF, r.t., 16 h, 75%.

3.3.3. Biological assessment

The biological data for the hits **72** and **73** collected in-house are presented in Figure 3.4. The original hit **72** was biologically active and inhibited BLM with an IC₅₀ of 31 μM in the primary screening assay. No biochemical or biophysical assay had yet been developed for orthogonal confirmation, although counter-screening showed the compound did not aggregate or bind DNA, nor did it compete with ATP for binding. However, **73** did not demonstrate any BLM inhibition in the unwinding assay despite showing 10-fold more potency than **72** in the BLM qHTS [AID2528].

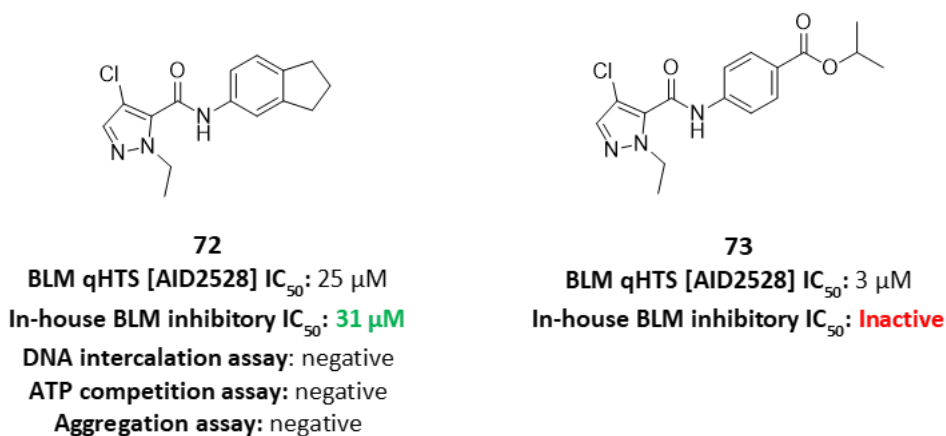


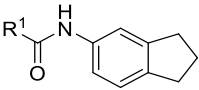
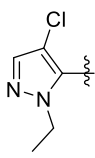
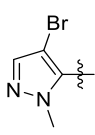
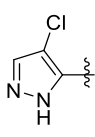
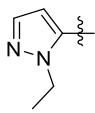
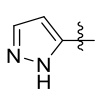
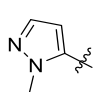
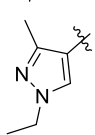
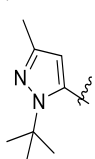
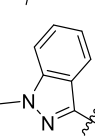
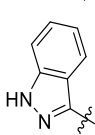
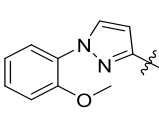
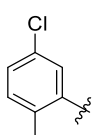
Figure 3.4. Biological data of **72** and **73**.

Various analogues of **72** were then synthesised to investigate the tractability of Series B through SAR studies. A flat SAR profile is suggestive of a non-specific mechanism of inhibiting DNA unwinding, while no SAR is indicative of a singleton and the hit may even be a PAINS compound.

In addition to those presented in Table 3.4, various compounds were synthesised in-house by Mr Kamlesh Bala, for which biological results are also available (Table 3.5). SAR probing occurred on the pyrazole moiety and all analogues of **72** were inactive in the BLM fluorescence quenching DNA unwinding assay.

Removal of the chloro (**76**), *N*-ethyl (**75**) and both (**7**) substituents resulted in no BLM inhibition. Other analogues of the pyrazole-3-carboxamide core (**74**, **79**, **81**, **82**, **83** and **84**) also showed no BLM activity. The same outcome occurred for the pyrazole-4-carboxamide **80** and phenyl **85**.

Table 3.5. Primary assay screening data of Series B.

<div style="text-align: center;">  </div>		
Compound	R ¹	BLM IC ₅₀ (μM)
72		31 ± 11 ^a
74		Inactive
75		Inactive
76		Inactive
78		Inactive
79		Inactive
80		Inactive
81		Inactive
82		Inactive
83		Inactive
84		Inactive
85		Inactive

^a n = 4

3.4. Series C hit validation

3.4.1. Rationale

CID2142222 (**86**) and CID2323972 (**87**) (Table 3.6) are isoquinolones that were reported as actives in the BLM qHTS assay with respective IC₅₀ values of 28 μ M and 31 μ M (Table 3.2). The fragment-like properties and good selectivity profile of this series made it a potential hit-like series for in-house assessment. The compounds were not available for commercial purchase and therefore needed to be synthesised to confirm BLM inhibition. The proposed synthetic route was a one-step synthesis which meant analogues could be synthesised in a relatively straightforward manner to aid determination of an initial SAR profile.

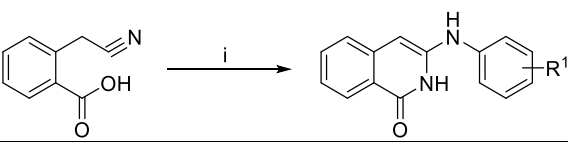
Table 3.6. Calculated physicochemical properties and reported biological data of Series C.

#	PubChem CID	Physicochemical properties				Pubchem Bioassay			
		MW	clogP	HBD	HBA	BLM qHTS 2528	WRN qHTS 651768	RECQ1 qHTS 2549	Bioactivity profile (active/tested)
86	2142222	254	3.4	2	3	28	Inactive	Inactive	78/ 833
87	2323972	254	3.0	2	3	31	Inactive	Inactive	75/812

3.4.2. Synthesis

Synthesis of analogues of compounds **86–90** proceeded through the introduction of various anilines into a reaction with 2-cyanomethylbenzoic acid to obtain different 3-arylamino-1,2-dihydro-1-isoquinolones (Table 3.7).²³⁹ The yields ranged from 3–36%. In all cases, observations by LCMS-LCQ revealed the reactions went mostly to completion. Purification by crystallisation in acetic acid resulted in the loss of a large amount of compound. As only small quantities were required for biological testing, no attempts were made to recover compounds remaining in solvent. ¹H-NMR exhibits signals of two NH protons illustrating the compounds are in the isoquinolone form rather than the isomeric isoquinolinols.

Table 3.7. Reagents and conditions: (i) chlorobenzene, 130 °C, 6 h.

		
Compound	R ¹	Yield (%)
86	2-CH ₃	3
87	4-F	3
88	3-Br, 4-Br	36
89	3-CF ₃ , 4-F	4
90	3-CN, 4-Br	11

3.4.3. Biological assessment

The synthesised HTS hits **86** and **87** showed no BLM inhibition in the fluorescence quenching assay (Table 3.8). Analogues **88–90** also did not inhibit BLM.

Table 3.8. Primary assay screening data of Series C.

Compound	BLM IC ₅₀ (μM)
86	Inactive
87	Inactive
88	Inactive
89	Inactive
90	Inactive

3.5. Series A hit confirmation

3.5.1. Rationale

CID5309875, also known as 2-(4-methoxyphenyl)-3-oxo-1H-isoindole-4-carboxylic acid (**91**) (Figure 3.5) is composed of an isoindolinone scaffold with a carboxylic acid at the 4-position and a *N*-substituted *para*-methoxy group. The low molecular weight (282 Da), clogP (2.2) and hydrogen bond donor and acceptor count qualify **91** as a fragment-like compound, which is advantageous because it allows structural growth without impacting the drug-likeness of the compound. The core contains two distinct synthetic handles available for SAR exploration: the carboxylic acid, and the nitrogen of the lactam ring. Series A also contained compound **92** (Figure 3.5), an isoindolinone analogue of **91**.

Isoindolinones are found in many natural products and have been associated with various biological activities,²⁴⁰ but the isoindolinone core is still unique in drug discovery with recent interest centred around its use as an inhibitor of the MDM2-p53 protein-protein interaction.²⁴¹ However, the construction of this core usually requires metal catalysts or inflexible multistep synthesis.²⁴⁰

91 was reported to have activity of 16 μM in the BLM qHTS assay [AID2528]. This compound was commercially sourced and biologically assessed by the in-house BLM DNA unwinding assay where its inhibitory activity was confirmed with an IC_{50} of 40 μM . Both the in-house and reported IC_{50} values were within a 3-fold range so were deemed to be in agreement. The isoindolinone analogue **92** was also active in the BLM qHTS screen with an IC_{50} of 18 μM . The additional 166 Da molecular weight did not significantly contribute to any increased activity, suggesting flat SAR in the region extending of the amide bond. **92** was also commercially sourced and its IC_{50} was determined to be 27 μM in-house. The use of counter-screen assays confirmed both compounds did not show off-target activity through alternative mechanisms such as DNA intercalation and protein aggregation. Series A also did not compete with ATP binding, which is a desirable feature of a human helicase inhibitor.

The PubChem Bioassay analysis tool has shown that **91** inhibits WRN and RECQ1 with a similar activity profile (Table 3.2). There is therefore a possibility that Series A compounds have pan RecQ helicase inhibitory properties, which could be of interest as a probe given its novelty. But a wider look at their biological screening profile reveals **91** was active in 34 out of 840 assays (4% hit rate) while **92** was active in 44 out of 866 assays (5% hit rate), which suggests these compounds are not inherently promiscuous otherwise a larger hit rate would be expected. Overall, the poor RECQ selectivity had meant Series A was given lower priority but was of interest for follow-up given its in-house confirmatory activity, unique core and fragment-like properties. Therefore, to

confirm this series as a potential hit it was necessary to resynthesise these compounds in-house.

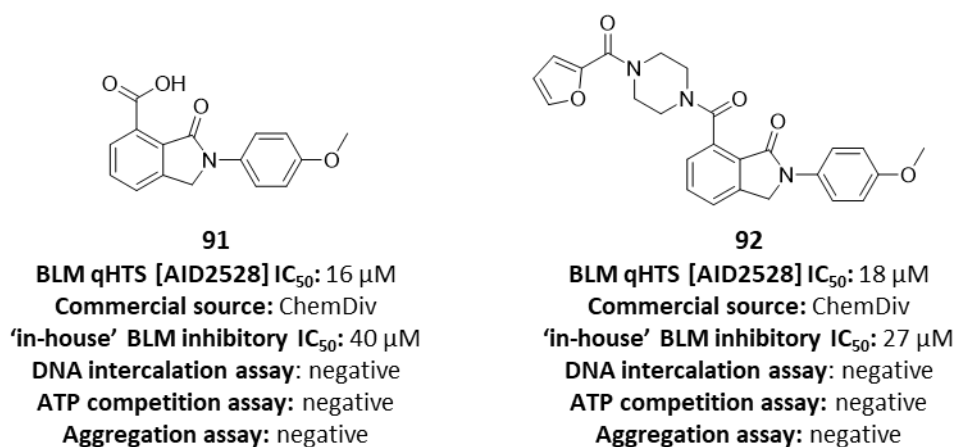
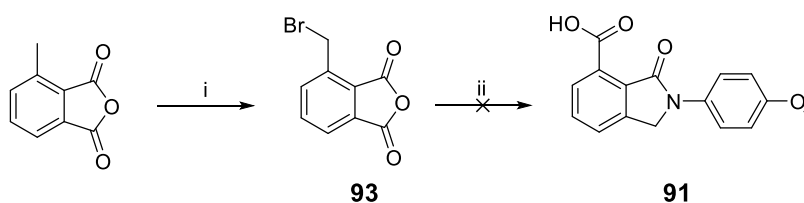


Figure 3.5. Biological data of **91** and **92**.

3.5.2. Synthesis

Initial synthesis of isoindolinone **91** began with commercially available 3-methylphthalic anhydride which was brominated with *N*-bromosuccinimide (NBS) in the presence of azobisisobutyronitrile (AIBN) to yield **93** (Scheme 3.2). This was followed by cyclisation with *p*-anisidine by refluxing in ethanol in the presence of potassium bicarbonate which was expected to produce compound **91** following a literature preparation where 4-benzyloxylaniline was used for cyclisation.²⁴²



Scheme 3.2. Reagents and conditions: (i) NBS, AIBN, MeCN, reflux, 16 h, 56%. (ii) *p*-anisidine, K₂CO₃, EtOH, reflux, 1–24 h.

Capelli showed through crystallographic structures that these conditions for 45 minutes can give various products depending on the aniline used, namely the isoindolinone and a carboximide (Figure 3.6).²⁴² Initially, running the reaction for 1 hour led to the isolation of a compound which was not a carboxylic acid and was likely to be the *N*-substituted product (Figure 3.6). This isolated compound was presumed not to be a carboxylic acid as the work-up extracted the compound into the organic layer and then

purification occurred on silica in relatively non-polar conditions. Figure 3.7 shows that allowing the reaction to run for 3 hours gave four peaks corresponding to the expected mass of the desired isoindolinone. Having later formed and isolated the desired isoindolinone through other protocols, it became clear that the first peak (retention time = 0.85 min) represented the desired product **91**. The remaining peaks represented other regioisomers, such as those in Figure 3.6. These side products were likely to be carboxylic acid derivatives because they were present as impurities when attempts were made to isolate **91** through an acidic work up.

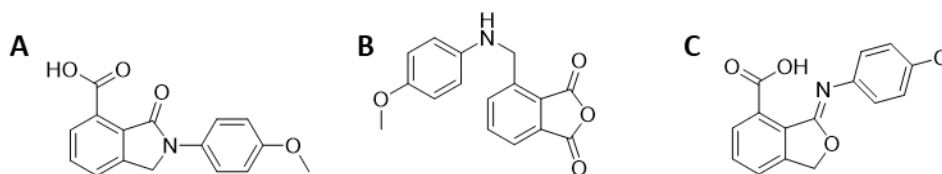


Figure 3.6. Potential products in cyclisation of isoindolinone synthesis via anhydride.

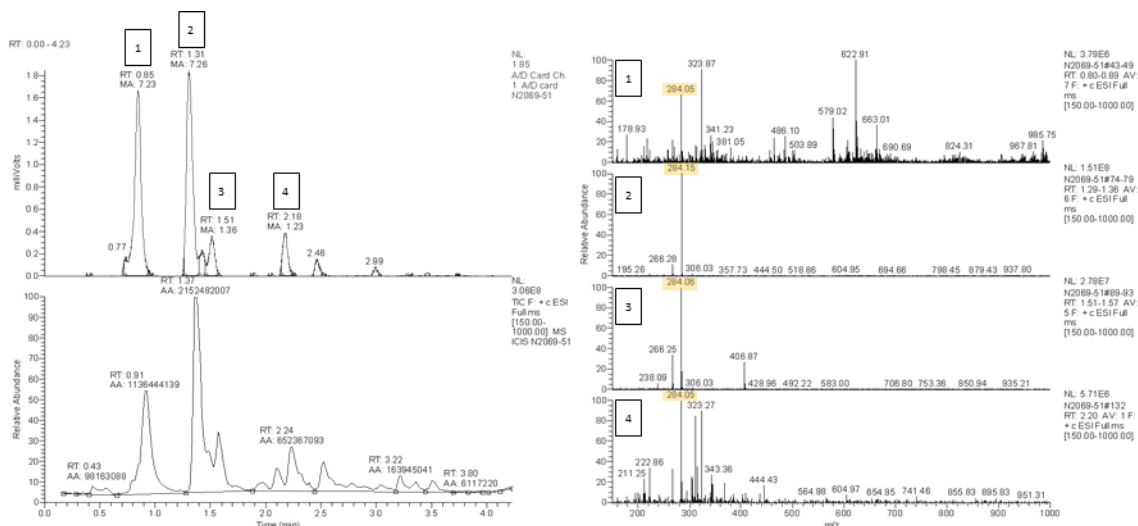
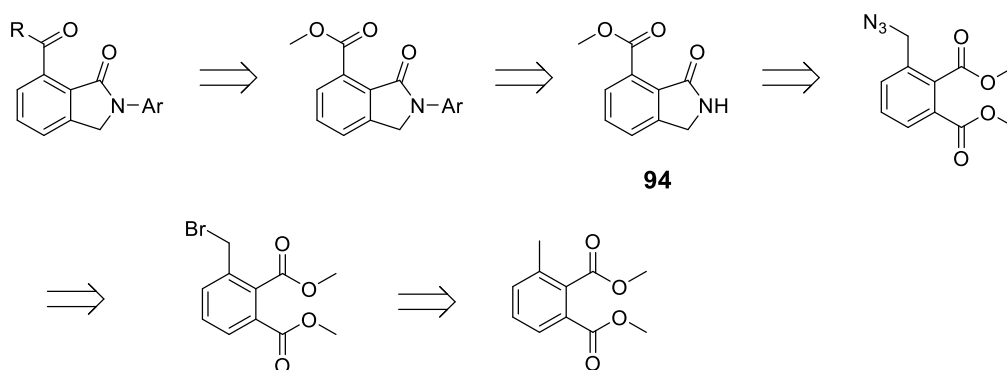


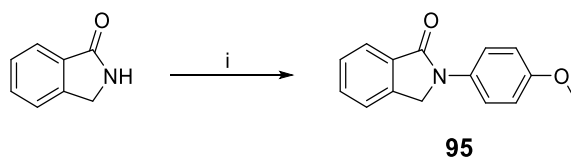
Figure 3.7. LCMS-LCQ of attempted formation of **91** (Scheme 3.4) shows four peaks corresponding to the same mass.

An alternative method to make **91** was via key intermediate **94** (Scheme 3.3), resulting in two accessible synthetic handles which would enable efficient SAR probing if required. The multistep route required the reduction of an azide to form an amine, which then cyclised *in situ* to the isoindolinone core **94** as described in the literature.²⁴³



Scheme 3.3. Retrosynthetic analysis of **91** and **92** via key isoindolinone intermediate **94**.

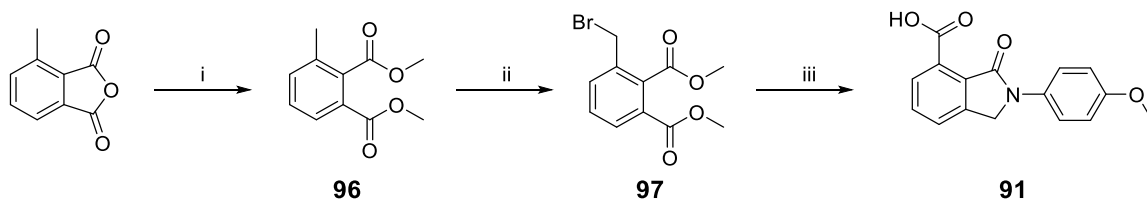
To assess the viability of this route, **95** was synthesised by the only Ullman coupling conditions available for this core in the literature.²⁴⁴ While Buchwald coupling conditions failed here, Ullman coupling worked well with good yields (Scheme 3.4) suggesting it would be possible to utilise this synthesis for late stage exploration of *N*-aryl functionalities.



Scheme 3.4. Test reaction to assess viability of proposed retrosynthesis in Scheme 3.3. (i) CuI, *trans*-*N,N'*-dimethylcyclohexane-1,2-diamine, toluene, 110 °C, 16 h, 70%.

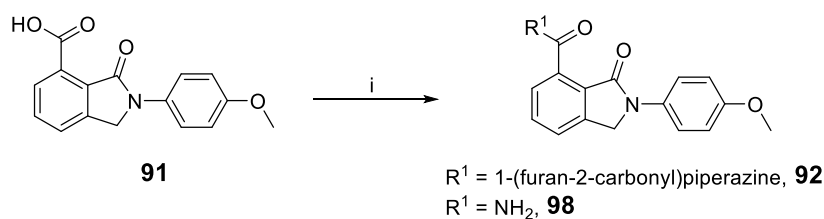
Synthesis began with 3-methylphthalic anhydride which was converted to the bis methyl ester **96** in the presence of concentrated sulphuric acid and methanol (Scheme 3.5). Treatment of **96** with NBS in acetonitrile with AIBN as a catalyst afforded the benzyl bromide **97**. In order to resynthesise **91** for hit confirmation, Capelli's conditions (described above) were attempted on the bis methyl ester **97**. Reflux of **97** in ethanol with potassium carbonate on this occasion resulted in the formation of the methyl ester of compound **91**. However, the weakly basic conditions did cause some hydrolysis resulting in a small amount of **91** forming in the crude reaction mixture. The reaction was therefore stopped after 2 hours and addition of 2 M sodium hydroxide allowed completion of hydrolysis to produce the desired carboxylic acid **91**. On this occasion, no other peaks with the appropriate mass were observed by LCMS-LCQ. Capelli found that isoindolinone carboxylic acid proton showed an unexpected strong intramolecular hydrogen-bonding interaction between the acid proton and lactam carbonyl which caused the acid proton peak to resonate at 15.5–15.7 ppm for their compound.²⁴²

^1H -NMR of **91** showed a broad singlet peak between 15–16 ppm, in strong agreement with this observation. Capelli *et al.* also found that the acid proton of the carboxyimide compound interacted strongly with the imide nitrogen by a peak seen at approximately 19 ppm, which was not observed for this compound when analysed in-house. Furthermore, the ^1H -NMR of **91** is consistent with literature data for this compound (see Experimental).



Scheme 3.5. Synthesis of isoindolinone 61. Reagents and conditions: (i) MeOH, H_2SO_4 , reflux, 3 d, 81%; (ii) NBS, AIBN, MeCN, reflux, 16 h, 76%; (iii) (a) *p*-anisidine, K_2CO_3 , EtOH, reflux, 2 h, then (b) 2 M NaOH, reflux, 1 h, 73% over 2 steps.

Compound **91** then underwent amide coupling with EDCI in the presence of HOBT and the amine 1-(furan-2-carbonyl)piperazine to form the second hit of this series **92** (Scheme 3.6). The same coupling conditions with methanolic ammonia gave the primary amide **98**. Again, strong intramolecular hydrogen bonding could be seen in the ^1H -NMR where the amide protons resonated at 7.7 and 10.2 ppm, a difference of approximately 2.5 ppm.



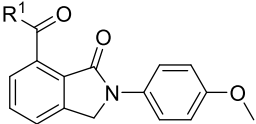
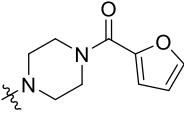
Scheme 3.6. Reagents and conditions: (i) 2 M NH_3 in MeOH or 1-(furan-2-carbonyl)piperazine, EDCI, HOBT, DIPEA, DMF, r.t., 16 h: (**92**, 79%; **98**, 53%).

3.5.3. Biological assessment

The activity data for BLM inhibitors based on CID5309875 (**91**) are presented in Table 3.9. Commercially-sourced **91** and **92** demonstrated activity in the BLM unwinding assay consistent with that in the BLM qHTS [AID2528], although both compounds were found to be inactive when synthesised in-house. The primary amide analogue **98** also showed no BLM inhibition, as expected given the inactivity of **91**.

Two LCMS analytical techniques (MDAP and LCQ) were used to assess commercially prepared **91** and **92** and no indication of a UV or ionisable impurity was observed. A similar LCMS-MDAP profile was observed for compounds prepared in-house.

Table 3.9. Primary assay screening data series A.

		
Compound	R ¹	BLM IC ₅₀ (μM)
91	H	Inactive
92		Inactive
98	NH ₂	Inactive

3.6. Series G hit confirmation

3.6.1. Rationale

CID 5299021, known as *N*-(2-methyl-5-sulfamoyl-phenyl)-4-(2-methylthiazol-4-yl)benzamide (**99**) was a qHTS hit against BLM with a reported IC₅₀ of 7 μM (Figure 3.8). Unlike most of the hits described in this chapter, **99** is not a fragment. The high MW, HBA count and calculated tPSA (Figure 3.8) indicates the compound does not conform to a lead-like compound.

PubChem Bioassay shows **99** was inactive against WRN but has not been tested against RECQ1 (Figure 3.8). Selectivity against WRN helicase is of real significance due to the close homology between BLM and WRN helicase as a good chemical probe will be selective against closely related proteins. A wider look at the biological screening profile of this compound reveals that **99** has been considered an active in 7 out of 530 assays, suggesting a good selectivity profile.

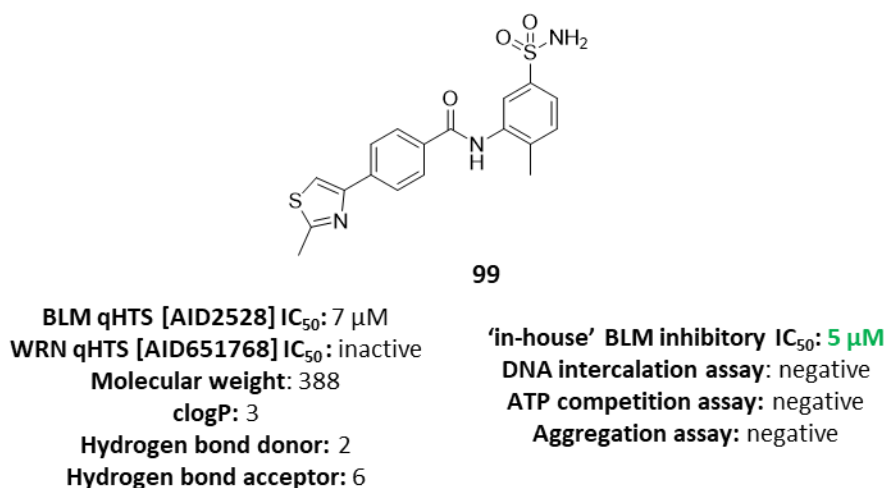


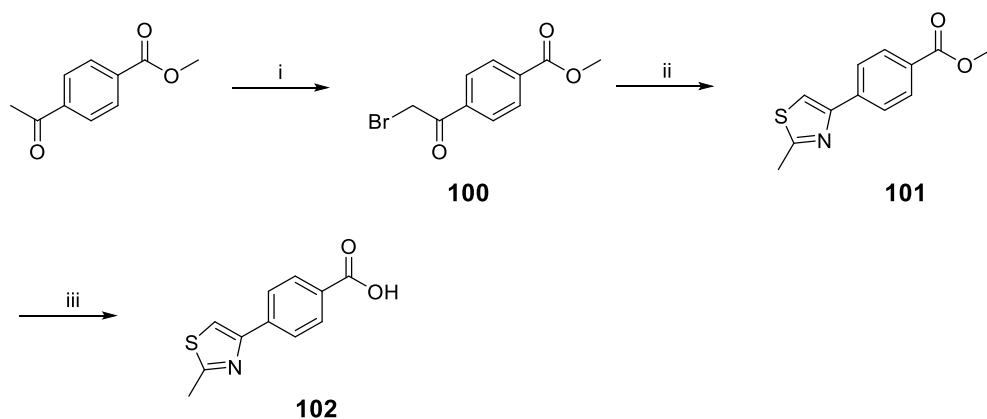
Figure 3.8. Biological data of **99**.

Commercially sourced **99** was confirmed to inhibit BLM helicase with an IC₅₀ of 7 μM when tested in-house. Counter-screen assays confirmed both compounds do not demonstrate activity through alternative mechanisms such as DNA intercalation and protein aggregation. This inhibitor also did not compete with ATP-binding.

It was important to then confirm Series G as a genuine hit in our screen through resynthesis of **99**. Once activity was confirmed, an initial and brief SAR profile was established.

3.6.2. Synthesis

Synthesis of amide **99** required the key acid intermediate **102**, which was synthesised on a relatively larger scale following the sequence described in Scheme 3.7. Bromination of the enol of methyl 4-acetylbenzoate in acidic conditions afforded **100** in 82% yield. Thioacetamide in DMF left overnight allowed cyclisation to proceed via the Hantzsch thiazole synthesis to afford **101** in good yield. Key intermediate **102** was then produced from basic hydrolysis of methyl ester **101**.

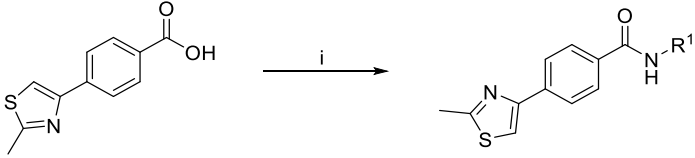
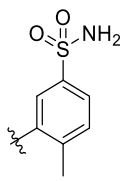
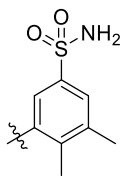
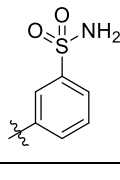
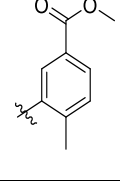
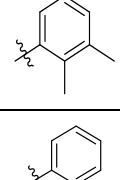
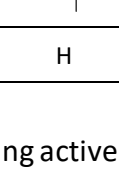


Scheme 3.7. Reagents and conditions: (i) NBS, *p*TsOH, 80 °C, MeCN, 82%; (ii) thioacetamide, DMF, 16 h, r.t., 73%; (iii) NaOH, H₂O/MeOH, r.t., 84%.

The initial amide conditions for production of the HTS hit **99** from carboxylic acid **102** used the amide coupling reagent HATU with DIPEA in DMF (Table 3.10). The reaction failed to go to completion, even on addition of further amine substrate, heating to 50 °C and running the reaction for 2 days. Exchanging HATU with HBTU produced the same result, but on this occasion the compound was isolated in low yields of 7% once purification conditions for **99** had been optimised.

As compound **99** demonstrated activity against BLM, various analogues were synthesised based on the in-house availability of starting material with a view to probe the existence of SAR. Compound **103** was also synthesised from the same HBTU conditions described above for **99** with similar yields (Table 3.10). Both HATU and HBTU conditions showed poor conversion for alternative substrates (data not shown) and were not looked at further.

Table 3.10. Optimisation of amide coupling conditions of carboxylic acid **102 using various anilines.**
Reagents and conditions: (i) HATU, DIPEA, DMF, r.t. – 50 °C, 2 d (ii) HBTU, DIPEA, DMF, r.t., 2 d; (iii) EDCI, HOBT, DIPEA, DMF, r.t., 16 h; (iv) EDCI, HOBT, 4-methylmorpholine, DMF, r.t., 16 h; (v) PCl₃, THF, 150 °C, MW, 15 min; (vi) T3P, Et₃N, DMF, r.t., 16 h; (vii) (a) oxalyl chloride, cat. DMF, DCM, r.t., 16 h, then (b) DCM, 2 h.

			
Compound	R ₁	Coupling conditions	Yield (%)
99		i	0
		ii	7
103		ii	7
		vii	16
104		v	0
		iv	32
105		i	0
		iv	11
		v	65
106		vi	-
		vii	45
107		vii	32
108	H	vii	24

Because Series G was producing active compounds, an effective amide coupling method was required to enable exploration of the aniline ring (right side aromatic ring). Accordingly, various coupling methods were employed to produce the remaining targets and the results are presented in Table 3.10. T3P coupling with various anilines failed to show any conversion. EDCI coupling with HOBT with DIPEA produced a low yield of compound **105** but failed for other anilines. Changing the base to 4-methylmorpholine

did produce compound **104**, however, the method was not transferable to other compounds in the series. Microwave-assisted phosphorous trichloride coupling,²⁴⁵ usually appropriate for electron poor anilines, successfully produced the methyl ester compound **104**, but again the method was not transferable across the series.

Acyl chloride formation with thionyl chloride in neat pyridine was not successful due to formation of a large amount of side product, which eventually resulted in a small conversion to the desired amide that proved difficult to isolate. Ultimately, acid chloride formation via the Vilsmeier reagent forming conditions of oxalyl chloride/DMF in DCM left overnight produced the acid chloride in high conversion. The reaction was optimised to a one-pot formation of amides in DCM to allow the synthesis of various analogues of **99** (Table 3.10).

3.6.3. Biological assessment

Data for BLM inhibitors of Series G are presented in Table 3.11. An IC₅₀ of 11 µM was determined for the resynthesised original hit **99** following biological analysis in the primary screening assay. No orthogonal biochemical or biophysical assay had yet been developed.

Various analogues were then synthesised to probe SAR and evaluate the tractability of this series. Addition of a methyl at the 3-position of the benzylcarboxamide (**103**) caused BLM inhibition to increase by 3-fold. However, removal of the methyl at 2- position of this aniline ring (**104**) resulted in loss of activity for the entire series. It was also shown that replacement of the sulphonamide with a methyl ester (**105**) retained potency against BLM. Furthermore, complete removal of the sulphonamide (compounds **106** and **108**) from compound **103** and **99**, respectively, only resulted a 2–3-fold reduction in activity. Complete removal of the amino aryl ring (**108**) resulted in no BLM inhibition observed in the primary screening assay.

Table 3.11. Primary assay screening data of Series G.

Compound	BLM IC ₅₀ (μM)
99	11
103	3
104	Inactive
105	13
106	6
107	30
108	Inactive

3.7. Discussion

3.7.1. Hit identification

High-throughput screening has become a much-favoured approach to discover biologically active compounds. The process involves rapidly screening tens to hundreds of thousands of compounds against a protein target to identify potential biological modulators. However, HTS libraries of such a size will inevitably contain a considerable amount of chemical matter that has little potential of being developed into drugs. Given that resources are often limited, particularly in academia, it is the role of medicinal chemists to triage HTS actives in order to direct the best use of such finite resources.

An informed triage strategy is essential for a successful HTS hit identification campaign.²³¹ Triage, when used in a hospital setting, determines the priority of a patient's treatment based on the severity of their condition. Originating from the battlefield, the term was used to classify soldiers who were likely to live, likely to die and those for whom immediate care could result in a positive outcome. Similarly, in HTS and hit identification, triage involves the classification and/or prioritisation of hits into those that can be further investigated, those that will not succeed as drugs or probes, and those that may succeed but would require intervention. Such processes are not an exact science but do require knowledge-based processes and medicinal chemistry experience. The work described in this chapter is the triage of HTS active compounds to identify chemical entities for a hit-to-lead program. This 'post-HTS workflow', using publicly available data, was designed to efficiently and rigorously eliminate compounds with

undesirable properties and was primarily focussed on the chemical properties of the hit matter over their activity profile.

Human helicases are a novel target class in drug discovery which make any hit identification campaign more of a challenge. Published crystal structures for BLM helicase do exist, but there are still many caveats to using a rational drug design philosophy or a virtual HTS. For instance, targeting the ATP-binding site would likely produce non-selective inhibitors for which there is no guarantee of potency, because unlike kinase inhibitors, there is no evidence for specific residues within the ATP site that would enable strong binding. Furthermore, it would be difficult to target a pocket in the nucleic acid binding site that would firstly, result in BLM inhibition, and secondly, bind with high affinity in such a polar site. Because of the limited target knowledge around helicases, HTS represents the most versatile powerful tool to discover inhibitors with novel binding mechanisms.

HTS facilities are rare in most academic drug discovery groups and often collaboration with industry is required. At the beginning of this study, the projected timeframe to run such a screen was over a year. Fortunately, more immediate methods to obtain chemical matter do exist. In particular, using known compounds from reported screens against the target of interest. Such data was publicly available for BLM helicase in PubChem. The qHTS screen [AID2528] of the MLSMR 355,000-compound library provided an opportunity to identify new hits from the resulting 672 actives. The data available also included a confirmatory assay using the same assay format to reassess 222 hits [AID2585] of which 85 were classed as active and another 83 as inconclusive. It was not clear why some results were classed as inconclusive and so the dose-response curves for these compounds were manually assessed. Hits were analysed from the original screen [AID2528] rather than the confirmatory screen [AID2528] because the probe reports did not reveal why only 222 out of 672 hits were chosen for the confirmatory screen. Some triage probably occurred but was not described in great detail. Accordingly, an in-house triage of the 672 hits was performed while the results of the confirmatory screen were used as justification for taking a series forward. Ultimately, all the series chosen for in-house assessment displayed activity in the BLM confirmatory assay [AID2585].

Chemical similarity is an important concept in drug discovery based on the principle that compounds with similar structures should exhibit similar biological activities.²⁴⁶ Defining chemical similarity in cheminformatics is a *known unknown* as there are no concrete definitions on describing whether compounds exhibit similarity.²⁴⁷ In this study, the initial clustering served as a 'net' to identify members from series of interest that may have been excluded by the subsequent screening processes. Whilst the eliminated compounds are not of interest for further development, if they share a core with a selected hit they can be useful for SAR studies and confirmation of series activity. For example, Series A originally included the inhibitor **72**. Revisiting the cluster of this compound revealed the hit **73** which was filtered out due to the ester metabolic liability. The addition of this second member to Series A would provide additional information during development of this series.

3.7.2. Cheminformatic analysis

Cheminformatic tools and methods enable the medicinal chemist to efficiently process and analyse large data sets.²⁴⁷ Despite increased investment in drug research and development activities, the attrition rates for small molecule drug candidates have remained largely the same. The emergence of HTS enabled the ability to generate large numbers of compounds with biological activity but have not significantly increased the number of new chemical entities.^{248,249} Contemporary drug discovery is thought to be focused too heavily on advancing leads with increased molecular weight and higher overall lipophilicity which then present challenges regarding toxicity, absorption and formulation.²⁵⁰ Defining physicochemical properties that predict long term viability of compounds began with Lipinski's³⁴ retrospective analysis of clinical candidates in addition to other formats that define boundaries of certain molecular physicochemical properties in order for compounds to conform to 'drug-likeness'.²⁴⁹ The physicochemical properties of a potential hit can be controlled which provides a reduced chance of attrition. In this study, the established parameters set out by Lipinski's 'rule of 5'³⁴ and Veber²³⁶ pertaining to oral bioavailability, referencing properties such as MW, clogP, HBA, HBD, and PSA, were calculated in Canvas and non-compliant compounds completely removed. The removal of 42% (292) of the library demonstrates that a

considerable proportion of BLM actives had poor calculated physicochemical properties. A recent analysis found that 25% of chemical matter in the MLSMR library (314,651 compounds in 2014)²³¹ did not meet REOS (rapid elimination of swill)²⁵¹ criteria. REOS uses physicochemical filters like Lipinski, but also includes over 200 functional group filters. The 42% of hits that were removed based on physicochemical properties alone is much higher than the amount of 'swill' in the MLSMR library, which could be because compounds with higher lipophilicity and molecular weight would generate enough potency to meet the 100 μ M threshold for a difficult-to-drug helicase. Other software exists to predict for properties such as toxicity^{252,253} and membrane permeability but they were not utilised here.

Compounds are generally more developable when they contain up to 3 aromatic rings and an increase in aromatic ring count decreases solubility and increases protein binding.²⁵⁴ Here, hits were not excluded based on aromatic ring count, but the count was considered during the cherry-picking process. Several binding indices, including ligand efficiency and lipophilic ligand efficiency, which relate physicochemical properties to potency, have also been introduced to guide medicinal chemists.^{255,256} Such indices would be more suitable for lead optimisation rather than hit selection in this study where compounds usually only vary by a log-fold in potency and are already limited by molecular weight parameters as only compounds below 500 Da were considered.

Large HTS libraries inevitably contain many compounds that have a small chance of being developed into drugs. To mitigate this occurrence, compounds with undesirable chemical structures which act as 'frequent hitters' or false positives — referred to as PAINS²³⁷ — are usually filtered out of HTS libraries. Many hundreds of these chemical scaffolds were described in a seminal paper by Baell and Holloway²³⁷ and were made available to the research community. There is consensus amongst medicinal chemists that compounds containing PAINS structures should be avoided in hit-to-lead programs.²³¹ However, many such structures still make their way into oncology studies despite widespread awareness of their reactivity. For example, the recently described WRN inhibitor NSC 19630 is a maleimide, a structure flagged as PAINS.¹²⁸

In this study, surprisingly, 300 compounds (75%) of the remaining actives were filtered out due to the compounds containing a PAINS or SMARTScreen feature. For example, catechols, quinones and hydroquinones were present in abundance, suggesting they may be protein-reactive compounds.²³⁷ Esters were part of the SMARTScreen filters (unlike the other substructure filters described in Table 3.1) so various compounds containing esters were removed as this group is a metabolic liability.

3.7.3. Manual triage

An analysis of the remaining 105 compounds was performed manually so resources could be focused on the most attractive remaining hits. Post-HTS triage requires both elimination of undesirable hits (e.g. poor physicochemical properties or false positives) and the prioritisation of promising hits. For the latter, the decision-making process may be more subjective, as it involves manual identification of 'drug-like' compounds. It has been proposed that pattern recognition is the forte of the medicinal chemists,²⁵⁷ who are capable of identifying drug-like compounds through their medicinal chemistry knowledge and experience. A study comparing the ability of chemists to assess drug-likeness revealed that chemists tend to agree on drug 'beauty' but are more inconsistent regarding 'ugly' compounds.²⁵⁸ In this study, cheminformatics was used to eliminate undesirable compounds while the skills of much more experienced medicinal chemists were used to prioritise promising hits. Chemical beauty is in the eye of the beholder and manual triage is expected to be influenced by personal biases. A different medicinal chemist may select a different final list of compounds for further analysis.

Compounds were deprioritised or eliminated during manual triage for reasons based on known chemistry principles. For example, various compounds with drug-like properties were assessed for their synthetic accessibility and tractability. Some hits required many steps (>5) for their synthesis or would require complex synthesis for SAR probing. Such compounds were not desirable in this project as they were beyond the capabilities of a single medicinal chemist. Therefore, by only allowing simple syntheses, a higher number of series could be assessed and taken forward. Compounds were also removed due to functionalities that were not identified during cheminformatic analysis. For instance, compounds with polycyclic structures and DNA base-like cores were removed on the

assumption that these compounds were likely binding in the DNA groove, which may be a non-selective site and difficult to drug given the high polarity of the pocket. Using PubChem data to identify bioassay promiscuity did not highly influence the selection process as the compounds that remained on the priority list were largely found to be active only in a small number of bioassays.

Also used during the cherry-picking process was the NIH HTS against RECQ1 and WRN helicase. In most cases, hits were progressed if they were selectively active against BLM, although additionally two of the selected hits were active against all three helicases. The rationale was that there would be an opportunity to develop a pan-RECQ family helicase inhibitor from the non-specific hits should development of a BLM inhibitor not be successful. Considering the priority of the project was to develop a tool compound, and that the RECQ helicase family plays an important role in DDR, a pan-RECQ helicase inhibitor would be highly beneficial for the research community. Other pan-family inhibitors of bromodomains have recently proven their significance, such as the pan-BET bromodomain inhibitor JQ1.²⁸ Overall, selection of the final 7 series from the 14 available clusters was largely heuristic and based on drug-likeness ('drug-beauty'), synthetic tractability and potential for chemical optimisation. Such processes are valid approaches to compound selection in HTS triage.

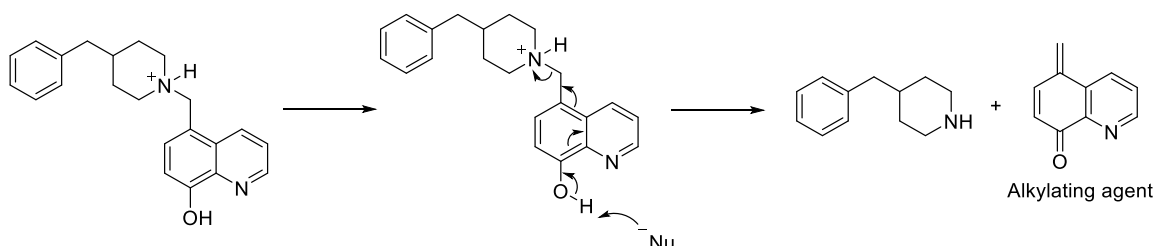
3.7.4. In-house biological data

Of the 7 series chosen for further investigation, 5 were available for commercial purchase and could therefore be tested promptly. At this stage, two series were identified as false positives. Both Series D and E did not demonstrate any activity against BLM helicase below 100 μ M. LCMS-MDAP of the compounds in these series showed sufficient purity (>90%). Therefore, it is possible these compounds displayed activity in the NIH screen through alternative mechanisms.

Compounds from Series A, F and G demonstrated activity, so these hits were resynthesised and retested to confirm biological activity against BLM helicase. Series F was a lower priority because although it was not flagged as a frequent hitter in the PubChem bioassay record, it contained the undesirable feature of a benzylamine para

to a phenol which could result in the amine being eliminated under assay conditions (Scheme 3.8). However, no promiscuous behaviour was noted for this Series F compound from WRN and RECQ qHTS data suggesting it may not be a PAINS.

Compounds from the successful series also underwent counter-screening and initial SAR probing while orthogonal assays were still under development. Counter-screens were used to identify whether any active compounds were assay artefacts caused by protein aggregation or DNA binding. Furthermore, selectivity for the ATP-binding site was studied to ensure ATP-binding site inhibitors were identified early, as these have less potential for development given the similarity of helicase ATP binding sites. No in-house counter-screens for protein selectivity were performed due to the resources not being available at the time. Furthermore, the PubChem bioassay record of this compound does not show it to be a frequent hitter in HTS assays. Therefore, the compound was still considered as a possible hit but of a lower priority.



Scheme 3.8. Proposed mechanism for Series F compound to form alkylating agent.

3.7.4.1. Series C

The isoquinolines based on the qHTS hit **86** and **87** were initially selected for in-house BLM inhibitory IC₅₀ determination because they conformed to the qualities expected of a lead-like compound and showed selective activity with two representative examples. The series was not available for commercial purchase and had to be synthesised in-house for biological evaluation. Analysis of the synthesised compound along with various analogues revealed the compounds did not demonstrate any inhibitory activity against BLM. Therefore, these hits were confirmed to be false positives from the qHTS and were not pursued further.

3.7.4.2. Series B

The qHTS hit (**72**) was identified as a fragment containing favourable features of a potential lead-like inhibitor of BLM helicase. The compound was synthesised in-house with straightforward amide coupling chemistry which confirmed the compound inhibited BLM with an IC₅₀ of 31 µM. Counter-screens showed this compound does not bind DNA, aggregate in the assay or quench the fluorescence signal. Orthogonal confirmation was not available at the time of study. Co-crystallisation trials with **72** were not successful.

In addition, the closely related analogue **73** was found to inhibit BLM with improved potency (4 µM) in the BLM qHTS [AID2528]. When **73** was synthesised, it was determined to be inactive against BLM, suggesting the compound was a false-positive. Consequently, Series B comprised only of the hit **72**.

Analogues of **72** were synthesised to investigate SAR. A series of small point changes as well as larger changes on the pyrazole ring resulted in 11 analogues with no activity against BLM. The purpose of the short SAR campaign was to generate active analogues and closely related inactive analogues which would place further confidence in the credibility of this series as BLM inhibitors in the absence of orthogonal and structural confirmation.

The synthesised hit **72** demonstrated BLM inhibition, lead-like properties and favourable results in the available counterscreens. However, because no SAR was established, further medicinal chemistry exploration was postponed, and Series B was considered a reserve in case no other series demonstrated hit-like properties.

3.7.4.3. Series A

The isoindolinone series based on the qHTS hit **91** was initially selected to assess in-house because it was a small fragment with lead-like properties. A problem identified early on was the poor selectivity between related RecQ helicases. Compound **91** and its analogue **92** were purchased and in-house assays showed both compounds to possess similar activity to that reported in the PubChem Bioassay database. LCMS-MDAP analysis of the compounds showed no signs of UV active or ionisable impurities in the

purchased compounds. Counter-screening on these batches also gave no indication of alternative mechanisms for activity against BLM helicase. However, resynthesised **91** and **92** showed no activity in the BLM helicase unwinding fluorescence-quenching assay. It is unknown why these compounds were flagged as hits in the original qHTS [AID2528], the confirmatory HTS [AID2585], and the in-house assay on the commercially supplied compounds. A probable explanation is the presence of some impurity, such as metals, which are not UV active and were present in commercially supplied compounds but not in the in-house synthesised compound. The series was therefore not taken forward for hit optimisation.

3.7.4.4. Series G

The qHTS hit **99** was identified as an inhibitor with favourable features for hit-to-lead development of a potent and selective BLM inhibitor. This hit displayed an IC_{50} of 7 μM in the BLM qHTS [AID2528], an in-house IC_{50} of 5 μM from commercial material, and 11 μM when the compound was resynthesised in-house. Such consistent biological data is supportive of **99** being a genuine BLM inhibitor.

The presence of an amide bond in this series presented a tractable disconnection for initial SAR investigations. Large quantities of the carboxylic acid derivative were synthesised to enable SAR investigations through amide coupling. However, such substrates were not amenable to the use of standard amide coupling reagents such as HATU, HBTU, T3P and EDCI/HOBt. It was found that the most versatile condition for this acid was via the acyl chloride derivative formed through the *in situ* generated Vilsmeier reagent.

SAR was investigated via changes on the aniline portion of the amide. The selected aniline moieties were selected on the basis of minor changes to the aniline ring and the in-house availability of substrates. The priority was synthesis of a small group of analogues of **99**, to investigate SAR and lend credibility to this hit. Therefore, the synthetic approach was primarily based on rapid production of the desired chemical target. Optimisation of various amide coupling reaction conditions were trialled against different substrates until reproducible conditions within the series were found.

Ultimately, the late stage diversification of the aniline moiety enabled efficient SAR probing and analogues of **99** were synthesised to assess SAR. The importance of the methyl at the 2-position of the carboxamide phenyl ring was established which indicated the presence of an activity cliff. Activity cliffs exist when pairs of compounds are highly similar but display IC₅₀ differences. In the case of **99** and **104**, the loss of a methyl group confers complete loss of BLM inhibitory activity. This is an important finding because a series possessing tractable SAR is suited to hit optimisation as it suggests that potent compounds can be designed through predictable modifications.

Other early SAR was also investigated. Addition of the 3-methyl (**103**) on the aniline portion resulted in a slight improvement to activity. Replacement of the sulphonamide with an ester or complete removal of the group itself resulted in no significant change in potency, suggesting the sulphonamide was easily replaceable. This finding is advantageous because sulphonamide groups may be classed as an undesirable functionality particularly due to reduced ability to permeate cells. Furthermore, it was also shown that replacing the sulphonamide with a bromine, an atom with a similar molecular weight, produced an inactive compound. Therefore, both the 3-position of the aniline moiety and the 5-position demonstrate SAR via small modifications.

Counter-screening of the hit **99** showed the compound did not aggregate, bind DNA, or cause fluorescence quenching in the absence of DNA. Adjusting the ATP concentrations in the primary screening assay had no effect, suggesting the inhibitor did not exert its effect by competing with ATP. Further, PubChem bioassay data has shown **99** is not active against the closely related WRN helicase and that its overall bioactivity profile is highly selective with only 7 actives in 544 assays.

The picture painted thus far reveals that Series G fulfils many of the requirements of a hit-to-lead candidate, therefore pursuing a hit optimisation campaign on this series to design and synthesise potent, selective BLM inhibitors with a drug-like physicochemical profile would be the best chance for success. While Series G does not possess the fragment-like qualities that others described in this chapter, it is the only series that demonstrates any tractable SAR which can enable synthesis of potent compounds. As a

result, the medicinal chemistry on this series will continue with a focus on understanding the SAR in the absence of orthogonal biological data and crystallographic information.

3.8. Conclusion

To identify starting points for the development of novel BLM inhibitors, a hit identification campaign was undertaken using the results of a NIH qHTS screen performed with the MLSMR compound set against BLM helicase and published in PubChem Bioassay. The screen of over 350,000 compounds resulted in 672 actives.

Several series of BLM helicase hits were produced via prioritisation of chemical matter through triaging potentially unfavourable compounds. This was accomplished by employing an array of cheminformatic filters to eliminate undesirable structures with non-lead-like physicochemical properties and promiscuous compounds such as PAINS. Such cheminformatic filters largely reduced the number of hits, highlighting that much of the active chemical matter did not satisfy criteria for drug-likeness. Further manual triaging isolated 7 series for which BLM IC_{50} values could be determined in-house. This process was largely heuristic and based on many factors including synthetic tractability, structural features, aromatic ring count and bioassay data.

Compounds were then commercially purchased and/or internally prepared to validate their activity in our in-house fluorescence quenching unwinding assay. Ideally, further confirmation would have occurred using orthogonal assays, but these were not available at the time. As a result, all hits validated in the primary assay were subject to counter-screens and initial SAR to aid confirmation of the respective series.

Compounds of Series C, D and E were shown to be inactive when tested in-house, therefore these series were not pursued further. Compounds of Series A were commercially sourced and validated in-house. However, further validation of these compounds by internal resynthesis failed, suggesting this series were false positives both in the HTS and internally, possibly due to impurities in the commercially prepared compounds. Accordingly, investigations on this series were discontinued. Compound **72** of series B was confirmed as a hit with similar IC_{50} values to the NIH qHTS screen, but its analogue **73** did not display any BLM inhibition. Furthermore, no SAR could be

ascertained following synthesis of a number of analogues. Series B was therefore deprioritised, despite having drug-like properties.

Ultimately, the most promising hit was compound **99** of series G, which successfully inhibited BLM when commercially sourced and also when internally resynthesised. Counter-screens on this series did not show these inhibitors worked by other mechanisms. When analogues were tested during the SAR studies, compound **103** was found to be highly active with an IC_{50} of 3 μ M — the most potent hit recorded in-house at the time. Therefore, it was decided that Series G would be investigated in greater depth from a medicinal chemistry standpoint to firstly, develop its SAR profile, and secondly, use this profile to improve compound potency.

To conclude, post-HTS triage of 672 actives from a NIH qHTS screen against BLM helicase resulted in the discovery of a potential hit **99** of Series G with lead-like properties. Investigative and optimisation studies of series G will continue in Chapter 4.

4. Series G Part One

4.1. Introduction

The development of a novel hit series targeting therapeutically relevant proteins is a challenge in the absence of structural or mechanistic binding data and typically consists of iterative SAR around the different parts of the hit molecule. Whilst the work described in Chapter 3 led to the identification of the novel hit **99**, the work described in this chapter focused on the development of this molecule into a probe-like compound. The discovery of a chemical probe targeting BLM is needed to enable further DDR research. Given the potential pharmacological consequences of BLM inhibition in DDR biochemistry, a compound with early lead-like properties would be valuable.

A chemical probe is a small molecule modulator of protein function that allows scientists to answer mechanistic and phenotypic questions about the molecular target in biochemical, cell based and animal studies.²⁶ Only high-quality molecular probes generate meaningful biological data. Although the properties of a defined probe are context dependent, properties such as potency, solubility, permeability and selectivity are generally important (Section 1.3). For example, the literature compound ML216, described in Chapter 2, would not be considered a high-quality probe, as it showed moderate potency, poor solubility, low permeability and bad selectivity.²⁰²

In advocating probes fit for purpose, Workman and Collins³² outlined fitness factors to assist in the discovery of high-quality chemical probes (Figure 1.3). Various criteria were proposed to ensure a BLM probe could meaningfully answer important biological questions (Table 4.1). Some parameter testing was not fully developed within the project timeframe or would only be considered once potency and solubility criteria were met. Therefore, the initial aim of this project was to develop a probe from hit **99** for use in experiments *in vitro*. As such the objective was to deliver inhibitors with IC₅₀ values against BLM helicase below 0.1 μ M and that additionally demonstrate aqueous thermodynamic solubility above 100 μ M.

Table 4.1. Proposed target properties for a chemical probe of BLM helicase.

Parameter	Target	Capabilities to assess criteria	Tested during PhD project?
Potency in biochemical assay	<0.1 μM	In-house DNA unwinding assay (Figure 1.13)	Yes
Solubility	>100 μM	In-house thermodynamic solubility	Yes
SAR and negative controls (inactive analogues)	Generate SARs and synthesise closely related inactive analogues	Synthesis described in this thesis	Yes
Permeability	Proven passive membrane permeability or defined active transport mechanisms	Outsourced at cost	No
Selectivity profile	>30-fold activity in closely related helicases	Biochemical assays for WRN and RECQ5 under development in-house	No
Potency in cellular studies	<10 μM in cell-based assays and proven target engagement	Cell-based assays under development in-house	No

4.1.1. Microscale thermophoresis (MST)

Microscale thermophoresis (MST) is an emerging technique based on the directed movement of molecules in a temperature gradient.²⁵⁹ Its highly sensitive nature in detecting changes in molecular properties makes it a powerful biophysical technique to quantify biomolecular interactions. Whilst the SAR exploration in this series, the development of an orthogonal biophysical assay by Ms Chen to characterise binding of BLM helicase with inhibitors was successful and confirmed various members of series G as BLM inhibitors. This represented the first example of MST experiments used to characterize biomolecular binding of a helicase to an inhibitor. Described in Section 3.6, **103** is an analogue of the original hit **99** which contains an additional methyl at the 3-position of the right side aniline ring and inhibited BLM with an IC_{50} of 3 μM in the biochemical DNA unwinding assay. The measured K_d for **103** using MST was 10 μM , a result consistent with the primary helicase unwinding assay (Figure 4.1). Interestingly, MST experiments demonstrated that the inhibitor binds to BLM helicase only in the presence of ssDNA. This suggests that a conformational change of the apo BLM, following exposure to ADP and DNA, is required for binding of the inhibitor. It is important to note that no binding is observed when the inhibitor is in the presence of

ssDNA without protein. The results of this experiment gave further confidence in the mode of action of Series G and emphasized the need to optimize both potency and chemical probe-like properties.

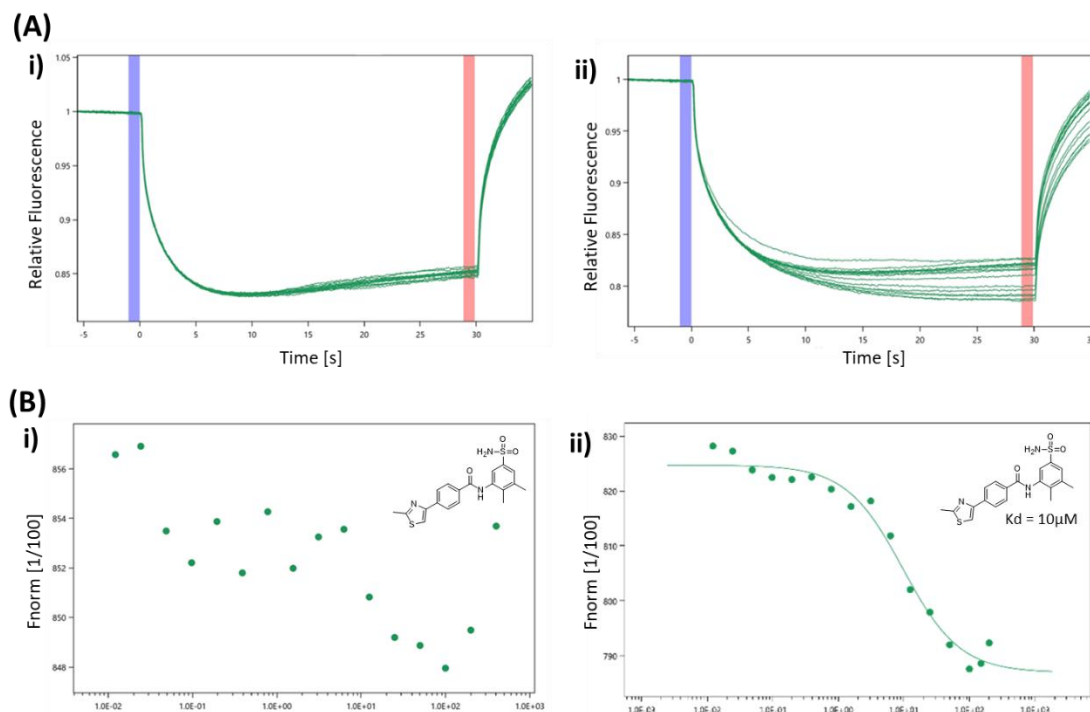


Figure 4.1. (A) MST thermogram of i) BLM, ATP and **103** and ii) BLM, ssDNA and **103**. (B) MST experimental binding curve of i) BLM, ATP and **103** ii) BLM, ssDNA and **103**. The obtained K_d for **103** was 10 μM . **103** has an activity of 3 μM in the DNA unwinding assay.

4.1.2. Aims

The aim of the work described in this chapter was to improve potency and the physicochemical properties through modification of the aniline ring of hit **99**. In order to achieve this objective, the following points were explored:

1. Design and synthesise a library of compounds exploring different substituents and substitution patterns around the aniline
2. Design and synthesise analogues with markedly improved physicochemical properties by the introduction of solubilising groups off the aniline ring.
3. Assess the impact of substituting the aniline with heterocycles on potency and physicochemical properties.

4.2. SAR studies of the aniline ring

4.2.1. Rationale

Preliminary hit optimisation efforts, described in Section 3.6, produced a small number of analogues of the hit **99** (Figure 4.2). The importance of the 2-methyl of the aniline ring in maintaining potency is demonstrated by compound **104**, whilst the addition of a 3-methyl results in a small potency gain as shown by compounds **103** and **106**. Furthermore, replacement of the sulphonamide group with a methyl ester did not lead to a reduction in potency. It was later shown that, complete removal of the bulky and polar sulphonamide group did not cause any significant loss of activity (Figure 4.2).

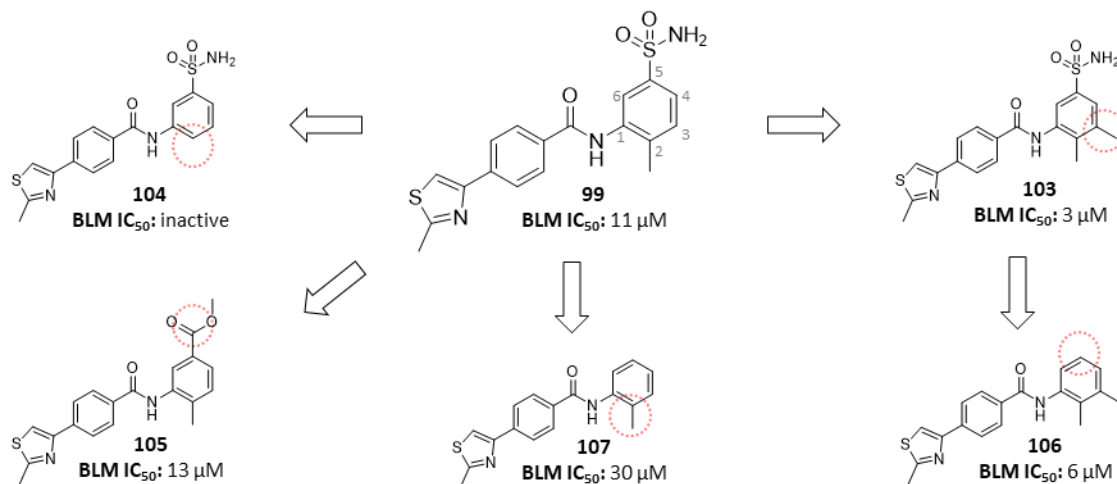


Figure 4.2. Preliminary SAR focussed on the aniline ring conducted on Series G during hit identification (See Section 3.6).

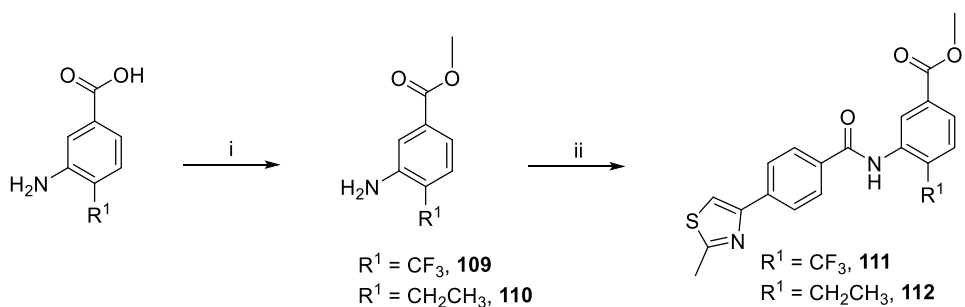
As modification of the aniline had demonstrated some positive and negative SARs, it was decided to conduct a broader SAR exploration around the peptidic bound. The presence of an amide bond allowed late stage diversification to introduce various amines. The selection of anilines used for the synthesis of Series G analogues largely focussed on commercially or in-house available anilines to assess the impact of point changes. Of the compounds discussed in this section, a considerable number were synthesised using widely applicable amide coupling conditions for carboxylic acid **102** which had been determined during the hit identification (Section 3.6.2). The primary amide forming conditions were *via* the acyl chloride of **102** from the Vilsmeier reagent forming conditions of oxalyl chloride/DMF (Table 4.2).

Table 4.2. Synthesis of analogues of 99 exploring changes to the aniline ring. *Reagents and Conditions:* (a) oxalyl chloride, *cat.* DMF, DCM, r.t., 16 h, then (b) DCM, 0.5–16 h.

Compound	R ¹	Yield (%)	Compound	R ¹	Yield (%)
113	2-CN	11	130	2-CH ₃ , 5-CH ₃	40
114	2-Cl, 3-CH ₃	7	131	2-CH ₃ , 5-Br	26
115	3-CH ₃	32	132	2-CH ₃ , 5-CF ₃	25
116		45	133	2-CH ₃ , 5-OH	35
117	2-CH ₃ , 3-OH	10	134	2-CH ₃ , 5-CN	24
118	2-CH ₃ , 3-Cl	17	135	2-CH ₃ , 5-OMe	46
119	2-CH ₃ , 3-CF ₃	46	136	2-CH ₃ , 5-F	10
122	2-CH ₃ , 4-CH ₃	11	137	2-CH ₃ , 6-OMe	20
124	2-CH ₃ , 4-Cl	17	138	2-CH ₃ , 6-CH ₃	28
125	2-CH ₃ , 5-CN	26			

4.2.2. Synthesis and SAR at the 2-position

The importance of the 2-methyl was initially demonstrated by compound **104** where its absence resulted in diminished activity. A selection of analogues were synthesised to draw further conclusions about the role of the methyl at the 2-position. Through the use of aminobenzoic acids, the impact of methyl replacement with the larger trifluoro and ethyl groups was explored (Scheme 4.1). To allow direct comparison with compound **105**, esterification with thionyl chloride and methanol of 3-amino-4-(trifluoromethyl)benzoic acid and 3-amino-4-ethylbenzoic acid produced the methyl esters **109** and **110**, respectively (Scheme 4.1). These amino benzoates underwent amide coupling to form **111** and **112**, respectively, under microwave-assisted PCl₃ conditions which had been successful for the synthesis of **105** (Section 3.6.2). In these instances, lower yields were observed as the reactions failed to go to completion.



Scheme 4.1. Reagents and conditions: (i) SOCl_2 , MeOH, r.t., 16 h: **109**, 84%; **110**, 87%; (ii) PCl_3 , THF/MeCN (3:2), 150 °C, MW, 15 min: **111**, 31%; **112**, 15%.

Replacement of the methyl group with a nitrile (**113**) and chloro (**114**) was also trialled and investigated. These analogues were synthesised from the acyl chloride precursor (Table 4.2). **115** was synthesised (Table 4.2) to understand if the 2-methyl group was still required in the presence of a methyl at the 3-position. Given that the 2,3-dimethyl substitution (**106**) displayed moderate potency, indane **116** was synthesised (Table 4.2) to explore whether these methyls could be further extended and cyclised in the form of an indane and if additional lipophilicity in this part of the molecule could lead to further gains in potency.

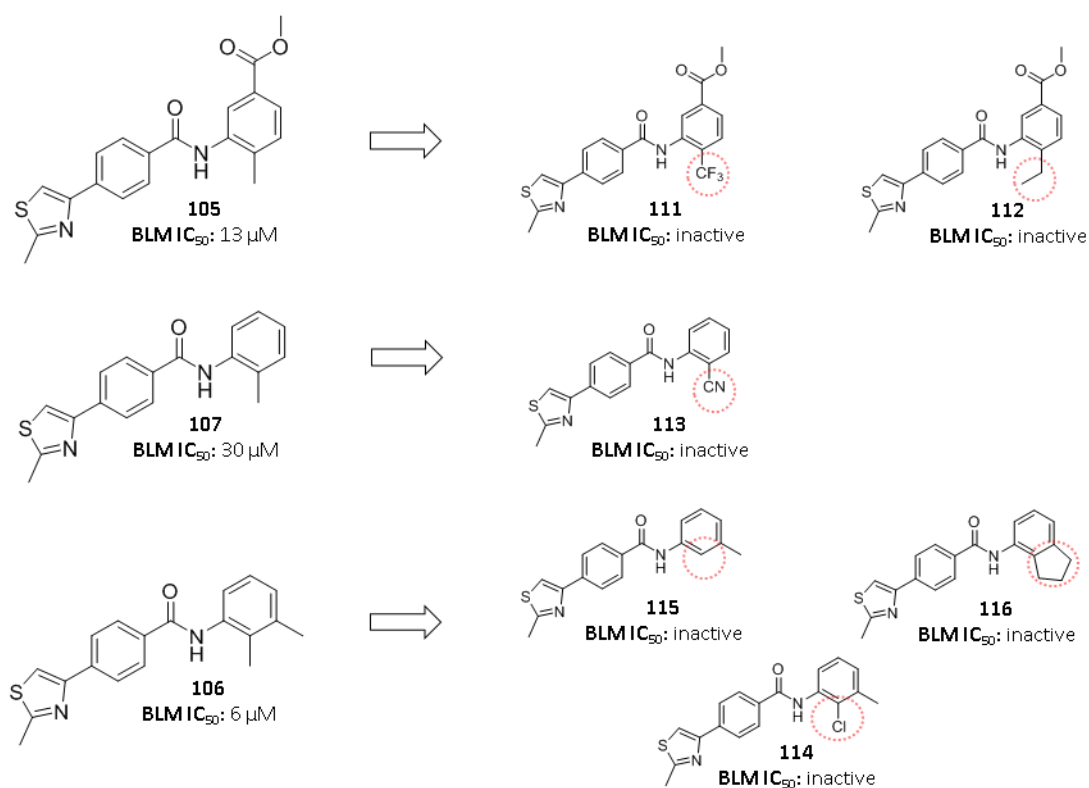


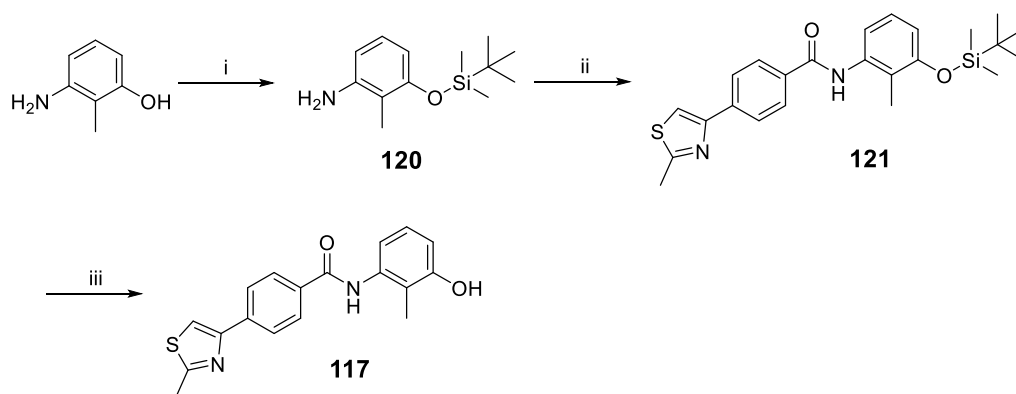
Figure 4.3. SAR pertaining to the replacement of the 2-methyl.

The BLM inhibitory activity data for compounds **111–116** are presented in Figure 4.3. In each case, there is diminished activity which highlights the importance of the methyl in the original hit (**99**). These results demonstrate that a methyl group is the preferred substituent at the 2-position of the phenyl ring.

4.2.2. Synthesis and SAR at the 3, 4, 5 and 6-position

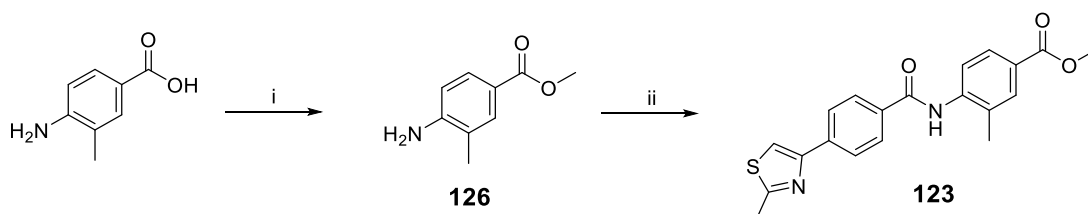
Since replacement the methyl at the 2-position of the aniline is not tolerated, it was decided to retain that group while investigating the SAR around the other positions of the ring. A variety of small 3-, 4-, 5- and 6-position substituents (e.g. methyl, chloro, hydroxyl, etc) were introduced on the 2-methylaniline motif to assess potential potency gains and develop an understanding of what position of the aniline could also be substituted. In broad terms, the aniline substrates undergoing amide coupling were chosen based on their in-house and commercial availability to grant a rapid and cost-effective SAR profile of Series G.

In addition to the initially explored 2,3-dimethyl **106**, substituents trialled at the 3-position included hydroxy (**117**), chloro (**118**) and trifluoro (**119**) which were synthesised from the acyl chloride precursor (Table 4.2). Larger amounts of the phenol derivative **117** were required for further biological testing, and on this occasion, amide coupling occurred following protection of the phenol. Isolation of **117** without protection of the hydroxyl group proceeded in poor yields (Table 4.2) because of the formation of various side-products caused by coupling of the phenol with the acid chloride substrate. Protection of 3-amino-2-methylphenol with a *tert*-butyldimethylsilyl (TBS) group was achieved in good yield in the presence of triethylamine and catalytic 4-(dimethylamino)pyridine (DMAP) (Scheme 4.2). The protected aniline **120** underwent amide coupling with **102** in high yield using HATU as the coupling reagent to produce **121** in good yield. This was followed by tetrabutylammonium fluoride (TBAF) deprotection to give **117**. This route allowed a scale-up of **117** and did not require any complicated purifications.



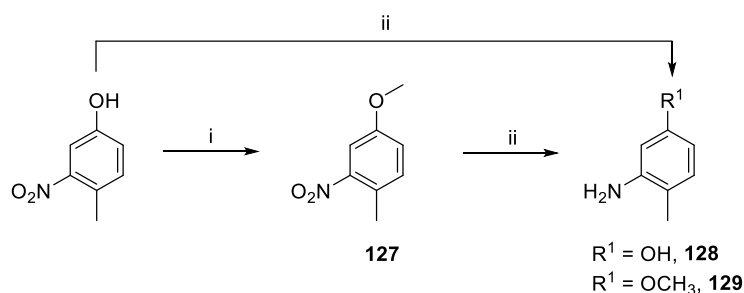
Scheme 4.2. Reagents and conditions: (i) TMSCl, DMAP, Et₃N, r.t., 18 h, 78%; (ii) **102**, HATU, DIPEA, DMF, r.t., 16 h, 90%; (ii) TBAF, THF, 0 °C, 5 min, then r.t., 10 min, 24%.

Similar substituents such as methyl (**122**), chloro (**125**) and nitrile (**124**) were introduced at the 4-position (Table 4.2). In order to assess the impact of shifting the methyl ester group from the 5-position (as in **105**) to the 4-position, esterification of 4-amino-3-methylbenzoic acid with thionyl chloride followed by microwave-assisted PCl₃ amide coupling afforded the analogue **123** (Scheme 4.3).



Scheme 4.3. Reagents and conditions: (i) SOCl₂, MeOH, r.t., 16 h, 85%; (ii) PCl₃, THF/MeCN (3:2), 150 °C, MW, 15 min, 30%.

The role of substituents at the 5-position was explored more thoroughly as early SAR knowledge of this series demonstrated that the bulkier sulphonamide and methyl ester groups were tolerated at this position. Again, small substituents with varying electronic effects were trialled (Figure 4.5). The precursor anilines of **133** and **135** (Table 4.2) were synthesised from 4-methyl-3-nitrophenol (Scheme 4.4). Methylation with iodomethane produced the methoxy derivative **127** in high yields, and along with 4-methyl-3-nitrophenol, was reduced in the presence of zinc/acetic acid to produce the desired aniline derivatives **128** and **129**, respectively (Scheme 4.4).



Scheme 4.4. Reagents and conditions: (i) MeI, NaOH, DMSO, r.t., 16 h, 90%; (ii) Zn, MeOH, AcOH, 50 °C, 1 h: **128**, 90%; **129**, 75%.

Substituents at the 6-position of the phenyl ring were explored to a lesser degree because the alternative *ortho* position was less tolerant and it was suspected that similar implications could be observed due to steric clashes and conformational consequences. The exploration included methyl (**137**) and methoxy (**138**) substituents (Table 4.2).

The broad SAR exploration carried out on the 3, 4, 5, and 6 positions of the aniline ring did not yield a more potent compound than **103**. The biological results of BLM inhibition presented in Figure 4.4 demonstrate that several substitution patterns can negatively affect the inhibitory activity but none of the explored substituents significantly enhanced activity. The movement of a methyl group around these positions (**106**, **122**, **130** and **138**) resulted in consistent BLM inhibitory effects between 3–6 μM . This was also the case for the other electron donating hydroxy (**117** and **133**) and methoxy (**135** and **137**) substituents at various positions. The addition of these substituents resulted in 5–10-fold increase in potency when compared to the mono-methyl analogue **107**. On the other hand, the electron-withdrawing substituents such as the nitrile, halogen and trifluoro groups were not tolerated with the exception of 3-chloro compound **118**.

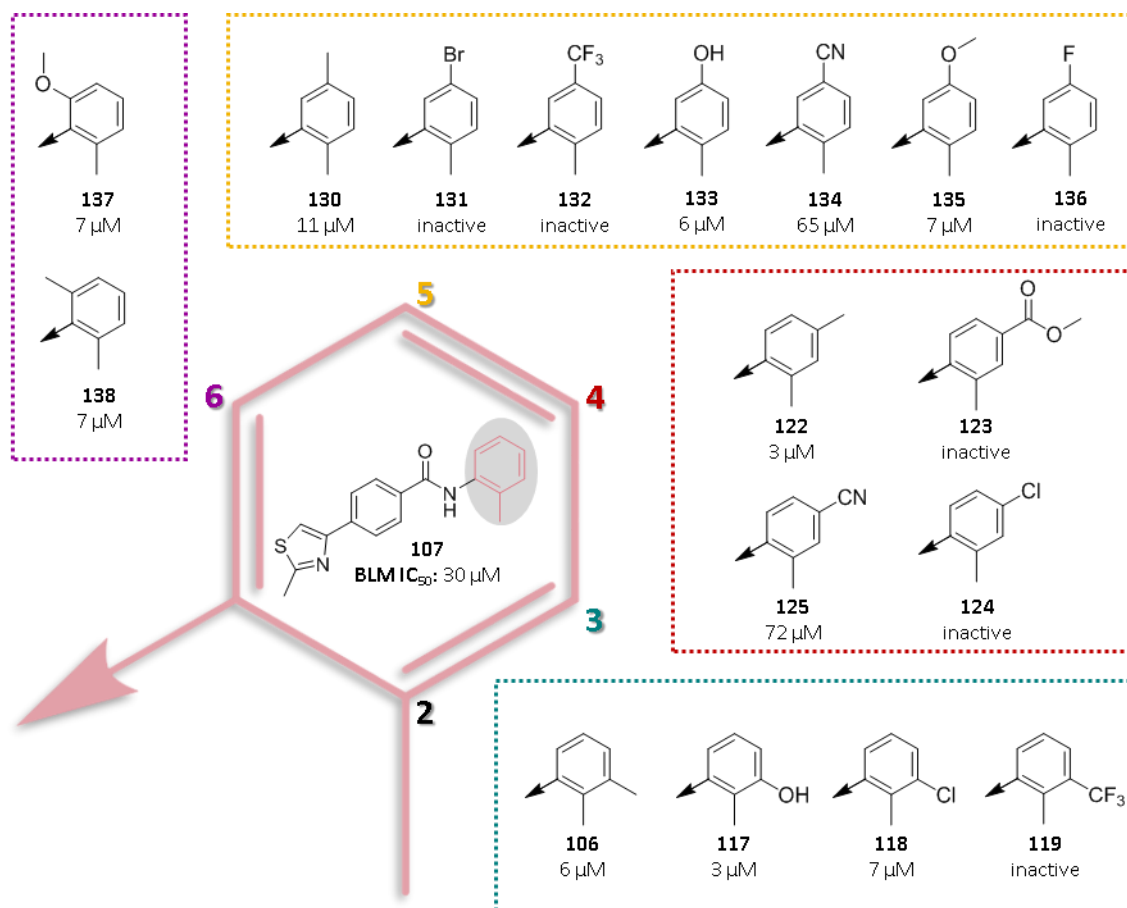


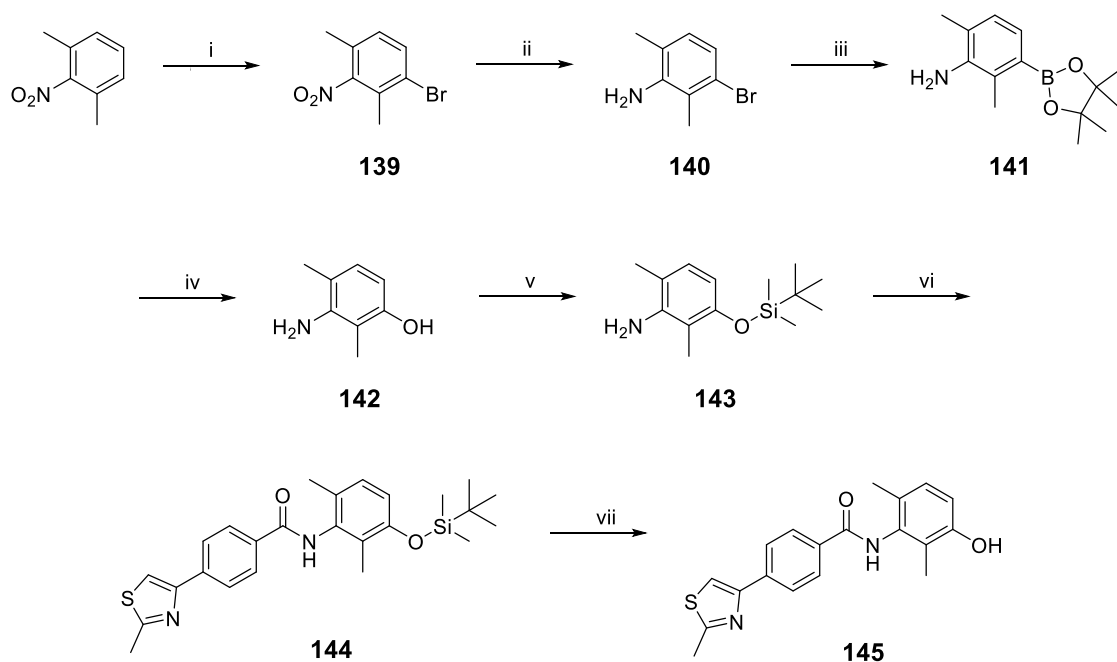
Figure 4.4. BLM inhibitory data for compounds assessing aniline ring SAR.

4.2.3. Third substituent effect – synthesis and SAR

Introduction of an additional methyl or hydroxy group at any position resulted in approximately a 5–10-fold increase in potency compared to mono-methyl analogue **107**. To ascertain whether the addition of a third substituent would yield similar gains in potency, it was decided to incorporate a hydroxy at the 3-position of the 2,6-dimethyl compound **138**. The commercial availability of substituted aniline substrates is limited and the 2,6-dimethyl aniline template allowed the most convenient synthesis for the introduction of a third group in a selective manner due to its symmetry. Compound **117** demonstrated that a 3-hydroxy substituent provided the best potency and while the addition of a 3-methyl (as in **116**) may be equally effective, it would raise the lipophilicity of the compound.

For the synthesis of the key tri-substituted aniline **142** (Scheme 4.5), a synthetic route described in a 2015 patent²⁶⁰ from Cancer Research UK was followed. The initial step

required bromination of 2,6-dimethylnitrobenzene with *N*-bromosuccinimide in the presence of catalytic iron in trifluoroacetic acid (Scheme 4.5). Following the patent conditions of 2 equivalents of *N*-bromosuccinimide resulted in a 20% yield of the desired mono-brominated **139** and a 40% yield of the 3,5-di-brominated compound. Furthermore, the reaction had reached completion within a day as opposed to the 5 days specified in the patent. The reaction was repeated with 1 equivalent of *N*-bromosuccinimide and proceeded for 5 days. It allowed isolation of mono-brominated compound **139** in 40% yield and there was no sign of the di-brominated side-product. However, of the 1 g of starting material in the reaction, only 330 mg was collected after purification, demonstrating the reaction did not go to completion. The patent being followed quoted a yield of 60% for this reaction suggesting the authors may have had similar difficulties around di-bromination and failure of the reaction to go to completion. Ultimately, sufficient quantities of **139** were obtained and further optimisation of this bromination was not conducted.



Scheme 4.5. *Reagents and conditions:* (i) NBS, TFA, 65 °C, 5 d, 40%; (ii) Fe, AcOH, 80 °C, 16 h, 78%; (iii) B₂pin₂, Pd(dppf)Cl₂, KOAc, 1,4-dioxane, 100 °C, 2 h, 95%; (iv) BNaO₃·H₂O, THF/H₂O, r.t., 16 h, 71%; (v) TMSCl, DMAP, Et₃N, r.t., 18 h, 71%; (vi) 4-(2-methylthiazol-4-yl)benzoyl chloride, Et₃N, cat. DMAP, DCM, r.t., 16 h, 35%; (vii) TBAF, THF, 0 °C, 5 min, then r.t., 10 min, 71%.

139 was reduced in presence of iron/acetic acid to produce the desired aniline derivative **140** which underwent borylation in high yields (Scheme 4.5). Finally, oxidative hydroxylation of the aryl boronate ester **141** with sodium perborate under mild

conditions produced the key aniline substrate **142**. As with the revised synthesis of compound **117** (Scheme 4.2), to avoid problems with side products, **141** was protected with a TBS group, followed by an amide coupling with **102** and a deprotection to give analogue **145** containing three substituents on the phenyl ring.

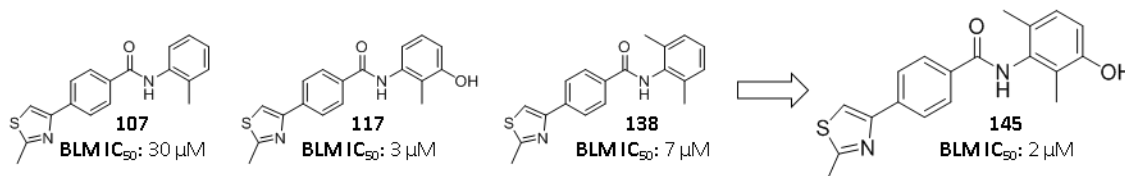


Figure 4.5. BLM inhibitory data of compound **145**.

The biological activity of compound **145** is presented Figure 4.5. Whilst there may be a 3.5-fold increase in potency relative to **138**, there is almost no increase in potency when compared with **117**. At this juncture, **145** represented the most potent analogue of Series G but, along with **103**, demonstrated that a third substituent on the aniline ring does not generate substantial gains in potency. Given the complex synthetic routes involved in producing highly substituted phenyl rings, **145** was the only example prepared in this investigation.

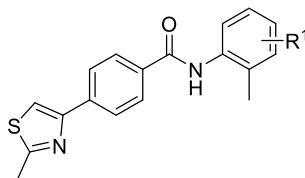
4.2.4. Solubility

In predicting solubility, the precise relationship between solubility and other molecular properties are still open to debate and the academic response has been the proposal of diverse solubility methods. Most of these are usually based on hydrophobicity in combination with other descriptors. Demonstrated by Ritchie and MacDonald,²²⁰ increased aromatic ring counts are associated with reduced solubility. Solubility prediction indexes such Physical Forecast Index (PFI) take into account $\log D_{PH7.4}$ and the aromatic ring count as simple, effective tools to predict the solubility of drug-like compounds.

Analogues of **99** were synthesised to assess basic SAR around the aniline ring. Of that small library, various compounds that demonstrated moderate potency (1–10 μ M) had their solubility measured and the results are presented in Table 4.3. In cases where the lower solubility limit is between 1 and 100 μ M, a compound is considered to have moderate (or partial) solubility, and above 100 μ M denotes high solubility. As there is a

consistent aromatic ring count, the clogD values are listed to assess the impact of hydrophobicity on solubility for this series thus far.

Table 4.3. Physicochemical and *in-vitro* solubility data for selected analogues.



Compound	R ¹	MW	clogD	tPSA (Å ²)	Sol (μM)
103	3-CH ₃ , 5-SO ₂ NH ₂	401	3.5	102	10
106	3-CH ₃	322	4.9	42	16
117	3-OH	324	4.1	62	58
133	5-OH	324	4.1	62	21
135	5-OMe	338	4.2	51	91
137	6-OMe	338	4.2	51	33
145	3-OH, 6-CH ₃	338	4.6	62	54

One of the early analogues synthesised, compound **103**, presented with relatively poor *in-vitro* aqueous solubility despite the lowered hydrophobicity of this compound (Table 4.3). Dimethyl benzene compounds, such as **106**, presented with moderate potency, and as expected due to their high hydrophobicity, demonstrated poor aqueous solubility. On the other hand, the less hydrophobic phenol and methoxybenzene compounds such as **117** and **135** had better solubility profiles. Overall, all compounds assessed for solubility had moderate solubility.

4.2.5. Summary

Various analogues of hit **99** were synthesised to evaluate the SAR around the aniline. It was determined the 2-methyl group was crucial for activity. Substituents were more tolerated around the remaining positions of the phenyl ring with hydroxy, methoxy and methyl substituents demonstrating moderate BLM inhibition between 2–10 μM. Overall, these simple changes did not yield any significant gains in potency to meet the probe like criteria set out (<0.1 μM). However, the synthesis of various inactive analogues demonstrated SAR and can be biologically useful in providing negative controls. In addition, solubility measurements determined various members of this

series demonstrated moderate solubility. As the phenyl ring was shown to tolerate various substituents, it can be possible to improve the solubility of Series G through further modifications on this ring.

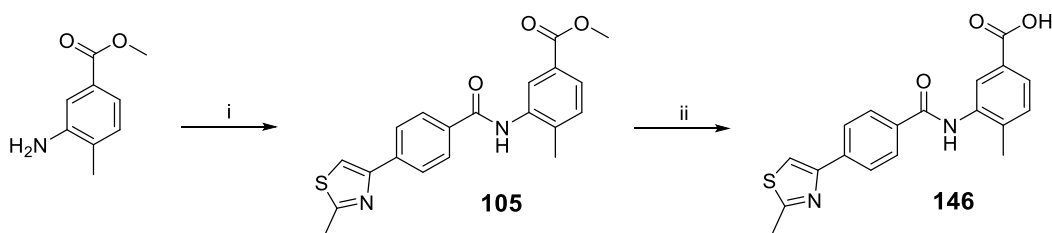
4.3. Amide library at the 5-position

4.3.1. Rationale

Exploration of the aniline substitution highlighted that the hydroxy, methoxy and methyl substituents at the 5-position enhanced activity and previous exploration had shown that a sulphonamide and methyl ester functionality yielded comparable results. Therefore, extension of the molecule from the 5-position was expected to be tolerated. Previous SAR suggested that potential handles of exploration could include sulphonamide or ether linkages. Furthermore, as the methyl ester demonstrated activity, an amide functionality may also be used. Given synthetic tractability and substrate availability, amide substituents were explored with the aim to improve potency and solubility.

4.3.2. Synthesis

In order to synthesise the key carboxylic acid intermediate **146**, microwave-assisted PCl_3 coupling of **102** with methyl 3-amino-4-methylbenzoate produced amide **105** which was hydrolysed under basic conditions (Scheme 4.6). Carboxylic acid **146** was obtained in high purity (>95%) for biological assessment.

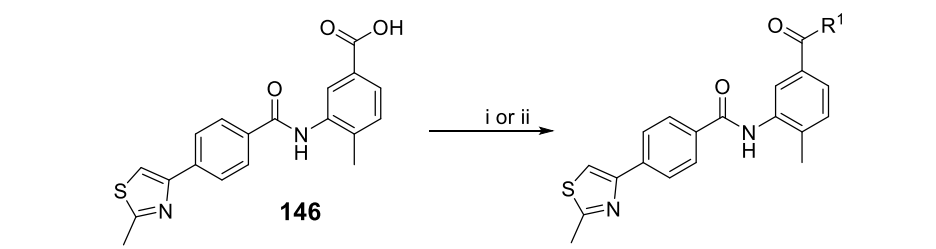


Scheme 4.6. Reagents and conditions: (i) **102**, PCl_3 , THF/MeCN (3:2), 150 °C, MW, 15 min, 65%; (ii) NaOH, $\text{H}_2\text{O}/\text{MeOH}$, 50 °C, 2 h, 99%.

Amide substituents were introduced *via* a final amide coupling step (Table 4.4). For the synthesis of **147–149**, poor yields were observed with EDCI/HOBt conditions due to failure of the reaction to go to completion and poor separation during purification. Changing to a T3P-mediated coupling resulted in slightly better yields as reduced side-

product formation enabled easier purifications despite the reactions still not going to completion.

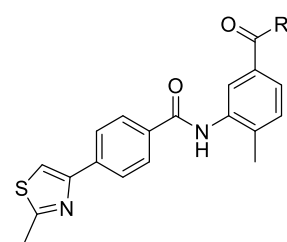
Table 4.4. Amide coupling in the synthesis of *N*-acylated groups. *Reagents and conditions:* (i) appropriate amine, EDCI, HOBt, DIPEA, DMF, r.t., 16 h; (ii) T3P, Et₃N, DMF, r.t., 16 h.

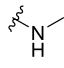
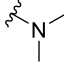
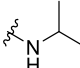
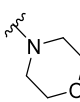
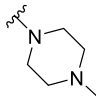


Compound	R ¹	Method	Yield (%)
147	NH ₂	i	37
148	NHCH ₃	i	10
149	N(CH ₃) ₂	i	9
150	NCH(CH ₃) ₂	ii	47
151	Morpholine	ii	63
152	Methylpiperazine	ii	30

4.3.3. SAR

Carboxylic acid **146** and primary amide **147** demonstrated similar BLM inhibitory activity (Table 4.5). In general, the biological results showed that expansion from the amide correlated with loss of activity. Overall, none of these compounds presented with improved activity over the methyl ester **105** and sulphonamide **99**. While these amide derivatives are associated with reduced clogD and increased tPSA, solubility measurements were not conducted due to their poor BLM inhibitory activity.

Table 4.5. BLM inhibitory activity and physicochemical properties of amide series.


Compound	R ¹	clogP	clogD	tPSA (Å ²)	BLM IC ₅₀ (μM)
105	OCH ₃	4.4	4.4	69	13
146	OH	3.9	1.0	79	17
147	NH ₂	3.2	3.2	85	19
148		3.5	3.5	72	36
149		3.7	3.7	62	70
150		4.2	4.2	71	55
151		3.5	3.5	72	89
152		3.5	3.4	66	inactive

4.3.4. Summary

A small set of 5 amide derivatives were prepared *via* amide coupling to assess the potential growth of this compound series from the 5-position of the phenyl ring. Positioning small amide derivatives in the space previously occupied by sulphonamide and methyl ester functionalities was expected to increase the solubility profile of this series and potentially gain new molecular interactions for potency enhancement. However, the biological results demonstrated that growing out of the amide through alkyl linkers resulted in loss of potency.

4.4. Heterocyclic replacement of the aniline ring

4.4.1. Rationale

To widen the scope of investigation around the aniline SAR, heterocyclic replacements were synthesised and evaluated. The changes focused initially on the classic isosteric

replacement of phenyls with pyridines which would lower the clogD and may improve the solubility and potentially improve the potency of Series G. However, pyridyl replacements did not improve potency of this series and so a more a diverse group of small heterocyclic replacements, also with removed clogD, were synthesised and evaluated.

4.4.2. Synthesis and SAR of pyridyl analogues

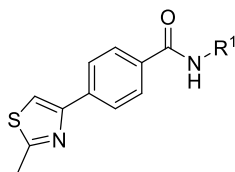
Five amino pyridyl substrates, containing mono- or dimethyl substituents to allow comparison to various compounds in this series, underwent amide coupling (Table 4.6). Compounds **153** and **156**, containing the 3-pyridyl, were less nucleophilic and required heating up to 50 °C. The yield for **156** was particularly poor as not only did the reaction fail to go to completion, but three rounds of chromatographic purification were required.

Table 4.6. *Reagents and Conditions:* (a) oxalyl chloride, cat. DMF, DCM, r.t., 16 h, then (b) DCM, 0.5–16 h, r.t. – 50 °C.

Compound	R ¹	Yield (%)
153		18
154		8
155		33
156		3
157		45

Table 4.7 illustrates the biological activity and calculated physicochemical parameters of the pyridyl replacements when compared to the phenyl ring. The replacement of a phenyl ring with a pyridine improved the clogD of these compounds by 1 to 2 log units. **157** was inactive which was expected given that a pyridyl nitrogen had replaced the essential 2-methyl. The SAR shows that the presence of a 2- or 3-pyridyl ring does not affect the biological activity of these compounds. Compound **156** was of high interest as this analogue demonstrated potency comparable to the best compounds in this series but presented with much favourable physicochemical properties. Assessment of the solubility of compound **156** indicated that the compound has excellent aqueous solubility. Interestingly, compound **155**, possessing similar calculated physicochemical properties to **156** was significantly less soluble.

Table 4.7. Biological activity and physicochemical properties of pyridines compared to corresponding phenyl analogues.



Compound		R ¹	clogD		tPSA (Å ²)		Sol (μM)		BLM IC ₅₀ (μM)	
X = C	X = N		X = C	X = N	X = C	X = N	X = C	X = N	X = C	X = N
107	153		4.4	3.2	42	55	nd	nd	30	23
107	154		4.4	3.8	42	55	nd	nd	30	44
122	155		4.9	2.9	42	55	nd	28	3	13
138	156		4.9	3.3	42	55	nd	244	7	4
115	157		4.4	3.4	42	55	nd	nd	>100	>100

4.4.3. Diverse heterocycles

Modifications of the aniline ring of the hit **99** had proved difficult in terms of major advancements in potency. In the absence of knowledge of the binding mechanism of this series to BLM helicase, various modifications on this aniline ring were trialled without any success. To scaffold hop from the phenyl ring, a small library of diverse derivatives was synthesised through amide coupling protocols used extensively in this chapter (Table 4.8). A structure search of in-house amines was conducted to identify aromatic and aliphatic heterocycles that could occupy the same region as the phenyl ring. The most potent analogues generally had a clogD just above 4 and it was preferable to keep the hydrophobicity of the small library below this to ensure sufficient solubility.

The replacement of the aniline ring with various small heteroaromatics such as an isoxazole, pyrrazole and thiazole scaffold and with aliphatic heterocycles resulted in an absence of BLM inhibition. While only a limited number of heterocyclic scaffolds were assessed, replacing the 6-membered aromatic ring consisting of small substituents is likely to be a challenging task in the absence of binding site knowledge.

Table 4.8. Physicochemical properties, synthesis and SAR of analogues of 99 exploring modification of the right side aromatic ring. *Reagents and Conditions:* (a) oxalyl chloride, *cat.* DMF, DCM, r.t., 16 h, then (b) DCM, 0.5–16 h, r.t. – 50 °C.

Reaction scheme: A 4-(4-methylthiazol-2-yl)benzoic acid derivative reacts under conditions (i) to form a 4-(4-methylthiazol-2-yl)benzoate derivative with an R¹ group.

Compound	R ¹	Yield (%)	clogD	tPSA (Å ²)	BLM IC ₅₀ (μM)
158		17	3.0	68	Inactive
159		16	2.3	71	Inactive
160		40	2.4	68	Inactive
161		41	3.9	55	Inactive
162		8	3.6	71	Inactive
163		31	0.6	79	Inactive
164		10	0.7	45	Inactive
165		25	3.3	33	Inactive

4.4.4. Summary

It has been demonstrated that the phenyl ring can be replaced with a pyridine while maintaining similar levels of potency and substantially increasing the solubility of this series. Attempts to scaffold hop away from the phenyl ring to a heterocyclic system with

a preferred physicochemical profile was unsuccessful following the synthesis of a small set of diverse amide derivatives.

4.5. Discussion

The identification of hit **99** was followed by limited SAR examination on the right side aniline ring to establish rapid SAR to further endorse continuing research on this hit series. Such rapid SAR was possible as established amide coupling chemistry utilising Vilsmeier reagent forming conditions of oxalyl chloride/DMF demonstrated a wide scope with the carboxylic acid moiety **102** that composed the remainder of the hit.

Through the use of readily accessible substrates, SAR investigations revealed that the presence of a 2-methyl was paramount for inhibitory activity. This could likely be due to the small pocket that the methyl points towards where larger groups don't fit and this *ortho* substituent allows conformational change by inducing twists in the molecule. This result led to all subsequent investigations of the phenyl ring to be conducted with 2-methyl group.

The ease of the synthetic route allowed a small library of aniline derivatives to be synthesised that investigated structurally similar analogues through isosteric modifications at the 3, 4, 5, and 6-position of the phenyl ring. The SAR presented was relatively flat with no significant gains in potency achieved. Various compounds presented with moderate potency and moderate solubility at this point. In general, the SAR pattern could be attributed to electronic effects where the more electron donating methyl, hydroxy and methoxy groups have superior activity over electron-withdrawing groups such as nitrile, halogens and trifluoromethyl groups. The results show that a sulphonamide, primary amide and methyl ester are all tolerated at the 5-position, but they don't bring the roughly 5–10-fold potency gains that the small electron donating groups did. Furthermore, whilst the addition of a second methyl or hydroxy resulted in such potency gains, a third addition of this substituent did not result in significant potency gains which suggests the electron-density of the benzene ring may be maximally influenced.

To further the improvement in solubility and continue the search for additional interactions to enhance activity, a small library of amide derivatives were used to occupy the space of the sulphonamide and potentially grow further into this pocket. The SAR demonstrated that as the molecule got larger, activity began to decrease. The small hydrophobic and polar chains coming off the amide did not gain additional molecular interactions despite there being space for the molecule to grow into the pocket. One could speculate this is because the area points into solvent space or an undruggable pocket. However, not a broad spectrum of potential linkers and moieties were assessed for a conclusive judgement to be reached regarding the druggable space discussed here.

Continuing with medicinal chemistry strategies which involved small alterations to gain SAR knowledge, a small pyridine replacement program of the phenyl ring ensued. The result was no significant difference in activity between the two aromatic ring structures, but that pyridine replacement resulted in improved solubility for the moderately potent compound **156**. This example fulfilled the solubility criteria of $>100\ \mu\text{M}$ for the desired BLM probe that was sought. Additionally, it was decided to use parallel chemistry on a very small scale, to synthesise small heterocyclic replacements of the aniline ring. None of these compounds were active but given the exploratory nature of this library, success would more likely result from making hundreds to thousands of compounds rather than in the tens. The resources in the project was not suited for such a campaign and it was judged that resources should be used to explore other regions of the molecule for potency gains as SAR around the aniline only led to limited success.

4.6. Conclusion

In the absence of a crystal structure, conventional medicinal chemistry strategies have been followed which involved modifying substituents and the ring system on the aniline in attempts to rationalise alterations in activity. However, despite the synthesis of a significant number of analogues, no further improvements in potency had resulted. Furthermore, an attempt to scaffold hop also proved unsuccessful and was not followed up on a large scale.

The SAR exploration was paired with improvements in solubility through the reduction in clogD and increasing tPSA of this compound series. This yielded various analogues

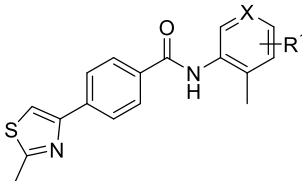
with moderate potency and moderate to high solubility. Furthermore, the generation of closely related inactive analogues is also useful for this series as a biological tool. Ultimately, the goal remains to further explore SAR for significant gains in potency.

5. Series G Part Two

5.1. Introduction

Series G, a novel series of BLM inhibitors, underwent SAR exploration of the aniline ring, ultimately leading to identification of various analogues with the potential to be optimised and developed into a good chemical probe (Chapter 4). Table 5.1 presents four leads progressed to the next round of development which were selected based on their activity, solubility and calculated physicochemical parameters. Compound **103** was an early hit with reasonable predicted physicochemical properties but was found to have poor solubility. Compound **117** demonstrated relatively good solubility for this series but required multiple steps for synthesis and **156** demonstrated excellent solubility but required expensive starting material that amide coupled in very low yields. Whilst compound **106** was relatively lipophilic ($\text{clogD} = 4.9$), the 2,3-dimethyl carboxamide core was considered the most synthetically tractable. Overall, the predicted physicochemical properties and solubility data indicated this core was adequate for use in assessing SAR, particularly as exploration would generally aim to increase potency whilst preserving solubility.

Table 5.1. Comparison of biological activity, physicochemical parameters, solubility data and synthetic tractability for selected analogues.



Compound	X	R ¹	BLM IC ₅₀ (μM)	MW	clogD	tPSA (\AA^2)	Sol (μM)	Comment on synthetic tractability
103	C	3-CH ₃ , 5-SO ₂ NH ₂	3	401	3.5	102	10	Low yield (16%), expensive substrate
106	C	3-CH ₃	6	322	4.9	42	16	Moderate yield (45%)
117	C	3-OH	3	324	4.1	62	58	Requires protection steps
156	N	6-CH ₃	3	323	3.3	55	244	Very low yield (3%), expensive substrate

5.1.1. Aims

The aim of the work presented in this chapter was to design and synthesise analogue compounds with changes around the amide bond, core phenyl ring and the thiazole ring in order to investigate and draw useful conclusions about the SAR and physicochemical properties of the series.

5.2. SAR exploration of the amide bond

5.2.1. Rationale

Figure 5.1 depicts the various strategies used to design compounds for exploring the role of the amide bond in binding. It was hypothesised that the components of the amide bond could be involved in hydrogen bonding interactions. To study SAR, it was proposed that synthesis of a reduced amide (to form an amine) could indicate whether the oxygen atom acts as a hydrogen bond acceptor, and synthesis of an *N*-methylated amide could indicate whether the amide proton acts as a hydrogen bond donor. Additionally, synthesising the reversal of the amide would illustrate the impact of changing the relative position of the potential hydrogen bond donors and acceptors. Finally, an alkyl linker was placed between the amide bond and the aniline ring to determine the repercussion of adding an extra rotatable bond. Furthermore, three of these four compounds designed might positively impact solubility (Figure 5.1), through reduction of the planarity and reduction of intermolecular hydrogen bonding.

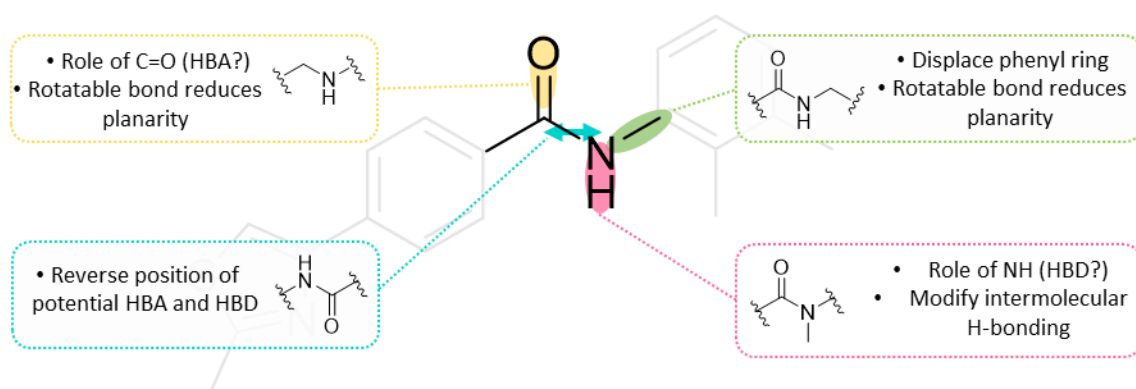
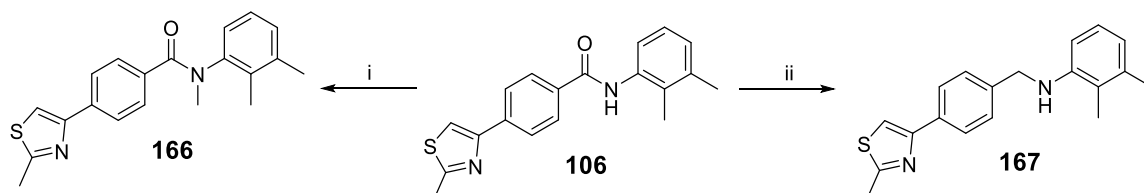


Figure 5.1. Strategies used to gain insights into amide bond SAR.

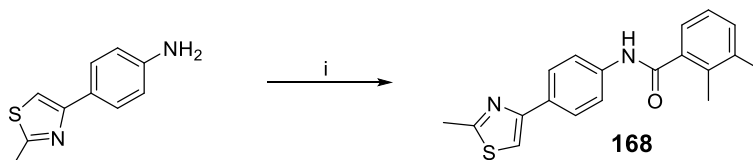
5.2.2. Synthesis and SAR

Synthesis of the *N*-methylated amide (**166**) and the reduced amide (**167**) involved one-step protocols from the parent analogue **106** (Scheme 5.1). Amide bond *N*-methylation *via* sodium hydride deprotonation and iodomethane as the methylating agent, and amide bond reduction with borane proceeded in moderate yields.

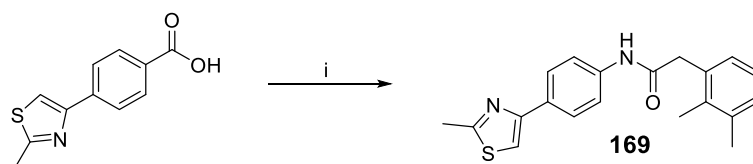


Scheme 5.1. Reagents and conditions: (i) MeI, NaH, DMF, r.t., 16 h, 43%; (ii) BH₃.THF, THF, 50 °C, 2 h, 23%.

The commercial availability of 4-(2-methyl-1,3-thiazol-4-yl)aniline and 2,3-dimethylbenzoic acid allowed a one-step amide coupling to access reverse amide analogue **168** using standard HATU conditions (Scheme 5.2). Amide coupling was also employed for the synthesis of **169**, on this occasion *via* the acyl chloride intermediate (Scheme 5.3).



Scheme 5.2. Reagents and conditions: (i) 2,3-dimethylbenzoic acid, HATU, DIPEA, DMF, r.t., 16 h, 47%.



Scheme 5.3. Reagents and conditions: (i) (a) oxalyl chloride, *cat.* DMF, DCM, r.t., 16 h, then (b) 2,3-dimethylbenzylamine, DCM, 16 h, 64%.

Biological evaluation of compounds **166–169** indicated that BLM inhibitory activity was not retained upon alteration of the amide bond. This suggested that the specific orientation of the amide bond in this inhibitor series is crucial for activity and should not be further modified.

5.2.3. Summary

Four analogues that impacted the amide bond were designed, synthesised and evaluated. These compounds were all inactive against BLM. As a result, it was determined the amide bond is crucial for activity.

5.3. Introduction of *ortho* methyl substitution and pyridyl replacement of the core phenyl ring

5.3.1. Rationale

Due to the reactivity of the thiazole motif, specifically the 2-methyl-1,3,thiazole contained within this inhibitor series, selective C-4 arylation is not well documented.²⁶¹ The reactivity of this motif is discussed in more detail in Section 6.2.2. Ultimately, arylation of the 2-methylthiazole motif will occur preferentially at the C-5 position due to its more nucleophilic nature. As a result, formation of a 4-arylthiazole requires synthesis through more traditional methods such as classical Hantzsch thiazole synthesis (connecting α -haloketones and thioamides in a convergent manner), as was the case for the synthesis of carboxylic acid **102** (Section 3.6.2). Consequently, such protracted syntheses render it difficult to rapidly construct libraries that assess the core phenyl ring.

In generating limited SAR on the core phenyl motif, more emphasis was placed on designing analogues that could be used to improve the solubility of the compound series. Compound **156** had demonstrated that replacement of the aniline ring for a pyridine resulted in a significant improvement in solubility. Therefore, a similar strategy was applied to the core phenyl ring where a reduction in clogD was sought through the introduction of a more hydrophilic pyridine (Figure 5.2).

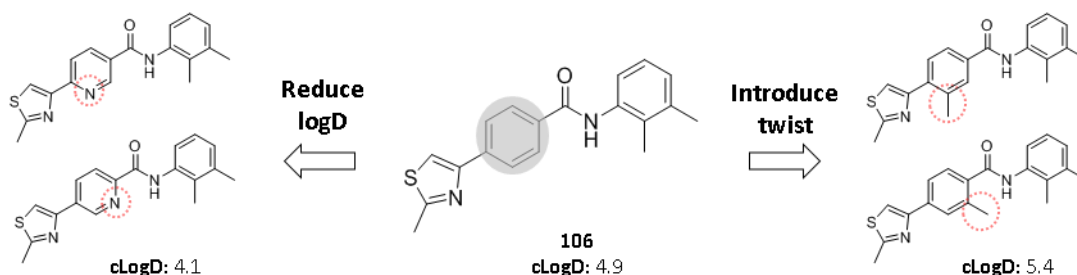
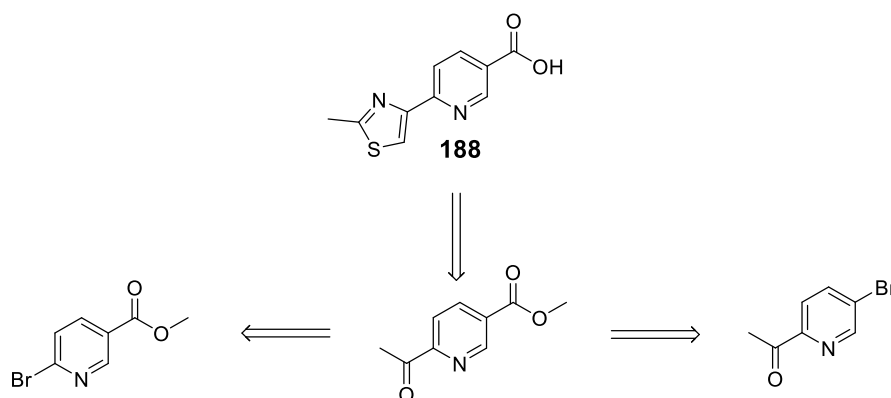


Figure 5.2. Introduction of *ortho* methyl and replacement with pyridine for improved solubility.

Additionally, improvements in solubility were sought through *ortho*-substitution of the aryl ring. The biaryl amide is likely to sit in a highly planar fashion, and the addition of a methyl *ortho*-substituent on the phenyl ring neighbouring the amide and thiazole motif would be expected to improve solubility by reducing the overall planarity and symmetry of the compounds, thereby causing disruption of π - π stacking.²⁰⁸ This culminates in a twisted conformation thought to result in the lowest energy conformation, reducing solid phase crystal packing and increasing the rate of solid dissolution into solvent. Overall, the use of a pyridine and methyl substituent would be useful as a combination strategy to improve solubility.²⁶² It was also the intention that both the pyridine nitrogen and the methyl group may be able to pick additional molecular interactions that could be combined with other SAR improvements.

5.3.2. Synthesis and SAR

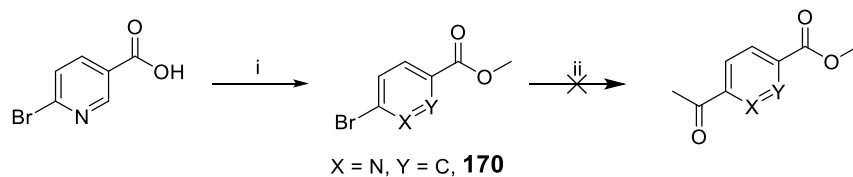
Synthesis of analogues with modified core phenyl rings required the formation of biarylcarboxylic acid intermediates. As discussed in the previous section, such arylthiazoles can be synthesised *via* α -haloketones. Therefore, the proposed analogues would be synthesised from substrates containing an acylated and a carbonylated moiety *para* to their relative positions (Scheme 5.4). Due to the limited commercial availability of such substrates, it would require at least one of these groups to be functionalised from purchased starting material. For example, synthesis of **188** would require acylation of the bromoester or carbonylation of the bromoketone, both of which can be obtained commercially (Scheme 5.4).



Scheme 5.4. Retrosynthetic analysis for synthesis of pyridyl containing core.

Three methods for the synthesis of an acylated pyridyl ester were attempted using methyl 6-bromonicotinate and methyl 5-bromo-2-pyridinecarboxylate as substrates (Table 5.2). Initially, methyl 6-bromonicotinate (**170**) was synthesised in-house by esterification of 6-bromonicotinic acid and then commercially obtained. Based on availability of the respective pyridine esters at that juncture, acylation optimisation occurred on both pyridine isomers. Given that both the starting material and final compound ionised, reactions were typically followed by LCMS-LCQ. Standard halogen exchange conditions with *n*-BuLi followed by DMA in both diethyl ether and tetrahydrofuran were ineffective and resulted in remaining starting material as well as formation of various side-products (Table 5.2). Additionally, conditions utilising a turbo Grignard reagent were trialled but resulted primarily in starting material suggesting lithium-halogen exchange did not occur. (Table 5.2)

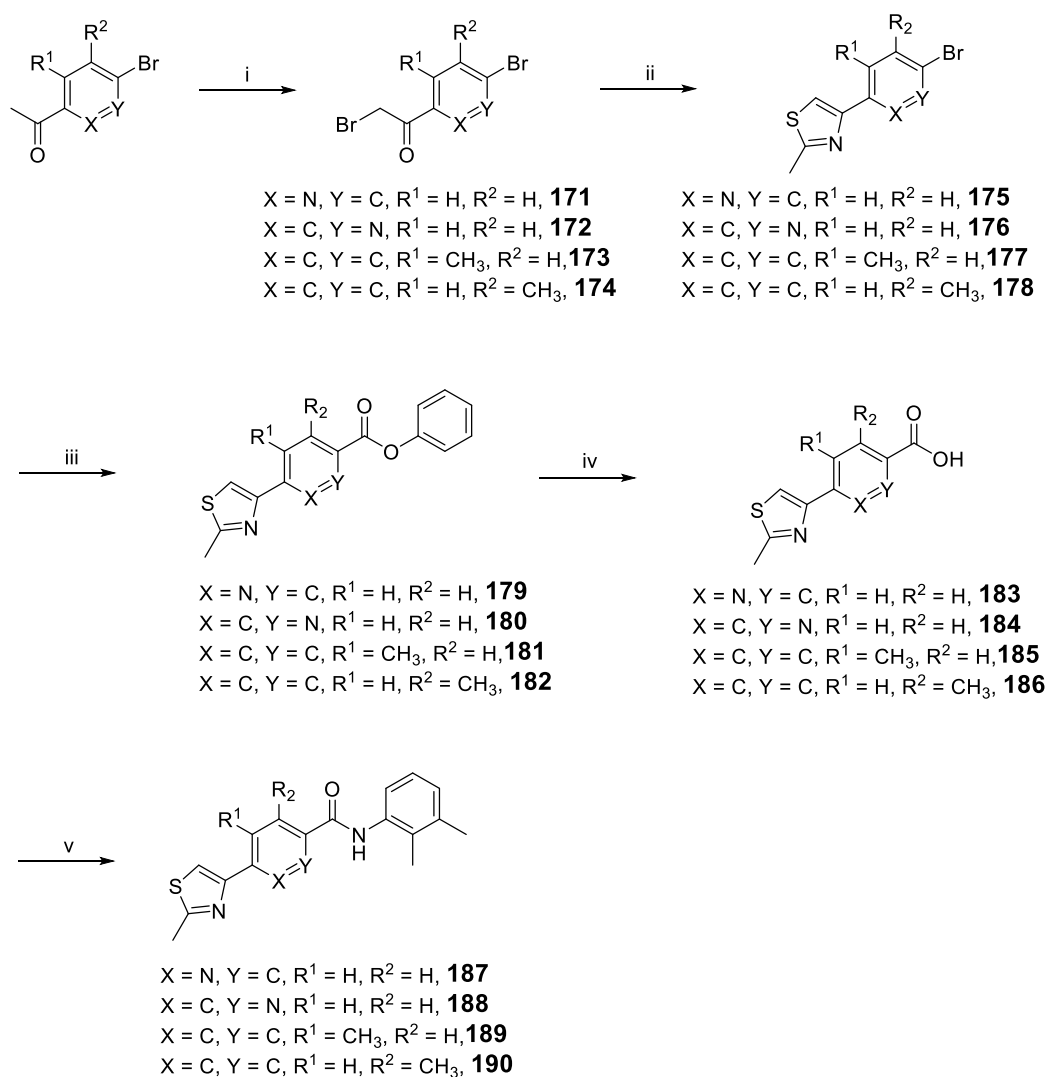
Alternatively, literature reports for the synthesis of these desired compounds had pointed to the use of regioselective Heck arylation of electron rich olefins such as butoxyethene, whereby the resulting α -arylated vinyl ethers were acidified *in situ* to form the desired aryl ketone.^{263,264} Using various proposed conditions from Mo 2004,²⁶⁴ solvent removal, temperature and base changes were trialled with no success in producing more than trace desired product (Table 5.2). In all cases, homocoupling of the pyridyl moiety was observed.

Table 5.2. Acylation test reactions. *Reagents and conditions: (i) H₂SO₄, MeOH, 65 °C, 4 h, 29%.*

#	X	Y	ii	Reaction outcome
1	N	C	<i>n</i> -BuLi, Et ₂ O, -78 °C, 5 min then DMA, r.t., 24 h	Some starting material and side-products and no product ^{a,b}
2	N	C	<i>n</i> -BuLi, THF, -78 °C, 5 min then DMA, r.t., 24 h	Some starting material and side-products and no product ^a
3	C	N	<i>i</i> -PrMgCl·LiCl, THF, r.t., 2 h then CH ₃ COCl, 16 h	Mostly starting material, some side-products and no product ^a
4	C	N	<i>i</i> -PrMgCl·LiCl, THF, -40 °C, 1 h then CH ₃ COCl, -60 °C, then r.t., 2.5 h	Mostly starting material, some side-products and no product ^a
5	C	N	Butoxyethene, Pd(OAc) ₂ , DPPP, BMIM, <i>i</i> Pr ₂ NH, DMSO, 115 °C, 6 h	Mostly homocoupled product, and trace product ^{a,b}
6	N	C	Butoxyethene, Pd(OAc) ₂ , DPPP, BMIM, <i>i</i> Pr ₂ NH, DMSO, 80 °C, 16 h	Mostly homocoupled product, and trace product ^{a,b}
7	N	C	Butoxyethene, Pd(OAc) ₂ , DPPP, BMIM, Et ₃ N, DMSO, 80 °C, 24 h	Mostly homocoupled product, and trace product ^{a,b}
8	N	C	Butoxyethene, Pd(OAc) ₂ , DPPP, BMIM, Et ₃ N, 80 °C, 24 h	Mostly homocoupled product, and trace product ^{a,b}

^a As judged by LCMS-LCQ; ^b As judge by ¹H-NMR

Given the challenges in functionalising bromopyridines with an acyl functionality, carbonylation was attempted to alternatively introduce a carboxylic acid functionality on acylated bromopyridines. It was decided that carbonylation would be performed once the Hantzsch thiazole synthesis had occurred. Palladium catalysed carbonylation conditions with phenyl formate²⁶⁵ were utilised to afford the phenyl ester that was isolated in all cases and then hydrolysed to give the desired carboxylic acid intermediate. Scheme 5.5 demonstrates that this synthetic route, starting with the acyl functionalised aromatic ring, was used to successfully synthesise four analogues of **106** with a modified core phenyl ring. For the bromide **177**, it was found that Pd(OAc)₂/TTBT or Pd(dppf)₂Cl₂ catalytic conditions did not give sufficient conversion to the carboxylic acid precursor. However, the use of Pd(PhCN)₂Cl₂ /xantphos was effective and therefore also used for the regioisomeric phenyl **178**.



Scheme 5.5. Reagents and conditions: (i) NBS, *p*TsOH, MeCN, 80 °C, 16 h: (**171**, 59%; **172**, 55%; **173**, 100%; **174**, 55%); (ii) thioacetamide, DMF, r.t., 16 h: (**175**, 32%; **176**, 64%; **177**, 57%; **178**, 99%); (iii) (a) phenyl formate, Pd(OAc)₂, TTBT, Et₃N, MeCN: (**179**, 69%; **180**, 53%) or (b) phenyl formate, Pd(PhCN)₂Cl₂, xantphos, Et₃N, DMF: (**181**, 53%; **182**, 90%); (iv) NaOH, H₂O/THF, r.t., 16 h: (**183**, 50%; **184**, 35%; **185**, 89%; **186**, 41%); (v) oxalyl chloride, cat. DMF, DCM, r.t., 16 h, then 2,3-dimethylaniline, NaH or Et₃N/*cat.* DMAP, DCM, 2–16 h: (**187**, 20%; **188**, 22%; **189**, 27%; **190**, 28%).

Unlike with the 4-(2-methylthiazol-4-yl)benzoic acid core utilised in the previous chapter, the couplings for these modified carboxylic acids were not successful when using 2,3-dimethylaniline with DIPEA as the base on addition to the *in-situ* formed acid chlorides. Alternatively, the use of either sodium hydride or triethylamine/*cat.* DMAP was successful in pushing the reaction to completion. It was found that the pyridine-2-carboxamide analogue **188** demonstrated poor solubility in organic solvents which prevented successful purification by column chromatography. Unlike most analogues in the series thus far, **188** was poorly soluble in methanol and as a result was purified by trituration in methanol.

5.3.3. SAR

The BLM inhibitory data and thermodynamic solubility data for analogues **187–190** are presented in Table 5.3 for comparison to compound **106**.

Table 5.3. BLM inhibitory and solubility data for pyridyl and methyl phenyl analogues.

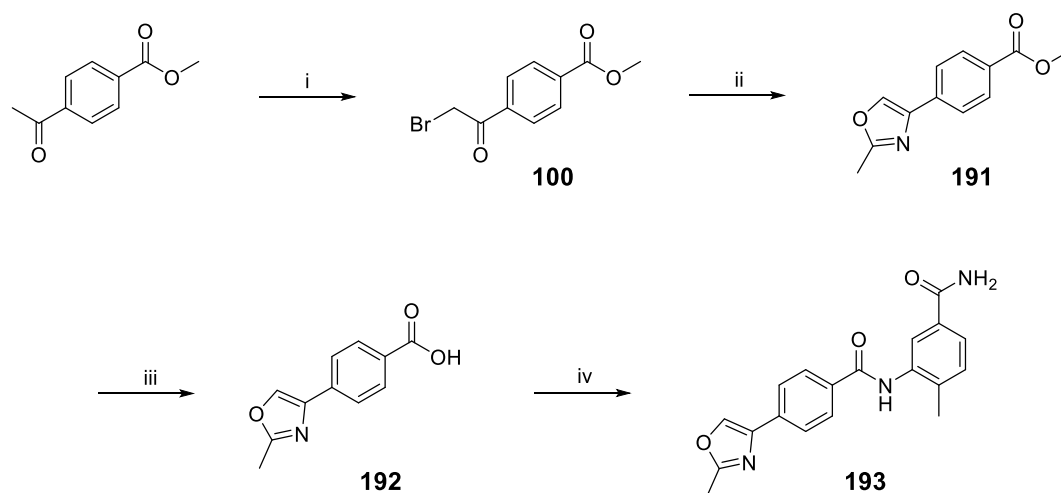
Compound	R ¹	BLM IC ₅₀ (μM)	Sol (μM)
106		6	16
187		4	37
188		Inactive	nd
189		Inactive	16
190		Inactive	39

The pyridine-3-carboxamide **187** was equipotent to its phenyl analogue demonstrating that an improvement in clogD can be achieved with this core without negatively impacting potency. Ultimately, the increase in clogD by 0.8 units resulted in a 2-fold improvement in solubility. In contrast, the pyridine-2-carboxamide **188** was not active against BLM helicase and due to its demonstrably poor solubility in organic solvents was not assessed for aqueous solubility. Both phenyl analogues, containing methyls to induce twists, were also inactive. Despite having an increased clogD, the 3-methyl benzamide (**189**) possessed a similar solubility to **106**, whilst the 2-methyl benzamide (**190**) had greater solubility thereby demonstrating the impact of *ortho* substituents on breaking the planarity of the aromatic ring system.

5.4. Synthesis of thiazole replacements utilising Suzuki-Miyaura cross-coupling

5.4.1. Rationale

Early SAR probing on the aniline ring included synthesis of an oxazole analogue of **147** (Scheme 5.6). Synthesis of the key oxazole carboxylic acid occurred in an analogous manner to that of the thiazole (**102**) (Scheme 2.7). In this instance the Hantzsch synthesis utilised neat acetamide and high temperature conditions instead of thioacetamide in DMF and ambient temperature (Scheme 5.6). Compound **193**, an analogue of **147**, demonstrated that the thiazole and oxazole isostere possess similar levels of potency (Table 5.4).



Scheme 5.6. *Reagents and conditions:* (i) NBS, *p*TsOH, MeCN, 80 °C, 16 h, 82%; (ii) acetamide, DMF, 160 °C, 2 h, 73%; (iii) NaOH, H₂O/MeOH, r.t., 84%; (iv) oxalyl chloride, *cat.* DMF, DCM, r.t., 16 h, then 2,3-dimethylaniline, DIPEA, DCM, 16 h, 55%.

The biological data of **193** demonstrated that a sulphur can be modified to an oxygen in this 5-membered aromatic system with minimal penalty to potency (Table 5.4), as would be expected for such a closely related isostere. No substantial gain in potency occurred from this change. It was proposed that a campaign focusing on small point changes on the thiazole substructure would result in a time-consuming and complicated synthesis due to the nature of the 1,3-thiazole substituted at the 4-position. Suzuki-Miyaura cross-coupling was used to generate a small library of compounds consisting of various heterocycles to depart from this less synthetically tractable thiazole to a scaffold that was preferable for SAR investigations and demonstrated greater gains in potency.

Table 5.4. BLM inhibitory data of oxazole derivative **193**.

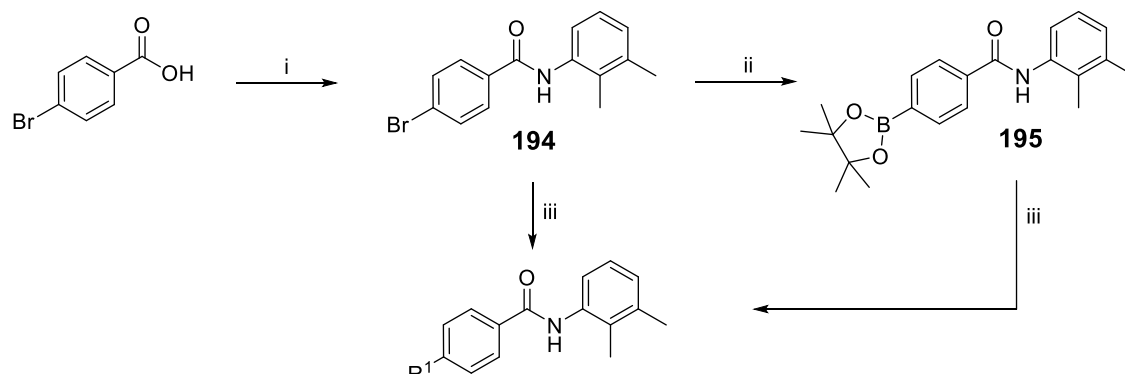
Compound	X	BLM IC ₅₀ (μM)
47	S	19
193	O	28

As in the previous section, the 2,3-dimethylaniline template of compound **106** was employed due to synthetic tractability. Furthermore, both bromide (**194**) and boronate ester (**195**) are substrates in Suzuki couplings (Table 5.5). Therefore, a search of in-house boronic acids/boronate esters, iodide and bromide compounds was conducted, and 23 substrates were then selected for Suzuki-Miyaura cross-coupling (Table 5.5). Substrates were considered for their ability to occupy a similar chemical space to that of the methyl thiazole and possess a clogD similar to or less than that of the methyl thiazole (< 5). A few compounds slightly exceeded this clogD threshold but were considered to be of interest with regards to their potential ability to probe for new molecular interactions. Unlike the 1,3-methylthiazole and 1,3-methyloxazole, the isosteric imidazole is relatively reactive at the 4-position due to its exhibited tautomerism and subsequently is readily available with a bromide substituted at this position thus allowing it to be a substrate in Suzuki-Miyaura cross-coupling.

5.4.2. Synthesis

Enabling late-stage diversification for thiazole replacement required the synthesis of aryl bromide **194** and aryl boronate ester **195**. Amide coupling of 4-bromobenzoic acid and 2,3-dimethylaniline was achieved using standard HATU conditions to produce **194** in good yield which was then converted to the boronate ester. Both reactions were found to be scalable when attempted with 2 g of starting material.

Table 5.5. Reagents and conditions: (i) 2,3-dimethylaniline, HATU, DIPEA, DMF, 16 h, r.t., 87 %; (ii) B₂pin₂, Pd(dppf)Cl₂, KOAc, 1,4-dioxane, 100 °C, 3 h, 87%; (iii) appropriate substrate, Pd(dppf)Cl₂, Na₂CO₃, 1,4-dioxane/water, MW, 120 °C, 20 min or appropriate borate, Pd(PPh₃)₄, Cs₂CO₃, DME/water for compounds **204**, **207**, **208** and **209**.



Cpd	Substrate type	R ¹	Yield (%)	Cpd	Substrate type	R ¹	Yield (%)
196	Aryl bromide		50	205	Boronic acid		32
197	Boronate ester		45	206	Boronic acid		61
198	Boronate ester		46	207	Boronate ester		17
199	Boronate ester		41	208	Boronic acid		13
200	Aryl bromide		24	209	Boronic acid		32
201	Aryl bromide		28	210	Boronic acid		44
202	Aryl bromide		40	211	Boronic acid		10
203	Boronate ester		52	212	Boronic acid		75
204	Boronate ester		21	213	Boronic acid		64

The substrates used for the synthesis of this library consisted mostly of boronate derivatives. For compounds **204**, **207**, **208** and **209**, Suzuki-Miyaura cross-coupling occurred in the presence of $\text{Pd}(\text{PPh}_3)_4$ and caesium carbonate under conventional heating (Table 5.5). These conditions resulted in consumption of the substrate within an hour, but it was found that removal of the triphenylphosphine oxide by-product required multiple purification efforts and resulted in loss of material in impure fractions. Consequently, yields for these conditions were poor. Instead, microwave-assisted coupling using $\text{Pd}(\text{dppf})\text{Cl}_2$ and sodium carbonate resulted in improved yields due to relatively straightforward purifications. Overall, these conditions for the Suzuki-Miyaura cross-coupling had a moderate scope but various substrates did not couple effectively (Figure 5.3). These included two thiophene boronate esters and three aryl bromide derivatives of which two contained hydroxy functionalities. Accordingly, these scaffolds were deprioritised and ultimately not further pursued in consideration of the biological data returned from the 18 compounds presented in Table 5.5.

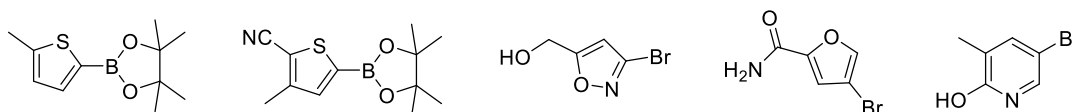
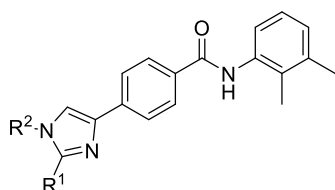


Figure 5.3. Substrates that did not couple effectively in Suzuki-Miyaura cross-coupling with reaction (iii) of Table 5.5.

5.4.3. SAR

With the exception of compounds **201** and **202** (Table 5.6), the biological data of compounds assessing SAR around the thiazole core demonstrated no inhibitory activity against BLM helicase. Compound **201**, where the thiazole sulphur was replaced by a tautomeric nitrogen or protonated nitrogen displayed a loss of over 5-fold in activity. For the other imidazole **202**, the movement of the methyl from the 2-position to the 3-position of the imidazole resulted in an almost 2-fold drop in potency when compared to **201**. Various thiazoles with an aryl attachment at the 5-position rather than the 4-position demonstrated no activity. Other small heterocyclic structures like pyrazoles and furans were also inactive. Additionally, various 6-membered aromatic ring-containing motifs demonstrated a similar lack of activity.

Table 5.6. BLM inhibitory activity of imidazoles **201** and **202**.


Compound	R ¹	R ²	BLM IC ₅₀ (μM)
201	CH ₃	H	31
202	H	CH ₃	49

5.4.4. Summary

Synthesis of a library of structurally diverse aryl derivatives was performed using Suzuki-Miyaura cross-coupling from substrates available in-house. It was found that the imidazole isostere of the thiazole showed reduced activity while more diverse structures were not tolerated. Overall, the thiazole motif also demonstrated tight SAR.

5.5. Discussion

The role of the amide bond in this inhibitor series was methodically assessed through changes to the functionality. Methylation of the amide nitrogen resulted in complete loss of activity which suggests it may be acting as a hydrogen bond donor. The inactivity of **167** indicates the carbonyl is crucial for activity and could be acting as a hydrogen bond acceptor. The amide functionality was transposed to form the reversed amide which showed no potency against BLM helicase demonstrating the importance configuration of the amide bond. When designing peptidomimetics with pseudo amide bonds such as retroamides and reduced amides, stable peptides can be produced, suggesting some isosteric and conformation similarities exists.^{266,267} In this series, the amide proton and the amide carbonyl are essential for activity and it is may be possible that these might form key interactions, specifically hydrogen bonding, in the binding pocket.

Additionally, it was found that the CH₂ linked amide of the parent analogue **106** was also inactive which, in agreement with the conclusions of the previous chapter, highlights the importance of the interaction of the phenyl ring in the pocket. The alkyl linker shifted

the position and/or altered the conformation of the phenyl ring and consequently was unable to interact with the pocket.

The phenyl ring within the core of the molecule connected to a 1,3-thiazole at the 4-position prevents late-stage diversification and therefore extensive SAR investigations into replacement of this ring is limited. Given the tight SAR demonstrated in this series thus far, synthetic efforts probing the core phenyl ring of the analogues focussed on two small changes that had a higher probability of improving the solubility profile of the series, which could be incorporated into analogue design later in the project. The change from a phenyl ring to a methyl substituted analogue, or alternatively a pyridyl ring, also presented an opportunity for gains in potency, however the incorporation of a methyl substituent on the core phenyl ring was also not tolerated. The compounds continued to demonstrate moderate solubility despite raising the clogD of the compound by 0.6 units to 5.4. One possible outcome of the resulting conformational twist is that the loss of planarity may prevent the compound accessing a relatively planar or narrow pocket.

The pyridine-3-carboxamide change (**187**) resulted in no loss of activity and a 2.5-fold improvement in solubility. The outcome was beneficial because this SAR knowledge could be utilised during later stage development to reduce lipophilicity and potentially any metabolic liabilities concerning the phenyl ring.

Conversely, the pyridine-2-carboxamide change (**188**) resulted in complete loss of activity. One cause could be the presence of an intramolecular hydrogen bond in the pyridine-2-carboxamide core. Generally, two conformations can exist in this scenario: one where intramolecular hydrogen bonding is occurring (closed conformation) and one where the polar groups are exposed to the solvent (open conformation). An analysis of the Cambridge structural database (CSD) and the protein data bank (PDB) by Kuhn and co-workers demonstrated a relatively high propensity for certain atom topologies to form intramolecular hydrogen bonds in various cyclic systems.²⁶⁸ Six membered rings containing two sp²-hybridized linker atoms (such as amides) are planar, conjugated systems that have a high probability of internal hydrogen bond formation. Such intramolecular hydrogen bonding is termed resonance-assisted hydrogen bonding and results in relatively highly stable bonding due to π -delocalization.²⁶⁹ For example,

Figure 5.4 demonstrates the internal hydrogen bonding occurring in a pyridine carboxamide substructure of c-Jun NH₂-terminal kinase inhibitor taken from the PDB [2H96].²⁷⁰ The motif represented is identical to that of compound **188** and Kuhn and co-workers found a probability of 67% that intramolecular hydrogen bond formation occurs for such a topology.²⁶⁸ The consequence of such bonding within **188** are 2-fold within the context of this discussion. Firstly, if it is the case, as suggested earlier, that the amide of this inhibitor series is involved in important hydrogen bonding interactions with BLM, then the presence of intramolecular hydrogen bonding can make the amide proton less available for such interactions. Secondly, there is a reduction in solubility due to the polar components of the inhibitor being removed from solvent exposure and enhancement of the rigidity of the planar substructure.



Figure 5.4. Internal H-bonding demonstrated by c-Jun NH₂-terminal kinase inhibitor consisting of a pyridine carboxamide [PDB:2H96].

A set of structurally diverse aryl derivatives were prepared to replace the 2-methyl-1,3-thiazole core connected at the 4-position to produce a more potent inhibitor with preferred synthetic versatility. The amide bond within the core of the compound presents a straightforward disconnection that readily permits diverse exploration. Given the nature of this drug discovery project, where comprehensive exploration is expected to occur in the absence of structural binding data for a series demonstrating tight SAR, a simple disconnection, such as Suzuki coupling, between the core phenyl and connecting aryl ring would also be preferred. However, continuing the trend of tight SAR, only the closely related imidazole analogues were found to be suitable replacements of the methyl thiazole. Other aryl cores that could potentially occupy similar space to the methyl thiazole of this inhibitor series were not tolerated and displayed inactivity. These results suggest closer exploration of the methyl thiazole will need to be conducted in order to further understand the SAR surrounding this motif.

5.6. Conclusion

In lieu of computationally enabled structure-based design, analogues were designed to probe the SAR and improve physicochemical properties of the three remaining motifs of this inhibitor series: core amide, core phenyl ring and the thiazole ring. Investigation of the amide motif highlighted the importance of both acceptor carbonyl and donor hydrogen of this core. Replacement of the core phenyl ring with a pyridine-3-carboxamide was tolerated and improved the physicochemical properties, including solubility, of this series. Finally, it was found that substitution of the thiazole motif with similarly sized heteroaryl structures was not permitted. Overall, following exploration of the right side aniline ring (Chapter 4), core amide and phenyl motifs, and the thiazole ring, it was not possible to achieve considerable improvements in potency.

6. Series G Part Three

6.1. Introduction

The SAR exploration of the four distinct parts composing this inhibitor series did not lead to the expected significant potency gains required to obtain an optimal BLM helicase chemical probe (Section 4.1). Examination of the aniline ring through the synthesis of a library of 50 analogues illustrated a narrow SAR profile in this region whilst a less rigorous assessment of the core amide and phenyl ring moieties depicted the presence of activity cliffs. The approach taken to explore the thiazole ring was based on optimising the synthetic tractability of this series alongside physicochemical and biological properties. The evaluation of a Suzuki coupled library containing heterocyclic replacements for this core demonstrated the loss of BLM inhibition suggesting a core highly similar to the 4-substituted 2-methyl-1,3-thiazole was preferred. The efforts in this chapter sought to resolve the SAR around the thiazole ring. With an extensive SAR identified on this series, additional compounds would be synthesised to serve as early leads for this novel series of BLM inhibitors.

6.1.1. Employing a miniaturised BLM assay to assess BLM inhibition

During SAR investigations discussed in this chapter, primary biochemical evaluation of BLM inhibition by Ms Chen was concluded and inhibitors produced during the remainder of this project were tested by a miniaturised assay developed in the SDDC by Mr Marcus Hanley and Mr Will Pearce. The new assay was developed for a HTS against BLM helicase for a separate program. Table 6.1 compares the concentrations of various components between the two fluorescent quenching assays developed in-house and that developed for the BLM qHTS conducted on the MLSMR library (Section 3.1.2). During this changeover period between assay formats, a bottleneck in testing meant that a large number of compounds were generated and their biological activity were determined in one iteration.

Table 6.1. Comparison of the components of fluorescence-quenching DNA unwinding BLM inhibition assays developed in-house and presented in the literature.

Assay	Nguyen et al ¹	In-house Protocol 1 (Ms Chen)	In house Protocol 2 (Mr Pearce)
Purpose	qHTS for BLM helicase [AID 2528]	Screening of compounds discussed in Chapters 2, 3, 4 and 5.	Developed for a HTS for BLM helicase. Utilised for screening of compound in Chapters 6 and 7.
Buffer	50mM Tris.HCl (pH 8.0) 5mM NaCl 2mM MgCl ₂ 0.01% Tween-20 2.5µg/ml Poly(dI-dC) 1mM DTT	50mM Tris.HCl (pH 8.0) 50mM NaCl 2mM MgCl ₂ 0.01% Tween-20 2.5µg/ml Poly(dI-dC) 1mM DTT	50mM Tris.HCl (pH8.0) 50mM NaCl 2mM MgCl ₂ 0.1% Tween-20 1.25µg/ml Poly(dI-dC) 1mM DTT
Final DMSO concentration	1%	5%	2%
Substrate and protein concentration	[DNA]: 200nM [ATP]: 2000µM [BLM]: 50nM	[DNA]: 75nM [ATP]: 120µM [BLM]: 3.75nM	[DNA]: 10nM [ATP]: 180µM [BLM]: 0.625nM
Final volume	4 µL	41 µL	7 µL

The biological assay data ultimately revealed that compounds containing the 2,3-dimethylbenzamide motif demonstrate poor solubility, likely due to their high clogD, and were not suitable for assessment in this newer format. Precipitation of the inhibitors at higher concentrations in the assay prevented accurate analysis of inhibitory values which further highlighted the necessity to synthesise compounds with improved physicochemical properties.

6.1.2. Aims

The aims of the work in this chapter were as follows:

1. A concentrated SAR campaign on the 4-substituted 2-methyl-1,3-thiazole scaffold would focus on the methyl substituent and on closely related aryl replacements of this scaffold.

2. Develop analogues in this inhibitor series with the most favourable physicochemical and biological properties based on SAR identified across the series.

6.2. SAR investigations of thiazole motif with closely related analogues

6.2.1. Rationale

The initial SAR looking at replacing the thiazole ring (see Section 5.4) indicated that small changes in this part of the molecule could abolish the activity. It was decided to follow two strategies while designing compounds that closely resemble the original thiazole motif. Firstly, extension from the thiazole 2-position with small alkyl substituents linked to the ring by a carbon, a nitrogen and an oxygen would probe for additional binding interactions. These rotatable substituents could help reduce the planarity of the molecules and lead to an increase in the aqueous solubility. Secondly, the design and synthesis of heterocyclic isosteres of the 2-methyl-1,3-thiazole may result in the identification of a core with improved potency and higher synthetic tractability.

6.2.2. Exploration of the potential use of CH activation chemistry on the 4-position of 1,3-thiazoles

Traditional aryl-aryl coupling chemistry on the 1,3-thiazole core could not be used in this case as arylation preferentially occurs at the position α to the sulphur atom (C-5) (Figure 6.1)

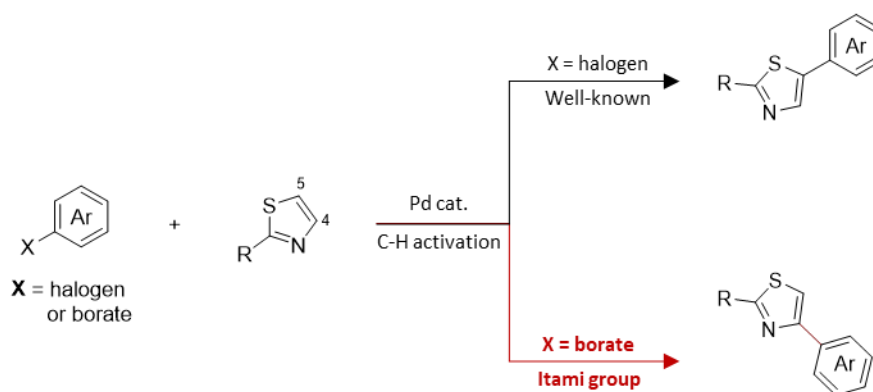
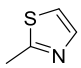
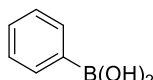
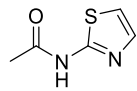
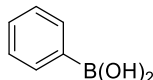
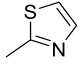
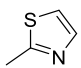


Figure 6.1. Reactivity of 1,3-thiazole motif in the presence of palladium catalysts.

The Itami group have developed novel C–H activation chemistry which allows aryl groups to be installed directly onto the thiazole ring at the C-4 position with arylboronic acid substrates under Pd/TEMPO catalysis.^{261,271–274} Utilising this oxidative biaryl coupling method had the potential to couple thiazole building blocks with regioselective control in order to further explore the thiazole motif SAR for this inhibitor series. Additionally, such a synthetic tool could enable more convenient and efficient SAR when assessing the other motifs of this inhibitor series. Other methods for selective C-4 arylation of thiazoles in this manner did not exist at the time of publication.

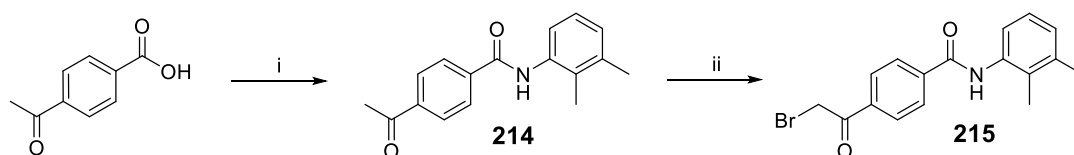
Implementing various conditions for this selective C–H activation, test reactions were conducted (Entry 1-2, Table 6.2) with 2-methylthiazole and 2-acetamidothiazole with the aryl borate phenylboronic acid resulting in yields of 34% and 32%, respectively. Whilst these yields were approximately 30-50% lower than those presented by Kirchberg and Itami for other substrates,²⁷¹ these results demonstrated the possibility of achieving selective C-4 arylation of the thiazole. However, these yields did not translate when using **195** as the boronate substrate in order to synthesise **106**. It was found that the use of two sets of conditions (Entry 3 and 4, Table 6.2) established for selective C-4 arylation of thiazoles failed when applied to our aryl borate substrate **195**. As a result, the C–H activation methodology was abandoned.

Table 6.2. Test reactions pertaining to regioselective C–H activation of thiazoles.

Entry	Thiazole substrate	Aryl borate (4 eq.)	Reagents	Conditions	Yield (%)	Comments
1			Pd(OAc) ₂ , TEMPO, LiBF ₄ , 1,10-phen, DMAc	115 °C, 2 d	34	
2			Pd(OAc) ₂ , TEMPO, LiBF ₄ , 1,10-phen, DMAc	115 °C, 2 d	32	
3		195	Pd(OAc) ₂ , TEMPO, LiBF ₄ , 1,10-phen, DMAc	115 °C, 2 d	0	Trace desired product observed
4		195	Pd(OAc) ₂ , TEMPO, bipy, C ₆ H ₅ CF ₃	80 °C, 2 d	0	Trace desired product observed

6.2.3. Extension of the methyl substituent

To investigate growth of the methyl group at the 2-position of the thiazole ring, late-stage thiazole functionalisation was preferred to ensure efficient synthesis. Similarly to the previous thiazole SAR exploration, the 2,3-dimethylaniline unit was used because it would be synthetically compatible with this objective. Given the unsuccessful C-H activation attempts described previously, it was decided to revert to classical Hantzsch thiazole synthesis to synthesise suitable analogues. The α -bromoketone **214** was required to aid convergent synthesis with thioamides to produce the thiazole analogues. This compound was synthesised by bromination of ketone **215** which was generated by HATU amide coupling of 2,3-dimethylaniline and 4-acetylbenzoic acid (Scheme 6.1).

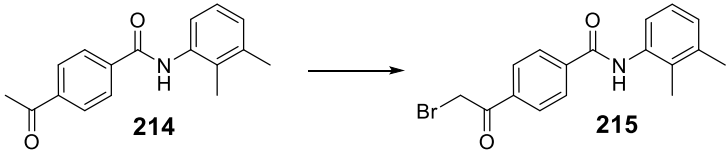


Scheme 6.1. Reagents and conditions: (i) 2,3-dimethylaniline, HATU, DIPEA, DMF, 16 h, r.t., 64 %; (ii) LiHMDS (1 M in THF), THF, -78°C , 30 min, then TMSCl , 60°C , 2 h, then NBS, -78°C , 5 min 72%.

To prepare the key intermediate **215** from the acetyl **214**, several brominating agents such as NBS, bromine and tetrabutylammonium tribromide were trialled (Table 6.3). However, undesired aromatic bromination on the dimethylaniline ring occurred in these experiments that utilised such direct brominating agents (Entry 1-4, Table 6.3). Table 6.3 Entry 1 depicts conditions that have been used previously for selective α -bromination on simpler substrates in this thesis. Entry 3 and 4 were literature conditions that enabled selective α -bromination on substrates containing 2,3-dimethyl phenyl ring systems. It was presumed that the electron donating methyl substituents decreased the nucleophilicity of the aniline ring making it more reactive than the α -carbon. To overcome this, it was proposed that a more nucleophilic carbonyl α -carbon would undergo α -bromination more readily. As a result, a highly nucleophilic enolate such as a trimethylsilyl (TMS) enolate would be produced before bromination. Literature conditions which promoted enolate formation with lithium bis(trimethylsilyl) amide were followed (Scheme 6.1).²⁷⁵ It was found that silyl intermediate did not form sufficiently at room temperature overnight, but heating at 60°C aided successful silylation. Finally, dropwise addition of NBS in THF at -78°C resulted in immediate

formation of the desired α -bromoketone **215** and no signs of undesired bromination were detected (Scheme 6.1).

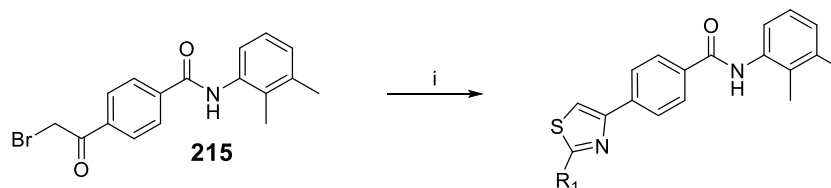
Table 6.3. Unsuccessful attempts for selective α -bromination.

			
Entry	Conditions	Reaction outcome	Ref
1	p-TsOH, NBS, MeCN, 80 °C, 16 h	Substrate consumed and bromination occurs on aniline ring. No production of desired product.	
2	Br ₂ , CHCl ₃ , r.t., 2 h	Substrate consumed and bromination occurs on aniline. No production of desired product.	
3	Br ₂ , 1,4-dioxane/Bu ₂ O, 0 °C, 45 min	Substrate consumed and bromination occurs on aniline. No production of desired product.	276
4	TBABr ₃ , r.t., 5 h, then 80 °C, 16 h	Substrate consumed and bromination occurs on aniline (50%) and produces desired product (50%).	277

The convergent synthesis of thioamides and the α -bromoketone **215** resulted in the synthesis of thiazole analogues **216–218** (Table 6.4). These thioamide substrates were available in-house and assessed small alkyl growth in the form of ethyl, isopropyl and acetonitrile substituents. The Hantzsch cyclisation occurred in poor to moderate yields (Table 6.4).

6.2.4. Extension of the methyl substituent with *N*-alkylation

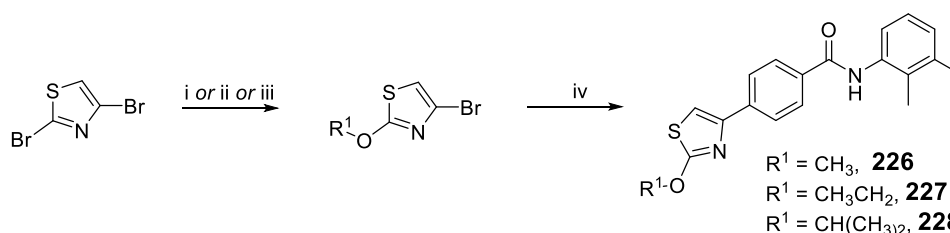
Thiazole derivatives with nitrogen-linked small alkyl substituents were also prepared using the methodology described in the Section 6.2.3 (Table 6.4). The replacement of the methyl with a primary amine would produce analogues with the potential to engage in hydrogen bond interactions. Additionally, incorporation of a nitrogen could improve the solubility. In this instance, compounds **218–222** were synthesised in moderate yields utilising precursor thiourea derivatives in ethanol at ambient temperature.

Table 6.4. *Reagents and conditions:* (i) appropriate thioamide or thiourea, DMF or EtOH, r.t., 2–6 h.


Compound	R ¹	Yield (%)
216	CH ₂ CH ₃	28
217	CH(CH ₃) ₂	22
218	CHCN	40
219	NH ₂	55
220	NHCH ₃	37
221	NHCH ₂ CH ₃	64
222	NHCH(CH ₃) ₂	46

6.2.5. Extension of the methyl substituent with *O*-alkylation

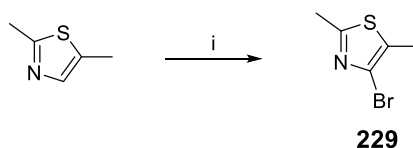
Finally, oxygen-linked thiazole analogues were also synthesised to complete the small set of compounds exploring the space extending from the thiazole 2-position which would have improved solubility due to the addition of the polar oxygen. Unlike the synthesis of the analogous nitrogen linked compounds, late-stage convergent Hantzsch synthesis was not possible to create oxygen linked substituents. Instead, the appropriate thiazole substrates suitable to undergo Suzuki coupling reactions were synthesised. Starting from 2,4-dibromothiazole, an S_NAr reaction was carried out with appropriate alkoxides (Scheme 6.2). The reaction selectively occurs at the 2-bromine as it is more activated α to the sulphur. Finally, the bromo thiazoles underwent Suzuki-Miyaura cross-coupling using standard microwave-assisted coupling with Pd(dppf)Cl₂ and sodium carbonate to produce oxygen linked methyl (**226**), ethyl (**227**) and isopropyl (**228**) thiazole analogues.

**Scheme 6.2.** *Reagents and conditions:* (i) NaOMe, MeOH, 65 °C, 16 h: (R¹ = CH₃, **223**, 54%); (ii) NaOEt, THF, 50 °C, 16 h: (R¹ = CH₃CH₂, **224**, 74%); (iii) KOiPr, *i*PrOH, 50 °C, 3 h: (R¹ = CH(CH₃)₂, **225**, 99%); (iv) **195**, Pd(dppf)Cl₂, Na₂CO₃, 1,4-dioxane/water, MW, 120 °C, 20 min: (**226**, 41%; **227**, 20%; **228**, 68%).

6.2.6. Replacement with thiazole regioisomers and assessment of methyl substituents

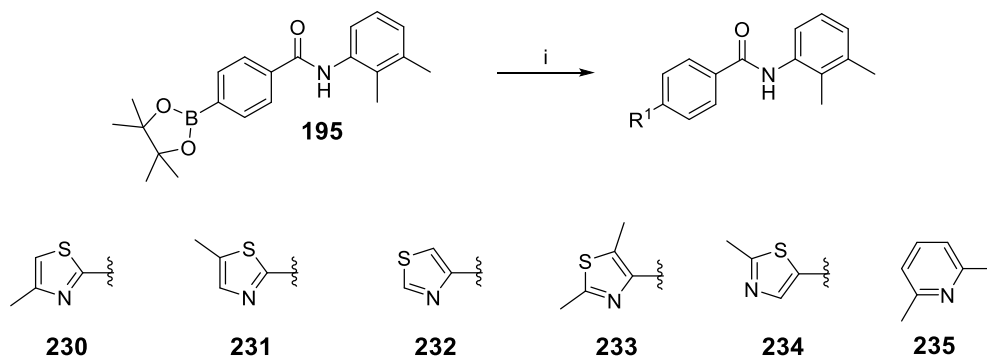
SAR studies presented in Section 5.4 show that the replacement of the 2-methyl-1,3-thiazole motif with heterocycles similar in size was detrimental to the BLM inhibitory activity of this compound series. Preparation of more closely related analogues was of interest to understand the tolerance of point changes and regioisomeric replacements for this motif.

Described in Section 5.3, the addition of methyl substituents on the core phenyl ring connecting to the thiazole was detrimental to the activity of this series and it could be hypothesised to be due to the loss of planarity preventing binding in a flat pocket. To further test this hypothesis, the addition of a methyl functionality at the 5-position of the thiazole was assessed. Brominating the vacant C-4 of the thiazole with bromine produced the aryl bromide **229** (Scheme 6.3) which then underwent Suzuki-Miyaura cross-coupling to result in the dimethyl thiazole analogue **233** (Scheme 6.4).



Scheme 6.3. Reagents and conditions: (i) Br₂, CHCl₃/CH₃CN, r.t., 16 h, 76%.

Additionally, compound **232** was synthesised to assess the impact of having an unsubstituted thiazole and regioisomeric methylthiazoles **230**, **231** and **234** were synthesised (Scheme 6.4).

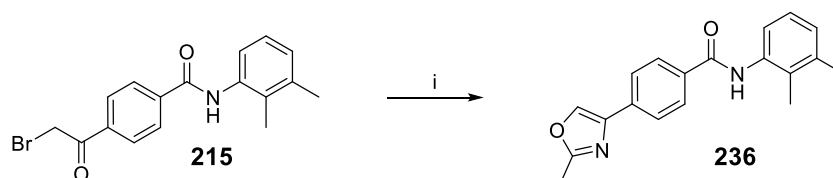


Scheme 6.4. Reagents and conditions: (i) appropriate aryl bromide, Pd(dppf)Cl₂, Na₂CO₃, 1,4-dioxane/water, MW, 120 °C, 20 min: (**230**, 31%; **231**, 43%; **232**, 27%; **233**, 49%; **234**, 55%; **235**, 31%).

6.2.7. Replacement with classical thiazole isomers

Traditionally, the C-C double bond has been considered isosteric to a sulphur atom. Therefore, when applying this to thiazoles, a pyridine can be considered a classical isosteric replacement. Therefore, to assess alternatives to the thiazole core, the 2-methyl pyridine compound **235** was synthesised utilising available Suzuki coupling chemistry (Scheme 6.4).

In Section 5.4, the replacement of the thiazole sulphur with a nitrogen to produce the imidazole derivative **201** resulted in an analogue with approximate a 5-fold loss in potency. Furthermore, using a different scaffold to the 2,3-dimethylaniline, it was shown that the oxazole derivative showed similar activity to the thiazole. In order to verify this result with the 2,3-dimethylaniline scaffold, the match pair compound **236** was synthesised by cyclisation of α -bromoketone **215** with acetamide under high temperatures. A low yield of desired product was obtained due to the reduced nucleophilicity of the acetamide (compared to thioamide) which required high temperatures resulting in the formation of numerous side products.

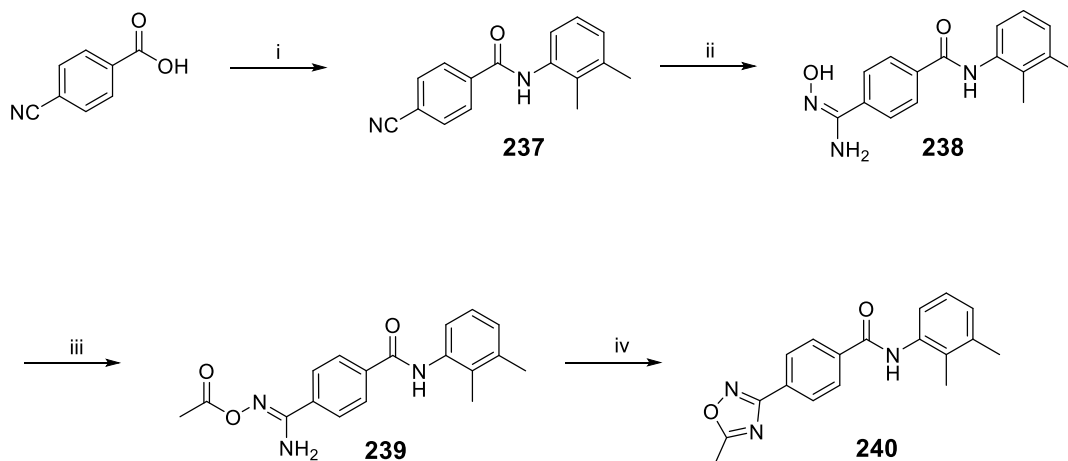


Scheme 6.5. Reagents and conditions: (i) acetamide, DMF, 130 °C, 3 h, 28%.

Another heterocyclic isostere of the thiazole that was desired for biological evaluation was the 1,2,4-thiadiazole motif. However, the required halogenated 5-methyl-1,2,4-thiadiazole was not commercially available and the complete synthesis of a final compound containing this motif was considered complex and time-consuming given optimisation of reaction conditions would be necessary due to the rare nature of this motif in chemistry literature.

Instead, a 1,2,4-oxadiazole analogue was synthesised that could be compared to **236** for biological activity. Whilst this synthesis consisted of four steps, more robust and precedented routes existed. The nitrile precursor **237** was synthesised by standard HATU coupling (Scheme 6.6.). The key amidoxime intermediate **238** was synthesised by

nucleophilic addition of hydroxylamine to nitrile **237**. Low yields were obtained for this reaction despite complete consumption of the starting material. **238** was then reacted with acetyl chloride to produce **239** which underwent cyclisation with KOH/DMSO affording the desired compound **240**.²⁷⁸



Scheme 6.6. *Reagents and conditions:* (i) 2,3-dimethylaniline, HATU, DIPEA, DMF, 16 h, r.t., 63 %; (ii) $\text{NH}_2\text{OH}\cdot\text{HCl}$, Et_3N , EtOH, 80 °C, 1 h, 24%; (iii) CH_3COCl , Et_3N , acetone, r.t., 12 h, 37%; (iv) KOH, DMSO, r.t., 12 h, 68%.

6.2.8. SAR

The analogues described in this chapter were designed and synthesised in a single iteration. Ultimately, the biological testing of these compounds in the miniaturised BLM DNA unwinding assay revealed inconsistent results to those described in the previous chapter. For example, compound **106**, whose template had been used for probing of the thiazole SAR, was found to possess a 10-fold loss in activity in the miniaturised assay. Figure 6.2 shows two examples of IC_{50} curves generated for this compound from the two assays. It can be seen that the cause of the lower IC_{50} for **106** in the miniaturised assay is due to unreliable readings generated for this compound above 10 μM . This was likely due to the compound precipitating under the assay conditions. Compound **106** has a clogD of 4.9 and an aqueous solubility of 15 μM and in the previous assay format (conducted by Ms Chen) displayed signs of inconsistent readings only at the top concentration of 100 μM . On the other hand, compound **117**, a structurally related analogue, possesses a lower clogD (4.1) and higher solubility (60 μM) profile and

demonstrates consistent IC_{50} curves across both assays, thereby highlighting the impact of compound solubility on generating reliable data for this assay.

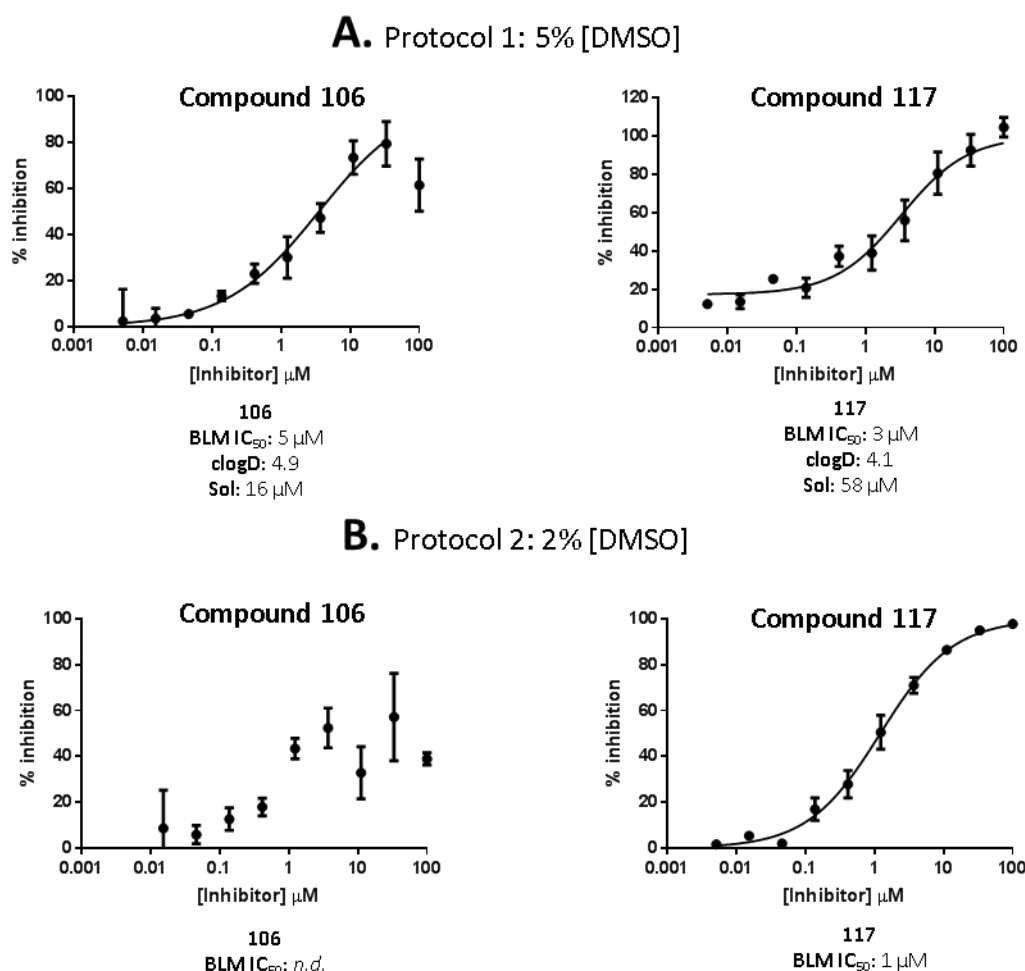
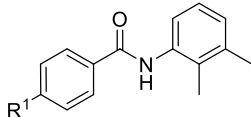
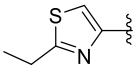
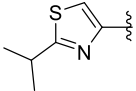
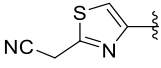
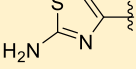
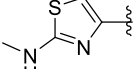
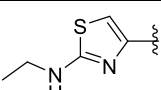
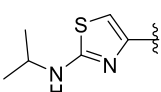
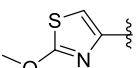
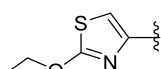
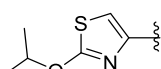
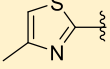
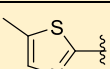
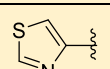
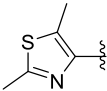
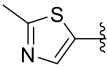
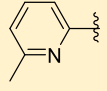
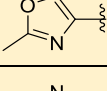
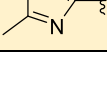


Figure 6.2. (A) IC_{50} curves of compound **106** and **117** conducted with protocol 1 (Table 6.1). (B) IC_{50} curves of compound **106** and **117** in the newer miniaturised assay conducted with protocol 2 (Table 6.1).

Due to the poor solubility of compounds containing a 2,3-dimethylaniline template, unreliable data points were generated from 10 μ M compound concentration and therefore an accurate IC_{50} determination was not possible (Table 6.5). Analogues of **116** synthesised to determine close SAR of the thiazole motif displayed similar or lower clogD values and were therefore not suitable for testing in this assay (Table 6.5). However, it was possible to analyse the IC_{50} curves to gain basic understanding of which motifs were likely to demonstrate activity when attached to a more soluble scaffold.

Table 6.5. Percentage inhibition between 1 and 100 μM of compounds assessing the thiazole ring SAR. The table attempts to aid understanding of compounds with potential BLM inhibitory activity in the DNA unwinding helicase assay Protocol 2 (Table 6.1). Highlighted in yellow are compounds that demonstrated activity between 3 and 30 μM . Inhibition values in red are values suggested to be affected by compound precipitation.

								
Compound	R ¹	clogD	% inhibition at substrate concentrations					BLM IC ₅₀ (μM)
			1 μM	3 μM	10 μM	30 μM	100 μM	
216		4.9	0	0	0	0	0	> 100
217		6.2	0	0	0	0	0	> 100
218		4.9	0	0	0	0	0	> 100
219		4.6	20	38	69	46	52	nd
220		4.9	0	0	8	13	19	> 100
221		5.3	0	0	0	0	21	> 100
222		5.7	0	0	0	0	20	> 100
226		5.3	0	0	0	6	17	> 100
227		6.1	0	0	0	0	0	> 100
228		5.7	0	0	0	0	0	> 100
230		4.9	0	10	10	13	18	nd
231		4.9	0	0	10	25	18	nd
232		4.8	11	32	25	35	29	nd

233		5.6	0	0	0	0	0	> 100
234		4.9	0	0	0	0	0	> 100
235		5.0	0	4	25	22	28	<i>nd</i>
236		4.2	0	13	48	38	41	<i>nd</i>
240		4.4	0	0	28	25	25	<i>nd</i>

Compounds **216–218** which assessed growth of the thiazole methyl showed flat inhibition curves suggesting these compounds do not bind and inhibit BLM helicase (Table 6.5). Similarly, the nitrogen-linked and oxygen-linked methyl, ethyl and isopropyl thiazoles (**220–222** and **226–228**) also displayed flat curves. These results suggest there is no space for growth from the 2-position of the thiazole. Compound **229**, which replaced the 2-methyl with a primary amine showed up to 69% BLM inhibition at 10 μM before precipitation was observed at higher concentrations.

Activity of closely related isosteres of the thiazole was assessed and **230**, **231**, **232**, **235**, **236** and **240** produced inhibition of BLM from at least a concentration of 10 μM but did not produce reliable IC_{50} curves due to them demonstrating similarly poor solubility to compound **106** (Table 6.5). Compound **233**, which contained a methyl at the C-5 thiazole did not produce any inhibition across all compound concentrations suggesting this modification causes complete loss of activity. Compound **234** where the thiazole is connected to the core at the 5-position rather than the 4-position was also inactive.

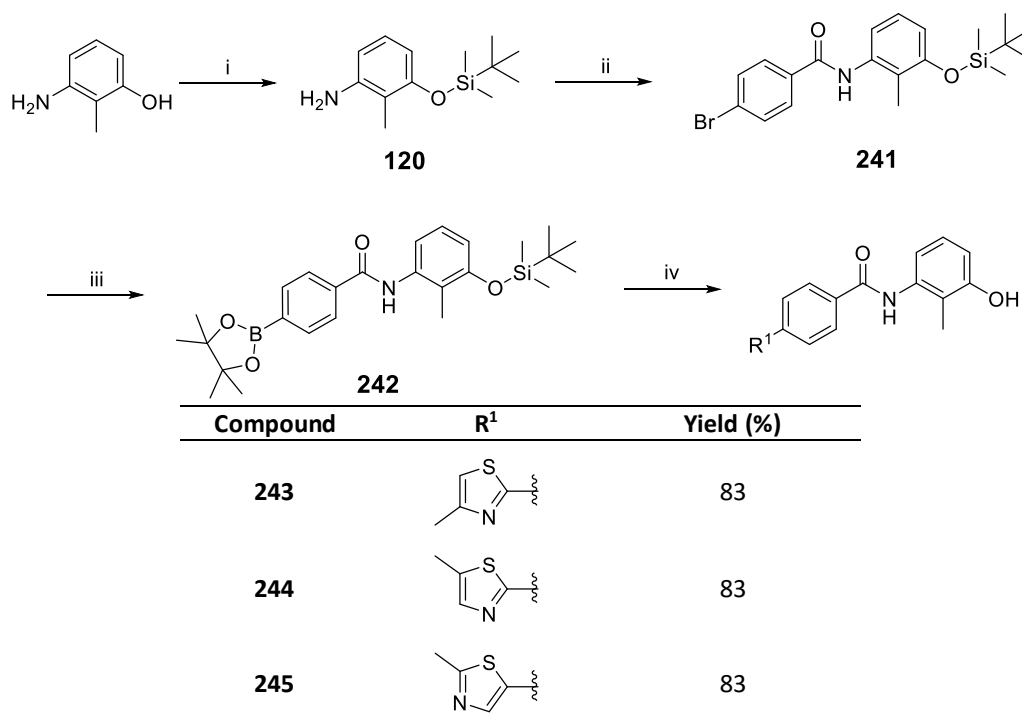
6.2.9. Synthesis of selected thiazole analogues with a more soluble scaffold

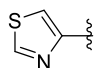
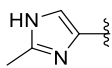
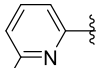
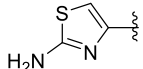
To ascertain the exact SAR profile of the methyl thiazole motif with the compounds presented in the previous section, selected hits were synthesised incorporating the phenol containing motif from compound **117** that demonstrated acceptable solubility. The motifs for resynthesis that were chosen based on the indication of significant activity at compound concentrations between 3 and 30 μM (highlighted in table 6.5).

The oxadiazole motif of compound **240** was not selected based on the observation that it had not shown improved inhibition over its oxazole isostere and would require a complex synthetic route. Additionally, the motif of **234** was synthesised to assess whether this core would also demonstrate a complete lack of activity on this newer scaffold thereby acting as a negative control when testing the hypothesis that the inhibition data presented in Table 6.5 is suitable to infer BLM activity.

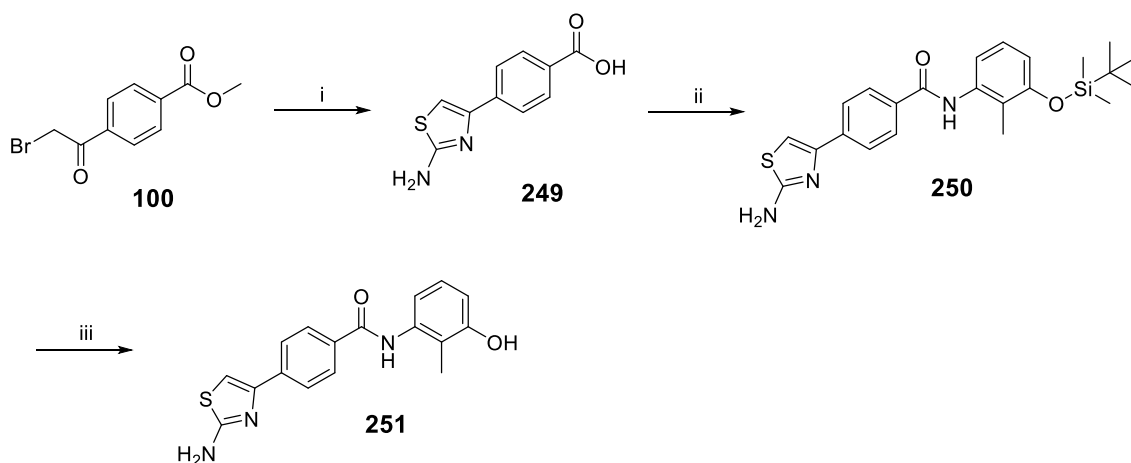
Various analogues would again be produced from late stage Suzuki-Miyaura cross-coupling. Synthesis began with TBS protection of 3-amino-2-methylphenol, followed by HATU amide coupling to 4-bromobenzoic acid and subsequent borylation to produce the key intermediate **242** (Table 6.6). All steps proceeded in good yields. Finally, various aryl bromides underwent Suzuki-Miyaura cross-coupling using standard microwave-assisted coupling with Pd(dppf)Cl₂ and sodium carbonate to produce the desired desilylated final compound. In general, Suzuki yields were improved when compared to the equivalent 2,3-dimethylaniline template and this was likely due to the improved solubility of the final compounds enabling an easier purification.

Table 6.6. *Reagents and conditions:* (i) TMSCl, DMAP, Et₃N, r.t., 18 h, 78%; (ii) 4-bromobenzoic acid, HATU, DIPEA, DMF, r.t., 16 h, 78%; (iii) B₂pin₂, Pd(dppf)Cl₂, KOAc, 1,4-dioxane, 100 °C, 16 h, 77%; (iv) appropriate aryl bromide, Pd(dppf)Cl₂, Na₂CO₃, 1,4-dioxane/water, MW, 120 °C, 20 min.



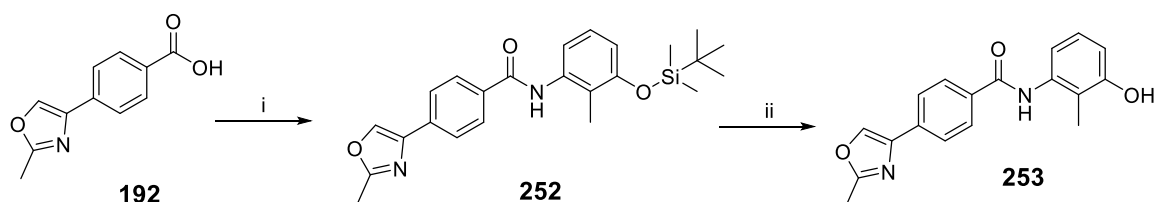
246		63
247		19
248		35
251		0

Compound **251** was attempted to be synthesised by Suzuki coupling. However, the reaction did not produce any of the desired product **251** (Table 6.6). Therefore, amino thiazole **251** was synthesised (Scheme 6.7) using the Hantzsch synthesis method employed in the synthesis of carboxylic acid **102** (Section 3.6.2). The low yield in the amide coupling step to synthesise **250** could be attributed to the poor purity associated with the protected phenol **120**.



Scheme 6.7. Reagents and conditions: (i) thiourea, MeOH, r.t., 1 h, then NaOH, H₂O/MeOH, r.t., 89%; (ii) **120**, HATU, DIPEA, DMF, r.t., 16 h, 30%; (iii) TBAF, THF, 0 °C, 5 min, then r.t., 10 min, 92%.

In a similar fashion to **251**, the oxazole derivative **253** was also synthesised *via* an amide coupling with subsequent deprotection (Scheme 6.8).

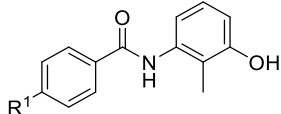
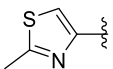
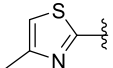
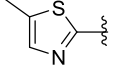
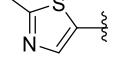
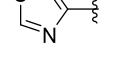
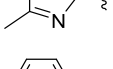
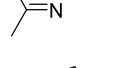
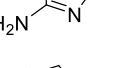
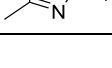


Scheme 6.8. Reagents and conditions: (i) oxalyl chloride, cat. DMF, DCM, r.t., 16 h, then **120**, DIPEA, DCM, 16 h, 68%; (ii) TBAF, THF, 0 °C, 5 min, then r.t., 10 min, 50%.

6.2.10. SAR of thiazole motif

Improved solubility in the helicase unwinding assay (Protocol 2) of the thiazole analogues described in Section 6.2.9 allowed accurate measurement of BLM inhibition in the miniaturised assay (Table 6.7). Compound **117** was used as a positive control and demonstrated similar activity to that described in Chapter 4.

Table 6.7. BLM inhibition of closely related analogues of **117** assessing SAR of the thiazole motif.

			
Compound	R ¹	clogD	BLM IC ₅₀ (μM)
117		4.1	4
243		4.1	16
244		4.1	34
245		4.1	0
246		4.0	6
247		3.3	30
248		4.2	11
251		3.9	6
253		3.4	7

SAR studies of the various methyl thiazole regioisomers reveal that those connected to the core at the 2-position (**243** and **244**) display reduced activity compared to the original hit motif connected at the 4-position going from 4 μM to 16 and 32 μM, respectively. Additionally, it has been confirmed that there is complete loss of activity when the methyl thiazole is connected to the 5-position (**245**). Interestingly, compound **246**, which bore an unsubstituted thiazole, had a similar activity profile to **117** suggesting

the methyl does not significantly contribute to inhibition. Inhibitor **251**, which replaced the methyl with an amino functionality, demonstrated comparable activity to **117**.

It had been shown in Section 5.4.1 that the change from a thiazole to an oxazole did not significantly cause a drop-in activity and this was confirmed again with compound **253**. Similarly, the imidazole motif (**247**) was also reconfirmed with this scaffold to cause a roughly 10-fold drop in activity. The pyridine isostere **248** displayed a roughly 3-fold loss in activity.

6.2.11. Summary

This section describes synthetic efforts to closely examine the SAR around the thiazole ring in attempts bring about improved potency for this inhibitor series. Following from the work in the previous chapter, the use of the 2,3-dimethylaniline core was maintained for these investigations but due to its high lipophilicity demonstrated poor solubility in a new miniaturised assay and consequently did not provide accurate IC₅₀ values. However, it was clear upon testing these compounds that extending the methyl of the thiazole by carbon, oxygen and nitrogen linkages resulted in considerable or complete loss of activity.

To ascertain SAR for various thiazole analogues that had demonstratable BLM inhibition with a 2,3-dimethylaniline core, compounds were resynthesised with a 2-methyl-3-hydroxy core analogous to inhibitor **117**. The inhibitory data shows that the thiazole motif still has a tight SAR profile as no substantial gains in potency were found. The results did demonstrate that the methyl of the thiazole can be removed or replaced by a primary amine with no significant loss of activity.

6.3. Design, synthesis and evaluation of analogues comprised of favoured motifs

6.3.1. Rationale

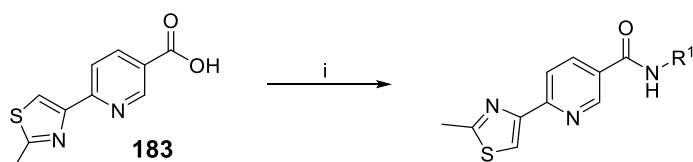
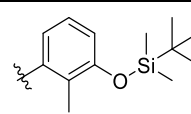
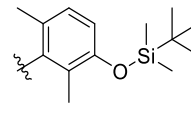
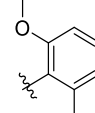
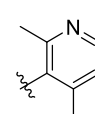
In the absence of knowledge of the binding site of this novel series of BLM inhibitors, a comprehensive SAR profile was undertaken resulting in the synthesis of 100 analogues

which aimed to improve potency and solubility to develop a chemical probe-like compound. Overall, it was found that some motifs encouraged noticeable improvements in calculated and measured physicochemical parameters, but various structural changes did improve the BLM inhibitory activity of the series. Given that various knowledge of the SAR of this series had been gained over this campaign, it was decided to design and synthesise analogues that would most closely fit the BLM chemical probe criteria set out in Section 4.1 in order to aid the development of cellular assays. The four analogues were synthesised with varied aniline moieties, maintained the thiazole ring found in the original hit but replaced the core phenyl ring with a pyridine ring to reduce lipophilicity.

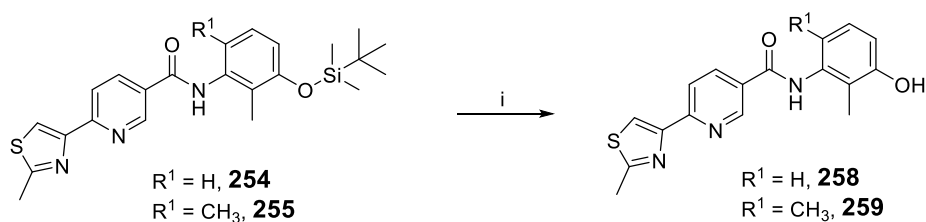
6.3.2. Synthesis

Amides **254–257** were formed from the key carboxylic acid intermediate **183** utilising acyl chloride forming conditions of oxalyl chloride/DMF and subsequent treatment with the appropriate aniline (Table 6.8).

Table 6.8. *Reagents and Conditions:* (a) oxalyl chloride, cat. DMF, DCM, r.t., 16 h, then (b) appropriate aniline, DCM, 0.5–16 h.

		
Compound	R ¹	Yield (%)
254		20
255		11
256		81
257		25

Subsequently, deprotection of **254** and **255** in standard TBAF conditions produced the phenols **258** and **259** in good yields.

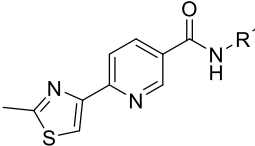
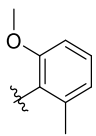
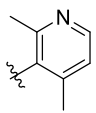
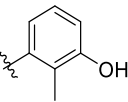
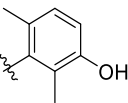


Scheme 6.9. Reagents and conditions: (i) TBAF, THF, 0 °C, 5 min, then r.t., 10 min: (**258**, 73%; **259**, 65%)

6.3.3. SAR

Compounds **256** and **257** are moderately potent BLM inhibitors that contain a core pyridine ring and demonstrate similar activity to their phenyl counterparts (Table 6.9). These inhibitors have good calculated physicochemical properties and resulted in marked improved solubility over some of the early hit optimisation compounds such as **103** (Table 6.9). In particular, **257** contains two pyridine rings and has excellent solubility making it a suitable chemical probe.

Table 6.9. BLM inhibition of compounds **256–259**.

								
Compound	R ¹	MW	HBD	HBA	clogD	tPSA (Å ²)	Sol (μM)	BLM IC ₅₀ (μM)
256		339	1	5	3.4	64	54	4
257		324	1	5	2.5	68	490	7
258		325	2	5	3.2	75	66	2
259		339	2	5	3.8	75	nd	5

6.3.4. Summary

Four compounds were prepared in an effort to incorporate potent and soluble moieties to establish probe compounds of BLM helicase that could be used to assist the development of in-house cellular assays. These compounds demonstrated moderate potency and good solubility with **257** demonstrating excellent solubility.

6.4. Discussion

The small- SAR exploration around the thiazole motif presented in Section 5.4 demonstrated that it may be difficult to identify a structurally different motif. It was therefore necessary to carefully evaluate the SAR of the methyl thiazole ring with small structural modifications. The compounds were designed to answer specific questions about the role of the thiazole motif in BLM inhibition concerning the significance of the heteroatoms within the ring structure, the preference of thiazole regioisomers and substituents at the 2- and 5- positions of the thiazole.

Similar to the previous exploration of the thiazole motif described in Section 5.4, the 2,3-dimethylaniline was used as the common core in order to maintain consistency to allow efficient and rapid synthesis. That scaffold enabled late stage diversification *via* Hantzsch synthesis and Suzuki coupling.

The consequence of using the 2,3-dimethylaniline scaffold in fixed core was that the inhibitors generally had clogD values above 4.5. This was not expected to be a problem as these values were similar to the early hit compound **106** which was known to have an IC₅₀ value of 3 μ M (Section 3.6). The current set of analogues described in this chapter were expected to have a similar solubility profile to **106**. Whilst various analogues that grew from the 2-position with alkyl chains possessed higher clogD values, it was expected that the addition of flexible side chains, and in some cases a polar oxygen and nitrogen atom, would not dramatically diminish solubility.

The miniaturised DNA unwinding assay, used to test compounds prepared in this chapter (Protocol 2, Table 6.1), had an improved assay detection window due to the use of more recently produced BLM protein and DNA substrate which allowed for a significant reduction in concentration of these components. However, the impact of this

newer miniaturised assay also containing reduced percentage of DMSO had caused unreliable data for this compound set from approximately 10 μM and 30 μM compound concentration. Previously, compounds with the 2,3-dimethylaniline core, presenting with clogD values around 5, were not found to precipitate at low concentrations, although analysis of this data has shown some examples that do indeed record lower inhibition at the 100 μM cut-off which ultimately did not dramatically affect their final IC_{50} value. In summary, compounds containing the 2,3-dimethylaniline motif had sufficient solubility in the previous assay format (Protocol 1, Table 6.1) to generate reliable data, but these analogues did not solubilise in Protocol 2 to a similar extent primarily due to the reduction in DMSO concentration from 5 to 2%.

In order to obtain reliable IC_{50} values, compounds were redesigned to contain a soluble core, in the form of the 3-amino-2-methylphenol from compounds **117**, which reduced clogD by roughly one unit. This strategy was successful and lead to the synthesis of more soluble compounds which did not precipitate in the miniaturised assay and reliable IC_{50} curves were determined.

Using the data generated in this chapter, various SAR observations around the thiazole motif can be made (Figure 6.3). The methyl of the thiazole motif does not contribute significantly to potency and can be removed with 1.5-fold loss of potency but a small reduction in clogD is also gained. This methyl was also replaced by an amino group which again displayed similar potency with the benefit of a small reduction in lipophilicity. However, extension of this methyl group to larger alkyl groups diminished activity of the compound. Similarly, the use of oxygen and nitrogen linkers to extend alkyl functionality was detrimental. This suggests that the methyl points towards a narrow space where only small groups such an amino group can be placed. Additionally, there may not be much scope for additional binding interactions as the hydrogen bond donor and acceptor capabilities of the amine did not lead to any improvement in potency.

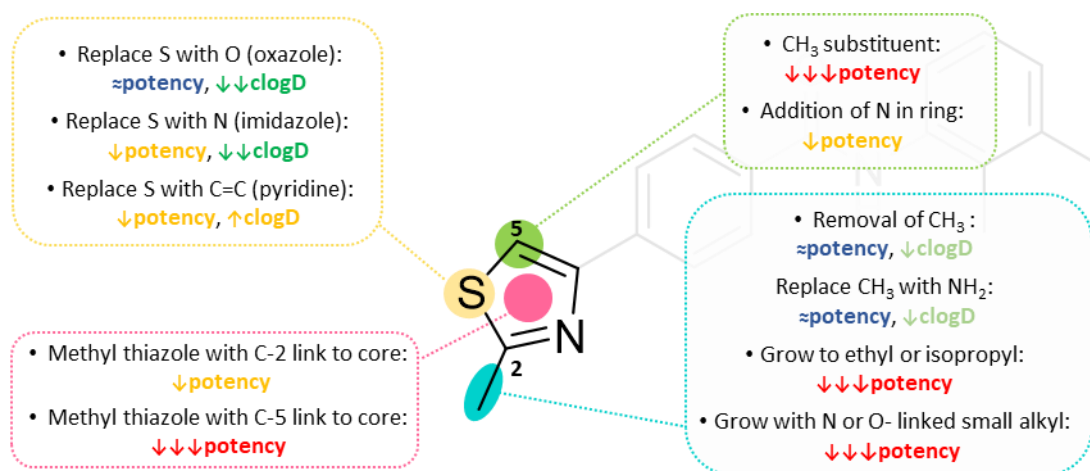


Figure 6.3. Summary of the SAR of the thiazole motif. \approx (blue): maintained potency; \downarrow : small reduction in potency (yellow), large reduction in potency (red), small reduction in clogD (lime), moderate reduction in clogD (green).

The C-5 of the thiazole, previously unsubstituted, was functionalised with a methyl group which diminished BLM inhibitory activity. One cause could be that the introduction of the methyl group may generate a twist in conformation preventing the compound from binding properly into a potentially narrow pocket. Further substitutions at this position are required to develop a better SAR profile and should be considered as potential future work. Such substitution could be accessed *via* thiazole ring forming methods.

Additionally, an oxadiazole analogue, placing a nitrogen at the C-5, was found to have less inhibitory activity than its isosteric oxazole, suggesting a 1,2,4-thiadiazole might not be superior to the thiazole. The data supporting this conclusion is based on the analysis of inhibition values of oxadiazole **240** at lower concentrations.

To ascertain the relevance of the appropriate orientation of the thiazole ring, two methyl thiazole regioisomers which were linked via C-2 and C-5 position were prepared. Compounds **243** and **244**, substituted to the core at the C-2 position, were found to be 4- and 8- fold less active against BLM compared to the C-4 linked thiazole. Therefore, this thiazole regioisomer could be followed up further as it presents two points, C-4 and C-5, for functionalisation. Compound **196**, a C-2 linked thiazole which lacked a methyl component, had demonstrated some inhibition at higher compound concentrations but an accurate IC₅₀ was not generated. Compound **245**, connecting the thiazole to the core

at the C-5 position, was found to be inactive. This result might suggest that the aromatic thiazole nitrogen needs to be neighbouring the carbon connected to the core phenyl ring for the compound to be active.

The oxazole **253**, imidazole **247** and pyridine **248** which possess aromatic nitrogen's between the methyl group and the connection to the core phenyl ring were all found to demonstrate BLM inhibitory activity. The oxazole and imidazole replacements reduce the clogD by 0.7 units and the oxazole maintains potency whilst a 7.5-fold drop in potency occurs with the imidazole. Additionally, the pyridine isostere results in a 3-fold drop in potency whilst maintaining a similar lipophilic character to the thiazole. This compound may be of interest as it is more accessible for further functionalisation at various positions allowing exploration and extension from vectors not possible with the thiazole motifs.

The SAR studies conducted around the thiazole motif closely examined the role of the 2-methyl substituent, the preferred ring systems and configuration of the aromatic motifs, and whether methylation of the C-5 position of the thiazole was possible. None of the compounds evaluated had any significant improvement in biological activity when compared to the original thiazole motif present in this series. Nonetheless, the knowledge that it is possible to remove the methyl or replace it with an amino functionality and replace the system with an isosteric oxazole without significantly disturbing the potency is useful, in particular, if there is a requirement to further reduce the lipophilicity of the compound. Furthermore, identifying that it may be possible to use a pyridine scaffold or a thiazole regioisomer as an alternative to explore different or multiple vectors coming off the aromatic ring system can aid further SAR campaigns for this series.

Invariably, the development of a chemical series involves optimising multiple physicochemical and biological properties simultaneously. Over the course of the SAR investigation conducted on this novel series, various of the explored motifs maintained the potency and had improved physicochemical properties, in particular with regard to solubility. Synthetic efforts were made to generate the four compounds presented in Table 6.9 to form early lead-like inhibitors of BLM helicase that could be utilised as

moderately potent chemical probes. These inhibitors pertain to the properties expected of an early-lead by demonstrating clogP values in the region of 3, molecular weight below 350, less than two hydrogen bond donors and less than five hydrogen acceptors, suggesting that they represent a series that has potential to be a high quality chemical probe or drug against BLM helicase. Unfortunately, the shallow SAR profile seen over the course of this investigation makes this series less tractable and medicinal chemistry optimisation on this series was halted until structural binding knowledge became available.

6.5. Conclusion

A set of analogues replacing the thiazole motif were synthesised and biologically evaluated to understand the SAR around this chemical space given that previous investigations had revealed the thiazole motif may sit in a relatively tight pocket. The SAR investigations revealed some alternative scaffolds that maintain potency and could be utilised to reduce lipophilicity of the inhibitor series or explore substituents and chemical growth from vectors not available in the original thiazole motif.

Having completed an extensive SAR campaign on this inhibitor series, four analogues were synthesised to represent BLM inhibitors with lead-like properties that can be used as preliminary chemical probes for cellular biology optimisation and investigation.

7. Analysis of the BLM helicase co-crystal structure

7.1. Introduction

A co-crystallisation strategy developed and implemented by Ms Xiangrong Chen successfully yielded multiple BLM inhibitors of Series G, discussed in Chapters 4–6, crystallised with a truncated form of BLM helicase (642-1070) — a novel discovery with human DNA helicases. Recently, an XChem fragment screen run at Diamond revealed a crystal structure with a fragment bound to human RECQL5 at an allosteric site that was subsequently submitted to the Protein Data Bank [PDB:5LBA]. However, no biochemical information, as of yet, has been published regarding this fragment. No other human DNA helicases have reported crystal structures of bound inhibitors.

The revelation of this novel BLM crystal structure bound to the amide inhibitor series, for which significant improvements in potency have not been possible, presented an opportunity for a structure-based drug discovery approach. The research detailed in this chapter describes analysis of the inhibitor binding site to assess whether it is a suitable site to develop a new generation of more potent BLM inhibitors based on the inhibitors described in Chapters 4–6.

7.2. Methods

7.2.1. Binding site analysis

The co-crystal complex of BLM₆₄₂₋₁₀₇₀ and **147** with a 3.1 Å X-ray resolution was primarily used for binding site analysis. The crystal structure was prepared using the ‘Protein Preparation Wizard’ panel of Maestro. In particular, using the “pre-process the Workplace structure’ tool, bond orders were assigned, hydrogen atoms were added, disulfide bonds were created, water molecules in a greater distance than 5 Å from heterogroups were deleted and Epik was used to generate appropriate ionisation and tautomeric states for heterogroups. The binding site was analysed using the Maestro workspace.

7.2.2. Druggability analysis

DoGSiteScorer employs a difference of Gaussian (DoG) filter to detect pockets on the protein surface. The resulting pockets can then be characterised by druggability scores based on three descriptors; depth, volume and relative number of apolar amino acids.²⁷⁹ The co-crystal complex of BLM₆₄₂₋₁₀₇₀ and **193** with a 3.1 Å X-ray resolution was submitted for analysis. Default parameters were set and the software was run using the website server.²⁸⁰ Pockets were considered druggable if they had a druggability score of 0.80. The pocket was identified by the presence of the ligand. Results were viewed in Pymol.²⁸¹

7.2.3. Sequence alignment

Sequences for each RECQ helicase were obtained from Uniprot.²⁸² The sequence position of the domains of each helicase was taken from Pfam.²⁸³ The five RECQ helicase sequences then underwent multiple sequence alignment using the ClustalW web tool at EMBL-EBI.

7.3 Results

7.3.1 Analysis of the inhibitor binding site

The X-ray crystal structure of **147**, **105** and **193** bound to BLM helicase revealed that this ligand series binds in a small opening between the core helicase D1 and D2 subdomains that form a pocket by the movement of the flexible zinc binding domain towards the D1 subdomain (Figure 7.1A) that we have termed the allosteric binding pocket.

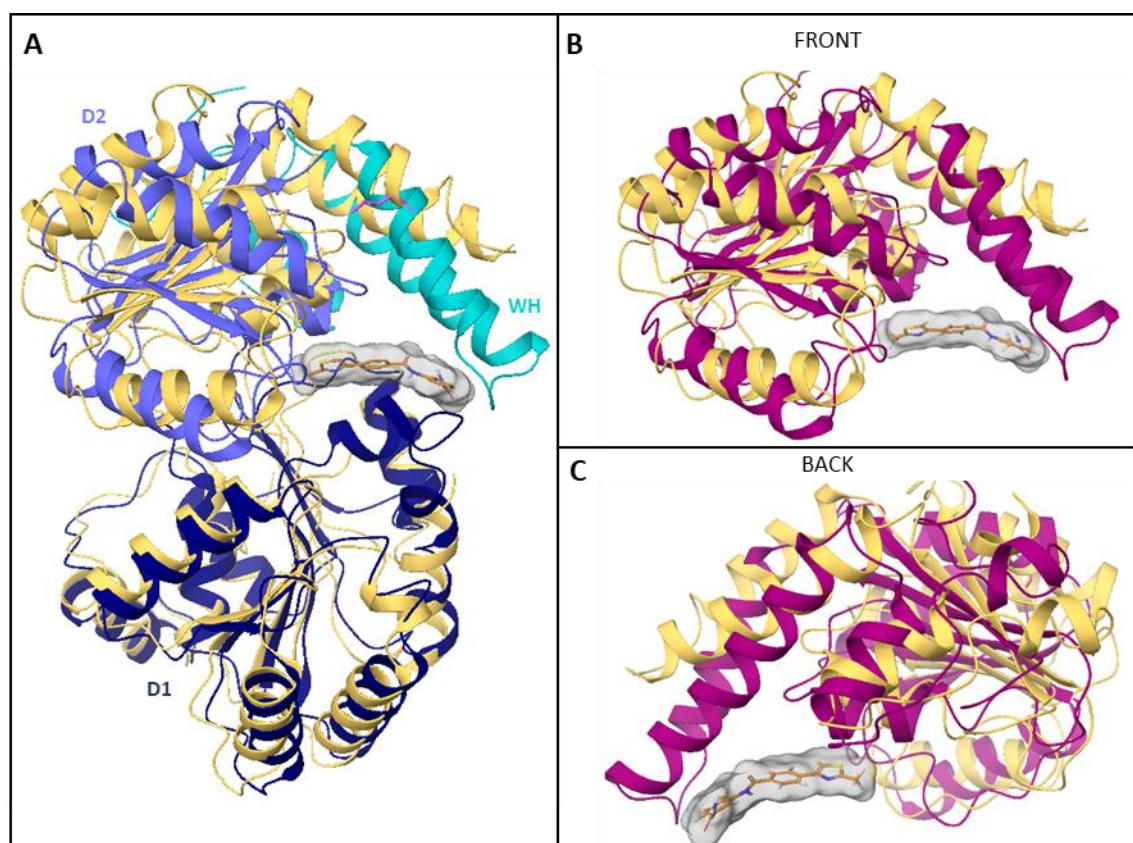


Figure 7.1. (A) Superimposition of BLM holoenzyme [PDB:4O3M] (gold) and BLM complex with **147** (orange sticks) consisting of the D1 core helicase domain (dark blue), D2 core helicase domain (sky blue) and the winged helix containing RQC domain (teal). (B) Front view of the superimposition of BLM holoenzyme [PDB:4O3M] (gold) and BLM complex (purple) with **147** (orange sticks). (C) Back view of the superimposition of BLM holoenzyme [PDB:4O3M] (gold) and BLM complex (purple) with **147** (orange sticks).

Structural comparison of the conformations of RecQ helicases that have been crystallised suggest that RecQ helicases can exist in multiple open conformations due to the flexibility between domains when they are not bound to DNA, but can only exist in one closed conformation that allows DNA binding.¹⁴⁰ A comparison of the ternary BLM structure with DNA (4O3M)¹⁴⁰ (closed conformation) and BLM structure without DNA (4CDG)¹⁴¹ (open conformation) for example highlights the mobility.

A comparison of the ternary BLM structure and DNA (4O3M) (closed conformation) with the co-crystal structure of bound **147** reveals the zinc binding subdomain extends roughly 9.6 Å towards the D1 subdomain (Figure 7.1A). This comparison also shows that the positioning of the D1 domain itself remains largely consistent (Figure 7.1A) but a ligand-induced shift occurs to the D2 and zinc-binding subdomains. In particular, a major

structural shift occurs to the two antiparallel-helices (994-1032) of the zinc binding subdomain (Figure 7.1B and C). It can be hypothesised that inhibitor binding locks the protein in a unique closed conformation to which DNA remains bound but does not undergo unwinding.

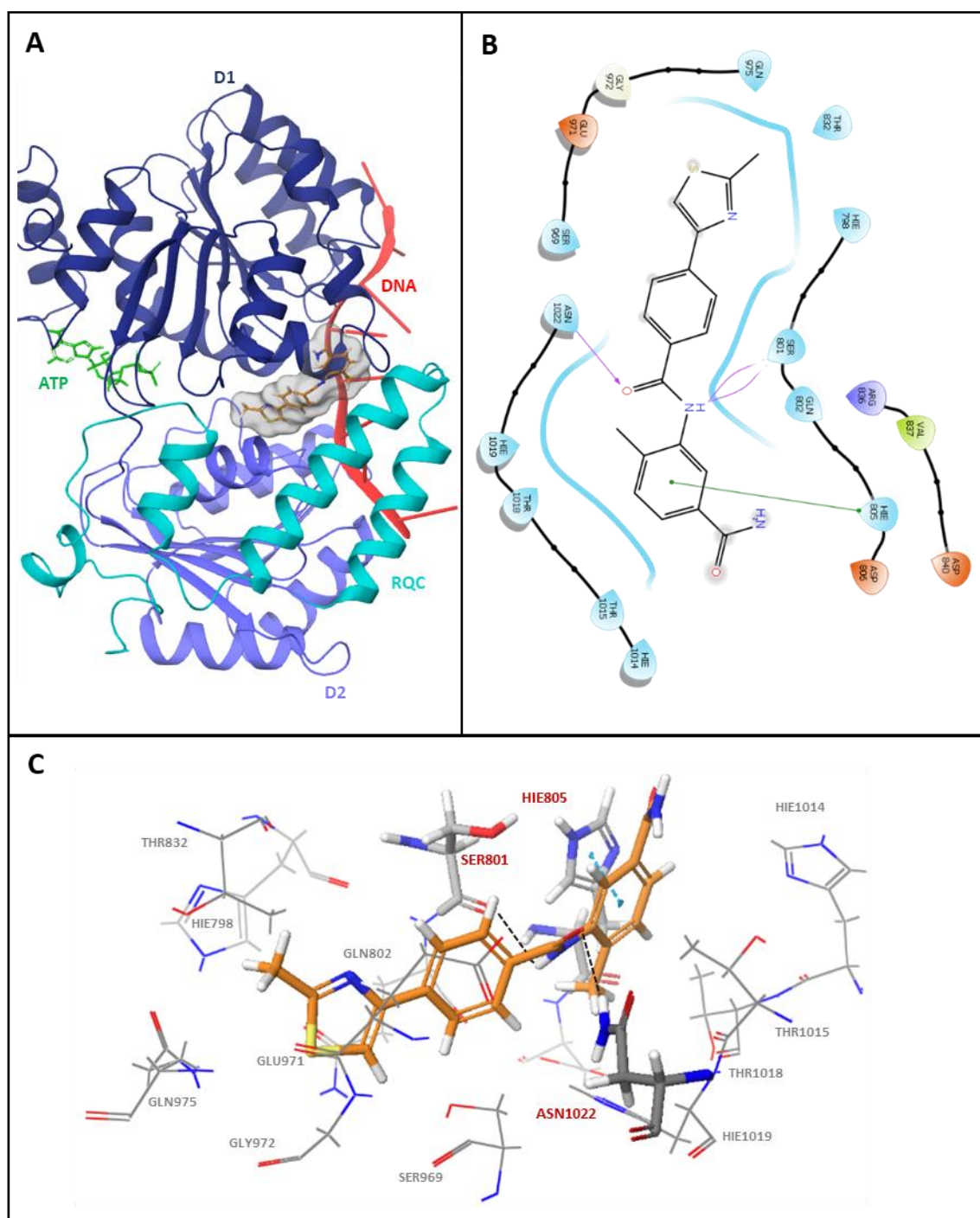


Figure 7.2. **(A)** X-ray crystal structure of **147** bound to BLM helicase (orange sticks) at an allosteric site situated between the D1 (dark blue) and D2 (purple) core helicase domains and the winged-helix domain (yellow). ATP (green sticks) and ssDNA (red) are also present. **(B)** Ligand interaction diagram for **147**. The inhibitor binds via two hydrogen bonds (purple arrows) and aromatic π -stacking (green arrows). Enzyme residues are coloured accordingly: polar (blue), negatively charged (red), positively charged (blue) and hydrophobic (green). **(C)** Inhibitor **147** bound to the BLM allosteric site is shown. The inhibitor carbon atoms are shown in green, hydrogen bonds are shown by black dotted lines and π - π stacking is shown by blue dotted lines.

7.3.2 Structural Analysis of the allosteric binding site

Within the SF2 superfamily of helicases, 13 characteristic motifs with high sequence conservation that are involved in ATP binding and hydrolysis, co-ordination between the ATP and DNA binding site, and in DNA binding, are present (described in Section 1.5.1). Members of this superfamily usually contain a conserved motif II, known as a DExD/H motif, and in fact, many of these helicase families are named on this basis, such as the RNA helicase families DEAD (DDX), DEAH and DExH (DHX).

Series G inhibitors bind in the allosteric binding pocket by forming a π -stacking interaction with His805 and two hydrogen bond interactions with Ser801 and Asn1022 of BLM helicase (Figure 7.2B and C). The neutral form of the His802 residue directly interacts with the aniline ring system of this inhibitor series (Figure 7.2C). Asn1022 forms a hydrogen bond by donating a proton from its side chain terminal amide to the amide oxygen in the inhibitor whilst the peptide bonded oxygen of Ser801 accepts a proton from the inhibitors amide nitrogen.

His798 of BLM helicase, a residue of the DEAH conserved motif II, is contained within the binding site 4.8 Å away from the thiazole motif of this inhibitor series. These important motif II residues located in the cleft between the two core D1 and D2 domains are involved in ATP binding and hydrolysis. Glu975 of motif VI, which sits just as close to this methyl is also involved in ATP binding and hydrolysis. Additionally, contained within the binding is site Thr832 which sits less than 4 Å away from the thiazole methyl group. This residue is a conserved motif III component which is primarily implicated in the coordination of ATP and the nucleic acid binding sites. Overall, the pocket largely consists of polar residues between the cleft of D1 and D2 subdomain, in addition to the residues His1014, Thr1015, Thr1018, His1019 and Asn1022 of the RQC domain that make up the remainder of the binding pocket.

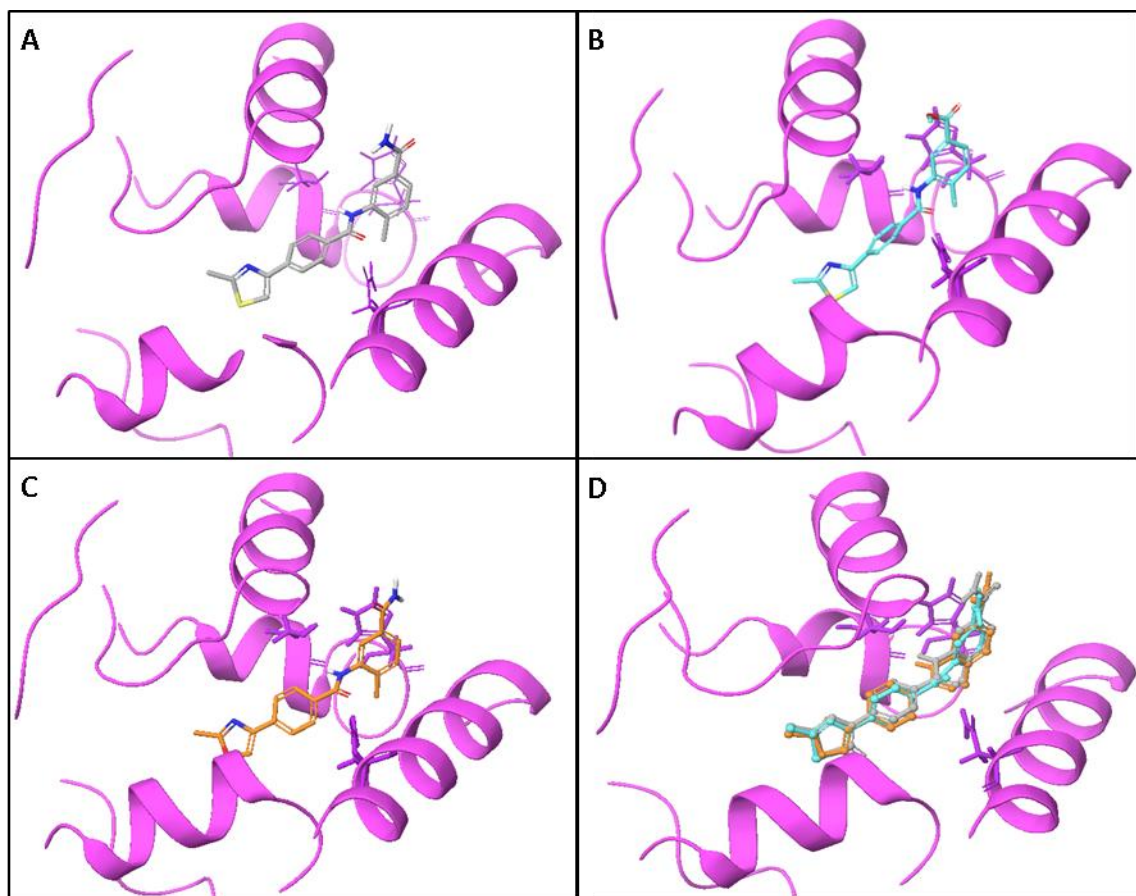


Figure 7.3. X-ray crystal structure of BLM (purple) in complex with (A) **147**, (B) **105**, (C) **193** and (D) superimposed structures of **147** (grey sticks), **105** (blue sticks) and **193** (orange sticks).

Co-crystal structures of BLM was achieved with three inhibitors; **147**, **105**, and **193** (Figure 7.3). The inhibitors demonstrate a consistent binding mode that is composed of 3 aromatic rings roughly in a plane with a perpendicular amide bond placed between two of these aromatic ring systems. The amide bond points this way to form crucial hydrogen bonds. The oxazole or thiazole motifs which bind between residues of the D1 and D2 subdomains overlay closely between inhibitors. The connecting core phenyl ring also overlay well but are more varied in their conformation. The aniline ring adopts consistent conformations with the *ortho* methyls pointing in the same directions. Large parts of the ring are exposed to solvent space and the *meta* substituents do not adopt consistent conformations.

7.3.3 Druggability analysis of the allosteric binding pocket

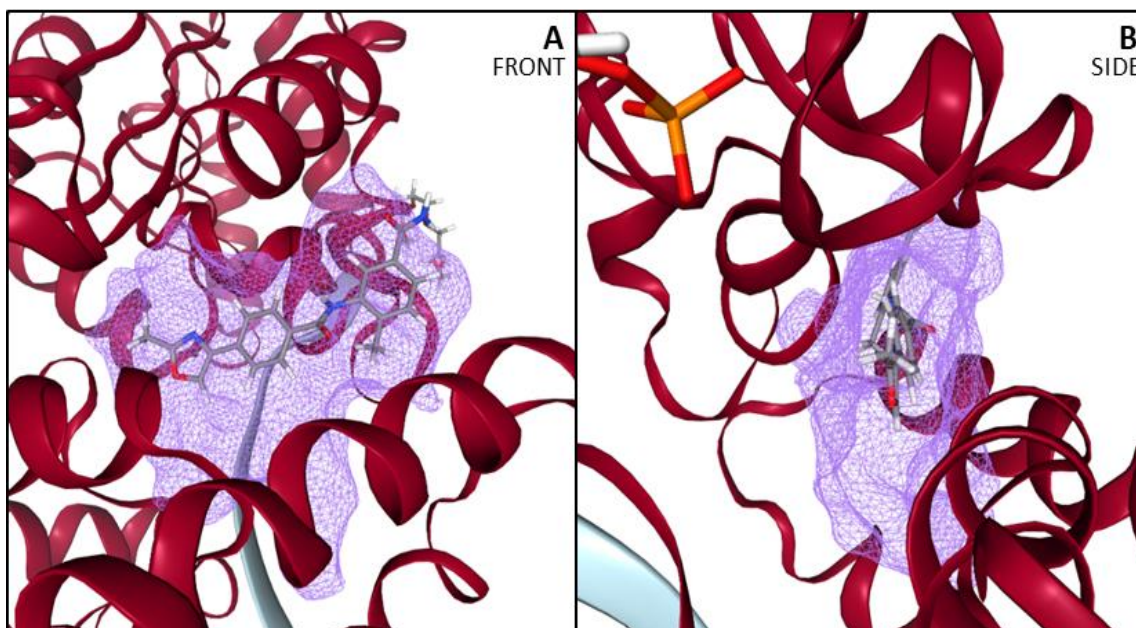


Figure 7.4. Druggability prediction by DoGSiteScorer of the binding pocket of **193** (grey sticks) in BLM helicase with the predicted druggable pocket represented by a purple mesh in the **(A)** Front view and **(B)** Side view. Made in Pymol.

Introduced in 2002, the concept of the ‘druggable genome’ related to genes that coded for proteins that could be modulated by small drug-like proteins.¹⁷ The druggability of a protein refers to therapeutic protein targets that have the ability to bind small molecules due to the presence of protein folds that favour interactions with small drug-like molecules. These small drug-like molecules will generally follow Lipinski’s Ro5.³⁴

The three dimensional structure of a target protein allows identification of cavities on its surface which can then be assessed for its likely druggability based on various parameters^{279,284–286}. To assess opportunities for adapting the inhibitor by adding extra chemical moieties within the binding pocket, a druggability analysis was conducted on the crystal structure of **193** using DoGSiteScorer (Figure 7.5).

Assessment of the pocket from a side on view reveals the pocket is narrow (Figure 7.4B) and the three aromatic rings contained in the inhibitor need to adopt conformations within the same plane. Whilst the *meta* and *para* positions of the aniline point towards solvent space, the *ortho* positions point towards a small pocket. The amide bond is vital in forming hydrogen bonds and is placed in the narrowest portion of the pocket. There

is opportunity for growth from certain vectors of the phenyl and thiazole/oxazole ring such as the C-5 of the thiazole should this not cause the aromatic rings to change plane and therefore not fit in the narrow pocket.

7.3.4 Selectivity analysis of the allosteric binding pocket

	D1										D2			RQC				
BLM	His798	Ser801	Gln803	His805	Asp806	Thr832	Arg836	Val837	Asp840	Ser969	Glu971	Gly972	Gln975	His1014	Thr1015	Thr1018	His1019	Asn1022
	H	S	Q	H	D	T	R	V	D	S	E	G	Q	H	T	T	H	N
RECQ1	H	S	Q	H	D	T	H	V	D	S	E	R	Q					
WRN	H	S	E	H	D	T	S	I	D	D	E	S	Q	K	F	Y	K	M
RECQ4	H	S	Q	H	D	T	R	T	D	S	E	R	Q					
RECQ5	H	S	Q	H	D	T	Q	V	D	S	A	G	Q					

Figure 7.5. Comparison of BLM binding-site sequence to other human RECQ helicases. In red are residues that are different from human BLM helicase. Sequence alignment performed in ClustalW2.²⁸⁷

A multiple sequence alignment was undertaken with EMBL-EBI ClustalW2 tool in attempt to assess the potential for selectivity at this site against other RECQ family members (Figure 7.5). As expected, binding site residues from the D1 and D2 subdomain showed a high degree of conservation with BLM but some differences existed for each RECQ family helicase. More importantly, only the closely related WRN helicase contains a RQC domain and the conservation for those residues forming the binding are very poor. Based on these findings, it was proposed that there was a high chance of achieving tool inhibitors that are selective for this binding-site against BLM helicase.

7.4. Conclusion

Analysis of the co-crystal structure of **147**, **105** and **193** demonstrated a novel binding mode that revealed a new allosteric pocket in BLM helicase. The inhibitors form key hydrogen bonds to BLM helicase through the amide bond moiety. Druggability analysis predict the binding site as druggable. The binding site is also composed of 5 residues from the zinc binding domain which can be targeted to improve selectivity of ligands. The binding pocket also offers multiple routes for exploration of further binding

interactions. These crystal structures offer new opportunities in the development of novel inhibitors of BLM helicase.

8. Computer-aided drug design

8.1. Introduction

The analysis of the allosteric binding site suggest it is a promising binding site for structure-based drug design approaches. The research detailed in this chapter describes the structure-based molecular design, organic synthesis and biological assessment to develop a new generation of more potent BLM inhibitors based on the inhibitors described in Chapters 4–6.

8.1.1. Structure Based Drug Design (SBDD)

Structure-based drug design (SBDD) is a prominent modern medicinal chemistry approach where computational modelling is used to aid hit identification and optimisation in drug discovery. SBDD employs the use of three-dimensional structural information of biological targets to enable the design of ligands containing the necessary features for high binding affinity at its binding pocket. The core hypothesis for this approach is that a ligands ability to interact with and exert biological effects on a protein is closely related to its ability to possess molecular interactions with a binding site on this protein. Prominent SBDD methods include *de novo* drug design, molecular docking, structure-based virtual screening (SBVS) and molecular dynamics (MD) and have seen increasing use and advancement as biomolecular spectroscopic strategies such as X-ray crystallography and NMR have progressed hand-in-hand. Unlike ligand-based drug design (LBDD) methods, which employ properties based on the chemical diversity of ligands with appropriate experimental parameters in processes such as QSAR modelling and pharmacophore generation, SBDD focus on the analysis of molecular recognition events such as molecular interactions and binding energies.²⁸⁸

Docking is a prediction of a ligand's conformation and orientation within the target pocket. Molecular docking is one of the most common used methods in SBDD as it can predict with a substantial degree of accuracy, the conformation and binding energies of ligands in binding sites.²⁸⁹ Algorithms that can model the chemical force fields generated by both ligand and protein, such as the Merck molecular force field (MMFF94)²⁸¹²⁹⁰ and

the assisted model building with energy refinement (AMBER)282 force field,²⁹¹ enable prediction of molecular interactions. As a result, it is possible to generate a score indicating how well a particular ligand binds when computationally placed into a pocket on the protein. Together, this can allow a SBVS as it is possible to rank docked ligands in their predicted binding modes. Whilst these predictions may not necessarily reflect the results obtained from biological screens, it enables medicinal chemists to reduce the number of compounds that must be synthesised in order to achieve high potency. Through the use of pharmacophores and other constraints, specific interactions and structural features necessary for good binding of lead compounds can be sought to identify molecules that may bind in a similar way.²⁹²

Concerning hit optimisation of inhibitor series whose binding mode have been deduced by X-ray crystallography or NMR, molecular docking can be utilised to increase the efficiency and effectiveness of wet science by aiding selection of molecular targets for chemical synthesis and subsequent biological evaluation. Usually, this is achieved in an iterative process that relies on experimental data as feedback to optimise future generations of compounds with improved properties. In general, such a structure-based strategy consists of the following steps: (i) compound selection; (ii) molecular target preparation; (iii) molecular docking; and (iv) post-docking analysis.²⁹³

To perform a virtual screen, a virtual library must be available for screening. In the case of lead optimisation, libraries are likely needed to be constructed using computational and combinatorial tools to form targeted libraries for the specific pocket of the protein target. Additionally, these libraries should be enriched with compounds that can be easily synthesised and are drug-like. Virtual libraries have the advantages of saving time and money by reducing the number of compounds to be experimentally tested and to eliminate compounds which are unlikely to bind to the target in addition to improving the drug discovery success rate.

8.1.2. Utilising structure-based drug discovery to develop potent tools of BLM helicase

As discussed in Chapter 6, a challenge encountered during the development of Series G was that the observed SAR profile was shallow and no clear interpretations to aid significant potency gains could be deduced. By having three co-crystal structures of Series G inhibitors solved, the acquired structural knowledge should allow the design of compounds with better potency. The strategy described in this chapter is based on a SBVS strategy for which libraries of analogues of this inhibitor series were screened against the pocket to identify inhibitors with improved binding affinity.

Analysis of the allosteric binding pocket shows the part of the pocket deeper into the protein, where the methyl thiazole and oxazole motifs were bound, was identified as an area where a number of ligand binding interactions could be gained. This area was preferred for exploration over the aniline ring which pointed to the solvent space from the *meta* and *para* positions, to the amide bond which was involved in two key hydrogen bond interactions and to the core phenyl ring for which it would be preferable to not contain substituents.

8.1.3. Aims

The aim of this chapter was to undertake computational experiments in order to facilitate the design of Series G analogues with an improved potency profile. More specifically, replacements for the thiazole motif would specifically be assessed whilst the remaining scaffolds of the inhibitor series would remain consistent.

The steps undertaken to achieve this aim were as follows:

4. Creation of a synthetically accessible structurally diverse focussed virtual library and subsequent virtual screening, post-docking analysis, and compound selection.
5. Synthesis and biological evaluation of selected hits.

8.2 Methods and Results

The hit optimisation efforts conducted on Series G did not produce an inhibitor with the desired IC_{50} of less than $0.1\ \mu\text{M}$ despite the synthesis of over 160 analogues. A virtual screening strategy was implemented to find such desired gains in potency through the identification of diverse motifs that can interact with additional residues within the binding pocket or alternative chemical starting points that would be easier to optimise. Due to time constraints in this project, only one iteration of docking, synthesis and biological evaluation could be performed.

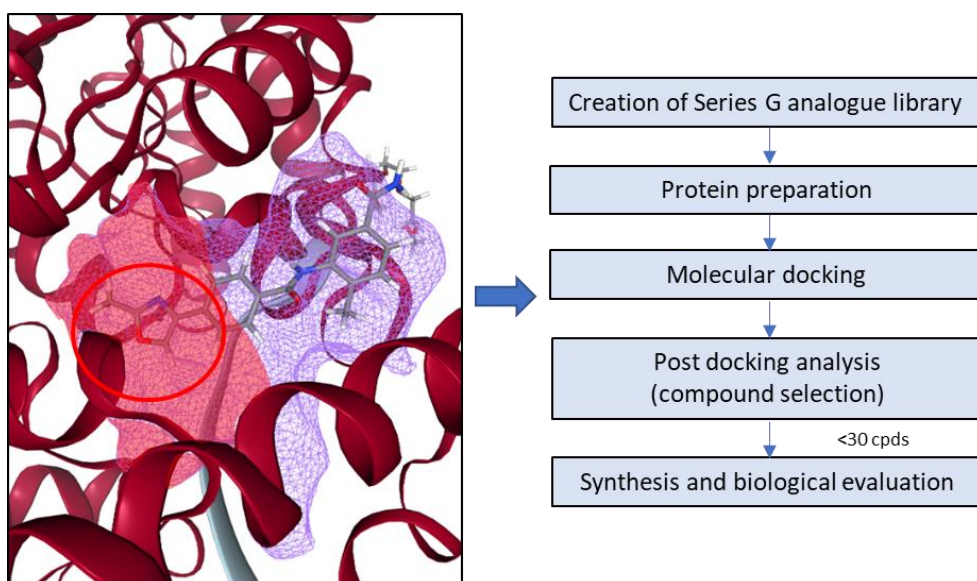


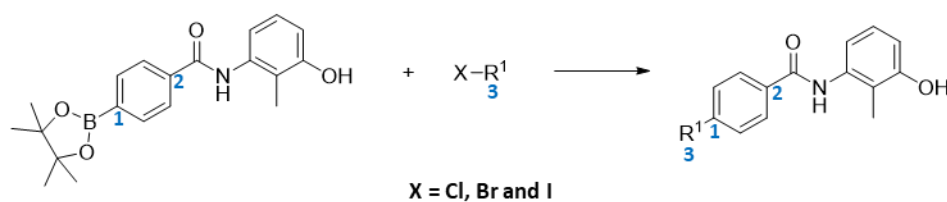
Figure 8.1. The computational design sequence followed to enable synthesis and biological evaluation of Series G analogues.

Figure 8.1 describes the steps implemented to perform this virtual screening strategy. A compound library set was generated (see below) that maintained the core phenyl, amide and aniline moieties of Series G, and contained diverse aromatic systems in place of the thiazole. The molecular docking would ensure that these consistent parts of the molecule still maintained vital hydrogen bonding and pi-stacking interactions. It was decided that the analogue **117** would be used as the template when synthesis compounds to allow direct comparison to the results of the analogues discussed in Section 6.2.10.

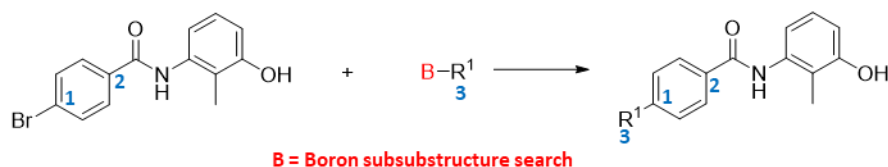
8.2.1. Compound selection

The SAR exploration of the thiazole motif conducted in Chapters 5 and 6 primarily utilised Suzuki-Miyaura coupling chemistry which enabled late-stage diversification. In other cases, a late-stage amide coupling step was required if certain motifs were not suitable for Suzuki chemistry. In order to elaborate our molecule from this point using previously reliable chemistry, the synthetic space was explored by the use of virtual chemical reactions that can generate predicted synthetic products. As before, aryl derivatives connected to the core phenyl ring *para* to the amide bond were of interest (Figure 8.2). Additionally, *ortho* linked aryl derivatives and bicyclic derivatives connecting aryl rings to the 3 and 4-position of the core phenyl were also considered to explore the pocket from these vectors.

1), 2) and 3) Suzuki-Miyaura reaction



4) Suzuki-Miyaura reaction



5) Amide-coupling reaction

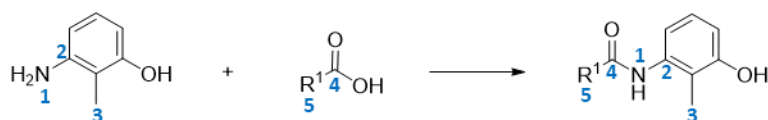


Figure 8.2. Use of ChemAxon Reactor to generate virtual analogue libraries. Numbers represent the mapping of atoms with this tool to ensure appropriate transformation.

An in-house library, termed EDEN, which contains approximately 300,000 building blocks from preferred commercial suppliers, was filtered for compounds containing appropriate aryl halides, aryl borate and benzoic acid derivatives that could be

appropriately reacted against the Series G intermediates, with the use of Canvas substructure searching.

The ChemAxon Reactor tool was used to produce the desired library of analogues by conducting virtual reactions. The 'initial reactant', which is the molecule desired to be modified was placed in its desired reaction scheme (Figure 8.2) where reactions are expressed as transformations in mapped atoms and bonds between reactants and product. The initial reactant was then reacted with the imported sdf file containing the halide, borate derivative or carboxylic acid library to produce analogue libraries of Series G compounds.

As described in Section 3.2.1, Lipinski, PAINS and SMARTScreen filters were applied to ensure final compounds remained in drug-like space for this series. Additionally, duplicates and compounds of excessive cost were then removed. This led to the production of a library of 8,030 analogues of **117**.

Compounds were then imported into Schrodinger Maestro (v2017.1) and were prepared using Ligprep. Ligand minimisation was achieved with orthogonal partial least squares 3 (OPLS3) force field and protonation and tautomer states were applied using Epik at pH 7.0 (+/-1).

8.2.2. Molecular docking

In addition to compound preparation, protein preparation and molecular docking were carried out in Schrödinger. The Glide SP docking algorithm was used for all docking runs. Glide is a popular docking tool that is routinely used in SBVS with significant success.²⁹⁴ The tool predicts binding modes with acceptable accuracy and has contributed to the discovery of potent drug-like ligands in many cases.

8.2.2.1. Preparation of protein file

The co-crystal complex of BLM₆₄₂₋₁₀₇₀ and **147** with a 3.1 Å X-ray resolution was chosen for molecular docking calculations. The crystal structure was prepared using the 'Protein Preparation Wizard' panel of Maestro. In particular, using the "pre-process the Workplace structure' tool, bond orders were assigned, hydrogen atoms were added,

disulfide bonds were created, water molecules in a greater distance than 5 Å from heterogroups were deleted and Epik was used to generate appropriate ionisation and tautomeric states for heterogroups.

8.2.2.2. Controls

Given that a significant number of compounds of Series G had been synthesised and experimentally assessed for biological activity, and that the library created for screening were analogues of this series, a control set was used to gauge a better understanding of the model. For positive controls, only compounds that demonstrated a complete IC₅₀ curve were chosen, as some compounds had shown poor solubility and were therefore not suitable for use as controls. For negative controls, only compounds with acceptable predicted solubility were selected, and for this series, it had been found that those with a clogP below 4 and tPSA above 50 were genuine inactives and not limited by their solubility *in vitro*. Overall, 48 compounds were selected, and this included 32 positive controls and 16 negative controls.

The 'Receptor Grid Generation' tool of Glide was used to define the binding site using the native ligand **147**. The scaling factor and partial charge cut-off of van der Waals radius scaling were 0.25 Å and 1 Å, respectively. The generation of this grid assists the ligands to bind in more than one possible conformation. As the controls were from the same series and expected to have similar binding modes, constraints were set to ensure the amide bond of the inhibitor underwent hydrogen bonding with Ser801 and Asn1022 and loose spatial constraints ensure that the three aromatic rings were also binding in their expected region. Other parameters such as site, rotatable groups and excluded volume were default.

Molecular docking in using Glide SP of the 48 control ligands of Series G was carried out with the generated receptor grid. To soften the potential for nonpolar parts of the ligands, the 'scaling of van der Waals radii' was used with scaling factor of 0.6 and partial charge cut-off of 0.15.

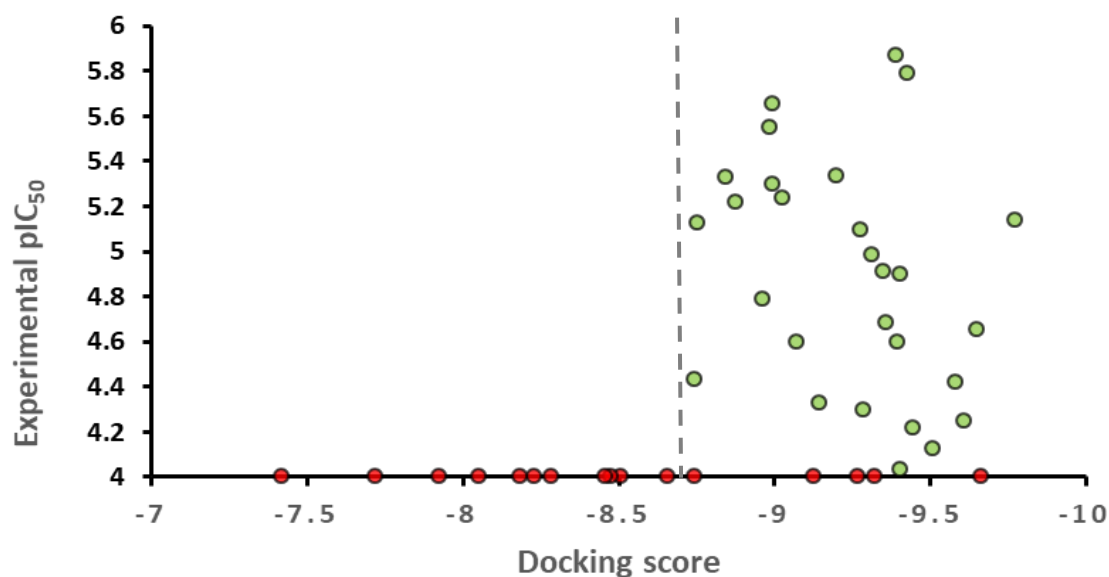


Figure 8.3. Graph correlating docking score with experimental potency for control compounds. Green are positive controls and red are negative controls.

The molecular docking carried out using 48 Series G compounds at their binding site produced Glide docking scores which were compared to their experimental affinity (Figure 8.3). The main observation found from the control run was that 11 of the 16 inactive compounds had a docking score below -8.7, whilst all active compounds had a binding affinity above this threshold, demonstrating a clear cut-off between active and inactive compounds. However, no correlation between experimental affinity and binding affinity for biological active compounds was seen. The data itself was not suitable for the identification of such correlation as there was little variation in data (i.e. up to 2 log units). The results for this control run show that the *in silico* model may predict inactivity but it may be more difficult to correlate Glide binding affinity to experimental activity. Therefore, not only was the Glide docking score to be used, but other factors such as conformation, strain and specific residue binding should be looked at when selecting compounds for experimental evaluation.

8.2.2.3. Virtual screening

As with the previous section, the 'Receptor Grid Generation' tool of Glide was used to define the binding site using the native ligand **147** and constraints were set to ensure

the amide bond of the inhibitor underwent hydrogen bonding with Ser801 and Asn1022. Additionally, a tight spatial constraint was set to ensure the aniline ring remained consistently in place for all compounds screened to ensure that the binding energy differences correlated primarily due to the regions of the molecule which were different i.e. where the phenyl thiazole motif lay.

In this study, Glide SP was used for the molecular docking of 8,730 analogues of **117** and included the controls described above. The force field used for the docking was OPLS3. The highest-scoring docking pose (orientation plus conformation) returned for these hits were overlaid with the BLM protein complex. The top 1000 compounds were manually analysed and inhibitors which demonstrated large surface clashes and inappropriate amide bond angles were discarded. The remaining inhibitors were clustered into 14 groups and compounds were then cherry-picked from each cluster based on their docking scores, calculated physicochemical properties and the amino acid contacts they made. In total 31 compounds were chosen for assessment as inhibitors for BLMs. This included 18 inhibitors required Suzuki coupling for synthesis and represented a relatively diverse group of contacts with amino acids of the pocket were chosen for synthesis (Figure 8.4) and 13 inhibitors that required synthesis by amide coupling were also chosen.

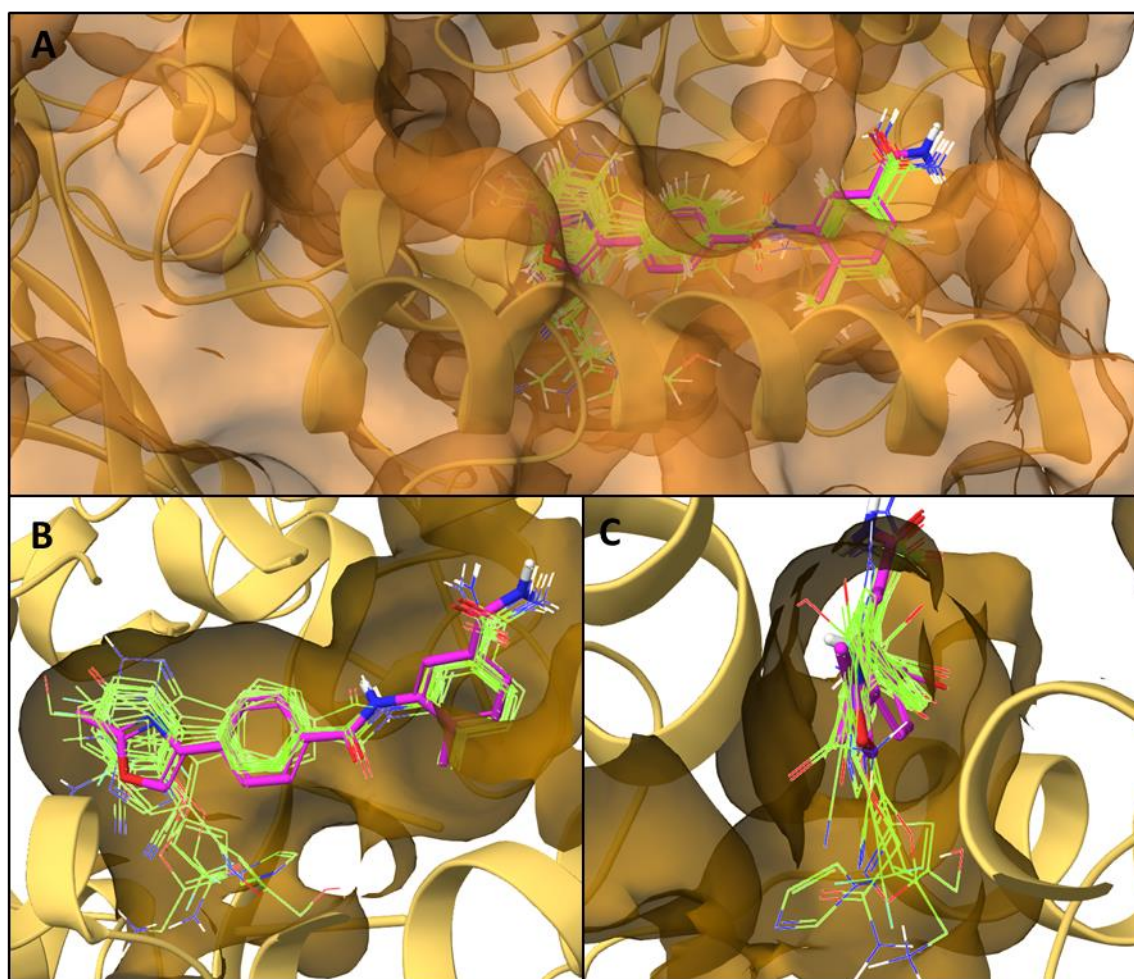
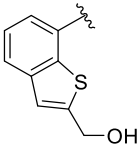
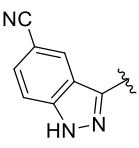
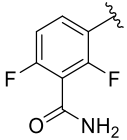
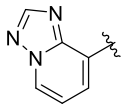
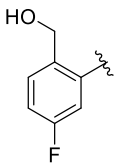
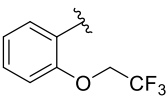
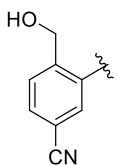
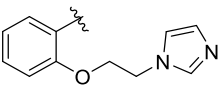
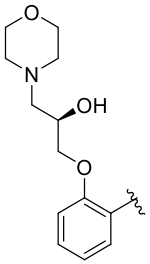
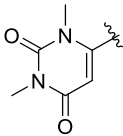
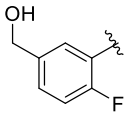
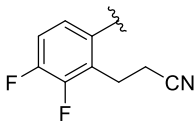
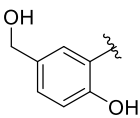
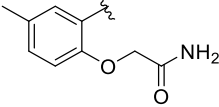
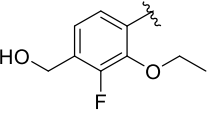
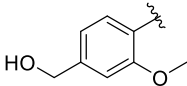
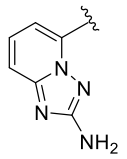
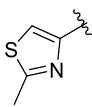
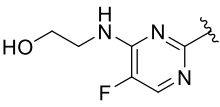


Figure 8.4. Overlay of crystallised inhibitor **147** with the selected 18 hits to be synthesised for experimental activity evaluation shown with **(A)** full surface view, **(B)** back surface view and **(C)** side surface view.

Overall, these compounds had much better docking scores than the control compounds and the various representatives of clusters accessed distinct parts of the pocket allowing us to explore if novel interactions could be gained. For example, Figure 8.4 depicts 18 analogues that are *para*-linked to the core phenyl ring with substituted aryl moieties that access different parts of the binding pocket. The structure and docking energies of these compounds are available in Table 8.1, and these *para*-linked hits were found to have the best docking scores. Hits that required amide coupling were generally biaryl rings (Table 8.3) and those with *meta*-linked aryl rings (Table 8.4) had lower docking scores but were selected so that we could explore novel chemical space. Overall, all analogues chosen for synthesis demonstrated better binding energies than the control thiazole motif.

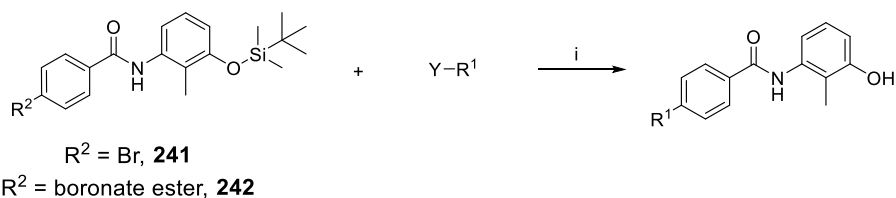
Table 8.1. Docking energies of the selected 18 compounds for synthesis and control **117**.

Cpd	R ¹	Docking score	Cpd	R ¹	Docking score
260		-11.55	270		-11.17
261		-11.45	271		-11.16
262		-11.40	272		-11.10
263		-11.38	273		-11.08
264		-11.28	274		-11.07
265		-11.27	275		-11.06
266		-11.26	276		-11.02
267		-11.25	277		-10.99
268		-11.21	117 (Control)		-9.65
269		-11.19			

8.2.3. Synthesis

The computational design process led to the selection of 18 compounds that were to be synthesised by Suzuki coupling and 8 compounds that were to be synthesised by amide coupling. For compounds **260–277** (Table 8.2), standard Suzuki coupling conditions presented previously for this series of compounds that also remove the protecting TMS group in one step was utilised to synthesise a Suzuki library through small scale reactions (30 mg starting material). Yields varied from 8–62%, with failure of reactions to go to completion being the main contributing factor for those with yields below 30%.

Table 8.2. *Reagents and conditions:* (i) appropriate aryl bromide, Pd(dppf)Cl₂, Na₂CO₃, 1,4-dioxane/water, MW, 120 °C, 20 min.



Cpd	R ²	Y	Yield (%)	IC ₅₀ (μM)	Cpd	R ²	Y	Yield (%)	IC ₅₀ (μM)
260	Br	B(OH) ₂	32	>100	269	Boronic ester	Cl	37	41
261	Br	B(OH) ₂	9	>100	270	Boronic ester	Br	8	>100
262	Boronic ester	Br	46	>100	271	Boronic ester	Br	62	>100
263	Boronic ester	Br	42	>100	272	Boronic ester	Br	22	>100
264	Boronic ester	Br	11	>100	273	Boronic ester	Br	38	>100
265	Boronic ester	Br	46	>100	274	Boronic ester	Cl	8	>100
266	Boronic ester	Br	36	39	275	Br	B(OH) ₂	34	>100
267	Br	B(OH) ₂	11	>100	276	Boronic ester	Br	41	>100
268	Boronic ester	Br	32	>100	277	Boronic ester	Br	22	>100

Compounds **286–293** were synthesised after HATU coupling of **120** with the appropriate benzoic acid derivatives followed by TBAF deprotection (Table 8.3).

Table 8.3. *Reagents and conditions:* (i) HATU, DIPEA, DMF, r.t., 16 h; (ii) Pd(dppf)Cl₂, Na₂CO₃, 1,4-dioxane/water, MW, 120 °C, 20 min.

120				
R ¹	(i) Cpd, Yield (%)	(ii) Cpd, Yield (%)	Docking score	IC ₅₀ (μM)
	278 , 72%	286 , 58%	-10.53	>100
	279 , 64%	287 , 44%	-10.51	>100
	280 , 78%	288 , 3%	-10.20	>100
	281 , 72%	289 , 58%	-10.01	>100
	282 , 92%	290 , 47%	-9.83	>100
	283 , 57%	291 , 59%	-9.74	>100
	284 , 85%	292 , 37%	-9.52	>100
	285 , 27%	293 , 20%	-9.00	>100

Compounds **295–299** were of interest as they had shown good docking scores and were connected to the core phenyl ring at the *meta* position rather than the *para* position as is usually the case with this series (Table 8.4). Whilst these compounds were in the

library through a virtual amide coupling, it was decided to synthesise these compounds by Suzuki coupling due to the significantly reduced cost of the Suzuki substrates over the benzoic acid derivatives. Amide coupling of 3-bromobenzoic acid to **120** was achieved with HATU conditions to produce **294** in good yields. Suzuki coupling with the appropriate boronic acids resulted in the five examples used to assess growth of this vector.

Table 8.4. Reagents and conditions: (i) *m*-bromobenzoic acid, HATU, DIPEA, DMF, r.t., 16 h, 78%; (ii) appropriate aryl bromide, Pd(dppf)Cl₂, Na₂CO₃, 1,4-dioxane/water, MW, 120 °C, 20 min.

Cpd	R ¹	Yield (%)	Docking score	Ic ₅₀
295		31	-10.41	>100
296		58	-10.37	>100
297		83	-10.23	>100
298		5	-9.41	>100
299		5	-9.39	>100

8.2.4. Biological activity of the novel compounds

Of the 31 compounds selected for synthesis, two were determined to be active *in vitro* although the activities measured were not better than those derived in Section 6.3. The biological screening of the computationally designed compounds **260–277** (Table 8.2) and **286–293** (Table 8.3) did not reveal any inhibitors with improved BLM inhibitory activity. With the exception of **266** and **269**, inhibitors that replaced with the thiazole

motif with alternative aromatic ring systems did not have an IC_{50} below 100 μM . Inhibitors **266** and **269** demonstrated weak potency with IC_{50} values of 39 and 41 μM , respectively. Additionally, inhibitors **286–293** of which most were chosen to assess the possibility of using bicyclic aromatic systems to explore the pocket were also inactive. Similarly, those compounds that extended of the *meta* position were also found to be inactive.

8.3. Discussion

The structure-based drug design process involved a virtual screening approach of a designed analogue library of Series G compounds. A manual analysis of the binding pocket using the Schrodinger workspace and a druggability analysis of the binding pocket with DoGSiteScorer revealed a large cavity where the thiazole motif of the inhibitor series resides. Within this cavity, a large number of residues were present that were not in close contact to the thiazole motif of Series G. As a result, the screening of a large number of synthetically accessible analogues was expected to produce hits that would possess molecular interactions with these residues lying deeper into this cavity. As a result, the top docked compounds were clustered and a few examples from each cluster was chosen based on their binding to these novel residues. These residues include Ala833, Thr832, Val837, Glu971, Ile947, Glu976, Lys968 and Ser969. Overall, a diverse group of hits were chosen based on their ability to interact with different residues of this area of the binding pocket.

The 18 compounds chosen in Table 8.1 was the result of manual selection of the top 100 hits after clustering. These hits were aryl moieties linked to the core phenyl ring at the *para* position. These compounds were mostly derivatives of phenyl rings whilst some examples of bicyclic heterocycles and six membered heterocycles were also present. It was found that the substituents generally contained hydrogen bond acceptors and donors, usually in the case of an alcohol group. Given the number of highly polar residues within this cavity, it is not surprising that hydrogen bond interactions were predicted for these compounds which led to their subsequent high docking scores. The synthesis of these compounds occurred *via* straightforward Suzuki couplings and the resultant biological evaluation revealed no BLM inhibitory activity in most cases except

for **266** and **269**. These two hits interacted with different residues according to their docking pose but were less than 10-fold potent than the best hits in these series. There were various compounds that were structurally similar to **266** which demonstrated no activity below 100 μM . However, these two compounds do show that it may be possible to use a phenyl ring or pyridazine ring system in place of 5-membered heterocycles which can allow for multiple vectors of growth.

13 compounds from the amide coupling library with good binding energies were also chosen for synthesis as they allowed exploration of the binding site from new vectors. 8 of these were to be synthesised *via* amide coupling, of which 7 of these represented substituted bicyclic aryl moieties. Such systems allowed exploration of the pocket below the core phenyl and thiazole rings whilst also exploring areas of the binding pocket where the thiazole resides with various functional groups. Additionally, 5 compounds which contained aryl rings linked to the core phenyl ring now at the *meta* position were also chosen as they also explore similar areas of the binding pocket. However, it was more cost efficient to synthesise these hits *via* Suzuki coupling rather than purchase the amide coupling partners. Ultimately the 13 compounds exploring regions from different vectors of the core phenyl ring were found to be inactive.

48 compounds, described in Chapters 4–6, were used as positive and negative controls to validate the docking model. The results showed a clear cut-off between inactive and active compounds demonstrating that the model can predict compounds that are inactive. However, no correlation of biological activity and binding energies were demonstrated which showed that the compounds with the best binding energies may not necessarily be the most potent as the docking model was not able to predict this. As a result, the top 200 docked compounds were initially assessed to select hits and this was then pushed to the top 1000 compounds to widen the scope of compounds. Rather than select the top 30 compounds with the best binding energies, compounds that showed good binding energy but were interacting with novel residues in the binding pocket were then selected for synthesis. It must be noted that **260** was the best docked compound and was chosen for this reason.

With the exception of **266** and **269**, the 31 compounds selected for biological evaluation from the virtual screen demonstrated no biological activity. The hits selected for synthesis represented a diverse group of scaffolds to replace the methyl thiazole motif of the hit Series G. The results show that the docking model was not successful in identifying more potent hits despite the selected hits demonstrating better docking binding energies over control hits.

An alternative idea would be to create libraries based around generating interactions with components of the RQC domain which is the area that is largely induced, and by forming stronger interactions with this component will further lock the protein in this ligand-induced conformation.

8.4. Conclusion

In conclusion, computational chemistry strategies such as Library creation and molecular docking allowed a structure based virtual screening strategy against BLM helicase against analogues of the inhibitor Series G. The docking scores and poses of these drug-like compounds were used to select analogues that were synthetically accessible and were found to generate novel interactions with residues in the ligand binding pocket. The subsequent synthesis and biological evaluation revealed these inhibitors were not more potent than previously described inhibitors of this series.

9. Conclusions and Future Work

Due to the high cost of modern drug discovery, it is imperative that high quality research is undertaken to identify and validate potential cancer targets to reduce overall attrition rates in the clinical phase. High quality tool inhibitors provide an excellent mechanism to test therapeutic hypotheses regarding novel biology and potential targets. The DNA damage response represents a rich potential source of anticancer targets, as inhibiting this network can potentially provide chemotherapeutic options possessing greater therapeutic windows and more selective targeting of tumour cells than traditional chemotherapy. This project was initiated with the aim of designing and characterising tool inhibitors of helicase involved in DNA damage response as this class of protein is significantly involved in DNA damage repair, yet chemical matter targeting such helicases is underrepresented.³⁶

The helicase of primary focus was BLM helicase, a RECQ helicase whose members are all highly involved in DNA damage repair. BLM is especially involved in homologous recombination and other processes of DNA double strand break repair. The primary aim of the project was to identify chemical probes that can be used for detailed mechanistic biochemical studies of BLM in order to aid elucidation of its roles in DNA damage repair.

In an attempt to produce a functional fit-for-purpose probe of BLM helicase, the recently published first-in-class probe, ML216, which was reported to display low micromolar potency, selectivity, and *in vitro* on-target activity, was selected as a starting point. In this thesis, optimisation of four cores of this molecule were attempted with the aim to improve both potency and ADMET properties, with the primary focus on the probes' aqueous solubility profile. The employed strategies took into consideration previously reported SAR and involved introducing solubilising groups, reducing planarity and lowering lipophilicity. Biological activity evaluations of ML216 and reported analogues revealed significantly reduced activities of these inhibitors, which were likely due to their poor solubility. Analogues designed in-house did not produce compounds with demonstrable potency and solubility, even to a moderate extent. Subsequent biological investigations revealed ML216 was binding to DNA rather than BLM helicase, rendering ML216 not fit-for-purpose as a probe. As a result, medicinal chemistry optimisation on

this series was discontinued. Multiple examples of poor chemical probes exist³³ and they are polluting the scientific literature due to bad practice that does not implement reproducible and robust science, resulting in a waste of time and resources. In fact, the use of ML216 to modulate BLM activity is still being described in current research papers.²⁹⁵ Therefore, it was of vital importance to design a probe fit-for-purpose helicase BLM helicase.

The post-HTS triage of 672 actives from a NIH qHTS screen against BLM helicase aided discovery of a novel hit series of BLM inhibitors. PubChem Bioassay, a database that was created to bridge the gap between HTS data generation and data sharing, facilitates the early discovery process, particularly in academia where HTS is difficult to implement. The post-HTS triage conducted in this thesis focussed on using computational and heuristic methods to identify hits with preferred physicochemical, structural and selectivity parameters. The successful post-triage campaign led to the identification of a hit series possessing moderate potency, acceptable physicochemical parameters, demonstratable SAR and orthogonal binding confirmation.

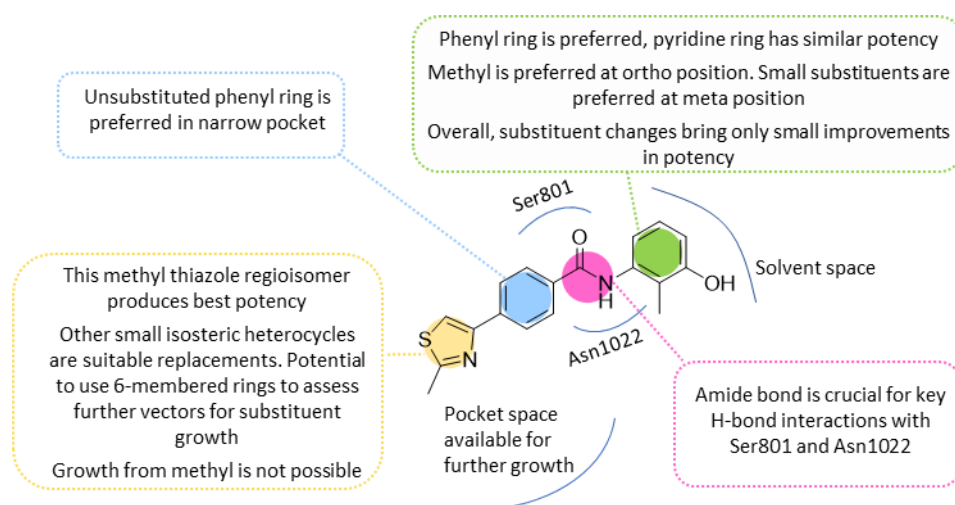
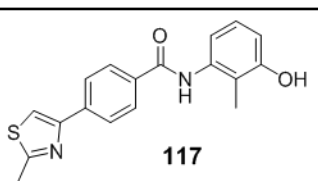


Figure 9.1. SAR summary of Series G at a novel allosteric binding site of BLM helicase.

In the absence of structural and binding site knowledge, the work in Chapters 4–6 describe the optimisation of the amide hit **99** towards a probe-like compound possessing improved potency and solubility. The SAR summary of this inhibitor series is represented in Figure 9.1. Invariably, the development of a chemical series involves optimizing multiple physicochemical and biological properties simultaneously. The

development of over 100 analogues of this series ultimately did not reveal major gains in potency but physicochemical parameters and aqueous solubility was impacted through the introduction of more polar functionalities. A tight SAR profile was observed for this series and is demonstrated by the fact that the starting hit compound possesses a similar scaffold to the best probe-like hits. The conversion of the core phenyl ring to a pyridine ring and substituent changes to the right-side aniline ring positively impacted the solubility profile. The subsequent identification of a crystal structure of BLM bound to these inhibitors led to the implementation of a single iteration of a structure-based approach, wherein virtual analogues were docked to aid future design. However, the chosen analogues did not reveal compounds with improved potency.

Chemistry		Potency	
Structure	Discrete chemical species Characterised spectroscopically Defined structure with reproducible synthetic method	Bio-chemical	Helicase unwinding assay: 3 μM Other series members have 1 μM MST biophysical: binding proven at 10 μM
Stability	Defined purity Defined stability No non-specific chemical reactivity	Cellular	Not yet undertaken
Solubility	Solubility: 66 μM . Other members also show good solubility	SAR	Many related structures with similar activity
Permeability	Permeability assessment not yet undertaken	In vivo	In vivo DMPK assessment not yet undertaken

Context		 117
Genetic methods	Not yet undertaken	
Target	Not yet undertaken. Sister chromatid exchange assays undergoing	
Application	Many related structures with similar activity	
Availability	Can be available in accessible quantities and use without restrictions	

Selectivity	
Profile	No activity against RECQ5 and UVRD Selectivity against other RECQ helicase not yet undertaken
Inactive analog	Closely related analogs have shown no activity in helicase and MST assay
Other chemotypes	No other chemical classes with similar activity
Chemo-informatics	PubChem data of original hit demonstrates this is hit series is highly selective

Figure 9.2. Summary of the probe-like criteria of compound **117** of the inhibitor Series G in the context of the fitness-factors described by Workman and Collins.³²

Overall, the extensive SAR campaign has led to the development of multiple analogues that demonstrate some probe-like properties, of which some have been extensively characterised biologically. Table 6.9 describes four examples compounds of this series that could be used as chemical tools targeting BLM helicase. Described in Figure 9.2,

compound **117** was an early compound that has undertaken further biological studies and is an example of a compound in this series that meets many of the fitness factors for a probe described by Workman and Collins (Section 1.3). Permeability and *in vivo* pharmacokinetic determinations should be determined for select members of this series.

Furthermore, various cellular and target-based assays should be undertaken. A sister chromatid exchange assay that determine increased levels of sister chromatid exchange due to BLM inhibition is an example to determine the downstream effects of such blockage. The use of cell proliferation assays followed by colony survival assays to determine whether the inhibitor is cytostatic or cytotoxic should also be undertaken. As BLM is implicated in the replication stress response, measuring DNA synthesis and mitogenic capacity in proliferative cells can provide further proof that BLM inhibition leads to replication stalling, restart failure and DNA damage at the fork. These studies can lead to assays that can aid target validation such as cell-based experiments with the inhibitors and DNA damaging agents or other DNA repair inhibitors to assess the effect of such combination therapy. Finally, these tools can be used in cell-based studies to assess genetic based synthetic lethality and find potential synthetic lethal partners.

The discovery of a crystal structure demonstrating this novel series of inhibitors binding at an allosterically induced site can aid efforts to target DNA repair helicases involved in cancer. Targeting the ATP-binding site would most likely lead to non-selective inhibitors whilst the nucleic-acid binding site is not considered druggable due to its polar and groove-like pockets. Allosteric inhibitors of helicases therefore present the best opportunity to produce potent and selective inhibitors. Alongside the recently deposited crystal structure of the RNA helicase BRR2, the co-crystal structure of compounds **147**, **105** and **193** with BLM helicase are unique examples of human helicases that are structurally enabled for drug discovery. The field of helicase drug discovery would greatly benefit from more structurally enabled targets as producing compounds with sub-micromolar potency against these proteins is uncommon. Overcoming the bottleneck between hit identification and crystallography is now possible and its implementation has resulted in the discovery of an allosteric binding fragment against RECQ5 [PDB:5LBA]. Conducting such a fragment screen against BLM helicase can reveal

fragments that bind at novel allosteric sites which can potentially be amenable to small molecule binding and aid the development of sub-micromolar inhibitors. In this project, only one iteration of analogue docking was conducted. The same principles can be applied to generate and dock analogues of the inhibitors targeting other parts of the Series G scaffold. Alternatively, *de novo* design can be used to guide further SAR on this series. RECQ helicases has been reported to have a degree of structural 'plasticity' due to the flexibility of their domains. It may be possible to apply molecular dynamics (MD) simulations to assess how this flexibility impacts the binding site and the ability of inhibitors to enter it. To generate more potent hits, a virtual screen can be conducted against this allosteric pocket.

Analysis of the literature reveals that none of the probes targeting human helicases meet the criteria required to be considered of high-quality. Series G possesses various qualities to meet such criteria and further optimisation and biological characterisation can impact the field significantly as a high-quality chemical probe of BLM helicase can be used to understand the role of this protein in DNA repair and assess potential synthetic lethality protein partners. Furthermore, it can help jump start the field of human helicase drug discovery by demonstrating the need for high-quality probes against this important protein class in DNA repair.

10. References

1. Nguyen, G. H. *et al.* A small molecule inhibitor of the BLM helicase modulates chromosome stability in human cells. *Chem. Biol.* **20**, 55–62 (2013).
2. Kim, S. *et al.* PubChem Substance and Compound databases. *Nucleic Acids Res.* **44**, D1202–13 (2016).
3. Ferlay, J. *et al.* Cancer incidence and mortality worldwide: Sources, methods and major patterns in GLOBOCAN 2012: Globocan 2012. *Int. J. Cancer* **136**, E359–E386 (2015).
4. UK, C. R. Worldwide cancer statistics. *Cancer Res. UK* **2012**, 2012–2015 (2014).
5. Blair, L. P. & Yan, Q. Cancer Genetics and Epigenetics: Two Sides of the Same Coin?. *DNA Cell Biol.* **31**, S49–S61 (2012).
6. Stratton MR Campbell PJ, F. P. A. The cancer genome. *Nature* **458**, 719 (2009).
7. Hanahan, D. & Weinberg, R. A. Hallmarks of cancer: the next generation. *Cell* **144**, 646–74 (2011).
8. Hanahan D, W. R. The hallmarks of cancer. *Cell* **100**, 57–70 (2000).
9. DeVita, V. T. & Chu, E. A history of cancer chemotherapy. *Cancer Res.* **68**, 8643–53 (2008).
10. Hoelder, S., Clarke, P. A. & Workman, P. Discovery of small molecule cancer drugs: Successes, challenges and opportunities. *Mol. Oncol.* **6**, (2012).
11. Hoelder, S., Clarke, P. A. & Workman, P. Discovery of small molecule cancer drugs: successes, challenges and opportunities. *Mol. Oncol.* **6**, 155–76 (2012).
12. Druker, B. J., Guilhot, F. & O'Brien *et al.*, S. G. Five-year follow-up of patients receiving imatinib for chronic myeloid leukemia. *N. Engl. J. Med.* **355**, 2408–17 (2006).
13. Gajria, D. & Chandarlapaty, S. HER2-amplified breast cancer: Mechanisms of trastuzumab resistance and novel targeted therapies. *Expert Review of Anticancer Therapy* **11**, 263–275 (2011).
14. O'Connor, M. J. Targeting the DNA Damage Response in Cancer. *Mol. Cell* **60**, 547–60 (2015).
15. Hughes, J. P., Rees, S., Kalindjian, S. B. & Philpott, K. L. Principles of early drug discovery. *Br. J. Pharmacol.* **162**, 1239–49 (2011).
16. DiMasi, J. A., Grabowski, H. G. & Hansen, R. W. Innovation in the pharmaceutical industry: New estimates of R&D costs. *J. Health Econ.* **47**, 20–33 (2016).
17. Hopkins, A. L. & Groom, C. R. The druggable genome. *Nat. Rev. Drug Discov.* **1**, 727–30 (2002).
18. Mayr, L. M. & Bojanic, D. Novel trends in high-throughput screening. *Current Opinion in Pharmacology* **9**, 580–588 (2009).
19. Hann, M. M. *et al.* Molecular obesity, potency and other addictions in drug discovery. *Medchemcomm* **2**, 349 (2011).
20. Scannell, J. W., Blanckley, A., Boldon, H. & Warrington, B. Diagnosing the decline in pharmaceutical R&D efficiency. *Nature Reviews Drug Discovery* **11**, 191–200 (2012).
21. Sams-Dodd, F. Target-based drug discovery: Is something wrong? *Drug Discovery Today* **10**, 139–147 (2005).
22. Waring, M. J. *et al.* An analysis of the attrition of pharmaceutical companies. *Nat. Publ. Gr.* **14**, 475–486 (2015).
23. Plenge, R. M. Disciplined approach to drug discovery and early development. *Sci. Transl. Med.* **8**, (2016).
24. Workman, P. & Collins, I. Probing the Probes: Fitness Factors For Small Molecule Tools. *Chem. Biol.* **17**, 561–577 (2010).
25. Bunnage, M. E., Chekler, E. L. P. & Jones, L. H. Target validation using chemical probes. *Nat. Chem. Biol.* **9**, 195–199 (2013).
26. Arrowsmith, C. H. *et al.* The promise and peril of chemical probes. *Nat. Chem. Biol.* **11**, 536–541 (2015).
27. Bunnage, M. E., Chekler, E. L. P. & Jones, L. H. Target validation using chemical probes. *Nat. Chem. Biol.* **9**, 195–199 (2013).
28. Filippakopoulos, P. *et al.* Selective inhibition of BET bromodomains. *Nature* **468**, 1067–73 (2010).
29. Nicodeme, E. *et al.* Suppression of inflammation by a synthetic histone mimic. *Nature* **468**, 1119–1123 (2010).
30. Austin, C. P., Brady, L. S., Insel, T. R. & Collins, F. S. MOLECULAR BIOLOGY: NIH Molecular Libraries Initiative. *Science (80-.)*. **306**, 1138–1139 (2004).
31. Oprea, T. I. *et al.* A crowdsourcing evaluation of the NIH chemical probes. *Nat. Chem. Biol.* **5**, 441–7 (2009).
32. Workman, P. & Collins, I. Probing the probes: fitness factors for small molecule tools. *Chem. Biol.* **17**, 561–77 (2010).
33. Blagg, J. & Workman, P. Choose and Use Your Chemical Probe Wisely to Explore Cancer Biology. *Cancer Cell* **32**, 9–25 (2017).
34. Lipinski, C. A., Lombardo, F., Dominy, B. W. & Feeney, P. J. Experimental and computational approaches to estimate solubility and permeability in drug discovery and development settings. *Adv. Drug Deliv. Rev.* **46**, 3–26 (2001).
35. Bouwman, P. & Jonkers, J. The effects of deregulated DNA damage signalling on cancer chemotherapy response and resistance. *Nat. Rev. Cancer* **12**, 587–598 (2012).
36. Pearl, L. H., Schierz, A. C., Ward, S. E., Al-Lazikani, B. & Pearl, F. M. G. Therapeutic opportunities within the DNA damage response. *Nat. Rev. Cancer* **15**, 166–180 (2015).
37. Helleday, T., Petermann, E., Lundin, C., Hodgson, B. & Sharma, R. A. DNA repair pathways as targets for

- cancer therapy. *Nat. Rev. Cancer* **8**, 193–204 (2008).
38. Curtin, N. J. DNA repair dysregulation from cancer driver to therapeutic target. *Nat. Rev. Cancer* **12**, 801–817 (2012).
 39. Hanahan, D. & Weinberg, R. A. Hallmarks of cancer: The next generation. *Cell* **144**, 646–674 (2011).
 40. Lord, C. J. & Ashworth, A. The DNA damage response and cancer therapy. *Nature* **481**, 287–94 (2012).
 41. Jackson, S. P. & Bartek, J. The DNA-damage response in human biology and disease. *Nature* **461**, 1071–8 (2009).
 42. Maréchal, A. & Zou, L. DNA damage sensing by the ATM and ATR kinases. *Cold Spring Harb. Perspect. Biol.* **5**, a012716 (2013).
 43. Lovejoy, C. A. & Cortez, D. Common mechanisms of PIKK regulation. *DNA Repair (Amst)*. **8**, 1004–1008 (2009).
 44. Lee, J.-H. & Paull, T. T. Direct activation of the ATM protein kinase by the Mre11/Rad50/Nbs1 complex. *Science* **304**, 93–6 (2004).
 45. Jette, N. & Lees-Miller, S. P. The DNA-dependent protein kinase: A multifunctional protein kinase with roles in DNA double strand break repair and mitosis. *Prog. Biophys. Mol. Biol.* **117**, 194–205 (2015).
 46. Sirbu, B. M. & Cortez, D. DNA damage response: three levels of DNA repair regulation. *Cold Spring Harb. Perspect. Biol.* **5**, a012724 (2013).
 47. Godon, C. *et al.* PARP inhibition versus PARP-1 silencing: different outcomes in terms of single-strand break repair and radiation susceptibility. *Nucleic Acids Res.* **36**, 4454–64 (2008).
 48. Le May, N., Egly, J.-M. & Coin, F. True lies: the double life of the nucleotide excision repair factors in transcription and DNA repair. *J. Nucleic Acids* **2010**, (2010).
 49. Hanawalt, P. C. Subpathways of nucleotide excision repair and their regulation. *Oncogene* **21**, 8949–56 (2002).
 50. Marteijn, J. A., Lans, H., Vermeulen, W. & Hoeijmakers, J. H. J. Understanding nucleotide excision repair and its roles in cancer and ageing. *Nat. Rev. Mol. Cell Biol.* **15**, 465–81 (2014).
 51. Nowosińska, A. & Marinus, M. G. Cisplatin induces DNA double-strand break formation in Escherichia coli dam mutants. *DNA Repair (Amst)*. **4**, 773–81 (2005).
 52. Moynahan, M. E. & Jasin, M. Mitotic homologous recombination maintains genomic stability and suppresses tumorigenesis. *Nat. Rev. Mol. Cell Biol.* **11**, 196–207 (2010).
 53. Wu, L. *et al.* BLAP75/RMI1 promotes the BLM-dependent dissolution of homologous recombination intermediates. *Proc. Natl. Acad. Sci. U. S. A.* **103**, 4068–73 (2006).
 54. Pastwa, E. & Błasiak, J. Non-homologous DNA end joining. *Acta Biochim. Pol.* **50**, 891–908 (2003).
 55. Zhu, Z., Chung, W.-H., Shim, E. Y., Lee, S. E. & Ira, G. Sgs1 helicase and two nucleases Dna2 and Exo1 resect DNA double-strand break ends. *Cell* **134**, 981–94 (2008).
 56. Mimitou, E. P. & Symington, L. S. DNA end resection--unraveling the tail. *DNA Repair (Amst)*. **10**, 344–8 (2011).
 57. Nimmonkar, A. V. *et al.* BLM-DNA2-RPA-MRN and EXO1-BLM-RPA-MRN constitute two DNA end resection machineries for human DNA break repair. *Genes Dev.* **25**, 350–62 (2011).
 58. Baumann, P., Benson, F. E. & West, S. C. Human Rad51 Protein Promotes ATP-Dependent Homologous Pairing and Strand Transfer Reactions *In Vitro*. *Cell* **87**, 757–766 (1996).
 59. Benson, F. E., Stasiak, A. & West, S. C. Purification and characterization of the human Rad51 protein, an analogue of E. coli RecA. *EMBO J.* **13**, 5764–71 (1994).
 60. Hühn, D., Bolck, H. A. & Sartori, A. A. Targeting DNA double-strand break signalling and repair: recent advances in cancer therapy. *Swiss Med. Wkly.* **143**, w13837 (2013).
 61. Kaelin, W. G. The concept of synthetic lethality in the context of anticancer therapy. *Nat. Rev. Cancer* **5**, 689–98 (2005).
 62. Bryant, H. E. *et al.* Specific killing of BRCA2-deficient tumours with inhibitors of poly(ADP-ribose) polymerase. *Nature* **434**, 913–7 (2005).
 63. Farmer, H. *et al.* Targeting the DNA repair defect in BRCA mutant cells as a therapeutic strategy. *Nature* **434**, 917–21 (2005).
 64. Tutt, A. *et al.* Oral poly(ADP-ribose) polymerase inhibitor olaparib in patients with BRCA1 or BRCA2 mutations and advanced breast cancer: a proof-of-concept trial. *Lancet* **376**, 235–44 (2010).
 65. Macheret, M. & Halazonetis, T. D. DNA Replication Stress as a Hallmark of Cancer. *Annu. Rev. Pathol. Mech. Dis.* **10**, 425–448 (2015).
 66. Cimprich, K. A. & Cortez, D. ATR: an essential regulator of genome integrity. *Nat. Rev. Mol. Cell Biol.* **9**, 616–627 (2008).
 67. Domínguez-Kelly, R. *et al.* Wee1 controls genomic stability during replication by regulating the Mus81-Eme1 endonuclease. *J. Cell Biol.* **194**, 567–579 (2011).
 68. Reaper, P. M. *et al.* Selective killing of ATM- or p53-deficient cancer cells through inhibition of ATR. *Nat. Chem. Biol.* **7**, 428–430 (2011).
 69. Barazzuol, L. *et al.* Evaluation of poly (ADP-ribose) polymerase inhibitor ABT-888 combined with radiotherapy and temozolomide in glioblastoma. *Radiat. Oncol.* **8**, 65 (2013).
 70. Leijen, S. *et al.* Phase II Study of WEE1 Inhibitor AZD1775 Plus Carboplatin in Patients With TP53-Mutated Ovarian Cancer Refractory or Resistant to First-Line Therapy Within 3 Months. *J. Clin. Oncol.* **34**, 4354–4361

- (2017).
71. O'Connor, M. J. *et al.* Abstract 4420: Generating preclinical models to assess bone marrow toxicity induced by the PARP inhibitor olaparib in combination with chemotherapy. *Cancer Res.* **73**, 4420–4420 (2013).
 72. Prakash, A., Garcia-Moreno, J., Brown, J. & Bourke, E. Clinically Applicable Inhibitors Impacting Genome Stability. *Molecules* **23**, 1166 (2018).
 73. Boucher, D. *et al.* Abstract P5-06-05: Preclinical characterization of VX-984, a selective DNA-dependent protein kinase (DNA-PK) inhibitor in combination with doxorubicin in breast and ovarian cancers. *Cancer Res.* **77**, P5-6-5-P5-6–5 (2017).
 74. Willmore, E. *et al.* A novel DNA-dependent protein kinase inhibitor, NU7026, potentiates the cytotoxicity of topoisomerase II poisons used in the treatment of leukemia. *Blood* **103**, 4659–4665 (2004).
 75. Chohan, T. A., Qian, H., Pan, Y. & Chen, J.-Z. Cyclin-dependent kinase-2 as a target for cancer therapy: progress in the development of CDK2 inhibitors as anti-cancer agents. *Curr. Med. Chem.* **22**, 237–63 (2015).
 76. Pommier, Y., O'Connor, M. J. & de Bono, J. Laying a trap to kill cancer cells: PARP inhibitors and their mechanisms of action. *Sci. Transl. Med.* **8**, 362ps17–362ps17 (2016).
 77. Degorce, S. L. *et al.* Discovery of Novel 3-Quinoline Carboxamides as Potent, Selective, and Orally Bioavailable Inhibitors of Ataxia Telangiectasia Mutated (ATM) Kinase. *J. Med. Chem.* **59**, 6281–6292 (2016).
 78. Velic, D. *et al.* DNA Damage Signalling and Repair Inhibitors: The Long-Sought-After Achilles' Heel of Cancer. *Biomolecules* **5**, 3204–59 (2015).
 79. Fokas, E. *et al.* Targeting ATR *in vivo* using the novel inhibitor VE-822 results in selective sensitization of pancreatic tumors to radiation. *Cell Death Dis.* **3**, e441 (2012).
 80. Daud, A. I. *et al.* Phase I Dose-Escalation Trial of Checkpoint Kinase 1 Inhibitor MK-8776 As Monotherapy and in Combination With Gemcitabine in Patients With Advanced Solid Tumors. *J. Clin. Oncol.* **33**, 1060–1066 (2015).
 81. Lainchbury, M. *et al.* Discovery of 3-alkoxyamino-5-(pyridin-2-ylamino)pyrazine-2-carbonitriles as selective, orally bioavailable CHK1 inhibitors. *J. Med. Chem.* **55**, 10229–40 (2012).
 82. Gavande, N. S. *et al.* DNA repair targeted therapy: The past or future of cancer treatment? *Pharmacol. Ther.* **160**, 65–83 (2016).
 83. Spies, M. *DNA helicases and DNA motor proteins.* (Springer Science+Business Media, 2013).
 84. Gupta, R. & Brosh, R. M. Helicases as prospective targets for anti-cancer therapy. *Anticancer. Agents Med. Chem.* **8**, 390–401 (2008).
 85. Umate, P., Tuteja, N. & Tuteja, R. Genome-wide comprehensive analysis of human helicases. *Commun. Integr. Biol.* **4**, 1–20 (2011).
 86. Gorbalenya, A. E. & Koonin, E. V. Helicases: amino acid sequence comparisons and structure-function relationships. *Curr. Opin. Struct. Biol.* **3**, 419–429 (1993).
 87. Gorbalenya, A. E., Koonin, E. V., Donchenko, A. P. & Blinov, V. M. Two related superfamilies of putative helicases involved in replication, recombination, repair and expression of DNA and RNA genomes. *Nucleic Acids Res.* **17**, 4713–30 (1989).
 88. Fairman-Williams, M. E., Guenther, U.-P. & Jankowsky, E. SF1 and SF2 helicases: family matters. *Curr. Opin. Struct. Biol.* **20**, 313–24 (2010).
 89. Banroques, J., Doère, M., Dreyfus, M., Linder, P. & Tanner, N. K. Motif III in superfamily 2 'helicases' helps convert the binding energy of ATP into a high-affinity RNA binding site in the yeast DEAD-box protein Ded1. *J. Mol. Biol.* **396**, 949–66 (2010).
 90. Caruthers, J. M. & McKay, D. B. Helicase structure and mechanism. *Curr. Opin. Struct. Biol.* **12**, 123–133 (2002).
 91. Mazin, A. V., Mazina, O. M., Bugreev, D. V & Rossi, M. J. Rad54, the motor of homologous recombination. *DNA Repair (Amst).* **9**, 286–302 (2010).
 92. Dynan, W. S. & Yoo, S. Interaction of Ku protein and DNA-dependent protein kinase catalytic subunit with nucleic acids. *Nucleic Acids Res.* **26**, 1551–9 (1998).
 93. Popuri, V., Croteau, D. L., Brosh, Jr., R. M. & Bohr, V. A. RECQ1 is required for cellular resistance to replication stress and catalyzes strand exchange on stalled replication fork structures. *Cell Cycle* **11**, 4252–4265 (2012).
 94. Croteau, D. L., Popuri, V., Opresko, P. L. & Bohr, V. A. Human RecQ helicases in DNA repair, recombination, and replication. *Annu. Rev. Biochem.* **83**, 519–52 (2014).
 95. Cooper, M. P. *et al.* Ku complex interacts with and stimulates the Werner protein. *Genes Dev.* **14**, 907–12 (2000).
 96. Li, B. & Comai, L. Functional interaction between Ku and the werner syndrome protein in DNA end processing. *J. Biol. Chem.* **275**, 28349–52 (2000).
 97. Yannone, S. M. *et al.* Werner Syndrome Protein Is Regulated and Phosphorylated by DNA-dependent Protein Kinase. *J. Biol. Chem.* **276**, 38242–38248 (2001).
 98. Doherty, K. M. *et al.* RECQ1 helicase interacts with human mismatch repair factors that regulate genetic recombination. *J. Biol. Chem.* **280**, 28085–94 (2005).
 99. Aggarwal, M., Sommers, J. A., Morris, C. & Brosh, R. M. Delineation of WRN helicase function with EXO1 in the replicational stress response. *DNA Repair (Amst).* **9**, 765–76 (2010).
 100. Opresko, P. L., Sowd, G. & Wang, H. The Werner syndrome helicase/exonuclease processes mobile D-loops

- through branch migration and degradation. *PLoS One* **4**, e4825 (2009).
101. LeRoy, G., Carroll, R., Kyin, S., Seki, M. & Cole, M. D. Identification of RecQL1 as a Holliday junction processing enzyme in human cell lines. *Nucleic Acids Res.* **33**, 6251–7 (2005).
 102. Karow, J. K., Constantinou, A., Li, J. L., West, S. C. & Hickson, I. D. The Bloom's syndrome gene product promotes branch migration of holliday junctions. *Proc. Natl. Acad. Sci. U. S. A.* **97**, 6504–8 (2000).
 103. Bachrati, C. Z., Borts, R. H. & Hickson, I. D. Mobile D-loops are a preferred substrate for the Bloom's syndrome helicase. *Nucleic Acids Res.* **34**, 2269–79 (2006).
 104. Wu, Y. Unwinding and rewinding: double faces of helicase? *J. Nucleic Acids* **2012**, 140601 (2012).
 105. Sun, W. *et al.* The FANCM ortholog Fml1 promotes recombination at stalled replication forks and limits crossing over during DNA double-strand break repair. *Mol. Cell* **32**, 118–28 (2008).
 106. Gari, K., Décaillet, C., Stasiak, A. Z., Stasiak, A. & Constantinou, A. The Fanconi anemia protein FANCM can promote branch migration of Holliday junctions and replication forks. *Mol. Cell* **29**, 141–8 (2008).
 107. Barber, L. J. *et al.* RTEL1 maintains genomic stability by suppressing homologous recombination. *Cell* **135**, 261–71 (2008).
 108. Litman, R. *et al.* BACH1 is critical for homologous recombination and appears to be the Fanconi anemia gene product FANCF. *Cancer Cell* **8**, 255–65 (2005).
 109. Rafnar, T. *et al.* Mutations in BRIP1 confer high risk of ovarian cancer. *Nat. Genet.* **43**, 1104–7 (2011).
 110. Sommers, J. A. *et al.* FANCF uses its motor ATPase to destabilize protein-DNA complexes, unwind triplexes, and inhibit RAD51 strand exchange. *J. Biol. Chem.* **284**, 7505–17 (2009).
 111. Coin, F., Oksenyich, V. & Egly, J.-M. Distinct roles for the XPB/p52 and XPD/p44 subcomplexes of TFIIH in damaged DNA opening during nucleotide excision repair. *Mol. Cell* **26**, 245–56 (2007).
 112. Cai, W. *et al.* Wanted DEAD/H or Alive: Helicases Winding Up in Cancers. *J. Natl. Cancer Inst.* **109**, djw278 (2017).
 113. Capp, C., Wu, J. & Hsieh, T.-S. RecQ4: the second replicative helicase? *Crit. Rev. Biochem. Mol. Biol.* **45**, 233–42 (2010).
 114. Mendoza-Maldonado, R. *et al.* The human RECQ1 helicase is highly expressed in glioblastoma and plays an important role in tumor cell proliferation. *Mol. Cancer* **10**, 83 (2011).
 115. Arai, A. *et al.* RECQL1 and WRN proteins are potential therapeutic targets in head and neck squamous cell carcinoma. *Cancer Res.* **71**, 4598–607 (2011).
 116. Sharma, S. & Brosh, R. M. Human RECQ1 is a DNA damage responsive protein required for genotoxic stress resistance and suppression of sister chromatid exchanges. *PLoS One* **2**, e1297 (2007).
 117. Futami, K. *et al.* Induction of mitotic cell death in cancer cells by small interference RNA suppressing the expression of RecQL1 helicase. *Cancer Sci.* **99**, 71–80 (2008).
 118. Ramamoorthy, M. *et al.* RECQL5 cooperates with Topoisomerase II alpha in DNA decatenation and cell cycle progression. *Nucleic Acids Res.* **40**, 1621–35 (2012).
 119. Brosh, R. M. DNA helicases involved in DNA repair and their roles in cancer. *Nat. Rev. Cancer* **13**, 542–58 (2013).
 120. Gagou, M. E. *et al.* Suppression of apoptosis by PIF1 helicase in human tumor cells. *Cancer Res.* **71**, 4998–5008 (2011).
 121. Chisholm, K. M. *et al.* A genomewide screen for suppressors of Alu-mediated rearrangements reveals a role for PIF1. *PLoS One* **7**, e30748 (2012).
 122. Cheng, W.-H. *et al.* Targeting Werner syndrome protein sensitizes U-2 OS osteosarcoma cells to selenium-induced DNA damage response and necrotic death. *Biochem. Biophys. Res. Commun.* **420**, 24–8 (2012).
 123. Chaganti, R. S., Schonberg, S. & German, J. A manyfold increase in sister chromatid exchanges in Bloom's syndrome lymphocytes. *Proc. Natl. Acad. Sci. U. S. A.* **71**, 4508–12 (1974).
 124. Patel, S. S. & Donmez, I. Mechanisms of helicases. *J. Biol. Chem.* **281**, 18265–8 (2006).
 125. Shadrack, W. R. *et al.* Discovering new medicines targeting helicases: challenges and recent progress. *J. Biomol. Screen.* **18**, 761–81 (2013).
 126. Kleymann, G. *et al.* New helicase-primase inhibitors as drug candidates for the treatment of herpes simplex disease. *Nat. Med.* **8**, 392–8 (2002).
 127. Crute, J. J. *et al.* Herpes simplex virus helicase-primase inhibitors are active in animal models of human disease. *Nat. Med.* **8**, 386–91 (2002).
 128. Aggarwal, M., Sommers, J. A., Shoemaker, R. H. & Brosh, R. M. Inhibition of helicase activity by a small molecule impairs Werner syndrome helicase (WRN) function in the cellular response to DNA damage or replication stress. *Proc. Natl. Acad. Sci. U. S. A.* **108**, 1525–30 (2011).
 129. Banerjee, T., Aggarwal, M. & Brosh, R. M. A new development in DNA repair modulation: discovery of a BLM helicase inhibitor. *Cell Cycle* **12**, 713–4 (2013).
 130. Liu, W. *et al.* A Selective Small Molecule DNA2 Inhibitor for Sensitization of Human Cancer Cells to Chemotherapy. *EBioMedicine* **6**, 73–86 (2016).
 131. Radi, M. *et al.* Discovery of the first small molecule inhibitor of human DDX3 specifically designed to target the RNA binding site: towards the next generation HIV-1 inhibitors. *Bioorg. Med. Chem. Lett.* **22**, 2094–8 (2012).
 132. Ito, M. *et al.* Discovery of Novel 1,4-Diacylpiperazines as Selective and Cell-Active eIF4A3 Inhibitors. *J. Med.*

- Chem.* **60**, 3335–3351 (2017).
133. Iwatani-Yoshihara, M. *et al.* Discovery of Allosteric Inhibitors Targeting the Spliceosomal RNA Helicase Brr2. *J. Med. Chem.* **60**, 5759–5771 (2017).
 134. Li, K. *et al.* Optimization of potent hepatitis C virus NS3 helicase inhibitors isolated from the yellow dyes thioflavine S and primuline. *J. Med. Chem.* **55**, 3319–30 (2012).
 135. Aiello, D. *et al.* Discovery, characterization and comparison of inhibitors of *Bacillus anthracis* and *Staphylococcus aureus* replicative DNA helicases. *Bioorg. Med. Chem.* **17**, 4466–76 (2009).
 136. Radi, M. *et al.* Discovery of the first small molecule inhibitor of human DDX3 specifically designed to target the RNA binding site: towards the next generation HIV-1 inhibitors. *Bioorg. Med. Chem. Lett.* **22**, 2094–8 (2012).
 137. Ito, M. *et al.* Discovery of selective ATP-competitive eIF4A3 inhibitors. *Bioorg. Med. Chem.* **25**, 2200–2209 (2017).
 138. Iwatani-Yoshihara, M. *et al.* Discovery and Characterization of a Eukaryotic Initiation Factor 4A-3-Selective Inhibitor That Suppresses Nonsense-Mediated mRNA Decay. *ACS Chem. Biol.* **12**, 1760–1768 (2017).
 139. Chu, W. K. & Hickson, I. D. RecQ helicases: multifunctional genome caretakers. *Nat. Rev. Cancer* **9**, 644–54 (2009).
 140. Swan, M. K. *et al.* Structure of human Bloom's syndrome helicase in complex with ADP and duplex DNA. *Acta Crystallogr. Sect. D Biol. Crystallogr.* **70**, 1465–1475 (2014).
 141. Newman, J. A. *et al.* Crystal structure of the Bloom's syndrome helicase indicates a role for the HRDC domain in conformational changes. *Nucleic Acids Res.* (2015). doi:10.1093/nar/gkv373
 142. Estep, K. N. & Brosh, R. M. RecQ and Fe-S helicases have unique roles in DNA metabolism dictated by their unwinding directionality, substrate specificity, and protein interactions. *Biochem. Soc. Trans.* **46**, 77–95 (2018).
 143. Kitano, K. Structural mechanisms of human RecQ helicases WRN and BLM. *Front. Genet.* **5**, 366 (2014).
 144. Kim, S.-Y., Hakoshima, T. & Kitano, K. Structure of the RecQ C-terminal domain of human Bloom syndrome protein. *Sci. Rep.* **3**, 3294 (2013).
 145. Sato, A. *et al.* Solution structure of the HRDC domain of human Bloom syndrome protein BLM. *J. Biochem.* **148**, 517–25 (2010).
 146. Wu, L. *et al.* The HRDC domain of BLM is required for the dissolution of double Holliday junctions. *EMBO J.* **24**, 2679–87 (2005).
 147. German, J. Bloom's syndrome. I. Genetical and clinical observations in the first twenty-seven patients. *Am. J. Hum. Genet.* **21**, 196–227 (1969).
 148. Bloom, D. Congenital telangiectatic erythema resembling lupus erythematosus in dwarfs; probably a syndrome entity. *AMA. Am. J. Dis. Child.* **88**, 754–8 (1954).
 149. Ellis, N. A. *et al.* The Bloom's syndrome gene product is homologous to RecQ helicases. *Cell* **83**, 655–66 (1995).
 150. German, J. Bloom's syndrome. XX. The first 100 cancers. *Cancer Genet. Cytogenet.* **93**, 100–106 (1997).
 151. German, J., Sanz, M. M., Ciocci, S., Ye, T. Z. & Ellis, N. A. Syndrome-causing mutations of the BLM gene in persons in the Bloom's Syndrome Registry. *Hum. Mutat.* **28**, 743–53 (2007).
 152. German, J. Bloom syndrome: A Mendelian prototype of somatic mutational disease. *Medicine* **72**, 393–406 (1993).
 153. Larsen, N. B. & Hickson, I. D. RecQ Helicases: Conserved Guardians of Genomic Integrity. *Adv. Exp. Med. Biol.* **767**, 161–84 (2013).
 154. Manthei, K. A. & Keck, J. L. The BLM dissolvasome in DNA replication and repair. *Cell. Mol. Life Sci.* **70**, 4067–84 (2013).
 155. Karow, J. K., Chakraverty, R. K. & Hickson, I. D. The Bloom's syndrome gene product is a 3'-5' DNA helicase. *J. Biol. Chem.* **272**, 30611–4 (1997).
 156. Huber, M. D. G4 DNA unwinding by BLM and Sgs1p: substrate specificity and substrate-specific inhibition. *Nucleic Acids Res.* **30**, 3954–3961 (2002).
 157. Popuri, V. *et al.* The Human RecQ helicases, BLM and RECQ1, display distinct DNA substrate specificities. *J. Biol. Chem.* **283**, 17766–76 (2008).
 158. Mohaghegh, P. The Bloom's and Werner's syndrome proteins are DNA structure-specific helicases. *Nucleic Acids Res.* **29**, 2843–2849 (2001).
 159. Karow, J. K., Newman, R. H., Freemont, P. S. & Hickson, I. D. Oligomeric ring structure of the Bloom's syndrome helicase. *Curr. Biol.* **9**, 597–600 (1999).
 160. Beresten, S. F. *et al.* Purification of overexpressed hexahistidine-tagged BLM N431 as oligomeric complexes. *Protein Expr. Purif.* **17**, 239–48 (1999).
 161. Xue, Y. *et al.* A Minimal Exonuclease Domain of WRN Forms a Hexamer on DNA and Possesses both 3'-5' Exonuclease and 5'-Protruding Strand Endonuclease Activities †. *Biochemistry* **41**, 2901–2912 (2002).
 162. Janscak, P. *et al.* Characterization and mutational analysis of the RecQ core of the bloom syndrome protein. *J. Mol. Biol.* **330**, 29–42 (2003).
 163. Yang, Y. *et al.* Kinetic mechanism of DNA unwinding by the BLM helicase core and molecular basis for its low processivity. *Biochemistry* **49**, 656–68 (2010).
 164. Xu, Y.-N. *et al.* Multimeric BLM is dissociated upon ATP hydrolysis and functions as monomers in resolving

- DNA structures. *Nucleic Acids Res.* **40**, 9802–14 (2012).
165. Bischof, O. *et al.* Regulation and Localization of the Bloom Syndrome Protein in Response to DNA Damage. *J. Cell Biol.* **153**, 367–380 (2001).
 166. Eladad, S. *et al.* Intra-nuclear trafficking of the BLM helicase to DNA damage-induced foci is regulated by SUMO modification. *Hum. Mol. Genet.* **14**, 1351–65 (2005).
 167. Dutertre, S. *et al.* Cell cycle regulation of the endogenous wild type Bloom's syndrome DNA helicase. *Oncogene* **19**, 2731–8 (2000).
 168. Champoux, J. J. DNA Topoisomerases : Structure, Function, and Mechanism. *Annu. Rev. Biochem.* **70**, 369–413 (2001).
 169. Hu, P. *et al.* Evidence for BLM and Topoisomerase III α interaction in genomic stability. *Hum. Mol. Genet.* **10**, 1287–98 (2001).
 170. Wu, L. & Hickson, I. D. The Bloom's syndrome helicase stimulates the activity of human topoisomerase III α . *Nucleic Acids Res.* **30**, 4823–9 (2002).
 171. Wu, L. & Hickson, I. D. The Bloom's syndrome helicase suppresses crossing over during homologous recombination. *Nature* **426**, 870–4 (2003).
 172. Yin, J. *et al.* BLAP75, an essential component of Bloom's syndrome protein complexes that maintain genome integrity. *EMBO J.* **24**, 1465–76 (2005).
 173. Wu, L. *et al.* BLAP75/RMI1 promotes the BLM-dependent dissolution of homologous recombination intermediates. *Proc. Natl. Acad. Sci. U. S. A.* **103**, 4068–73 (2006).
 174. Xu, D. *et al.* RMI, a new OB-fold complex essential for Bloom syndrome protein to maintain genome stability. *Genes Dev.* **22**, 2843–55 (2008).
 175. Raynard, S., Bussen, W. & Sung, P. A double Holliday junction dissolvase comprising BLM, topoisomerase III α , and BLAP75. *J. Biol. Chem.* **281**, 13861–4 (2006).
 176. Yang, J., Bachrati, C. Z., Ou, J., Hickson, I. D. & Brown, G. W. Human topoisomerase III α is a single-stranded DNA decatenase that is stimulated by BLM and RMI1. *J. Biol. Chem.* **285**, 21426–36 (2010).
 177. van Brabant, A. J. *et al.* Binding and melting of D-loops by the Bloom syndrome helicase. *Biochemistry* **39**, 14617–25 (2000).
 178. Sung, P., Krejci, L., Van Komen, S. & Sehorn, M. G. Rad51 recombinase and recombination mediators. *J. Biol. Chem.* **278**, 42729–32 (2003).
 179. Bugreev, D. V., Mazina, O. M. & Mazin, A. V. Bloom syndrome helicase stimulates RAD51 DNA strand exchange activity through a novel mechanism. *J. Biol. Chem.* **284**, 26349–59 (2009).
 180. Bugreev, D. V., Yu, X., Egelman, E. H. & Mazin, A. V. Novel pro- and anti-recombination activities of the Bloom's syndrome helicase. *Genes Dev.* **21**, 3085–94 (2007).
 181. Rao, V. A. *et al.* Endogenous γ -H2AX-ATM-Chk2 Checkpoint Activation in Bloom's Syndrome Helicase Deficient Cells Is Related to DNA Replication Arrested Forks. *Mol. Cancer Res.* **5**, 713–724 (2007).
 182. Davies, S. L., North, P. S., Dart, A., Lakin, N. D. & Hickson, I. D. Phosphorylation of the Bloom's Syndrome Helicase and Its Role in Recovery from S-Phase Arrest. *Mol. Cell. Biol.* **24**, 1279–1291 (2004).
 183. Beamish, H. *et al.* Functional Link between BLM Defective in Bloom's Syndrome and the Ataxia-telangiectasia-mutated Protein, ATM. *J. Biol. Chem.* **277**, 30515–30523 (2002).
 184. Sengupta, S. *et al.* BLM helicase-dependent transport of p53 to sites of stalled DNA replication forks modulates homologous recombination. *EMBO J.* **22**, 1210–1222 (2003).
 185. Petermann, E. & Helleday, T. Pathways of mammalian replication fork restart. *Nat. Rev. Mol. Cell Biol.* **11**, 683–687 (2010).
 186. Ralf, C., Hickson, I. D. & Wu, L. The Bloom's Syndrome Helicase Can Promote the Regression of a Model Replication Fork. *J. Biol. Chem.* **281**, 22839–22846 (2006).
 187. Machwe, A., Karale, R., Xu, X., Liu, Y. & Orren, D. K. The Werner and Bloom Syndrome Proteins Help Resolve Replication Blockage by Converting (Regressed) Holliday Junctions to Functional Replication Forks. *Biochemistry* **50**, 6774–6788 (2011).
 188. de Renty, C. & Ellis, N. A. Bloom's syndrome: Why not premature aging?: A comparison of the BLM and WRN helicases. *Ageing Res. Rev.* **33**, 36–51 (2017).
 189. Chan, K. L. & Hickson, I. D. New insights into the formation and resolution of ultra-fine anaphase bridges. *Semin. Cell Dev. Biol.* **22**, 906–912 (2011).
 190. Chan, K.-L., North, P. S. & Hickson, I. D. BLM is required for faithful chromosome segregation and its localization defines a class of ultrafine anaphase bridges. *EMBO J.* **26**, 3397–3409 (2007).
 191. Ke, Y. *et al.* PICH and BLM limit histone association with anaphase centromeric DNA threads and promote their resolution. *EMBO J.* **30**, 3309–3321 (2011).
 192. Bhattacharyya, S. *et al.* Telomerase-associated Protein 1, HSP90, and Topoisomerase II α Associate Directly with the BLM Helicase in Immortalized Cells Using ALT and Modulate Its Helicase Activity Using Telomeric DNA Substrates. *J. Biol. Chem.* **284**, 14966–14977 (2009).
 193. Lillard-Wetherell, K. *et al.* Association and regulation of the BLM helicase by the telomere proteins TRF1 and TRF2. *Hum. Mol. Genet.* **13**, 1919–1932 (2004).
 194. Opresko, P. L. *et al.* POT1 Stimulates RecQ Helicases WRN and BLM to Unwind Telomeric DNA Substrates. *J. Biol. Chem.* **280**, 32069–32080 (2005).

195. Croteau, D. L., Popuri, V., Opresko, P. L. & Bohr, V. A. Human RecQ helicases in DNA repair, recombination, and replication. *Annu. Rev. Biochem.* **83**, 519–52 (2014).
196. Tacar, O., Sriamornsak, P. & Dass, C. R. Doxorubicin: an update on anticancer molecular action, toxicity and novel drug delivery systems. *J. Pharm. Pharmacol.* **65**, 157–70 (2013).
197. Bachur, N. R. *et al.* Helicase inhibition by anthracycline anticancer agents. *Mol. Pharmacol.* **41**, 993–998 (1992).
198. Stepankova, J. *et al.* DNA interactions of 2-pyrrolinodoxorubicin, a distinctively more potent daunosamine-modified analogue of doxorubicin. *Biochem. Pharmacol.* **82**, 227–35 (2011).
199. Gewirtz, D. A critical evaluation of the mechanisms of action proposed for the antitumor effects of the anthracycline antibiotics adriamycin and daunorubicin. *Biochem. Pharmacol.* **57**, 727–741 (1999).
200. Brosh, R. M. Potent inhibition of Werner and Bloom helicases by DNA minor groove binding drugs. *Nucleic Acids Res.* **28**, 2420–2430 (2000).
201. Li, J.-L. *et al.* Inhibition of the Bloom's and Werner's Syndrome Helicases by G-Quadruplex Interacting Ligands †. *Biochemistry* **40**, 15194–15202 (2001).
202. Rosenthal, A. S. *et al.* Discovery of ML216, a Small Molecule Inhibitor of Bloom (BLM) Helicase. Probe Reports from the NIH Molecular Libraries Program (National Center for Biotechnology Information (US), 2010).
203. Rosenthal, A. S. *et al.* Synthesis and SAR studies of 5-(pyridin-4-yl)-1,3,4-thiadiazol-2-amine derivatives as potent inhibitors of Bloom helicase. *Bioorganic Med. Chem. Lett.* **23**, 5660–5666 (2013).
204. Austin, C. P., Brady, L. S., Insel, T. R. & Collins, F. S. NIH Molecular Libraries Initiative. *Science* **306**, 1138–9 (2004).
205. Wang, Y., Cheng, T. & Bryant, S. H. PubChem BioAssay: A Decade's Development toward Open High-Throughput Screening Data Sharing. *SLAS Discov. Adv. Life Sci. R&D* **22**, 655–666 (2017).
206. Wang, Y. *et al.* PubChem BioAssay: 2014 update. *Nucleic Acids Res.* **42**, D1075–82 (2014).
207. Hill, A. P. & Young, R. J. Getting physical in drug discovery: a contemporary perspective on solubility and hydrophobicity. *Drug Discov. Today* **15**, 648–655 (2010).
208. Ishikawa, M. & Hashimoto, Y. Improvement in aqueous solubility in small molecule drug discovery programs by disruption of molecular planarity and symmetry. *J. Med. Chem.* **54**, 1539–54 (2011).
209. Saunders, J. H. & Slocombe, R. J. The Chemistry of the Organic Isocyanates. *Chem. Rev.* **43**, 203–218 (1948).
210. Eckert, H. & Forster, B. Triphosgene, a Crystalline Phosgene Substitute. *Angew. Chemie Int. Ed. English* **26**, 894–895 (1987).
211. Alan R. Katritzky, David P. M. Pleyne, and Yang, B. A General Synthesis of Unsymmetrical Tetrasubstituted Ureas. (1997). doi:10.1021/JO962245T
212. Simon, M.; Turoczy, M.C.; Badea, V.; Csunderlik, C. Bis(o-nitrophenyl) carbonate, a valid alternative reagent to phosgene in symmetrical N,N-diaryl ureas synthesis. *Rev. Chim.* 383–386 (2006).
213. Batey, R. A., Santhakumar, V., Yoshina-Ishii, C. & Taylor, S. D. An efficient new protocol for the formation of unsymmetrical tri- and tetrasubstituted ureas. *Tetrahedron Lett.* **39**, 6267–6270 (1998).
214. Gallou, I. Unsymmetrical ureas. Synthetic methodologies and application in drug design. *Org. Prep. Proced. Int.* **39**, 355–383 (2007).
215. Bogolubsky, A. V. *et al.* A facile synthesis of unsymmetrical ureas. *Tetrahedron* **67**, 3619–3623 (2011).
216. Díaz, D. J., Darko, A. K. & McElwee-White, L. Transition Metal-Catalyzed Oxidative Carbonylation of Amines to Ureas. *European J. Org. Chem.* **2007**, 4453–4465 (2007).
217. Li, K. & Chen, W. A new convenient way to synthesize 1,3,4-thiadiazol-2-yl urea derivatives under microwave irradiation. *Heteroat. Chem.* **19**, 621–629 (2008).
218. Castanedo, G., Liu, Y., Crawford, J. J. & Braun, M.-G. Synthesis of Fused Imidazole-Containing Ring Systems via Dual Oxidative Amination of C(sp³)–H Bonds. *J. Org. Chem.* **81**, 8617–8624 (2016).
219. Amgen Inc, Zeng, Q., Chenguang, C., Yao, G. & Xianghong Wang. Thiadiazole modulators of pkb. (2011).
220. Ritchie, T. J. & Macdonald, S. J. F. The impact of aromatic ring count on compound developability – are too many aromatic rings a liability in drug design? *Drug Discov. Today* **14**, 1011–1020 (2009).
221. Platts, J. A., Maarof, H., Harris, K. D. M., Lim, G. K. & Willock, D. J. The effect of intermolecular hydrogen bonding on the planarity of amides. *Phys. Chem. Chem. Phys.* **14**, 11944–52 (2012).
222. Ritchie, T. J., Macdonald, S. J. F. & Pickett, S. D. Insights into the impact of N- and O-methylation on aqueous solubility and lipophilicity using matched molecular pair analysis. *Medchemcomm* **6**, 1787–1797 (2015).
223. Kurt, B. Z., Gazioglu, I., Sonmez, F. & Kucukislamoglu, M. Synthesis, antioxidant and anticholinesterase activities of novel coumarylthiazole derivatives. *Bioorg. Chem.* **59**, 80–90 (2015).
224. Kumbhare, R. M. *et al.* Synthesis and anticancer evaluation of novel triazole linked N-(pyrimidin-2-yl)benzo[d]thiazol-2-amine derivatives as inhibitors of cell survival proteins and inducers of apoptosis in MCF-7 breast cancer cells. *Bioorg. Med. Chem. Lett.* **25**, 654–8 (2015).
225. Tahir, S., Badshah, A. & Hussain, R. A. Guanidines from 'toxic substances' to compounds with multiple biological applications - Detailed outlook on synthetic procedures employed for the synthesis of guanidines. *Bioorganic Chemistry* **59**, 39–79 (2015).
226. Ishikawa, T. & Kumamoto, T. Guanidines in organic synthesis. *Synthesis* 737–752 (2006). doi:10.1055/s-2006-926325
227. Ramadas, K., Janarthanan, N. & Pritha, R. A Short and Concise Synthesis of Guanidines. *Synlett* **1997**, 1053–

- 1054 (1997).
228. Katritzky, A. R. & Rogovoy, B. V. Recent developments in guanylate agents. *Nikolai Zefirov Ark.* 49–87 (2005). doi:10.3998/ark.5550190.0006.406
 229. Atkinson, R. C. *et al.* Intramolecular arylation of amino acid enolates. *Chem. Commun. (Camb)*. **49**, 9734–6 (2013).
 230. Andresen, B., AnthonY, N. J., Haidle, A., Miller, T. & Osimbon, E. 2-pyridyl carboxamide-containing spleen tyrosine kinase (syk) inhibitors. (2014).
 231. Dahlin, J. L. & Walters, M. A. The essential roles of chemistry in high-throughput screening triage. *Future Med. Chem.* **6**, 1265–1290 (2014).
 232. Wilhelm, S. M. *et al.* Preclinical overview of sorafenib, a multikinase inhibitor that targets both Raf and VEGF and PDGF receptor tyrosine kinase signaling. *Mol. Cancer Ther.* **7**, 3129–40 (2008).
 233. Thorne, N., Auld, D. S. & Inglese, J. Apparent activity in high-throughput screening: origins of compound-dependent assay interference. *Curr. Opin. Chem. Biol.* **14**, 315–324 (2010).
 234. Bleicher, K. H., Böhm, H.-J., Müller, K. & Alanine, A. I. Hit and lead generation: beyond high-throughput screening. *Nat. Rev. Drug Discov.* **2**, 369–78 (2003).
 235. Wang, Y., Cheng, T. & Bryant, S. H. PubChem BioAssay: A Decade's Development toward Open High-Throughput Screening Data Sharing. *SLAS Discov. Adv. Life Sci. R D* **22**, 655–666 (2017).
 236. Veber, D. F. *et al.* Molecular properties that influence the oral bioavailability of drug candidates. *J. Med. Chem.* **45**, 2615–23 (2002).
 237. Baell, J. & Walters, M. A. Chemistry: Chemical con artists foil drug discovery. *Nature* **513**, 481–483 (2014).
 238. Weininger, D. SMILES, a chemical language and information system. 1. Introduction to methodology and encoding rules. *J. Chem. Inf. Model.* **28**, 31–36 (1988).
 239. Kucherenko, T. T., Gutsul, R., Kisel, V. M. & Kovtunencko, V. A. Fused isoquinolines: 3-aryl-2,3,4,5-tetrahydro-1H-pyrrolo[2,3-c]isoquinoline-1,5-dione-2-spiro-4'-(1'-alkyl-1',4'-dihydropyridine)s. *Tetrahedron* **60**, 211–217 (2004).
 240. Petronzi, C. *et al.* Synthesis and Reactivity of the 3-Substituted Isoindolinone Framework to Assemble Highly Functionalized Related Structures. *European J. Org. Chem.* **2012**, 5357–5365 (2012).
 241. Watson, A. F. *et al.* MDM2-p53 protein–protein interaction inhibitors: A-ring substituted isoindolinones. *Bioorg. Med. Chem. Lett.* **21**, 5916–9 (2011).
 242. Cappelli, A. *et al.* Design, synthesis, and preliminary biological evaluation of pyrrolo[3,4-c]quinolin-1-one and oxoisoindoline derivatives as aggrecanase inhibitors. *ChemMedChem* **5**, 739–48 (2010).
 243. Hughes, T. V *et al.* 7-[1H-Indol-2-yl]-2,3-dihydro-isoindol-1-ones as dual Aurora-A/VEGF-R2 kinase inhibitors: design, synthesis, and biological activity. *Bioorg. Med. Chem. Lett.* **18**, 5130–3 (2008).
 244. Marugan, J. J. *et al.* No Title. (2015).
 245. Colombo, M., Bossolo, S. & Aramini, A. Phosphorus trichloride-mediated and microwave-assisted synthesis of a small collection of amides bearing strong electron-withdrawing group substituted anilines. *J. Comb. Chem.* **11**, 335–7 (2009).
 246. Yvonne C. Martin, James L. Kofron, and & Traphagen, L. M. Do Structurally Similar Molecules Have Similar Biological Activity? (2002). doi:10.1021/JM020155C
 247. Muchmore, S. W., Edmunds, J. J., Stewart, K. D. & Hajduk, P. J. Cheminformatic Tools for Medicinal Chemists. *J. Med. Chem.* **53**, 4830–4841 (2010).
 248. Darrow, J. J. & Kesselheim, A. S. Drug Development and FDA Approval, 1938–2013. *N. Engl. J. Med.* **370**, e39 (2014).
 249. Tian, S., Wang, J., Li, Y., Li, D. & Xu, L. The application of in silico drug-likeness predictions in pharmaceutical research. *Adv. Drug Deliv. Rev.* **86**, 2–10 (2015).
 250. Meanwell, N. A. Improving Drug Candidates by Design: A Focus on Physicochemical Properties As a Means of Improving Compound Disposition and Safety. *Chem. Res. Toxicol.* **24**, 1420–1456 (2011).
 251. Walters, W. P. & Murcko, M. A. Prediction of 'drug-likeness'. *Adv. Drug Deliv. Rev.* **54**, 255–71 (2002).
 252. Cruciani, G., Pastor, M. & Guba, W. VolSurf: a new tool for the pharmacokinetic optimization of lead compounds. *Eur. J. Pharm. Sci.* **11 Suppl 2**, S29-39 (2000).
 253. Cheng, F. *et al.* admetSAR: A Comprehensive Source and Free Tool for Assessment of Chemical ADMET Properties. *J. Chem. Inf. Model.* **52**, 3099–3105 (2012).
 254. Ritchie, T. J. & Macdonald, S. J. F. The impact of aromatic ring count on compound developability - are too many aromatic rings a liability in drug design? *Drug Discovery Today* **14**, 1011–1020 (2009).
 255. Hopkins, A. L., Keserü, G. M., Leeson, P. D., Rees, D. C. & Reynolds, C. H. The role of ligand efficiency metrics in drug discovery. *Nat. Rev. Drug Discov.* **13**, 105–21 (2014).
 256. Leeson, P. D. & Springthorpe, B. The influence of drug-like concepts on decision-making in medicinal chemistry. *Nat. Rev. Drug Discov.* **6**, 881–890 (2007).
 257. Lipinski, C. A. in 1–24 (Springer, Berlin, Heidelberg, 2009). doi:10.1007/7355_2009_4
 258. Michael S. Lajiness, Gerald M. Maggiora, and Shanmugasundaram, V. Assessment of the Consistency of Medicinal Chemists in Reviewing Sets of Compounds. (2004). doi:10.1021/JM049740Z
 259. Jerabek-Willemsen, M. *et al.* MicroScale Thermophoresis: Interaction analysis and beyond. *J. Mol. Struct.* **1077**, 101–113 (2014).

260. Goldberg, Kristin; Hamilton, Niall; Jones, Stuart; Jordan, Allan; Lyons, Amanda; Newton, Rebecca; Ggilvie, Donald; Waszkowycz, B. Quinazoline compounds. (2015).
261. Tani, S., Uehara, T. N., Yamaguchi, J. & Itami, K. Programmed synthesis of arylthiazoles through sequential C–H couplings. *Chem. Sci.* **5**, 123–135 (2014).
262. Ishikawa, M. & Hashimoto, Y. Improvement in Aqueous Solubility in Small Molecule Drug Discovery Programs by Disruption of Molecular Planarity and Symmetry. *J. Med. Chem.* **54**, 1539–1554 (2011).
263. Mo, J., Liu, S. & Xiao, J. Palladium-catalyzed regioselective Heck arylation of electron-rich olefins in a molecular solvent-ionic liquid cocktail. *Tetrahedron* **61**, 9902–9907 (2005).
264. Jun Mo, Lijin Xu, and & Xiao*, J. Ionic Liquid-Promoted, Highly Regioselective Heck Arylation of Electron-Rich Olefins by Aryl Halides. (2004). doi:10.1021/JA0450861
265. Ueda, T., Konishi, H. & Manabe, K. Palladium-Catalyzed Carbonylation of Aryl, Alkenyl, and Allyl Halides with Phenyl Formate. *Org. Lett.* **14**, 3100–3103 (2012).
266. Dauber-Osguthorpe, P., Campbell, M. M. & Osguthorpe, D. J. Conformational analysis of peptide surrogates. Reduced and retro-amide links in blocked alanine and in secondary structures. *Int. J. Pept. Protein Res.* **38**, 357–77 (1991).
267. Chorev, M. & Goodman, M. A dozen years of retro-inverso peptidomimetics. *Acc. Chem. Res.* **26**, 266–273 (1993).
268. Kuhn, B., Mohr, P. & Stahl, M. Intramolecular Hydrogen Bonding in Medicinal Chemistry. *J. Med. Chem.* **53**, 2601–2611 (2010).
269. Gilli, G., Bellucci, F., Ferretti, V. & Bertolasi, V. Evidence for resonance-assisted hydrogen bonding from crystal-structure correlations on the enol form of the .beta.-diketone fragment. *J. Am. Chem. Soc.* **111**, 1023–1028 (1989).
270. Hongyu Zhao, * *et al.* Discovery of Potent, Highly Selective, and Orally Bioavailable Pyridine Carboxamide c-Jun NH2-Terminal Kinase Inhibitors. (2006). doi:10.1021/JM060465L
271. Kirchberg, S. *et al.* Oxidative Biaryl Coupling of Thiophenes and Thiazoles with Arylboronic Acids through Palladium Catalysis: Otherwise Difficult C4-Selective C–H Arylation Enabled by Boronic Acids. *Angew. Chemie Int. Ed.* **50**, 2387–2391 (2011).
272. Sekizawa, H. *et al.* Late-Stage C–H Coupling Enables Rapid Identification of HDAC Inhibitors: Synthesis and Evaluation of NCH-31 Analogues. *ACS Med. Chem. Lett.* **5**, 582–586 (2014).
273. Lohrey, L. *et al.* 2,4- and 2,5-Disubstituted Arylthiazoles: Rapid Synthesis by C–H Coupling and Biological Evaluation. *European J. Org. Chem.* **2014**, 3387–3394 (2014).
274. Yamaguchi, J., Yamaguchi, A. D. & Itami, K. C–H Bond Functionalization: Emerging Synthetic Tools for Natural Products and Pharmaceuticals. *Angew. Chemie Int. Ed.* **51**, 8960–9009 (2012).
275. Han, Y. T., Wang, Z. & Bae, E. J. Synthesis of the Proposed Structure of Damaurone D and Evaluation of Its Anti-inflammatory Activity. *Chem. Pharm. Bull. (Tokyo)*. **63**, 907–912 (2015).
276. WIRTH, David D.; HUDSPETH, R. No Title. 11 (2010).
277. Lau, J. & Huang, J.-J. Modulators Of HEC1 Activity And Methods Therefore. (2010).
278. Baykov, S. *et al.* A convenient and mild method for 1,2,4-oxadiazole preparation: cyclodehydration of O-acylamidoximes in the superbase system MOH/DMSO. *Tetrahedron Lett.* **57**, 2898–2900 (2016).
279. Volkamer, A., Kuhn, D., Grombacher, T., Rippmann, F. & Rarey, M. Combining global and local measures for structure-based druggability predictions. *J. Chem. Inf. Model.* **52**, 360–72 (2012).
280. Volkamer, A., Kuhn, D., Rippmann, F. & Rarey, M. DoGSiteScorer: a web server for automatic binding site prediction, analysis and druggability assessment. *Bioinformatics* **28**, 2074–5 (2012).
281. DeLano, W. L. The PyMOL Molecular Graphics System. *Schrödinger LLC www.pymol.org Version 1.*, <http://www.pymol.org> (2002).
282. UniProt Consortium, T. U. UniProt: a hub for protein information. *Nucleic Acids Res.* **43**, D204-12 (2015).
283. Finn, R. D. *et al.* Pfam: the protein families database. *Nucleic Acids Res.* **42**, D222-30 (2014).
284. Fauman, E. B., Rai, B. K. & Huang, E. S. Structure-based druggability assessment—identifying suitable targets for small molecule therapeutics. *Curr. Opin. Chem. Biol.* **15**, 463–468 (2011).
285. Le Guilloux, V., Schmidtke, P. & Tuffery, P. Fpocket: an open source platform for ligand pocket detection. *BMC Bioinformatics* **10**, 168 (2009).
286. Halgren, T. A. Identifying and Characterizing Binding Sites and Assessing Druggability. *J. Chem. Inf. Model.* **49**, 377–389 (2009).
287. Goujon, M. *et al.* A new bioinformatics analysis tools framework at EMBL-EBI. *Nucleic Acids Res.* **38**, W695–W699 (2010).
288. Anderson, A. C. The Process of Structure-Based Drug Design. *Chem. Biol.* **10**, 787–797 (2003).
289. Pagadala, N. S., Syed, K. & Tuszynski, J. Software for molecular docking: a review. *Biophys. Rev.* **9**, 91–102 (2017).
290. Cheng, A., Best, S. A., Merz, K. M. & Reynolds, C. H. GB/SA water model for the Merck molecular force field (MMFF). *J. Mol. Graph. Model.* **18**, 273–82 (2000).
291. Case, D. A. *et al.* The Amber biomolecular simulation programs. *J. Comput. Chem.* **26**, 1668–1688 (2005).
292. Klebe, G. Virtual ligand screening: strategies, perspectives and limitations. *Drug Discov. Today* **11**, 580–594 (2006).

293. Ferreira, L., dos Santos, R., Oliva, G. & Andricopulo, A. Molecular Docking and Structure-Based Drug Design Strategies. *Molecules* **20**, 13384–13421 (2015).
294. Zhou, Z., Felts, A. K., Friesner, R. A. & Levy, R. M. Comparative performance of several flexible docking programs and scoring functions: Enrichment studies for a diverse set of pharmaceutically relevant targets. *J. Chem. Inf. Model.* **47**, 1599–1608 (2007).
295. Tripathi, V. *et al.* MRN complex-dependent recruitment of ubiquitylated BLM helicase to DSBs negatively regulates DNA repair pathways. *Nat. Commun.* **9**, 1016 (2018).
296. Castro- Palomino, Laria Julio Cesar; Camacho, Gómez Juan Alberto; Mendoza Lizalde, A. derivatives of 2-aminopyridine as adenosine a2b receptor antagonists and ligands of the melatonin mt3 receptorS. (2016).
297. Iida, H. *et al.* Efficient and rapid synthesis of phenolic analogs of 4-phenylbutanoic acid using microwave-assisted Michael addition as a key reaction. *Synth. Commun.* **46**, 581–585 (2016).
298. HARKI, D. A., Harris, R. S., Perkins-Harki, A. & Li, M. O. Small molecule inhibitors of apobec3g and apobec3b. (2015).
299. Nozawa-Kumada, K., Kadokawa, J., Kameyama, T. & Kondo, Y. Copper-Catalyzed sp^3 C–H Aminative Cyclization of 2-Alkyl- *N* -arylbenzamides: An Approach for the Synthesis of *N* -Aryl-isindolinones. *Org. Lett.* **17**, 4479–4481 (2015).
300. Thangavelu, B., Bhansali, P. & Viola, R. E. Elaboration of a fragment library hit produces potent and selective aspartate semialdehyde dehydrogenase inhibitors. *Bioorg. Med. Chem.* **23**, 6622–31 (2015).
301. Sander, K. *et al.* Development of Fluorine-18 Labeled Metabolically Activated Tracers for Imaging of Drug Efflux Transporters with Positron Emission Tomography. *J. Med. Chem.* **58**, 6058–6080 (2015).
302. Qi, C. A. S. *et al.* Trka kinase inhibitors, compositions and methods thereof. (2015).
303. Li, Y. *et al.* Pyrrolidinobenzoic acid inhibitors of influenza virus neuraminidase: The hydrophobic side chain influences type A subtype selectivity. *Bioorg. Med. Chem.* **20**, 4582–4589 (2012).
304. Limited, S. L. S. Muscarinic M1 receptor positive allosteric modulators. (2018).

11. Experimental information

11.1. Experimental information

All reactions were conducted under an atmosphere of nitrogen unless otherwise stated. Anhydrous solvents were used as purchased or were purified under nitrogen as follows using activated molecular sieves.

Thin layer chromatography was performed on glass plates pre-coated with Merck silica gel 60 F254. Visualisation was achieved with U.V. fluorescence (254 nm) or by staining with a phosphomolybdic acid dip or a potassium permanganate dip.

Flash column chromatography was carried out using pre-packed columns filled with Aldrich silica gel (40-63 μm) on an ISCO Combiflash R_f, or a Biotage Isolera Prime.

Proton nuclear magnetic resonance spectra were recorded at 500 MHz on a Varian 500 spectrometer (at 30 °C), using residual isotopic solvent (CHCl_3 , $\delta_{\text{H}} = 7.27$ ppm, DMSO $\delta_{\text{H}} = 2.50$ ppm, 3.33 ppm (H_2O)) as an internal reference. Chemical shifts are quoted in parts per million (ppm). Coupling constants (J) are recorded in Hertz (Hz).

Carbon nuclear magnetic resonance spectra were recorded at 125 MHz on a Varian 500 spectrometer and are proton decoupled, using residual isotopic solvent (CHCl_3 , $\delta_{\text{C}} = 77.00$ ppm, DMSO $\delta_{\text{C}} = 39.52$ ppm) as an internal reference. Carbon spectra assignments are supported by HSQC and DEPT editing and chemical shifts (δ_{C}) are quoted in ppm.

Infrared spectra were recorded on a Perkin Elmer FT-IR One spectrometer as either an evaporated film or liquid film on sodium chloride plates. Absorption maxima are reported in wave numbers (cm^{-1}). Only significant absorptions are presented in the data, with key stretches identified in brackets.

LCMS data was recorded on a Waters 2695 HPLC using a Waters 2487 UV detector and a Thermo LCQ ESI-MS. Samples were eluted through a Phenomenex Lunar 3 μ C18 50 mm \times 4.6 mm column, using acetonitrile and water acidified by 0.01% formic acid in three methods: method 1 (3:7 to 7:3 acetonitrile and water over 7 minutes), method 2 (3:7 to 7:3 acetonitrile and water over 4 minutes) and method 3 (19:1 to 1:19 acetonitrile and water over 10 minutes),

High resolution mass spectrometry (HRMS) spectra were recorded on Bruker Daltonics Apex III ESI-MS, with an Apollo ESI probe using a methanol spray. Only molecular ions, fragments from molecular ions and other major peaks are reported as mass/charge (m/z) ratios.

Microwave reactions were performed using a Biotage Initiator 8+ microwave reactor.

All novel compounds used for biological testing are fully characterised unless specified. Novel compounds of Series G used for biological testing have assigned NMR spectra except when part of library synthesis, for which only a single or few compounds contain assigned NMR spectra.

11.2. Experimental for ML216 series

11.2.1. General procedures

General procedure A: To a suspension of phenyl *N*-(5-(4-pyridyl)-1,3,4-thiadiazol-2-yl)carbamate (**11**) (1 mol eq.) in toluene was added the appropriate aniline (1 mol eq.). The reaction mixture was heated in a microwave reactor at 150 °C for 30 min and the resulting suspension was cooled to rt. The crude product was purified by either column chromatography and/or trituration with appropriate solvents.

General procedure B: To an ice-cold solution of triphosgene (0.4 mol eq.) in dichloromethane was added the appropriate aniline (1 mol eq.) in dichloromethane and triethylamine (2 mol eq.). The reaction mixture was stirred at ambient temperature for 1.5 h. The solvent was removed under reduced pressure. The appropriate amine (0.6–0.8 mol eq.) was added to the crude mixture in *N,N*-dimethylformamide and stirred at 90 °C for 2 h. The crude product was purified by flash column chromatography using appropriate solvents or recrystallised.

General procedure C: To the appropriate carboxylic acid (1 mol eq.), HATU (1.2 mol eq.), *N,N*-diisopropylethylamine (2 mol eq.) in *N,N*-dimethylformamide was added the appropriate amine (1.2 mol eq.). The reaction mixture was stirred for 16 h. Upon completion, the solvent was removed under reduced pressure to yield a crude product. The crude product was purified by either column chromatography and/or trituration with appropriate solvents.

General procedure D: Sodium periodate (1.2 mol eq.) was added to a mixture of the appropriate thiourea (1 mol eq.) and the appropriate amine (1.5 mol eq.) in an appropriate mixture of *N,N*-dimethylformamide and water. The reaction mixture was heated to 80 °C and stirred for 1 h. Upon completion, the reaction mixture was cooled to rt, aq. sodium hydroxide was added and the mixture was stirred for 20 min. The crude product was then filtered or concentrated under reduced pressure and then purified by column chromatography.

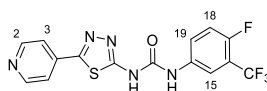
General procedure E: Iodomethane (1 mol eq.) was added to a mixture of the appropriate amine (1 mol eq.) and K_2CO_3 (1 mol eq.) in acetonitrile. The reaction mixture was stirred for 16 h at 80 °C. Upon completion, the reaction mixture was taken up in water (15 mL) and extracted with ethyl acetate (2 × 15 mL). The organics components were combined and washed with brine (10 mL), dried with $MgSO_4$, filtered and concentrated under reduced pressure. The crude product was purified by column chromatography.

6. General procedure F: To 2-(5-(4-pyridyl)-1,3,4-thiadiazol-2-yl)acetic acid (**59**) (1 mol eq.), T3P (1 mol eq.), triethylamine (3 mol eq.) in *N,N*-dimethylformamide was added the appropriate amine (1.2 mol eq.). The reaction mixture was stirred at r.t. for 16 h. Upon completion, the reaction mixture was concentrated under reduced pressure. The crude product was taken up in saturated aq. $NaHCO_3$ (5 mL) and extracted with ethyl acetate (3 × 10 mL). The combined organic components were then washed with brine (10 mL), dried over $MgSO_4$, filtered and concentrated under reduced pressure. The crude product was purified by column chromatography with appropriate solvents.

General procedure G: A solution of 6-bromopyridin-2-amine (1 mol eq.) in dioxane/water (4:1) was charged with nitrogen for 5 min. To this solution, cesium carbonate (3 mol eq.), the appropriate pyridyl boronic acid (1 mol eq.) and (1,1'-bis(diphenylphosphino)ferrocene)dichloropalladium(II) (0.1 mol eq.) were added. The resulting mixture was heated at 120 °C for 3 h. Upon cooling, the reaction mixture was filtered through Celite and the filtrate was concentrated under reduced pressure. The crude was purified by column chromatography with appropriate solvents.

11.2.1. Synthetic procedures

1-(4-Fluoro-3-(trifluoromethyl)phenyl)-3-(5-(4-pyridyl)-1,3,4-thiadiazol-2-yl)urea (**1**)²⁰³



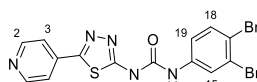
1st procedure: Compound **1** was synthesised according to general procedure A, using the following reagents: phenyl *N*-(5-(4-pyridyl)-1,3,4-thiadiazol-2-yl)carbamate (**11**) (150 mg, 0.50 mmol), 4-fluoro-3-(trifluoromethyl)aniline (65 μ L, 0.50 mmol) and toluene (5 mL). The reaction mixture was concentrated under reduced pressure. The resulting solid

was triturated with dichloromethane (5 mL) and further triturated with 5% methanol in dichloromethane (3 mL) to yield the desired compound **1** as an orange solid (82 mg, 46%).

2nd procedure: Compound **1** was synthesised according to general procedure B, using the following reagents: triphosgene (240 mg, 0.80 mmol), 5-amino-2-fluorobenzotrifluoride (26 μ L, 2.0 mmol), dichloromethane (22 mL), triethylamine (0.56 mL, 4.0 mmol), 5-(4-pyridyl)-1,3,4-thiadiazol-2-yl-amine (**1**) (250 mg, 1.4 mmol) and *N,N*-dimethylformamide (10 mL). The hot crude was added to hot methanol (10 mL) and recrystallized overnight to yield the desired compound **1** as an orange solid (121 mg, 21%).

¹H-NMR (500 MHz, DMSO-*d*₆) δ 11.61 (s, 1H, *NH*-urea), 9.52 (s, 1H, *NH*-urea), 8.73 (d, *J* 5.9, 2H, H-2), 8.06 (s, 1H, H-15), 7.89 (d, *J* 5.3, 2H, H-3), 7.77 (s, 1H, H-19), 7.49 (t, *J* 9.7, 1H, H-18); **LCMS (LCQ)** *R*_t = 2.7 min (method 1), *m/z* (ESI⁺) 384.0 [M+H]⁺. ¹H-NMR consistent with literature data.²⁰³

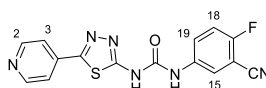
1-(3,4-Dibromophenyl)-3-(5-(4-pyridyl)-1,3,4-thiadiazol-2-yl) (**2**)²⁰³



Compound **2** was synthesised according to general procedure A, using the following reagents: phenyl *N*-(5-(4-pyridyl)-1,3,4-thiadiazol-2-yl)carbamate (**11**) (150 mg, 0.50 mmol), 3,4-dibromoaniline (130 mg, 0.50 mmol) and toluene (5 mL). The reaction mixture was concentrated under reduced pressure. The crude was purified by flash column chromatography (silica, 0 to 5% methanol in dichloromethane) to yield the desired urea (**2**) as an orange solid (160 mg, 70%).

¹H-NMR (500 MHz, DMSO-*d*₆) δ 9.69 (s, 1H, *NH*-urea), 8.72 (d, *J* 5.2, 2H, H-2), 8.06 (d, *J* 2.5, 1H, H-15), 7.86 (d, *J* 5.1, 2H, H-3), 7.67 (d, *J* 8.7, 1H, H-18), 7.43 (dd, *J* 9.0, 2.5, 1H, H-19). Note: urea NH not visible; **LCMS (LCQ)** *R*_t = 3.3 min (method 1), *m/z* (ESI⁺) 455.8 [M+H]⁺. ¹H-NMR consistent with literature data.²⁰³

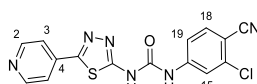
1-(3-Cyano-4-fluoro-phenyl)-3-(5-(4-pyridyl)-1,3,4-thiadiazol-2-yl)urea (**3**)²⁰³



Compound **3** was synthesised according to general procedure A, using the following reagents: phenyl *N*-(5-(4-pyridyl)-1,3,4-thiadiazol-2-yl)carbamate (**11**) (100 mg, 0.34 mmol), 5-amino-2-fluorobenzonitrile (50 mg, 0.34 mmol) and toluene (5 mL). The reaction suspension was filtered and the resulting solid was triturated with 5% methanol in dichloromethane (5 mL) to yield the desired compound **3** as an orange solid (52 mg, 46%).

¹H-NMR (500 MHz, DMSO-*d*₆) δ 9.53 (s, 1H, *NH*-urea), 8.73 (d, *J* 5.2, 2H, H-2), 8.04 (s, 1H, H-15), 7.86 (m, 3H, H-3, H-19), 7.51 (t, *J* 9.1, 1H, H-18). Note: urea NH not visible; **LCMS (LCQ)** *R*_t = 1.9 min (method 1), *m/z* (ESI⁺) 341.0 [M+H]⁺. ¹H-NMR consistent with literature data.²⁰³

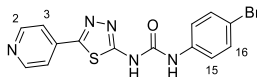
1-(3-Chloro-4-cyano-phenyl)-3-(5-(4-pyridyl)-1,3,4-thiadiazol-2-yl)urea (**4**)²⁰³



Compound **4** was synthesised according to general procedure A, using the following reagents: phenyl *N*-(5-(4-pyridyl)-1,3,4-thiadiazol-2-yl)carbamate (**11**) (100 mg, 0.34 mmol), 4-amino-2-chloro-benzonitrile (50 mg, 0.34 mmol) and toluene (5 mL). The reaction mixture was concentrated under reduced pressure. The resulting solid was triturated with methanol (5 mL) to yield the desired compound **4** as a yellow/orange solid (52 mg, 44%).

¹H-NMR (500 MHz, DMSO-*d*₆) δ 9.95 (s, 1H, *NH*-urea), 8.73 (d, *J* 5.1, 2H, H-2), 8.01 (s, 1H, H-15), 7.88 (m, 3H, H-3, H-19), 7.63 (d, *J* 8.6, 1H, H-18). Note: urea NH not visible; **LCMS (LCQ)** Rt = 2.3 min (method 1), *m/z* (ESI⁺) 356.9 [M(³⁵Cl)+H]⁺, 358.9 [M(³⁷Cl)+H]⁺. ¹H-NMR consistent with literature data.²⁰³

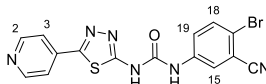
1-(4-Bromophenyl)-3-(5-(4-pyridyl)-1,3,4-thiadiazol-2-yl)urea (5)²⁰³



Compound **5** was synthesised according to general procedure A, using the following reagents: phenyl *N*-(5-(4-pyridyl)-1,3,4-thiadiazol-2-yl)carbamate (**11**) (80 mg, 0.27 mmol), 4-bromoaniline (50 mg, 0.27 mmol) and toluene (4 mL). The reaction suspension was filtered and the resulting solid was triturated with hot methanol (2 × 5 mL) to yield the desired compound **5** as a colourless solid (50 mg, 50%).

¹H-NMR (500 MHz, DMSO-*d*₆) δ 11.38 (s, 1H, *NH*-urea), 9.28 (s, 1H, *NH*-urea), 8.72 (d, *J* 5.3, 2H, H-2), 7.87 (d, *J* 5.8, 2H, H-3), 7.51 (m, 4H, H-15, H-16); **LCMS (LCQ)** Rt = 2.3 min (method 1), *m/z* (ESI⁺) 375.9 [M(⁷⁹Br)+H]⁺, 377.9 [M(⁸¹Br)+H]⁺. ¹H-NMR consistent with literature data.²⁰³

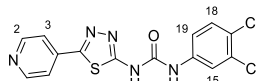
1-(4-Bromo-3-cyano-phenyl)-3-(5-(4-pyridyl)-1,3,4-thiadiazol-2-yl)urea (6)²⁰³



Compound **6** was synthesised according to general procedure B, using the following reagents: triphosgene (480 mg, 1.62 mmol), 5-amino-2-bromobenzonitrile (800 mg, 4.06 mmol), dichloromethane (20 mL), triethylamine (1.1 mL, 8.12 mmol), 5-(4-pyridyl)-1,3,4-thiadiazol-2-yl-amine (**10**) (250 mg, 1.40 mmol) and *N,N*-dimethylformamide (10 mL). The reaction mixture was allowed to cool and the solid was collected by filtration and recrystallised in *N,N*-dimethylformamide. The recrystallised solid was taken up in 50% *N,N*-dimethylformamide in ethyl acetate and washed with aq. NaHCO₃ at 90 °C for 30 min to remove excess triethylamine. On cooling, the resulting solid was collected by filtration to yield the desired compound **6** as a pale yellow solid (550 mg, 27%).

¹H-NMR (500 MHz, DMSO-*d*₆) δ 10.67 (s, 1H, *NH*-urea), 8.65 (d, *J* 5.0, 2H, H-2), 8.28 (s, 1H, H-15), 7.91 (dd, *J* 8.8, 1.5, 1H, H-19), 7.80 (d, *J* 5.0, 2H, H-3), 7.73 (d, *J* 8.9, 1H, H-18). Note: urea NH not visible; **LCMS (LCQ)** Rt = 1.7 min (method 2), *m/z* (ESI⁺) 400.9 [M(⁷⁹Br)+H]⁺, 402.9 [M(⁸¹Br)+H]⁺. ¹H-NMR consistent with literature data.²⁰³

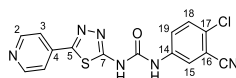
1-(3,4-Dichlorophenyl)-3-(5-(4-pyridyl)-1,3,4-thiadiazol-2-yl)urea (7)²⁰³



Compound **7** was synthesised according to general procedure B, using the following reagents: triphosgene (170 mg, 0.56 mmol), 3,4-dichloroaniline (230 mg, 1.41 mmol), dichloromethane (5 mL), triethylamine (0.39 mL, 2.81 mmol), 5-(4-pyridyl)-1,3,4-thiadiazol-2-yl-amine (**10**) (180 mg, 0.99 mmol) and *N,N*-dimethylformamide (4 mL). The reaction mixture was filtered while hot and the resulting solid was recrystallised in *N,N*-dimethylformamide to yield the desired compound **7** as an orange solid (40 mg, 7%).

¹H-NMR (500 MHz, DMSO-*d*₆) δ 11.63 (s, 1H, *NH*-urea), 9.44 (s, 1H, *NH*-urea), 8.69 (d, *J* 4.8 Hz, 2H, H-2), 7.88 (s, 1H, H-15), 7.83 (d, *J* 5.0 Hz, 2H, H-3), 7.53 (d, *J* 8.8 Hz, 1H, H-19), 7.43 (d, *J* 8.2 Hz, 1H, H-18) **LCMS (LCQ)** Rt = 2.4 min (method 2), *m/z* (ESI⁺) 365.9 [M(³⁵Cl³⁵Cl)+H]⁺, 367.9 [M(³⁵Cl³⁷Cl)+H]⁺. ¹H-NMR consistent with literature data.²⁰³

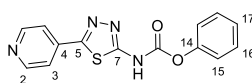
1-(4-chloro-3-cyano-phenyl)-3-(5-(4-pyridyl)-1,3,4-thiadiazol-2-yl)urea (8)²⁰³



Compound **7** was synthesised according to general procedure **B**, using the following reagents: triphosgene (170 mg, 0.56 mmol), 5-amino-2-chlorobenzonitrile (215 mg, 1.41 mmol), dichloromethane (5 mL), triethylamine (0.39 mL, 2.81 mmol), 5-(4-pyridyl)-1,3,4-thiadiazol-2-yl-amine (**10**) (200 mg, 1.13 mmol) and *N,N*-dimethylformamide (4 mL). The reaction mixture was filtered while hot and the resulting solid was recrystallised in *N,N*-dimethylformamide to yield the desired compound **7** as a yellow solid (117 mg, 22%).

¹H-NMR (500 MHz, DMSO-*d*₆) δ 11.56 (s, 1H, NH-urea), 9.48 (s, 1H, NH-urea), 8.73 (d, *J* 5.1, 2H, H-2), 7.92 (s, 1H, H-15), 7.87 (d, *J* 4.0, 2H, H-3), 7.58 (d, *J* 8.8 Hz, 1H, H-19), 7.47 (d, *J* 8.8 Hz, 1H, H-18). **LCMS (LCQ)** Rt = 2.4 min (method 2), *m/z* (ESI⁺) 365.9 [M(³⁵Cl)+H]⁺, 367.9 [M(³⁷Cl)+H]⁺. ¹H-NMR consistent with literature data.²⁰³

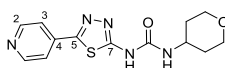
Phenyl-5-(4-pyridyl)-1,3,4-thiadiazol-2-ylcarbamate (**11**)



Sodium hydride (700 mg, 33.7 mmol) was slowly added to a suspension of 5-(4-pyridyl)-1,3,4-thiadiazol-2-yl-amine (2.00 g, 11.2 mmol) in tetrahydrofuran (40 mL) at 0 °C. The resulting reaction mixture was stirred at 0 °C for 2 h. Diphenyl carbonate (2.89 g, 13.5 mmol) was added and the reaction mixture was stirred at 0 °C for 30 min. The reaction mixture was warmed to r.t. and stirred overnight. Dichloromethane (40 mL) and brine (10 mL) was added to the reaction mixture and the solid precipitate was collected by filtration to yield the desired compound **11** as a crystalline off-white solid (3.10 g, 93%).

R_f 0.52 (dichloromethane:methanol 19:1); **m.p.** 278–280 °C; **¹H-NMR** (500 MHz, DMSO-*d*₆) δ 8.58 (d, *J* 4.9, 2H, H-2), 7.70 (d, *J* 4.9, 2H, H-3), 7.33 (t, *J* 7.6, 2H, H-15), 7.11 (t, *J* 7.4, 1H, H-17), 7.07 (d, *J* 7.7, 2H, H-16); **¹³C-NMR** (126 MHz DMSO-*d*₆) δ = 174.7 (CO), 162.1 (ArC), 155.1 (ArC), 153.7 (C-14), 150.7 (C-2), 140.1 (ArC), 129.2 (C-15), 124.0 (C-17), 122.4 (C-16), 120.2 (C-3); **IR** (neat, *v*_{max}, cm⁻¹) 3542, 3118, 2417, 1604, 1460, 1319, 1296, 1208, 1113; **LCMS (LCQ)** Rt = 1.8 min (method 2), *m/z* (ESI⁺) 299.03 [M+H]⁺; **HRMS** (ESI): calcd. for C₁₄H₁₁N₄O₂S [M+H]⁺ 299.0598, found 299.0597.

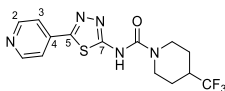
1-(5-(4-Pyridyl)-1,3,4-thiadiazol-2-yl)-3-tetrahydropyran-4-yl-urea (**12**)



Compound **12** was synthesised according to general procedure **A**, using the following reagents: phenyl *N*-(5-(4-pyridyl)-1,3,4-thiadiazol-2-yl)carbamate (**11**) (100 mg, 0.34 mmol), tetrahydropyran-4-amine (34 μL, 0.34 mmol) and toluene (5 mL). The reaction suspension was filtered and the resulting solid was purified by flash column chromatography (silica, 0 to 5% methanol in dichloromethane) to yield the desired urea **12** as a colourless solid (50 mg, 49%).

R_f 0.31 (dichloromethane:methanol, 19:1); **m.p.** >300 °C; **¹H-NMR** (500 MHz, DMSO-*d*₆) δ 10.95 (s, 1H, NH-urea), 8.70 (d, *J* 5.6, 2H, H-2), 7.84 (dd, *J* 4.6, 1.5, 2H, H-3), 6.77 (brs, 1H, CH₂NH), 3.83 (dt, *J* 11.8, 3.7, 2H, CHCH₂CH_AO), 3.75 (dtd, *J* 0.8, 6.8, 4.2, 1H, CHCH₂CH₂O), 3.39 (td, *J* = 11.4, 2.3, 2H, CHCH₂CH_BO) 1.85 – 1.76 (m, 2H, CHCH_{A+B}CH₂O), 1.46 (dtd, *J* 12.7, 10.8, 4.3, 2H, CHCH_{A+B}CH₂O). **¹³C-NMR** (126 MHz, DMSO-*d*₆) δ 161.9 (C=O), 159.2 (ArC), 153.0 (ArC), 151.1 (C-2), 137.8 (C-4), 121.0 (C-3), 66.1 (CHCH₂CH₂O), 46.6 (CHCH₂CH₂O), 33.1 (CHCH₂CH₂O); **IR** (neat, *v*_{max}, cm⁻¹) 3397, 2862, 2699, 1698, 1577, 1525, 1440, 1393, 1245, 1137, 1080; **LCMS (LCQ)** Rt = 0.68 min (method 2), *m/z* (ESI⁺) 306.0 [M+H]⁺; **HRMS** *m/z* (ESI): calcd. for C₁₃H₁₆N₅O₂S [M+H]⁺ 306.1019, found 306.1021.

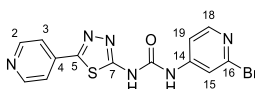
N-(5-(4-pyridyl)-1,3,4-thiadiazol-2-yl)-4-(trifluoromethyl)piperidine-1-carboxamide (**13**)



Compound **13** was synthesised according to general procedure A, using the following reagents: phenyl *N*-(5-(4-pyridyl)-1,3,4-thiadiazol-2-yl)carbamate (**11**) (100 mg, 0.34 mmol), 4-(trifluoromethyl)piperidine hydrochloride (60 mg, 0.34 mmol) and toluene (5 mL). The reaction suspension was filtered and the resulting solid was purified by flash column chromatography (silica, 0 to 2.5% methanol in dichloromethane) to yield the desired urea **13** as a yellow solid (53 mg, 42%).

R_f 0.51 (dichloromethane:methanol, 19:1); **m.p.** 238–240 °C; **¹H-NMR** (500 MHz, DMSO-*d*₆) δ 11.71 (s, 1H, NH), 8.71 (d, *J* 4.3, 2H, H-2), 7.84 (d, *J* 4.3, 2H, H-3), 4.35 (d, *J* 13.2, 2H, NCH_{AB}CH₂CH), 2.92 (t, *J* 12.8, 2H, NCH_{AB}CH₂CH), 2.67 – 2.60 (m, 1H, NCH₂CH₂CH), 1.86 (d, *J* 11.9, 2H, NCH₂CH_{AB}CH), 1.38 (qd, *J* 12.6, 3.6, 2H, NCH₂CH_{AB}CH); **¹³C-NMR** (126 MHz, DMSO-*d*₆) δ 151.1 (C-2), 137.8 (C-4), 120.9 (C-3), 42.9 (NCH₂CH₂CH), 24.5 (NCH₂CH₂CH). CO, C-5 and C-7 not visible. NCH₂CH₂CH covered by the solvent peak.; **IR** (neat, *v*_{max}, cm⁻¹) 3542, 3118, 1417, 1604, 1460, 1319, 1296, 1208, 1113; **LCMS** (LCQ) Rt = 1.85 min (method 2), *m/z* (ESI⁺) 358.7 [M+H]⁺; **HRMS** *m/z* (ESI): calcd. for C₁₄H₁₄F₃N₅OS [M+H]⁺ 357.0871, found 357.0873.

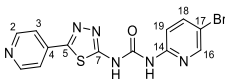
1-(2-Bromo-4-pyridyl)-3-(5-(4-pyridyl)-1,3,4-thiadiazol-2-yl)urea (**14**)



Compound **14** was synthesised according to general procedure A, using the following reagents: phenyl *N*-(5-(4-pyridyl)-1,3,4-thiadiazol-2-yl)carbamate (**11**) (60 mg, 0.20 mmol), 4-amino-2-bromopyridine (30 mg, 0.20 mmol) and toluene (4 mL). The reaction suspension was filtered and the resulting solid was triturated with hot methanol (2 × 5 mL) to yield the desired compound **14** as an orange solid (30 mg, 40%).

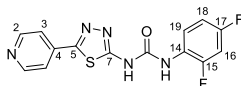
R_f 0.31 (dichloromethane:methanol, 19:1); **m.p.** >300 °C; **¹H-NMR** (500 MHz, DMSO-*d*₆) δ 9.92 (s, 1H, NH-urea), 8.74 (d, *J* 5.5, 2H, H-2), 8.21 (d, *J* 5.6, 1H, H-18), 7.92 – 7.82 (m, 3H, H-3, H-15), 7.51 (dd, *J* 5.7, 1.9, 1H, H-19). Note: urea NH not visible; **¹³C-NMR** (126 MHz, DMSO-*d*₆) δ 151.8 (C-2, C-18), 142.4 (ArC), 121.0 (C-3), 116.2 (C-15) 113.2 (ArC), 110.0 (ArC), 88.2 (ArC). CO and 3 × ArC not visible; **IR** (neat, *v*_{max}, cm⁻¹) 2631, 1706, 1634, 1566, 1548, 1512, 1410, 1217, 1236, 1121, 1206, 1033; **LCMS** (LCQ) Rt = 0.67 min (method 2), *m/z* (ESI⁺) 376.9 [M(⁷⁹Br)+H]⁺, 378.9 [M(⁸¹Br)+H]⁺; **HRMS** *m/z* (ESI): calcd. for C₁₃H₁₀BrN₆OS [M(⁷⁹Br)+H]⁺ 376.9815, found 376.9818.

1-(5-Bromo-2-pyridyl)-3-(5-(4-pyridyl)-1,3,4-thiadiazol-2-yl)urea (**15**)



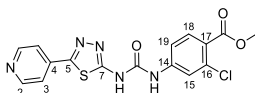
Compound **15** was synthesised according to general procedure A, using the following reagents: phenyl *N*-(5-(4-pyridyl)-1,3,4-thiadiazol-2-yl)carbamate (**11**) (60 mg, 0.20 mmol), 2-amino-5-bromopyridine (30 mg, 0.20 mmol) and toluene (4 mL). The reaction suspension was filtered and the resulting solid was triturated with hot methanol (2 × 5 mL) to yield the desired compound **15** as a colourless solid (35 mg, 46%).

R_f 0.47 (dichloromethane:methanol, 19:1); **m.p.** >300 °C; **¹H-NMR** (500 MHz, DMSO-*d*₆) δ 11.94 (s, 1H, NH-urea), 9.90 (s, 1H, NH-urea), 8.73 (d, *J* 5.7, 2H, H-2), 8.48 (d, *J* 2.4, 1H, H-16), 8.06 (dd, *J* 8.8, 2.5, 1H, H-19), 7.90 (d, *J* 6.0, 2H, H-3), 7.73 (d, *J* 8.9, 1H, H-18); **¹³C-NMR** (126 MHz, DMSO-*d*₆) 151.2 (C-2), 150.9 (C-4), 148.6 (16), , 141.7 (C-19), 137.5 (C-14), 121.1 (C-13), 114.6 (C-18), 113.6 (C-17). CO, C-5 and C-7 not visible; **IR** (neat, *v*_{max}, cm⁻¹) 3363, 3020, 2601, 1634, 1567, 1514, 1447, 1369, 1316, 1291, 1267, 1248, 1011; **LCMS** (LCQ) Rt = 1.61 min (method 2), *m/z* (ESI⁺) 376.9 [M(⁷⁹Br)+H]⁺, 378.9 [M(⁸¹Br)+H]⁺; **HRMS** *m/z* (ESI): calcd. for C₁₃H₁₀BrN₆OS [M(⁷⁹Br)+H]⁺ 376.9815, found 376.9817.

1-(2,4-Difluorophenyl)-3-(5-(4-pyridyl)-1,3,4-thiadiazol-2-yl)urea (16**)**

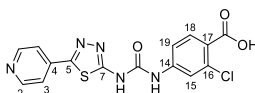
Compound **16** was synthesised according to general procedure A, using the following reagents: phenyl *N*-(5-(4-pyridyl)-1,3,4-thiadiazol-2-yl)carbamate (**11**) (100 mg, 0.34 mmol), 2,4-difluoroaniline (34 μ L, 0.34 mmol) and toluene (4 mL). The reaction suspension was filtered and the resulting solid was triturated with hot 10% methanol in dichloromethane (10 mL) to yield the desired urea **16** as a colourless solid (48 mg, 43%).

R_f 0.42 (dichloromethane:methanol, 19:1); **m.p.** >300 °C; **¹H-NMR** (500 MHz, DMSO-*d*₆) δ 11.50 (s, 1H, *NH*-urea), 8.94 (s, 1H, *NH*-urea), 8.71 (d, *J* 5.6, 2H, H-2), 7.99 (td, *J* 9.1, 6.0, 1H, H-19), 7.86 (d, *J* 5.7, 2H, H-3), 7.35 (ddd, *J* 11.4, 8.8, 2.9, 1H, H-16), 7.10 (ddd, *J* 10.7, 6.4, 2.0, 1H, H-18); **¹³C-NMR** (126 MHz, DMSO-*d*₆) δ 158.41 (dd, *J* 242.9, 11.2, ArC), 153.47 (dd, *J* 247.2, 13.1, ArC), 151.15 (C-2), 137.61 (C-4), 123.6 (dd, *J* 8.8, 1.9, 14-C), 123.0 (dd, *J* 11.6, 3.6, C-19), 121.1 (C-3), 111.8 (dd, *J* 21.9, 3.8, C-18), 104.6 (dd, *J* 27.0, 23.7, C-16). CO, C-5 and C-7 not visible; **IR** (neat, ν_{\max} , cm⁻¹) 3380, 2995, 2665, 1716, 1592, 1545, 1458, 1445, 1276, 1200, 1146, 1132, 1101; **LCMS** (LCQ) *R_t* = 1.82 min (method 2), *m/z* (ESI⁺) 378.9 [M+H]⁺; **HRMS** *m/z* (ESI): calcd. for C₁₄H₁₀F₂N₅OS [M+H]⁺ 334.0569, found 334.0569.

Methyl 2-chloro-4-((5-(4-pyridyl)-1,3,4-thiadiazol-2-yl)carbamoylamino)benzoate (23**)**

Compound **23** was synthesised according to general procedure B, using the following reagents: triphosgene (320 mg, 0.56 mmol), methyl 4-amino-2-chlorobenzoate (500 mg, 2.69 mmol), dichloromethane (10 mL), triethylamine (0.75 mL, 5.39 mmol), 5-(4-pyridyl)-1,3,4-thiadiazol-2-yl-amine (**10**) (384 mg, 2.16 mmol) and *N,N*-dimethylformamide (15 mL). The reaction mixture was filtered while hot and the resulting solid was washed with ethyl acetate to yield the desired urea **23** as an off-white solid (489 mg, 47%).

R_f 0.29 (dichloromethane:methanol, 19:1); **m.p.** >300 °C; **¹H-NMR** (500 MHz, DMSO-*d*₆) δ 9.37 (s, 1H, *NH*-urea), 8.57 (dd, *J* 4.5, 1.5, 2H, H-2), 7.96 (d, *J* 1.9, 1H, H-15), 7.73 (d, *J* 8.8, 1H, H-18), 7.70 (dd, *J* 4.5, 1.5, 2H, H-3), 7.57 (dd, *J* 8.7, 2.0, 1H, H-19), 3.79 (s, 3H, COOCH₃). One urea not visible; **IR** (neat, ν_{\max} , cm⁻¹) 2905, 2490, 1920, 1695, 1616, 1292; **LCMS** (LCQ) *R_t* = 1.34 min (method 2), *m/z* (ESI⁺) 390.2 [M(³⁵Cl)+H]⁺, 391.9 [M(³⁷Cl)+H]⁺; **HRMS** *m/z* (ESI): calcd. for C₁₆H₁₃ClN₅O₃S [M(³⁵Cl)+H]⁺ 390.0422, found 390.0428. The high insolubility of the compound prevented the preparation of a sufficiently concentrated sample for ¹³C-NMR.

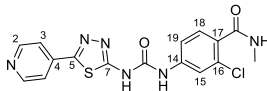
2-Chloro-4-((5-(4-pyridyl)-1,3,4-thiadiazol-2-yl)carbamoylamino)benzoic acid (24**)**

To methyl 2-chloro-4-((5-(4-pyridyl)-1,3,4-thiadiazol-2-yl)carbamoylamino)benzoate (**23**) (200 mg, 0.51 mmol) in water (4 mL) and methanol (12 mL) was added sodium hydroxide (205 mg, 5.13 mmol) and the reaction mixture was stirred at 65 °C for 16 h. The reaction mixture was concentrated under reduced pressure. The crude was taken up in water (10 mL), washed with ethyl acetate (15 mL) then acidified to pH of 2-3 using 2 M aq. hydrochloric acid solution. The resulting precipitate was collected by filtration to yield the desired compound **24** as a yellow solid (88 mg, 91%).

m.p. >300 °C; **¹H-NMR** (500 MHz, DMSO-*d*₆) δ 12.74 (s, 1H), 10.66 (s, 1H, *NH*-urea), 8.72 (dd, *J* 4.5, 1.7, 2H, H-2), 7.90 – 7.87 (m, 3H, H-3, H-15), 7.85 (d, *J* 8.6, 1H, H-18), 7.58 (dd, *J* 8.6, 1.6, 1H, H-19); **¹³C-NMR** (126 MHz, DMSO-*d*₆) δ 166.9 (CO), 151.1 (C-2), 143.1 (ArC), 137.9 (C-4), 133.6 (ArC), 133.0 (ArC), 132.9 (ArC), 121.0 (C-3), 119.8 (C-15), 116.8

(C-19). CO, C-5 and C-7 not visible; **IR** (neat, ν_{\max} , cm^{-1}) 3391, 3045, 2826, 2732, 1700, 1630, 1567, 1505, 1441, 1411, 1384, 1291, 1234; **LCMS** (LCQ) $R_t = 0.40$ min (method 2), m/z (ESI⁺) 375.9 [M(³⁵Cl)+H]⁺, 377.9 [M(³⁷Cl)+H]⁺; **HRMS** m/z (ESI): calcd. for C₁₅H₁₁ClN₅O₃S [M(³⁵Cl)+H]⁺ 376.0266, found 376.0271.

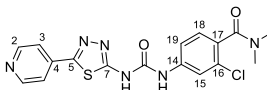
2-Chloro-*N*-methyl-4-((5-(4-pyridyl)-1,3,4-thiadiazol-2-yl)carbamoylamino)benzamide (25)



Compound **25** was synthesised according to general procedure C, using the following reagents: 2-chloro-4-((5-(4-pyridyl)-1,3,4-thiadiazol-2-yl)carbamoylamino)benzoic acid (**24**) (60 mg, 0.16 mmol), HATU (70 mg, 0.19 mmol), *N,N*-diisopropylethylamine (56 μL , 0.32 mmol), methylamine (25%) in water (9 μL , 0.19 mmol) and *N,N*-dimethylformamide (2.5 mL). The crude was purified by column chromatography (amino silica, 0 to 20% methanol in dichloromethane) and further purified by column chromatography (C-18 silica, 0 to 100% methanol in water) to yield the desired compound **25** as a yellow solid (15 mg, 23%).

R_f 0.20 (dichloromethane:methanol, 8:2, amino silica); **m.p.** 252–254 °C; **¹H-NMR** (500 MHz, DMSO-*d*₆) δ 9.99 (s, 1H, NH-urea), 8.73 (d, *J* 5.1, 2H, H-2), 8.23 (s, 1H, COONHCH₃), 7.94 – 7.78 (m, 3H, H-3, H-15), 7.52 (d, *J* 8.4, 1H, H-19), 7.41 (d, *J* 8.3, 1H, H-18), 2.75 (d, *J* 4.6, 3H, COONHCH₃); **¹³C-NMR** (126 MHz, DMSO-*d*₆) δ 166.8 (CO), 151.1 (C-2), 141.5 (ArC), 137.9 (C-4), 131.0 (ArC), 130.9 (ArC), 130.0 (C-18), 120.8 (C-3), 119.2 (C-15), 117.1 (C-19), 26.4 (COONHC). CO, C-5 and C-7 not visible; **IR** (neat, ν_{\max} , cm^{-1}) 3352, 2928, 2714, 1702, 1627, 1602, 1519, 1443, 1412, 1386, 1303, 1243, 1210; **LCMS** (LCQ) $R_t = 0.52$ min (method 2), m/z (ESI⁺) 388.9 [M(³⁵Cl)+H]⁺, 390.8 [M(³⁷Cl)+H]⁺; **HRMS** m/z (ESI): calcd. for C₁₆H₁₄ClN₆O₂S [M(³⁵Cl)+H]⁺ 389.0587, found 389.0587.

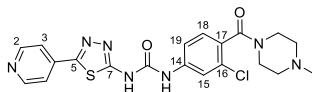
2-Chloro-*N,N*-dimethyl-4-((5-(4-pyridyl)-1,3,4-thiadiazol-2-yl)carbamoylamino)benzamide (26)



Compound **26** was synthesised according to general procedure C, using the following reagents: 2-chloro-4-((5-(4-pyridyl)-1,3,4-thiadiazol-2-yl)carbamoylamino)benzoic acid (**24**) (70 mg, 0.19 mmol), HATU (85 mg, 0.22 mmol), *N,N*-diisopropylethylamine (65 μL , 0.37 mmol), dimethylamine (2 M) in tetrahydrofuran (0.11 mL, 0.32 mmol) and *N,N*-dimethylformamide (2.5 mL). The crude was purified by column chromatography (amino silica, 0 to 15% methanol in dichloromethane) to yield the desired compound **26** as a yellow solid (52 mg, 66%).

R_f 0.25 (dichloromethane:methanol, 17:3, amino silica); **m.p.** 221–224 °C; **¹H-NMR** (500 MHz, DMSO-*d*₆) δ 10.02 (s, 1H, NH-urea), 8.72 (d, *J* 5.3, 2H, H-2), 7.92 – 7.81 (m, 3H, H-3, H-15), 7.58 (d, *J* 8.3, 1H, H-19), 7.30 (d, *J* 8.3, 1H, H-18), 3.00 (s, 3H, COONH(CH₃)₂), 2.80 (s, 3H, COONH(CH₃)₂); **¹³C-NMR** (126 MHz, DMSO-*d*₆) δ 167.5 (CO), 151.1 (C-2), 141.1 (ArC), 137.9 (C-4), 130.6 (ArC), 129.9 (ArC), 128.8 (C-18), 120.9 (C-3), 119.0 (C-15), 117.9 (C-19), 38.1 (COONHC), 34.54 (COONHC). CO, C-5 and C-7 not visible; **IR** (neat, ν_{\max} , cm^{-1}) 3375, 2923, 2851, 1703, 1601, 1521, 1443, 1387, 1304, 1241, 1202; **LCMS** (LCQ) $R_t = 1.13$ min (method 2), m/z (ESI⁺) 402.9 [M(³⁵Cl)+H]⁺, 404.9 [M(³⁷Cl)+H]⁺; **HRMS** m/z (ESI): calcd. for C₁₇H₁₆ClN₆O₂S [M(³⁵Cl)+H]⁺ 403.0738, found 403.0738.

1-(3-Chloro-4-(4-methylpiperazine-1-carbonyl)phenyl)-3-(5-(4-pyridyl)-1,3,4-thiadiazol-2-yl)urea (27)

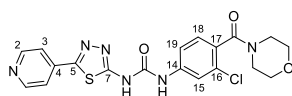


Compound **27** was synthesised according to general procedure C, using the following reagents: 2-chloro-4-((5-(4-pyridyl)-1,3,4-thiadiazol-2-yl)carbamoylamino)benzoic acid (**24**) (100 mg, 0.27 mmol), HATU (120 mg, 0.32 mmol),

N,N-diisopropylethylamine (92 μ L, 0.53 mmol), 1-methylpiperazine (35 μ L, 0.32 mmol) and *N,N*-dimethylformamide (3 mL). The crude was purified by column chromatography (silica, 0 to 5% methanol in dichloromethane) and further purified by column chromatography (amino silica, 0 to 20% methanol in dichloromethane) to yield the desired compound **27** as a yellow/orange solid (79 mg, 58%).

R_f 0.20 (dichloromethane:methanol, 4:1, amino silica); **m.p.** 198–201 °C; **¹H-NMR** (500 MHz, DMSO-*d*₆) δ 10.58 (s, 1H, *NH*-urea), 8.72 (d, *J* 5.1, 2H, H-2), 7.98 (s, 1H, H-15), 7.88 (d, *J* 5.1, 2H, H-3), 7.68 (d, *J* 8.4, 1H, H-19), 7.31 (d, *J* 8.3, 1H, H-18), 3.68–3.61 (br s, 4H, CONCH₂), 3.22–3.12 (m, 4H, CONCH₂CH₂), 2.23 (s, 3H, NCH₃). One urea NH not visible; **¹³C-NMR** (126 MHz, DMSO-*d*₆) δ 166.0 (CO), 164.8 (CO), 158.0 (ArC), 154.7 (ArC), 151.1 (C-2), 141.6 (ArC), 138.0 (C-4), 130.0 (ArC), 129.7 (ArC), 128.9 (C-18), 120.8 (C-3), 118.9 (C-15), 117.7 (C-19), 46.5 (CONCH₂CH₂), 45.8 (NCH₃), 41.3 (CONCH₂); **IR** (neat, ν_{\max} , cm⁻¹) 3185, 3046, 2926, 2859, 2805, 1691, 1598, 1517, 1429, 1380, 1295, 1241, 1219; **LCMS** (LCQ) *Rt* = 0.31 min (method 2), *m/z* (ESI⁺) 458.0 [M(³⁵Cl)+H]⁺, 459.9 [M(³⁷Cl)+H]⁺; **HRMS** *m/z* (ESI): calcd. for C₂₀H₂₁ClN₇O₂S [M(³⁵Cl)+H]⁺ 458.1162, found 458.1160.

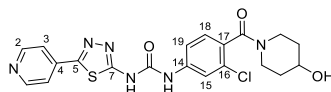
1-(3-Chloro-4-(morpholine-4-carbonyl)phenyl)-3-(5-(4-pyridyl)-1,3,4-thiadiazol-2-yl)urea (**28**)



Compound **28** was synthesised according to general procedure C, using the following reagents: 2-chloro-4-((5-(4-pyridyl)-1,3,4-thiadiazol-2-yl)carbamoylamino)benzoic acid (**24**) (80 mg, 0.21 mmol), HATU (100 mg, 0.26 mmol), *N,N*-diisopropylethylamine (0.11 mL, 0.64 mmol), morpholine (22 μ L, 0.26 mmol) and *N,N*-dimethylformamide (2.5 mL). The resulting crude solid was triturated in ethyl acetate then dichloromethane to yield the desired compound **28** as a yellow solid (36 mg, 40%).

R_f 0.30 (dichloromethane:methanol, 4:1, amino silica); **m.p.** 202–204 °C; **¹H-NMR** (500 MHz, DMSO-*d*₆) δ 9.53 (s, 1H, 13-NH), 8.73 (d, *J* 5.6, 2H, 2-CH), 7.87 (d, *J* 5.2, 2H, 3-CH), 7.81 (s, 1H, 15-CH), 7.49 (d, *J* 7.9, 1H, 19-CH), 7.34 (d, *J* 8.3, 1H, 18-CH), 3.64 (br s, 4H, CONCH₂), 3.54 (t, *J* 4.8, 2H, CONCH₂CH_{AB}O), 3.16 (t, *J* 4.8, 2H, CONCH₂CH_{AB}O). One urea NH not visible; **¹³C-NMR** (126 MHz, DMSO-*d*₆) δ 166.0 (CO), 151.1 (C-2), 140.7 (ArC), 137.6 (ArC), 130.0 (ArC), 129.0 (C-18), 121.0 (C-3), 119.3 (C-15), 118.2 (C-19), 110.00 (ArC), 66.6 (CONCH₂), 66.4 (CONCH₂), 47.2 (CONCH₂CH₂O), 42.1 (CONCH₂CH₂O). CO, C-5 and C-7 not visible; **IR** (neat, ν_{\max} , cm⁻¹) 3289, 1972, 2861, 1717, 1602, 1526, 1460, 1438, 1415, 1388, 1301, 1280; **LCMS** (LCQ) *Rt* = 0.58 min (method 2), *m/z* (ESI⁺) 444.9 [M(³⁵Cl)+H]⁺, 446.9 [M(³⁷Cl)+H]⁺; **HRMS** *m/z* (ESI): calcd. for C₁₉H₁₈ClN₆O₃S [M(³⁵Cl)+H]⁺ 445.0844, found 445.0840.

1-(3-Chloro-4-(4-hydroxypiperidine-1-carbonyl)phenyl)-3-(5-(4-pyridyl)-1,3,4-thiadiazol-2-yl)urea (**29**)

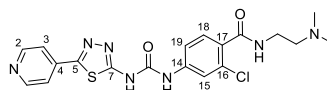


Compound **29** was synthesised according to general procedure C, using the following reagents: 2-chloro-4-((5-(4-pyridyl)-1,3,4-thiadiazol-2-yl)carbamoylamino)benzoic acid (**24**) (80 mg, 0.21 mmol), HATU (97 mg, 0.26 mmol), *N,N*-diisopropylethylamine (0.11 mL, 0.64 mmol), 4-hydroxypiperidine (26 mg, 0.26 mmol) and *N,N*-dimethylformamide (2.5 mL). The resulting crude solid was triturated in ethyl acetate then dichloromethane to yield the desired compound **29** as an orange solid (40 mg, 41%).

R_f 0.40 (dichloromethane:methanol, 9:1, amino silica); **m.p.** 208–210 °C; **¹H-NMR** (500 MHz, DMSO-*d*₆) δ 9.52 (s, 1H, *NH*-urea), 8.73 (d, *J* 5.1, 2H, H-2), 7.87 (d, *J* 5.3, 2H, H-3), 7.80 (s, 1H, H-15), 7.49 (d, *J* 8.2, 1H, H-19), 7.30 (dd, *J* 12.8, 8.1, 1H, H-18), 4.78 (s, 1H, OH), 4.11–3.94 (m, 1H), 3.73 (s, 1H), 3.25–3.16 (m, 1H), 3.09–2.94 (m, 1H), 1.86–1.73

(m, 1H), 1.67 (s, 1H), 1.46 – 1.19 (m, 2H). One urea NH not visible and one piperidine H is under water peak; $^{13}\text{C-NMR}$ (126 MHz, DMSO- d_6) δ 165.7 (CO), 151.1 (C-2), 140.4 (ArC), 137.6 (C-4), 130.9 (ArC), 129.9 (ArC), 128.7 (C-18), 121.0 (C-3), 119.9 (C-15), 118.2 (C-19), 65.8 (COH), 44.3 (NCH₂CH₂COH), 39.0 (NCH₂CH₂COH), 34.8 (NCH₂CH₂COH), 34.1 (NCH₂CH₂COH). CO, C-5 and C-7 not visible; **IR** (neat, ν_{max} , cm⁻¹) 3345, 2925, 2869, 1708, 1593, 1524, 1441, 1388, 1303, 1240, 1204; **LCMS** (LCQ) Rt = 0.48 min (method 2), m/z (ESI⁺) 459.0 [M(³⁵Cl)+H]⁺, 461.0 [M(³⁷Cl)+H]⁺; **HRMS** m/z (ESI): calcd. for C₂₀H₂₀ClN₆O₃S [M(³⁵Cl)+H]⁺ 459.1001, found 459.1003.

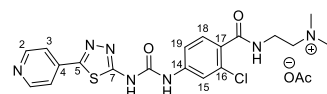
2-Chloro-*N*-(2-(dimethylamino)ethyl)-4-((5-(4-pyridyl)-1,3,4-thiadiazol-2-yl)carbamoylamino)-benzamide (**30**)



Compound **30** was synthesised according to general procedure C, using the following reagents: 2-chloro-4-((5-(4-pyridyl)-1,3,4-thiadiazol-2-yl)carbamoylamino)benzoic acid (**24**) (80 mg, 0.21 mmol), HATU (97 mg, 0.26 mmol), *N,N*-diisopropylethylamine (65 μL , 0.4 mmol), *N,N*-dimethylethylenediamine (35 μL , 0.26 mmol) and *N,N*-dimethylformamide (3 mL). The crude product was purified by column chromatography (amino silica, 0 to 20% methanol in dichloromethane) to yield the desired compound **30** as a pale brown solid (74 mg, 79%).

R_f 0.20 (dichloromethane:methanol, 4:1, amino silica); **m.p.** 230–232 °C; $^1\text{H-NMR}$ (500 MHz, DMSO- d_6) δ 10.56 (s, 1H, NH-urea), 8.70 (d, J 5.1, 2H, H-2), 8.26 (t, J 5.6, 1H, CONHCH₂), 7.99 (s, 1H, H-15), 7.86 (d, J 5.1, 2H, H-3), 7.68 (d, J 8.4, 1H, H-19), 7.42 (d, J 8.4, 1H, H-18), 2.61 (t, J 6.8, 2H, CONHCH₂CH₂N(CH₃)₂), 2.35 (s, 6H, CONHCH₂CH₂N(CH₃)₂). One urea NH not visible and CONHCH₂CH₂N(CH₃)₂ is covered by water peak; $^{13}\text{C-NMR}$ (126 MHz, DMSO- d_6) δ 166.59 (CO), 166.5 (CO), 157.2 (ArC), 155.9 (ArC), 151.0 (C-1), 142.6 (ArC), 138.4 (C-4), 130.9 (ArC), 130.2 (ArC), 129.8 (ArC), 120.6 (C-3), 119.0 (C-15), 116.7 (C-19), 57.8 (CONHCH₂CH₂), 45.0 (CONHCH₂CH₂N(CH₃)₂), 37.1 (CONHCH₂); **IR** (neat, ν_{max} , cm⁻¹) 3269, 3050, 2926, 2850, 2716, 1696, 1624, 1606, 1566, 1491, 1437, 1312, 1246, 1232; **LCMS** (LCQ) Rt = 0.20 min (method 2), m/z (ESI⁺) 446.0 [M(³⁵Cl)+H]⁺, 448.0 [M(³⁷Cl)+H]⁺; **HRMS** m/z (ESI): calcd. for C₁₉H₂₁ClN₇O₂S [M(³⁵Cl)+H]⁺ 446.1160, found 446.1157.

2-((2-Chloro-4-((5-(4-pyridyl)-1,3,4-thiadiazol-2-yl)carbamoylamino)benzoyl)amino)ethyl-dimethyl-ammonium acetate (**31**)

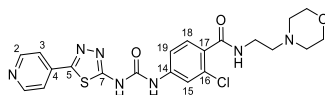


Compound **31** was synthesised according to general procedure C, using the following reagents: 2-chloro-4-((5-(4-pyridyl)-1,3,4-thiadiazol-2-yl)carbamoylamino)benzoic acid (**24**) (100 mg, 0.27 mmol), HATU (120 mg, 0.32 mmol), *N,N*-diisopropylethylamine (92 μL , 0.53 mmol), *N,N*-dimethylethylenediamine (35 μL , 0.32 mmol) and *N,N*-dimethylformamide (3 mL). The crude product was purified by column chromatography (amino silica, 0 to 20% methanol in dichloromethane and 0.5% acetic acid) to yield the desired compound **31** as the acetate salt of **30** as a pale brown solid (73 mg, 54%).

R_f 0.20 (dichloromethane:methanol, 4:1, amino silica); **m.p.** 236–238 °C; $^1\text{H-NMR}$ (500 MHz, DMSO- d_6) δ 10.89 (s, 1H, NH-urea), 8.70 (dd, J 4.6, 1.5, 2H, H-2), 8.28 (t, J 5.7, 1H, ArCONHCH₂), 8.02 (d, J 2.1 Hz, 1H, H-15), 7.87 (dd, J 4.5, 1.8, 2H, H-3), 7.72 (dd, J 8.4, 2.1, 1H, H-19), 7.44 (d, J 8.4, 1H, H-18), 3.39 (q, J 6.4, 2H, ArCONHCH₂), 2.65 (t, J 6.8, 2H, ArCONHCH₂CH₂), 2.38 (s, 6H, N(CH₃)₂), 1.90 (s, 3H, ⁻OCOCH₃). Note: one urea NH not visible; $^{13}\text{C-NMR}$ (126 MHz, DMSO- d_6) δ 172.5 (CO), 166.6 (CO), 166.5 (CO), 157.3 (C-7), 155.9 (C-5), 151.0 (C-2), 142.7 (ArC), 138.4 (C-4), 131.0

(ArC), 130.2 (ArC), 129.8 (ArC), 120.7 (C-3), 119.0 (C-15), 116.7 (C-19), 57.8 (ArCONHCH₂CH₂), 44.9 (N(CH₃)₂), 37.0 (ArCONHCH₂CH₂), 21.6 (CH₃COO⁻); **IR** (neat, ν_{\max} , cm⁻¹) 3747, 3263, 3040, 2929, 2715, 1700, 1635, 1601, 1575, 1524, 1490, 1430, 1408, 1305, 1245; **LCMS** (LCQ) Rt = 0.3 min (method 2), m/z (ESI⁺) 446.0 [M(³⁵Cl)+H]⁺, 448.1 [M(³⁷Cl)+H]⁺; **HRMS** m/z (ESI): calcd. for C₁₉H₂₁ClN₇O₂S [M(³⁵Cl)+H]⁺ 446.1160, found 446.1156.

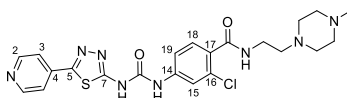
2-Chloro-*N*-(2-morpholinoethyl)-4-((5-(4-pyridyl)-1,3,4-thiadiazol-2-yl)carbamoylamino)-benzamide (32)



Compound **32** was synthesised according to general procedure C, using the following reagents: 2-chloro-4-((5-(4-pyridyl)-1,3,4-thiadiazol-2-yl)carbamoylamino)benzoic acid (**24**) (100 mg, 0.27 mmol), HATU (120 mg, 0.32 mmol), *N,N*-diisopropylethylamine (93 μ L, 0.53 mmol), *N*'-ethyl-*N*'-(2-methoxyethyl)ethane-1,2-diamine (47 μ L, 0.32 mmol) and *N,N*-dimethylformamide (3 mL). The crude product was purified by column chromatography (amino silica, 0 to 20% methanol in dichloromethane) to yield the desired compound **32** as an orange solid (76 mg, 58%);

R_f 0.30 (dichloromethane:methanol, 4:1, amino silica); **m.p.** 246–248 °C; **¹H-NMR** (500 MHz, DMSO-*d*₆) δ 9.73 (s, 1H, NH-urea), 8.73 (d, *J* 5.7, 2H, H-2), 8.26 (t, *J* 5.4, 2H, ArCONHCH₂), 7.88 (d, *J* 5.7, 2H, H-3), 7.82 (d, *J* 1.3, 1H, H-15), 7.51 (dd, *J* 8.4, 1.5, 1H, H-19), 7.42 (d, *J* 8.3, 1H, H-18), 3.64–3.55 (t, 4H, NCH₂CH₂O), 3.42–3.34 (m, 2H, ArCONHCH₂CH₂). One urea NH not visible. ArCONHCH₂CH₂ and ArCONCH₂CH₂ are covered by the solvent peak. Peak at 3.42-3.34 is partially impeded by water peak. **¹³C-NMR** (126 MHz, DMSO-*d*₆) δ 166.4 (CO), 163.1 (CO), 158.6 (ArC), 153.6 (ArC), 151.1 (C-2), 141.3 (ArC), 137.7 (C-4), 131.1 (ArC), 130.9 (ArC), 130.1 (C-18), 120.9 (C-3), 119.5 (C-15), 117.4 (C-19), 66.4 (NCH₂CH₂O), 57.3 (NCH₂CH₂O), 53.5 (ArCONHCH₂CH₂), 36.60 (ArCONHCH₂CH₂); **IR** (neat, ν_{\max} , cm⁻¹) 3651, 3293, 2945, 2820, 1701, 1649, 1603, 1526, 1503, 1451, 1413, 1297, 1247; **LCMS** (LCQ) Rt = 0.5 min (method 3), m/z (ESI⁺) 488.0 [M(³⁵Cl)+H]⁺, 490.0 [M(³⁷Cl)+H]⁺; **HRMS** m/z (ESI): calcd. for C₂₁H₂₃ClN₇O₃S [M(³⁵Cl)+H]⁺ 488.1266, found 488.1259.

2-Chloro-*N*-(2-(4-methylpiperazin-1-yl)ethyl)-4-((5-(4-pyridyl)-1,3,4-thiadiazol-2-yl)carbamoylamino)benzamide (33)

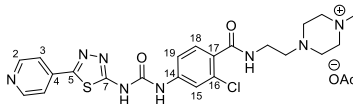


Compound **33** was synthesised according to general procedure C using the following reagents: 2-chloro-4-((5-(4-pyridyl)-1,3,4-thiadiazol-2-yl)carbamoylamino)benzoic acid (**24**) (90 mg, 0.24 mmol), HATU (109 mg, 0.29 mmol), *N,N*-diisopropylethylamine (83 μ L, 0.48 mmol), 2-(4-methyl-piperazin-1-yl)-ethylamine (51 μ L, 0.29 mmol) and *N,N*-dimethylformamide (3 mL). The crude product was purified by column chromatography (amino silica 12 g, 0 to 20% methanol in dichloromethane) to yield the desired compound **33** as a cream solid (89 mg, 74%).

R_f 0.25 (dichloromethane:methanol, 4:1, amino silica); **m.p.** 218–220 °C; **¹H-NMR** (500 MHz, DMSO-*d*₆) δ 10.58 (s, 1H, NH-urea), 8.71 (d, *J* 5.0, 2H, H-2), 8.20 (t, *J* 5.6, 1H, ArCONHCH₂), 7.98 (s, 1H, H-15), 7.87 (d, *J* 5.0, 2H, H-3), 7.68 (d, *J* 8.4, 1H, H-19), 7.42 (d, *J* 8.3, 1H, H-18), 2.62 (m, 4H), 2.35 (s, 3H, NCH₂CH₂NCH₃). One urea NH not visible, ArCONCH₂CH₂ is under water peak and ArCONHCH₂CH₂N and 2 \times piperazine-CH₂ under solvent peak; **¹³C-NMR** (126 MHz, DMSO-*d*₆) δ 166.4 (CO), 166.2 (CO), 157.42 (C-7), 155.6 (C-5), 151.0 (C-2), 142.4 (ArC), 138.3 (C-4), 130.9 (ArC), 130.2 (ArC), 130.1 (ArC), 120.7 (C-3), 119.1 (C-15), 116.8 (C-19), 56.7 (ArCONCH₂CH₂), 54.6, 52.0, 45.0 (NCH₂CH₂NCH₃), 37.0 (ArCONCH₂CH₂); **IR** (neat, ν_{\max} , cm⁻¹) 3525, 3040, 2938, 2817, 1695, 1631, 1605, 1536, 1490, 1425, 1387, 1305,

1237, 1203; **LCMS** (LCQ) Rt = 0.5 min (method 1), m/z (ESI⁺) 501.0 [M(³⁵Cl)+H]⁺, 503.0 [M(³⁷Cl)+H]⁺; **HRMS** m/z (ESI): calcd. for C₂₂H₂₆ClN₈O₂S [M(³⁵Cl)+H]⁺ 501.1582, found 501.1569.

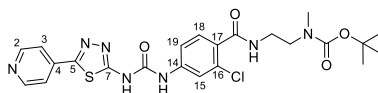
2-Chloro-*N*-(2-(4-methylpiperazin-4-ium-1-yl)ethyl)-4-((5-(4-pyridyl)-1,3,4-thiadiazol-2-yl)carbamoylamino)benzamide acetate (34**)**



Compound **34** was synthesised according to general procedure C, using the following reagents: 2-chloro-4-((5-(4-pyridyl)-1,3,4-thiadiazol-2-yl)carbamoylamino)benzoic acid (**24**) (100 mg, 0.27 mmol), HATU (120 mg, 0.32 mmol), *N,N*-diisopropylethylamine (92 μ L, 0.53 mmol), 2-(4-methyl-piperazin-1-yl)-ethylamine (57 μ L, 0.32 mmol) and *N,N*-dimethylformamide (3 mL). The crude product was purified by column chromatography (amino silica, 0 to 20% methanol in dichloromethane and 0.5% acetic acid) to yield the desired compound **34** as the acetate salt of **33** as a pale yellow solid (100 mg, 67%).

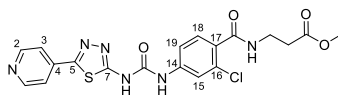
R_f 0.25 (dichloromethane:methanol, 4:1, amino silica); **m.p.** 212–213 °C; **¹H-NMR** (500 MHz, DMSO-*d*₆) δ 10.25 (s, 1H, *NH*-urea), 8.64 (d, *J* 6.0, 2H, H-2), 8.11 (t, *J* 5.7, 1H, ArCONHCH₂), 7.98 (d, *J* 2.0, 1H, H-15), 7.79 (d, *J* 5.4, 2H, H-3), 7.63 (d, *J* 8.1, 1H, H-19), 7.35 (d, *J* 8.5, 1H, H-18), 2.46 (t, *J* 7.0, 2H, ArCONHCH₂CH₂N), 2.40 – 2.27 (m, 4H), 2.17 (s, 3H, NCH₂CH₂NCH₃), 1.91 (s, 3H, CH₃COO⁻). One urea NH not visible, ArCONCH₂CH₂ is under water peak and ArCONHCH₂CH₂N and 2 \times piperazine-CH₂ under solvent peak; **¹³C-NMR** (126 MHz, DMSO-*d*₆) δ 172.9 (CH₃COO⁻), 169.1 (CO), 166.5 (CO), 158.3 (ArC), 155.6 (ArC), 150.8 (C-2), 143.8 (ArC), 139.3 (C-4), 130.8 (ArC), 130.0 (ArC), 128.9 (ArC), 120.4 (C-3), 118.3 (C-15), 116.1 (C-19), 57.0 (ArCONCH₂CH₂), 55.2, 53.0, 46.08 (NCH₂CH₂N⁺CH₃), 37.20 (ArCONCH₂CH₂), 21.78 (CH₃COO⁻); **IR** (neat, ν_{\max} , cm⁻¹) 3752, 3276, 3040, 2933, 2728, 1695, 1640, 1605, 1571, 1545, 1490, 1430, 1305, 1250; **LCMS** (LCQ) Rt = 0.3 min (method 2), m/z (ESI⁺) 501.0 [M(³⁵Cl)+H]⁺, 503.0 [M(³⁷Cl)+H]⁺; **HRMS** m/z (ESI): calcd. for C₂₂H₂₆ClN₈O₂S [M(³⁵Cl)+H]⁺ 501.1582, found 501.1578.

***Tert*-butyl *N*-(2-((2-chloro-4-((5-(4-pyridyl)-1,3,4-thiadiazol-2-yl)carbamoylamino)benzoyl)-amino)ethyl)-*N*-methyl-carbamate (**35**)**



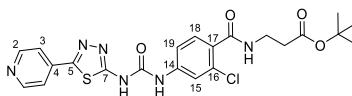
Compound **35** was synthesised according to general procedure C, using the following reagents: 2-chloro-4-((5-(4-pyridyl)-1,3,4-thiadiazol-2-yl)carbamoylamino)benzoic acid (**24**) (120 mg, 0.32 mmol), HATU (146 mg, 0.38 mmol), *N,N*-diisopropylethylamine (0.11 mL, 0.64 mmol), *tert*-butyl (2-aminoethyl)methylcarbamate (69 μ L, 0.38 mmol) and *N,N*-dimethylformamide (4 mL). The crude product was twice purified by column chromatography (silica, 0 to 5% methanol in dichloromethane) to yield the desired compound **35** as an orange solid (65 mg, 38%).

R_f 0.35 (dichloromethane:methanol, 19:1, amino silica); **m.p.** 238–240 °C; **¹H-NMR** (500 MHz, DMSO-*d*₆) δ 9.53 (s, 1H, *NH*-urea), 8.74 (s, 2H, H-2), 8.45 – 8.28 (m, 1H, ArCONHCH₂), 7.88 (d, *J* 5.2, 2H, H-3), 7.77 (s, 1H, H-15), 7.46 (d, *J* 6.9, 1H, H-19), 7.40 (d, *J* 8.4, 1H, H-18), 2.84 (s, 3H, NCH₃), 1.40 (s, 9H, COOC(CH₃)₃). One urea NH not visible, ArCONCH₂CH₂ is under water peak and ArCONHCH₂CH₂N is under solvent peak; **¹³C-NMR** (126 MHz, DMSO-*d*₆) δ 166.4 (CO), 151.1 (C-2), 140.9 (ArC), 137.6 (ArC), 130.9 (ArC), 130.1 (C-18), 121.0 (C-3), 119.6 (C-15), 117.4 (C-19), 79.0 (COOC(CH₃)₃), 37.5 (ArCONCH₂CH₂), 34.8 (NCH₃), 28.54 (COOC(CH₃)₃). CO, C-5, C-7 and ArC not visible. ArCONCH₂CH₂ is under solvent peak; **IR** (neat, ν_{\max} , cm⁻¹) 3280, 2929, 2869, 1640, 1585, 1521, 1489, 1446, 1414, 1390, 1365, 1302, 1239, 1204; **LCMS** (LCQ) Rt = 1.3 min (method 2), m/z (ESI⁺) 432.0 [M(³⁵Cl)+H]⁺, 434.0 [M(³⁷Cl)+H]⁺. Removal of boc group occurs during ionization; **HRMS** m/z (ESI): calcd. for C₂₃H₂₆ClN₅O₄S [M(³⁵Cl)+H]⁺ 532.1528, found 532.1532.

Methyl 3-((2-chloro-4-((5-(4-pyridyl)-1,3,4-thiadiazol-2-yl)carbamoylamino)benzoyl)amino)-propanoate (36)

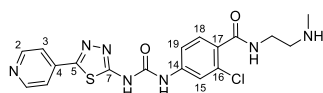
Compound **36** was synthesised according to general procedure C, using the following reagents: 2-chloro-4-((5-(4-pyridyl)-1,3,4-thiadiazol-2-yl)carbamoylamino)benzoic acid (**24**) (130 mg, 0.35 mmol), HATU (157 mg, 0.42 mmol), *N,N*-diisopropylethylamine (0.18 mL, 1.04 mmol), methyl 3-aminopropanoate (42 mg, 0.42 mmol) and *N,N*-dimethylformamide (4 mL). The crude product was purified by column chromatography (silica, 0 to 5% methanol in dichloromethane). The resulting solid was triturated in ethyl acetate then dichloromethane to yield the desired compound **36** as an orange solid (45 mg, 28%).

R_f 0.45 (dichloromethane:methanol, 19:1); **m.p.** 245–247 °C; **¹H-NMR** (500 MHz, DMSO-*d*₆) δ 9.69 (s, 1H, *NH*-urea), 8.73 (d, *J* 4.7, 2H, H-2), 8.42 (t, *J* 5.3 Hz, 1H, ArCONHCH₂), 7.88 (d, *J* 5.5, 2H, H-3), 7.78 (s, 1H, H-15), 7.47 (d, *J* 8.8 Hz, 1H, H-19), 7.39 (d, *J* 8.4 Hz, 1H, H-18), 3.62 (s, 3H, COOCH₃), 3.45 (q, *J* 6.5 Hz, 2H, ArCONCH₂CH₂), 2.58 (t, *J* 6.8, 2H, ArCONHCH₂CH₂N); **¹³C-NMR** (126 MHz, DMSO-*d*₆) δ 172.1 (CO), 166.4 (CO), 151.2 (2-CH), 139.9 (ArC), 137.6 (C-4), 131.3 (ArC), 130.9 (ArC), 130.1 (C-18), 121.0 (C-3), 119.5 (C-15), 117.4 (C-19), 51.8 (COOCH₃), 35.7 (ArCONCH₂CH₂), 33.9 (ArCONCH₂CH₂). CO, C-5 and C-7 not visible; **IR** (neat, *v*_{max}, cm⁻¹) 3263, 3079, 2749, 1725, 1637, 1513, 1414, 1382, 1304, 1246, 1232, 1207; **LCMS** (LCQ) *R*_t = 0.5 min (method 2), *m/z* (ESI⁺) 460.9 [M(³⁵Cl)+H]⁺, 462.8 [M(³⁷Cl)+H]⁺; **HRMS** *m/z* (ESI): calcd. for C₁₉H₁₈ClN₆O₄S [M(³⁵Cl)+H]⁺ 461.0793, found 461.0793.

***Tert*-butyl 3-((2-Chloro-4-((5-(4-pyridyl)-1,3,4-thiadiazol-2-yl)carbamoylamino)benzoyl)-aminopropanoate (37)**

Compound **37** was synthesised according to general procedure C, using the following reagents: 2-chloro-4-((5-(4-pyridyl)-1,3,4-thiadiazol-2-yl)carbamoylamino)benzoic acid (**24**) (100 mg, 0.27 mmol), HATU (120 mg, 0.32 mmol), *N,N*-diisopropylethylamine (93 μL, 0.53 mmol), *tert*-butyl-aminopropanoate hydrochloride (58 mg, 0.32 mmol) and *N,N*-dimethylformamide (3.5 mL). The crude product was purified by column chromatography (silica, 0 to 10% methanol in dichloromethane) and further purified by column chromatography (C-18 silica 30 g, 0 to 80% methanol in water) to yield the desired compound **37** as a colourless solid (42 mg, 40%).

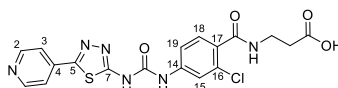
R_f 0.30 (dichloromethane:methanol, 19:1); **m.p.** 237–239 °C; **¹H-NMR** (500 MHz, DMSO-*d*₆) δ 11.51 (s, 1H, *NH*-urea), 9.46 (s, 1H, *NH*-urea), 8.73 (d, *J* 5.3, 2H, H-2), 8.38 (t, *J* 5.6, 1H, ArCONHCH₂), 7.88 (d, *J* 5.5, 2H, H-3), 7.77 (s, 1H, H-15), 7.46 (d, *J* 8.5, 1H, H-19), 7.38 (d, *J* 8.3, 1H, H-18), 3.41 (q, *J* 6.6, 2H, ArCONCH₂CH₂), 1.42 (s, 9H, COOC(CH₃)₃). ArCONHCH₂CH₂ is under solvent peak; **IR** (neat, *v*_{max}, cm⁻¹) 3366, 2926, 1709, 1600, 1522, 1443, 1410, 1390, 1303, 1242, 1203; **LCMS** (LCQ) *R*_t = 1.4 min (method 2), *m/z* (ESI⁺) 502.7 [M(³⁵Cl)+H]⁺, 504.7 [M(³⁷Cl)+H]⁺; **HRMS** *m/z* (ESI): calcd. for C₂₂H₂₄ClN₆O₄S [M(³⁵Cl)+H]⁺ 503.1263, found 503.1264. Not enough material for ¹³C-NMR.

2-Chloro-*N*-(2-(methylamino)ethyl)-4-((5-(4-pyridyl)-1,3,4-thiadiazol-2-yl)carbamoylamino)-benzamide (38)

To *tert*-butyl *N*-((2-chloro-4-((5-(4-pyridyl)-1,3,4-thiadiazol-2-yl)carbamoylamino)benzoyl)-amino)ethyl)-*N*-methyl-carbamate (**35**) (65 mg, 0.12 mmol) in dichloromethane (1 mL) was added trifluoroacetic acid (1 mL, 13.1 mmol). The reaction mixture was stirred at r.t. for 16 h. The reaction mixture was concentrated under reduced pressure. The crude was purified by column chromatography (amino silica, 0 to 20% methanol in dichloromethane) to yield the desired compound **38** as a pale yellow solid (38 mg, 73%).

R_f 0.30 (dichloromethane:methanol, 4:1, amino silica); **m.p.** 208–212 °C; **¹H-NMR** (500 MHz, DMSO-*d*₆) δ 10.34 (s, 1H, *NH*-urea), 8.62 (d, *J* 5.1, 2H, H-2), 8.32 (t, *J* 5.6, 1H, ArCONHCH₂), 7.99 (s, 1H, H-15), 7.77 (d, *J* 5.1, 2H, *NH*CH₃), 7.67 (d, *J* 8.5, 1H, H-19), 7.43 (d, *J* 8.4, 1H, H-18), 3.43 (q, *J* 6.6, 2H, ArCONCH₂CH₂), 2.96 (t, *J* 6.4, 2H, ArCONHCH₂CH₂), 2.53 (s, 3H, *NH*CH₃). **¹³C-NMR** (126 MHz, DMSO-*d*₆) δ 169.1 (CO), 167.1 (CO), 158.1 (ArC), 155.9 (ArC), 150.9 (C-2), 144.0 (ArC), 139.16 (ArC), 131.1 (ArC), 130.3 (C-18), 128.3 (ArC), 120.4 (C-3), 118.5 (C-15), 116.0 (C-19), 49.0 (ArCONHCH₂CH₂), 37.0 (ArCONCH₂CH₂), 34.0 (*NH*CH₃); **IR** (neat, *v*_{max}, cm⁻¹) 3263, 3036, 2933, 2852, 2728, 1700, 1627, 1601, 1545, 1490, 1430, 1387, 1305, 1250, 1211; **LCMS** (LCQ) *R*_t = 0.3 min (method 2), *m/z* (ESI⁺) 431.9 [M(³⁵Cl)+H]⁺, 433.9 [M(³⁷Cl)+H]⁺; **HRMS** *m/z* (ESI): calcd. for C₁₈H₁₉ClN₇O₂S [M(³⁵Cl)+H]⁺ 432.1004, found 432.1004.

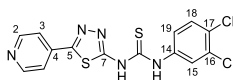
3-((2-Chloro-4-((5-(4-pyridyl)-1,3,4-thiadiazol-2-yl)carbamoylamino)benzoyl)amino)propanoic acid (**39**)



To *tert*-butyl 3-((2-chloro-4-((5-(4-pyridyl)-1,3,4-thiadiazol-2-yl)carbamoylamino)benzoyl)-aminopropanoate (**37**) (35 mg, 0.07 mmol) in dichloromethane (1 mL) was added trifluoroacetic acid (1 mL, 13.1 mmol) and the reaction mixture was stirred at r.t. for 4 h. The reaction mixture was concentrated under reduced pressure. The crude was taken up in water/ethyl acetate (1:1) (10 mL) and the resulting precipitate was filtered and washed with water (10 mL) to yield the desired compound **39** as a colourless solid (17 mg, 52%).

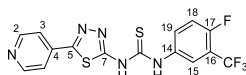
R_f 0.35 (dichloromethane:methanol, 9:1); **m.p.** 228–230 °C; **¹H-NMR** (500 MHz, DMSO-*d*₆) δ 10.01 (s, 1H, *NH*-urea), 8.87 (d, *J* 5.9, 2H, 2-CH), 8.40 (t, *J* 5.6, 1H, ArCONHCH₂), 8.19 (d, *J* 5.6, 2H, H-3), 7.75 (s, 1H, H-15), 7.48 – 7.33 (m, 2H, H-18, H-19), 3.42 (q, *J* 6.7, 2H, ArCONCH₂CH₂). One urea NH not visible and ArCONHCH₂CH₂ is under solvent peak; **¹³C-NMR** (126 MHz, DMSO-*d*₆) δ 173.1 (CO), 166.3 (CO), 162.9 (ArC), 157.7 (ArC), 145.9 (C-2), 143.0 (ArC), 140.7 (ArC), 131.4 (ArC), 131.0 (ArC), 130.2 (C-18), 123.0 (C-3), 119.3 (C-15), 117.2 (C-19), 35.8 (ArCONCH₂CH₂), 34.1 (ArCONHCH₂CH₂); **IR** (neat, *v*_{max}, cm⁻¹) 3456, 3381, 3233, 3097, 2916, 2851, 1751, 1703, 1600, 1534, 1508, 1447, 1381, 1301, 1235; **LCMS** (LCQ) *R*_t = 0.5 min (method 2), *m/z* (ESI⁺) 446.9 [M(³⁵Cl)+H]⁺, 448.9 [M(³⁷Cl)+H]⁺; **HRMS** *m/z* (ESI): calcd. for C₁₈H₁₅ClN₆O₄S [M(³⁵Cl)+H]⁺ 447.0637, found 447.0638.

1-(3,4-Dichlorophenyl)-3-(5-(4-pyridyl)-1,3,4-thiadiazol-2-yl)thiourea (**42**)²⁰³



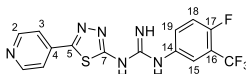
Sodium hydride (269 mg, 6.74 mmol) was slowly added to a suspension of 5-(4-pyridyl)-1,3,4-thiadiazol-2-yl-amine (1.00 g, 5.61 mmol) in tetrahydrofuran (75 mL) at 0 °C and the resulting suspension was stirred for 30 min at 0 °C. 1,2-Dichloro-4-isothiocyanatobenzene (1.21 mL, 8.42 mmol) was added and the reaction mixture was stirred 50 °C for 24 h. The reaction mixture was filtered and the resulting solid was washed with dichloromethane (100 mL) to yield the sodium salt **41** of the desired thiourea **42**. The salt was taken up in water and acidified to pH of 2–3 using 2 M aq. hydrochloric acid solution. The resulting precipitate was collected by filtration and washed with water to afford the desired compound **42** as a yellow/orange solid (1.47 g, 68%).

¹H-NMR (500 MHz, DMSO-*d*₆) δ 10.67 (s, 1H, *NH*-thiourea), 8.73 (d, *J* 5.2, 2H, H-2), 8.11 (d, *J* 2.5, 1H, H-15), 7.86 (d, *J* 5.2, 2H, H-3), 7.74 (dd, *J* 9.0, 2.5, 1H, H-19), 7.56 (d, *J* 8.8, 1H, H-18). One urea NH not visible; **LCMS** (LCQ) *R*_t = 2.4 min (method 1), *m/z* (ESI⁺) 382.1 [M(³⁵Cl³⁵Cl)+H]⁺, 384.0 [M(³⁵Cl³⁷Cl)+H]⁺. ¹H-NMR corresponds to literature data.²⁰³

1-(4-Fluoro-3-(trifluoromethyl)phenyl)-3-(5-(4-pyridyl)-1,3,4-thiadiazol-2-yl)thiourea (43)

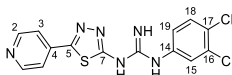
2-Fluoro-4-isothiocyano-1-(trifluoromethyl)benzene (210 μ L, 1.35 mmol) was added to a suspension of 5-(4-pyridyl)-1,3,4-thiadiazol-2-yl-amine (200 mg, 1.12 mmol) in *N,N*-dimethylformamide (5 mL) and the reaction mixture stirred for 16 h at 90 °C. Upon completion, ethyl acetate (20 mL) was added to the reaction mixture and the resulting precipitate was filtered. The crude filtrate was purified by column chromatography (silica, 0 to 5% methanol in water) to yield the desired compound **43** as a yellow solid (172 mg, 37%).

R_f 0.28 (dichloromethane:methanol, 19:1); **m.p.** 278–280 °C; **¹H-NMR** (500 MHz, DMSO-*d*₆) δ 10.78 (s, 1H, *NH*-thiourea), 8.75 (d, *J* 5.3, 2H, H-2), 8.12–8.00 (m, 2H, H-15, H-19), 7.87 (d, *J* 5.2, 2H, H-3), 7.50 (app t, *J* 9.7, 1H, H-18); **¹³C-NMR** (126 MHz, DMSO-*d*₆) δ 184.5 (HNCSNH), 154.3 (d, *J* 428.1, C-17), 150.5 (C-2), 137.2 (C-4), 136.2 (d, *J* 2.9, C-14), 128.9 (d, *J* 12.0, C-19), 125.7–120.2 (m, CF₃), 120.9–120.6 (m, C-16), 120.4 (C-3), 117.7 (d, *J* 22.2, C-15), 117.2 (d, *J* 21.1, C-18). C-5 and C-7 peaks are not visible; **LCMS** (LCQ) *R*_t = 2.4 min (method 1), *m/z* (ESI⁺) 400.0 [M+H]⁺.

1-(4-Fluoro-3-(trifluoromethyl)phenyl)-3-(5-(4-pyridyl)-1,3,4-thiadiazol-2-yl)guanidine (44)

Compound **44** was synthesised according to general procedure D, using the following reagents: 1-(4-fluoro-3-(trifluoromethyl)phenyl)-3-(5-(4-pyridyl)-1,3,4-thiadiazol-2-yl)thiourea (**43**) (136 mg, 0.34 mmol), ammonium hydroxide solution (28%) (40 μ L, 1.02 mmol), sodium periodate (80 mg, 0.37 mmol), *N,N*-dimethylformamide (3 mL). The reaction was quenched by the addition of 10% aq. sodium hydroxide (0.5 mL). The reaction mixture was filtered and the resulting solid was washed with water. The crude was twice purified by column chromatography (silica, 0 to 5% methanol in dichloromethane) to yield the desired compound **44** as a yellow solid (35 mg, 25%).

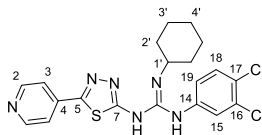
R_f 0.41 (dichloromethane:methanol, 19:1); **m.p.** 218–220 °C; **¹H-NMR** (500 MHz, DMSO-*d*₆) δ 9.37 (s, 1H, *NH*-guanidine), 8.69 (d, *J* 5.1 Hz, 2H, H-2), 8.00 (dd, *J* 6.7, 2.6, 1H, H-15), 7.89–7.82 (m, 2 \times guanidine *NH*), 7.79 (d, *J* 5.1, 2H, H-3), 7.77–7.71 (m, 1H, H-19), 7.48 (app t, *J* 9.7, 1H, H-18). **¹³C-NMR** (126 MHz, DMSO-*d*₆) δ 176.3 (C-guanidine), 157.3 (ArC), 155.8 (ArC), 152.5 (d, *J* 333.1, C-17), 151.0 (C-2), 138.1 (C-4), 136.1 (d, *J* 2.0, C-14), 127.3 (d, *J* 9.5, C-19), 122.2 (q, *J* 662.0, CF₃), 120.9 (C-3), 119.34 (d, *J* 5.6, C-15), 118.0 (d, *J* 21.4, C-18); **IR** (neat, ν_{max} , cm⁻¹) 3451, 3296, 3121, 1641, 1594, 1538, 1505, 1459, 1434, 1411, 1385; **LCMS** (LCQ) *R*_t = 1.8 min (method 2), *m/z* (ESI⁺) 383.0 [M+H]⁺; **HRMS** *m/z* (ESI): calcd. for C₁₅H₁₁F₄N₆S [M+H]⁺ 383.0697, found 383.0682.

1-(3,4-Dichlorophenyl)-3-(5-(4-pyridyl)-1,3,4-thiadiazol-2-yl)guanidine (45)²⁰³

Compound **45** was synthesised according to general procedure D, using the following reagents: 1-(3,4-dichlorophenyl)-3-(5-(4-pyridyl)-1,3,4-thiadiazol-2-yl)thiourea (**42**) (200 mg, 0.52 mmol), ammonium hydroxide solution (28%) (31 μ L, 0.78 mmol), sodium periodate (123 mg, 0.58 mmol), *N,N*-dimethylformamide (2 mL) and water (2 mL). The reaction was quenched by the addition of 10% aq. sodium hydroxide (0.5 mL). The reaction mixture was filtered and the resulting solid was washed with water. The crude was purified by column chromatography (silica, 0 to 10% methanol in dichloromethane) to yield the desired compound **45** as a yellow solid (94 mg, 49%).

¹H-NMR (500 MHz, DMSO-*d*₆) δ 9.49 (s, 1H, *NH*-guanidine), 8.73 (s, 2H, H-2), 7.96 – 7.81 (m, 3H, H-3, H-15), 7.57 (d, *J* 8.6, 1H, H-19), 7.46 (d, *J* 7.8, 1H, H-18). 2 × guanidine *NH* not visible; **LCMS** (LCQ) *R*_t = 1.8 min (method 1), *m/z* (ESI⁺) 365.9 [M(³⁵Cl³⁵Cl)+H]⁺, 367.9 [M(³⁵Cl³⁷Cl)+H]⁺. ¹H-NMR corresponds to literature data.²⁰³

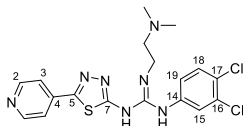
2-Cyclohexyl-1-(3,4-dichlorophenyl)-3-(5-(4-pyridyl)-1,3,4-thiadiazol-2-yl)guanidine (46)



Compound **46** was synthesised according to general procedure D, using the following reagents: 1-(3,4-dichlorophenyl)-3-(5-(4-pyridyl)-1,3,4-thiadiazol-2-yl)thiourea (**42**) (200 mg, 0.52 mmol), cyclohexylamine (90 μL, 0.78 mmol), sodium periodate (123 mg, 0.58 mmol), *N,N*-dimethylformamide (2 mL) and water (2 mL). The reaction was quenched by the addition of 10% aq. sodium hydroxide (0.5 mL). The reaction mixture was filtered and the resulting solid was washed with water. The crude was triturated with 50% methanol in water to yield the desired compound **46** as a colourless solid (55 mg, 24%).

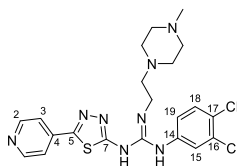
*R*_f 0.25 (dichloromethane:methanol, 19:1, amino silica); *m.p.* 211–213 °C; **¹H-NMR** (500 MHz, DMSO-*d*₆) δ 9.17 – 8.87 (br s, 2H, *NH*-guanidine), 8.68 (d, *J* 5.1, 2H, H-2), 7.76 (d, *J* 4.7, 3H, H-3, H-15), 7.57 (d, *J* 8.7, 1H, H-18), 7.47 (d, *J* 7.9, 1H, H-19), 3.86 (s, 1H, H-1'), 2.03 – 1.90 (m, 2H, H-2'), 1.72 (dd, *J* 10.2, 5.3, 2H, H-3'), 1.62 – 1.52 (m, 1H, H-4'_A), 1.47 – 1.31 (m, 4H, H-2'_B, H-3'_B), 1.27 (t, *J* 11.6, 1H, H-4'_B); **δ_c** (126 MHz, DMSO-*d*₆) δ 162.2 (C-guanidine), 156.7 (ArC), 152.0 (ArC), 151.0 (C-2), 139.6 (ArC), 138.1 (C-4), 131.0 (ArC), 130.6 (C-18), 124.5 (C-3 or C-15), 123.2 (C-19), 120.9 (C-3 or C-15), 50.1 (C-1'), 33.0 (C-2'), 25.4 (C-4'), 24.4 (C-3'); **IR** (neat, *v*_{max}, cm⁻¹) 3250, 3100, 2938, 2861, 1610, 1597, 1580, 1528, 1442, 1344, 1323; **LCMS** (LCQ) *R*_t = 3.9 min (method 2), *m/z* (ESI⁺) 447.1 [M(³⁵Cl³⁵Cl)+H]⁺, 449.1 [M(³⁵Cl³⁷Cl)+H]⁺; **HRMS** *m/z* (ESI): calcd. for C₂₀H₂₁Cl₂N₆S [M(³⁵Cl³⁵Cl)+H]⁺ 447.0920, found 447.0911.

1-(3,4-Dichlorophenyl)-2-(2-(dimethylamino)ethyl)-3-(5-(4-pyridyl)-1,3,4-thiadiazol-2-yl)guanidine (47)



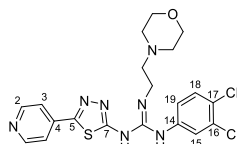
Compound **47** was synthesised according to general procedure D, using the following reagents: 1-(3,4-dichlorophenyl)-3-(5-(4-pyridyl)-1,3,4-thiadiazol-2-yl)thiourea (**42**) (250 mg, 0.65 mmol), *N,N*-dimethylethylenediamine (0.11 mL, 0.98 mmol), sodium periodate (167 mg, 0.78 mmol), *N,N*-dimethylformamide (5 mL). The reaction was quenched by the addition of 10% aq. sodium hydroxide (0.5 mL). The crude was purified by column chromatography (C18-silica, 0 to 100% methanol in water and 0.5% NH₃) and further purified by column chromatography (silica, 0 to 5% methanol in dichloromethane) to yield the desired compound **47** as a yellow solid (64 mg, 23%).

*R*_f 0.35 (dichloromethane:methanol, 19:1); *m.p.* 173–175 °C; **¹H-NMR** (500 MHz, DMSO-*d*₆) δ 10.24 (s, 1H, *NH*-guanidine), 8.96 (s, 1H, *NH*-guanidine), 8.68 (d, *J* 5.0, 2H, H-2), 7.89 – 7.74 (m, 3H, H-3, H-15), 7.57 (d, *J* 8.8, 1H, H-19), 7.39 (s, 1H, H-18), 3.57 – 3.44 (br s, 2H, CNCH₂CH₂NC(CH₃)₂), 2.57 (t, *J* 5.4, 2H, CNCH₂CH₂NC(CH₃)₂), 2.30 (s, 6H, CNCH₂CH₂NC(CH₃)₂); **¹³C-NMR** (126 MHz, DMSO-*d*₆) δ 157.0 (ArC), 151.0 (C-2), 139.8 (ArC), 138.2 (ArC), 131.2 (ArC), 130.8 (ArC), 125.3, 123.7 (C-19), 122.4 (C-15), 120.9 (C-13), 59.1 (CNCH₂CH₂NC(CH₃)₂), 45.2 (CNCH₂CH₂NC(CH₃)₂). C-guanidine, C-5 and 7-C not visible and CNCH₂CH₂NC(CH₃)₂ shift is covered by solvent peak; **IR** (neat, *v*_{max}, cm⁻¹) 3226, 2959, 2776, 1701, 1611, 1583, 1429, 1406, 1366, 1342, 1308, 1254; **LCMS** (LCQ) *R*_t = 0.5 min (method 2), *m/z* (ESI⁺) 435.9 [M(³⁵Cl³⁵Cl)+H]⁺, 437.9 [M(³⁵Cl³⁷Cl)+H]⁺; **HRMS** *m/z* (ESI): calcd. for C₁₈H₂₀Cl₂N₇O₃S [M(³⁵Cl)+H]⁺ 436.0872, found 436.0862.

1-(3,4-Dichlorophenyl)-2-(2-(4-methylpiperazin-1-yl)ethyl)-3-(5-(4-pyridyl)-1,3,4-thiadiazol-2-yl)guanidine (48)


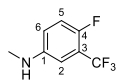
Compound **48** was synthesised according to general procedure D, using the following reagents: 1-(3,4-dichlorophenyl)-3-(5-(4-pyridyl)-1,3,4-thiadiazol-2-yl)thiourea (**42**) (250 mg, 0.65 mmol), 2-(4-methyl-piperazin-1-yl)-ethylamine (174 μ L, 0.98 mmol), sodium periodate (168 mg, 0.78 mmol), *N,N*-dimethylformamide (5 mL). The reaction was quenched by the addition of 10% aq. sodium hydroxide (0.5 mL). The crude was purified by column chromatography (C18-silica, 0 to 100% methanol in water and 0.5% NH_3) to yield the desired compound **48** as a yellow solid (145 mg, 45%).

R_f 0.40 (methanol, C-18 silica); **m.p.** 166–168 °C; **¹H-NMR** (500 MHz, $\text{DMSO-}d_6$) δ 9.58 (s, 1H, *NH*-guanidine), 8.88 (s, 1H, *NH*-guanidine), 8.68 (d, *J* 5.1, 2H, H-2), 7.76 (d, *J* 5.2, 3H, H-3, H-15), 7.59 (d, *J* 8.6, 1H, H-18), 7.47 (s, 1H, H-19), 3.51 (br s, 2H, $\text{C}=\text{NCH}_2\text{CH}_2\text{N}$), 2.58 (t, *J* 5.9, 2H, $\text{C}=\text{NCH}_2\text{CH}_2\text{N}$), 2.43 – 2.21 (m, 6H, 6 \times H-piperazine), 2.15 (s, 3H, NCH_3). 2 \times H-piperazine is under DMSO peak; **¹³C-NMR** (126 MHz, $\text{DMSO-}d_6$) δ 156.9 (C-14), 151.0 (C-2), 138.2 (C-4), 131.2 (ArC or C-18), 130.8 (ArC or C-18), 125.6 (ArC), 124.4 (C-15), 123.1 (C-19), 120.8 (C-3), 57.2 ($\text{C}=\text{NCH}_2\text{CH}_2\text{N}$), 55.1 (C-piperazine), 55.0 (C-piperazine), 53.0 (C-piperazine), 52.9 (C-piperazine), 46.16 (NCH_3). C-guanidine, C-5, C-7 peaks are not visible and $\text{C}=\text{NCH}_2\text{CH}_2\text{N}$ shift is covered by solvent peak; **IR** (neat, ν_{max} , cm^{-1}) 3252, 3181, 3119, 2932, 2798, 1599, 1571, 1525, 1448, 1435, 1369, 1309, 1285; **LCMS** (LCQ) *R_t* = 0.5 min (method 2), *m/z* (ESI⁺) 491.1 [$\text{M}^{(35}\text{Cl})+\text{H}$]⁺, 493.0 [$\text{M}^{(35}\text{Cl}^{37}\text{Cl})+\text{H}$]⁺; **HRMS** *m/z* (ESI): calcd. for $\text{C}_{12}\text{H}_{24}\text{Cl}_2\text{N}_8\text{S}$ [$\text{M}^{(35}\text{Cl})+\text{H}$]⁺ 491.1277, found 491.1291.

1-(3,4-Dichlorophenyl)-2-(2-morpholinoethyl)-3-(5-(4-pyridyl)-1,3,4-thiadiazol-2-yl)guanidine (49)


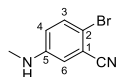
Compound **49** was synthesised according to general procedure 4, using the following reagents: 1-(3,4-dichlorophenyl)-3-(5-(4-pyridyl)-1,3,4-thiadiazol-2-yl)thiourea (**42**) (250 mg, 0.65 mmol), 4-(2-aminoethyl)morpholine (129 μ L, 0.98 mmol), sodium periodate (168 mg, 0.78 mmol), *N,N*-dimethylformamide (6 mL). The reaction was quenched by the addition of 10% aq. sodium hydroxide (0.5 mL). The crude was purified by column chromatography (C18-silica, 0 to 80% methanol in water and 0.5% NH_3) to yield the desired compound **49** as a yellow solid (188 mg, 60%).

R_f 0.40 (water:methanol:ammonia 20:80:1, C-18 silica); **m.p.** 173–175 °C; **¹H-NMR** (500 MHz, $\text{DMSO-}d_6$) δ 9.43 (s, 1H, *NH*-guanidine), 8.87 (s, 1H, *NH*-guanidine), 8.67 (d, *J* 5.1, 2H, H-2), 7.76 (d, *J* 5.2, 3H, H-3, H-15), 7.58 (d, *J* 8.7, 1H, H-18 or H-19), 7.48 – 7.38 (d, *J* 6.4, 1H, H-18 or H-19), 3.62 (t, *J* 4.5, 4H, $\text{NCH}_2\text{CH}_2\text{O}$), 3.57 – 3.46 (m, 2H, $\text{C}=\text{NCH}_2\text{CH}_2\text{N}$), 2.58 (t, *J* 6.0, 2H, $\text{C}=\text{NCH}_2\text{CH}_2\text{N}$). $\text{NCH}_2\text{CH}_2\text{O}$ under solvent peak; **¹³C-NMR** (126 MHz, $\text{DMSO-}d_6$) δ 156.87 (ArC), 153.13 (ArC), 150.99 (C-2), 138.27 (C-4), 131.18 (18-C or ArC), 130.78 (18-C or ArC), 124.24 (C-15), 122.97 (C-19), 120.82 (C-3), 109.99, 66.66 ($\text{NCH}_2\text{CH}_2\text{O}$), 57.30 ($\text{C}=\text{NCH}_2\text{CH}_2\text{N}$), 53.47 ($\text{NCH}_2\text{CH}_2\text{O}$). $\text{C}=\text{NCH}_2\text{CH}_2\text{N}$ shift is under DMSO peak and C-5 or C-7 and ArC are not visible; **IR** (neat, ν_{max} , cm^{-1}) 3212, 2954, 2858, 1582, 1546, 1428, 1307; **LCMS** (LCQ) *R_t* = 0.7 min (method 2), *m/z* (ESI⁺) 478.0 [$\text{M}^{(35}\text{Cl}^{35}\text{Cl})+\text{H}$]⁺, 480.0 [$\text{M}^{(35}\text{Cl}^{37}\text{Cl})+\text{H}$]⁺; **HRMS** *m/z* (ESI): calcd. for $\text{C}_{20}\text{H}_{22}\text{Cl}_2\text{N}_7\text{OS}$ [$\text{M}^{(35}\text{Cl})+\text{H}$]⁺ 478.0978 found 478.0971.

4-Fluoro-*N*-methyl-3-(trifluoromethyl)aniline (50)

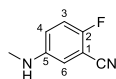
Compound **50** was synthesised according to general procedure E, using the following reagents: 5-amino-2-fluorobenzotrifluoride (0.72 mL, 5.58 mmol), potassium carbonate (770 mg, 5.58 mmol), iodomethane (0.35 mL, 5.58 mmol) and acetonitrile (15 mL). The crude was purified by column chromatography (silica, 0 to 10% ethyl acetate in petroleum ether) to yield the desired compound **50** as a pale yellow solid (420 mg, 37%).

¹H-NMR (500 MHz, DMSO-*d*₆) δ 7.19 (t, *J* 9.8, 1H, H-6), 6.81 – 6.71 (m, 2H, *NHCH*₃, H-3), 6.01 (d, *J* 5.5, 1H, H-5), 2.68 (d, *J* 5.0, 3H, *NHCH*₃); **LCMS** (LCQ) *R*_t = 2.0 min (method 2), no ionisation observed.

2-Bromo-5-(methylamino)benzonitrile (51)

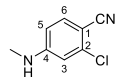
Compound **51** was synthesised according to general procedure E, using the following reagents: 5-amino-2-bromobenzonitrile (1.50 g, 7.61 mmol), potassium carbonate (1.06 g, 7.61 mmol), iodomethane (0.47 mL, 7.61 mmol) and acetonitrile (20 mL). The crude was purified by column chromatography (silica, 0 to 10% ethyl acetate in petroleum ether) to yield the desired compound **51** as an orange solid (440 mg, 26%).

¹H-NMR (500 MHz, Chloroform-*d*₆) δ 7.39 (d, *J* 8.9, 1H, H-6), 6.83 (d, *J* 2.9, 1H, H-3), 6.68 (dd, *J* 8.9, 2.9, 1H, H-5), 2.84 (s, 3H, *NHCH*₃). **LCMS** (LCQ) *R*_t = 2.5 min (method 2), *m/z* (ESI⁺) 211.1 [*M*(⁷⁹Br)+H]⁺, 213.1 [*M*(⁸¹Br)+H]⁺.

2-Fluoro-5-(methylamino)benzonitrile (52)

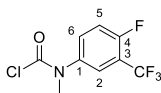
Compound **52** was synthesised according to general procedure 5, using the following reagents: 5-amino-2-fluorobenzonitrile (1.00 g, 7.35 mmol), potassium carbonate (1.02 g, 7.35 mmol), iodomethane (0.46 mL, 7.35 mmol) and acetonitrile (15 mL). The crude was purified by column chromatography (silica, 0 to 15% ethyl acetate in petroleum ether) to yield the desired compound **52** as a yellow solid (310 mg, 27%).

¹H-NMR (500 MHz, DMSO-*d*₆) δ 7.21 (app t, *J* 9.2, 1H, H-6), 6.88 (m, 1H, H-5), 6.80 (dd, *J* 5.1, 3.0, 1H, H-3), 6.05 (d, *J* 5.7, 1H, *NHCH*₃), 2.66 (d, *J* 5.0, 3H, *NHCH*₃); **LCMS** (LCQ) *R*_t = 2.6 min (method 2), no ionisation observed.

2-Chloro-4-(methylamino)benzonitrile (53)

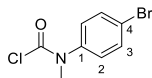
Compound **53** was synthesised according to general procedure 5, using the following reagents: 4-amino-2-chlorobenzonitrile (0.72 mL, 6.55 mmol), potassium carbonate (906 mg, 6.55 mmol), iodomethane (0.41 mL, 6.55 mmol) and acetonitrile (15 mL). The crude was purified by column chromatography (silica, 0 to 20% ethyl acetate in petroleum ether) to yield the desired compound **53** as a yellow solid (144 mg, 13%).

¹H-NMR (500 MHz, DMSO-*d*₆) δ 7.51 (d, *J* 8.7, 1H, H-6), 7.01 (s, 1H, *NHCH*₃), 6.69 (d, *J* 2.3, 1H, H-3), 6.57 (dd, *J* 8.7, 2.2, 1H, H-5), 2.73 (d, *J* = 4.9 Hz, 3H, *NHCH*₃). **LCMS** (LCQ) *R*_t = 0.5 min (method 2), no ionisation observed.

***N*-(4-fluoro-3-(trifluoromethyl)phenyl)-*N*-methyl-carbamoyl chloride (54)**

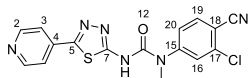
To a solution of triphosgene (307 mg, 1.04 mmol) in dichloromethane (10 mL), cooled at -78 °C, was added dropwise pyridine (0.60 mL, 7.42 mmol), followed by a solution of 4-fluoro-*N*-methyl-3-(trifluoromethyl)aniline (400 mg, 2.07 mmol) in dichloromethane (1 mL). The reaction mixture was stirred at rt for 16 h. The reaction was quenched by cautious addition of 1 M aq. hydrochloric acid solution (5 mL). The aqueous layer was extracted with dichloromethane (3 × 4 mL). The combined organic components were washed with water (5 mL) and brine (5 mL), dried over MgSO₄, filtered and concentrated under reduced pressure. The crude was purified by column chromatography (silica, 0 to 5% ethyl acetate in petroleum ether) to yield the desired compound **54** as a crude pale yellow liquid (238 mg, 36%).

¹H NMR (500 MHz, DMSO-*d*₆) δ 8.03 (s, 1H, *ArH*), 7.88 (d, *J* 8.4, *ArH*), 7.64 (t, *J* 9.7, *ArH*), 3.31 (s, 3H, NCH₃); LCMS (LCQ) Rt = 2.8 min (method 2), no ionisation observed.

***N*-(4-bromophenyl)-*N*-methyl-carbamoyl chloride (55)**

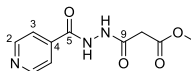
To a solution of triphosgene (160 mg, 0.54 mmol) in dichloromethane (5 mL), cooled at -78 °C, was added dropwise pyridine (0.30 mL, 3.71 mmol), followed by a solution of 4-bromo-*N*-methylaniline (135 μL, 1.08 mmol) in dichloromethane (0.5 mL). The reaction mixture was stirred at rt for 16 h. The reaction was quenched by cautious addition of 1 M aq. hydrochloric acid solution (2 mL). The aqueous layer was extracted with dichloromethane (3 × 3 mL). The combined organic components were washed with water (3 mL) and brine (3 mL), dried over MgSO₄, filtered and concentrated under reduced pressure. The crude was purified by column chromatography (silica, 0 to 20% ethyl acetate in petroleum ether) to yield the desired compound **55** as a pale yellow solid (106 mg, 38%).

¹H NMR (500 MHz, DMSO-*d*₆) δ 7.28 (d, *J* 8.3, 2H, H-2), 6.88 (d, *J* 8.2, 2H, H-3), 3.06 (s, 3H, NCH₃); LCMS (LCQ) Rt = 3.25 min (method 2), no ionisation observed.

1-(3-Chloro-4-cyano-phenyl)-1-methyl-3-[5-(4-pyridyl)-1,3,4-thiadiazol-2-yl]urea (56)

2-Chloro-4-(methylamino)benzonitrile (**56**) (150 mg, 0.90 mmol) was added to a suspension of phenyl *N*-(5-(4-pyridyl)-1,3,4-thiadiazol-2-yl)carbamate (270 mg, 0.90 mmol) in toluene (8 mL). The resulting mixture was heated in a microwave reactor at 200 °C for 30 min. Upon cooling, the solid was collected by filtration. The crude was purified by column chromatography (silica, 0 to 3% methanol in dichloromethane) to yield the desired compound **56** as a colourless solid (8 mg, 2%).

¹H-NMR (500 MHz, DMSO-*d*₆) δ 8.73 (d, *J* 4.7, 2H, H-2), 7.99 (d, *J* 8.5 Hz, 1H, 19-CH), 7.90 (d, *J* 1.9, 1H, H-16), 7.84 (d, *J* 5.0, 2H, H-3), 7.61 (dt, *J* 8.6, 1.6, 1H, H-20), 3.45 (s, 3H, NCH₃); LCMS (LCQ) Rt = 1.3 min (method 2), *m/z* (ESI⁺) 371.0 [M(³⁵Cl³⁵Cl)+H]⁺, 373.1 [M(³⁵Cl³⁷Cl)+H]⁺. Not enough material for ¹³C-NMR, IR, m.p. and HRMS determination.

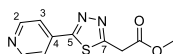
Methyl 3-oxo-3-(2-(pyridine-4-carbonyl)hydrazine)propanoate (57)

Methyl malonyl chloride (1.17 mL, 10.9 mmol) was added to isoniazid (1.50 g, 10.9 mmol) in *N,N*-dimethylformamide (22 mL) at 0 °C and the reaction mixture stirred at 0 °C for 3 h. The reaction mixture was neutralised by the addition

of pyridine (0.8 mL) and then concentrated under reduced pressure. The crude was purified by column chromatography (silica, 0 to 5% methanol in dichloromethane) to yield the desired compound **57** as a light yellow solid (602 mg, 22%).

R_f 0.14 (dichloromethane:methanol, 19:1); **m.p.** 218–220 °C; **¹H-NMR** (500 MHz, DMSO-*d*₆) δ 10.82 (s, 1H, NH), 10.32 (s, 1H, NH), 8.76 (dd, *J* 4.6, 1.6, 2H, H-2), 7.77 (dd, *J* 4.5, 1.6, 2H, H-3), 3.65 (s, 3H, OCH₃), 3.40 (s, 2H, CH₂). **¹³C-NMR** (126 MHz, DMSO-*d*₆) δ 168.0 (CO), 164.7 (CO), 164.2 (CO), 150.8 (C-2), 139.8 (C-4), 121.8 (C-3), 52.4 (CH₂), 40.9 (OCH₃); **IR** (neat, *v*_{max}, cm⁻¹) 3220, 2941, 2844, 1729, 1648, 1535, 1433, 1323, 1201; **LCMS** (LCQ) *R*_t = 0.5 min (method 2), *m/z* (ESI⁺) 238.0 [M+H]⁺; **HRMS** *m/z* (ESI): calcd. for C₁₀H₁₁N₃O₄ [M+H]⁺ 237.0750 found 237.0751.

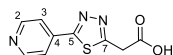
Methyl 2-(5-(4-pyridyl)-1,3,4-thiadiazol-2-yl)acetate (**58**)



Lawesson's reagent (1.02 g, 2.53 mmol) was added to methyl 3-oxo-3-(2-(pyridine-4-carbonyl)hydrazine)propanoate (**57**) (200 mg, 0.84 mmol) in 1,4-dioxane (6 mL) and the mixture stirred at 100 °C for 24 h. The reaction mixture was concentrated under reduced pressure. The crude was purified by column chromatography (silica, 0 to 3% methanol in dichloromethane) and then further purified by column chromatography (amino silica, dichloromethane) to yield the desired compound **58** as a yellow solid (90 mg, 42%).

R_f 0.53 (dichloromethane:methanol, 97:3); **¹H-NMR** (500 MHz, DMSO-*d*₆) δ 8.76 (dd, *J* 4.4, 1.7, 2H, H-2), 7.94 (dd, *J* 4.7, 1.6, 2H, H-3), 4.44 (s, 2H, CH₂), 3.71 (s, 3H, CH₃); **LCMS** (LCQ) *R*_t = 0.7 min (method 2), *m/z* (ESI⁺) 236.2 [M+H]⁺. Compound not suitable for HRMS.

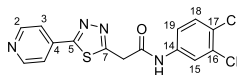
2-(5-(4-Pyridyl)-1,3,4-thiadiazol-2-yl)acetic acid (**59**)



To methyl 2-(5-(4-pyridyl)-1,3,4-thiadiazol-2-yl)acetate (300 mg, 1.28 mmol) (**58**) in tetrahydrofuran (4 mL) and water (1.5 mL) was added lithium hydroxide (1.07 g, 25.5 mmol) and the reaction mixture stirred at an r.t. for 16 h. The reaction mixture was concentrated under reduced pressure. The crude product was taken up in water (8 mL) and washed with ethyl acetate (10 mL). The aqueous component was acidified with 2 M aq. hydrochloric acid solution to pH 3 and then extracted with ethyl acetate (3 × 8 mL). The organic components were combined, dried over MgSO₄, filtered and concentrated under reduced pressure to reveal the desired acid **59** as a brown gum (83 mg, 23%).

¹H-NMR (500 MHz, DMSO-*d*₆) δ 8.76 (dd, *J* 4.5, 1.6, 2H, H-2), 7.90 (dd, *J* 4.5, 1.6, 2H, H-3), 2.82 (s, 2H, CH₂). **¹³C-NMR** (126 MHz, DMSO-*d*₆) δ 151.3 (C-2), 121.8 (C-3), 15.9 (CH₂). CO, C-4, C-5 and C-7 are not visible; **IR** (neat, *v*_{max}, cm⁻¹) 3359, 1601, 1509, 1443, 1415, 1385, 1244; **LCMS** (LCQ) *R*_t = 0.6 min (method 2), *m/z* (ESI⁺) 222.0 [M+H]⁺. Compound not suitable for HRMS.

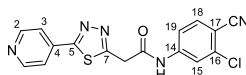
N-(3,4-dichlorophenyl)-2-[5-(4-pyridyl)-1,3,4-thiadiazol-2-yl]acetamide (**60**)



Compound **60** was synthesised according to general procedure F, using the following reagents: 2-(5-(4-pyridyl)-1,3,4-thiadiazol-2-yl)acetic acid (**59**) (100 mg, 0.45 mmol), T3P (0.15 mL, 0.45 mmol), trimethylamine (0.18 mL, 1.35 mmol), 3,4-dichloroaniline (90 mg, 0.54 mmol), and *N,N*-dimethylformamide (3 mL). The crude was purified by column chromatography (amino silica, 0 to 2.5% methanol in dichloromethane) and further purified by column chromatography (silica, 0 to 3% methanol in dichloromethane) to yield the desired product **60** as a light yellow solid (10 mg, 6%).

R_f 0.44 (dichloromethane:methanol, 39:1); **¹H-NMR** (500 MHz, DMSO-*d*₆) δ 10.78 (s, 1H, CONH), 8.77 (d, *J* 5.0, 2H, H-2), 7.99 (d, *J* 2.4, 1H, H-15), 7.95 (d, *J* 5.1, 2H, H-3), 7.60 (d, *J* 8.8, 1H, H-18), 7.50 (dd, *J* 8.8, 2.4, 1H, H-19), 4.45 (s, 2H, ArCH₂); **¹³C-NMR** (126 MHz, DMSO-*d*₆) δ 167.3 (CO), 166.8 (ArC), 165.3 (ArC), 151.1 (C-2), 139.1 (ArC), 137.3 (ArC), 131.6 (ArC), 131.3 (C-18), 125.8 (ArC), 121.9 (C-3), 121.1 (C-15), 119.9 (C-19), 38.0 (ArCH₂); **LCMS** (LCQ) Rt = 1.7 min (method 2), *m/z* (ESI⁺) 365.1 [M(³⁵Cl³⁵Cl)+H]⁺, 367.1 [M(³⁵Cl³⁷Cl)+H]⁺; **HRMS** *m/z* (ESI): calcd. for C₁₅H₁₁Cl₂N₄OS [M+H]⁺ 365.0025, found 365.0026. Not enough material for IR and m.p. determination.

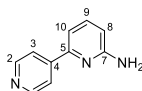
***N*-(3-Chloro-4-cyano-phenyl)-2-[5-(4-pyridyl)-1,3,4-thiadiazol-2-yl]acetamide (61)**



Compound **61** was synthesised according to general procedure F, using the following reagents: 2-(5-(4-pyridyl)-1,3,4-thiadiazol-2-yl)acetic acid (**59**) (120 mg, 0.54 mmol), T3P (0.18 mL, 0.54 mmol), trimethylamine (0.24 mL, 1.62 mmol), 4-amino-2-chlorobenzonitrile (100 mg, 0.65 mmol), and *N,N*-dimethylformamide (3 mL). The crude was purified by column chromatography (silica, 0 to 5% methanol in dichloromethane) to yield the desired compounds **61** as a yellow solid (15 mg, 7%).

R_f 0.45 (dichloromethane:methanol, 19:1); **¹H-NMR** (500 MHz, DMSO-*d*₆) δ 11.08 (s, 1H, 13-NH), 8.77 (d, *J* 5.5, 2H, H-2), 8.05 (d, *J* 1.9, 1H, H-15), 7.98 – 7.91 (m, 3H, H-3, H-18), 7.63 (dd, *J* 8.6, 2.0, 1H, H-19), 4.50 (s, 2H); **IR** (neat, *v*_{max}, cm⁻¹) 3169, 2951, 2227, 1698, 1633, 1595, 1537, 1489, 1440, 1401, 1310, 1219; **LCMS** (LCQ) Rt = 1.6 min (method 2), *m/z* (ESI⁺) 356.1 [M(³⁵Cl)+H]⁺, 358.1 [M(³⁷Cl)+H]⁺; **HRMS** *m/z* (ESI): calcd. for C₁₆H₁₁ClN₅OS [M+H]⁺ 356.0373, found 356.0368. Not enough material for ¹³C-NMR and m.p. determination.

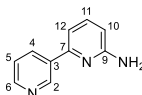
6-(4-Pyridyl)pyridin-2-amine²⁹⁶ (63)



Compound **63** was synthesised according to general procedure G, using the following reagents: pyridine-4-boronic acid hydrate (0.71 g, 5.78 mmol), cesium carbonate (5.64 g, 17.3 mmol), 6-bromopyridin-2-amine (1.00 g, 5.78 mmol) and (1,1'-bis(diphenylphosphino)ferrocene)dichloropalladium(II) (0.42 g, 0.58 mmol), 1,4-dioxane (10 mL) and water (2.5 mL). The crude was purified by column chromatography (silica, 0 to 70% ethyl acetate in petroleum ether) and further purified by column chromatography (amino silica, 3% methanol in dichloromethane) to yield the desired compound **63** as a crude brown solid which was carried forward without further purification (400 mg, 32%).

R_f 0.10 (dichloromethane:methanol, 19:1); **¹H-NMR** (500 MHz, DMSO-*d*₆) δ 8.62 (dd, *J* 4.6, 1.7, 2H, H-2), 7.92 (dd, *J* = 4.5, 1.8, 2H, H-3), 7.52 (app t, *J* 8.0, 1H, H-9), 7.20 (d, *J* 7.2, 1H, ArH), 6.53 (d, *J* 8.1, 1H, ArH), 6.11 (s, 2H, ArNH₂); **LCMS** (LCQ) Rt = 0.5 min (method 2), *m/z* (ESI⁺) 172.3 [M+H]⁺. ¹H-NMR consistent with literature data.²⁹⁶

6-(3-Pyridyl)pyridin-2-amine²⁹⁶ (64)

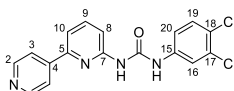


Compound **64** was synthesised according to general procedure G, using the following reagents: pyridine-3-boronic acid (426 mg, 3.47 mmol), cesium carbonate (3.39 g, 10.4 mmol), 6-bromopyridin-2-amine (600 mg, 3.47 mmol) and (1,1'-bis(diphenylphosphino)ferrocene)dichloropalladium(II) (253 mg, 0.35 mmol) and 1,4-dioxane (9 mL) and water (2.25 mL). The crude was purified by column chromatography (silica, 5% methanol in dichloromethane)

and further purified by column chromatography (amino silica, 3% methanol in dichloromethane) to yield the desired compound **64** as a brown solid (399 mg, 63%).

R_f 0.10 (dichloromethane:methanol, 19:1); **¹H-NMR** (500 MHz, DMSO-*d*₆) δ 9.14 (d, *J* 2.3 Hz, 1H, H-2), 8.56 (dd, *J* 4.8, 1.6, 1H, H-6), 8.29 (dt, *J* 8.0, 2.0, 1H, H-4), 7.53 – 7.38 (m, 2H, H-5, H-11), 7.12 (d, *J* 7.4, 1H, ArH), 6.47 (d, *J* 8.2, 1H, ArH), 6.06 (s, 2H, ArNH₂); **LCMS** (LCQ) Rt = 0.4 min (method 2), *m/z* (ESI⁺) 172.3 [M+H]⁺. ¹H-NMR consistent with literature data.²⁹⁶

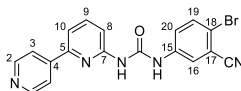
1-(3,4-Dichlorophenyl)-3-(6-(4-pyridyl)-2-pyridyl)urea (**65**)²⁰³



Compound **65** was synthesised according to general procedure B, using the following reagents: triphosgene (150 mg, 0.49 mmol), 3,4-dichloroaniline (200 mg, 1.23 mmol), triethylamine (0.34 mL, 2.47 mmol), dichloromethane (5 mL), 6-(4-pyridyl)pyridin-2-amine (**63**) (169 mg, 0.99 mmol) and *N,N*-dimethylformamide (4 mL). The crude was purified by column chromatography (silica, 2% methanol in dichloromethane) and further purified by column chromatography (silica, 2% methanol in dichloromethane) to yield the desired urea **65** as a colourless solid (15 mg, 3%).

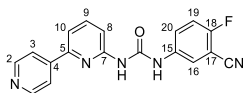
R_f = 0.47 (DCM:MeOH 19:1); **¹H-NMR** (500 MHz, DMSO-*d*₆) 10.33 (s, 1H, NH-urea), 9.65 (s, 1H, NH-urea), 8.73 (dd, *J* 5.0, 1.5, 2H, H-2), 8.00 – 7.90 (m, 4H, H-3, H-9, H-16, H-17), 7.71 (dd, *J* 12.4, 7.9, 2H, H-8, H-10), 7.57 (d, *J* 8.8, 1H, H-19), 7.35 (dd, *J* 8.7, 2.6, 1H, H-20). **LCMS** (LCQ) Rt = 1.3 min (method 2), *m/z* (ESI⁺) 359.0 [M(³⁵Cl³⁵Cl)+H]⁺, 361.1 [M(³⁵Cl³⁷Cl)+H]⁺; **HRMS** *m/z* (ESI): calcd. for C₁₇H₁₃Cl₂N₄O [M+H]⁺ 359.0461, found 359.0465. ¹H-NMR consistent with literature data.²⁰³

1-(4-Bromo-3-cyano-phenyl)-3-(6-(4-pyridyl)-2-pyridyl)urea (**66**)



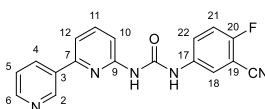
Compound **66** was synthesised according to general procedure B, using the following reagents: triphosgene (160 mg, 0.52 mmol), 5-amino-2-bromobenzonitrile (260 mg, 1.31 mmol), triethylamine (0.37 mL, 2.62 mmol), dichloromethane (5 mL) followed by 6-(4-pyridyl)pyridin-2-amine (**63**) (130 mg, 0.79 mmol) and *N,N*-dimethylformamide (4 mL). The crude was purified by column chromatography (silica, 2% methanol in dichloromethane) and further purified by column chromatography (silica, 2% methanol in dichloromethane) to yield the desired urea **66** as a colourless solid (22 mg, 4%).

R_f 0.33 (dichloromethane:methanol, 19:1); **m.p.** 260–262 °C; **¹H-NMR** (500 MHz, DMSO-*d*₆) 10.10 (s, 1H, NH-urea), 8.71 (dd, *J* 4.6, 1.6, 2H, H-2), 8.09 (d, *J* 2.6, 1H, H-16), 7.96 (dd, *J* 4.8, 1.5, 2H, H-3), 7.92 (app t, *J* 7.9, 1H, H-9), 7.78 (d, *J* 8.8, 1H, H-19), 7.72 (dd, *J* 10.3, 7.9, 2H, H-8, H-10), 7.63 (dd, *J* 8.9, 2.7, 1H, H-20). **¹³C-NMR** (126 MHz, DMSO-*d*₆) δ 153.0 (ArC or CO), 152.6 (ArC or CO), 152.1 (ArC or CO), 150.1 (C-2), 145.6 (C-4), 140.3 (C-15), 134.1 (C-19), 125.3 (C-20), 124.1 (C-16), 121.2 (C-3), 117.6 (ArC or ArCN), 116.5 (ArC or ArCN), 115.8 (ArC or ArCN), 115.0 (C-10), 113.2 (C-8); **LCMS** (LCQ) Rt = 2.0 min (method 2), *m/z* (ESI⁺) 393.9 [M+H]⁺; **HRMS** *m/z* (ESI): calcd. for C₁₈H₁₂BrN₅O [M+Na]⁺ 416.0117, found 416.0117.

1-(3-Cyano-4-fluoro-phenyl)-3-[6-(4-pyridyl)-2-pyridyl]urea (67)

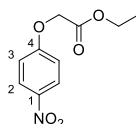
Compound **67** was synthesised according to general procedure 1, using the following reagents: triphosgene (130 mg, 0.44 mmol), 5-amino-2-fluorobenzonitrile (150 mg, 1.10 mmol), triethylamine (0.31 mL, 2.20 mmol), dichloromethane (6 mL), 6-(4-pyridyl)pyridin-2-amine (**63**) (110 mg, 0.66 mmol) and *N,N*-dimethylformamide (5 mL). The crude was purified by column chromatography (silica, 2% methanol in dichloromethane) and further purified by column chromatography (silica, 2% methanol in dichloromethane) to yield the desired urea **67** as a colourless solid (6 mg, 2%).

R_f 0.35 (dichloromethane:methanol, 47:3); **¹H-NMR** (500 MHz, DMSO-*d*₆) 10.29 (s, 1H, urea-NH), 9.68 (s, 1H urea-NH), 8.73 (d, *J* = 5.0 Hz, 2H, 2-CH), 8.06 (dd, *J* = 5.8, 2.7 Hz, 1H, 16-CH), 7.98 (d, *J* = 5.1 Hz, 2H, 3-CH), 7.94 (t, *J* = 8.0 Hz, 1H, 9-CH), 7.74 (q, *J* = 8.1, 7.6 Hz, 3H, 8-CH +10-CH +20-CH), 7.51 (t, *J* = 9.1 Hz, 1H, 19-CH). **LCMS** (LCQ) *R_t* = 0.8 min (method 2), *m/z* (ESI⁺) 334.1 [M(⁷⁹Br)+H]⁺, 336.0 [M(⁸¹Br)+H]⁺; **HRMS** *m/z* (ESI): calcd. for C₁₈H₁₂FN₅O [M+Na]⁺ 356.0918, found 356.0922. Not enough material for and ¹³C-NMR, m.p. and IR determination.

1-(3-Cyano-4-fluoro-phenyl)-3-(6-(3-pyridyl)-2-pyridyl)urea (68)

Compound **68** was synthesised according to general procedure 1, using the following reagents: triphosgene (130 mg, 0.44 mmol), 5-amino-2-fluorobenzonitrile (150 mg, 1.10 mmol), triethylamine (0.31 mL, 2.20 mmol), dichloromethane (6 mL) followed by 6-(4-pyridyl)pyridin-2-amine (**64**) (110 mg, 0.66 mmol) and *N,N*-dimethylformamide (5 mL). The crude was purified by column chromatography (silica, 2% methanol in dichloromethane) and further purified by column chromatography (silica, 2% methanol in dichloromethane) to yield the desired urea **68** as a colourless solid (12 mg, 3%).

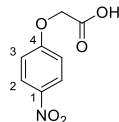
R_f 0.32 (dichloromethane:methanol, 47:3); **¹H-NMR** (500 MHz, DMSO-*d*₆) δ 10.35 (s, 1H, NH-urea), 9.66 (s, 1H), 9.22 (s, 1H), 8.66 (d, *J* 4.6, 1H), 8.37 (d, *J* 7.9, 1H), 8.09 – 8.01 (m, 1H), 7.91 (t, *J* 8.0, 1H), 7.75 (app dt, *J* 7.9, 3.5, 1H), 7.66 (app t, *J* 9.3, 2H), 7.61 – 7.39 (m, 2H). One NH-urea not visible; **¹³C-NMR** (126 MHz, DMSO-*d*₆) δ 153.0, 152.6, 152.4, 150.5, 148.2, 140.2, 136.5 (d, *J* 27.0), 134.2 (d, *J* 28.3), 126.6 (d, *J* 8.7), 124.2, 123.0, 117.6 (d, *J* 20.6), 115.4 (d, *J* 2.3), 114.4 (d, *J* 1.6), 112.0, 110.0; **LCMS** (LCQ) *R_t* = 0.5 min (method 2), *m/z* (ESI⁺) 334.1 [M+H]⁺; **HRMS** *m/z* (ESI): calcd. for C₁₈H₁₂FN₅O [M+Na]⁺ 356.0918, found 356.0920. Not enough material for IR and m.p. determination.

Ethyl 2-(4-nitrophenoxy)acetate (69)

Ethyl chloroacetate (213 μL, 2.16 mmol) was added to a mixture of 4-nitrophenol (236 μL, 2.16 mmol) and potassium carbonate (298 mg, 2.16 mmol) in acetonitrile (2 mL). The reaction mixture was stirred at 80 °C for 16 h. Upon completion, the reaction mixture was taken up in water (6 mL) and extracted with ethyl acetate (3 × 6 mL). The combined organic components were washed with 1 M aq. sodium hydroxide solution (3 × 6 mL) and water (3 × 6 mL), dried over MgSO₄, filtered and concentrated under reduced pressure to yield the desired compound **69** as a colourless solid (364 mg, 71%).

R_f = 0.27 (petroleum ether: ethyl acetate, 1:1); $^1\text{H-NMR}$ (500 MHz, Chloroform- d) δ 8.24 – 8.19 (m, 2H, H-2), 6.99 – 6.95 (m, 2H, H-3), 4.72 (s, 2H, OCH_2COO), 4.29 (q, J 7.2, 2H, $\text{COOCH}_2\text{CH}_3$), 1.31 (app td, J 7.2, 0.9, 3H, $\text{COOCH}_2\text{CH}_3$); **LCMS** (LCQ) R_t = 2.5 min (method 2), m/z (ESI $^+$) 226.1 $[\text{M}+\text{H}]^+$.

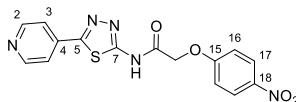
2-(4-Nitrophenoxy)acetic acid (**70**)²⁹⁷



Sodium hydroxide (1.70 g, 42.2 mmol) was added to a solution of ethyl 2-(4-nitrophenoxy)acetate (**69**) (955 mg, 4.24 mmol) in methanol (6 mL) and water (2 mL). The reaction mixture was stirred at 65 °C for 16 h. The reaction mixture was concentrated under reduced pressure. The crude product was taken up in water (12 mL) and washed with ethyl acetate (12 mL). The aqueous layer was acidified to a pH of 2–3 with 2 M aq. hydrochloric acid solution and then extracted with ethyl acetate (12 mL). The organic components were dried over MgSO_4 , filtered and concentrated under reduced pressure to reveal the desired acid **70** as a yellow solid (110 mg, 13%).

$^1\text{H-NMR}$ (500 MHz, DMSO- d_6) δ 8.20 (dd, J 7.3, 2.0, 2H, H-2), 7.13 (dd, J 7.2, 1.8, 2H, H-3), 4.87 (s, 2H, OCH_2); **LCMS** (LCQ) R_t = 0.6 min (method 2), no ionisation observed. $^1\text{H-NMR}$ corresponds to literature data.²⁹⁷

2-(4-Nitrophenoxy)-*N*-[5-(4-pyridyl)-1,3,4-thiadiazol-2-yl]acetamide (**71**)



Compound **71** was synthesised according to general procedure C, using the following reagents: 2-(4-nitrophenoxy)acetic acid (**70**) (120 mg, 0.61 mmol), HATU (280 mg, 0.73 mmol), *N,N*-diisopropylethylamine (212 μL , 1.22 mmol), 5-(4-pyridyl)-1,3,4-thiadiazol-2-yl-amine (130 mg, 0.73 mmol). and *N,N*-dimethylformamide (4 mL). The crude product was purified by column chromatography (amino silica, 0 to 5% methanol in dichloromethane). The resulting solid was triturated with methanol to yield the desired compound **70** as a colourless solid (30 mg, 13%).

R_f 0.33 (dichloromethane:methanol, 19:1); **m.p.** 261–263 °C; $^1\text{H-NMR}$ (500 MHz, DMSO- d_6) δ 13.19 (s, 1H, NH-amide), 8.72 (dd, J 4.4, 1.2, 2H, H-2), 8.21 (d, J 8.7, 2H, H-17), 7.90 (dd, J 4.4, 1.2, 2H, H-3), 7.22 (d, 8.8, 2H, H-16), 5.15 (s, 2H, OCH_2). $^{13}\text{C-NMR}$ (126 MHz, DMSO- d_6) δ 167.3 (C=O), 163.3 (ArC), 160.6 (ArC), 159.6 (ArC), 151.2 (C-2), 137.5 (C-18), 132.8 (C-4), 126.2 (C-17), 121.3 (C-3), 115.8 (C-16), 67.1 (OCH_2); **IR** (neat, ν_{max} , cm^{-1}) 3294, 2976, 1673, 1608, 1551, 1489, 1437, 1403, 1332, 1252; **LCMS** (LCQ) R_t = 0.5 min (method 2), m/z (ESI $^+$) 358.1 $[\text{M}+\text{H}]^+$; **LCMS** (ESI) retention time: 0.52 min, m/z 358.12 $[\text{M}+\text{H}]^+$, method 2; **HRMS** m/z (ESI): calcd. for $\text{C}_{15}\text{H}_{11}\text{N}_5\text{O}_4\text{S}$ $[\text{M}+\text{Na}]^+$ 380.0424, found 380.0408.

11.3. Experimental for hit identification

11.2.1. General procedures

General procedure H: To the appropriate acid (1 mol eq.), HATU (1.2 mol eq.) *N,N*-diisopropylethylamine (2 mol eq.) in *N,N*-dimethylformamide was added 5-indanamine (1.2 mol eq.). The reaction mixture was stirred at r.t. for 16 h. Upon completion, the solvent was removed under reduced pressure to yield a crude product. The crude was dissolved in EtOAc (5 mL), saturated aq. NaHCO_3 (5 mL), brine (5 mL), dried over MgSO_4 and concentrated under reduced pressure. The crude product was purified by column chromatography with appropriate solvents.

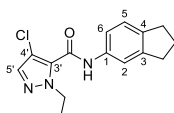
General procedure I: To 2-(cyanomethyl)benzoic acid (1 mol eq.) was added the appropriate amine (1 mol eq.) in chlorobenzene and the resulting suspension was heated to 130 °C and stirred for 6 h. Upon completion, the solvent was removed under reduced pressure. The crude product was then triturated with 2-propanol, filtered and then washed with 2-propanol. The crude product was purified by crystallisation from acetic acid.

General procedure J: To the appropriate substrate (1 mol eq.) in acetonitrile, was added AIBN (0.1 mol eq.) and the reaction mixture is heated to 78 °C. Upon heating, NBS (1.3 mol eq.) was added to the reaction mixture and stirred for 16 h. Upon completion, the solvent was removed under reduced pressure to yield a crude product. The crude product was purified by column chromatography with appropriate solvents.

General procedure K: To the appropriate acid (1 mol eq.), EDCI (1.2 mol eq.), HOBT (1.2 mol eq.) *N,N*-diisopropylethylamine (1.2–2 mol eq.) in *N,N*-dimethylformamide was added the appropriate amine (1–3 mol eq.). The reaction mixture was stirred at ambient temperature for 16 h. Upon completion, the solvent was removed under reduced pressure to yield a crude product. The crude was dissolved in EtOAc (5 mL), washed with 1M HCl (4 mL), saturated aq. NaHCO₃ (4 mL), brine (4 mL), dried over MgSO₄ and concentrated under reduced pressure. The crude product was purified by column chromatography with appropriate solvents.

11.2.1. Synthetic procedures

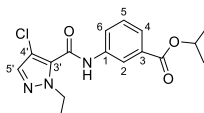
2-Ethyl-*N*-indan-5-yl-pyrazole-3-carboxamide (**72**)



Compound **72** was synthesised according to general procedure H, using the following reagents: 4-chloro-1-ethyl-1H-pyrazole-5-carboxylic acid (157 mg, 0.90 mmol), 5-indanamine (144 mg, 1.08 mmol), HATU (411 mg, 1.08 mmol), *N,N*-diisopropylethylamine (0.32 mL, 1.80 mmol) and *N,N*-dimethylformamide (4 mL). The crude was purified by column chromatography (silica 12 g, 0 to 5% ethyl acetate in petroleum ether) to yield the desired amide **72** as a white solid (107 mg, 39%).

R_f 0.27 (petroleum ether:ethyl acetate, 19:1); **m.p.** 180–182 °C; **¹H-NMR** (500 MHz, DMSO-*d*₆) δ 10.46 (s, 1H, CONH), 7.68 (s, 1H, H-5'), 7.61 (s, 1H, H-2), 7.41 (d, *J* 8.1, 1H, H-6), 7.20 (d, *J* 8.1, 1H, H-5), 4.26 (dd, *J* 14.1, 7.5 Hz, 2H, NCH₂CH₃), 2.84 (dt, *J* 15.4, 7.4, 4H, ArCH₂CH₂), 2.07 – 1.96 (m, 2H, ArCH₂CH₂), 1.33 (t, *J* 7.2, 3H, NCH₂CH₃); **¹³C-NMR** (126 MHz, DMSO-*d*₆) δ 157.0 (CO), 144.8 (C-3), 140.3 (C-4), 136.9 (C-5'), 136.8 (C-5), 134.8 (C-3'), 124.7 (C-1), 118.5 (C-6), 116.6 (C-2), 108.8 (C-4'), 46.8 (NCH₂CH₃), 32.9 (ArCH₂CH₂), 32.3 (ArCH₂CH₂), 25.6 (ArCH₂CH₂), 15.9 (NCH₂CH₃); **IR** (neat, ν_{max}, cm⁻¹) 3294, 3075, 1671, 1608, 1551, 1489, 1471, 1332; **LCMS** (LCQ) *R_t* = 3.0 min (method 2), *m/z* (ESI⁺) 290.1 [M(³⁵Cl)+H]⁺, 292.0 [M(³⁷Cl)+H]⁺; **HRMS** *m/z* (ESI): calcd. for C₁₅H₁₆ClN₃O [M(³⁵Cl)+Na]⁺ 312.0874, found 312.0862.

Isopropyl 4-((4-chloro-2-ethyl-pyrazole-3-carbonyl)amino)benzoate (**73**)

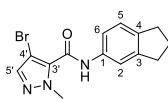


Compound **73** was synthesised according to general procedure H, using the following reagents: 4-chloro-1-ethyl-1H-pyrazole-5-carboxylic acid (100 mg, 0.57 mmol), isopropyl 3-aminobenzoate (**77**) (205 mg, 0.69 mmol), HATU (261 mg, 0.69 mmol), *N,N*-diisopropylethylamine (200 μL, 1.15 mmol) and *N,N*-dimethylformamide (3 mL). The crude

was purified by column chromatography (silica 12 g, 0 to 25% ethyl acetate in petroleum ether) to yield the desired amide **73** as a white solid (155 mg, 75%).

R_f 0.22 (petroleum ether:ethyl acetate, 3:1); **m.p.** 79–81 °C; **¹H-NMR** (500 MHz, DMSO-*d*₆) δ 10.82 (s, 1H, CONH), 8.33 (s, 1H, H-5'), 7.96 (d, *J* 7.8, 1H, H-4), 7.73 (d, *J* 7.7, 1H, H-6), 7.71 (d, *J* 1.2, 1H, H-2), 7.53 (t, *J* 7.9, 1H, H-5), 5.15 (hept, *J* 6.6, 1H, OCH(CH₃)₂), 4.28 (q, *J* 7.2, 2H, NCH₂CH₃), 1.38 – 1.30 (m, 9H, OCH(CH₃)₂, NCH₂CH₃); **¹³C-NMR** (126 MHz, DMSO-*d*₆) δ 165.4 (CO), 157.6 (CO), 138.9 (ArC), 137.0 (ArC), 134.4 (ArC), 131.4 (ArC), 129.8 (C-5), 125.5 (C-6), 124.8 (C-4), 120.8 (C-5'), 109.2 (C-4'), 68.8 (OCH(CH₃)₂), 46.9 (NCH₂CH₃), 22.1 (OCH(CH₃)₂), 15.9 (NCH₂CH₃); **IR** (neat, *v*_{max}, cm⁻¹) 3305, 3128, 2976, 1726, 1647, 1546, 1491, 1282, 1235; **LCMS** (LCQ) *R*_t = 4.8 min (method 2), *m/z* (ESI⁺) 335.8 [M(³⁵Cl)+H]⁺, 337.5 [M(³⁷Cl)+H]⁺. Compound not suitable for HRMS.

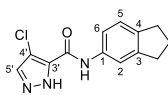
4-Bromo-*N*-indan-5-yl-2-methyl-pyrazole-3-carboxamide (**74**)



Compound **74** was synthesised according to general procedure H, using the following reagents: 4-bromo-2-methyl-pyrazole-3-carboxylic acid (140 mg, 0.70 mmol), 5-indanamine (111 mg, 0.86 mmol), HATU (333 mg, 0.86 mmol), *N,N*-diisopropylethylamine (0.25 mL, 1.43 mmol) and *N,N*-dimethylformamide (4 mL). The crude was purified by column chromatography (silica 12 g, 0 to 25% ethyl acetate in petroleum ether) to yield the desired amide **74** as a white solid (123 mg, 52%).

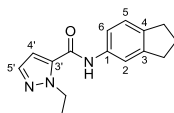
R_f 0.21 (petroleum ether:ethyl acetate, 4:1); **m.p.** 65–67 °C; **¹H-NMR** (500 MHz, DMSO-*d*₆) δ 10.39 (s, 1H, CONH), 7.65 (s, 1H, H-5'), 7.61 (s, 1H, H-2), 7.42 (d, *J* 8.1, 1H, H-6), 7.20 (d, *J* 8.1, 1H, H-5), 3.93 (s, 3H, NCH₃), 2.85 (dt, *J* 15.5, 7.4, 4H, ArCH₂CH₂), 2.02 (p, *J* 7.4, 2H, ArCH₂CH₃); **¹³C-NMR** (126 MHz, DMSO-*d*₆) δ 157.3 (CO), 144.8 (C-3), 140.2 (C-4), 139.0 (C-5'), 137.2 (ArC), 136.8 (ArC), 124.7 (C-5), 118.5 (C-6), 116.6 (C-2), 93.5 (C-4'), 39.1 (NCH₃), 33.0 (ArCH₂CH₂), 32.3 (ArCH₂CH₂), 25.6 (ArCH₂CH₃); **IR** (neat, *v*_{max}, cm⁻¹) 3280, 2945, 1679, 1635, 1512, 1487, 1420, 1419, 1293, 1251; **LCMS** (LCQ) *R*_t = 3.2 min (method 2), *m/z* (ESI⁺) 320.1 [M(⁷⁹Br)+H]⁺, 322.3 [M(⁸¹Br)+H]⁺; **HRMS** *m/z* (ESI): calcd. for C₁₄H₁₄BrN₃NaO₁ [M(⁷⁹Br)+Na]⁺ 342.0212, found 342.0215.

4-Chloro-*N*-indan-5-yl-1H-pyrazole-5-carboxamide (**75**)



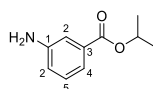
Compound **75** was synthesised according to general procedure H, using the following reagents: 4-chloro-1H-pyrazole-5-carboxylic acid (100 mg, 0.68 mmol), 5-indanamine (110 mg, 0.82 mmol), HATU (310 mg, 0.82 mmol), *N,N*-diisopropylethylamine (0.24 mL, 1.36 mmol) and *N,N*-dimethylformamide (3 mL). The crude was purified by column chromatography (silica 12 g, 0 to 30% ethyl acetate in petroleum ether) to yield the desired amide **75** as a white solid (72 mg, 38%).

R_f 0.35 (dichloromethane:methanol, 7:3); **m.p.** 204–206 °C; **¹H-NMR** (500 MHz, DMSO-*d*₆) δ 13.64 (s, 1H, NH-pyrazole), 9.93 (s, 1H, CONH), 8.13 (s, 1H, H-5'), 7.67 (s, 1H, H-2), 7.47 (d, *J* 8.3, 1H, H-6), 7.15 (d, *J* 8.1, 1H, H-5), 2.83 (dt, *J* 14.6, 7.4, 4H, ArCH₂CH₂), 2.01 (p, *J* 6.9, 6.3, 2H, ArCH₂CH₃); **¹³C-NMR** (126 MHz, DMSO-*d*₆) δ 159.5 (CO), 144.4 (C-3), 141.8 (C-4'), 139.3 (C-4), 137.2 (C-1), 130.1 (C-5'), 124.5 (C-5), 118.8 (C-6), 116.8 (C-2), 109.6 (C-4'), 33.0 (ArCH₂CH₂), 32.3 (ArCH₂CH₂), 25.6 (ArCH₂CH₃); **IR** (neat, *v*_{max}, cm⁻¹) 3265, 2914, 1680, 1603, 1587, 1540, 1475, 1328, 1305, 1223; **LCMS** (LCQ) *R*_t = 3.5 min (method 2), *m/z* (ESI⁺) 262.1 [M(³⁵Cl)+H]⁺, 263.0 [M(³⁷Cl)+H]⁺; **HRMS** *m/z* (ESI): calcd. for C₁₃H₁₃ClN₃O₁ [M(³⁵Cl)]⁺ 262.0742, found 262.0745.

2-Ethyl-*N*-indan-5-yl-pyrazole-3-carboxamide (76)

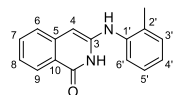
Compound **76** was synthesised according to general procedure H, using the following reagents: 2-ethylpyrazole-3-carboxylic acid (100 mg, 0.71 mmol), 5-indanamine (111 mg, 0.86 mmol), HATU (333 mg, 0.86 mmol), *N,N*-diisopropylethylamine (0.25 mL, 1.43 mmol) and *N,N*-dimethylformamide (3 mL). The crude was purified by column chromatography (silica 12 g, 0 to 50% ethyl acetate in petroleum ether) to yield the desired amide **76** as a white solid (175 mg, 91%).

R_f 0.37 (petroleum ether:ethyl acetate, 1:1); **m.p.** 79–81 °C; **¹H-NMR** (500 MHz, DMSO-*d*₆) δ 10.05 (s, 1H, CONH), 7.63 (s, 1H, H-2), 7.53 (s, 1H, H-5'), 7.41 (d, *J* 8.2, 1H, H-6), 7.18 (d, *J* 8.2 Hz, 1H, H-5), 7.02 (s, 1H, H-4'), 4.51 (q, *J* 7.3, 2H, NCH₂CH₃), 2.84 (dt, *J* 16.0, 7.5, 4H, ArCH₂CH₂), 2.02 (p, *J* 7.5, 2H, ArCH₂CH₂), 1.34 (t, *J* 7.2 Hz, 3H, NCH₂CH₃); **¹³C-NMR** (126 MHz, DMSO-*d*₆) δ 158.4 (CO), 144.5 (C-3), 139.8 (C-5), 137.7 (C-7'), 137.0 (ArC), 135.3 (ArC), 124.5 (C-5), 119.2 (C-6), 117.3 (C-2), 108.4 (C-4'), 46.4 (NCH₂CH₃), 32.9 (ArCH₂CH₂), 32.3 (ArCH₂CH₂), 25.6 (ArCH₂CH₂), 16.3 (NCH₂CH₃); **IR** (neat, ν_{\max} , cm⁻¹) 3243, 2974, 2845, 1714, 1654, 1594, 1537, 1460, 1405, 1328, 1205; **LCMS** (LCQ) *R_t* = 0.7 min (method 2), *m/z* (ESI⁺) 256.2 [M+H]⁺. Compound not suitable for HRMS.

Isopropyl 3-aminobenzoate (77)

Thionyl chloride (2.66 mL, 36.5 mmol) was added dropwise to 3-amino-benzoic acid (500 mg, 3.65 mmol) in 2-propanol (20 mL). The reaction mixture was stirred at 90 °C for 16 h. The solvent was removed under reduced pressure. The crude product was taken up in saturated aq. NaHCO₃ (10 mL) and extracted with ethyl acetate (3 × 10 mL). The combined organic components were then washed with water (20 mL), dried over MgSO₄, filtered and concentrated under reduced pressure to yield the intermediate **77** as a yellow oil (518 mg, 40%) and was carried forward without further purification (<50 % purity).

R_f 0.23 (petroleum ether:ethyl acetate, 9:1); **¹H-NMR** (500 MHz, DMSO-*d*₆) δ 7.73 – 7.65 (m, 1H, ArCH), 7.21 – 7.19 (m, 1H, ArCH), 7.14 – 7.12 (m, 1H, ArCH), 6.82 (dt, *J* = 7.5, 2.0 Hz, 1H, H-5), 5.63 (s, 2H, ArNH₂), 5.09 (hept, *J* 6.3, 1H, OCH(CH₃)₂), 1.29 (d, *J* 6.3, 6H, OCH(CH₃)₂); **LCMS** (LCQ) *R_t* = 2.2 min (method 2), *m/z* (ESI⁺) 180.0 [M+H]⁺.

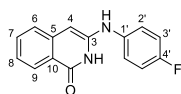
3-(2-Methylanilino)-2H-isoquinolin-1-one (86)

Compound **86** was synthesised according to general procedure I, using the following reagents: 2-(cyanomethyl)benzoic acid (161 mg, 1.00 mmol), *o*-toluidine (0.11 mL, 1.00 mmol) and chlorobenzene (1.5 mL). The crude was purified by crystallisation from acetic acid to yield the desired compound **86** as a light pink solid (8 mg, 3%).

m.p. 210–212 °C; **¹H-NMR** (500 MHz, DMSO-*d*₆) δ 10.72 (s, 1H, CONH), 7.98 (d, *J* 8.0, 1H, H-9), 7.45 (app t, *J* 7.6, 1H, H-7), 7.29 (m, 4H, H-6 + ArNH + H-3' + H-6'), 7.23 (app t, *J* 7.7, 1H, H-8), 7.12 (app t, *J* 7.5, 1H, H-5'), 7.07 (app t, *J* 7.5, 1H, H-4'), 5.55 (s, 1H, H-4), 2.23 (s, 3H, CH₃); **¹³C-NMR** (126 MHz, DMSO-*d*₆) δ 162.5 (CO), 143.3 (ArC), 140.7 (ArC), 138.5 (ArC), 138.2 (ArC), 132.80 (C-7), 131.5 (ArC), 131.4 (ArC), 127.3 (ArC), 127.0 (ArC), 125.0 (ArC), 124.7 (H-4'), 123.4 (H-6'), 122.7 (ArC), 121.0 (ArC), 83.2 (C-4), 18.0 (CH₃); **IR** (neat, ν_{\max} , cm⁻¹) 3294, 3254, 3075, 2934, 1671, 1608,

1551, 1505, 1472, 1332, 1310, 1280; **LCMS** (LCQ) Rt = 2.2 min (method 2), m/z (ESI⁺) 251.2 [M+H]⁺; **HRMS** m/z (ESI): calcd. for C₁₆H₁₅N₂O [M+H]⁺ 251.1179, found 251.1179.

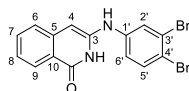
3-(4-Fluoroanilino)-2H-isoquinolin-1-one (87)



Compound **87** was synthesised according to general procedure I, using the following reagents: 2-(cyanomethyl)benzoic acid (161 mg, 1.00 mmol), 4-fluoroaniline (95 μ L, 1.00 mmol) and chlorobenzene (1.5 mL). The crude was purified by crystallisation from acetic acid to yield the desired compound (**87**) as a white solid (71 mg, 3%).

m.p. 192–194 °C; **¹H-NMR** (500 MHz, DMSO-*d*₆) δ 10.77 (s, 1H, CONH), 8.00 (dd, J 8.0, 1.3, 1H, H-9), 7.87 (s, 1H, ArNH), 7.49 (ddd, J 8.3, 6.9, 1.4, 1H, H-7), 7.36 (d, J 8.0, 1H, H-6), 7.25 – 7.12 (m, 5H, 8-CH + 2'+6'-CH + 3'+5'-CH), 5.89 (s, 1H, 4-CH); **¹³C-NMR** (126 MHz, DMSO-*d*₆) δ 162.6 (CO), 158.26 (d, J 238.8, ArCF), 142.8 (ArC), 140.5 (ArC), 137.4 (d, J 2.5, 1'-C), 132.8 (C-7), 127.0 (C-9), 125.2 (C-6), 123.1 (C-8), 122.5 (d, J 8.1, C-2'), 121.5 (C-5), 116.4 (d, J 22.5, C-3'), 84.5 (C-5); **IR** (neat, ν_{\max} , cm⁻¹) 3301, 1719, 1643, 1607, 1546, 1510, 1477, 1409, 1333, 1293, 1217; **LCMS** (LCQ) Rt = 0.57 min (method 2), m/z (ESI⁺) 255.2 [M+H]⁺; **HRMS** m/z (ESI): calcd. for C₁₅H₁₁FN₂O [M+Na]⁺ 277.0748, found 277.0737.

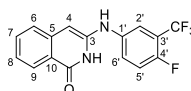
3-(3,4-Dibromoanilino)-2H-isoquinolin-1-one (88)



Compound **88** was synthesised according to general procedure I, using the following reagents: 2-(cyanomethyl)benzoic acid (161 mg, 1.00 mmol), 3,4-dibromoaniline (250 mg, 1.00 mmol) and chlorobenzene (1.5 mL). The crude was purified by crystallisation from acetic acid to yield the desired compound **88** as a white solid (148 mg, 36%).

m.p. 221–223 °C; **¹H-NMR** (500 MHz, DMSO-*d*₆) δ 11.07 (s, 1H, CONH), 8.33 (s, 1H, ArNH), 8.05 (dd, J 8.1, 0.3, 1H, H-9), 7.61 (d, J 8.7, 1H, H-5'), 7.56 (ddd, J 8.2, 7.0, 1.4, 1H, H-7), 7.48 (d, J 8.0, 1H, H-6), 7.42 (d, J 2.6, 1H, H-2'), 7.26 (ddd, J 8.0, 6.9, 1.2, 1H, H-8), 7.06 (dd, J 8.8, 2.6, 1H, H-6'), 6.16 (s, 1H, H-4); **¹³C-NMR** (126 MHz, DMSO-*d*₆) δ 162.8 (CO), 143.3 (ArC), 140.3 (ArC), 139.8 (ArC), 134.5 (C-5'), 132.9 (C-7), 127.0 (C-9), 125.7 (C-6), 124.6 (C-3'), 124.3 (C-8), 122.7 (C-2'), 122.6 (C-10), 119.3 (C-6), 114.4 (C-4'), 89.50 (C-4); **IR** (neat, ν_{\max} , cm⁻¹) 3293, 1661, 1639, 1609, 1581, 1552, 1512, 1464, 1433, 1330; **LCMS** (LCQ) Rt = 3.2 min (method 2), m/z (ESI⁺) 395.0 [M(⁷⁹Br⁸¹Br)+H]⁺; **HRMS** m/z (ESI): calcd. for C₁₅H₁₁Br₂N₂O [M(⁷⁹Br⁷⁹Br)+H]⁺ 394.9218, found 394.9204.

3-(4-Fluoro-3-(trifluoromethyl)anilino)-2H-isoquinolin-1-one (89)

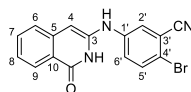


Compound **89** was synthesised according to general procedure I, using the following reagents: 2-(cyanomethyl)benzoic acid (150 mg, 0.93 mmol), 5-amino-2-fluorobenzotrifluoride (0.12 mL, 0.93 mmol) and chlorobenzene (1.5 mL). The crude was purified by crystallisation from acetic acid to yield the desired compound **89** as a white solid (12 mg, 4%).

m.p. 192–194 °C; **¹H-NMR** (500 MHz, DMSO-*d*₆) δ 11.09 (s, 1H, CONH), 8.26 (s, 1H, ArNH), 8.04 (d, J 8.0, 1H, H-9), 7.54 (ddd, J 8.2, 7.0, 1.4, 1H, H-7), 7.50 – 7.37 (m, 4H, H-6 + H-2' + H-5' + H-6'), 7.24 (ddd, J 8.1, 7.0, 1.2, 1H, H-8), 6.05 (s, 1H, H-4). **IR** (neat, ν_{\max} , cm⁻¹) 3222, 2942, 1729, 1645, 1535, 1411, 1323, 1201; **LCMS** (LCQ) Rt = 2.9 min (method 2),

m/z (ESI⁺) 323.2 [M+H]⁺; **HRMS** m/z (ESI): calcd. for C₁₆H₁₀F₄N₂O [M+Na]⁺ 345.0621, found 345.0609. Not enough material for ¹³C NMR.

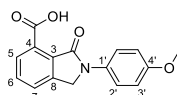
2-Bromo-5-((1-oxo-2H-isoquinolin-3-yl)amino)benzonitrile (**90**)



Compound **90** was synthesised according to general procedure I using the following reagents: 2-(cyanomethyl)benzoic acid (150 mg, 0.93 mmol), 5-amino-2-bromobenzonitrile (183 mg, 0.93 mmol) and chlorobenzene (1.5 mL). The crude was purified by crystallisation from acetic acid to yield the desired compound **90** as a white solid (36 mg, 11%).

m.p. 255–257 °C; **¹H-NMR** (500 MHz, DMSO-*d*₆) δ 11.15 (s, 1H, CONH), 8.57 (s, 1H, ArNH), 8.07 (d, *J* 8.0, 1H, H-9), 7.71 (d, *J* 8.9, 1H, H-5'), 7.57 (app dt, *J* 6.8, 4.0, 2H, H-7 + H-2'), 7.51 (d, *J* 8.0, 1H, H-6), 7.32 (dd, *J* 8.8, 2.8, 1H, H-6'), 7.28 (t, *J* 7.5, 1H, H-8), 6.23 (s, 1H, H-4); **¹³C-NMR** (126 MHz, DMSO-*d*₆) δ 162.8 (CO), 142.2 (C-1'), 139.7 (ArC), 139.6 (ArC), 134.2 (ArC), 132.8 (C-7), 127.0 (C-9), 125.9 (C-6), 124.5 (C-8), 124.4 (C-10), 122.9 (C-6'), 122.8 (C-2'), 117.66 (C-4), 115.3 (ArC or CN), 114.4 (ArC or CN), 90.4 (C-4); **IR** (neat, ν_{\max} , cm⁻¹) 3301, 3114, 1640, 1595, 1539, 1505, 1460, 1435, 1386, 1264; **LCMS** (LCQ) Rt = 0.6 min (method 2), m/z (ESI⁺) 340.1 [M(⁷⁹Br)+H]⁺, 342.2 [M(⁸¹Br)+H]⁺; **HRMS** m/z (ESI): calcd. for C₁₆H₁₀BrN₃O [M+Na]⁺ 361.9899, found 361.9868.

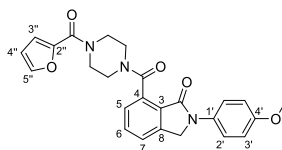
2-(4-Methoxyphenyl)-3-oxo-isoindoline-4-carboxylic acid (**91**)



To dimethyl 3-(bromomethyl)benzene-1,2-dicarboxylate (1.40 g, 4.88 mmol) in ethanol (30 mL) was added *p*-anisidine (660 mg, 5.36 mmol) and potassium carbonate (740 mg, 5.36 mmol). The mixture was stirred at 78 °C for 1.15 h. The reaction mixture was cooled and 2 M aq. sodium hydroxide (7.31 mL, 14.6 mmol) was added and the mixture stirred at reflux for 1 h. The solvent was removed under reduced pressure to give the crude product. The crude taken up in water (50 mL) and washed with ethyl acetate (2 × 50 mL). The aqueous layer was acidified with 2 M aq. hydrochloric acid solution until pH 3 and the resulting precipitate was filtered and dried under reduced pressure to reveal the desired acid **91** as a white solid (960 mg, 66%).

m.p. 180–182 °C; **¹H-NMR** (500 MHz, DMSO-*d*₆) δ 15.44 (brs, 1H, COOH) 8.15 (d, *J* 7.6, 1H, H-7), 7.94 (d, *J* 7.6, 1H, H-5), 7.86 (app t, *J* 7.6, 1H, H-6), 7.74 (dd, *J* 7.0, 2.3, 2H, H-2'), 7.07 (dd, *J* 6.9, 2.4, 2H, H-3'), 5.18 (s, 2H, NCH₂), 3.80 (s, 3H, OCH₃); **¹³C-NMR** (126 MHz, DMSO-*d*₆) δ 168.2 (NCO), 165.5 (COOH), 157.9 (C-4'), 143.1 (C-8), 133.1 (C-6), 132.0 (C-7), 131.1 (C-4), 129.8 (ArC), 129.5 (ArC), 127.7 (C-5), 123.8 (C-2'), 114.8 (C-3'), 55.9 (NCH₂), 53.08 (OCH₃); **IR** (neat, ν_{\max} , cm⁻¹) 2950, 2227, 1701, 1595, 1492, 1473, 1402, 1310, 1246; **LCMS** (LCQ) Rt = 3.0 min (method 1), m/z (ESI⁺) 284.0 [M+H]⁺; **HRMS** m/z (ESI): calcd. for C₁₆H₁₃NO₄ [M+Na]⁺ 306.0737, found 306.0739. ¹H-NMR corresponds to literature data.²⁹⁸

7-(4-(Furan-2-carbonyl)piperazine-1-carbonyl)-2-(4-methoxyphenyl)isoindolin-1-one (**92**)

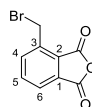


Compound **92** was synthesised according to general procedure K, using the following reagents: 2-(4-methoxyphenyl)-3-oxo-isoindoline-4-carboxylic acid (**91**) (100 mg, 0.35 mmol), EDCI (82 mg, 0.42 mmol), HOBT (65 mg, 0.42 mmol),

N,N-diisopropylethylamine (0.12 mL, 0.71 mmol), 1-(furan-2-carbonyl)piperazine (80 mg, 0.42 mmol), and *N,N*-dimethylformamide (1.5 mL). The crude was purified by column chromatography (silica 12 g, 0 to 2% methanol in dichloromethane), followed by crystallisation in ether to yield the desired amide **92** as a white solid (131 mg, 79%).

R_f 0.38 (dichloromethane:methanol, 19:1); **m.p.** 210–212 °C; **¹H-NMR** (500 MHz, DMSO-*d*₆) δ 7.82 (s, 1H, H-5), 7.79 – 7.74 (m, 2H, H-2'), 7.74 – 7.67 (m, 2H, H-6, H-5'), 7.39 (dd, *J* = 6.7, 1.7 Hz, 1H, H-7), 7.06 – 6.97 (m, 3H, H-3', H-4''), 6.61 (s, 1H, H-3''), 5.02 (d, *J* 17.2, 1H, NCH_{AB}), 5.01 (d, *J* = 17.6 Hz, 1H, NCH_{AB}), 3.86 – 3.80 (m, 2H, 2 × H-piperazine), 3.79 – 3.76 (m, 4H, OCH₃, H-piperazine), 3.74 – 3.67 (m, 1H, H-piperazine), 3.65 – 3.53 (m, 2H, 2 × H-piperazine), 3.23 – 3.18 (m, 2H, 2 × H-piperazine); **¹³C-NMR** (126 MHz, DMSO-*d*₆) δ 167.1 (CO), 165.4 (CO), 159.0 (CO), 156.6 (C-4'), 147.3 (ArC), 145.3 (ArC), 141.9 (ArC), 133.7 (ArC), 132.8 (C-6), 132.7 (ArC), 128.9 (ArC), 126.3 (C-7), 124.1 (C-6), 121.9 (C-2'), 116.2 (C-4''), 114.6 (C-3'), 111.8 (C-3''), 55.8 (OCH₃), 51.2 (NCH₂), 46.7 (C-piperazine), 41.8 (C-piperazine); **IR** (neat, ν_{max}, cm⁻¹) 2923, 1680, 1628, 1511, 1482, 1423, 1390, 1270, 1250; **LCMS** (LCQ) Rt = 2.5 min (method 1), *m/z* (ESI⁺) 446.1 [M+H]⁺; **HRMS** *m/z* (ESI): calcd. for C₂₅H₂₃N₃O₅ [M+Na]⁺ 468.1530, found 468.1530.

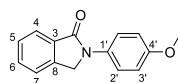
4-(Bromomethyl)isobenzofuran-1,3-dione (**93**)



Compound **93** was synthesised according to general procedure J, using the following reagents: methylphthalic anhydride (1.0 g, 6.17 mmol), AIBN (100 mg, 0.62 mmol), NBS (1.43 g, 8.02 mmol) and acetonitrile (30 mL). The crude was purified by column chromatography (silica 24 g, 0 to 10% ethyl acetate in petroleum ether) to yield the desired compound **93** as a crystalline white solid (930 mg, 56%).

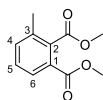
R_f 0.18 (petroleum ether:ethyl acetate, 9:1); **¹H-NMR** (500 MHz, Chloroform-*d*) δ 7.97 (d, *J* 7.4, 1H, ArCH), 7.93 (d, *J* 7.8, 1H, ArCH), 7.88 (app t, *J* 7.6, 1H, H-5), 4.92 (s, 2H, ArCH₂); **LCMS** (LCQ) Rt = 0.6 min (method 2), *m/z* (ESI⁺) 242.3 [M(⁷⁹Br)+H]⁺.

2-(4-Methoxyphenyl)isoindolin-1-one (**95**)



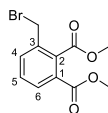
A microwave vial was charged with isoindolinone (80 mg, 0.60 mmol), 4-iodoanisole (117 mg, 0.50 mmol), *trans*-*N,N'*-dimethylcyclohexane-1,2-diamine (16 μL, 0.10 mmol), copper iodide (4.77 mg, 0.03 mmol) and potassium carbonate (138 mg, 1 mmol) in toluene (3 mL). The mixture was stirred at 110 °C for 16 h. The reaction mixture was concentrated under reduced pressure. The crude was purified by column chromatography (silica 12 g, 0 to 50% ethyl acetate in petroleum ether) to yield the desired product **95** as a white solid (88 mg, 70%).

R_f 0.77 (petroleum ether:ethyl acetate 1:1); **¹H-NMR** (500 MHz, Chloroform-*d*) δ 7.92 (d, *J* 7.6 Hz, 1H, H-4), 7.74 (dd, *J* 8.9, 1.6, 2H, H-2'), 7.58 (app td, *J* 7.4, 1.3, 1H, H-6), 7.53 – 7.46 (m, 2H, H-5, H-7), 6.97 (d, *J* 9.0, 2H, C-3'), 4.82 (s, 2H, NCH₂), 3.83 (s, 3H, OCH₃); **LCMS** (LCQ) Rt = 0.6 min (method 2), *m/z* (ESI⁺) 240.2 [M+H]⁺. ¹H-NMR consistent with literature data.²⁹⁹

Dimethyl 3-methylbenzene-1,2-dicarboxylate (96)

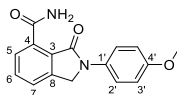
To methylphthalic anhydride (5.50 g, 33.9 mmol) in methanol (12.5 mL) was added sulphuric acid (2.71 mL, 50.9 mmol) dropwise and the mixture stirred at 65 °C for 3 d. Upon completion, the solvent was removed under reduced pressure to yield a crude product. The crude was taken up in saturated aq. NaHCO₃ (100 mL) and extracted with EtOAc (3 × 100 mL). The combined organics were then washed with water (100 mL), brine (100 mL) and dried over MgSO₄ and concentrated under reduced pressure to yield the desired compound **96** as a clear orange liquid (6.76 g, 91%).

R_f 0.83 (petroleum ether:ethyl acetate, 3:1); **¹H-NMR** (500 MHz, Chloroform-*d*) δ 7.83 (d, *J* 7.6, 1H, H-6), 7.40 (d, *J* 7.6, 1H, H-4), 7.36 (app t, *J* 7.7, 1H, H-5), 3.95 (d, *J* 1.2, 3H, OCH₃), 3.89 (d, *J* 1.3, 3H, OCH₃), 2.35 (s, 3H, ArCH₃); **LCMS** (LCQ) **R_t** = 2.2 min (method 2), no ionisation observed. ¹H-NMR corresponds to literature data.³⁰⁰

Dimethyl 3-(bromomethyl)benzene-1,2-dicarboxylate (97)

Compound **97** was synthesised according to general procedure J, using the following reagents: dimethyl 3-methylbenzene-1,2-dicarboxylate (**96**) (1.95 g, 9.37 mmol), AIBN (150 mg, 0.94 mmol), NBS (2.17 g, 12.2 mmol) and acetonitrile (50 mL). The crude was purified by column chromatography (silica 40 g, 0 to 10% ethyl acetate in petroleum ether) to yield the desired compound **96** as a crystalline white solid (2.15 g, 76%).

R_f 0.29 (petroleum ether:ethyl acetate, 9:1); **¹H-NMR** (500 MHz, Chloroform-*d*) δ 7.92 (d, *J* 7.7, 1H, H-6), 7.64 (d, *J* 7.6, 1H, H-4), 7.48 (app t, *J* 7.8, 1H, H-5), 4.54 (s, 2H, ArCH₂), 3.97 (s, 3H, OCH₃), 3.90 (s, 3H, OCH₃); **LCMS** (LCQ) **R_t** = 2.5 min (method 2), no ionisation observed. ¹H-NMR corresponds to literature data.³⁰⁰

2-(4-Methoxyphenyl)-3-oxo-isindoline-4-carboxamide (98)

Compound **98** was synthesised according to general procedure K, using the following reagents: 2-(4-methoxyphenyl)-3-oxo-isindoline-4-carboxylic acid (**91**) (100 mg, 0.35 mmol), EDCI (82 mg, 0.42 mmol), HOBT (65 mg, 0.42 mmol), *N,N*-diisopropylethylamine (0.12 mL, 0.71 mmol), 2 M ammonia in methanol (0.53 mL, 1.06 mmol), and *N,N*-dimethylformamide (1.5 mL). The crude was purified by column chromatography (silica 12 g, 0 to 2% methanol in dichloromethane) to yield the desired primary amide **98** as a white solid (59 mg, 53%).

R_f 0.38 (dichloromethane:methanol, 49:1); **m.p.** 274–276 °C; **¹H-NMR** (500 MHz, DMSO-*d*₆) δ 10.16 (s, 1H, CONH), 8.15 (d, *J* 7.3, 1H, H-5), 7.81 – 7.76 (m, 2H, CONH + ArCH), 7.75 – 7.67 (m, 3H, Ar-CH, H-2'), 7.03 (d, *J* 9.0, 2H, H-3'), 5.03 (s, 2H, NCH₂), 3.78 (s, 3H, OCH₃); **¹³C-NMR** (126 MHz, DMSO-*d*₆) δ 159.5 (ArCO), 144.4 (ArC), 141.9 (ArC), 139.3 (ArC), 137.2 (ArC), 130.1 (ArC), 124.5 (ArC), 118.8 (C-2'), 116.8 (C-3'), 109.6 (ArC). 2 × ArCO not visible. NCH₂ and OCH₃ are also not visible without explanation; **IR** (neat, ν_{\max} , cm⁻¹) 3231, 1663, 1622, 1598, 1512, 1445, 1392, 1303, 1246, 1169; **LCMS** (LCQ) **R_t** = 1.8 min (method 1), *m/z* (ESI⁺) 283.1 [M+H]⁺; **HRMS** *m/z* (ESI): calcd. for C₁₆H₁₄N₂O₃ [M+Na]⁺ 305.0897, found 305.0897.

11.3. Experimental for Series G

11.2.1. General procedures

General procedure L: To 4-(2-methyl-1,3-thiazol-4-yl)benzoic acid (**102**) (1 mol eq.), HBTU (1.2 mol eq.), *N,N*-diisopropylethylamine (2 mol eq.) in *N,N*-dimethylformamide was added the appropriate amine (1 mol eq.). The reaction mixture was stirred at ambient temperature for 16 h. Upon completion, the solvent was removed under reduced pressure. The crude product was taken up in ethyl acetate (5 mL), washed with saturated aq. NaHCO₃ (4 mL), brine (4 mL), dried over MgSO₄, filtered and concentrated under reduced pressure. The crude product was purified by column chromatography with appropriate solvents.

General procedure M: To 4-(2-methyl-1,3-thiazol-4-yl)benzoic acid (**102**) (1 mol eq.) in dichloromethane was added oxalyl chloride (1.2 mol eq.) in a dropwise manner followed by the addition of a few drops of *N,N*-dimethylformamide. The reaction mixture was stirred at ambient temperature for 16 h. The crude acyl chloride was then added to a stirred mixture of the appropriate amine (1 mol eq.) followed by the addition of *N,N*-diisopropylethylamine (5 mol eq.). The reaction mixture was stirred at ambient temperature for 2-16 h. The solvent was removed under reduced pressure. The crude product was taken up in saturated aq. NaHCO₃ (5 mL) and extracted with ethyl acetate (3 × 10 mL). The combined organic components were then washed with brine (10 mL), dried over MgSO₄, filtered and concentrated under reduced pressure. The crude product was purified by column chromatography with appropriate solvents.

General procedure N: To 4-(2-methyl-1,3-thiazol-4-yl)benzoic acid (**102**) (1 mol eq.), EDCI (1.3 mol eq.), HOBT (1.3 mol eq.), 4-methylmorpholine (2 mol eq.) in *N,N*-dimethylformamide was added the appropriate amine (1.3 mol eq.). The reaction mixture was stirred at ambient temperature for 16 h. The solvent was removed under reduced pressure. The crude product was taken up in saturated aq. NaHCO₃ (5 mL) and extracted with ethyl acetate (3 × 10 mL). The combined organic components were then washed with brine (10 mL), dried over MgSO₄, filtered and concentrated under reduced pressure. The crude product was purified by column chromatography with appropriate solvents.

General procedure O: To 4-(2-methyl-1,3-thiazol-4-yl)benzoic acid (**102**) (1 mol eq.) and the appropriate aniline (2.5 mol eq.) in tetrahydrofuran was added phosphorus trichloride (1 mol eq.). The reaction mixture was heated in a microwave reactor for 20 min at 150 °C. The crude product was taken up in saturated aq. NaHCO₃ (5 mL) and extracted with ethyl acetate (3 × 10 mL). The combined organic components were then washed with brine (10 mL), dried over MgSO₄, filtered and concentrated under reduced pressure. The crude product was purified by column chromatography with appropriate solvents.

General procedure P: To the appropriate acid (1 mol eq.), EDCI (1.2 mol eq.), HOBT (1.2 mol eq.) *N,N*-diisopropylethylamine (1.2–2 mol eq.) in *N,N*-dimethylformamide was added the appropriate amine (1–3 mol eq.). The reaction mixture was stirred at ambient temperature for 16 h. The solvent was removed under reduced pressure. The crude product was taken up in ethyl acetate (5 mL), washed with 1 M aq. hydrochloric acid solution. (4 mL), saturated aq. NaHCO₃ (4 mL), brine (4 mL), dried over MgSO₄, filtered and concentrated under reduced pressure. The crude product was purified by column chromatography with appropriate solvents.

General procedure Q: To the appropriate acid (1 mol eq.) in the appropriate solvent was added thionyl chloride (10 mol eq.). The reaction mixture was stirred at ambient temperature for 16 h. The solvent was removed under reduced pressure. The crude product was taken up in saturated aq. NaHCO₃ and extracted with ethyl acetate. The

combined organic components were then washed with water, dried over MgSO_4 , filtered and concentrated under reduced pressure.

General procedure R: To the appropriate carboxylic acid (1 mol eq.), HATU (1.2 mol eq.), *N,N*-diisopropylethylamine (2 mol eq.) in *N,N*-dimethylformamide was added the appropriate amine (1.2 mol eq.). The reaction mixture was stirred for 16 h. Upon completion, the solvent was removed under reduced pressure to yield a crude product. The crude product was taken up in saturated aq. NaHCO_3 (5 mL) and extracted with ethyl acetate (3×10 mL). The combined organic components were then washed with 1 M aq. hydrochloric acid solution (10 mL), brine (10 mL), dried over MgSO_4 , filtered and concentrated under reduced pressure. The crude product was purified by column chromatography with appropriate solvents.

General procedure S: To 4-methyl-3-((4-(2-methylthiazol-4-yl)benzoyl)amino)benzoic acid (**102**) (1 mol eq.), T3P (1.2 mol eq.), triethylamine (3 mol eq.) in *N,N*-dimethylformamide was added the appropriate amine (2 mol eq.). The reaction mixture was stirred at ambient temperature for 16 h. The solvent was removed under reduced pressure. The crude product was taken up in saturated aq. NaHCO_3 (5 mL) and extracted with ethyl acetate (3×10 mL). The combined organic components were then washed with brine (10 mL), dried over MgSO_4 , filtered and concentrated under reduced pressure. The crude product was purified by column chromatography with appropriate solvents.

General procedure T: To 4-bromo-*N*-(2,3-dimethylphenyl)benzamide (**194**) (1 mol eq.) in water and dimethoxyethane was added the appropriate boronic acid (2 mol eq.), tetrakis(triphenylphosphine)palladium(0) (10% mol eq.) and caesium carbonate (8 mol eq.). The reaction mixture was stirred at 80 °C for 0.5 h. The crude product was taken up in brine (5 mL) and extracted with ethyl acetate (2×5 mL). The combined organic components were then washed with brine (5 mL), dried over MgSO_4 , filtered and concentrated under reduced pressure. The crude product was purified by column chromatography with appropriate solvents.

General procedure U: To the appropriate aryl bromide in 1,4-dioxane was added bis(pinacolato)diboron (1.2 mol eq.), (1,1'-bis(diphenylphosphino)ferrocene)dichloropalladium(II) (5% mol eq.) and potassium acetate (3 mol eq.). The reaction mixture was stirred at 100 °C for 3-16 h. Upon cooling, the reaction mixture was filtered through Celite and the filtrate was concentrated under reduced pressure. The crude product was purified by column chromatography with appropriate solvents.

General procedure V: To the appropriate aryl boronic ester (1 mol eq.) in 1,4-dioxane and water (1:1) was added the appropriate aryl halide (1 mol eq.), (1,1'-bis(diphenylphosphino)ferrocene)dichloropalladium(II) (5% mol eq.) and sodium carbonate (10 mol eq.). The reaction mixture was heated in a microwave reactor for 20 min at 120 °C. The crude product was taken up in brine (5 mL) and extracted with ethyl acetate (2×5 mL). The combined organic components were then washed with brine (5 mL), dried over MgSO_4 , filtered and concentrated under reduced pressure. The crude product was purified by column chromatography with appropriate solvents.

General procedure W: To the appropriate aryl bromide (1 mol eq.) in acetonitrile was added phenyl formate (2 mol eq.), palladium(II) acetate (3% mol eq.), tri-*tert*-butylphosphonium tetrafluoroborate (0.12 mol eq.) and triethylamine (2 mol eq.). The reaction mixture was heated in a microwave reactor for 30 min at 150 °C. The crude product was taken up in brine (5 mL) and extracted with ethyl acetate (2×5 mL). The combined organic components were dried over MgSO_4 , filtered and concentrated under reduced pressure. The crude product was purified by column chromatography with appropriate solvents.

General procedure X: To the appropriate aryl bromide (1 mol eq.) in *N,N*-dimethylformamide was added phenyl formate (2 mol eq.), bis(benzonitrile)palladium(II) chloride (5% mol eq.), xantphos (0.06 mol eq.) and triethylamine

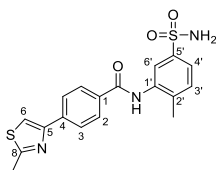
(2 mol eq.). The reaction mixture was heated in a microwave reactor for 30 min at 150 °C. The crude product was taken up in brine (5 mL) and extracted with ethyl acetate (2 × 5 mL). The combined organic components were dried over MgSO₄, filtered and concentrated under reduced pressure. The crude product was purified by column chromatography with appropriate solvents.

General procedure Y: To 4-(2-methyl-1,3-thiazol-4-yl)benzoic acid (**102**) (1 mol eq.) in dichloromethane was added oxalyl chloride (1.2 mol eq.) in a dropwise manner followed by the addition of a few drops of *N,N*-dimethylformamide. The reaction mixture was stirred at ambient temperature for 16 h. The crude acyl chloride was then added to a stirred mixture of the appropriate amine (1 mol eq.), triethylamine (1 mol eq.) and 4-(dimethylamino)pyridine (0.1 mol eq.). The reaction mixture was stirred at ambient temperature for 2-16 h. The solvent was removed under reduced pressure. The crude product was taken up in saturated aq. NaHCO₃ (5 mL) and extracted with ethyl acetate (3 × 10 mL). The combined organic components were then washed with brine (10 mL), dried over MgSO₄, filtered and concentrated under reduced pressure. The crude product was purified by column chromatography with appropriate solvents.

General procedure Z: To the appropriate acid (1 mol eq.) in dichloromethane was added oxalyl chloride (1.2 mol eq.) in a dropwise manner followed by the addition of a few drops of *N,N*-dimethylformamide. The reaction mixture was stirred at ambient temperature for 16 h. The crude acyl chloride was then added to a stirred mixture of the appropriate amine (1 mol eq.) followed by the addition of sodium hydride (60% dispersion in mineral oil) (4 mol eq.). The reaction mixture was stirred at ambient temperature for 2-16 h. The solvent was removed under reduced pressure. The crude product was taken up in saturated aq. NaHCO₃ (5 mL) and extracted with ethyl acetate (3 × 10 mL). The combined organic components were then washed with brine (10 mL), dried over MgSO₄, filtered and concentrated under reduced pressure. The crude product was purified by column chromatography with appropriate solvents.

11.2.1. Synthetic procedures

N-(2-methyl-5-sulfamoyl-phenyl)-4-(2-methylthiazol-4-yl)benzamide (**99**)

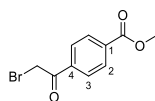


Compound **99** was synthesised according to general procedure L, using the following reagents: 4-(2-methyl-1,3-thiazol-4-yl)benzoic acid (**102**) (120 mg, 0.55 mmol), HBTU (153 mg, 0.66 mmol), *N,N*-diisopropylethylamine (191 µL, 1.09 mmol), 3-amino-4-methylbenzenesulfonamide (102 mg, 0.55 mmol) and *N,N*-dimethylformamide (2 mL). The crude was purified by column chromatography (silica 12 g, 0 to 55% ethyl acetate in petroleum ether) and further purified by column chromatography (amino silica 4 g, 0 to 5% methanol in dichloromethane) to yield the desired amide **99** as a white solid (15 mg, 7%).

R_f 0.14 (petroleum ether:ethyl acetate 9:11); **m.p.** 261–263 °C; **¹H-NMR** (500 MHz, DMSO-*d*₆) δ 10.11 (s, 1H, CONH), 8.15 – 8.09 (m, 3H, H-3, H-6), 8.06 (d, *J* 8.2, 2H, H-2), 7.87 (s, 1H, H-6'), 7.62 (d, *J* 8.0, 1H, H-4'), 7.48 (d, *J* 8.0, 1H, H-9'), 7.34 (s, 2H, SO₂NH₂), 2.75 (s, 3H, 8-CH₃), 2.32 (s, 3H, 2'-CH₃); **¹³C-NMR** (126 MHz, DMSO-*d*₆) δ 166.4 (CO), 165.5 (C-8), 153.3 (C-5), 142.5 (C-5'), 138.3 (C-1), 137.6 (C-2'), 137.2 (C-2'), 133.6 (C-4), 131.2 (C-3'), 128.75 (C-2), 126.3 (C-3), 124.1 (C-6'), 123.4 (C-4'), 116.1 (C-6), 19.4 (8-CH₃), 18.44 (2'-CH₃); **IR** (neat, ν_{max}, cm⁻¹) 3258, 2923, 1630, 1572,

1516, 1444, 1403, 1304, 1154; **LCMS** (LCQ) Rt = 2.7 min (method 1), m/z (ESI⁺) 388.1 [M+H]⁺; **HRMS** m/z (ESI): calcd. for C₁₈H₁₇N₃O₃S₂ [M+H]⁺ 388.6847, found 388.6850.

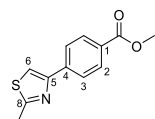
Methyl 4-(2-bromoacetyl)benzoate (**100**)



A solution of methyl 4-acetylbenzoate (1.00 g, 5.61 mmol) and *p*-toluenesulfonic acid monohydrate (54 mg, 0.28 mmol) in acetonitrile (30 mL) was treated with *N*-bromosuccinimide (0.99 g, 5.61 mmol) and the reaction mixture heated to 80 °C for 16 h. The solvent was removed under reduced pressure. The crude product was taken up in saturated aq. NaHCO₃ (15 mL) and extracted with ethyl acetate (3 × 15 mL). The combined organic components were then washed with brine (15 mL), dried over MgSO₄, filtered and concentrated under reduced pressure. The crude product was purified by column chromatography (silica 24 g, 0 to 10% ethyl acetate in petroleum ether) to yield the desired compound **100** as a light yellow solid (1.12 g, 70%).

R_f 0.66 (petroleum ether:ethyl acetate, 9:1); **¹H-NMR** (500 MHz, DMSO-*d*₆) δ 8.14 – 8.01 (m, 4H, H-2, H-3), 4.98 (s, 2H, COCH₂Br), 3.89 (s, 3H, COOCH₃). ¹H-NMR corresponds to literature data.³⁰¹

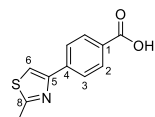
Methyl 4-(2-methylthiazol-4-yl)benzoate (**101**)



To methyl 4-(2-bromoacetyl)benzoate (2.12 g, 8.23 mmol) (**100**) in *N,N*-dimethylformamide (30 mL) was added thioacetamide (931 mg, 12.4 mmol) and the reaction mixture stirred at ambient temperature for 16 h. Upon completion, water was added to the reaction mixture. The resulting precipitate was collected by vacuum filtration and dried under reduced pressure to afford the desired compound **101** as a white solid (1.48 g, 73%).

m.p. 223–225 °C; **¹H-NMR** (500 MHz, DMSO-*d*₆) δ 8.14 (s, 1H, H-6), 8.08 (d, *J* 8.2, 2H, H-2), 8.01 (d, *J* 8.2, 2H, H-3), 3.87 (s, OCH₃), 2.73 (s, CH₃); **¹³C-NMR** (126 MHz, DMSO-*d*₆) δ 166.5 (CO), 166.4 (C-8), 153.0 (C-5), 138.9 (C-4), 130.2 (C-2), 129.1 (C-1), 126.5 (C-3), 116.8 (C-6), 52.5 (OCH₃), 19.4 (CH₃); **IR** (neat, ν_{max} , cm⁻¹) 3106, 2943, 1713, 1606, 1436, 1409, 1270, 1170; **LCMS** (LCQ) Rt = 2.9 min (method 2), m/z (ESI⁺) 234.2 [M+H]⁺; **HRMS** m/z (ESI): calcd. for C₁₂H₁₁NO₂S [M+H]⁺ 234.0583, found 234.0583.

4-(2-Methylthiazol-4-yl)benzoic acid (**102**)

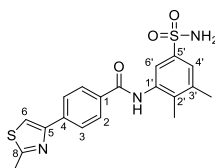


To methyl 4-(2-methylthiazol-4-yl)benzoate (1.46 g, 6.26 mmol) (**101**) in methanol (24 mL) and water (8 mL) was added sodium hydroxide (502 mg, 12.5 mmol) and the reaction mixture stirred at an ambient temperature for 16 h. Upon completion, the reaction mixture was acidified to pH of 2–3 using 2 M aq. hydrochloric acid solution. The resulting precipitate was collected by vacuum filtration and dried under reduced pressure to afford the desired acid **102** as a white solid (1.21 g, 84%).

m.p. 250–252 °C; **¹H-NMR** (500 MHz, DMSO-*d*₆) δ 8.10 (s, 1H, H-6), 8.05 (d, *J* 8.2, 2H, H-3), 7.99 (d, *J* 8.1, 2H, H-2), 2.73 (s, 3H, CH₃); **¹³C-NMR** (126 MHz, DMSO-*d*₆) δ 167.5 (CO), 166.4 (C-8), 153.2 (C-5), 138.5 (C-4), 130.3 (C-2), 126.4 (C-3), 116.5 (C-6), 19.4 (CH₃). Quaternary 5-C not visible; **IR** (neat, ν_{max} , cm⁻¹) 2826, 1667, 1608, 1573, 1421, 1290, 1169;

LCMS (LCQ) Rt = 0.6 min (method 1), m/z (ESI⁺) 220.2 [M+H]⁺; **HRMS** m/z (ESI): calcd. for C₁₁H₉NO₂S [M+H]⁺ 220.0427, found 220.0428.

***N*-(2,3-dimethyl-5-sulfamoyl-phenyl)-4-(2-methylthiazol-4-yl)benzamide (103)**

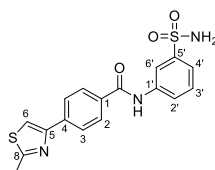


1st procedure: Compound **103** was synthesised according to general procedure L, using the following reagents: 4-(2-methyl-1,3-thiazol-4-yl)benzoic acid (**102**) (120 mg, 0.55 mmol), HBTU (153 mg, 0.66 mmol), *N,N*-diisopropylethylamine (0.19 mL, 1.09 mmol), 3-amino-4,5-dimethylbenzenesulfonamide (110 mg, 0.55 mmol) and *N,N*-dimethylformamide (3 mL). The crude was purified by column chromatography (silica 12 g, 0 to 60% ethyl acetate in petroleum ether) to yield the desired amide **103** as a white solid (15 mg, 7%).

2nd procedure: Compound **103** was synthesised according to general procedure M, using the following reagents: 4-(2-methyl-1,3-thiazol-4-yl)benzoic acid (**102**) (100 mg, 0.46 mmol), oxalyl chloride (46 μ L, 0.55 mmol), *N,N*-dimethylformamide (10 μ L) and dichloromethane (3 mL) and stirred for 16 h. Followed by 3-amino-4,5-dimethylbenzenesulfonamide (109 mg, 0.55 mmol), *N,N*-diisopropylethylamine (397 μ L, 2.28 mmol) and dichloromethane (1 mL) and stirred for 16 h. The crude was purified by column chromatography (silica 12 g, 0 to 60% ethyl acetate in petroleum ether) and further purified by column chromatography (amino silica 12 g, 0 to 100% ethyl acetate in petroleum ether) to yield the desired amide **103** as a white solid (30 mg, 16%).

R_f 0.12 (petroleum ether:ethyl acetate 1:1); **m.p.** 246–248 °C; **¹H-NMR** (500 MHz, DMSO-*d*₆) δ 10.17 (s, 1H, CONH), 8.13 – 8.08 (m, 3H, H-3, H-6), 8.05 (d, *J* 8.4, 2H, H-2), 7.64 (d, *J* 1.9, 1H, H-4'), 7.54 (d, *J* 1.9, 1H, H-3'), 7.28 (s, 2H, SO₂NH₂), 2.74 (s, 3H, 8-CH₃), 2.36 (s, 3H, 3'-CH₃), 2.17 (s, 3H, 2'-CH₃); **¹³C-NMR** (126 MHz, DMSO-*d*₆) δ 166.4 (CO), 165.7 (C-8), 153.3 (C-5), 141.6 (C-5'), 138.5 (C-1), 137.6 (ArC), 137.5 (ArC), 137.1 (ArC), 133.7 (C-4), 128.7 (C-2), 126.3 (C-3), 124.6 (C-6'), 122.3 (C-4'), 116.1 (C-6), 20.7 (3'-CH₃), 19.4 (8-CH₃), 15.0 (2'-CH₃); **IR** (neat, ν_{\max} , cm⁻¹) 3258, 2923, 1630, 1572, 1516, 1444, 1403, 1304, 1154; **LCMS** (LCQ) Rt = 2.0 min (method 1), m/z (ESI⁺) 402.1 [M+H]⁺; **HRMS** m/z (ESI): calcd. for C₁₉H₁₉N₃O₃S₂ [M+H]⁺ 401.0868, found 401.0866.

4-(2-Methylthiazol-4-yl)-*N*-(3-sulfamoylphenyl)benzamide (104)

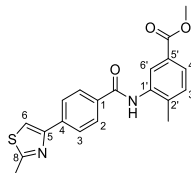


Compound **104** was synthesised according to general procedure N, using the following reagents: 4-(2-methyl-1,3-thiazol-4-yl)benzoic acid (**102**) (120 mg, 0.55 mmol), EDCI (137 mg, 0.71 mmol), HOBt (109 mg, 0.71 mmol), 4-methylmorpholine (120 μ L, 1.09 mmol), methyl 3-aminobenzenesulfonamide (120 mg, 0.71 mmol), and *N,N*-dimethylformamide (1 mL). The crude was purified by column chromatography (amino silica 12 g, 0 to 5% methanol in dichloromethane) to yield the desired amide **104** as a white solid (68 mg, 32%).

R_f 0.22 (petroleum ether:ethyl acetate 1:1); **m.p.** 220–222 °C; **¹H-NMR** (500 MHz, DMSO-*d*₆) δ 10.54 (s, 1H, CONH), 8.37 (s, 1H, H-6'), 8.15 – 8.08 (m, 3H, H-3, H-6), 8.06 (d, *J* 8.2, 2H, H-2), 7.98 (d, *J* 6.3, 1H, H-4'), 7.55 (d, *J* 6.2, 2H, H-2', H-3'), 7.36 (s, 2H, SONH₂), 2.74 (s, 3H, CH₃); **¹³C-NMR** (126 MHz, DMSO-*d*₆) δ 166.4 (-CO), 165.7 (C-8), 153.3 (C-5), 145.1 (C-5'), 140.0 (C-1'), 137.7 (C-1), 133.9 (C-4), 129.7 (C-3'), 128.8 (C-2), 126.3 (C-3), 123.7 (C-4'), 121.2 (C-2'), 117.9

(C-6'), 116.2 (C-6), 19.4 (CH₃); **IR** (neat, ν_{\max} , cm⁻¹) 3297, 1643, 1594, 1523, 1419. 1305, 1249, 1149; **LCMS** (LCQ) R_t = 2.4 min (method 1), m/z (ESI⁺) 374.1 [M+H]⁺; **HRMS** m/z (ESI): calcd. for C₁₇H₁₅N₃O₃S₂ [M+Na]⁺ 396.0447, found 396.0451.

Methyl 4-methyl-3-((4-(2-methylthiazol-4-yl)benzoyl)amino)benzoate (105)

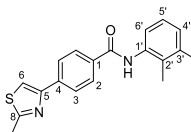


Procedure 1: Compound **105** was synthesised according to general procedure O, using the following reagents: 4-(2-methyl-1,3-thiazol-4-yl)benzoic acid (**102**) (800 mg, 3.65 mmol), methyl 3-amino-4-methylbenzoate (52 μ L, 9.12 mmol), phosphorus trichloride (0.32 mL, 3.65 mmol), tetrahydrofuran (15 mL). The crude was purified by column chromatography (amino silica 12 g, 0 to 50% ethyl acetate in petroleum ether) to yield the desired amide **105** as a white solid (920 mg, 65%).

Procedure 2: Compound **105** was synthesised according to general procedure P, using the following reagents: 4-(2-methyl-1,3-thiazol-4-yl)benzoic acid (**102**) (100 mg, 0.46 mmol), EDCI (105 mg, 0.55 mmol), HOBT (83 mg, 0.55 mmol), *N,N*-diisopropylethylamine (100 μ L, 0.55 mmol), methyl 3-amino-4-methylbenzoate (80 mg, 0.46 mmol), and *N,N*-dimethylformamide (3 mL). The crude was purified by column chromatography (silica 12 g, 0 to 75% ethyl acetate in petroleum ether) and further purified by column chromatography (amino silica 12 g, 0 to 50% ethyl acetate in petroleum ether) to yield the desired amide **105** as a white solid (20 mg, 11%).

R_f 0.23 (petroleum ether:ethyl acetate 3:1); **m.p.** 179–181 °C; **¹H-NMR** (500 MHz, DMSO-*d*₆) δ 10.03 (s, 1H, CONH), 8.14–8.07 (m, 3H, H-3, H-6), 8.05 (d, *J* 8.3, 2H, H-2), 8.00 (d, *J* 1.8, 1H, H-6'), 7.76 (dd, *J* 7.9, 1.8, 1H, H-4'), 7.44 (d, *J* 7.9, 1H, H-9'), 3.85 (s, 3H, OCH₃), 2.74 (s, 3H, 8-CH₃), 2.33 (s, 3H, 2'-CH₃); **¹³C-NMR** (126 MHz, DMSO-*d*₆) δ 166.4 (CO), 165.6 (C-8), 153.3 (C-5), 140.0 (C-8'), 137.6 (C-1), 137.3 (C-7'), 133.7 (C-4), 131.3 (C-3'), 128.8 (C-2), 128.1 (C-6'), 127.5 (C-5'), 126.9 (C-4'), 126.3 (C-3), 116.1 (C-6), 52.5 (OCH₃), 19.4 (8-CH₃), 18.6 (2'-CH₃). COO not visible; **IR** (neat, ν_{\max} , cm⁻¹) 3256, 1726, 1643, 1523, 1432, 1296, 1171, 1110; **LCMS** (LCQ) R_t = 2.6 min (method 1), m/z (ESI⁺) 367.0 [M+H]⁺; **HRMS** m/z (ESI): calcd. for C₂₀H₁₈N₂O₃S [M+Na]⁺ 389.0930, found 389.0931.

***N*-(2,3-dimethylphenyl)-4-(2-methylthiazol-4-yl)benzamide (106)**

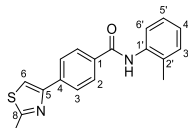


Compound **106** was synthesised according to general procedure M, using the following reagents: 4-(2-methyl-1,3-thiazol-4-yl)benzoic acid (**102**) (160 mg, 0.73 mmol), oxalyl chloride (74 μ L, 0.88 mmol), *N,N*-dimethylformamide (10 μ L) and dichloromethane (3 mL) and stirred for 16 h. Followed by 2,3-dimethylaniline (107 μ L, 0.55 mmol), *N,N*-diisopropylethylamine (397 μ L, 2.28 mmol) and dichloromethane (1 mL) and stirred for 1 h. The crude was purified by column chromatography (silica 12 g, 0 to 25% ethyl acetate in petroleum ether) to yield the desired amide **106** as a white solid (71 mg, 29%).

R_f 0.23 (petroleum ether:ethyl acetate 3:1); **m.p.** 193–195 °C; **¹H-NMR** (500 MHz, DMSO-*d*₆) δ 9.94 (s, 1H, CONH), 8.11 (s, 1H, H-6), 8.08 (d, *J* 8.3, 2H, H-3), 8.05 (d, *J* 8.3, 2H, H-2), 7.17–7.05 (m, 3H, H-4', H-5', H-6'), 2.75 (s, 3H, 8-CH₃), 2.29 (s, 3H, 2'-CH₃), 2.11 (s, 3H, 3'-CH₃); **¹³C-NMR** (126 MHz, DMSO-*d*₆) δ 166.4 (CO), 165.4 (C-8), 153.4 (C-5), 137.4 (ArC), 137.3 (ArC), 136.8 (ArC), 134.1 (ArC), 133.2 (ArC), 128.6 (C-2), 128.0 (ArC), 126.2 (C-3), 125.7 (ArC), 125.2

(ArC), 115.9 (C-6), 20.6 (2'-CH₃), 19.4 (8-CH₃), 14.7 (3'-CH₃); **IR** (neat, ν_{\max} , cm⁻¹) 3106, 1636, 1603, 1521, 1452, 1303, 1275; **LCMS** (LCQ) Rt = 0.8 min (method 1), m/z (ESI⁺) 323.0 [M+H]⁺; **HRMS** m/z (ESI): calcd. for C₁₉H₁₈N₂NaOS [M+Na]⁺ 345.1032, found 345.1032.

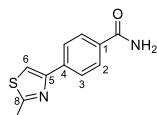
4-(2-Methylthiazol-4-yl)-*N*-(*o*-tolyl)benzamide (107)



Compound **107** was synthesised according to general procedure M, using the following reagents: 4-(2-methyl-1,3-thiazol-4-yl)benzoic acid (**102**) (100 mg, 0.46 mmol), oxalyl chloride (46 μ L, 0.55 mmol), *N,N*-dimethylformamide (10 μ L) and dichloromethane (3 mL) and stirred for 16 h. Followed *o*-toluidine (58 μ L, 0.55 mmol), *N,N*-diisopropylethylamine (397 μ L, 2.28 mmol) and dichloromethane (1 mL) and stirred for 2 h. The crude was purified by column chromatography (silica 12 g, 0 to 25% ethyl acetate in petroleum ether) to yield the desired amide **107** as a white solid (41 mg, 28%).

R_f 0.25 (petroleum ether:ethyl acetate 3:1); **m.p.** 210–211 °C; **¹H-NMR** (500 MHz, DMSO-*d*₆) δ 9.90 (s, 1H, CONH), 8.14 – 8.07 (m, 3H, H-3, H-6), 8.05 (d, *J* 8.2, 2H, H-2), 7.35 (d, *J* 7.8, 1H, H-6'), 7.28 (d, *J* 7.4, 1H, H-3'), 7.23 (t, *J* 7.5, 1H, H-5'), 7.18 (t, *J* 7.4, 1H, H-4'), 2.75 (s, 3H, 8-CH₃), 2.25 (s, 3H, 2'-CH₃); **¹³C-NMR** (126 MHz, DMSO-*d*₆) δ 166.4 (CO), 165.3 (C-8), 153.4 (C-5), 137.4 (C-1), 136.9 (C-8'), 134.2 (C-3'), 134.0 (C-4), 130.7 (C-5'), 128.7 (C-2), 127.1 (C-6'), 126.4 (C-4'), 126.2 (C-3), 116.0 (C-6), 19.4 (8-CH₃), 18.4 (3'-CH₃); **IR** (neat, ν_{\max} , cm⁻¹) 2921, 1633, 1610, 1519, 1454, 1305, 1263, 1168; **LCMS** (LCQ) Rt = 0.8 min (method 1), m/z (ESI⁺) 309.1 [M+H]⁺; **HRMS** (ESI): calcd. for C₁₈H₁₆N₂OS [M+Na]⁺ 331.0876, found 331.0862.

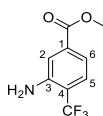
4-(2-Methylthiazol-4-yl)benzamide (108)



Compound **108** was synthesised according to general procedure M, using the following reagents: 4-(2-methyl-1,3-thiazol-4-yl)benzoic acid (**102**) (100 mg, 0.46 mmol), oxalyl chloride (46 μ L, 0.55 mmol), *N,N*-dimethylformamide (10 μ L) and dichloromethane (3 mL) and stirred for 16 h. Followed 2 M ammonia solution in methanol (3.42 mL, 6.74 mmol) and dichloromethane (1 mL) and stirred for 8 h. The crude was purified by column chromatography (silica 12 g, 0 to 5% methanol in dichloromethane) to yield the desired amide **108** as a white solid (15 mg, 24%).

R_f 0.11 (dichloromethane:methanol, 19:1); **m.p.** 172–174 °C; **¹H-NMR** (500 MHz, DMSO-*d*₆) δ 8.06 (s, 1H, H-6), 8.04 – 7.96 (m, 3H, H-3, NH), 7.93 (d, *J* 8.1, 2H, H-2), 7.34 (s, 1H, 3NH), 2.73 (s, 3H, CH₃); **¹³C-NMR** (126 MHz, DMSO-*d*₆) δ 168.0 (CO), 166.3 (C-8), 153.5 (C-5), 137.1 (C-1), 133.8 (C-4), 128.5 (C-2), 126.1 (C-3), 115.7 (H-6), 19.4 (CH₃); **LCMS** (LCQ) Rt = 0.8 min (method 1), m/z (ESI⁺) 319.1 [M+H]⁺; **HRMS** (ESI): calcd. for C₂₃H₁₉BrN₄NaO₃S [M+Na]⁺ 553.0253, found 553.0253.

Methyl 3-amino-4-(trifluoromethyl)benzoate (109)

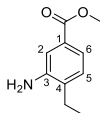


Compound **109** was synthesised according to general procedure Q, using the following reagents: thionyl chloride (1.25 mL, 17.1 mmol), 3-amino-4-(trifluoromethyl)benzoic acid (500 mg, 2.4 mmol), methanol (20 mL), to yield the

intermediate **109** as a brown solid (473 mg, 84%) which was carried forward without further purification. $^1\text{H-NMR}$ consistent with literature data.³⁰²

R_f 0.85 (petroleum ether:ethyl acetate 1:1); $^1\text{H-NMR}$ (500 MHz, DMSO- d_6) δ 7.48 (s, 1H, H-2), 7.45 (d, J 8.3, 1H, ArH), 7.14 (d, J 8.2, 1H, ArH), 5.89 (s, 2H, NH₂), 3.84 (s, 3H, OCH₃); **LCMS** (LCQ) R_t = 2.5 min (method 1), m/z (ESI⁺) 220.0 [M+H]⁺.

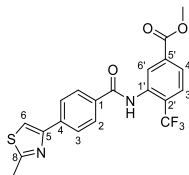
Methyl 3-amino-4-ethylbenzoate (**110**)



Compound **110** was synthesised according to general procedure Q, using the following reagents: thionyl chloride (1.25 mL, 17.14 mmol), 3-amino-4-ethylbenzoic acid (300 mg, 1.82 mmol), methanol (20 mL), to yield the intermediate **110** as a brown solid (298 mg, 87%) which was carried forward without further purification.

R_f 0.77 (petroleum ether:ethyl acetate 1:1); $^1\text{H-NMR}$ (500 MHz, DMSO- d_6) δ 7.25 (s, 1H, H-2), 7.11 (d, J 6.6, 1H, H-6), 7.03 (d, J 7.8, 1H, H-5), 5.12 (s, 2H, NH₂), 3.78 (s, 3H, OCH₃), 2.48 – 2.43 (m, 2H, CH₂CH₃), 1.13 (t, J 7.5, 3H, CH₂CH₃); **LCMS** (LCQ) R_t = 1.8 min (method 1), m/z (ESI⁺) 180.2 [M+H]⁺.

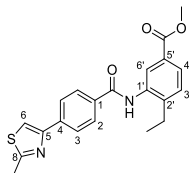
Methyl 3-((4-(2-methylthiazol-4-yl)benzoyl)amino)-4-(trifluoromethyl)benzoate (**111**)



Compound **111** was synthesised according to general procedure O, using the following reagents: 4-(2-methylthiazol-4-yl)benzoic acid (**102**) (100 mg, 0.46 mmol), methyl 3-amino-4-(trifluoromethyl)benzoate (250 mg, 1.14 mmol), phosphorus trichloride (40 μL , 0.46 mmol), tetrahydrofuran (3 mL) and acetonitrile (2 mL). The crude was purified by column chromatography (silica 12 g, 0 to 25% ethyl acetate in petroleum ether) to yield the desired amide **111** as a white solid (62 mg, 31%).

R_f 0.32 (petroleum ether:ethyl acetate 3:1); **m.p.** 235–237 °C; $^1\text{H-NMR}$ (500 MHz, DMSO- d_6) δ 10.31 (s, 1H, NH), 8.16 – 8.09 (m, 3H, H-3, H-6), 8.07 (d, J 5.6, 2H, 2 \times ArH), 8.03 (d, J 8.1, 2H, H-2), 7.98 (d, J 8.7, 1H, H-4'), 3.92 (s, 3H, OCH₃), 2.75 (s, 3H, 8-CH₃); **LCMS** (LCQ) R_t = 4.5 min (method 1), m/z (ESI⁺) 421.1 [M+H]⁺; **HRMS (ESI)**: calcd. for C₂₀H₁₅F₃N₂NaO₃S [M+Na]⁺ 443.0648, found 443.0627.

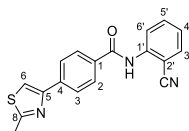
Methyl 4-ethyl-3-((4-(2-methylthiazol-4-yl)benzoyl)amino)benzoate (**112**)



Compound **112** was synthesised according to general procedure O, using the following reagents: 4-(2-methylthiazol-4-yl)benzoic acid (**102**) (80 mg, 0.36 mmol), methyl 3-amino-4-ethylbenzoate (160 mg, 0.91 mmol), phosphorus trichloride (31 μL , 0.36 mmol), tetrahydrofuran (3 mL) and acetonitrile (2 mL). The crude was purified by column chromatography (silica 12 g, 0 to 25% ethyl acetate in petroleum ether) to yield the desired amide **112** as a light pink solid (21 mg, 15%).

R_f 0.57 (petroleum ether:ethyl acetate 1:1); **m.p.** 211–213 °C; **¹H-NMR** (500 MHz, DMSO-*d*₆) δ 10.05 (s, 1H, NH), 8.11 (d, *J* 12.3, 3H, H-3, H-6), 8.05 (d, *J* 8.0, 2H, H-2), 7.94 (s, 1H, H-6'), 7.83 (d, *J* 8.1, 1H, H-4'), 7.47 (d, *J* 8.0, 1H, H-3'), 3.86 (s, 3H, OCH₃), 2.75 (s, 3H, 8-CH₃), 2.73 – 2.68 (m, 2H, CH₂CH₃), 1.17 (t, *J* 7.6, 3H, CH₂CH₃); **¹³C-NMR** (126 MHz, DMSO-*d*₆) δ 166.4 (CO), 165.9 (C-8), 152.2 (C-5), 145.8 (C-2'), 137.5 (C-1), 136.6 (C-1'), 133.7 (C-4), 129.4 (C-3'), 128.7 (C-2), 128.5 (ArC), 128.1 (ArC), 127.4 (C-4'), 126.3 (C-3), 116.1 (C-6), 52.5 (OCH₃), 24.5 (CH₂CH₃), 19.4 (8-CH₃), 14.1 (CH₂CH₃). CO not visible; **LCMS** (LCQ) Rt = 3.1 min (method 1), *m/z* (ESI⁺) 381.1 [M+H]⁺; Not enough material for IR and HRMS determination.

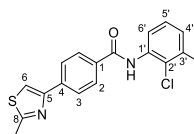
***N*-(2-cyanophenyl)-4-(2-methylthiazol-4-yl)benzamide (113)**



Compound **113** was synthesised according to general procedure M, using the following reagents: 4-(2-methyl-1,3-thiazol-4-yl)benzoic acid (**102**) (100 mg, 0.46 mmol), oxalyl chloride (46 µL, 0.55 mmol), *N,N*-dimethylformamide (10 µL) and dichloromethane (3 mL) and stirred for 16 h. Followed by 2-aminobenzonitrile (65 mg, 0.55 mmol), *N,N*-diisopropylethylamine (397 µL, 2.28 mmol) and dichloromethane (1 mL) and stirred for 16 h. The crude was purified by column chromatography (silica 12 g, 0 to 30% ethyl acetate in petroleum ether) and further purified by column chromatography (amino silica 12 g, 0 to 60% ethyl acetate in petroleum ether) to yield the desired amide **113** as a white solid (17 mg, 11%).

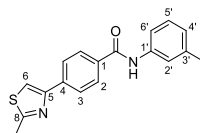
R_f 0.22 (petroleum ether:ethyl acetate 4:1); **m.p.** 220–222 °C; **¹H-NMR** (500 MHz, DMSO-*d*₆) δ 10.63 (s, 1H, CONH), 8.18 – 8.10 (m, 3H, H-6, H-3), 8.07 (d, *J* 8.2, 2H, H-2), 7.88 (d, *J* 7.4, 1H, H-3'), 7.76 (t, *J* 8.1, 1H, H-5'), 7.60 (d, *J* 8.1, 1H, H-6'), 7.44 (t, *J* 7.6, 1H, H-4'), 2.75 (s, 3H, CH₃); **¹³C-NMR** (126 MHz, DMSO-*d*₆) δ 166.6 (CO), 165.7 (C-8), 153.2 (C-5), 140.8 (ArC), 137.9 (C-1), 134.2 (ArC), 133.5 (ArC), 132.9 (ArC), 128.9 (C-2), 127.3 (C-6'), 126.9 (C-4'), 126.4 (C-3), 117.4 (ArC), 116.4 (C-6), 109.9 (C-2'), 19.4 (8-CH₃); **IR** (neat, ν_{max} , cm⁻¹) 3280, 2643, 1607, 1582, 1524, 1448, 1304, 1167; **LCMS** (LCQ) Rt = 3.3 min (method 1), *m/z* (ESI⁺) 320.2 [M+H]⁺; **HRMS (ESI)**: calcd. for C₁₈H₁₃N₃NaOS [M+Na]⁺ 342.0672, found 342.0676.

***N*-(2-chloro-3-methyl-phenyl)-4-(2-methylthiazol-4-yl)benzamide (114)**



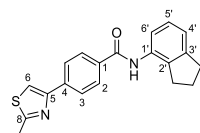
Compound **114** was synthesised according to general procedure M, using the following reagents: 4-(2-methyl-1,3-thiazol-4-yl)benzoic acid (**102**) (100 mg, 0.46 mmol), oxalyl chloride (46 µL, 0.55 mmol), *N,N*-dimethylformamide (10 µL) and dichloromethane (3 mL) and stirred for 16 h. Followed by 2-chloro-3-methylaniline (59 µL, 0.46 mmol), *N,N*-diisopropylethylamine (397 µL, 2.28 mmol) and dichloromethane (1 mL) and stirred for 1 h. The crude was purified by column chromatography (silica 12 g, 0 to 20% ethyl acetate in petroleum ether) to yield the desired amide **114** as a cream solid (11 mg, 7%).

R_f 0.19 (petroleum ether:ethyl acetate 3:1); **m.p.** 157–159 °C; **¹H-NMR** (500 MHz, DMSO-*d*₆) δ 10.04 (s, 1H), 8.13 (s, 1H), 8.10 (d, *J* 8.4, 2H), 8.05 (d, *J* 8.5, 2H), 7.44 (s, 1H), 7.33 – 7.25 (m, 2H), 2.74 (s), 2.39 (s, 3H); **¹³C-NMR** (126 MHz, DMSO-*d*₆) δ 166.4, 165.4, 153.3, 137.6, 136.9, 135.7, 128.9, 128.7, 127.0, 126.3, 116.2, 20.7, 19.4; **IR** (neat, ν_{max} , cm⁻¹) 3309, 2918, 1610, 1520, 1470, 1424, 1288, 1169; **LCMS** (LCQ) Rt = 4.9 min (method 1), *m/z* (ESI⁺) 343.2 [M+H]⁺; **HRMS (ESI)**: calcd. for C₁₈H₁₆ClN₂OS [M+H]⁺ 343.0666, found 342.0672.

4-(2-Methylthiazol-4-yl)-*N*-(*m*-tolyl)benzamide (115)

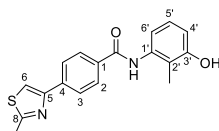
Compound **115** was synthesised according to general procedure M, using the following reagents: 4-(2-methyl-1,3-thiazol-4-yl)benzoic acid (**102**) (100 mg, 0.46 mmol), oxalyl chloride (46 μ L, 0.55 mmol), *N,N*-dimethylformamide (10 μ L) and dichloromethane (3 mL) and stirred for 16 h. Followed by *m*-toluidine (58 μ L, 0.55 mmol), *N,N*-diisopropylethylamine (397 μ L, 2.28 mmol) and dichloromethane (1 mL) and stirred for 2 h. The crude was purified by column chromatography (silica 12 g, 0 to 25% ethyl acetate in petroleum ether) to yield the desired amide **115** as a white solid (48 mg, 32%).

R_f 0.24 (petroleum ether:ethyl acetate 3:1); **m.p.** 138–140 °C; **¹H-NMR** (500 MHz, DMSO-*d*₆) δ 10.17 (s, 1H), 8.11 (s, 1H), 8.08 (d, *J* 8.2, 2H), 8.02 (d, *J* 8.2, 2H), 7.63 (s, 1H), 7.58 (d, *J* 8.1, 1H), 7.23 (t, *J* 7.8, 1H), 6.93 (d, *J* 7.5, 1H), 2.74 (s, 3H), 2.32 (s, 3H); **¹³C-NMR** (126 MHz, DMSO-*d*₆) δ 166.4, 165.4, 153.4, 139.5, 138.2, 137.4, 134.4, 128.9, 128.7, 126.2, 124.8, 121.5, 118.1, 116.0, 21.7, 19.4; **IR** (neat, ν_{max} , cm⁻¹); **LCMS** (LCQ) *R_t*=4.1 min (method 1), *m/z* (ESI⁺) 309.1 [M+H]⁺; **HRMS (ESI)**: calcd. for C₁₈H₁₆N₂NaOS [M+Na]⁺ 331.0876, found 342.0877.

***N*-indan-4-yl-4-(2-methylthiazol-4-yl)benzamide (116)**

Compound **116** was synthesised according to general procedure M, using the following reagents: 4-(2-methyl-1,3-thiazol-4-yl)benzoic acid (**102**) (100 mg, 0.46 mmol), oxalyl chloride (46 μ L, 0.55 mmol), *N,N*-dimethylformamide (10 μ L) and dichloromethane (3 mL) and stirred for 16 h. Followed by 4-indanamine (55 μ L, 0.55 mmol), *N,N*-diisopropylethylamine (397 μ L, 2.28 mmol) and dichloromethane (1 mL) and stirred for 2 h. The crude was purified by column chromatography (silica 12 g, 0 to 20% ethyl acetate in petroleum ether) to yield the desired amide **116** as a cream solid (73 mg, 45%).

R_f 0.26 (petroleum ether:ethyl acetate 3:1); **m.p.** 157–159 °C; **¹H-NMR** (500 MHz, DMSO-*d*₆) δ 9.94 (s, 1H), 8.12 (s, 1H), 8.08 (d, *J* 8.1, 2H), 8.03 (d, *J* 8.0, 2H), 7.25 (d, *J* 7.4, 1H), 7.15 (t, *J* 7.6, 1H), 7.10 (d, *J* 6.7, 1H), 2.92 (t, *J* 6.8, 2H), 2.85 (t, *J* 7.1, 2H), 2.74 (s, 3H), 2.00 (p, *J* 7.5, 2H); **¹³C-NMR** (126 MHz, DMSO-*d*₆) δ 166.4, 165.0, 153.3, 145.3, 139.0, 137.3, 134.7, 134.2, 128.8, 126.8, 126.2, 122.8, 121.7, 116.0, 40.2, 33.2, 31.3, 25.0, 19.4; **IR** (neat, ν_{max} , cm⁻¹) 3095, 1624, 1581, 1473, 1377, 1300, 1172, 1060; **LCMS** (LCQ) *R_t*=4.6 min (method 1), *m/z* (ESI⁺) 335.2 [M+H]⁺; **HRMS (ESI)**: calcd. for C₂₀H₁₉ClN₂OS [M+H]⁺ 335.1213, found 335.1208.

***N*-(3-hydroxy-2-methyl-phenyl)-4-(2-methylthiazol-4-yl)benzamide (117)**

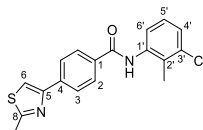
Procedure 1: Compound **117** was synthesised according to general procedure M, using the following reagents: 4-(2-methyl-1,3-thiazol-4-yl)benzoic acid (**102**) (80 mg, 0.36 mmol), oxalyl chloride (37 μ L, 0.44 mmol), *N,N*-dimethylformamide (10 μ L) and dichloromethane (3 mL) and stirred for 16 h. Followed by 3-amino-2-methylphenol (54 mg, 0.44 mmol), *N,N*-diisopropylethylamine (397 μ L, 2.28 mmol) and dichloromethane (1 mL) and stirred for

16 h. The crude was purified by column chromatography (silica 12 g, 0 to 40% ethyl acetate in petroleum ether) to yield the desired amide **117** as a colourless solid (13 mg, 10%).

Procedure 2: *N*-(3-(tert-butyl(dimethyl)silyl)oxy-2-methyl-phenyl)-4-(2-methylthiazol-4-yl)benzamide (**121**) (85 mg, 0.19 mmol) in tetrahydrofuran (1 mL) and was cooled to 0 °C and to the reaction mixture was added tetrabutylammonium fluoride (380 µL, 0.39 mmol). The reaction mixture was stirred at 0 °C for 5 min and at ambient temperature for 10 min. The reaction mixture was concentrated under reduced pressure. The crude was purified by column chromatography (silica 12 g, 0 to 5% methanol in dichloromethane), followed by trituration in ether to yield the desired amide **117** as a colourless solid (16 mg, 24%).

R_f 0.47 (petroleum ether:ethyl acetate 1:1); **m.p.** 238–240 °C; **¹H-NMR** (500 MHz, DMSO-*d*₆) δ 9.84 (s, 1H, CONH), 9.35 (s, 1H, OH), 8.10 (s, 1H, H-6), 8.07 (d, *J* 8.2, 2H, H-3), 8.03 (d, *J* 8.3, 2H, H-2), 7.00 (t, *J* 7.9, 1H, H-5'), 6.79 (d, *J* 7.8, 1H, H-6'), 6.73 (d, *J* 8.0, 1H, H-4'), 2.74 (s, 3H, 8-CH₃), 2.03 (s, 3H, 2'-CH₃); **¹³C-NMR** (126 MHz, DMSO-*d*₆) δ 166.4 (CONH), 165.3 (C-8), 156.2 (C-5), 153.4 (C-3'), 137.9 (ArC), 137.3 (ArC), 134.1 (ArC), 128.7 (H-2), 126.2 (H-3), 126.0 (ArC), 121.3 (ArC), 118.0 (C-6'), 116.0 (C-6), 112.9 (C-4'), 19.4, (C-8) 11.4 (C-2'); **IR** (neat, *v*_{max}, cm⁻¹) 3291, 1640, 1607, 1499, 1466, 1307, 1174; **LCMS** (LCQ) *R*_t=2.5 min (method 1), *m/z* (ESI⁺) 325.1 [M+H]⁺; **HRMS (ESI)**: calcd. for C₁₈H₁₆NaN₂OS [M+Na]⁺ 347.0825, found 347.0827.

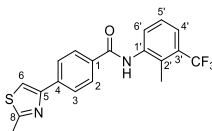
***N*-(3-chloro-2-methyl-phenyl)-4-(2-methylthiazol-4-yl)benzamide (118)**



Compound **118** was synthesised according to general procedure M, using the following reagents: 4-(2-methyl-1,3-thiazol-4-yl)benzoic acid (**102**) (80 mg, 0.36 mmol), oxalyl chloride (37 µL, 0.44 mmol), *N,N*-dimethylformamide (10 µL) and dichloromethane (3 mL) and stirred for 16 h. Followed by 3-chloro-2-methylaniline5-methoxy-2-methylaniline (52 µL, 0.44 mmol), *N,N*-diisopropylethylamine (397 µL, 2.28 mmol) and dichloromethane (1 mL) and stirred for 2 h. The crude was purified by column chromatography (silica 12 g, 0 to 25% ethyl acetate in petroleum ether) to yield the desired amide **118** as a white solid (22 mg, 17%).

R_f 0.22 (petroleum ether:ethyl acetate 3:1); **m.p.** 201–203 °C; **¹H-NMR** (500 MHz, DMSO-*d*₆) δ 10.15 (s, 1H), 8.11 (s, 1H), 8.09 (d, *J* 8.4, 2H), 8.05 (d, *J* 8.4, 2H), 7.37 (d, *J* 7.8), 7.32 (d, *J* 7.7), 7.26 (t, *J* 7.9, 1H), 2.74 (s, 3H), 2.26 (s, 3H); **¹³C-NMR** (126 MHz, DMSO-*d*₆) δ 166.4, 165.6, 153.6, 138.6, 137.6, 134.3, 133.6, 132.7, 128.7, 127.3, 127.2, 126.3, 126.3, 116.1, 19.4, 15.8; **IR** (neat, *v*_{max}, cm⁻¹) 3337, 1640, 1607, 1506, 1434, 1289, 1167; **LCMS** (LCQ) *R*_t=4.3 min (method 2), *m/z* (ESI⁺) 343.2 [M+H]⁺; **HRMS (ESI)**: calcd. for C₁₈H₁₆NaN₂OS [M+Na]⁺ 343.0666, found 343.0665.

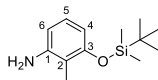
4-(2-Methylthiazol-4-yl)-*N*-(2-methyl-3-(trifluoromethyl)phenyl)benzamide (119)



Compound **119** was synthesised according to general procedure M, using the following reagents: 4-(2-methyl-1,3-thiazol-4-yl)benzoic acid (**102**) (80 mg, 0.36 mmol), oxalyl chloride (37 µL, 0.44 mmol), *N,N*-dimethylformamide (10 µL) and dichloromethane (3 mL) and stirred for 16 h. Followed by 2-methyl-3-(trifluoromethyl)aniline (77 mg, 0.44 mmol), *N,N*-diisopropylethylamine (397 µL, 2.28 mmol) and dichloromethane (1 mL) and stirred for 2 h. The crude was purified by column chromatography (silica 12 g, 0 to 20% ethyl acetate in petroleum ether) to yield the desired amide **119** as a white solid (32 mg, 46%).

R_f 0.32 (petroleum ether:ethyl acetate 3:1); **m.p.** 197–199 °C; **¹H-NMR** (500 MHz, DMSO-*d*₆) δ 10.16 (s, 1H), 8.15 – 8.09 (m, 3H), 8.07 (d, *J* 8.2, 2H), 7.64 (m, 2H), 7.45 (t, *J* 7.9, 1H), 2.75 (s, 3H), 2.34 (s, 3H); **¹³C-NMR** (126 MHz, DMSO-*d*₆) δ 166.5, 165.7, 153.2, 138.7, 137.6, 133.4, 131.8, 128.7, 126.8, 126.3, 124.0, 116.1, 19.3, 14.3; **IR** (neat, ν_{max} , cm⁻¹) 3337, 1640, 1607, 1506, 1434, 1289, 1167; **LCMS** (LCQ) Rt = 4.5 min (method 1), *m/z* (ESI⁺) 377.1 [M+H]⁺; **HRMS (ESI)**: calcd. for C₁₉H₁₆F₃N₂OS [M+H]⁺ 377.0930, found 377.0932

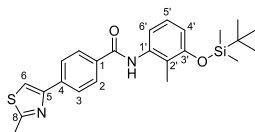
3-(*Tert*-butyl(dimethyl)silyloxy)-2-methyl-aniline (**120**)



To 3-amino-2-methylphenol (100 mg, 0.81 mmol), 4-(dimethylamino)pyridine (10 mg, 0.08 mmol) and triethylamine (340 μL, 2.44 mmol) in dichloromethane was added *tert*-butyldimethylsilyl chloride (367 mg, 2.44 mmol). The reaction mixture was stirred at ambient temperature for 18 h. The reaction mixture was taken up in water (3 mL) and the components separated. The organic components were concentrated under reduced pressure. The crude was purified by column chromatography (silica 12 g, 0 to 15% ethyl acetate in petroleum ether) to yield the desired product **120** as a pale yellow oil (168 mg, 78%).

R_f 0.85 (petroleum ether:ethyl acetate 1:1); **¹H-NMR** (500 MHz, DMSO-*d*₆) δ 6.72 (t, *J* 8.0, 1H, H-5), 6.25 (d, *J* 8.0, 1H, ArH), 6.04 (d, *J* 7.9, 1H, ArH), 4.78 (s, 2H, NH₂), 1.89 (s, 3H, ArCH₃), 0.97 (s, 9H, OSi(CH₃)₂(CH₃)₃), 0.15 (s, 6H, OSi(CH₃)₂(CH₃)₃); **LCMS** (LCQ) Rt = 3.7 min (method 1), *m/z* (ESI⁺) 238.2 [M+H]⁺.

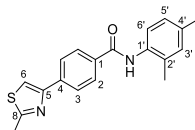
N-(3-(*tert*-butyl(dimethyl)silyloxy)-2-methyl-phenyl)-4-(2-methylthiazol-4-yl)benzamide (**121**)



Compound **121** was synthesised according to general procedure R, using the following reagents: 4-(2-methyl-1,3-thiazol-4-yl)benzoic acid (**102**) (70 mg, 0.32 mmol), HATU (120 mg, 0.32 mmol), *N,N*-diisopropylethylamine (111 μL, 0.64 mmol), 3-(*tert*-butyl(dimethyl)silyloxy)-2-methyl-aniline (**120**) (182 mg, 0.38 mmol) and *N,N*-dimethylformamide (1 mL). The crude was purified by column chromatography (silica, 0 to 25% ethyl acetate in petroleum ether) to yield the desired compound **121** as a white solid (85 mg, 90%).

R_f 0.85 (petroleum ether:ethyl acetate 1:1); **¹H-NMR** (500 MHz, DMSO-*d*₆) δ 9.93 (s, 1H, CONH), 8.10 (s, 1H, H-6), 8.06 (d, *J* 8.5, 2H, H-3), 8.01 (d, *J* 7.8, 2H, H-2), 7.08 (t, *J* 7.8, 1H, H-5'), 6.93 (d, *J* 7.3, 1H, ArH), 6.74 (d, *J* 7.7, 1H, ArH), 2.72 (s, 3H, 8-CH₃), 2.04 (s, 3H, 2'-CH₃), 0.98 (s, 9H, OSi(CH₃)₂(CH₃)₃), 0.21 (s, 6H, OSi(CH₃)₂(CH₃)₃); **LCMS** (LCQ) Rt = 6.4 min (method 1), *m/z* (ESI⁺) 439.2 [M+H]⁺.

N-(2,4-dimethylphenyl)-4-(2-methylthiazol-4-yl)benzamide (**122**)

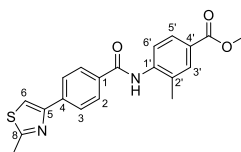


Compound **122** was synthesised according to general procedure M, using the following reagents: 4-(2-methyl-1,3-thiazol-4-yl)benzoic acid (**102**) (100 mg, 0.46 mmol), oxalyl chloride (46 μL, 0.55 mmol), *N,N*-dimethylformamide (10 μL) and dichloromethane (3 mL) and stirred for 16 h. Followed by 2,4-dimethylaniline (68 μL, 0.55 mmol), *N,N*-diisopropylethylamine (397 μL, 2.28 mmol) and dichloromethane (1 mL) and stirred for 16 h. The crude was purified

by column chromatography (silica 12 g, 0 to 25% ethyl acetate in petroleum ether) to yield the desired amide **112** as a cream solid (17 mg, 11%).

R_f 0.23 (petroleum ether:ethyl acetate 3:1); **m.p.** 188–190 °C; **¹H-NMR** (500 MHz, DMSO-*d*₆) δ 9.82 (s, 1H), 8.10 (s, 1H), 8.08 (d, *J* 8.2, 2H), 8.03 (d, *J* 8.1, 2H), 7.20 (d, *J* 7.9), 7.09 (s, 1H), 7.02 (d, *J* 8.3), 2.74 (s, 3H), 2.29 (s, 3H), 2.20 (s, 3H); **¹³C-NMR** (126 MHz, DMSO-*d*₆) δ 166.4, 165.4, 153.4, 137.3, 135.5, 134.3, 134.1, 134.0, 131.2, 128.6, 127.0, 126.9, 126.2, 115.9, 21.0, 19.4, 18.3; **IR** (neat, *v*_{max}, cm⁻¹) 3337, 1640, 1607, 1506, 1434, 1289, 1167; **LCMS** (LCQ) *R*_t = 4.1 min (method 1), *m/z* (ESI⁺) 323.1 [M+H]⁺; **HRMS (ESI)**: calcd. for C₁₉H₁₆F₃N₂OS [M+H]⁺ 377.0930, found 377.0932. Not enough material for HRMS determination.

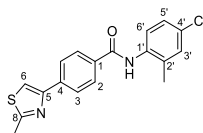
Methyl 3-methyl-4-((4-(2-methylthiazol-4-yl)benzoyl)amino)benzoate (**123**)



Compound **123** was synthesised according to general procedure O, using the following reagents: 4-(2-methylthiazol-4-yl)benzoic acid (80 mg, 0.36 mmol), methyl 4-amino-3-methyl-benzoate (151 mg, 0.91 mmol), phosphorus trichloride (31 μL, 0.36 mmol), tetrahydrofuran (3 mL) and acetonitrile (2 mL). The crude was purified by column chromatography (silica 12 g, 0 to 50% ethyl acetate in petroleum ether) to yield the desired amide **123** as a white solid (42 mg, 30%).

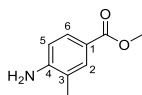
R_f 0.53 (petroleum ether:ethyl acetate 1:1); **m.p.** 191–193 °C; **¹H-NMR** (500 MHz, DMSO-*d*₆) δ 10.01 (s, 1H), 8.13 (s, 1H), 8.10 (d, *J* 8.3, 2H), 8.05 (d, *J* 8.4, 2H), 7.89 (d, *J* 2.0, 1H), 7.83 (dd, *J* 8.4, 2.1, 1H), 7.63 (d, *J* 8.3, 1H), 3.86 (s, 3H), 2.75 (s, 3H), 2.34 (s, 3H); **IR** (neat, *v*_{max}, cm⁻¹) 2923, 1716, 1646, 1607, 1587, 1520, 1437, 1318, 1273, 1170; **LCMS** (LCQ) *R*_t = 0.7 min (method 1), *m/z* (ESI⁺) 367.1 [M+H]⁺; **HRMS (ESI)**: calcd. for C₂₀H₁₈N₂NaO₃S [M+Na]⁺ 389.0930, found 389.0921.

N-(4-chloro-2-methyl-phenyl)-4-(2-methylthiazol-4-yl)benzamide (**124**)



Compound **124** was synthesised according to general procedure M, using the following reagents: 4-(2-methyl-1,3-thiazol-4-yl)benzoic acid (**102**) (80 mg, 0.36 mmol), oxalyl chloride (37 μL, 0.44 mmol), *N,N*-dimethylformamide (10 μL) and dichloromethane (3 mL) and stirred for 16 h. Followed by 3-chloro-2-methylaniline (52 μL, 0.44 mmol), *N,N*-diisopropylethylamine (397 μL, 2.28 mmol) and dichloromethane (1 mL) and stirred for 1 h. The crude was purified by column chromatography (silica 12 g, 0 to 25% ethyl acetate in petroleum ether) to yield the desired amide **124** as a white solid (22 mg, 17%).

R_f 0.29 (petroleum ether:ethyl acetate 3:1); **m.p.** 219–221 °C; **¹H-NMR** (500 MHz, DMSO-*d*₆) δ 9.94 (s, 1H), 8.12 (s, 1H), 8.09 (d, *J* 8.5, 2H), 8.04 (d, *J* 8.0, 2H), 7.42 – 7.36 (m, 2H), 7.28 (dd, *J* 8.4, 2.6, 1H), 2.74 (s, 3H), 2.25 (s, 3H); **¹³C-NMR** (126 MHz, DMSO-*d*₆) δ 166.5, 165.5, 153.3, 137.5, 136.6, 135.9, 133.7, 130.4, 130.3, 128.7, 128.6, 126.3, 126.2, 116.1, 19.4, 18.2; **IR** (neat, *v*_{max}, cm⁻¹) 3280, 1633, 1604, 1513, 1484, 1394, 1304, 1271; **LCMS** (LCQ) *R*_t = 4.4 min (method 1), *m/z* (ESI⁺) 343.2 [M+H]⁺; **HRMS (ESI)**: calcd. for C₁₈H₁₆ClN₂OS [M+H]⁺ 343.0666, found 343.0668.

Methyl 4-amino-3-methyl-benzoate (126)

Compound **126** was synthesised according to general procedure Q, using the following reagents: thionyl chloride (1.25 mL, 17.1 mmol), 4-amino-3-methylbenzoic acid (500 mg, 2.4 mmol), methanol (20 mL), to yield the intermediate **126** as a brown solid (493 mg, 85%) which was carried forward without further purification.

R_f 0.59 (petroleum ether:ethyl acetate 1:1); **¹H-NMR** (500 MHz, DMSO-*d*₆) δ 7.59 – 7.49 (m, 2H, H-2, H-6), 6.61 (d, *J* 8.3, 1H, H-5), 5.69 (s, 2H, NH₂), 3.73 (s, 3H, OCH₃), 2.07 (s, 3H, CH₃); **LCMS** (LCQ) *R_t* = 0.6 min (method 1), *m/z* (ESI⁺) 166.4 [M+H]⁺. ¹H-NMR consistent with literature data.³⁰³

4-Methoxy-1-methyl-2-nitro-benzene (127)

Iodomethane (183 μL, 2.94 mmol) and sodium hydroxide (117 mg, 2.94 mmol) were added to a solution of 4-methyl-3-nitrophenol (300 mg, 1.96 mmol) in dimethyl sulfoxide (2 mL) at *Rt*. The reaction mixture was stirred at ambient temperature for 16 h. Water (5 mL) was added to the reaction and the reaction mixture extracted with ethyl acetate (15 mL). The combined organic extracts were then washed with water (2 × 5 mL), brine (5 mL), dried over MgSO₄, filtered and concentrated under reduced pressure to yield the intermediate **127** as a yellow oil (309 mg, 90%) which was carried forward without further purification.

¹H-NMR (500 MHz, DMSO-*d*₆) δ 7.49 (d, *J* 2.6, 1H, H-3), 7.40 (d, *J* 8.5, 1H, H-6), 7.22 (dd, *J* 8.6, 2.6, 1H, H-5), 3.82 (s, 3H, OCH₃), 2.42 (s, 3H, CH₃); **LCMS** (LCQ) *R_t* = 3.8 min (method 1), no ionisation observed.

3-amino-4-methyl-phenol (128)

Zinc (854 mg, 13.1 mmol) was added to a solution of 4-methyl-3-nitrophenol (200 mg, 1.31 mmol) in methanol (13 mL) and acetic acid (6 mL) at 0 °C. The reaction mixture was stirred at 50 °C for 1 h. Upon cooling, the reaction mixture was filtered through Celite and the filtrate was concentrated under reduced pressure. The crude was taken up in water (10 mL) and alkalisied with ammonia solution to a pH of neutral. The aqueous layer was extracted with ethyl acetate (3 × 10 mL). The combined organic components were washed with water (10 mL) and brine (10 mL), dried over MgSO₄, filtered and concentrated under reduced pressure to yield the desired intermediate **128** as a light grey solid (153 mg, 90%).

¹H-NMR (500 MHz, DMSO-*d*₆) δ 8.58 (s, 1H, OH), 6.65 (d, *J* 8.0, 1H, H-6), 6.05 (d, *J* 2.4, 1H, H-3), 5.89 (dd, *J* 8.0, 2.4, 1H, H-4), 4.61 (s, 2H, NH₂), 1.92 (s, 3H, CH₃); **LCMS** (LCQ) *R_t* = 0.6 min (method 1), no ionisation observed.

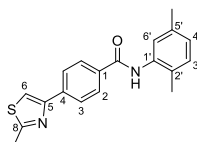
5-Methoxy-2-methyl-aniline (129)

Zinc (1.21 g, 18.5 mmol) was added to a solution of 4-methoxy-1-methyl-2-nitro-benzene (**127**) (309 mg, 1.85 mmol) in methanol (4 mL) and acetic acid (4 mL) at 0 °C. The reaction mixture was stirred at 50 °C for 1 h. Upon cooling, the reaction mixture was filtered through Celite and the filtrate was concentrated under reduced pressure. The crude

was taken up in water (10 mL) and alkalisied with ammonia solution to a pH of neutral. The aqueous layer was extracted with ethyl acetate (3 × 10 mL). The combined organic components were washed with water (10 mL) and brine (10 mL), dried over MgSO₄, filtered and concentrated under reduced pressure to yield the desired intermediate **129** as a yellow oil (200 mg, 75%) which crystallised overnight to a brown solid.

¹H-NMR (500 MHz, DMSO-*d*₆) δ 6.78 (d, *J* 8.2, 1H, H-6), 6.20 (d, *J* 2.5, 1H, H-3), 6.04 (dd, *J* 8.2, 2.6, 1H, H-4), 4.77 (s, 2H, NH₂), 3.62 (s, 3H, OCH₃), 1.96 (s, 3H, CH₃); **LCMS** (LCQ) Rt = 1.1 min (method 1), no ionisation observed.

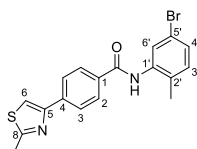
***N*-(2,5-dimethylphenyl)-4-(2-methylthiazol-4-yl)benzamide (130)**



Compound **130** was synthesised according to general procedure M, using the following reagents: 4-(2-methyl-1,3-thiazol-4-yl)benzoic acid (**102**) (80 mg, 0.36 mmol), oxalyl chloride (37 µL, 0.44 mmol), *N,N*-dimethylformamide (10 µL) and dichloromethane (3 mL) and stirred for 16 h. Followed by 2,5-dimethylaniline (55 µL, 0.44 mmol), *N,N*-diisopropylethylamine (397 µL, 2.28 mmol) and dichloromethane (1 mL) and stirred for 2 h. The crude was purified by column chromatography (silica 12 g, 0 to 25% ethyl acetate in petroleum ether) to yield the desired amide **130** as a white solid (41 mg, 40%).

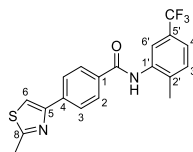
R_f 0.25 (petroleum ether:ethyl acetate 3:1); **m.p.** 182–184 °C; **¹H-NMR** (500 MHz, DMSO-*d*₆) δ 9.83 (s, 1H), 8.11 (s, 1H), 8.08 (d, *J* 8.5, 2H), 8.04 (d, *J* 8.0, 2H), 7.18 – 7.12 (m, 2H), 6.99 (d, *J* 7.6, 1H), 2.75 (s, 3H), 2.29 (s, 3H), 2.20 (s, 3H); **¹³C-NMR** (126 MHz, DMSO-*d*₆) δ 166.4, 165.3, 153.4, 137.3, 136.7, 135.5, 134.1, 131.0, 130.6, 128.6, 127.6, 127.1, 126.2, 115.9, 20.9, 19.4, 17.9; **IR** (neat, ν_{max}, cm⁻¹) 3327, 2918, 1640, 1607, 1531, 1459, 1412, 1289, 1167; **LCMS** (LCQ) Rt = 3.8 min (method 1), *m/z* (ESI⁺) 323.1 [M+H]⁺; **HRMS (ESI)**: calcd. for C₁₉H₁₉N₂OS [M+H]⁺ 323.1213, found 323.1215.

***N*-(5-bromo-2-methyl-phenyl)-4-(2-methylthiazol-4-yl)benzamide (131)**



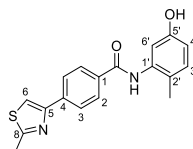
Compound **131** was synthesised according to general procedure M, using the following reagents: 4-(2-methyl-1,3-thiazol-4-yl)benzoic acid (**102**) (100 mg, 0.46 mmol), oxalyl chloride (46 µL, 0.55 mmol), *N,N*-dimethylformamide (10 µL) and dichloromethane (3 mL) and stirred for 16 h. Followed by 5-Bromo-2-methylaniline (101 mg, 0.55 mmol), *N,N*-diisopropylethylamine (397 µL, 2.28 mmol) and dichloromethane (1 mL) and stirred for 16 h. The crude was purified by column chromatography (silica 12 g, 0 to 25% ethyl acetate in petroleum ether) to yield the desired amide **131** as a white solid (48 mg, 26%).

R_f 0.72 (petroleum ether:ethyl acetate 1:1); **m.p.** 202–204 °C; **¹H-NMR** (500 MHz, DMSO-*d*₆) δ 9.97 (s, 1H), 8.15 – 8.07 (m, 3H), 8.04 (d, *J* 8.0, 2H), 7.62 (s, 1H), 7.36 (d, *J* 8.2, 1H), 7.25 (d, *J* 8.2, 1H), 2.75 (s, 3H), 2.23 (s, 3H); **¹³C-NMR** (126 MHz, DMSO-*d*₆) δ 166.4, 165.5, 153.3, 138.6, 137.6, 133.6, 133.3, 132.6, 129.2, 128.9, 128.7, 126.2, 118.3, 116.1, 19.4, 17.9; **IR** (neat, ν_{max}, cm⁻¹) 3293, 1637, 1536, 1498, 1329, 1291, 1169; **LCMS** (LCQ) Rt = 4.6 min (method 1), *m/z* (ESI⁺) 387.0 [M+H]⁺; **HRMS (ESI)**: calcd. for C₁₈H₁₅BrN₂NaOS [M+Na]⁺ 408.9981, found 408.9975.

4-(2-Methylthiazol-4-yl)-N-(2-methyl-5-(trifluoromethyl)phenyl)benzamide (132)

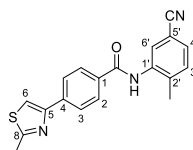
Compound **132** was synthesised according to general procedure M, using the following reagents: 4-(2-methyl-1,3-thiazol-4-yl)benzoic acid (**102**) (100 mg, 0.46 mmol), oxalyl chloride (46 μ L, 0.55 mmol), *N,N*-dimethylformamide (10 μ L) and dichloromethane (3 mL) and stirred for 16 h. Followed 2-methyl-5-(trifluoromethyl)aniline (160 mg, 0.46 mmol), *N,N*-diisopropylethylamine (397 μ L, 2.28 mmol) and dichloromethane (1 mL) and stirred for 16 h. The crude was purified by column chromatography (silica 12 g, 0 to 25% ethyl acetate in petroleum ether) to yield the desired amide **132** as a white solid (45 mg, 25%).

R_f 0.25 (petroleum ether:ethyl acetate 3:1); **m.p.** 163–165 °C; **¹H-NMR** (500 MHz, DMSO-*d*₆) δ 10.08 (s, 1H), 8.14 – 8.08 (m, 3H), 8.06 (d, *J* 7.5, 2H), 7.78 (s, 1H), 7.53 (s, 2H), 2.75 (s, 3H), 2.35 (s, 3H); **IR** (neat, ν_{max} , cm⁻¹) 3229, 1638, 1535, 1490, 1329, 1163; **LCMS** (LCQ) *R_t* = 4.8 min (method 1), *m/z* (ESI⁺) 377.1 [M+H]⁺; **HRMS (ESI)**: calcd. for C₁₉H₁₅F₃N₂NaOS [M+Na]⁺ 399.0749, found 399.0749.

N-(5-hydroxy-2-methyl-phenyl)-4-(2-methylthiazol-4-yl)benzamide (133)

Compound **133** was synthesised according to general procedure M, using the following reagents: 4-(2-methyl-1,3-thiazol-4-yl)benzoic acid (**102**) (80 mg, 0.36 mmol), oxalyl chloride (37 μ L, 0.44 mmol), *N,N*-dimethylformamide (10 μ L) and dichloromethane (3 mL) and stirred for 16 h. Followed by 3-amino-4-methylphenol (54 mg, 0.44 mmol), *N,N*-diisopropylethylamine (397 μ L, 2.28 mmol) and dichloromethane (1 mL) and stirred for 1.5 h. The crude was purified by column chromatography (silica 12 g, 0 to 40% ethyl acetate in petroleum ether) and further purified by column chromatography (amino silica 12 g, 0 to 40% ethyl acetate in petroleum ether) to yield the desired amide **133** as a white solid (44 mg, 35%).

R_f 0.27 (petroleum ether:ethyl acetate 3:1); **m.p.** 210–212 °C; **¹H-NMR** (500 MHz, DMSO-*d*₆) δ 9.73 (s, 1H), 9.22 (s, 1H), 8.10 (s, 1H), 8.07 (d, *J* 8.2, 2H), 8.02 (d, *J* 8.3, 2H), 7.03 (d, *J* 8.3, 1H), 6.84 (s, 1H), 6.58 (dd, *J* 8.1, 2.0, 1H), 2.74 (s, 3H), 2.13 (s, 3H); **¹³C-NMR** (126 MHz, DMSO-*d*₆) δ 166.4, 165.2, 155.8, 153.4, 137.4, 137.3, 134.1, 131.1, 128.6, 126.2, 123.8, 115.9, 113.8, 113.5, 19.4, 17.5; **IR** (neat, ν_{max} , cm⁻¹) 3186, 1658, 1600, 1546, 1445, 1268, 1235, 1174; **LCMS** (LCQ) *R_t* = 2.7 min (method 1), *m/z* (ESI⁺) 325.1 [M+H]⁺; **HRMS (ESI)**: calcd. for C₁₈H₁₆N₂NaO₂S [M+Na]⁺ 347.0825, found 347.0828.

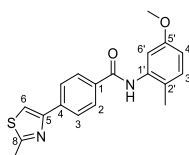
N-(5-cyano-2-methyl-phenyl)-4-(2-methylthiazol-4-yl)benzamide (134)

Compound **134** was synthesised according to general procedure M, using the following reagents: 4-(2-methyl-1,3-thiazol-4-yl)benzoic acid (**102**) (100 mg, 0.46 mmol), oxalyl chloride (46 μ L, 0.55 mmol), *N,N*-dimethylformamide (10 μ L) and dichloromethane (3 mL) and stirred for 16 h. Followed 3-amino-*p*-tolunitrile (72 mg, 0.55 mmol), *N,N*-diisopropylethylamine (397 μ L, 2.28 mmol) and dichloromethane (1 mL) and stirred for 16 h. The crude was purified

by column chromatography (silica 12 g, 0 to 25% ethyl acetate in petroleum ether) to yield the desired amide **134** as a white solid (38 mg, 24%).

R_f 0.11 (petroleum ether:ethyl acetate 3:1); **m.p.** 204–206 °C; **¹H-NMR** (500 MHz, DMSO-*d*₆) δ 10.07 (s, 1H, 3'-NH), 8.20–8.07 (m, 3H, 1+3-CH + 11-CH), 8.04 (d, *J* 8.1, 2H, 4+6-CH), 7.86 (s, 1H, 9'-CH), 7.63 (d, *J* 7.7, 1H, 7'-CH), 7.50 (d, *J* 8.0, 1H, 6'-CH), 2.74 (s, 3H, 12-CH₃), 2.34 (s, 3H, 10'-CH₃); **¹³C-NMR** (126 MHz, DMSO-*d*₆) δ 166.4, 165.6, 153.3, 140.4, 137., 137.7, 133.5, 132.2, 130.1, 129.8, 128.8, 126.3, 116.2, 109.3, 19.4, 18.7; **IR** (neat, *v*_{max}, cm⁻¹) 2924, 1732, 1673, 1610, 1519, 1418, 1286, 1033; **LCMS** (LCQ) *R*_t = 0.7 min (method 1), *m/z* (ESI⁺) 334.2 [M+H]⁺; **HRMS (ESI)**: calcd. for C₁₉H₁₅N₃OS [M+Na]⁺ 356.0828, found 356.0817.

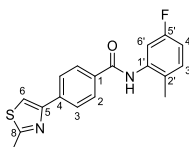
***N*-(5-methoxy-2-methyl-phenyl)-4-(2-methylthiazol-4-yl)benzamide (135)**



Compound **135** was synthesised according to general procedure M, using the following reagents: 4-(2-methyl-1,3-thiazol-4-yl)benzoic acid (**102**) (80 mg, 0.36 mmol), oxalyl chloride (37 μL, 0.44 mmol), *N,N*-dimethylformamide (10 μL) and dichloromethane (3 mL) and stirred for 16 h. Followed by 5-methoxy-2-methyl-aniline (60 mg, 0.44 mmol), *N,N*-diisopropylethylamine (397 μL, 2.28 mmol) and dichloromethane (1 mL) and stirred for 2 h. The crude was purified by column chromatography (silica 12 g, 0 to 30% ethyl acetate in petroleum ether) to yield the desired amide **135** as a white solid (60 mg, 46%).

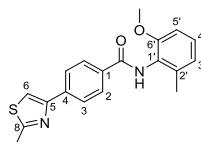
R_f 0.37 (petroleum ether:ethyl acetate 3:1); **m.p.** 173–175 °C; **¹H-NMR** (500 MHz, DMSO-*d*₆) δ 8.11 (s, 1H), 8.08 (d, *J* 8.0, 2H), 8.04 (d, *J* 8.0, 2), 7.17 (d, *J* 8.2, 1H), 6.98 (s, 1H), 6.77 (d, *J* 7.3, 1H), 3.74 (s, 3H), 2.74 (s, 3H), 2.17 (s, 3H); **¹³C-NMR** (126 MHz, DMSO-*d*₆) δ 166.4, 165.3, 157.9, 153.1, 137.6, 137.4, 134.0, 131.2, 128.7, 126.2, 125.8, 116.0, 112.1, 112.1, 55.6, 19.4, 17.5; **IR** (neat, *v*_{max}, cm⁻¹) 3272, 2911, 1680, 1651, 1586, 1524, 1452, 1275, 1253, 1159; **LCMS** (LCQ) *R*_t = 4.0 min (method 1), *m/z* (ESI⁺) 339.1 [M+H]⁺; **HRMS (ESI)**: calcd. for C₁₉H₁₈N₂NaOS [M+Na]⁺ 361.0981, found 361.0982.

***N*-(5-fluoro-2-methyl-phenyl)-4-(2-methylthiazol-4-yl)benzamide (136)**



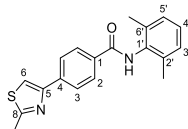
Compound **136** was synthesised according to general procedure M, using the following reagents: 4-(2-methyl-1,3-thiazol-4-yl)benzoic acid (**102**) (100 mg, 0.46 mmol), oxalyl chloride (46 μL, 0.55 mmol), *N,N*-dimethylformamide (10 μL) and dichloromethane (3 mL) and stirred for 16 h. Followed by 5-fluoro-2-methylaniline (68 mg, 0.55 mmol), *N,N*-diisopropylethylamine (397 μL, 2.28 mmol) and dichloromethane (1 mL) and stirred for 2 h. The crude was purified by column chromatography (silica 12 g, 0 to 25% ethyl acetate in petroleum ether) and further purified by column chromatography (amino silica 12 g, 0 to 40% ethyl acetate in petroleum ether) to yield the desired amide **136** as a white solid (16 mg, 10%).

R_f 0.44 (petroleum ether:ethyl acetate 3:1); **m.p.** 193–195 °C; **¹H-NMR** (500 MHz, DMSO-*d*₆) δ 9.92 (s, 1H), 8.16–8.07 (m, 3H), 8.04 (d, *J* 7.5, 2H), 7.35–7.24 (m, 2H), 7.01 (s, 1H), 2.74 (s, 3H), 2.24 (s, 3H); **IR** (neat, *v*_{max}, cm⁻¹) 3099, 1650, 1600, 1520, 1452, 1416, 1253, 1170; **LCMS** (LCQ) *R*_t = 4.1 min (method 1), *m/z* (ESI⁺) 327.1 [M+H]⁺; **HRMS (ESI)**: calcd. for C₁₈H₁₃N₃NaOS [M+Na]⁺ 342.0672, found 342.0676. Not enough material for ¹³C-NMR.

***N*-(2-methoxy-6-methyl-phenyl)-4-(2-methylthiazol-4-yl)benzamide (137)**

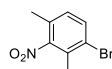
Compound **137** was synthesised according to general procedure M, using the following reagents: 4-(2-methyl-1,3-thiazol-4-yl)benzoic acid (**102**) (100 mg, 0.46 mmol), oxalyl chloride (46 μ L, 0.55 mmol), *N,N*-dimethylformamide (10 μ L) and dichloromethane (3 mL) and stirred for 16 h. Followed by 2-methoxy-6-methylaniline (75 mg, 0.55 mmol), *N,N*-diisopropylethylamine (397 μ L, 2.28 mmol) and dichloromethane (1 mL) and stirred for 16 h. The crude was purified by column chromatography (silica 12 g, 0 to 40% ethyl acetate in petroleum ether) to yield the desired amide **137** as a white solid (32 mg, 20%).

R_f 0.09 (petroleum ether:ethyl acetate 1:1); **m.p.** 176–178 °C; **¹H-NMR** (500 MHz, DMSO-*d*₆) δ 9.58 (s, 1H), 8.22 – 7.87 (m, 5H), 7.19 (t, J 8.1, 1H), 6.95 – 6.81 (m, 2H), 3.75 (s, 3H), 2.74 (s, 3H), 2.17 (s, 3H); **¹³C-NMR** (126 MHz, DMSO-*d*₆) δ 166.3, 165.1, 155.7, 153.4, 137.4, 137.2, 133.9, 128.6, 127.7, 126.2, 125.7, 122.4, 115.9, 109.7, 56.1, 19.4, 18.3; **IR** (neat, ν_{max} , cm⁻¹) 3265, 1647, 1603, 1506, 1462, 1427, 1289, 1267, 1173, 1090; **LCMS** (LCQ) *R_t* = 3.6 min (method 1), *m/z* (ESI⁺) 338.9 [M+H]⁺; **HRMS (ESI)**: calcd. for C₁₉H₁₈N₂NaO₂S [M+Na]⁺ 361.0981, found 361.0982.

***N*-(2,6-dimethylphenyl)-4-(2-methylthiazol-4-yl)benzamide (138)**

Compound **138** was synthesised according to general procedure M, using the following reagents: 4-(2-methyl-1,3-thiazol-4-yl)benzoic acid (**102**) (100 mg, 0.46 mmol), oxalyl chloride (46 μ L, 0.55 mmol), *N,N*-dimethylformamide (10 μ L) and dichloromethane (3 mL) and stirred for 16 h. Followed 2,6-dimethylaniline (67 μ L, 0.55 mmol), *N,N*-diisopropylethylamine (397 μ L, 2.28 mmol) and dichloromethane (1 mL) and stirred for 1.5 h. The crude was purified by column chromatography (silica 12 g, 0 to 25% ethyl acetate in petroleum ether) to yield the desired amide **138** as a white solid (18 mg, 28%).

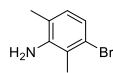
R_f 0.14 (petroleum ether:ethyl acetate 3:1); **m.p.** 194–196 °C; **¹H-NMR** (500 MHz, DMSO-*d*₆) δ 9.78 (s, 1H), 8.14 – 7.98 (m, 5H), 7.13 (m, 3H), 2.75 (s, 3H), 2.20 (s, 6H); **¹³C-NMR** (126 MHz, DMSO-*d*₆) δ 166.4, 165.1, 153.4, 137.3, 136.1, 135.8, 133.9, 128.5, 128.2, 127.1, 126.3, 115.9, 19.4, 18.5; **IR** (neat, ν_{max} , cm⁻¹) 3265, 1647, 1607, 1506, 1474, 1304, 1174; **LCMS** (LCQ) *R_t* = 3.8 min (method 1), *m/z* (ESI⁺) 323.1 [M+H]⁺; **HRMS (ESI)**: calcd. for C₁₉H₁₈N₂NaOS [M+Na]⁺ 345.1032, found 345.1032.

1-Bromo-2,4-dimethyl-3-nitro-benzene (139)

To 2,6-dimethylnitrobenzene (1.00 g, 6.62 mmol) in trifluoroacetic acid (7 mL) was added *N*-bromosuccinimide (2.35 g, 13.2 mmol) and the reaction mixture stirred at 65 °C for 16 h. The reaction mixture was concentrated under reduced pressure. The crude product was taken up in aq. saturated NaHCO₃ (20 mL) and extracted with ethyl acetate (3 \times 20 mL). The combined organic components were then washed with brine (10 mL), dried over MgSO₄, filtered and concentrated under reduced pressure. The crude product was purified by column chromatography (silica 30 g, 0 to 5% ethyl acetate in petroleum ether) to yield the desired compound **139** as a white solid (313 mg, 20%).

¹H-NMR (500 MHz, DMSO-*d*₆) δ 7.76 (d, *J* 8.3, 1H), 7.28 (d, *J* 8.3, 1H), 2.26 (s, 3H), 2.20 (s, 3H); **LCMS** (LCQ) Rt = 3.7 min (method 1), no ionisation observed.

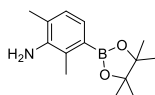
3-Bromo-2,6-dimethyl-aniline (**140**)



To 1-bromo-2,4-dimethyl-3-nitro-benzene (**139**) (900 mg, 3.91 mmol) in acetic acid (9 mL) was added iron (874 mg, 15.6 mmol) and the reaction mixture stirred at 80 °C for 16 h. The reaction mixture was concentrated under reduced pressure. The crude product was taken up in aq. saturated NaHCO₃ (30 mL) and extracted with ethyl acetate (3 × 30 mL). The combined organic components were then washed with brine (30 mL), dried over MgSO₄, filtered and concentrated under reduced pressure. The crude product was purified by column chromatography (silica 30 g, 0 to 10% ethyl acetate in petroleum ether) to yield the desired compound **140** as a yellow oil (640 mg, 78%).

¹H-NMR (500 MHz, DMSO-*d*₆) δ 6.73 (d, *J* 8.1, 1H), 6.69 (d, *J* 8.0, 1H), 4.88 (s, 2H), 2.18 (s, 3H), 2.03 (s, 3H); **LCMS** (LCQ) Rt = 3.8 min (method 1), *m/z* (ESI⁺) *m/z* (ESI⁺) 200.1 [M(⁷⁹Br)+H]⁺, 202.2 [M(⁸¹Br)+H]⁺.

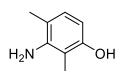
2,6-Dimethyl-3-(4,4,5,5-tetramethyl-1,3,2-dioxaborolan-2-yl)aniline (**141**)



Compound **141** was synthesised according to general procedure M, using the following reagents: 3-bromo-2,6-dimethyl-aniline (**140**) (540 mg, 2.70 mmol), bis(pinacolato)diboron (822 mg, 3.24 mmol), (1,1'-bis(diphenylphosphino)ferrocene)dichloropalladium(II) (143 mg, 0.18 mmol), potassium acetate (795 mg, 8.10 mmol) and 1,4-dioxane (7.5 mL) and stirred for 2 h. The crude was purified by column chromatography (silica 12 g, 0 to 10% ethyl acetate in petroleum ether) to yield the desired product **141** as a yellow solid (704 mg, 95%).

¹H-NMR (500 MHz, DMSO-*d*₆) δ 6.83 (d, *J* 7.4, 1H), 6.79 (d, *J* 7.4, 1H), 4.45 (s, 2H), 2.25 (s, 3H), 2.08 (s, 3H), 1.27 (s, 12H); **LCMS** (LCQ) Rt = 3.7 min (method 1), *m/z* (ESI⁺) 248.2 [M+H]⁺.

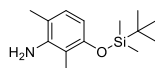
3-Amino-2,4-dimethyl-phenol (**142**)



To 2,6-dimethyl-3-(4,4,5,5-tetramethyl-1,3,2-dioxaborolan-2-yl)aniline (**141**) (400 mg, 1.62 mmol) in tetrahydrofuran (8 mL) and water (8 mL) was added sodium perborate monohydrate (565 mg, 5.66 mmol) and the reaction mixture stirred at ambient temperature for 16 h. The reaction mixture was concentrated under reduced pressure. The crude product was taken up in aq. saturated ammonium chloride (8 mL) and dichloromethane (20 mL) and stirred for 0.75 h. The mixture was passed through a hydrophobic frit and the organic components were purified by column chromatography (silica 12 g, 0 to 30% ethyl acetate in petroleum ether) to yield the desired compound **142** as a brown solid (167 mg, 71%).

¹H-NMR (500 MHz, DMSO-*d*₆) δ 8.65 (s, 1H), 6.54 (d, *J* 8.0, 1H), 6.01 (d, *J* 8.0, 1H), 4.35 (s, 2H), 1.95 (s, 3H), 1.88 (s, 3H); **LCMS** (LCQ) Rt = 1.0 min (method 1), no ionisation observed.

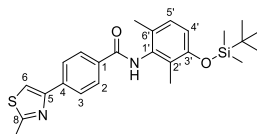
3-(*Tert*-butyl(dimethyl)silyl)oxy-2,6-dimethyl-aniline (**143**)



To 3-amino-2,4-dimethylphenol (**142**) (170 mg, 1.24 mmol), 4-(dimethylamino)pyridine (15 mg, 0.12 mmol) and triethylamine (518 μ L, 3.72 mmol) in dichloromethane was added *tert*-butyldimethylsilyl chloride (560 mg, 3.72 mmol). The reaction mixture was stirred at ambient temperature for 16 h. The reaction mixture was taken up in water (3 mL) and the components separated. The organic components were concentrated under reduced pressure. The crude was purified by column chromatography (silica 12 g, 0 to 5% ethyl acetate in petroleum ether) to yield the desired product **143** as a pale yellow oil (246 mg, 71%).

¹H-NMR (500 MHz, DMSO-*d*₆) δ 6.64 (d, *J* 7.9, 1H), 6.01 (d, *J* 7.6, 1H), 4.49 (s, 2H), 1.99 (s, 3H), 1.93 (s, 3H), 0.96 (s, 9H), 0.13 (s, 6H).

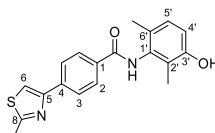
***N*-(3-(*tert*-butyl(dimethyl)silyl)oxy-2,6-dimethyl-phenyl)-4-(2-methylthiazol-4-yl)benzamide (**144**)**



Compound **144** was synthesised according to general procedure M, using the following reagents: : 4-(2-methyl-1,3-thiazol-4-yl)benzoic acid (**102**) (100 mg, 0.45 mmol), oxalyl chloride (96 μ L, 1.14 mmol), *N,N*-dimethylformamide (10 μ L) and dichloromethane (3 mL) and stirred for 16 h. Followed 3-(*tert*-butyl(dimethyl)silyl)oxy-2,6-dimethyl-aniline (171 mg, 0.68 mmol), triethylamine (190 μ L, 1.36 mmol), 4-(dimethylamino)pyridine (5.6 mg, 0.05 mmol) and dichloromethane (1 mL) and stirred for 16 h. The crude was purified by column chromatography (silica 12 g, 0 to 3% methanol in dichloromethane) to yield the desired amide **144** as a white solid (80 mg, 35%).

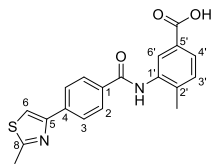
¹H-NMR (500 MHz, DMSO-*d*₆) δ 9.82 (s, 1H), 8.12 (s, 1H), 8.09 (d, *J* 8.4 Hz, 2H), 8.05 (d, *J* 8.3 Hz, 2H), 7.00 (d, *J* 8.3 Hz, 1H), 6.73 (d, *J* 8.3 Hz, 1H), 2.74 (s, 3H), 2.11 (s, 3H), 2.03 (s, 3H), 0.99 (s, 9H), 0.21 (s, 6H); **LCMS** (LCQ) *R*_t = 6.1 min (method 1), *m/z* (ESI⁺) 453.1 [M+H]⁺.

***N*-(3-hydroxy-2,6-dimethyl-phenyl)-4-(2-methylthiazol-4-yl)benzamide (**145**)**



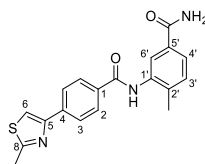
N-(3-(*tert*-butyl(dimethyl)silyl)oxy-2,6-dimethyl-phenyl)-4-(2-methylthiazol-4-yl)benzamide (**144**) (70 mg, 0.31 mmol) in tetrahydrofuran (2 mL) and was cooled to 0 °C and to the reaction mixture was added tetrabutylammonium fluoride (309 μ L, 0.31 mmol). The reaction mixture was stirred at 0 °C for 5 min and at ambient temperature for 10 min. The reaction mixture was concentrated under reduced pressure. The crude was purified by column chromatography (silica 12 g, 0 to 5% methanol in dichloromethane) to yield the desired amide **145** as a colourless solid (39 mg, 71%).

R_f 0.49 (petroleum ether:ethyl acetate 1:1); **m.p.** 245–247 °C; **¹H-NMR** (500 MHz, DMSO-*d*₆) δ 9.75 (s, 1H, CONH), 9.20 (s, 1H, OH), 8.13 – 8.11 (s, 1H, H-6), 8.08 (d, *J* 8.4, 2H, H-3), 8.05 (d, *J* 8.4, 2H, H-2), 6.90 (d, *J* 8.2, 1H, H-5'), 6.70 (d, *J* 8.2, 1H, H-4'), 2.74 (s, 3H, 8-CH₃), 2.07 (s, 3H, 2'-CH₃), 1.99 (s, 3H, 6'-CH₃); **¹³C-NMR** (126 MHz, DMSO-*d*₆) δ 166.4 (CO), 165.0 (C-8), 154.1 (ArC), 153.3 (ArC), 137.2 (ArC), 136.4 (ArC), 133.9 (ArC), 128.5 (C-2), 127.3 (C-5'), 126.2 (C-3), 126.0 (ArC), 122.7 (ArC), 115.9 (C-6), 113.6 (C-4'), 19.4 (8-CH₃), 18.0 (2'-CH₃), 11.6 (6'-CH₃); **IR** (neat, ν_{max} , cm⁻¹) 3203, 1644, 1595, 1493, 1448, 1434, 1418, 1326, 1295; **LCMS** (LCQ) *R*_t = 0.6 min (method 1), *m/z* (ESI⁺) 339.0 [M+H]⁺; **HRMS** (ESI): calcd. for C₁₉H₁₉N₂O₂S [M+H]⁺ 339.1162, found 339.1172.

4-Methyl-3-((4-(2-methylthiazol-4-yl)benzoyl)amino)benzoic acid (146)

To methyl 4-methyl-3-((4-(2-methylthiazol-4-yl)benzoyl)amino)benzoate (920 mg, 2.51 mmol) (**105**) in methanol (24 mL) was added 2 M aq. sodium hydroxide (12.6 mL, 25.1 mmol) and the mixture stirred at an ambient temperature for 16 h. The reaction mixture was then heated for 2 h at 50 °C. The solvent was removed under reduced pressure. The crude was taken up in water and the mixture was acidified to a pH of 2–3 with 2 M aq. hydrochloric acid solution. The resulting precipitate was collected by vacuum filtration and dried under reduced pressure to afford the desired acid **146** as a white solid (926 mg, 99%).

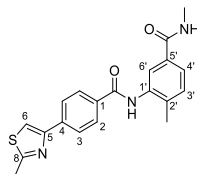
m.p. 254–256 °C; **¹H-NMR** (500 MHz, DMSO-*d*₆) δ 12.85 (s, 1H, COOH), 10.04 (s, 1H, CONH), 8.13 – 8.07 (m, 3H, H-3, H-6), 8.06 (d, *J* 8.3, 2H, H-2), 7.95 (d, *J* 1.7, 1H, H-6'), 7.74 (dd, *J* 7.9, 1.7, 1H, H-4'), 7.40 (d, *J* 7.9, 1H, H-3'), 2.74 (s, 3H, 8-CH₃), 2.32 (s, 3H, 2'-CH₃); **¹³C-NMR** (126 MHz, DMSO-*d*₆) δ 167.4 (COOH), 166.4 (CONH), 165.6 (C-8), 153.3 (C-5), 139.5 (C-2'), 137.5 (C-1), 137.1 (C-1'), 133.8 (C-4), 131.1 (C-3'), 129.3 (C-5'), 128.7 (C-2), 127.8 (C-6'), 127.2 (C-4'), 126.3 (C-3), 116.01 (C-6), 19.4 (8-CH₃), 18.59 (2'-CH₃); **IR** (neat, *v*_{max}, cm⁻¹) 2923, 1679, 1638, 1512, 1492, 1414, 1390, 1251, 1178; **LCMS** (LCQ) Rt = 3.0 min (method 1), *m/z* (ESI⁺) 353.0 [M+H]⁺; **HRMS (ESI)**: calcd. for C₁₉H₁₆N₂NaO₃S [M+Na]⁺ 375.0774, found 375.0774.

4-Methyl-3-((4-(2-methylthiazol-4-yl)benzoyl)amino)benzamide (147)

Procedure 1: Compound **147** was synthesised according to general procedure P, using the following reagents: 4-methyl-3-((4-(2-methylthiazol-4-yl)benzoyl)amino)benzoic acid (**146**) (100 mg, 0.28 mmol), EDCI (68 mg, 0.35 mmol), HOBT (54 mg, 0.35 mmol), *N,N*-diisopropylethylamine (100 μL, 0.57 mmol), 2 M ammonia in methanol (0.43 mL, 0.85 mmol), and *N,N*-dimethylformamide (1 mL). The crude was purified by column chromatography (amino silica 12 g, 0 to 5% methanol in dichloromethane) to yield the desired primary amide **147** as a white solid (39 mg, 37%).

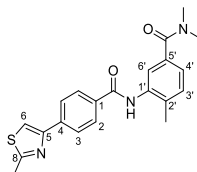
Procedure 2: Compound **147** was synthesised according to general procedure M, using the following reagents: 4-(2-methyl-1,3-thiazol-4-yl)benzoic acid (**102**) (90 mg, 0.41 mmol), oxalyl chloride (42 μL, 0.49 mmol), *N,N*-dimethylformamide (10 μL) and dichloromethane (3 mL) and stirred for 16 h. Followed by 3-amino-4-methylbenzamide (74 mg, 0.49 mmol), *N,N*-diisopropylethylamine (357 μL, 2.05 mmol) and dichloromethane (1 mL) and stirred for 16 h. The precipitation formed during the work up was collected by vacuum filtration and dried under reduced pressure to yield the desired amide **147** as a white solid (28 mg, 18%).

R_f 0.17 (dichloromethane:methanol 19:1); **m.p.** 215–217 °C; **¹H-NMR** (500 MHz, DMSO-*d*₆) δ 10.02 (s, 1H, CONH), 8.14 – 8.08 (m, 3H, H-3, H-6), 8.05 (d, *J* 8.5, 2H, H-2), 7.91 (s, 1H, 5'-CONH_{AB}), 7.86 (d, *J* 1.8, 1H, H-6'), 7.70 (dd, *J* 7.9, 1.8, 1H, H-4'), 7.35 (d, *J* 7.9, 1H, H-3'), 7.27 (s, 1H, 5'-CONH_{AB}), 2.74 (s, 3H, 8-CH₃), 2.28 (s, 3H, 2'-CH₃); **¹³C-NMR** (126 MHz, DMSO-*d*₆) δ 167.9 (CO), 166.4 (CO), 165.5 (C-8), 153.3 (C-5), 138.0 (C-2'), 137.5 (C-1), 136.8 (C-1'), 133.8 (C-4), 132.8 (C-5'), 130.6 (C-3'), 128.7 (C-2), 126.6 (C-6'), 126.3 (C-3), 125.6 (C-4), 116.0 (C-6), 19.4 (8-CH₃), 18.37 (2'-CH₃); **IR** (neat, *v*_{max}, cm⁻¹) 3108, 1713, 1668, 1608, 1571, 1501, 1436, 1410, 1278; **LCMS** (LCQ) Rt = 1.7 min (method 1), *m/z* (ESI⁺) 352.0 [M+H]⁺; **HRMS (ESI)**: calcd. for C₁₉H₁₇N₃NaO₂S [M+Na]⁺ 374.0934, found 374.0933.

***N,N*,4-dimethyl-3-((4-(2-methylthiazol-4-yl)benzoyl)amino)benzamide (148)**

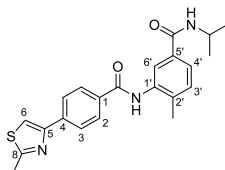
Compound **148** was synthesised according to general procedure P, using the following reagents: 4-methyl-3-((4-(2-methylthiazol-4-yl)benzoyl)amino)benzoic acid (**146**) (100 mg, 0.28 mmol), EDCI (68 mg, 0.35 mmol), HOBt (54 mg, 0.35 mmol), *N,N*-diisopropylethylamine (100 μ L, 0.57 mmol), 2 M methylamine in tetrahydrofuran (30 μ L, 0.85 mmol), and *N,N*-dimethylformamide (1 mL). The crude was purified by column chromatography (amino silica 12 g, 0 to 4% methanol in dichloromethane) to yield the desired amide **148** as a white solid (11 mg, 10%).

R_f 0.49 (dichloromethane:methanol 19:1); **m.p.** 228–230 °C; **¹H-NMR** (500 MHz, DMSO-*d*₆) δ 10.01 (s, 1H, 1-CONH), 8.37 (s, 1H, CONHCH₃), 8.16–7.98 (m, 5H, H-3, H-2, H-6), 7.83 (s, 1H, H-6'), 7.65 (d, *J* 7.9, 1H, H-4'), 7.35 (d, *J* 8.1, 1H, H-3'), 2.77 (s, 3H, CONHCH₃), 2.74 (s, 3H, 8-CH₃), 2.28 (s, 3H, 2'-CH₃); **¹³C-NMR** (126 MHz, DMSO-*d*₆) δ 166.5 (CO), 166.4 (CO), 165.5 (C-8), 153.4 (C-5), 137.6 (C-2'), 137.5 (C-1), 136.9 (C-1'), 133.8 (C-4), 133.0 (C-5'), 130.6 (C-3'), 128.7 (C-2), 126.3 (C-3), 126.1 (C-6'), 125.0 (C-4'), 116.0 (C-6), 26.7 (NCH₃), 19.4 (8-CH₃), 18.4 (2'-CH₃); **LCMS** (LCQ) *R_t* = 2.5 min (method 1), *m/z* (ESI⁺) 366.0 [M+H]⁺; **HRMS (ESI)**: calcd. for C₂₀H₁₉N₃NaO₂S [M+Na]⁺ 388.1090, found 388.1104. Not enough material for IR determination.

***N,N*,4-trimethyl-3-((4-(2-methylthiazol-4-yl)benzoyl)amino)benzamide (149)**

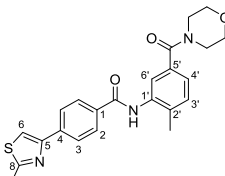
Compound **149** was synthesised according to general procedure P, using the following reagents: 4-methyl-3-((4-(2-methylthiazol-4-yl)benzoyl)amino)benzoic acid (**146**) (100 mg, 0.28 mmol), EDCI (68 mg, 0.35 mmol), HOBt (54 mg, 0.35 mmol), *N,N*-diisopropylethylamine (100 μ L, 0.57 mmol), 2 M dimethylamine in tetrahydrofuran (35 μ L, 0.85 mmol), and *N,N*-dimethylformamide (1 mL). The crude was purified by column chromatography (amino silica 12 g, 0 to 100% ethyl acetate in petroleum ether), followed by crystallisation in ether to yield the desired amide **149** as a white solid (9 mg, 8%).

R_f 0.45 (dichloromethane:methanol 19:1); **m.p.** 218–219 °C; **¹H-NMR** (500 MHz, DMSO-*d*₆) δ 9.96 (s, 1H, CONH), 8.20–8.07 (m, 3H, H-3, H-11), 8.04 (d, *J* 8.2, 2H, H-2), 7.42 (s, 1H, H-6'), 7.33 (d, *J* 7.7, 1H, H-3'), 7.21 (d, *J* 7.8, 1H, H-4'), 2.97 (s, 6H, N(CH₃)₂), 2.74 (s, 3H, 8-CH₃), 2.28 (s, 3H, 2'-CH₃); **¹³C-NMR** (126 MHz, DMSO-*d*₆) δ 170.1 (CO), 166.4 (CO), 165.5 (C-8), 153.3 (C-5), 137.5 (C-1), 136.7 (C-2'), 135.4 (C-1'), 134.6 (C-5'), 133.9 (C-4), 130.7 (C-3'), 128.7 (C-2), 126.3 (C-3), 125.6 (C-6'), 125.0 (C-4'), 116.1 (C-6), 19.4 (8-CH₃), 18.3 (2'-CH₃). N(CH₃)₂ under DMSO peak; **IR** (neat, ν_{\max} , cm⁻¹) 2922, 1664, 1607, 1571, 1537, 1497, 1395, 1290, 1171; **LCMS** (LCQ) *R_t* = 2.9 min (method 1), *m/z* (ESI⁺) 380.0 [M+H]⁺; **HRMS (ESI)**: calcd. for C₂₁H₂₁N₃NaO₂S [M+Na]⁺ 402.1247, found 402.1248.

***N*-isopropyl-4-methyl-3-((4-(2-methylthiazol-4-yl)benzoyl)amino)benzamide (150)**

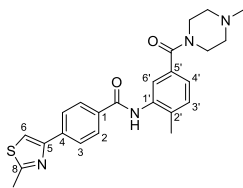
Compound **150** was synthesised according to general procedure S, using the following reagents: 4-methyl-3-((4-(2-methylthiazol-4-yl)benzoyl)amino)benzoic acid (**146**) (100 mg, 0.28 mmol), T3P (95 μ L, 0.34 mmol), triethylamine (119 μ L, 0.85 mmol), isopropylamine (146 μ L, 0.57 mmol), and *N,N*-dimethylformamide (1 mL). The crude was purified by column chromatography (amino silica 12 g, 0 to 5% methanol in dichloromethane) followed by crystallisation in ether to yield the desired amide **150** as a white solid (55 mg, 47%).

R_f 0.28 (dichloromethane:methanol 19:1); **m.p.** 212–214 °C; **¹H-NMR** (500 MHz, DMSO-*d*₆) 10.03 (s, 1H), 8.17 (d, *J* 7.7, 1H), 8.13 – 8.02 (m, 5H), 7.84 (s, 1H), 7.68 (d, *J* 7.8, 1H), 7.35 (d, *J* 7.9, 1H), 4.10 (dt, *J* 13.5, 6.8, 1H), 2.74 (s, 3H), 2.28 (s, 3H), 1.16 (d, *J* 6.6, 6H); **¹³C-NMR** (126 MHz, DMSO-*d*₆) δ 166.5, 165.6, 165.3, 153.3, 137.7, 137.5, 136.7, 133.7, 133.3, 130.6, 128.7, 126.3, 126.3, 125.4, 116.0, 41.4, 22.8, 19.4, 18.4; **IR** (neat, ν_{\max} , cm⁻¹) 3259, 2981, 1619, 1568, 1533, 1491, 1456, 1310, 1171; **LCMS** (LCQ) *R*_t = 3.4 min (method 1), *m/z* (ESI⁺) 394.1 [M+H]⁺; **HRMS (ESI)**: calcd. for C₂₂H₂₃N₃NaO₂S [M+Na]⁺ 416.1403, found 416.1410.

***N*-(2-methyl-5-(morpholine-4-carbonyl)phenyl)-4-(2-methylthiazol-4-yl)benzamide (151)**

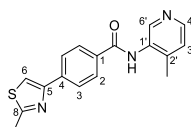
Compound **151** was synthesised according to general procedure S, using the following reagents: 4-methyl-3-((4-(2-methylthiazol-4-yl)benzoyl)amino)benzoic acid (**146**) (100 mg, 0.28 mmol), T3P (95 μ L, 0.34 mmol), triethylamine (119 μ L, 0.85 mmol), morpholine (56 μ L, 0.57 mmol), and *N,N*-dimethylformamide (1 mL). The crude was purified by column chromatography (amino silica 12 g, 0 to 10% methanol in dichloromethane) followed by crystallisation in ether to yield the desired amide **151** as a white solid (79 mg, 63%).

R_f 0.56 (dichloromethane:methanol 19:1); **m.p.** 185–187 °C; **¹H-NMR** (500 MHz, DMSO-*d*₆) 9.97 (s, 1H), 8.11 (s, 1H), 8.09 (d, *J* 8.3, 2H), 8.04 (d, *J* 8.2, 2H), 7.43 (s, 1H), 7.35 (d, *J* 7.8, 1H), 7.22 (d, *J* 7.8, 1H), 3.69 – 3.52 (m, 8H), 2.74 (s, 3H), 2.29 (s, 3H); **¹³C-NMR** (126 MHz, DMSO-*d*₆) δ 166.5, 165.6, 165.3, 153.3, 137.7, 137.5, 136.7, 133.7, 133.3, 130.6, 128.7, 126.3, 126.3, 125.4, 116.0, 41.4, 22.8, 19.4, 18.4. 1 \times C not visible; **IR** (neat, ν_{\max} , cm⁻¹) 2979, 1651, 1608, 1568, 1541, 1522, 1460, 1439, 1301, 1271, 1111; **LCMS** (LCQ) *R*_t = 2.8 min (method 1), *m/z* (ESI⁺) 422.0 [M+H]⁺; **HRMS (ESI)**: calcd. for C₂₃H₂₃N₃NaO₃S [M+Na]⁺ 444.1352, found 444.1351.

***N*-(2-methyl-5-(4-methylpiperazine-1-carbonyl)phenyl)-4-(2-methylthiazol-4-yl)benzamide (152)**

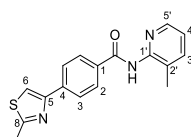
Compound **152** was synthesised according to general procedure S, using the following reagents: 4-methyl-3-((4-(2-methylthiazol-4-yl)benzoyl)amino)benzoic acid (**146**) (100 mg, 0.28 mmol), T3P (95 μ L, 0.34 mmol), triethylamine (119 μ L, 0.85 mmol), 1-methylpiperazine (63 μ L, 0.57 mmol), and *N,N*-dimethylformamide (1 mL). The crude was purified by column chromatography (amino silica 12 g, 0 to 10% methanol in dichloromethane) followed by crystallisation in ether to yield the desired amide **152** as a white solid (39 mg, 30%).

R_f 0.10 (dichloromethane:methanol 19:1); **m.p.** 156–160 °C; **¹H-NMR** (500 MHz, DMSO-*d*₆) 9.97 (s, 1H), 8.15 – 8.07 (m, 3H), 8.04 (d, *J* 8.2, 2H), 7.43 (s, 1H), 7.35 (d, *J* 7.8, 1H), 7.20 (d, *J* 7.8, 1H), 3.85 – 3.34 (m, 8H), 2.74 (s, 3H), 2.34 – 2.20 (m, 6H); **¹³C-NMR** (126 MHz, DMSO-*d*₆) δ 169.0, 166.4, 165.5, 153.3, 137.5, 136.8, 135.6, 133.9, 133.8, 130.9, 128.7, 126.3, 125.5, 124.9, 116.1, 65.3, 19.4, 18.3. 2 \times C not visible; **IR** (neat, ν_{max} , cm⁻¹) 2923, 1657, 1613, 1571, 1519, 1489, 1458, 1436, 1291, 1266; **LCMS** (LCQ) Rt = 0.5 min (method 1), *m/z* (ESI⁺) 435.1 [M+H]⁺; **HRMS (ESI)**: calcd. for C₂₄H₂₇N₄O₂S [M+H]⁺ 435.1849, found 435.1862.

***N*-(4-methyl-3-pyridyl)-4-(2-methylthiazol-4-yl)benzamide (153)**

Compound **153** was synthesised according to general procedure M, using the following reagents: 4-(2-methyl-1,3-thiazol-4-yl)benzoic acid (**102**) (100 mg, 0.46 mmol), oxalyl chloride (46 μ L, 0.55 mmol), *N,N*-dimethylformamide (10 μ L) and dichloromethane (3 mL) and stirred for 16 h. Followed 3-amino-4-methylpyridine (59 mg, 0.55 mmol), *N,N*-diisopropylethylamine (397 μ L, 2.28 mmol) and dichloromethane (1 mL) and stirred at 40 °C for 72 h. The crude was purified by column chromatography (silica 12 g, 0 to 3% methanol in dichloromethane) and further purified by column chromatography (amino silica 12 g, 0 to 3% methanol in dichloromethane) to yield the desired amide **153** as a white solid (27 mg, 18%).

R_f 0.12 (dichloromethane:methanol 19:1); **m.p.** 190–192 °C; **¹H-NMR** (500 MHz, DMSO-*d*₆) 10.12 (s, 1H, NH), 8.49 (s, 1H, H-6'), 8.33 (d, *J* 4.9, 1H, H-4'), 8.12 (d, *J* 5.7, 2H, H-3), 8.10 (s, 1H, H-6), 8.06 (d, *J* 8.2, 2H, H-2), 7.33 (d, *J* 4.9, 1H, H-3'), 2.75 (s, 3H, 8-CH₃), 2.27 (s, 3H, 2'-CH₃); **¹³C-NMR** (126 MHz, DMSO-*d*₆) δ 166.4 (CO), 165.8 (C-8), 153.3 (C-5), 147.9 (C-6'), 147.2 (C-4'), 143.4 (ArC), 137.6 (ArC), 134.0 (ArC), 133.4 (ArC), 128.8 (C-2), 126.3 (C-3), 125.7 (C-3'), 116.1 (C-6), 19.4 (8-CH₃), 17.8 (2'-CH₃).; **IR** (neat, ν_{max} , cm⁻¹) 3334, 1643, 1611, 1539, 1502, 1466, 1438, 13182, 1170; **LCMS** (LCQ) Rt = 0.6 min (method 1), *m/z* (ESI⁺) 310.2 [M+H]⁺; **HRMS (ESI)**: calcd. for C₁₇H₁₆N₃NaOS [M+H]⁺ 310.1009, found 310.1010.

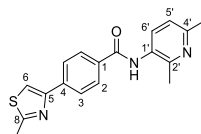
***N*-(3-methyl-2-pyridyl)-4-(2-methylthiazol-4-yl)benzamide (154)**

Compound **154** was synthesised according to general procedure M, using the following reagents: 4-(2-methyl-1,3-thiazol-4-yl)benzoic acid (**102**) (100 mg, 0.46 mmol), oxalyl chloride (46 μ L, 0.55 mmol), *N,N*-dimethylformamide

(10 μ L) and dichloromethane (3 mL) and stirred for 16 h. Followed 2-amino-3-methylpyridine (55 μ L, 0.55 mmol), *N,N*-diisopropylethylamine (397 μ L, 2.28 mmol) and dichloromethane (1 mL) and stirred for 16 h. The crude was purified by column chromatography (silica 12 g, 0 to 2.5% methanol in dichloromethane) to yield the desired amide **154** as a white solid (41 mg, 8%).

R_f 0.21 (dichloromethane:methanol 19:1); **m.p.** 213–214 °C; **¹H-NMR** (500 MHz, DMSO-*d*₆) 10.53 (s, 1H), 8.32 (d, *J* 4.0, 1H), 8.12 (s, 1H), 8.08 (s, 4H), 7.73 (dd, *J* 7.6, 1.7, 1H), 7.27 (dd, *J* 7.5, 4.8, 1H), 2.74 (s, 3H), 2.22 (s, 3H); **¹³C-NMR** (126 MHz, DMSO-*d*₆) δ 166.4, 165.5, 153.3, 150.8, 146.3, 139.7, 137.6, 133.4, 130.2, 128.9, 126.2, 122.5, 116.1, 19.4, 18.1; **LCMS** (LCQ) *R*_t = 1.9 min (method 1), *m/z* (ESI⁺) 310.1 [M+H]⁺; **HRMS (ESI)**: calcd. for C₁₇H₁₅N₃NaOS [M+H]⁺ 332.0828, found 332.0827. Not enough material for IR determination.

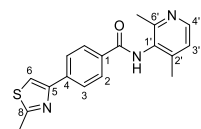
***N*-(2,6-dimethyl-3-pyridyl)-4-(2-methylthiazol-4-yl)benzamide (155)**



Compound **155** was synthesised according to general procedure M, using the following reagents: 4-(2-methyl-1,3-thiazol-4-yl)benzoic acid (**102**) (100 mg, 0.46 mmol), oxalyl chloride (46 μ L, 0.55 mmol), *N,N*-dimethylformamide (10 μ L) and dichloromethane (3 mL) and stirred for 16 h. Followed by 2,6-dimethyl-3-pyridinamine (56 mg, 0.46 mmol), *N,N*-diisopropylethylamine (397 μ L, 2.28 mmol) and dichloromethane (1 mL) and stirred for 2 h. The crude was purified by column chromatography (silica 12 g, 0 to 80% ethyl acetate in petroleum ether) to yield the desired amide **155** as a cream solid (52 mg, 33%).

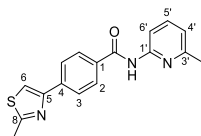
R_f 0.14 (petroleum ether:ethyl acetate 1:3); **m.p.** 182–184 °C; **¹H-NMR** (500 MHz, DMSO-*d*₆) 10.01 (s, 1H), 8.13 (s, 1H), 8.10 (d, *J* 8.0, 2H), 8.05 (d, *J* 8.1, 2H), 7.61 (d, *J* 8.0, 1H), 7.12 (d, *J* 8.0, 1H), 2.74 (s, 3H), 2.44 (s, 3H), 2.39 (s, 3H); **¹³C-NMR** (126 MHz, DMSO-*d*₆) δ 166.4, 165.6, 154.9, 153.5, 153.3, 137.5, 135.0, 133.6, 130.3, 128.7, 126.2, 121.1, 116.1, 24.0, 21.4, 19.4; **IR** (neat, ν_{max} , cm⁻¹) 3099, 2923, 1625, 1606, 1473, 1420, 1367, 1300, 1172; **LCMS** (LCQ) *R*_t = 0.7 min (method 1), *m/z* (ESI⁺) 324.3 [M+H]⁺; **HRMS (ESI)**: calcd. for C₁₈H₁₈N₃OS [M+H]⁺ 324.1165, found 324.1163.

***N*-(2,4-dimethyl-3-pyridyl)-4-(2-methylthiazol-4-yl)benzamide (156)**



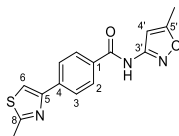
Compound **156** was synthesised according to general procedure M, using the following reagents: 4-(2-methyl-1,3-thiazol-4-yl)benzoic acid (**102**) (270 mg, 1.23 mmol), oxalyl chloride (156 μ L, 1.85 mmol), *N,N*-dimethylformamide (10 μ L) and dichloromethane (6 mL) and stirred for 16 h. Followed by 2,4-dimethylpyridin-3-amine (150 mg, 1.23 mmol), *N,N*-diisopropylethylamine (1.07 mL, 6.16 mmol) and dichloromethane (2 mL) and stirred for 2 h and at 50 °C for 16 h. The crude was purified by column chromatography (silica 12 g, 0 to 20% methanol in dichloromethane), further purified by column chromatography (amino silica 12 g, 0 to 20% methanol in dichloromethane) and further purified by column chromatography (amino silica 12 g, 0 to 2% methanol in ethyl acetate) to yield the desired amide **156** as a colourless solid (13 mg, 3%).

R_f 0.52 (petroleum ether:ethyl acetate 9:1); **¹H-NMR** (500 MHz, DMSO-*d*₆) 10.00 (s, 1H), 8.26 (d, *J* 4.9, 1H), 8.13 (s, 1H), 8.11 (d, *J* 8.4, 2H), 8.07 (d, *J* 8.3, 2H), 7.19 (d, *J* 4.9, 1H), 2.75 (s, 3H), 2.39 (s, 3H), 2.21 (s, 3H); **LCMS** (LCQ) *R*_t = 0.5 min (method 1), *m/z* (ESI⁺) 324.3 [M+H]⁺; **HRMS (ESI)**: calcd. for C₁₈H₁₈N₃OS [M+H]⁺ 324.1165, found 324.1162. Not enough material for mp, IR and ¹³C-NMR determination.

***N*-(6-methyl-2-pyridyl)-4-(2-methylthiazol-4-yl)benzamide (157)**

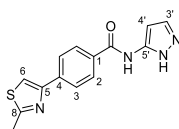
Compound **157** was synthesised according to general procedure M, using the following reagents: 4-(2-methyl-1,3-thiazol-4-yl)benzoic acid (**102**) (80 mg, 0.36 mmol), oxalyl chloride (37 μ L, 0.44 mmol), *N,N*-dimethylformamide (10 μ L) and dichloromethane (3 mL) and stirred for 16 h. Followed by 2-amino-6-methylpyridine (40 mg, 0.36 mmol), *N,N*-diisopropylethylamine (397 μ L, 2.28 mmol) and dichloromethane (1 mL) and stirred for 2 h. The crude was purified by column chromatography (silica 12 g, 0 to 45% ethyl acetate in petroleum ether) to yield the desired amide **157** as a colourless solid (54 mg, 45%).

R_f 0.48 (petroleum ether:ethyl acetate 1:1); **m.p.** 195–197 °C; **¹H-NMR** (500 MHz, DMSO-*d*₆) 10.69 (s, 1H), 8.13 (s, 1H), 8.10 (d, *J* 8.2, 2H), 8.06 (d, *J* 8.0, 2H), 8.02 (d, *J* 8.2, 1H), 7.73 (t, *J* 7.8, 1H), 7.03 (d, *J* 7.3, 1H), 2.74 (s, 3H), 2.46 (s, 3H); **¹³C-NMR** (126 MHz, DMSO-*d*₆) 166.4, 165.9, 157.0, 153.3, 152.0, 138.8, 137.6, 133.5, 129.1, 126.1, 119.5, 116.2, 112.1, 24.0, 19.4; **IR** (neat, ν_{max} , cm⁻¹) 3314, 2923, 1610, 1539, 1522, 1290, 1169; **LCMS** (LCQ) *R*_t = 3.1 min (method 1), *m/z* (ESI⁺) 310.1 [M+H]⁺; **HRMS (ESI)**: calcd. for C₁₇H₁₆N₃OS [M+H]⁺ 310.1009, found 310.1012.

***N*-(5-methylisoxazol-3-yl)-4-(2-methylthiazol-4-yl)benzamide (158)**

Compound **158** was synthesised according to general procedure M, using the following reagents: 4-(2-methyl-1,3-thiazol-4-yl)benzoic acid (**102**) (80 mg, 0.36 mmol), oxalyl chloride (37 μ L, 0.44 mmol), *N,N*-dimethylformamide (10 μ L) and dichloromethane (3 mL) and stirred for 16 h. Followed by 3-amino-5-methylisoxazole (36 mg, 0.36 mmol), *N,N*-diisopropylethylamine (397 μ L, 2.28 mmol) and dichloromethane (1 mL) and stirred for 2 h. The crude was purified by column chromatography (silica 12 g, 0 to 35% ethyl acetate in petroleum ether) to yield the desired amide **158** as a colourless solid (19 mg, 17%).

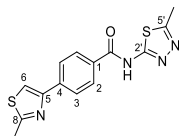
R_f 0.42 (petroleum ether:ethyl acetate 3:1); **m.p.** 235–239 °C; **¹H-NMR** (500 MHz, DMSO-*d*₆) 11.31 (s, 1H), 8.14 (s, 1H), 8.10 – 8.05 (m, 4H), 6.76 (s, 1H), 2.74 (s, 3H), 2.42 (s, 3H); **¹³C-NMR** (126 MHz, DMSO-*d*₆) 169.9, 165.4, 159.0, 153.1, 138.0, 136.1, 129.1, 126.2, 116.5, 97.4, 19.3, 12.6; **IR** (neat, ν_{max} , cm⁻¹) 3186, 1643, 1609, 1565, 1492, 1459, 1347, 1257, 1168; **LCMS** (LCQ) *R*_t = 0.5 min (method 2), *m/z* (ESI⁺) 300.0 [M+H]⁺; **HRMS (ESI)**: calcd. for C₁₅H₁₃N₃NaO₂S [M+H]⁺ 322.0621, found 322.0625.

4-(2-Methylthiazol-4-yl)-*N*-(1H-pyrazol-5-yl)benzamide (159)

Compound **159** was synthesised according to general procedure M, using the following reagents: 4-(2-methyl-1,3-thiazol-4-yl)benzoic acid (**102**) (80 mg, 0.36 mmol), oxalyl chloride (37 μ L, 0.44 mmol), *N,N*-dimethylformamide (10 μ L) and dichloromethane (3 mL) and stirred for 16 h. Followed by 1H-pyrazol-5-amine (23 mg, 0.36 mmol), *N,N*-diisopropylethylamine (397 μ L, 2.28 mmol) and dichloromethane (1 mL) and stirred for 2 h. The crude was purified by column chromatography (silica 12 g, 0 to 100% ethyl acetate in petroleum ether) to yield the desired amide **159** as a colourless solid (17 mg, 16%).

R_f 0.06 (ethyl acetate); **m.p.** 224–226 °C; **¹H-NMR** (500 MHz, DMSO-*d*₆) 12.44 (s, 1H), 10.81 (s, 1H), 8.11 (s, 1H), 8.06 (t, *J* 6.9, 4H), 7.66 (s, 1H), 6.65 (s, 1H), 2.74 (s, 3H); **¹³C-NMR** (126 MHz, DMSO-*d*₆) δ 166.4, 164.5, 153.3, 153.2, 137.3, 133.6, 128.8, 128.5, 126.1, 116.0, 97.4, 19.4; **IR** (neat, ν_{max} , cm⁻¹) 3185, 1643, 1610, 1565, 1492, 1459, 1327, 1257, 1168; **LCMS** (LCQ) *R*_t = 1.8 min (method 1), *m/z* (ESI⁺) 285.1 [M+H]⁺; **HRMS (ESI)**: calcd. for C₁₄H₁₃N₄OS [M+H]⁺ 285.0805, found 285.0812.

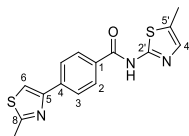
***N*-(5-methyl-1,3,4-thiadiazol-2-yl)-4-(2-methylthiazol-4-yl)benzamide (160)**



Compound **160** was synthesised according to general procedure M, using the following reagents: 4-(2-methyl-1,3-thiazol-4-yl)benzoic acid (**102**) (80 mg, 0.36 mmol), oxalyl chloride (37 μL, 0.44 mmol), *N,N*-dimethylformamide (10 μL) and dichloromethane (3 mL) and stirred for 16 h. Followed by 2-amino-5-methyl-1,3,4-thiadiazole (42 mg, 0.36 mmol), *N,N*-diisopropylethylamine (397 μL, 2.28 mmol) and dichloromethane (1 mL) and stirred for 2 h. The precipitation formed during the work up was collected by vacuum filtration and triturated in water then ethyl acetate to yield the desired amide **160** as a colourless solid (48 mg, 40%).

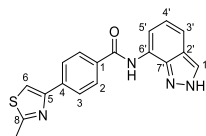
R_f 0.49 (petroleum ether:ethyl acetate 1:1); **m.p.** 230–232 °C; **¹H-NMR** (500 MHz, DMSO-*d*₆) 12.93 (s, 1H), 8.21 – 8.15 (m, 3H), 8.11 (d, *J* 8.1, 2H), 2.74 (s, 3H), 2.65 (s, 3H); **¹³C-NMR** (126 MHz, DMSO-*d*₆) δ 166.8, 160.2, 153.0, 138.4, 129.4, 126.4, 116.8, 110.0. 2 × C not visible; **IR** (neat, ν_{max} , cm⁻¹) 3301, 2914, 1610, 1540, 1522, 1470, 1289, 1169; **LCMS** (LCQ) *R*_t = 0.9 min (method 1), *m/z* (ESI⁺) 317.0 [M+H]⁺; **HRMS (ESI)**: calcd. for C₁₄H₁₃N₄OS₂ [M+H]⁺ 317.0525, found 317.0531.

4-(2-methylthiazol-4-yl)-*N*-(5-methylthiazol-2-yl)benzamide (161)



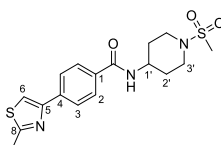
Compound **161** was synthesised according to general procedure M, using the following reagents: 4-(2-methyl-1,3-thiazol-4-yl)benzoic acid (**102**) (100 mg, 0.46 mmol), oxalyl chloride (46 μL, 0.55 mmol), *N,N*-dimethylformamide (10 μL) and dichloromethane (3 mL) and stirred for 16 h. Followed by 2-amino-5-methylthiazole (52 mg, 0.46 mmol), *N,N*-diisopropylethylamine (397 μL, 2.28 mmol) and dichloromethane (1 mL) and stirred for 2 h. The crude was purified by column chromatography (silica 12 g, 0 to 50% ethyl acetate in petroleum ether) to yield the desired amide **161** as a colourless solid (52 mg, 41%).

R_f 0.31 (petroleum ether:ethyl acetate 1:1); **m.p.** 232–235 °C; **¹H-NMR** (500 MHz, DMSO-*d*₆) 12.47 (s, 1H), 8.15 (m, *J* 8.8, 3H), 8.09 (d, *J* 6.8, 2H), 7.23 (s, 1H), 2.74 (s, 3H), 2.38 (s, 3H); **¹³C-NMR** (126 MHz, DMSO-*d*₆) δ 166.4, 164.9, 153.1, 138.1, 131.7, 130.3, 129.2, 126.9, 126.3, 116.5, 88.3, 19.4, 11.6; **IR** (neat, ν_{max} , cm⁻¹) 2920, 1655, 1608, 1524, 1443, 1301, 1286, 1174, 1158; **LCMS** (LCQ) *R*_t = 3.7 min (method 1), *m/z* (ESI⁺) 316.1 [M+H]⁺; **HRMS (ESI)**: calcd. for C₁₅H₁₄N₃OS₂ [M+H]⁺ 316.0573, found 316.0568.

***N*-(2H-indazol-7-yl)-4-(2-methylthiazol-4-yl)benzamide (162)**

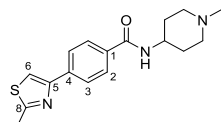
Compound **162** was synthesised according to general procedure M, using the following reagents: 4-(2-methyl-1,3-thiazol-4-yl)benzoic acid (**102**) (100 mg, 0.46 mmol), oxalyl chloride (46 μ L, 0.55 mmol), *N,N*-dimethylformamide (10 μ L) and dichloromethane (3 mL) and stirred for 16 h. Followed by 2H-indazol-7-amine (55 μ L, 0.46 mmol), *N,N*-diisopropylethylamine (397 μ L, 2.28 mmol) and dichloromethane (1 mL) and stirred for 1 h. The crude was purified by column chromatography (silica 12 g, 0 to 40% ethyl acetate in petroleum ether) and further purified by column chromatography (amino silica 4 g, 0 to 80% ethyl acetate in petroleum ether) to yield the desired amide **162** as a cream solid (12 mg, 8%).

R_f 0.50 (petroleum ether:ethyl acetate 1:4, amino silica); **m.p.** 263–265 °C; **¹H-NMR** (500 MHz, DMSO-*d*₆) 13.07 (s, 1H), 10.45 (s, 1H), 8.23 (s, 1H), 8.14 (s, 1H), 8.12 (d, *J* 8.3, 2H), 8.08 (d, *J* 8.3, 2H), 7.50 (t, *J* 7.9, 4.0, 1H), 7.36–7.31 (m, 2H), 2.75 (s, 3H); **IR** (neat, ν_{\max} , cm⁻¹) 3305, 1610, 1539, 1520, 1471, 1289, 1170; **LCMS** (LCQ) *R_t* = 0.8 min (method 1), *m/z* (ESI⁺) 335.2 [M+H]⁺; **HRMS (ESI)**: calcd. for C₁₈H₁₅N₄OS [M+H]⁺ 335.0961, found 335.0966. Not enough material for ¹³C-NMR determination.

***N*-(1-methylsulfonyl-4-piperidyl)-4-(2-methylthiazol-4-yl)benzamide (163)**

Compound **163** was synthesised according to general procedure M, using the following reagents: 4-(2-methyl-1,3-thiazol-4-yl)benzoic acid (**102**) (100 mg, 0.46 mmol), oxalyl chloride (46 μ L, 0.55 mmol), *N,N*-dimethylformamide (10 μ L) and dichloromethane (3 mL) and stirred for 16 h. Followed by 1-methanesulfonylpiperidin-4-amine (74 μ L, 0.46 mmol), *N,N*-diisopropylethylamine (397 μ L, 2.28 mmol) and dichloromethane (1 mL) and stirred for 2 h. The precipitation formed during the work up was collected by vacuum filtration and triturated in water then methanol to yield the desired amide **163** as a cream solid (57 mg, 31%).

R_f 0.62 (ethyl acetate); **m.p.** 177–179 °C; **¹H-NMR** (500 MHz, DMSO-*d*₆) 8.38 (d, *J* 8.0, 1H), 8.08 (s, 1H), 8.02 (d, *J* 7.6, 2H), 7.91 (d, *J* 7.6, 2H), 3.99–3.89 (m, 1H), 3.64–3.53 (m, 2H), 2.95–2.80 (m, 5H), 2.73 (s, 3H), 1.95–1.88 (m, 2H), 1.68–1.52 (m, 2H); **¹³C-NMR** (126 MHz, DMSO-*d*₆) δ 166.3, 165.8, 153.4, 137.0, 134.0, 128.3, 126.1, 115.8, 46.4, 45.2, 34.8, 31.3, 19.4; **IR** (neat, ν_{\max} , cm⁻¹) 3301, 2927, 1656, 1610, 1539, 1522, 1471, 1289, 1169; **LCMS** (LCQ) *R_t* = 2.5 min (method 1), *m/z* (ESI⁺) 380.1 [M+H]⁺; **HRMS (ESI)**: calcd. for C₁₇H₂₂N₃O₃S₂ [M+H]⁺ 380.1097, found 380.1105.

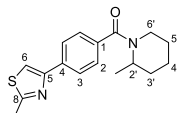
***N*-(1-methyl-4-piperidyl)-4-(2-methylthiazol-4-yl)benzamide (164)**

Compound **164** was synthesised according to general procedure M, using the following reagents: 4-(2-methyl-1,3-thiazol-4-yl)benzoic acid (**102**) (80 mg, 0.36 mmol), oxalyl chloride (37 μ L, 0.44 mmol), *N,N*-dimethylformamide (10 μ L) and dichloromethane (3 mL) and stirred for 16 h. Followed by 4-amino-1-methylpyridine (46 μ L, 0.36 mmol), *N,N*-diisopropylethylamine (397 μ L, 2.28 mmol) and dichloromethane (1 mL) and stirred for 2 h. The crude was

purified by column chromatography (silica 12 g, 0 to 20% methanol in dichloromethane) to yield the desired amide **164** as a colourless solid (12 mg, 10%).

m.p. 221–223 °C; **¹H-NMR** (500 MHz, DMSO-*d*₆) 8.29 (d, *J* 7.7, 1H), 8.06 (s, 1H), 8.00 (d, *J* 8.1, 2H), 7.90 (d, *J* 8.1, 2H), 3.82–3.70 (m, 1H), 2.88–2.79 (m, 2H), 2.73 (s, 3H), 2.21 (s, 3H), 2.11–1.99 (m, 2H), 1.82–1.75 (m, 2H), 1.61 (qd, *J* 12.1, 3.7, 2H); **¹³C-NMR** (126 MHz, DMSO-*d*₆) δ 166.3, 165.8, 153.4, 136.9, 134.2, 128.3, 126.0, 115.7, 54.7, 46.7, 45.9, 31.5, 19.4; **IR** (neat, ν_{\max} , cm⁻¹) 3301, 2918, 1610, 1539, 1522, 1290, 1272, 1169; **LCMS** (LCQ) *R*_t = 2.5 min (method 1), *m/z* (ESI⁺) 380.1 [M+H]⁺; **HRMS (ESI)**: calcd. for C₁₇H₂₂N₃OS [M+H]⁺ 316.1478, found 316.1486.

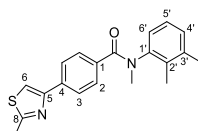
(2-Methyl-1-piperidyl)-(4-(2-methylthiazol-4-yl)phenyl)methanone (165)



Compound **165** was synthesised according to general procedure M, using the following reagents: 4-(2-methyl-1,3-thiazol-4-yl)benzoic acid (**102**) (100 mg, 0.46 mmol), oxalyl chloride (46 μL, 0.55 mmol), *N,N*-dimethylformamide (10 μL) and dichloromethane (3 mL) and stirred for 16 h. Followed by 2-methylpiperidine (51 μL, 0.46 mmol), *N,N*-diisopropylethylamine (397 μL, 2.28 mmol) and dichloromethane (1 mL) and stirred for 2 h. The crude was purified by column chromatography (silica 12 g, 0 to 20% ethyl acetate in petroleum ether) to yield the desired amide **165** as a colourless solid (36 mg, 25%).

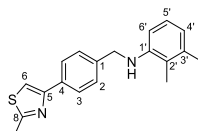
R_f 0.48 (petroleum ether:ethyl acetate 1:1); **m.p.** 140–142 °C; **¹H-NMR** (500 MHz, DMSO-*d*₆) 7.90 (d, *J* 8.0, 2H), 7.42 (d, *J* 7.9, 2H), 7.35 (s, 1H), 4.27 (brs, 2H), 3.00 (s, 1H), 2.78 (s, 3H), 1.84–1.61 (m, 4H), 1.59–1.39 (m, 2H), 1.24 (d, *J* 7.2 3H); **¹³C-NMR** (126 MHz, DMSO-*d*₆) δ 169.4, 166.2, 153.5, 136.7, 135.2, 127.3, 126.4, 115.1, 110.0, 88.3 30.3, 26.0, 19.4, 18.9, 16.3; **IR** (neat, ν_{\max} , cm⁻¹) 3289, 2910, 1610, 1521, 1470, 1273, 1170; **LCMS** (LCQ) *R*_t = 3.9 min (method 1), *m/z* (ESI⁺) 301.1 [M+H]⁺; **HRMS (ESI)**: calcd. for C₁₈H₁₈N₃OS [M+H]⁺ 324.1165, found 324.1166.

***N*-(2,3-dimethylphenyl)-*N*-methyl-4-(2-methylthiazol-4-yl)benzamide (166)**



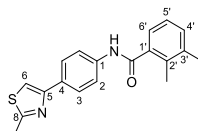
To *N*-(2,3-dimethylphenyl)-4-(2-methylthiazol-4-yl)benzamide (**106**) (40 mg, 0.12 mmol) in *N,N*-dimethylformamide was added iodomethane (23 μL, 0.37 mmol) and the reaction mixture was stirred at 0 °C. To the reaction mixture was slowly added sodium hydride (60% dispersion in mineral oil) (2.9 mg, 0.19 mmol). The reaction mixture was stirred at ambient temperature for 16 h. The crude product was taken up in water (2 mL) and extracted with ethyl acetate (2 × 3 mL). The combined organic components were dried over MgSO₄, filtered and concentrated under reduced pressure. The crude was purified by column chromatography (silica 4 g, 0 to 20% ethyl acetate in petroleum ether) to yield the desired product **166** as a white solid (19 mg, 43%).

R_f 0.29 (petroleum ether:ethyl acetate 3:1); **m.p.** 145–147 °C; **¹H-NMR** (500 MHz, DMSO-*d*₆) δ 7.92 (s, 1H, H-6), 7.72 (d, *J* 7.9, 2H, H-3), 7.25 (d, *J* 8.0, 2H, H-2), 7.05–6.98 (m, 3H, H-4', H-5', H-6'), 3.24 (s, 3H, NCH₃), 2.67 (s, 3H, 8-CH₃), 2.16 (s, 3H, 3'-CH₃), 2.08 (s, 3H, 2'-CH₃); **¹³C-NMR** (126 MHz, DMSO-*d*₆) δ 170.6 (CO), 167.0 (C-8), 153.0 (C-5), 143.2 (ArC), 138.6 (ArC), 135.7 (ArC), 135.1 (ArC), 133.7 (ArC), 129.5 (ArC), 128.6 (C-2), 126.7 (ArC), 126.6 (ArC), 125.4 (C-3), 115.4 (C-6), 37.7 (NCH₃), 20.2 (2'-CH₃), 19.0 (8-CH₃), 14.3 (3'-CH₃); **IR** (neat, ν_{\max} , cm⁻¹) 3096, 1625, 1604, 1563, 1474, 1418, 1367, 1173; **LCMS** (LCQ) *R*_t = 4.4 min (method 1), *m/z* (ESI⁺) 337.2 [M+H]⁺; **HRMS** *m/z* (ESI): calcd. for C₂₀H₂₁N₂OS [M+H]⁺ 337.1369, found 337.1373.

2,3-Dimethyl-*N*-((4-(2-methylthiazol-4-yl)phenyl)methyl)aniline (167)

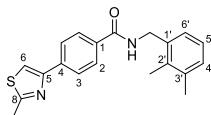
To a solution of *N*-(2,3-dimethylphenyl)-4-(2-methylthiazol-4-yl)benzamide (**106**) (30 mg, 0.90 mmol) in tetrahydrofuran (0.5 mL) at 0 °C was added dropwise borane tetrahydrofuran complex solution (1 M) (465 µL, 0.47 mmol) and the reaction mixture heated to 50 °C for 2 h. The crude product was taken up in acetate (2 mL) and washed with brine (2 mL). The organic components were dried over MgSO₄, filtered and concentrated under reduced pressure. The crude product was purified by column chromatography (silica 4 g, 0 to 10% ethyl acetate in petroleum ether) to yield the desired compound **167** as a colourless solid (7 mg, 23%).

R_f 0.11 (petroleum ether:ethyl acetate 9:1); **¹H-NMR** (500 MHz, DMSO-*d*₆) δ 7.89 – 7.78 (m, 3H, H-6, H-3), 7.38 (d, *J* 7.9, 2H, H-2), 6.75 (t, *J* 7.8, 1H, H-5'), 6.39 (d, *J* 7.5, 1H, ArH), 6.25 (d, *J* 8.1, 1H, ArH), 5.59 (d, *J* 6.2, 1H, NH), 4.35 (d, *J* 5.9, 2H, NHCH₂), 2.70 (s, 3H, 8-CH₃), 2.18 (s, 3H, 2'-CH₃), 2.07 (s, 3H, 3'-CH₃); **IR** (neat, *v*_{max}, cm⁻¹) 1724, 1678, 1484, 1418, 1394, 1303, 1246, 1165; **LCMS** (LCQ) *R*_t = 5.3 min (method 1), *m/z* (ESI⁺) 309.1 [M+H]⁺; **HRMS** *m/z* (ESI): calcd. for C₁₉H₂₁N₂S [M+H⁺ 309.1420, found 309.1423. Not enough material for mp and ¹³C-NMR determination.

2,3-Dimethyl-*N*-(4-(2-methylthiazol-4-yl)phenyl)benzamide (168)

Compound **168** was synthesised according to general procedure R, using the following reagents: 2,3-dimethylbenzoic acid (142 mg, 0.95 mmol), HATU (360 mg, 0.95 mmol), *N,N*-diisopropylethylamine (274 µL, 1.58 mmol), 4-(2-methyl-1,3-thiazol-4-yl)aniline (150 mg, 0.79 mmol) and *N,N*-dimethylformamide (1.5 mL). The crude was purified by column chromatography (silica, 0 to 20% ethyl acetate in petroleum ether) to yield the desired compound **168** as a white solid (125 mg, 47%).

R_f 0.33 (petroleum ether:ethyl acetate 3:1); **m.p.** 182–184 °C; **¹H-NMR** (500 MHz, DMSO-*d*₆) δ 10.38 (s, 1H, CONH), 7.90 (d, *J* 8.2, 2H, ArH), 7.82 (s, 1H, H-6), 7.80 (d, *J* 8.4, 2H, ArH), 7.30 – 7.23 (m, 2H, 2 × ArH), 7.19 (t, *J* 7.5, 1H, ArH), 2.71 (s, 3H), 2.30 (s, 3H), 2.26 (s, 3H); **¹³C-NMR** (126 MHz, DMSO-*d*₆) δ 169.1 (CO), 166.1 (C-8), 154.1 (C-5), 139.3 (ArC), 138.3 (ArC), 137.7 (ArC), 133.7 (ArC), 131.2 (ArC), 130.1 (ArC), 126.8 (ArC), 125.8 (ArC), 125.0 (ArC), 120.2 (ArC), 113.1 (C-6), 20.2 (2'-CH₃), 19.3 (8-CH₃), 16.5 (3'-CH₃); **IR** (neat, *v*_{max}, cm⁻¹) 3344, 1698, 1643, 1596, 1503, 1477, 1459, 1376, 1281; **LCMS** (LCQ) *R*_t = 4.2 min (method 1), *m/z* (ESI⁺) 323.2 [M+H]⁺; **HRMS** *m/z* (ESI): calcd. for C₁₉H₁₉N₂OS [M+H]⁺ 323.1213, found 323.1201.

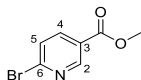
***N*-[(2,3-dimethylphenyl)methyl]-4-(2-methylthiazol-4-yl)benzamide (169)**

Compound **169** was synthesised according to general procedure M, using the following reagents: 4-(2-methyl-1,3-thiazol-4-yl)benzoic acid (**102**) (100 mg, 0.46 mmol), oxalyl chloride (46 µL, 0.55 mmol), *N,N*-dimethylformamide (10 µL) and dichloromethane (3 mL) and stirred for 16 h. Followed 2,3-dimethylbenzylamine (64 µL, 0.46 mmol), *N,N*-diisopropylethylamine (397 µL, 2.28 mmol) and dichloromethane (1 mL) and stirred for 16 h. The crude was purified

by column chromatography (silica 12 g, 0 to 30% ethyl acetate in petroleum ether) to yield the desired amide **169** as a white solid (104 mg, 64%).

R_f 0.73 (petroleum ether:ethyl acetate 1:1); **m.p.** 147–149 °C; **¹H-NMR** (500 MHz, DMSO-*d*₆) δ 8.89 (t, *J* 5.9, 1H, CONH), 8.07 (s, 1H, H-6), 8.03 (d, *J* 8.3, 2H, H-3), 7.96 (d, *J* 8.0, 2H, H-2), 7.11 (d, *J* 7.2, 1H, ArH), 7.09 – 7.02 (m, 2H, ArH), 4.48 (d, *J* 5.6, 2H, NHCH₂), 2.73 (s, 3H, 8-CH₃), 2.26 (s, 3H, 2'-CH₃), 2.21 (s, 3H, 3'-CH₃); **¹³C-NMR** (126 MHz, DMSO-*d*₆) δ 166.3 (C-8 or CO), 166.2 (C-8 or CO), 153.4 (C-5), 137.3 (ArC), 137.0 (ArC), 136.7 (ArC), 134.6 (ArC), 133.9 (ArC), 128.9 (ArC), 128.3 (C-2), 126.1 (C-3), 125.6 (ArC), 115.8 (C-6), 41.9 (NHCH₂), 20.5 (2'-CH₃), 19.4 (8-CH₃), 14.9 (3'-CH₃); **IR** (neat, ν_{max} , cm⁻¹) 3293, 1610, 1539, 1521, 1471, 1272, 1170; **LCMS** (LCQ) *R_t* = 4.4 min (method 1), *m/z* (ESI⁺) 337.1 [M+H]⁺; **HRMS** *m/z* (ESI): calcd. for C₂₀H₂₁N₂OS [M+H]⁺ 337.1369, found 337.1377.

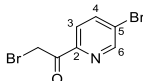
Methyl 6-bromopyridine-3-carboxylate (**170**)



To a solution of 6-bromonicotinic acid (200 mg, 1.00 mmol) in methyl alcohol (0.6 mL) was added dropwise sulphuric acid (79 μ L, 1.5 mmol) and the reaction mixture heated to 65 °C for 4 h. The solvent was removed under reduced pressure. The crude product was taken up in saturated aq. NaHCO₃ (5 mL) and extracted with ethyl acetate (3 \times 5 mL). The combined organic components were then washed with brine (5 mL), dried over MgSO₄, filtered and concentrated under reduced pressure. The crude product was purified by column chromatography (silica 12 g, 0 to 10% ethyl acetate in petroleum ether) to yield the desired compound **170** as a colourless solid (65 mg, 29 %).

¹H-NMR (500 MHz, DMSO-*d*₆) δ 8.89 – 8.86 (m, 1H, H-2), 8.20 (dd, *J* 8.3, 1.0, 1H, H-4), 7.84 (d, *J* 8.3, 1H, H-5), 3.89 (s, 3H, OCH₃); **LCMS** (LCQ) *R_t* = 2.6 min (method 1), *m/z* (ESI⁺) 216.2 [M(⁷⁹Br)+H]⁺, 218.3 [M(⁸¹Br)+H]⁺. ¹H-NMR corresponds to literature data.³⁰⁴

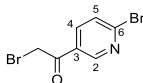
2-bromo-1-(5-bromo-2-pyridyl)ethanone (**171**)



A solution of 5-bromo-2-acetylpyridine (1.00 g, 5.00 mmol) and *p*-toluenesulfonic acid monohydrate (95 mg, 0.50 mmol) in acetonitrile (30 mL) was treated with *N*-bromosuccinimide (979 mg, 5.50 mmol) and the reaction mixture heated to 80 °C for 4 h. The solvent was removed under reduced pressure. The crude product was taken up in saturated aq. NaHCO₃ (20 mL) and extracted with ethyl acetate (3 \times 20 mL). The combined organic components were then washed with brine (20 mL), dried over MgSO₄, filtered and concentrated under reduced pressure. The crude product was purified by column chromatography (silica 24 g, 100% petroleum ether) to yield the desired compound **171** as a white solid (1.02 g, 59%).

¹H-NMR (500 MHz, DMSO-*d*₆) δ 8.90 (s, 1H, H-6), 8.34 – 8.29 (m, 1H, H-3), 7.96 (d, *J* 8.3, 1H, H-4), 4.98 (s, 2H, OCH₂Br); **LCMS** (LCQ) *R_t* = 0.8 min (method 1), *m/z* (ESI⁺) 278.2 [M(⁷⁹Br⁷⁹Br)+H]⁺, 280.1 [M(⁷⁹Br⁸¹Br)+H]⁺.

2-Bromo-1-(6-bromo-3-pyridyl)ethenone (**172**)



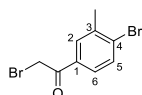
A solution of 1-(6-bromo-3-pyridyl)ethanone (500 mg, 2.5 mmol) and *p*-toluenesulfonic acid monohydrate (24 mg, 0.12 mmol) in acetonitrile (15 mL) was treated with *N*-bromosuccinimide (445 mg, 2.5 mmol) and the reaction mixture heated to 80 °C for 4 h. The solvent was removed under reduced pressure. The crude product was taken up

in saturated aq. NaHCO_3 (10 mL) and extracted with ethyl acetate (3×10 mL). The combined organic components were then washed with brine (10 mL), dried over MgSO_4 , filtered and concentrated under reduced pressure. The crude product was purified by column chromatography (silica 24 g, 0 to 10% ethyl acetate in petroleum ether) to yield the desired compound **172** as a white solid (480 mg, 55%).

$^1\text{H-NMR}$ (500 MHz, $\text{DMSO}-d_6$) δ 8.95 (s, 1H, H-2), 8.23 (d, J 9.2, 1H, H-4), 7.86 (d, J 8.6, 1H, H-5), 4.97 (s, 2H, COCH_2Br);

LCMS (LCQ) R_t = 2.9 min (method 1), m/z (ESI^+) 278.1 [$\text{M}(^{79}\text{Br}^{79}\text{Br})+\text{H}$] $^+$, 280.1 [$\text{M}(^{79}\text{Br}^{81}\text{Br})+\text{H}$] $^+$.

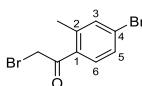
2-Bromo-1-(4-bromo-3-methyl-phenyl)ethenone (**173**)



A solution of 1-(4-bromo-3-methylphenyl)ethanone (200 mg, 0.94 mmol) and *p*-toluenesulfonic acid monohydrate (8.9 mg, 0.05 mmol) in acetonitrile (4 mL) was treated with *N*-bromosuccinimide (167 mg, 0.94 mmol) and the reaction mixture heated to 80°C for 16 h. The solvent was removed under reduced pressure. The crude product was taken up in saturated aq. NaHCO_3 (5 mL) and extracted with ethyl acetate (3×5 mL). The combined organic components were then washed with brine (5 mL), dried over MgSO_4 , filtered and concentrated under reduced pressure. The crude product was purified by column chromatography (silica 12 g, 0 to 3% ethyl acetate in petroleum ether) to yield the desired compound **173** as a white solid (158 mg, 55%).

$^1\text{H-NMR}$ (500 MHz, $\text{DMSO}-d_6$) δ 7.83 (d, J 8.9, 1H, H-2), 7.73 – 7.58 (m, 2H, H-5, H-6), 4.41 (s, 2H, OCH_2Br) 2.48 (s, 3H, ArCH_3); **LCMS** (LCQ) R_t = 3.5 min (method 1), no ionisation observed.

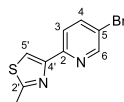
2-Bromo-1-(4-bromo-2-methyl-phenyl)ethenone (**174**)



A solution of 1-(4-bromo-2-methylphenyl)ethanone (500 mg, 2.35 mmol) and *p*-toluenesulfonic acid monohydrate (22 mg, 0.05 mmol) in acetonitrile (10 mL) was treated with *N*-bromosuccinimide (439 mg, 2.46 mmol) and the reaction mixture heated to 80°C for 16 h. The solvent was removed under reduced pressure. The crude product was taken up in saturated aq. NaHCO_3 (5 mL) and extracted with ethyl acetate (3×5 mL). The combined organic components were then washed with brine (5 mL), dried over MgSO_4 , filtered and concentrated under reduced pressure. The crude product was purified by column chromatography (silica 40 g, 0 to 3% ethyl acetate in petroleum ether) to yield the desired compound **174** as a white solid (720 mg, 100%).

$^1\text{H-NMR}$ (500 MHz, $\text{DMSO}-d_6$) δ 7.55 (d, J 8.3, 1H, H-6), 7.47 (s, 1H, H-3), 7.44 (d, J 8.3, 1H, H-5), 4.37 (s, 2H, OCH_2Br), 2.51 (s, 3H, ArCH_3).

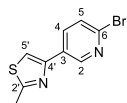
4-(5-Bromo-2-pyridyl)-2-methyl-thiazole (**175**)



To 2-bromo-1-(5-bromo-2-pyridyl)ethanone (**171**) (1.02 g, 2.93 mmol) in *N,N*-dimethylformamide (10 mL) was added thioacetamide (330 mg, 4.39 mmol) and the reaction mixture stirred at ambient temperature for 16 h. Upon completion, water was added to the reaction mixture. The resulting precipitate was collected by vacuum filtration and dried under reduced pressure to afford the desired compound **175** as a yellow solid (320 mg, 32%).

¹H-NMR (500 MHz, DMSO-*d*₆) δ 8.71 (d, *J* 2.3, 1H, H-6), 8.16 – 8.09 (m, 2H, H-4, H-5'), 7.98 (d, *J* 8.5, 1H, H-4), 2.73 (s, 3H, 2'-CH₃). **LCMS** (LCQ) Rt = 3.6 min (method 1), *m/z* (ESI⁺) 255.3 [M(⁷⁹Br)+H]⁺, 257.2 [M(⁸¹Br)+H]⁺.

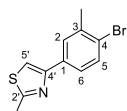
4-(6-Bromo-3-pyridyl)-2-methyl-thiazole (176)



To 2-bromo-1-(6-bromo-3-pyridyl)ethanone (**172**) (467 mg, 1.67 mmol) in *N,N*-dimethylformamide (5 mL) was added thioacetamide (189 mg, 2.51 mmol) and the reaction mixture stirred at ambient temperature for 16 h. Upon completion, water was added to the reaction mixture. The resulting precipitate was collected by vacuum filtration and dried under reduced pressure to afford the desired compound **176** as an off-white solid (289 mg, 64%).

¹H-NMR (500 MHz, DMSO-*d*₆) δ 8.94 (s, 1H, H-2), 8.24 (d, *J* 8.3, 1H, H-4), 8.18 (s, 1H, H-5'), 7.72 (d, *J* 8.3, 1H, H-5), 2.73 (s, 3H, CH₃); **LCMS** (LCQ) Rt = 0.9 min (method 1), *m/z* (ESI⁺) 255.1 [M(⁷⁹Br)+H]⁺, 257.2 [M(⁸¹Br)+H]⁺.

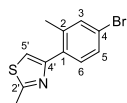
4-(4-Bromo-3-methyl-phenyl)-2-methyl-thiazole (177)



To 2-bromo-1-(4-bromo-3-methyl-phenyl)ethenone (**173**) (150 mg, 0.51 mmol) in *N,N*-dimethylformamide (1 mL) was added thioacetamide (58 mg, 0.78 mmol) and the reaction mixture stirred at ambient temperature for 16 h. The crude product was taken up in water (5 mL) and extracted with ethyl acetate (2 × 5 mL). The combined organic components were then washed with brine (5 mL), dried over MgSO₄, filtered and concentrated under reduced pressure. The crude product was purified by column chromatography (silica 12 g, 0 to 5% ethyl acetate in petroleum ether) to yield the desired compound **177** as a orange solid (144 mg, 99%).

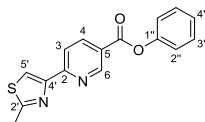
¹H-NMR (500 MHz, DMSO-*d*₆) δ 7.99 (s, 1H, H-5'), 7.93 (d, *J* 1.6, 1H, H-2), 7.69 (dd, *J* 8.3, 1.9, 1H, H-6), 7.62 (d, *J* 8.3, 1H, H-5), 2.71 (s, 3H, 2'-CH₃), 2.40 (s, 3H, 3-CH₃); **LCMS** (LCQ) Rt = 5.4 min (method 1), *m/z* (ESI⁺) 268.2 [M(⁷⁹Br)+H]⁺, 270.1 [M(⁸¹Br)+H]⁺.

4-(4-Bromo-2-methyl-phenyl)-2-methyl-thiazole (178)



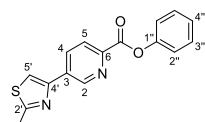
To 2-bromo-1-(4-bromo-2-methyl-phenyl)ethanone (**174**) (630 mg, 2.16 mmol) in *N,N*-dimethylformamide (6 mL) was added thioacetamide (243 mg, 3.24 mmol) and the reaction mixture stirred at ambient temperature for 16 h. The crude product was taken up in water (10 mL) and extracted with ethyl acetate (2 × 10 mL). The combined organic components were then washed with brine (5 mL), dried over MgSO₄, filtered and concentrated under reduced pressure. The crude product was purified by column chromatography (silica 12 g, 0 to 5% ethyl acetate in petroleum ether) to yield the desired compound **178** as a white solid (345 mg, 57%).

¹H-NMR (500 MHz, DMSO-*d*₆) δ 7.62 (s, 1H, H-5'), 7.53 (d, *J* 8.3, 1H, H-6), 7.51 (d, *J* 1.7, 1H, H-3), 7.42 (dd, *J* 8.3, 2.0, 1H, H-5), 2.68 (s, 3H, 2'-CH₃), 2.39 (s, 3H, 2-CH₃); **LCMS** (LCQ) Rt = 5.1 min (method 1), *m/z* (ESI⁺) 268.1 [M(⁷⁹Br)+H]⁺, 270.1 [M(⁸¹Br)+H]⁺.

Phenyl 6-(2-methylthiazol-4-yl)pyridine-3-carboxylate (179)

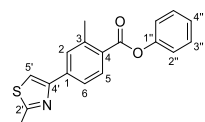
Compound **179** was synthesised according to general procedure W, using the following reagents: 4-(5-bromo-2-pyridyl)-2-methyl-thiazole (**175**) (300 mg, 1.18 mmol), phenyl formate (287 mg, 2.35 mmol), palladium(II) acetate (8 mg, 0.03 mmol), tri-tert-butylphosphonium tetrafluoroborate (41 mg, 0.12 mmol), triethylamine (328 μ L, 2.35 mmol) and acetonitrile (3 mL). The crude was purified by column chromatography (silica 12 g, 0 to 10% ethyl acetate in petroleum ether) to yield the desired product **179** as a yellow solid (266 mg, 69%).

¹H-NMR (500 MHz, DMSO-*d*₆) δ 9.26 (d, *J* 0.9, 1H, H-6), 8.56 (dd, *J* 8.3, 2.0, 1H, H-4), 8.36 (s, 1H, H-5'), 8.24 (d, *J* 8.3, 1H, H-3), 7.50 (app t, *J* 7.8, 2H, H-2''), 7.36 – 7.30 (m, 3H, H-3'', H-4''), 2.77 (s, 3H, ArCH₃); **LCMS** (LCQ) Rt = 4.3 min (method 1), *m/z* (ESI⁺) 297.2 [M+H]⁺.

Phenyl 5-(2-methylthiazol-4-yl)pyridine-2-carboxylate (180)

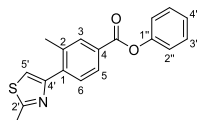
Compound **180** was synthesised according to general procedure W, using the following reagents: 4-(6-bromo-3-pyridyl)-2-methyl-thiazole (**176**) (300 mg, 1.18 mmol), phenyl formate (287 mg, 2.35 mmol), palladium(II) acetate (8 mg, 0.03 mmol), tri-tert-butylphosphonium tetrafluoroborate (41 mg, 0.12 mmol), triethylamine (328 μ L, 2.35 mmol) and acetonitrile (3 mL). The crude was purified by column chromatography (silica 12 g, 0 to 30% ethyl acetate in petroleum ether) to yield the desired product **180** as a white solid (196 mg, 53%).

¹H-NMR (500 MHz, DMSO-*d*₆) δ 9.36 (s, 1H, H-2), 8.55 (d, *J* 9.1, 1H, H-5), 8.39 (s, 1H, H-5'), 8.30 (d, *J* 8.2, 1H, H-4), 7.50 (app t, *J* 7.5, 2H, H-2''), 7.39 – 7.25 (m, 3H, H-3'', H-4''), 2.77 (s, 3H, CH₃); **LCMS** (LCQ) Rt = 3.5 min (method 1), *m/z* (ESI⁺) 297.0 [M+H]⁺.

Phenyl 2-methyl-4-(2-methylthiazol-4-yl)benzoate (181)

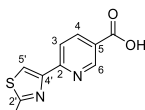
Compound **181** was synthesised according to general procedure X, using the following reagents: 4-(4-bromo-3-methyl-phenyl)-2-methyl-thiazole (**177**) (300 mg, 1.12 mmol), phenyl formate (251 μ L, 2.24 mmol), bis(benzonitrile)palladium(II) chloride (21 mg, 0.05 mmol), xantphos (32 mg, 0.06 mmol), triethylamine (311 μ L, 2.24 mmol) and *N,N*-dimethylformamide (1 mL). The crude was purified by column chromatography (silica 12 g, 0 to 10% ethyl acetate in petroleum ether) to yield the desired product **181** as a white solid (520 mg, 90%).

¹H-NMR (500 MHz, DMSO-*d*₆) δ 8.18 (s, 1H, H-2), 8.16 (d, *J* 8.2, 1H, H-5), 8.00 (s, 1H, H-5'), 7.97 (d, *J* 8.2, 1H, H-6), 7.48 (app t, *J* 7.7, 2H, H-2''), 7.34 – 7.26 (m, 3H, H-3'', H-4''), 2.74 (s, 3H, 2'-CH₃), 2.65 (s, 3H, 3-CH₃); **LCMS** (LCQ) Rt = 5.4 min (method 1), *m/z* (ESI⁺) 310.2 [M+H]⁺.

Phenyl 3-methyl-4-(2-methylthiazol-4-yl)benzoate (182)

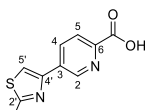
Compound **182** was synthesised according to general procedure X, using the following reagents: 4-(4-bromo-3-methyl-phenyl)-2-methyl-thiazole (**178**) (500 mg, 1.86 mmol), phenyl formate (418 μ L, 3.73 mmol), bis(benzonitrile)palladium(II) chloride (36 mg, 0.95 mmol), xantphos (54 mg, 0.09 mmol), triethylamine (520 μ L, 3.73 mmol) and *N,N*-dimethylformamide (5 mL). The crude was purified by column chromatography (silica 12 g, 0 to 15% ethyl acetate in petroleum ether) to yield the desired product **182** as a clear liquid (520 mg, 63%).

¹H-NMR (500 MHz, DMSO-*d*₆) δ 8.06 (s, 1H, H-5'), 8.01 (d, *J* 8.0, 1H, H-5), 7.88 (d, *J* 8.1, 1H, H-6), 7.83 (s, 1H, H-3), 7.49 (app t, *J* 7.9, 2H, H-2'), 7.36 – 7.23 (m, 3H, H-3'', H-4''), 2.74 (s, 3H, 2'-CH₃), 2.56 (s, 3H, 2-CH₃); LCMS (LCQ) Rt = 5.4 min (method 1), *m/z* (ESI⁺) 310.2 [M+H]⁺.

6-(2-Methylthiazol-4-yl)pyridine-3-carboxylic acid (183)

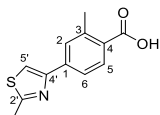
To phenyl 6-(2-methylthiazol-4-yl)pyridine-3-carboxylate (**179**) (260 mg, 0.88 mmol) in water (1 mL) and tetrahydrofuran (3 mL) was added sodium hydroxide (351 mg, 8.77 mmol) and the reaction mixture stirred at an ambient temperature for 16 h. The solvent was removed under reduced pressure. The crude product was taken up in water (5 mL) and washed with ethyl acetate (5 mL). The aqueous components were acidified to pH of 2-3 using 2 M aq. hydrochloric acid solution. The resulting precipitate was collected by vacuum filtration and dried under reduced pressure to afford the desired acid **183** as a yellow solid (108 mg, 50%).

¹H-NMR (500 MHz, DMSO-*d*₆) δ 9.07 (d, *J* 2.0, 1H, H-6), 8.35 (dd, *J* 8.2, 2.2, 1H, H-4), 8.27 (s, 1H, H-3), 8.15 (s, 1H, H-5'), 2.75 (s, 3H, CH₃); LCMS (LCQ) Rt = 0.7 min (method 1), *m/z* (ESI⁺) 221.3 [M+H]⁺.

5-(2-Methylthiazol-4-yl)pyridine-2-carboxylic acid (184)

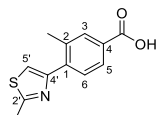
To phenyl 5-(2-methylthiazol-4-yl)pyridine-2-carboxylate (**180**) (200 mg, 0.67 mmol) in water (0.75 mL) and tetrahydrofuran (2.5 mL) was added sodium hydroxide (270 mg, 6.75 mmol) and the reaction mixture stirred at an ambient temperature for 16 h. The solvent was removed under reduced pressure. The crude product was taken up in water (5 mL) and washed with ethyl acetate (5 mL). The aqueous components were acidified to pH of 2-3 using 2 M aq. hydrochloric acid solution and were extracted with ethyl acetate (5 mL). The combined organic components were dried over MgSO₄, filtered and concentrated under reduced pressure to afford the desired acid **184** as an off-white solid (70 mg, 35%).

¹H-NMR (500 MHz, DMSO-*d*₆) δ 9.22 (s, 1H, H-2), 8.42 (d, *J* 7.9, 1H, H-4), 8.28 (s, 1H, H-5'), 8.08 (d, *J* 8.2, 1H, H-5), 2.75 (s, 3H, 2'-CH₃); LCMS (LCQ) Rt = 0.6 min (method 1), *m/z* (ESI⁺) 221.0 [M+H]⁺.

2-Methyl-4-(2-methylthiazol-4-yl)benzoic acid (185)

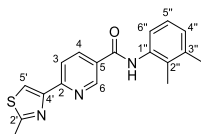
To phenyl 2-methyl-4-(2-methylthiazol-4-yl)benzoate (400 mg, 0.65 mmol) (**181**) in water (1.25 mL) and tetrahydrofuran (4 mL) was added sodium hydroxide (259 mg, 6.46 mmol) and the reaction mixture stirred at an ambient temperature for 16 h and at 50 °C for 1 h. The solvent was removed under reduced pressure. The crude product was taken up in water (15 mL) and washed with ethyl acetate (15 mL). The aqueous components were acidified to pH of 2-3 using 2 M aq. hydrochloric acid solution and were extracted with ethyl acetate (15 mL). The combined organic components were dried over MgSO_4 , filtered and concentrated under reduced pressure to afford the desired acid **185** as an off-white solid (65 mg, 41%).

$^1\text{H-NMR}$ (500 MHz, $\text{DMSO}-d_6$) δ 8.08 (s, 1H, H-5'), 7.88 (m, 2H, H-2, H-5), 7.83 (d, J 8.6, 1H, H-6), 2.73 (s, 3H, 2'- CH_3), 2.58 (s, 3H, 3- CH_3); **LCMS** (LCQ) R_t = 2.9 min (method 1), m/z (ESI^+) 234.2 $[\text{M}+\text{H}]^+$.

3-Methyl-4-(2-methylthiazol-4-yl)benzoic acid (186)

To phenyl 3-methyl-4-(2-methylthiazol-4-yl)benzoate (500 mg, 1.13 mmol) (**182**) in water (1.5 mL) and tetrahydrofuran (5 mL) was added sodium hydroxide (453 mg, 11.3 mmol) and the reaction mixture stirred at an ambient temperature for 5 h. The solvent was removed under reduced pressure. The crude product was taken up in water (15 mL) and washed with ethyl acetate (15 mL). The aqueous components were acidified to pH of 2-3 using 2 M aq. hydrochloric acid solution and were extracted with ethyl acetate (15 mL). The combined organic components were dried over MgSO_4 , filtered and concentrated under reduced pressure to afford the desired acid **186** as an off-white solid (390 mg, 89%).

$^1\text{H-NMR}$ (500 MHz, $\text{DMSO}-d_6$) δ 12.26 (s, 1H, COOH), 7.86 (s, 1H, H-5'), 7.81 (d, J 7.6, 1H, H-6), 7.76 – 7.72 (m, 2H, H-3, H-5), 2.72 (s, 3H, 2'- CH_3), 2.48 (s, 3H, 3- CH_3); **LCMS** (LCQ) R_t = 2.7 min (method 1), m/z (ESI^+) 234.2 $[\text{M}+\text{H}]^+$.

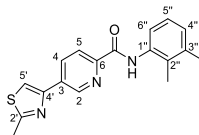
***N*-(2,3-dimethylphenyl)-6-(2-methylthiazol-4-yl)pyridine-3-carboxamide (187)**

Compound **187** was synthesised according to general procedure Z, using the following reagents: 5-(2-methylthiazol-4-yl)pyridine-2-carboxylic acid (**183**) (100 mg, 0.45 mmol), oxalyl chloride (58 μL , 0.68 mmol), *N,N*-dimethylformamide (10 μL) and dichloromethane (3 mL) and stirred for 16 h. Followed by 2,3-dimethylaniline (67 μL , 0.64 mmol), sodium hydride (60% dispersion in mineral oil) (26 mg, 1.09 mmol) and dichloromethane (1 mL) and stirred for 0.5 h. The crude was purified by column chromatography (silica 12 g, 0 to 40% ethyl acetate in petroleum ether), further purified by column chromatography (amino silica 12 g, 0 to 40% ethyl acetate in petroleum ether) to yield the desired amide **187** as a white solid (31 mg, 20%).

R_f 0.43 (petroleum ether:ethyl acetate 1:1); **m.p.** 184–186 °C; $^1\text{H-NMR}$ (500 MHz, $\text{DMSO}-d_6$) δ 10.14 (s, 1H, CONH), 9.15 (s, 1H, H-6), 8.42 (d, J 9.3, 1H, H-4), 8.27 (s, 1H, H-5'), 8.16 (d, J 8.6, 1H, H-3), 7.23 – 7.05 (m, 3H, H-4'', H-5'', H-6''), 2.76 (s, 3H, 2'- CH_3), 2.29 (s, 3H, 2''- CH_3), 2.13 (s, 3H, 3''- CH_3); $^{13}\text{C-NMR}$ (126 MHz, $\text{DMSO}-d_6$) δ 167.5 (CO), 164.6

(C-2'), 154.3 (ArC), 153.4 (ArC), 149.2 (C-6), 137.7 (C-4), 137.3 (ArC), 135.9 (ArC), 133.2 (ArC), 129.2 (ArC), 128.4 (ArC), 125.9 (ArC), 125.0 (ArC), 120.5 (C-3), 119.9 (C-5), 20.5 (2''-CH₃), 19.3 (2'-CH₃), 14.6 (3''-CH₃); **IR** (neat, ν_{\max} , cm⁻¹) 3245, 1636, 1610, 1500, 1447, 1294, 1173; **LCMS** (LCQ) Rt = 3.0 min (method 1), m/z (ESI⁺) 324.3 [M+H]⁺; **HRMS** m/z (ESI): calcd. for C₁₈H₁₈N₃O₂S [M+H]⁺ 324.1165, found 324.1174.

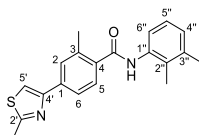
***N*-(2,3-dimethylphenyl)-5-(2-methylthiazol-4-yl)pyridine-2-carboxamide (188)**



Compound **188** was synthesised according to general procedure Z, using the following reagents: 5-(2-methylthiazol-4-yl)pyridine-2-carboxylic acid (**184**) (70 mg, 0.32 mmol), oxalyl chloride (40 , 0.48 mmol), *N,N*-dimethylformamide (10 μ L) and dichloromethane (3 mL) and stirred for 3 h. Followed by 2,3-dimethylaniline (67 μ L, 0.64 mmol), sodium hydride (60% dispersion in mineral oil) (31 mg, 1.27 mmol) and dichloromethane (1 mL) and stirred for 16 h. The crude was purified by column chromatography (silica 12 g, 0 to 70% ethyl acetate in petroleum ether), further purified by column chromatography (amino silica 12 g, 0 to 85% ethyl acetate in petroleum ether) and triturated in methanol to yield the desired amide **188** as a white solid (24 mg, 22%).

R_f 0.49 (petroleum ether:ethyl acetate 3:1); **m.p.** 178–180 °C; **¹H-NMR** (500 MHz, DMSO-*d*₆) δ 10.29 (s, 1H, CONH), 9.28 (d, *J* 2.1, 1H, H-2), 8.54 (dd, *J* 8.2, 2.1, 1H, H-4), 8.31 (s, 1H, H-5'), 8.20 (d, *J* 8.2, 1H, H-5), 7.56 (d, *J* 7.8, 1H, H-6''), 7.13 (t, *J* 7.7, 1H, H-5''), 7.06 (d, *J* 7.4, 1H, H-4''), 2.77 (s, 3H, 2'-CH₃), 2.30 (s, 3H, 2''-CH₃), 2.19 (s, 3H, 3''-CH₃); **¹³C-NMR** (126 MHz, DMSO-*d*₆) δ 167.2 (CO), 162.4 (C-2'), 150.4 (ArC), 149.1 (ArC), 146.4 (C-2), 137.3 (ArC), 136.2 (C-4), 135.2 (ArC), 132.8 (ArC), 127.3 (C-4''), 125.9 (C-5''), 122.9 (C-5), 122.5 (C-6'), 117.8 (C-5'), 20.6 (2''-CH₃), 19.4 (2'-CH₃), 14.2 (3''-CH₃); **IR** (neat, ν_{\max} , cm⁻¹) 3251, 1637, 1535, 1500, 1447, 1293, 1173; **LCMS** (LCQ) Rt = 5.0 min (method 1), m/z (ESI⁺) 324.1 [M+H]⁺; **HRMS** m/z (ESI): calcd. for C₁₈H₁₈N₃O₂S [M+H]⁺ 324.1165, found 324.1160.

***N*-(2,3-dimethylphenyl)-2-methyl-4-(2-methylthiazol-4-yl)benzamide (189)**

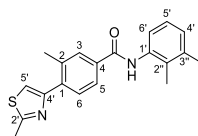


Compound **189** was synthesised according to general procedure Y, using the following reagents: : 4-(2-methyl-1,3-thiazol-4-yl)benzoic acid (**185**) (65 mg, 0.28 mmol), oxalyl chloride (35 μ L, 0.42 mmol), *N,N*-dimethylformamide (10 μ L) and dichloromethane (3 mL) and stirred for 16 h. Followed 2,3-dimethylaniline (41 μ L, 0.33 mmol), triethylamine (39 μ L, 0.28 mmol), 4-(dimethylamino)pyridine (3.4 mg, 0.28 mmol) and dichloromethane (1 mL) and stirred for 16 h. The crude was purified by column chromatography (silica 12 g, 0 to 20% ethyl acetate in petroleum ether) and further purified by column chromatography (amino silica 12 g, 0 to 20% ethyl acetate in petroleum ether) to yield the desired amide **189** as a white solid (28 mg, 28%).

R_f 0.61 (petroleum ether:ethyl acetate 3:1); **m.p.** 180–182 °C; **¹H-NMR** (500 MHz, DMSO-*d*₆) δ 9.87 (s, 1H, CONH), 8.04 (s, 1H, H-5'), 7.91 (s, 1H, H-2), 7.87 (d, *J* 7.8, 1H, H-5), 7.59 (d, *J* 7.8, 1H, H-6), 7.20 (d, *J* 7.5, 1H, ArH), 7.15 – 7.04 (m, 2H, 2 \times ArH), 2.74 (s, 3H, 2'-CH₃), 2.51 (s, 3H, 3-CH₃), 2.29 (s, 3H, 2''-CH₃), 2.17 (s, 3H, 3''-CH₃); **¹³C-NMR** (126 MHz, DMSO-*d*₆) δ 168.2 (CO), 166.2 (C-2'), 153.6 (ArC), 137.4 (ArC), 136.8 (ArC), 136.5 (ArC), 136.4 (ArC), 135.5 (ArC), 132.7 (ArC), 128.3 (C-5), 127.9 (C-6), 125.7 (ArC), 124.9 (ArC), 123.5 (ArC), 115.1 (C-5'), 110.0, 20.6 (2''-CH₃), 20.1(3-CH₃), 19.4 (2'-CH₃), 14.7 (3''-CH₃); **IR** (neat, ν_{\max} , cm⁻¹) 3267, 1693, 1652, 1594, 1565, 1478, 1438, 1385, 1308, 1272, 1177;

LCMS (LCQ) Rt = 4.3 min (method 1), m/z (ESI⁺) 337.1 [M+H]⁺; **HRMS** m/z (ESI): calcd. for C₂₀H₂₁N₂OS [M+H]⁺ 337.1369, found 337.1376.

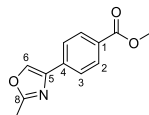
***N*-(2,3-dimethylphenyl)-3-methyl-4-(2-methylthiazol-4-yl)benzamide (190)**



Compound **190** was synthesised according to general procedure Z, using the following reagents: 3-methyl-4-(2-methylthiazol-4-yl)benzoic acid (**186**) (150 mg, 0.39 mmol), oxalyl chloride (49 μ L, 0.58 mmol), *N,N*-dimethylformamide (10 μ L) and dichloromethane (3 mL) and stirred for 16 h. Followed by 2,3-dimethylaniline (57 μ L, 0.46 mmol), sodium hydride (60% dispersion in mineral oil) (15 mg, 0.39 mmol) and dichloromethane (1 mL) and stirred for 2 h. The crude was purified by column chromatography (silica 12 g, 0 to 70% ethyl acetate in petroleum ether), further purified by column chromatography (amino silica 12 g, 0 to 60% ethyl acetate in petroleum ether) and triturated in methanol to yield the desired amide **190** as a white solid (37 mg, 27%).

R_f 0.58 (petroleum ether:ethyl acetate 3:1); **m.p.** 193–195 °C; **¹H-NMR** (500 MHz, DMSO-*d*₆) δ 9.96 (s, 1H, CONH), 7.91 (s, 1H, H-3), 7.86 (d, *J* 8.9, 1H, H-6), 7.76 (d, *J* 8.1, 1H, H-5), 7.73 (s, 1H, H-5'), 7.14 – 7.06 (m, 3H, H-4'', H-5'', H-6''), 2.74 (s, 3H, 2'-CH₃), 2.28 (s, 3H, 2''-CH₃), 2.10 (s, 3H, 3''-CH₃), 2-CH₃ under DMSO peak; **¹³C-NMR** (126 MHz, DMSO-*d*₆) δ 165.6 (ArC or CO), 165.1 (ArC or CO), 153.5 (ArC), 137.5 (ArC), 137.4 (ArC), 136.7 (ArC), 136.0 (ArC), 134.0 (ArC), 133.2 (ArC), 130.6 (C-3), 130.0 (H-5), 128.0 (ArC), 125.7 (ArC), 125.6 (ArC), 125.2 (ArC), 118.2 (C-5'), 21.7 (2-CH₃), 20.6 (2''-CH₃), 19.0 (2'-CH₃), 14.7 (3''-CH₃); **IR** (neat, ν_{\max} , cm⁻¹) 2543, 1670, 1603, 1566, 1421, 1307, 1257, 1171; **LCMS** (LCQ) Rt = 4.3 min (method 1), m/z (ESI⁺) 337.1 [M+H]⁺; **HRMS** m/z (ESI): calcd. for C₂₀H₂₁N₂OS [M+H]⁺ 337.1369, found 337.1212.

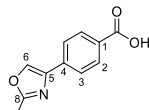
Methyl 4-(2-methyloxazol-4-yl)benzoate (191)



Methyl 4-(2-bromoacetyl)benzoate (**100**) (400 mg, 1.56 mmol) was stirred in neat acetamide (276 mg, 4.67 mmol) at 160 °C for 2 h. Water was added to the reaction mixture. The resulting precipitate was collected by vacuum filtration and dried under reduced pressure to afford the desired compound **191** as a brown solid (308 mg, 87%) which was carried forward without further purification.

¹H-NMR (500 MHz, DMSO-*d*₆) δ 8.07 (s, 1H, H-6), 8.00 (d, *J* 8.2, 2H, H-3), 7.89 (d, *J* 8.1, 2H, H-2), 3.86 (s, 3H, OCH₃), 2.48 (s, 3H, 8-CH₃).

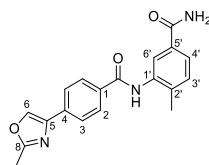
4-(2-Methyloxazol-4-yl)benzoic acid (192)



To methyl 4-(2-methyloxazol-4-yl)benzoate (**191**) (279 mg, 1.2 mmol) in methanol (5 mL) and water (1.5 mL) was added sodium hydroxide (150 mg, 3.86 mmol) and the reaction mixture stirred at ambient temperature for 16 h. Upon completion, the reaction mixture was acidified to pH of 2-3 using 2 M aq. hydrochloric acid solution. The resulting precipitate was collected by vacuum filtration and dried under reduced pressure to afford the desired acid **192** as a white solid (130 mg, 47%).

¹H-NMR (500 MHz, DMSO-*d*₆) δ 8.56 (s, 1H, 11, H-6), 7.97 (d, *J* 8.0, 2H, H-3), 7.85 (d, *J* 8.0, 2H, H-2), 2.47 (s, 3H, 8-CH₃); **LCMS** (LCQ) Rt = 0.5 min (method 1), *m/z* (ESI⁺) 204.2 [M+H]⁺.

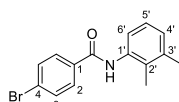
4-Methyl-3-((4-(2-methyloxazol-4-yl)benzoyl)amino)benzamide (193)



Compound **193** was synthesised according to general procedure M, using the following reagents: 4-(2-methyloxazol-4-yl)benzoic acid (**192**) (110 mg, 0.54 mmol), oxalyl chloride (0.05 mL, 0.65 mmol), *N,N*-dimethylformamide (10 μL) and dichloromethane (3 mL) and stirred for 16 h. Followed by 3-amino-4-methylbenzamide (98 mg, 0.65 mmol), *N,N*-diisopropylethylamine (0.47 mL, 2.71 mmol) and DCM (1 mL) and stirred for 16 h. The crude was purified by column chromatography (silica 12 g, 0 to 5% methanol in dichloromethane) to yield the desired amide **193** as a white solid (55 mg, 29%).

R_f 0.28 (dichloromethane:methanol 19:1); **m.p.** 260–262 °C; **¹H-NMR** (500 MHz, DMSO-*d*₆) δ 10.00 (s, 1H, CONH), 8.61 (s, 1H, H-6), 8.05 (d, *J* 8.1, 2H, H-3), 7.91 (d, *J* 8.4, 3H, H-2, 5'-CONH_{AB}), 7.86 (s, 1H, H-6'), 7.70 (dd, *J* 7.9, 1.9, 1H, H-4'), 7.35 (d, *J* 7.9, 1H, H-3'), 7.27 (s, 1H, 5'-CONH_{AB}) 2.28 (s, 3H, 2'-CH₃). 8-CH₃ under DMSO peak; **¹³C-NMR** (126 MHz, DMSO-*d*₆) δ 167.8 (CO), 165.4 (CO), 162.2 (C-8), 139.4 (C-5), 137.9 (C-2'), 136.8 (ArC), 136.3 (ArC), 134.6 (C-1), 133.8 (C-4), 132.8 (C-5'), 130.6 (C-3'), 128.7 (C-2), 126.6 (C-6'), 125.5 (C-4'), 125.33 (C-3), 18.4 (8-CH₃), 14.0 (2'-CH₃); **IR** (neat, ν_{max}, cm⁻¹) 3255, 1673, 1635, 1616, 1522, 1489, 1386, 1276, 1214; **LCMS** (LCQ) Rt = 0.8 min (method 1), *m/z* (ESI⁺) 336.1 [M+H]⁺; **HRMS (ESI)**: calcd. for C₁₉H₁₇N₃NaO₃ [M+Na]⁺ 358.1162, found 358.1150.

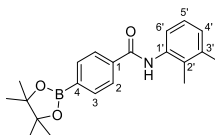
4-Bromo-*N*-(2,3-dimethylphenyl)benzamide (194)



Compound **194** was synthesised according to general procedure R, using the following reagents: *p*-bromobenzoic acid (200 mg, 0.99 mmol), HATU (454 mg, 1.19 mmol), *N,N*-diisopropylethylamine (347 μL, 1.99 mmol), 2,3-dimethylaniline (146 μL, 1.19 mmol) and *N,N*-dimethylformamide (3 mL). The crude was purified by column chromatography (silica, 0 to 10% ethyl acetate in petroleum ether) to yield the desired compound **194** as a white solid (277 mg, 87%).

¹H-NMR (500 MHz, DMSO-*d*₆) δ 9.98 (s, 1H, CONH), 7.92 (d, *J* 8.3, 2H, H-2), 7.74 (d, *J* 8.5, 2H, H-3), 7.13 – 7.08 (m, 3H, H-4', H-5', H-6'), 2.28 (s, 3H, 2'-CH₃), 2.09 (s, 3H, 3'-CH₃); **LCMS** (LCQ) Rt = 3.2 min (method 1), *m/z* (ESI⁺) 304.1 [M(⁷⁹Br)+H]⁺, 306.2 [M(⁸¹Br)+H]⁺.

N-(2,3-dimethylphenyl)-4-(4,4,5,5-tetramethyl-1,3,2-dioxaborolan-2-yl)benzamide (195)

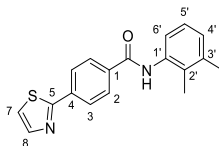


Compound **195** was synthesised according to general procedure U, using the following reagents: 4-bromo-*N*-(2,3-dimethylphenyl)benzamide (**194**) (200 mg, 0.66 mmol), bis(pinacolato)diboron (200 mg, 0.79 mmol), (1,1'-bis(diphenylphosphino)ferrocene)dichloropalladium(II) (24 mg, 0.03 mmol), potassium acetate (194 mg,

1.97 mmol) and 1,4-dioxane (1 mL) and stirred for 3 h. The crude was purified by column chromatography (silica 12 g, 0 to 20% ethyl acetate in petroleum ether) to yield the desired product **195** as a yellow solid (168 mg, 65%).

¹H-NMR (500 MHz, DMSO-*d*₆) δ 9.97 (s, 1H, CONH), 7.98 (d, *J* 7.6, 2H, H-2), 7.80 (d, *J* 7.6, 2H, H-3), 7.14 – 7.04 (m, 3H, H-4', H-5', H-6'), 2.28 (s, 3H, 2'-CH₃), 2.09 (s, 3H, 3'-CH₃), 1.32 (s, 12H, B(OC(CH₃)₂)₂); **LCMS** (LCQ) Rt = 3.7 min (method 1), *m/z* (ESI⁺) 352.2 [M+H]⁺.

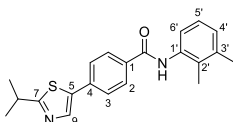
***N*-(2,3-dimethylphenyl)-4-thiazol-2-yl-benzamide (196)**



Compound **196** was synthesised according to general procedure V, using the following reagents: *N*-(2,3-dimethylphenyl)-4-(4,4,5,5-tetramethyl-1,3,2-dioxaborolan-2-yl)benzamide (**195**) (80 mg, 0.23 mmol), 2-bromo-1,3-thiazole (37 mg, 0.23 mmol), (1,1'-bis(diphenylphosphino)ferrocene)dichloropalladium(II) (17 mg, 0.02 mmol), sodium carbonate (242 mg, 2.28 mmol), 1,4-dioxane (1.5 mL) and water (1.5 mL). The crude was purified by column chromatography (silica 12 g, 0 to 30% ethyl acetate in petroleum ether) and further purified by column chromatography (amino silica 12 g, 0 to 70% ethyl acetate in petroleum ether) to yield the desired product **196** as a white solid (37 mg, 50%).

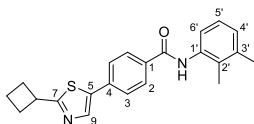
R_f 0.33 (petroleum ether:ethyl acetate 3:1); **m.p.** 198–200 °C; **¹H-NMR** (500 MHz, DMSO-*d*₆) δ 10.05 (s, 1H, CONH), 8.13 – 8.08 (m, 4H, H-2, H-3), 8.02 – 7.99 (m, 1H, H-7), 7.90 – 7.87 (m, 1H, H-8), 7.16 – 7.12 (m, 1H, H-5'), 7.12 – 7.06 (m, 2H, H-4', H-6'), 2.29 (s, 3H, 2'-CH₃), 2.11 (s, 3H, 3'-CH₃). **¹³C-NMR** (126 MHz, DMSO-*d*₆) δ 166.6 (C-5 or CO), 165.2 (C-5 or CO), 144.6 (C-8), 137.5 (ArC), 136.6 (ArC), 136.2 (ArC), 136.0 (ArC), 133.2 (ArC), 129.1 (C-3), 128.1 (ArC), 126.6 (C-2), 125.7 (ArC), 125.1 (C-7), 121.9 (ArC), 20.6 (2'-CH₃), 14.7 (3'-CH₃); **IR** (neat, *v*_{max}, cm⁻¹) 3298, 1677, 1624, 1610, 1544, 1524, 1419, 1274, 1250; **LCMS** (LCQ) Rt = 3.7 min (method 1), *m/z* (ESI⁺) 309.1 [M+H]⁺; **HRMS (ESI)**: calcd. for C₁₈H₁₇NOS [M+Na]⁺ 309.1056, found 309.1062.

***N*-(2,3-dimethylphenyl)-4-(2-isopropylthiazol-5-yl)benzamide (197)**



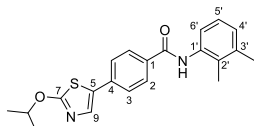
Compound **197** was synthesised according to general procedure V, using the following reagents: 4-bromo-*N*-(2,3-dimethylphenyl)benzamide (**194**) (100 mg, 0.33 mmol), 2-(propan-2-yl)-5-(tetramethyl-1,3,2-dioxaborolan-2-yl)-1,3-thiazole (166 mg, 0.66 mmol), (1,1'-bis(diphenylphosphino)ferrocene)dichloropalladium(II) (24 mg, 0.03 mmol), sodium carbonate (348 mg, 3.30 mmol), 1,4-dioxane (1.5 mL) and water (1.5 mL). The crude was purified by column chromatography (silica 12 g, 0 to 50% ethyl acetate in petroleum ether) to yield the desired product **197** as an off-white solid (54 mg, 45%).

R_f 0.29 (petroleum ether:ethyl acetate 3:1); **m.p.** 186–188 °C; **¹H-NMR** (500 MHz, DMSO-*d*₆) δ 9.96 (s, 1H, CONH), 8.20 (s, 1H, H-9), 8.04 (d, *J* 8.1, 2H, H-3), 7.79 (d, *J* 8.2, 2H, H-2), 7.15 – 7.06 (m, 3H, H-4', H-5', H-6'), 3.91 – 3.89 (m, 1H, CH(CH₃)₂), 2.29 (s, 3H, 2'-CH₃), 2.11 (s, 3H, 3'-CH₃), 1.38 (d, *J* 6.9, 6H, CH(CH₃)₂); **¹³C-NMR** (126 MHz, DMSO-*d*₆) δ 177.6 (CO), 165.2 (C-7), 139.6 (C-9), 137.4 (ArC), 136.9 (ArC), 136.8 (ArC), 134.5 (ArC), 134.2 (ArC), 133.2 (ArC), 129.1 (C-3), 128.0 (ArC), 126.5 (C-2), 125.7 (ArC), 125.2 (ArC), 33.2 (CH(CH₃)₂), 23.2 (CH(CH₃)₂), 20.6 (2'-CH₃), 14.7 (3'-CH₃); **IR** (neat, *v*_{max}, cm⁻¹) 3280, 1650, 1604, 1524, 1452, 1300, 1279; **LCMS** (LCQ) Rt = 3.8 min (method 1), *m/z* (ESI⁺) 351.2 [M+H]⁺; **HRMS (ESI)**: calcd. for C₂₁H₂₂N₂NaOS [M+Na]⁺ 373.1345, found 373.1341.

4-(2-Cyclobutylthiazol-5-yl)-*N*-(2,3-dimethylphenyl)benzamide (198)

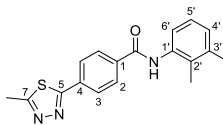
Compound **198** was synthesised according to general procedure V, using the following reagents: 4-bromo-*N*-(2,3-dimethylphenyl)benzamide (**194**) (100 mg, 0.33 mmol), 2-cyclobutyl-5-(tetramethyl-1,3,2-dioxaborolan-2-yl)-1,3-thiazole (174 mg, 0.66 mmol), (1,1'-bis(diphenylphosphino)ferrocene)dichloropalladium(II) (24 mg, 0.03 mmol), sodium carbonate (348 mg, 3.30 mmol), 1,4-dioxane (1.5 mL) and water (1.5 mL). The crude was purified by column chromatography (silica 12 g, 0 to 40% ethyl acetate in petroleum ether) to yield the desired product **198** as a pale yellow solid (58 mg, 46%).

R_f 0.37 (petroleum ether:ethyl acetate 3:1); **m.p.** 183–185 °C; **¹H-NMR** (500 MHz, DMSO-*d*₆) δ 9.95 (s, 1H), 8.22 (s, 1H), 8.03 (d, *J* 8.0, 2H), 7.79 (d, *J* 8.1, 2H), 7.16–7.05 (m, 3H), 3.89 (p, *J* 8.4, 1H), 2.29 (s, 3H), 2.11 (s, 3H), 1.08–1.06 (m, 6H); **¹³C-NMR** (126 MHz, DMSO-*d*₆) δ 139.8, 137.5, 137.2, 136.5, 134.2, 133.2, 129.0, 128.1, 126.5, 125.8, 125.1, 110.0, 38.1, 29.9, 25.3, 20.5, 18.3, 14.6. CO and ArC not visible; **IR** (neat, *v*_{max}, cm⁻¹) 3283, 1643, 1607, 1520, 1506, 1452, 1307, 1279; **LCMS** (LCQ) *R*_t = 4.9 min (method 1), *m/z* (ESI⁺) 363.2 [M+H]⁺; **HRMS (ESI)**: calcd. for C₂₂H₂₂N₂NaOS [M+Na]⁺ 385.1345, found 385.1347.

***N*-(2,3-dimethylphenyl)-4-(2-isopropoxythiazol-5-yl)benzamide (199)**

Compound **199** was synthesised according to general procedure V, using the following reagents: 4-bromo-*N*-(2,3-dimethylphenyl)benzamide (**194**) (100 mg, 0.33 mmol), 2-isopropoxy-5-(4,4,5,5-tetramethyl-1,3,2-dioxaborolan-2-yl)thiazole (178 mg, 0.66 mmol), (1,1'-bis(diphenylphosphino)ferrocene)dichloropalladium(II) (24 mg, 0.03 mmol), sodium carbonate (348 mg, 3.30 mmol), 1,4-dioxane (1.5 mL) and water (1.5 mL). The crude was purified by column chromatography (silica 12 g, 0 to 55% ethyl acetate in petroleum ether) and further purified by column chromatography (amino silica 12 g, 0 to 20% ethyl acetate in petroleum ether) to yield the desired product **199** as a white solid (52 mg, 41%).

R_f 0.39 (petroleum ether:ethyl acetate 3:1); **m.p.** 219–221 °C; **¹H-NMR** (500 MHz, DMSO-*d*₆) δ 9.92 (s, 1H), 8.00 (d, *J* 8.0, 2H), 7.77 (s, 1H), 7.67 (d, *J* 8.0, 2H), 5.18 (hept, *J* 6.2, 5.6, 1H), 2.29 (s, 3H), 2.10 (s, 3H), 1.39 (d, *J* 6.2, 6H); **¹³C-NMR** (126 MHz, DMSO-*d*₆) δ 173.3, 165.4, 137.5, 136.6, 134.8, 133.6, 133.2, 129.4, 128.9, 128.1, 125.7, 125.6, 125.2, 110.0, 76.5, 22.0, 20.5, 14.6; **IR** (neat, *v*_{max}, cm⁻¹) 3283, 1640, 1611, 1520, 1499, 1456, 1304, 1275, 1253; **LCMS** (LCQ) *R*_t = 5.1 min (method 1), *m/z* (ESI⁺) 367.1 [M+H]⁺; **HRMS (ESI)**: calcd. for C₂₁H₂₂N₂NaO₂S [M+Na]⁺ 389.1294, found 389.1298.

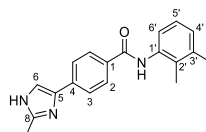
***N*-(2,3-dimethylphenyl)-4-(5-methyl-1,3,4-thiadiazol-2-yl)benzamide (200)**

Compound **200** was synthesised according to general procedure V, using the following reagents: *N*-(2,3-dimethylphenyl)-4-(4,4,5,5-tetramethyl-1,3,2-dioxaborolan-2-yl)benzamide (**195**) (100 mg, 0.33 mmol), 2-bromo-5-methyl-1,3,4-thiadiazole (51 mg, 0.33 mmol), (1,1'-bis(diphenylphosphino)ferrocene)dichloropalladium(II) (24 mg,

0.03 mmol), sodium carbonate (348 mg, 3.30 mmol), 1,4-dioxane (1.5 mL) and water (1.5 mL). The crude was purified by column chromatography (silica 12 g, 0 to 35% ethyl acetate in petroleum ether) to yield the desired product **200** as a white solid (23 mg, 24%).

R_f 0.22 (petroleum ether:ethyl acetate 3:1); **m.p.** 210–212 °C; **¹H-NMR** (500 MHz, DMSO-*d*₆) δ 10.09 (s, 1H), 8.13 (d, *J* 8.3, 2H), 8.09 (d, *J* 8.1, 2H), 7.17–7.06 (m, 3H), 2.81 (s, 3H), 2.29 (s, 3H), 2.11 (s, 3H); **¹³C-NMR** (126 MHz, DMSO-*d*₆) δ 167.8, 166.5, 165.1, 137.5, 137.0, 136.5, 133.2, 132.7, 129.1, 128.2, 128.0, 125.8, 125.1, 20.6, 15.8, 14.7; **IR** (neat, ν_{\max} , cm⁻¹) 3099, 1623, 1604, 1473, 1418, 1367, 1300, 1173; **LCMS** (LCQ) *R*_t = 2.9 min (method 1), *m/z* (ESI⁺) 324.2 [M+H]⁺; **HRMS (ESI)**: calcd. for C₁₈H₁₈N₃OS [M+H]⁺ 324.1165, found 324.1164.

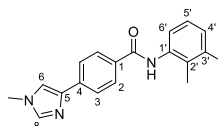
***N*-(2,3-dimethylphenyl)-4-(2-methyl-1H-imidazol-4-yl)benzamide (201)**



Compound **201** was synthesised according to general procedure V, using the following reagents: *N*-(2,3-dimethylphenyl)-4-(4,4,5,5-tetramethyl-1,3,2-dioxaborolan-2-yl)benzamide (**195**) (100 mg, 0.33 mmol), 4-bromo-2-methyl-1H-imidazole (46 mg, 0.33 mmol), (1,1'-bis(diphenylphosphino)ferrocene)dichloropalladium(II) (24 mg, 0.03 mmol), sodium carbonate (348 mg, 3.30 mmol), 1,4-dioxane (1.5 mL) and water (1.5 mL). The crude was purified by column chromatography (amino silica 12 g, 0 to 5% ethyl acetate in petroleum ether) to yield the desired product **201** as a brown solid (26 mg, 28%).

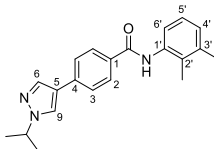
R_f 0.22 (petroleum ether:ethyl acetate 3:1); **m.p.** 145–147 °C; **¹H-NMR** (500 MHz, DMSO-*d*₆) δ 9.85 (s, 1H), 7.96 (d, *J* 7.8, 2H), 7.84 (d, *J* 8.2, 2H), 7.61 (d, *J* 5.9, 1H), 7.16–7.03 (m, 3H), 2.35 (s, 3H), 2.28 (s, 3H), 2.10 (s, 3H); **IR** (neat, ν_{\max} , cm⁻¹) 3306, 1677, 1624, 1610, 1544, 1419, 1272, 1167; **LCMS** (LCQ) *R*_t = 0.5 min (method 1), *m/z* (ESI⁺) 306.2 [M+H]⁺; **HRMS (ESI)**: calcd. for C₁₉H₂₀N₃O [M+H]⁺ 306.1601, found 306.1605.

***N*-(2,3-dimethylphenyl)-4-(1-methylimidazol-4-yl)benzamide (202)**



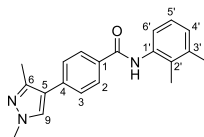
Compound **202** was synthesised according to general procedure V, using the following reagents: *N*-(2,3-dimethylphenyl)-4-(4,4,5,5-tetramethyl-1,3,2-dioxaborolan-2-yl)benzamide (**195**) (80 mg, 0.23 mmol), 4-bromo-1-methyl-1H-imidazole (37 mg, 0.23 mmol), (1,1'-bis(diphenylphosphino)ferrocene)dichloropalladium(II) (17 mg, 0.02 mmol), sodium carbonate (242 mg, 2.28 mmol), 1,4-dioxane (1.5 mL) and water (1.5 mL). The crude was purified by column chromatography (silica 12 g, 0 to 100% ethyl acetate in petroleum ether) to yield the desired product **202** as a white solid (29 mg, 40%).

R_f 0.13 (ethyl acetate); **m.p.** 240–242 °C; **¹H-NMR** (500 MHz, DMSO-*d*₆) δ 9.85 (s, 1H), 7.99–7.93 (m, 2H), 7.88–7.83 (m, 2H), 7.75 (s, 1H), 7.68 (s, 1H), 7.15–7.03 (m, 3H), 3.71 (s, 3H), 2.28 (s, 3H), 2.10 (s, 3H); **¹³C-NMR** (126 MHz, DMSO-*d*₆) δ 165.7, 140.2, 139.3, 138.1, 137.4, 136.8, 133.2, 132.4, 128.5, 127.9, 125.7, 125.2, 124.2, 118.7, 33.6, 20.6, 14.7; **IR** (neat, ν_{\max} , cm⁻¹) 3281, 1677, 1623, 1610, 1545, 1525, 1419, 1249, 1206, 1167; **LCMS** (LCQ) *R*_t = 0.6 min (method 1), *m/z* (ESI⁺) 306.2 [M+H]⁺; **HRMS (ESI)**: calcd. for C₁₉H₂₀N₃O [M+H]⁺ 306.1601, found 306.1603.

***N*-(2,3-dimethylphenyl)-4-(1-isopropylpyrazol-4-yl)benzamide (203)**

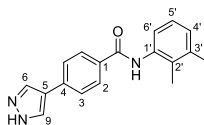
Compound **203** was synthesised according to general procedure V, using the following reagents: 4-bromo-*N*-(2,3-dimethylphenyl)benzamide (**195**) (100 mg, 0.33 mmol), 1-isopropyl-1H-pyrazole-4-boronic acid pinacol ester (155 mg, 0.66 mmol), (1,1'-bis(diphenylphosphino)ferrocene)dichloropalladium(II) (24 mg, 0.03 mmol), sodium carbonate (348 mg, 3.30 mmol), 1,4-dioxane (1.5 mL) and water (1.5 mL). The crude was purified by column chromatography (silica 12 g, 0 to 55% ethyl acetate in petroleum ether) and further purified by column chromatography (amino silica 12 g, 0 to 60% ethyl acetate in petroleum ether) to yield the desired product **203** as an off-white solid (60 mg, 52%).

R_f 0.47 (petroleum ether:ethyl acetate 1:1); **m.p.** 200–202 °C; **¹H-NMR** (500 MHz, DMSO-*d*₆) δ 9.85 (s, 1H), 8.35 (s, 1H), 8.00 – 7.91 (m, 3H), 7.73 (dd, *J* 8.2, 2.2, 2H), 7.16 – 7.04 (m, 3H), 4.52 (hept, *J* 14.2, 7.4, 1H), 2.29 (s, 3H), 2.11 (s, 3H), 1.47 (d, *J* 6.6, 6H); **¹³C-NMR** (126 MHz, DMSO-*d*₆) δ 165.5, 137.4, 136.9, 136.4, 133.2, 132.1, 128.7, 127.9, 125.9, 125.7, 125.2, 125.0, 121.1, 110.0, 53.7, 23.1, 20.6, 14.7; **IR** (neat, *v*_{max}, cm⁻¹) 3291, 1647, 1611, 1521, 1452, 1311, 1282; **LCMS** (LCQ) *R*_t = 2.9 min (method 1), *m/z* (ESI⁺) 334.2 [M+H]⁺; **HRMS (ESI)**: calcd. for C₂₁H₂₃N₃NaO [M+Na]⁺ 356.1733, found 356.1731.

***N*-(2,3-dimethylphenyl)-4-(1,3-dimethylpyrazol-4-yl)benzamide (204)**

Compound **204** was synthesised according to general procedure T, using the following reagents: 4-bromo-*N*-(2,3-dimethylphenyl)benzamide (**194**) (100 mg, 0.33 mmol), 1,3-dimethyl-1H-pyrazole-4-boronic acid pinacol ester (146 mg, 0.66 mmol), tetrakis(triphenylphosphine)palladium(0) (38 mg, 0.03 mmol), caesium carbonate (857 mg, 2.63 mmol), dimethoxyethane (4 mL) and water (1 mL). The crude was purified by column chromatography (silica 12 g, 0 to 60% ethyl acetate in petroleum ether) and further purified by column chromatography (amino silica 12 g, 0 to 80% ethyl acetate in petroleum ether) to yield the desired product **204** as a white solid (23 mg, 21%).

R_f 0.21 (petroleum ether:ethyl acetate 1:1); **m.p.** 216–218 °C; **¹H-NMR** (500 MHz, DMSO-*d*₆) δ 9.86 (s, 1H), 8.01 (s, 1H), 7.99 (d, *J* 8.1, 2H), 7.56 (d, *J* 8.1, 2H), 7.16 – 7.05 (m, 3H), 3.80 (s, 3H), 2.34 (s, 3H), 2.29 (s, 3H), 2.11 (s, 3H); **¹³C-NMR** (126 MHz, DMSO-*d*₆) δ 165.6, 144.9, 137.4, 137.2, 136.8, 133.2, 132.0, 130.6, 128.5, 127.9, 126.7, 125.7, 125.2, 119.3, 110.0, 20.6, 14.6, 13.8; **IR** (neat, *v*_{max}, cm⁻¹) 3287, 1640, 1611, 1520, 1506, 1452, 1307, 1282; **LCMS** (LCQ) *R*_t = 0.6 min (method 1), *m/z* (ESI⁺) 320.2 [M+H]⁺; **HRMS (ESI)**: calcd. for C₂₀H₂₁N₃NaO [M+Na]⁺ 342.1577, found 342.1576.

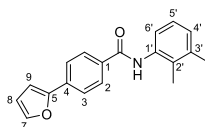
***N*-(2,3-dimethylphenyl)-4-(1H-pyrazol-4-yl)benzamide (205)**

Compound **205** was synthesised according to general procedure V, using the following reagents: 4-bromo-*N*-(2,3-dimethylphenyl)benzamide (**194**) (100 mg, 0.33 mmol), furan-2-boronic acid (127 mg, 0.66 mmol), (1,1'-

bis(diphenylphosphino)ferrocene)dichloropalladium(II) (24 mg, 0.03 mmol), sodium carbonate (348 mg, 3.30 mmol), 1,4-dioxane (1.5 mL) and water (1.5 mL). The crude was purified by column chromatography (silica 12 g, 0 to 35% ethyl acetate in petroleum ether) to yield the desired product **205** as a white solid (32 mg, 32%).

R_f 0.13 (petroleum ether:ethyl acetate 3:1); **m.p.** >300 °C; **¹H-NMR** (500 MHz, DMSO-*d*₆) δ 9.93 (s, 1H), 8.04 (d, *J* 8.1, 2H), 7.87 – 7.80 (m, 3H), 7.17 – 7.05 (m, 4H), 6.68 – 6.62 (m, 1H), 2.29 (s, 3H), 2.11 (s, 3H); **¹³C-NMR** (126 MHz, DMSO-*d*₆) δ 137.4, 136.6, 133.2, 128.7, 127.9, 125.7, 125.2, 120.9, 110.0, 20.6, 14.7. CO and 2 × ArC not visible; **IR** (neat, *v*_{max}, cm⁻¹) 2925, 1628, 1607, 1528, 1517, 1466, 1300, 1268; **LCMS** (LCQ) *R*_t = 2.7 min (method 1), *m/z* (ESI⁺) 292.2 [M+H]⁺; **HRMS (ESI)**: calcd. for C₁₈H₁₇N₃NaO [M+Na]⁺ 314.1264, found 314.1269.

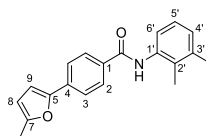
***N*-(2,3-dimethylphenyl)-4-(2-furyl)benzamide (206)**



Compound **206** was synthesised according to general procedure V, using the following reagents: 4-bromo-*N*-(2,3-dimethylphenyl)benzamide (**194**) (100 mg, 0.33 mmol), Furan-2-boronic acid (60 mg, 0.66 mmol), (1,1'-bis(diphenylphosphino)ferrocene)dichloropalladium(II) (24 mg, 0.03 mmol), sodium carbonate (348 mg, 3.30 mmol), 1,4-dioxane (1.5 mL) and water (1.5 mL). The crude was purified by column chromatography (silica 12 g, 0 to 30% ethyl acetate in petroleum ether) to yield the desired product **206** as a white solid (61 mg, 61%).

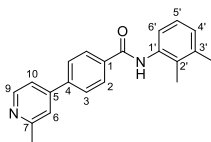
R_f 0.55 (petroleum ether:ethyl acetate 3:1); **m.p.** 189–190 °C; **¹H-NMR** (500 MHz, DMSO-*d*₆) δ 13.03 (s, 1H), 9.84 (s, 1H), 8.32 (s, 1H), 8.03 (s, 1H), 7.98 (d, *J* 8.0, 2H), 7.76 (d, *J* 7.9, 2H), 7.16 – 7.05 (m, 3H), 2.29 (s, 3H), 2.11 (s, 3H); **¹³C-NMR** (126 MHz, DMSO-*d*₆) δ 165.3, 152.7, 144.2, 137.4, 136.8, 133.2, 133.4, 133.2, 128.8, 128.0, 125.7, 125.2, 123.6, 112.8, 108.1, 20.6, 14.7; **IR** (neat, *v*_{max}, cm⁻¹) 3287, 1640, 1611, 1524, 1503, 1452, 1470, 100, 1279; **LCMS** (LCQ) *R*_t = 4.5 min (method 1), *m/z* (ESI⁺) 292.2 [M+H]⁺; **HRMS (ESI)**: calcd. for C₁₉H₁₇N₁NaO₂ [M+Na]⁺ 314.1151, found 314.1153.

***N*-(2,3-dimethylphenyl)-4-(5-methyl-2-furyl)benzamide (207)**



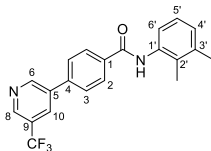
Compound **207** was synthesised according to general procedure T, using the following reagents: 4-bromo-*N*-(2,3-dimethylphenyl)benzamide (**194**) (100 mg, 0.33 mmol), 4,4,5,5-tetramethyl-2-(5-methylfuran-2-yl)-1,3,2-dioxaborolane (134 μL, 0.66 mmol), tetrakis(triphenylphosphine)palladium(0) (38 mg, 0.03 mmol), caesium carbonate (857 mg, 2.63 mmol), dimethoxyethane (4 mL) and water (1 mL). The crude was purified by column chromatography (silica 12 g, 0 to 20% ethyl acetate in petroleum ether) to yield the desired product **207** as a white solid (18 mg, 17%).

R_f 0.49 (petroleum ether:ethyl acetate 3:1); **m.p.** 167–168 °C; **¹H-NMR** (500 MHz, DMSO-*d*₆) δ 13.03 (s, 1H), 9.84 (s, 1H), 8.32 (s, 1H), 8.03 (s, 1H), 7.98 (d, *J* 8.0, 2H), 7.76 (d, *J* 7.9, 2H), 7.16 – 7.05 (m, 3H), 2.29 (s, 3H), 2.11 (s, 3H); **¹³C-NMR** (126 MHz, DMSO-*d*₆) δ 13C NMR (126 MHz, dmso) δ 165.6, 153.3, 151.0, 137.5, 136.6, 133.6, 133.2, 132.8, 128.8, 128.1, 125.7, 125.2, 123.0, 110.0, 109.1, 20.5, 14.7, 13.9; **IR** (neat, *v*_{max}, cm⁻¹) 3269, 1647, 1607, 1521, 1452, 1304, 1279; **LCMS** (LCQ) *R*_t = 4.8 min (method 1), *m/z* (ESI⁺) 306.1 [M+H]⁺; **HRMS (ESI)**: calcd. for C₂₀H₁₉N₁NaO₂ [M+Na]⁺ 328.1308, found 328.1307.

***N*-(2,3-dimethylphenyl)-4-(2-methyl-4-pyridyl)benzamide (208)**

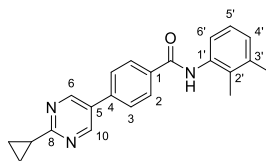
Compound **208** was synthesised according to general procedure T, using the following reagents: 4-bromo-*N*-(2,3-dimethylphenyl)benzamide (**194**) (100 mg, 0.33 mmol), (2-methylpyridin-4-yl)boronic acid (90 mg, 0.66 mmol), tetrakis(triphenylphosphine)palladium(0) (38 mg, 0.03 mmol), caesium carbonate (857 mg, 2.63 mmol), dimethoxyethane (4 mL) and water (1 mL). The crude was purified by column chromatography (silica 12 g, 0 to 60% ethyl acetate in petroleum ether), further purified by column chromatography (silica 12 g, 0 to 55% ethyl acetate in petroleum ether) and further purified by column chromatography (amino silica 12 g, 0 to 60% ethyl acetate in petroleum ether). To remove triphenylphosphine oxide residues, the remaining solid stirred with 2 M aq. hydrochloric acid solution to obtain *N*-pyridyl salt. The aqueous components were washed with ethyl acetate, alkalisied with sodium hydroxide until neutral pH and extracted with ethyl acetate. The combined organic components were then dried over MgSO_4 , filtered and concentrated under reduced pressure yield the desired product **208** as a white solid (14 mg, 13%).

R_f 0.26 (petroleum ether:ethyl acetate 1:1); **m.p.** 190–192 °C; **¹H-NMR** (500 MHz, $\text{DMSO}-d_6$) δ 10.06 (s, 1H), 8.54 (s, 1H), 8.12 (d, *J* 7.8, 2H), 7.94 (d, *J* 7.9, 2H), 7.67 (s, 1H), 7.58 (s, 1H), 7.19 – 7.01 (m, 3H), 2.29 (s, 3H), 2.12 (s, 3H), 1.60 (s, 3H); **IR** (neat, ν_{max} , cm^{-1}) 3280, 1640, 1604, 1531, 1510, 1463, 1304, 1170; **LCMS** (LCQ) *Rt* = 0.5 min (method 2), *m/z* (ESI^+) 317.3 [$\text{M}+\text{H}$]⁺; **HRMS (ESI)**: calcd. for $\text{C}_{21}\text{H}_{21}\text{N}_2\text{O}$ [$\text{M}+\text{H}$]⁺ 317.1648, found 317.1652. Not enough material for ^{13}C -NMR determination.

***N*-(2,3-dimethylphenyl)-4-(5-(trifluoromethyl)-3-pyridyl)benzamide (209)**

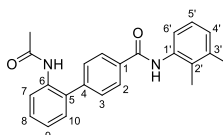
Compound **209** was synthesised according to general procedure T, using the following reagents: 4-bromo-*N*-(2,3-dimethylphenyl)benzamide (**194**) (100 mg, 0.33 mmol), (5-(trifluoromethyl)pyridin-3-yl)boronic acid (106 μL , 0.66 mmol), tetrakis(triphenylphosphine)palladium(0) (38 mg, 0.03 mmol), caesium carbonate (857 mg, 2.63 mmol), dimethoxyethane (4 mL) and water (1 mL). The crude was purified by column chromatography (silica 12 g, 0 to 50% ethyl acetate in petroleum ether) and further purified by column chromatography (silica 12 g, 0 to 55% ethyl acetate in petroleum ether) to yield the desired product **209** as a white solid (41 mg, 32%).

R_f 0.76 (petroleum ether:ethyl acetate 1:1); **m.p.** 198–200 °C; **¹H-NMR** (500 MHz, $\text{DMSO}-d_6$) δ 10.03 (s, 1H), 9.31 (s, 1H), 9.02 (s, 1H), 8.57 (s, 1H), 8.14 (d, *J* 8.0, 2H), 8.04 (d, *J* 7.9, 2H), 7.20 – 7.04 (m, 3H), 2.30 (s, 3H), 2.13 (s, 3H); **IR** (neat, ν_{max} , cm^{-1}) 3309, 1647, 1531, 1503, 1452, 1336, 1264, 1127; **LCMS** (LCQ) *Rt* = 4.5 min (method 1), *m/z* (ESI^+) 371.2 [$\text{M}+\text{H}$]⁺; **HRMS (ESI)**: calcd. for $\text{C}_{21}\text{H}_{17}\text{F}_3\text{N}_2\text{NaO}$ [$\text{M}+\text{H}$]⁺ 393.1185, found 393.1187. Not enough material for ^{13}C -NMR determination.

4-(2-Cyclopropylpyrimidin-5-yl)-*N*-(2,3-dimethylphenyl)benzamide (210)

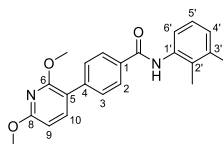
Compound **210** was synthesised according to general procedure V, using the following reagents: 4-bromo-*N*-(2,3-dimethylphenyl)benzamide (**194**) (100 mg, 0.33 mmol), (2-cyclopropylpyrimidin-5-yl)boronic acid (108 mg, 0.66 mmol), (1,1'-bis(diphenylphosphino)ferrocene)dichloropalladium(II) (24 mg, 0.03 mmol), sodium carbonate (348 mg, 3.30 mmol), 1,4-dioxane (1.5 mL) and water (1.5 mL). The crude was purified by column chromatography (amino silica 12 g, 0 to 20% ethyl acetate in petroleum ether) to yield the desired product **210** as a white solid (52 mg, 44%).

R_f 0.45 (petroleum ether:ethyl acetate 1:1); **m.p.** 218–220 °C; **¹H-NMR** (500 MHz, DMSO-*d*₆) 9.98 (s, 1H), 9.04 (d, *J* 2.1, 2H), 8.11 (d, *J* 7.3, 2H), 7.92 (d, *J* 7.0, 2H), 7.17–7.07 (m, 3H), 3.19–3.15 (m, 1H), 2.29 (s, 3H), 2.12 (s, 3H), 1.14–1.01 (m, 4H); **¹³C-NMR** (126 MHz, DMSO-*d*₆) δ 170.9, 165.3, 155.3, 137.5, 136.7, 134.7, 133.2, 129.6, 128.9, 128.1, 126.9, 125.7, 125.2; **IR** (neat, *v*_{max}, cm⁻¹) 3222, 1651, 1586, 1524, 1456, 1383, 1311, 1228; **LCMS** (LCQ) *R*_t = 3.8 min (method 1), *m/z* (ESI⁺) 344.4 [M+H]⁺; **HRMS (ESI)**: calcd. for C₂₂H₂₁N₃NaO [M+H]⁺ 366.1577, found 366.1580.

4-(3-Acetamidophenyl)-*N*-(2,3-dimethylphenyl)benzamide (211)

Compound **211** was synthesised according to general procedure V, using the following reagents: 4-bromo-*N*-(2,3-dimethylphenyl)benzamide (**194**) (100 mg, 0.33 mmol), 3-acetamidophenylboronic acid (118 mg, 0.66 mmol), (1,1'-bis(diphenylphosphino)ferrocene)dichloropalladium(II) (24 mg, 0.03 mmol), sodium carbonate (348 mg, 3.30 mmol), 1,4-dioxane (1.5 mL) and water (1.5 mL). The crude was purified by column chromatography (silica 12 g, 0 to 60% ethyl acetate in petroleum ether), further purified by column chromatography (amino silica 12 g, 0 to 85% ethyl acetate in petroleum ether) and recrystallised in ethanol to yield the desired product **211** as a white solid (12 mg, 10%).

R_f 0.18 (petroleum ether:ethyl acetate 1:1); **m.p.** 227–229 °C; **¹H-NMR** (500 MHz, DMSO-*d*₆) 10.07 (s, 1H), 9.98 (s, 1H), 8.09 (d, *J* 8.0, 2H), 7.97 (s, 1H), 7.75 (d, *J* 8.0, 2H), 7.61 (d, *J* 7.2, 1H), 7.45–7.37 (m, 2H), 7.16–7.12 (m, 1H), 7.12–7.07 (m, 2H), 2.29 (s, 3H), 2.12 (s, 3H), 2.08 (s, 3H); **¹³C-NMR** (126 MHz, DMSO-*d*₆) δ 168.9, 165.5, 143.5, 140.4, 140.2, 137.4, 136.7, 133.9, 133.2, 129.9, 128.8, 128.0, 127.0, 125.7, 125.2, 122.1, 119.1, 117.9, 24.5, 20.6, 14.7; **LCMS** (LCQ) *R*_t = 3.5 min (method 1), *m/z* (ESI⁺) 359.2 [M+H]⁺; **HRMS (ESI)**: calcd. for C₂₃H₂₃N₂O₂ [M+H]⁺ 359.1754, found 359.1748. Not enough material for IR determination.

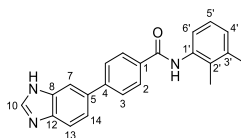
4-(2,6-dimethoxy-3-pyridyl)-*N*-(2,3-dimethylphenyl)benzamide (212)

Compound **212** was synthesised according to general procedure V, using the following reagents: 4-bromo-*N*-(2,3-dimethylphenyl)benzamide (**194**) (100 mg, 0.33 mmol), 2,6-dimethoxy-3-pyridineboronic acid (120 mg, 0.66 mmol), (1,1'-bis(diphenylphosphino)ferrocene)dichloropalladium(II) (24 mg, 0.03 mmol), sodium carbonate (348 mg,

3.30 mmol), 1,4-dioxane (1.5 mL) and water (1.5 mL). The crude was purified by column chromatography (silica 12 g, 0 to 30% ethyl acetate in petroleum ether) to yield the desired product **212** as a white solid (92 mg, 75%).

R_f 0.42 (petroleum ether:ethyl acetate 3:1); **m.p.** 204–206 °C; **¹H-NMR** (500 MHz, DMSO-*d*₆) 9.92 (s, 1H), 8.01 (d, *J* 7.9, 2H), 7.80 (d, *J* 8.1, 1H), 7.67 (d, *J* 7.9, 2H), 7.18 – 7.04 (m, 3H), 6.53 (dd, *J* 8.1, 1.8, 1H), 3.97 – 3.91 (m, 6H), 2.29 (s, 3H), 2.11 (s, 3H); **¹³C-NMR** (126 MHz, DMSO-*d*₆) δ 165.6, 162.6, 159.3, 142.4, 139.9, 137.4, 136.8, 133.1, 133.1, 129.0, 128.0, 125.7, 125.1, 114.6, 102.1, 53.8, 20.6, 14.6. ArC not visible; **IR** (neat, ν_{\max} , cm⁻¹) 3348, 2935, 1752, 1710, 1642, 1596, 1503, 1445, 1376, 1282; **LCMS** (LCQ) Rt = 5.1 min (method 1), *m/z* (ESI⁺) 363.2 [M+H]⁺; **HRMS (ESI)**: calcd. for C₂₂H₂₃N₂O₃ [M+H]⁺ 363.1703, found 363.1689.

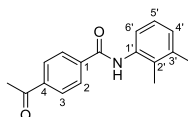
4-(3H-benzimidazol-5-yl)-*N*-(2,3-dimethylphenyl)benzamide (**213**)



Compound **213** was synthesised according to general procedure V, using the following reagents: *N*-(2,3-dimethylphenyl)-4-(4,4,5,5-tetramethyl-1,3,2-dioxaborolan-2-yl)benzamide (**195**) (80 mg, 0.23 mmol), 6-bromo-1H-1,3-benzodiazole (45 mg, 0.23 mmol), (1,1'-bis(diphenylphosphino)ferrocene)dichloropalladium(II) (17 mg, 0.02 mmol), sodium carbonate (242 mg, 2.28 mmol), 1,4-dioxane (1.5 mL) and water (1.5 mL). The precipitation formed during the work-up was collected by vacuum filtration, washed with water (5 mL) and ethyl acetate (5 mL), and dried under reduced pressure to yield the desired product **213** as a brown solid (52 mg, 64%).

¹H-NMR (500 MHz, DMSO-*d*₆) 10.01 (s, 1H), 8.26 (m, 1H), 8.09 (m, 2H), 7.93 (m, 2H), 7.84 (m, 2H), 7.69 (m, 1H), 7.58 (m, 1H), 7.20 – 6.98 (m, 3H), 2.28 (s, 3H), 2.11 (s, 3H); **LCMS** (LCQ) Rt = 5.8 min (method 1), *m/z* (ESI⁺) 342.2 [M+H]⁺.

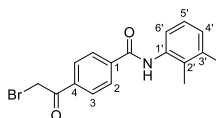
4-Acetyl-*N*-(2,3-dimethylphenyl)benzamide (**214**)



Compound **214** was synthesised according to general procedure R, using the following reagents: 4-acetylbenzoic acid (500 mg, 3.05 mmol), HATU (1.39 g, 3.65 mmol), *N,N*-diisopropylethylamine (1.06 mL, 6.09 mmol), 2,3-dimethylaniline (446 μL, 3.65 mmol) and *N,N*-dimethylformamide (5 mL). The precipitation formed during the work-up was collected by vacuum filtration and triturated with methanol to yield the desired product **214** as a whit solid (549 mg, 64%).

¹H-NMR (500 MHz, DMSO-*d*₆) δ 10.13 (s, 1H, CONH), 8.14 – 8.04 (m, 4H, H-2, H-3), 7.18 – 7.05 (m, 3H, H-4', H-5', H-6'), 2.65 (s, 3H, CO(CH₃)), 2.29 (s, 3H, 2'-CH₃), 2.10 (s, 3H, 3'-CH₃); **LCMS** (LCQ) Rt = 3.3 min (method 1), *m/z* (ESI⁺) 268.1 [M+H]⁺.

4-(2-Bromoacetyl)-*N*-(2,3-dimethylphenyl)benzamide (**215**)

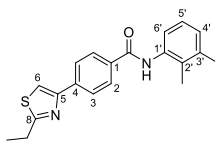


Lithium bis(trimethylsilyl)amide solution (1.0 M in tetrahydrofuran) (11.2 mL, 11.2 mmol) was added dropwise to a solution of 4-acetyl-*N*-(2,3-dimethylphenyl)benzamide (**214**) (1.00 g, 3.74 mmol) in tetrahydrofuran (25 mL) at –78 °C and the reaction mixture was stirred for 0.5 h. Chlorotrimethylsilane (1.89 mL, 15.0 mmol) was added to the reaction mixture which was stirred at 60 °C for 2 h. Upon formation of the silyl enolate, *N*-bromosuccinimide (732 mg,

4.11 mol) was added dropwise to the reaction mixture at -78°C and the reaction mixture stirred for 5 min. The reaction mixture was taken up in aq. saturated NaHCO_3 (30 mL) and extracted with ethyl acetate (3×30 mL). The combined organic components were washed with water (20 mL) and brine (20 mL), dried over MgSO_4 , filtered and concentrated under reduced pressure. The crude product was purified by column chromatography (silica 12 g, 0 to 70% ethyl acetate in petroleum ether) to yield the desired compound **215** as a white solid (1.27 g, 72%).

$^1\text{H-NMR}$ (500 MHz, $\text{DMSO-}d_6$) δ 10.15 (s, 1H, CONH), 8.15 – 8.07 (m, 4H, H-2, H-3), 7.16 – 7.07 (m, 3H, H-4', H-5', H-6'), 5.01 (s, 2H, OCH_2B), 2.29 (s, 3H, 2'- CH_3), 2.10 (s, 3H, 3'- CH_3); **LCMS** (LCQ) R_t = 3.9 min (method 1), m/z (ESI^+) 346.1 $[\text{M}(^{79}\text{Br})+\text{H}]^+$, 348.2 $[\text{M}(^{81}\text{Br})+\text{H}]^+$.

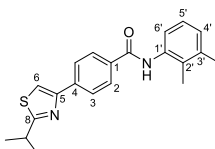
***N*-(2,3-dimethylphenyl)-4-(2-ethylthiazol-4-yl)benzamide (216)**



To 4-(2-bromoacetyl)-*N*-(2,3-dimethylphenyl)benzamide (**215**) (70 mg, 0.20 mmol) in *N,N*-dimethylformamide (1 mL) was added acetamide (36 mg, 0.60 mmol) and the reaction mixture stirred at 130°C for 3 h. The crude product was taken up in water (5 mL) and extracted with ethyl acetate (3×5 mL). The combined organic components were then washed with brine (10 mL), dried over MgSO_4 , filtered and concentrated under reduced pressure. The crude product was purified by column chromatography (silica 12 g, 0 to 60% ethyl acetate in petroleum ether) and further purified by column chromatography (amino silica 12 g, 0 to 50% ethyl acetate in petroleum ether) to yield the desired compound **216** as a white solid (18 mg, 28%).

$^1\text{H-NMR}$ (500 MHz, $\text{DMSO-}d_6$) δ 9.95 (s, 1H), 8.61 (s, 1H), 8.01 (d, J 8.2, 2H), 7.88 (d, J 8.2, 2H), 7.16 – 7.02 (m, 3H), 2.81 (q, J 7.6, 2H), 2.26 (s, 3H), 2.08 (s, 3H), 1.28 (t, J 7.6, 3H); **LCMS** (LCQ) R_t = 6.8 min (method 3), m/z (ESI^+) 321.5 $[\text{M}+\text{H}]^+$.

***N*-(2,3-dimethylphenyl)-4-(2-isopropylthiazol-4-yl)benzamide (217)**

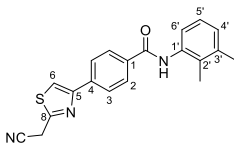


To 4-(2-bromoacetyl)-*N*-(2,3-dimethylphenyl)benzamide (**215**) (167 mg, 0.39 mmol) in *N,N*-dimethylformamide (3 mL) was added thioisobutyramide (60 mg, 0.58 mmol) and the reaction mixture stirred at ambient temperature for 1 h. The crude product was taken up in aq. saturated NaHCO_3 (5 mL) and extracted with ethyl acetate (3×5 mL). The combined organic components were then washed with brine (10 mL), dried over MgSO_4 , filtered and concentrated under reduced pressure. The crude product was purified by column chromatography (silica 12 g, 0 to 20% ethyl acetate in petroleum ether) and further purified by column chromatography (amino silica 12 g, 0 to 20% ethyl acetate in petroleum ether) to yield the desired compound **217** as a white solid (32 mg, 22%).

R_f 0.47 (petroleum ether:ethyl acetate 3:1); **m.p.** 179–181 $^{\circ}\text{C}$; **$^1\text{H-NMR}$** (500 MHz, $\text{DMSO-}d_6$) δ 9.99 (s, 1H, CONH), 8.16 (s, 1H, H-6), 8.10 (d, J 8.4, 2H, H-3), 8.05 (d, J 8.1, 2H, H-2), 7.17 – 7.05 (m, 3H, H-4', H-5', H-6'), 3.41 – 3.37 (m, 1H, $\text{CH}(\text{CH}_3)_2$), 2.29 (s, 3H, 2'- CH_3), 2.11 (s, 3H, 3'- CH_3), 1.40 (d, J 6.9, 6H, $\text{CH}(\text{CH}_3)_2$); **$^{13}\text{C-NMR}$** (126 MHz, $\text{DMSO-}d_6$) δ 177.8 (C-8), 165.4 (CO), 153.2 (ArC), 137.4 (ArC), 136.7 (ArC), 134.0 (ArC), 133.2 (ArC), 128.6 (C-3), 128.0 (ArC), 126.2 (C-2), 125.7 (ArC), 125.2 (ArC), 115.2 (C-6), 33.1 ($\text{CH}(\text{CH}_3)_2$), 23.3 ($\text{CH}(\text{CH}_3)_2$), 20.6 (2'- CH_3), 14.7 (3'- CH_3); **IR** (neat, ν_{max} ,

cm^{-1} 3247, 2956, 1693, 1636, 1594, 1566, 1532, 1439, 1384, 1272; **LCMS** (LCQ) $R_t = 5.2$ min (method 1), m/z (ESI⁺) 351.2 [M+H]⁺; **HRMS** m/z (ESI): calcd. for $\text{C}_{21}\text{H}_{23}\text{N}_2\text{OS}$ [M+H]⁺ 351.1526, found 351.1534.

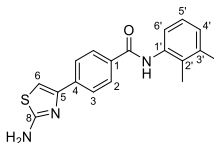
4-(2-(Cyanomethyl)thiazol-4-yl)-*N*-(2,3-dimethylphenyl)benzamide (**218**)



To 4-(2-bromoacetyl)-*N*-(2,3-dimethylphenyl)benzamide (**215**) (100 mg, 0.23 mmol) in *N,N*-dimethylformamide (2 mL) was added 2-cyanothioacetamide (35 mg, 0.35 mmol) and the reaction mixture stirred at ambient temperature for 2 h. The crude product was taken up in aq. saturated NaHCO_3 (5 mL) and extracted with ethyl acetate (3×5 mL). The combined organic components were then washed with brine (10 mL), dried over MgSO_4 , filtered and concentrated under reduced pressure. The crude product was purified by column chromatography (silica 12 g, 0 to 60% ethyl acetate in petroleum ether) and further purified by column chromatography (amino silica 12 g, 0 to 60% ethyl acetate in petroleum ether) to yield the desired compound **218** as a brown solid (34 mg, 95%).

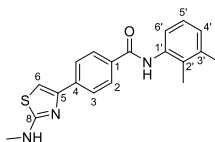
R_f 0.13 (petroleum ether:ethyl acetate 3:1); **m.p.** 188–190 °C; **¹H-NMR** (500 MHz, $\text{DMSO}-d_6$) δ 10.03 (s, 1H), 8.30 (s, 1H), 8.14 – 8.03 (m, 4H), 7.16 – 7.05 (m, 3H), 4.64 (s, 2H), 2.28 (s, 3H), 2.10 (s, 3H); **¹³C-NMR** (126 MHz, $\text{DMSO}-d_6$) δ 165.5, 159.8, 153.8, 137.5, 136.7, 136.6, 134.4, 133.2, 128.8, 128.1, 126.3, 125.7, 125.2, 117.8, 117.4, 29.9, 22.0, 20.6, 14.7; **IR** (neat, ν_{max} , cm^{-1}) 2947, 1692, 1565, 1478, 1438, 1385, 1272, 1218, 1178; **LCMS** (LCQ) $R_t = 3.5$ min (method 1), m/z (ESI⁺) 348.2 [M+H]⁺; **HRMS** m/z (ESI): calcd. for $\text{C}_{20}\text{H}_{18}\text{N}_3\text{OS}$ [M+H]⁺ 348.1165, found 348.1179.

4-(2-Aminothiazol-4-yl)-*N*-(2,3-dimethylphenyl)benzamide (**219**)



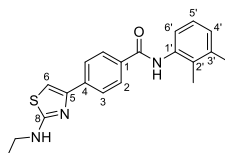
To 4-(2-bromoacetyl)-*N*-(2,3-dimethylphenyl)benzamide (**215**) (100 mg, 0.29 mmol) in ethanol (2 mL) was added thiourea (24 mg, 0.32 mmol) and the reaction mixture stirred at ambient temperature for 2 h. The crude product was taken up in aq. saturated NaHCO_3 (5 mL) and extracted with ethyl acetate (3×5 mL). The combined organic components were then washed with brine (10 mL), dried over MgSO_4 , filtered and concentrated under reduced pressure. The crude product was purified by column chromatography (silica 12 g, 50 to 100% ethyl acetate in petroleum ether) to yield the desired compound **219** as a white solid (54 mg, 55%).

R_f 0.41 (petroleum ether:ethyl acetate 1:1); **m.p.** 242–244 °C; **¹H-NMR** (500 MHz, $\text{DMSO}-d_6$) δ 9.93 (s, 1H, CONH), 7.98 (d, J 8.4, 2H, H-3), 7.93 (d, J 8.3, 2H, H-2), 7.21 (s, 1H, H-6), 7.15 (s, 2H, ArNH_2), 7.13 – 7.05 (m, 3H, H-4', H-5', H-6'), 2.28 (s, 3H, 2'- CH_3), 2.10 (s, 3H, 3'- CH_3); **¹³C-NMR** (126 MHz, $\text{DMSO}-d_6$) δ 168.8, 165.5, 137.4, 136.8, 133.3, 133.2, 128.4, 128.0, 125.8, 125.7, 125.2, 104.0, 30.0, 20.6, 14.7. ArC not visible; **IR** (neat, ν_{max} , cm^{-1}) 3306, 2923, 1645, 1607, 1513, 1450, 1300, 1274; **LCMS** (LCQ) $R_t = 2.2$ min (method 1), m/z (ESI⁺) 324.3 [M+H]⁺; **HRMS** m/z (ESI): calcd. for $\text{C}_{18}\text{H}_{17}\text{N}_3\text{NaOS}$ [M+Na]⁺ 346.0985, found 346.0972.

***N*-(2,3-dimethylphenyl)-4-[2-(methylamino)thiazol-4-yl]benzamide (220)**

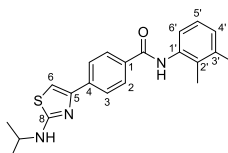
To 4-(2-bromoacetyl)-*N*-(2,3-dimethylphenyl)benzamide (**215**) (25 mg, 0.07 mmol) in ethanol (1 mL) was added 1-methyl-2-thiourea (9.7 mg, 0.11 mmol) and the reaction mixture stirred at ambient temperature for 6 h. The crude product was taken up in aq. saturated NaHCO₃ (5 mL) and extracted with ethyl acetate (3 × 5 mL). The combined organic components were then washed with brine (10 mL), dried over MgSO₄, filtered and concentrated under reduced pressure. The crude product was purified by column chromatography (silica 12 g, 0 to 60% ethyl acetate in petroleum ether) to yield the desired compound **220** as a white solid (9 mg, 37%).

R_f 0.57 (petroleum ether:ethyl acetate 1:1); **m.p.** 197–199 °C; **¹H-NMR** (500 MHz, DMSO-*d*₆) δ 9.93 (s, 1H), 7.99 (d, *J* 8.6, 2H), 7.96 (d, *J* 8.5, 2H), 7.65 (q, *J* 4.7, 1H), 7.27 (s, 1H), 7.15 – 7.05 (m, 3H), 2.89 (d, *J* 4.7, 3H), 2.28 (s, 3H), 2.10 (s, 3H); **¹³C-NMR** (126 MHz, DMSO-*d*₆) δ 169.9, 165.5, 149.8, 138.1, 137.4, 136.8, 133.2, 128.4, 128.0, 125.8, 125.7, 125.2, 103.3, 31.5, 20.6, 14.7; **IR** (neat, *v*_{max}, cm⁻¹) 2931, 1669, 1634, 1607, 1585, 1566, 1506, 1429, 1289; **LCMS** (LCQ) *R*_t = 2.8 min (method 1), *m/z* (ESI⁺) 338.1 [M+H]⁺; **HRMS** *m/z* (ESI): calcd. for C₁₉H₂₀N₃OS [M+H]⁺ 339.1162, found 339.1165.

***N*-(2,3-dimethylphenyl)-4-[2-(ethylamino)thiazol-4-yl]benzamide (221)**

To 4-(2-bromoacetyl)-*N*-(2,3-dimethylphenyl)benzamide (**215**) (95 mg, 0.22 mmol) in ethanol (2 mL) was added ethylthiourea (34 mg, 0.33 mmol) and the reaction mixture stirred at ambient temperature for 2 h. The crude product was taken up in aq. saturated NaHCO₃ (5 mL) and extracted with ethyl acetate (3 × 5 mL). The combined organic components were then washed with brine (10 mL), dried over MgSO₄, filtered and concentrated under reduced pressure. The crude product was purified by column chromatography (silica 12 g, 0 to 35% ethyl acetate in petroleum ether) to yield the desired compound **221** as a white solid (52 mg, 64%).

R_f 0.18 (petroleum ether:ethyl acetate 3:1); **m.p.** 198–201 °C; **¹H-NMR** (500 MHz, DMSO-*d*₆) δ 9.93 (s, 1H), 8.04 – 7.91 (m, 4H), 7.71 (t, *J* 5.2, 1H), 7.26 (s, 1H), 7.19 – 7.05 (m, 3H), 3.33 – 3.28 (m, 2H), 2.28 (s, 3H), 2.10 (s, 3H), 1.20 (t, *J* 7.1, 3H); **¹³C-NMR** (126 MHz, DMSO-*d*₆) δ 168.9, 165.5, 149.7, 138.1, 137.4, 136.8, 133.4, 133.2, 128.4, 127.9, 125.8, 125.7, 125.2, 103.1, 20.6, 14.9, 14.7; **IR** (neat, *v*_{max}, cm⁻¹) 3267, 1648, 1561, 1528, 1458, 1334, 1260; **LCMS** (LCQ) *R*_t = 3.1 min (method 1), *m/z* (ESI⁺) 352.2 [M+H]⁺; **HRMS** *m/z* (ESI): calcd. for C₂₀H₂₂N₃O₂S [M+H]⁺ 352.1478, found 352.1479.

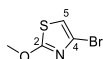
***N*-(2,3-dimethylphenyl)-4-[2-(isopropylamino)thiazol-4-yl]benzamide (222)**

To 4-(2-bromoacetyl)-*N*-(2,3-dimethylphenyl)benzamide (**215**) (100 mg, 0.23 mmol) in ethanol (2 mL) was added isopropylthiourea (41 mg, 0.35 mmol) and the reaction mixture stirred at ambient temperature for 2 h. The crude product was taken up in aq. saturated NaHCO₃ (5 mL) and extracted with ethyl acetate (3 × 5 mL). The combined organic components were then washed with brine (10 mL), dried over MgSO₄, filtered and concentrated under reduced pressure. The crude product was purified by column chromatography (silica 12 g, 0 to 70% ethyl acetate in

petroleum ether) and further purified by column chromatography (amino silica 12 g, 0 to 50% ethyl acetate in petroleum ether) to yield the desired compound **222** as a white solid (41 mg, 46%).

R_f 0.34 (petroleum ether:ethyl acetate 3:1); **m.p.** 182–184 °C; **¹H-NMR** (500 MHz, DMSO-*d*₆) δ 9.93 (s, 1H), 7.99 (d, *J* 8.3, 2H), 7.95 (d, *J* 8.2, 2H), 7.63 (d, *J* 7.4, 1H), 7.23 (s, 1H), 7.15 – 7.03 (m, 3H), 3.85 (h, *J* 6.6, 1H), 2.28 (s, 3H), 2.10 (s, 3H), 1.22 (d, *J* 6.4, 6H); **¹³C-NMR** (126 MHz, DMSO-*d*₆) δ 168.1, 165.6, 149.6, 138.2, 137.4, 136.7, 133.3, 133.2, 128.4, 128.0, 125.8, 125.7, 125.2, 103.0, 46.8, 22.8, 20.6, 14.7; **IR** (neat, ν_{\max} , cm⁻¹) 2948, 1692, 1565, 1479, 1438, 1385, 1308, 1272, 1218, 1176; **LCMS** (LCQ) Rt = 3.9 min (method 1), *m/z* (ESI⁺) 366.3 [M+H]⁺; **HRMS** *m/z* (ESI): calcd. for C₂₁H₂₄N₃O₂S [M+H]⁺ 366.1635, found 366.1639.

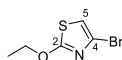
4-Bromo-2-methoxy-thiazole (**223**)



To 2,4-dibromothiazole (300 mg, 1.23 mmol) in methanol (7 mL) was added sodium methoxide (30%) in methanol (2.36 mL, 3.70 mmol) and the reaction mixture stirred at 65 °C for 16 h. The crude product was taken up in water (10 mL) and extracted with ethyl acetate (3 × 10 mL). The combined organic components were then washed with brine (20 mL), dried over MgSO₄, filtered and concentrated under reduced pressure to yield the desired compound **223** as a brown solid (137 mg, 54%).

¹H-NMR (500 MHz, DMSO-*d*₆) δ 7.17 (s, 1H, H-5), 4.02 (s, 3H, OCH₃); **LCMS** (LCQ) Rt = 3.1 min (method 1), *m/z* (ESI⁺) 194.1 [M(⁷⁹Br)+H]⁺, 196.1 [M(⁸¹Br)+H]⁺

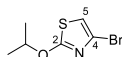
4-Bromo-2-ethoxy-thiazole (**224**)



To ethanol (139 μL, 2.47 mmol) in tetrahydrofuran (4 mL) was added portionwise sodium hydride (60% dispersion in mineral oil) (59 mg, 2.47 mmol) and the reaction mixture stirred at ambient temperature for 0.5 h. To the reaction mixture was added portionwise 2,4-dibromothiazole (300 mg, 1.23 mmol) and the reaction mixture stirred at 50 °C for 16 h. The crude product was taken up in water (10 mL) and extracted with ethyl acetate (3 × 10 mL). The combined organic components were then washed with brine (20 mL), dried over MgSO₄, filtered and concentrated under reduced pressure to yield the desired compound **224** as a brown oil (210 mg, 74%).

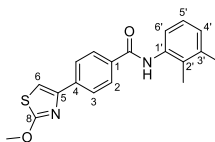
¹H-NMR (500 MHz, DMSO-*d*₆) δ 6.57 (s, 1H, H-5), 4.48 (q, *J* 6.5, 2H, OCH₂CH₃), 1.42 (t, *J* 6.2, 3H, OCH₂CH₃); **LCMS** (LCQ) Rt = 2.7 min (method 1), *m/z* (ESI⁺) 220.4 [M(⁷⁹Br)+H]⁺, 222.6 [M(⁸¹Br)+H]⁺.

4-Bromo-2-isopropoxy-thiazole (**225**)



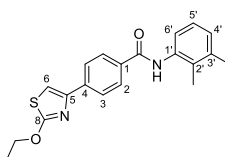
To 2,4-dibromothiazole (300 mg, 1.23 mmol) was added potassium isopropoxide (5%) in 2-propanol (185 mL, 3.70 mmol) and the reaction mixture stirred at 50 °C for 3 h. The crude product was taken up in water (10 mL) and extracted with ethyl acetate (3 × 10 mL). The combined organic components were then washed with brine (20 mL), dried over MgSO₄, filtered and concentrated under reduced pressure to yield the desired compound **225** as a brown oil (272 mg, 99%).

¹H-NMR (500 MHz, DMSO-*d*₆) δ 7.13 (s, 1H, H-5), 5.08 (hept, *J* 12.3, 6.1, 1.4, 1H, OCH(CH₃)₂), 1.34 (d, *J* 7.5, 6H, OCH(CH₃)₂); **LCMS** (LCQ) Rt = 2.6 min (method 1), no ionisation observed.

***N*-(2,3-dimethylphenyl)-4-(2-methoxythiazol-4-yl)benzamide (226)**

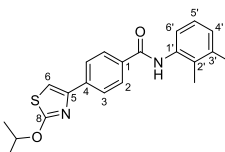
Compound **226** was synthesised according to general procedure V, using the following reagents: *N*-(2,3-dimethylphenyl)-4-(4,4,5,5-tetramethyl-1,3,2-dioxaborolan-2-yl)benzamide (**195**) (120 mg, 0.34 mmol), 4-bromo-2-methoxy-thiazole (**223**) (66 mg, 0.34 mmol), (1,1'-bis(diphenylphosphino)ferrocene)dichloropalladium(II) (25 mg, 0.03 mmol), sodium carbonate (362 mg, 3.42 mmol), 1,4-dioxane (2 mL) and water (2 mL). The crude was purified by column chromatography (silica 12 g, 0 to 20% ethyl acetate in petroleum ether) to yield the desired product **226** as a white solid (50 mg, 41%).

R_f 0.66 (petroleum ether:ethyl acetate 3:1); **m.p.** 175–177 °C; **¹H-NMR** (500 MHz, DMSO-*d*₆) δ 9.98 (s, 1H, CONH), 8.08 – 7.93 (m, 4H, H-2, H-3), 7.67 (s, 1H, H-6), 7.16 – 7.05 (m, 3H, H-4', H-5', H-6'), 4.13 (s, 3H, OCH₃), 2.28 (s, 3H, 2'-CH₃), 2.11 (s, 3H, 3'-CH₃); **¹³C-NMR** (126 MHz, DMSO-*d*₆) δ 174.6, 165.4, 147.6, 137.4, 137.2, 136.7, 134.0, 133.2, 128.6, 128.0, 125.8, 125.7, 125.2, 108.7, 59.3, 20.6, 14.7; **IR** (neat, ν_{max}, cm⁻¹) 2927, 1671, 1603, 1566, 1470, 1421, 1307, 1287, 1257; **LCMS** (LCQ) Rt = 4.6 min (method 1), *m/z* (ESI⁺) 339.1 [M+H]⁺; **HRMS** *m/z* (ESI): calcd. for C₁₉H₁₉N₂O₂S [M+H]⁺ 339.1162, found 339.1165.

***N*-(2,3-dimethylphenyl)-4-(2-ethoxythiazol-4-yl)benzamide (227)**

Compound **227** was synthesised according to general procedure V, using the following reagents: *N*-(2,3-dimethylphenyl)-4-(4,4,5,5-tetramethyl-1,3,2-dioxaborolan-2-yl)benzamide (**195**) (120 mg, 0.34 mmol), 4-bromo-2-ethoxy-thiazole (**224**) (71 mg, 0.34 mmol), (1,1'-bis(diphenylphosphino)ferrocene)dichloropalladium(II) (25 mg, 0.03 mmol), sodium carbonate (362 mg, 3.42 mmol), 1,4-dioxane (2 mL) and water (2 mL). The crude was purified by column chromatography (silica 12 g, 25 to 60% ethyl acetate in petroleum ether) and further purified by column chromatography (amino silica 12 g, 0 to 70% ethyl acetate in petroleum ether) to yield the desired product **227** as a light orange solid (26 mg, 21%).

R_f 0.60 (petroleum ether:ethyl acetate 3:1); **m.p.** 171–173 °C; **¹H-NMR** (500 MHz, DMSO-*d*₆) δ 9.95 (s, 1H), 8.01 (d, *J* 8.4, 2H), 7.97 (d, *J* 8.4, 2H), 7.63 (s, 1H), 7.13 – 7.04 (m, 3H), 4.51 (q, *J* 7.0, 2H), 2.26 (s, 3H), 2.08 (s, 3H), 1.39 (t, *J* 7.0, 3H); **¹³C-NMR** (126 MHz, DMSO-*d*₆) δ 173.9, 165.4, 147.6, 137.4, 137.3, 136.7, 134.0, 133.2, 128.6, 128.0, 125.8, 125.7, 125.2, 108.4, 68.4, 20.6, 14.8, 14.7; **IR** (neat, ν_{max}, cm⁻¹) 3256, 1636, 1520, 1474, 1455, 1298, 1232; **LCMS** (LCQ) Rt = 3.6 min (method 1), *m/z* (ESI⁺) 353.1 [M+H]⁺; **HRMS** *m/z* (ESI): calcd. for C₂₀H₂₁N₂O₂S [M+H]⁺ 353.1318, found 353.1327.

***N*-(2,3-dimethylphenyl)-4-(2-isopropoxythiazol-4-yl)benzamide (228)**

Compound **228** was synthesised according to general procedure V, using the following reagents: *N*-(2,3-dimethylphenyl)-4-(4,4,5,5-tetramethyl-1,3,2-dioxaborolan-2-yl)benzamide (**195**) (100 mg, 0.28 mmol), 4-bromo-2-isopropoxy-thiazole (**224**) (63 mg, 0.28 mmol), (1,1'-bis(diphenylphosphino)ferrocene)dichloropalladium(II) (21 mg,

0.03 mmol), sodium carbonate (302 mg, 2.85 mmol), 1,4-dioxane (2 mL) and water (2 mL). The crude was purified by column chromatography (silica 12 g, 0 to 18% ethyl acetate in petroleum ether) to yield the desired product **228** as a white solid (75 mg, 68%).

R_f 0.50 (petroleum ether:ethyl acetate 3:1); **m.p.** 174–176 °C; **¹H-NMR** (500 MHz, DMSO-*d*₆) δ 9.98 (s, 1H), 8.03 (d, *J* 8.3, 2H), 7.99 (d, *J* 8.4, 2H), 7.62 (s, 1H), 7.16 – 7.05 (m, 3H), 5.24 (hept, *J* 6.2, 1H), 2.28 (s, 3H), 2.10 (s, 3H), 1.41 (d, *J* 6.1, 6H); **¹³C-NMR** (126 MHz, DMSO-*d*₆) δ 173.4, 165.4, 147.7, 137.4, 137.3, 136.7, 133.9, 133.2, 128.6, 128.0, 125.8, 125.7, 125.2, 108.1, 60.2, 22.0, 20.6, 14.7; **IR** (neat, *v*_{max}, cm⁻¹) 2947, 1693, 1594, 1565, 1478, 1438, 1384, 1272, 1217; **LCMS** (LCQ) *R*_t = 5.2 min (method 1), *m/z* (ESI⁺) 367.0 [M+H]⁺; **HRMS** *m/z* (ESI): calcd. for C₂₁H₂₃N₂O₂S [M+H]⁺ 367.1475, found 367.1487.

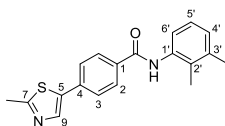
4-Bromo-2,5-dimethyl-thiazole (229)



To a solution of 2,5-dimethyl-1,3-thiazole (89 μL, 0.88 mmol) in chloroform (1 mL) and acetonitrile (1 mL) was added bromine (136 μL, 2.65 mmol) and the reaction mixture stirred at ambient temperature for 16 h. The crude product was taken up in saturated aq. NaHCO₃ (3 mL) and extracted with ethyl acetate (3 × 3 mL). The combined organic components were then washed with brine (10 mL), dried over MgSO₄, filtered and concentrated under reduced pressure. The crude was purified by column chromatography (silica 12 g, 0 to 10% ethyl acetate in petroleum ether) to yield the desired product **229** as a colourless oil (136 mg, 76%).

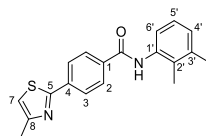
¹H-NMR (500 MHz, DMSO-*d*₆) δ 6.57 (s, 1H, H-5), 4.48 (q, *J* 6.5, 2H, OCH₂CH₃), 1.42 (t, *J* 6.2, 3H, OCH₂CH₃); **LCMS** (LCQ) *R*_t = 3.0 min (method 1), *m/z* (ESI⁺) 192.1 [M(⁷⁹Br)+H]⁺, 194.1 [M(⁸¹Br)+H]⁺.

N-(2,3-dimethylphenyl)-4-(2-methylthiazol-5-yl)benzamide (234)



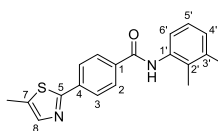
Compound **234** was synthesised according to general procedure V, using the following reagents: *N*-(2,3-dimethylphenyl)-4-(4,4,5,5-tetramethyl-1,3,2-dioxaborolan-2-yl)benzamide (**195**) (100 mg, 0.33 mmol), 5-bromo-2-methyl-1,3-thiazole (60 mg, 0.33 mmol), (1,1'-bis(diphenylphosphino)ferrocene)dichloropalladium(II) (24 mg, 0.03 mmol), sodium carbonate (348 mg, 3.30 mmol), 1,4-dioxane (1.5 mL) and water (1.5 mL). The crude was purified by column chromatography (silica 12 g, 0 to 30% ethyl acetate in petroleum ether) to yield the desired product **234** as a white solid (61 mg, 55%).

R_f 0.50 (petroleum ether:ethyl acetate 1:1); **m.p.** 188–190 °C; **¹H-NMR** (500 MHz, DMSO-*d*₆) δ 9.94 (s, 1H, CONH), 8.18 (s, 1H, H-9), 8.03 (d, *J* 8.0, 2H, H-3), 7.77 (d, *J* 7.9, 2H, H-2), 7.16 – 7.05 (m, 3H, H-3', H-4', H-5'), 2.70 (s, 3H, 7-CH₃), 2.29 (s, 3H, 2'-CH₃), 2.11 (s, 3H, 3'-CH₃); **¹³C-NMR** (126 MHz, DMSO-*d*₆) δ 166.5, 165.4, 139.6, 137.7, 137.5, 136.5, 134.4, 134.1, 133.2, 129.0, 128.1, 126.5, 125.8, 125.1, 20.5, 19.4, 14.6; **IR** (neat, *v*_{max}, cm⁻¹) 3233, 1651, 1607, 1520, 1452, 1304, 1271, 1170; **LCMS** (LCQ) *R*_t = 3.7 min (method 1), *m/z* (ESI⁺) 323.3 [M+H]⁺; **HRMS** (ESI): calcd. for C₁₉H₁₈N₂NaOS [M+Na]⁺ 345.1032, found 345.1032.

***N*-(2,3-dimethylphenyl)-4-(4-methylthiazol-2-yl)benzamide (230)**

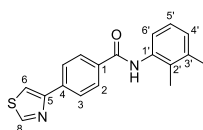
Compound **230** was synthesised according to general procedure V, using the following reagents: *N*-(2,3-dimethylphenyl)-4-(4,4,5,5-tetramethyl-1,3,2-dioxaborolan-2-yl)benzamide (**195**) (120 mg, 0.34 mmol), 2-bromo-4-methylthiazole (37 μ L, 0.34 mmol), (1,1'-bis(diphenylphosphino)ferrocene)dichloropalladium(II) (25 mg, 0.03 mmol), sodium carbonate (362 mg, 3.42 mmol), 1,4-dioxane (2 mL) and water (2 mL). The crude was purified by column chromatography (silica 12 g, 0 to 90% ethyl acetate in petroleum ether) and purified by column chromatography (amino silica 12 g, 0 to 40% ethyl acetate in petroleum ether) to yield the desired product **230** as a white solid (36 mg, 31%).

R_f 0.26 (petroleum ether:ethyl acetate 3:1); **m.p.** 185–187 °C; **¹H-NMR** (500 MHz, DMSO-*d*₆) δ 10.08 (s, 1H), 8.08 (d, *J* 8.5, 2H), 8.05 (d, *J* 8.3, 2H), 7.43 (s, 1H), 7.15 – 7.06 (m, 3H), 2.46 (s, 3H), 2.29 (s, 3H), 2.10 (s, 3H); **¹³C-NMR** (126 MHz, DMSO-*d*₆) δ 165.7, 165.2, 154.2, 137.5, 136.6, 136.1, 136.0, 133.2, 129.0, 128.1, 126.3, 125.7, 125.1, 116.2, 20.6, 17.3, 14.7; **IR** (neat, ν_{max} , cm⁻¹) 3276, 1645, 1588, 1508, 1455, 1300, 1281; **LCMS** (LCQ) *R_t* = 4.1 min (method 1), *m/z* (ESI⁺) 323.2 [M+H]⁺; **HRMS** *m/z* (ESI): calcd. for C₁₉H₁₉N₂O₂S [M+H]⁺ 323.1213, found 323.1221.

***N*-(2,3-dimethylphenyl)-4-(5-methylthiazol-2-yl)benzamide (231)**

Compound **231** was synthesised according to general procedure V, using the following reagents: *N*-(2,3-dimethylphenyl)-4-(4,4,5,5-tetramethyl-1,3,2-dioxaborolan-2-yl)benzamide (**195**) (100 mg, 0.28 mmol), 2-bromo-5-methyl-1,3-thiazole (51 mg, 0.28 mmol), (1,1'-bis(diphenylphosphino)ferrocene)dichloropalladium(II) (21 mg, 0.03 mmol), sodium carbonate (302 mg, 2.85 mmol), 1,4-dioxane (2 mL) and water (2 mL). The crude was purified by column chromatography (silica 12 g, 0 to 30% ethyl acetate in petroleum ether) to yield the desired product **231** as a white solid (42 mg, 43%).

R_f 0.24 (petroleum ether:ethyl acetate 3:1); **m.p.** 208–210 °C; **¹H-NMR** (500 MHz, DMSO-*d*₆) δ 10.05 (s, 1H), 8.08 (d, *J* 8.1, 2H), 8.01 (d, *J* 8.1, 2H), 7.69 (s, 1H), 7.17 – 7.05 (m, 3H), 2.53 (s, 3H), 2.29 (s, 3H), 2.11 (s, 3H); **¹³C-NMR** (126 MHz, DMSO-*d*₆) δ 165.2, 164.7, 142.6, 137.5, 136.6, 136.2, 135.8, 135.8, 133.2, 129.0, 128.1, 126.1, 125.7, 125.1, 25.4, 20.6, 14.7, 12.2; **IR** (neat, ν_{max} , cm⁻¹) 3259, 2948, 1693, 1652, 1594, 1565, 1439, 1384, 1308, 1271, 1218; **LCMS** (LCQ) *R_t* = 4.4 min (method 1), *m/z* (ESI⁺) 323.2 [M+H]⁺; **HRMS** *m/z* (ESI): calcd. for C₁₉H₁₉N₂O₂S [M+H]⁺ 323.1213, found 323.1219.

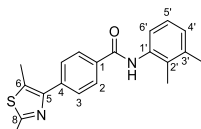
***N*-(2,3-dimethylphenyl)-4-thiazol-4-yl-benzamide (232)**

Compound **232** was synthesised according to general procedure V, using the following reagents: *N*-(2,3-dimethylphenyl)-4-(4,4,5,5-tetramethyl-1,3,2-dioxaborolan-2-yl)benzamide (**195**) (120 mg, 0.34 mmol), 4-bromothiazole (30 μ L, 0.34 mmol), (1,1'-bis(diphenylphosphino)ferrocene)dichloropalladium(II) (25 mg, 0.03 mmol), sodium carbonate (362 mg, 3.42 mmol), 1,4-dioxane (2 mL) and water (2 mL). The crude was purified by column

chromatography (silica 12 g, 0 to 50% ethyl acetate in petroleum ether) to yield the desired product **232** as a white solid (30 mg, 27%).

R_f 0.24 (petroleum ether:ethyl acetate 3:1); **m.p.** 217–219 °C; **¹H-NMR** (500 MHz, DMSO-*d*₆) δ 10.00 (s, 1H), 9.25 (s, 1H), 8.37 (s, 1H), 8.15 (d, *J* 7.4, 2H), 8.07 (d, *J* 7.6, 2H), 7.20 – 7.01 (m, 3H), 2.29 (s, 3H), 2.11 (s, 3H); **¹³C-NMR** (126 MHz, DMSO-*d*₆) δ 165.4, 155.4, 154.7, 137.4, 137.2, 136.7, 134.2, 133.2, 128.7, 128.0, 126.4, 125.7, 125.2, 116.4, 20.6, 14.7; **IR** (neat, ν_{max} , cm⁻¹) 3314, 2918, 1645, 1607, 1513, 1450, 1299, 1274; **LCMS** (LCQ) *R_t* = 3.2 min (method 1), *m/z* (ESI⁺) 309.1 [M+H]⁺; **HRMS** *m/z* (ESI): calcd. for C₁₈H₁₇N₂O₂S [M+H]⁺ 309.1056, found 309.1059.

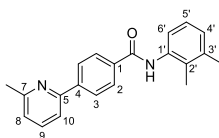
***N*-(2,3-dimethylphenyl)-4-(2,5-dimethylthiazol-4-yl)benzamide (233)**



Compound **233** was synthesised according to general procedure V, using the following reagents: *N*-(2,3-dimethylphenyl)-4-(4,4,5,5-tetramethyl-1,3,2-dioxaborolan-2-yl)benzamide (**195**) (120 mg, 0.34 mmol), 4-bromo-2,5-dimethyl-thiazole (**229**) (66 mg, 0.34 mmol), (1,1'-bis(diphenylphosphino)ferrocene)dichloropalladium(II) (25 mg, 0.03 mmol), sodium carbonate (362 mg, 3.42 mmol), 1,4-dioxane (2 mL) and water (2 mL). The crude was purified by column chromatography (silica 12 g, 0 to 30% ethyl acetate in petroleum ether) to yield the desired product **233** as a light pink solid (59 mg, 49%).

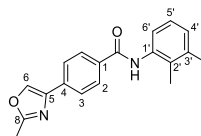
R_f 0.17 (petroleum ether:ethyl acetate 3:1); **m.p.** 186–188 °C; **¹H-NMR** (500 MHz, DMSO-*d*₆) δ 10.01 (s, 1H), 8.05 (d, *J* 8.3, 2H), 7.80 (d, *J* 8.4, 2H), 7.15 – 7.02 (m, 3H), 2.64 (s, 3H), 2.55 (s, 3H), 2.28 (s, 3H), 2.11 (s, 3H); **¹³C-NMR** (126 MHz, DMSO-*d*₆) δ 165.9, 162.5, 148.7, 138.0, 137.6, 136.5, 133.4, 133.3, 129.7, 128.4, 128.2, 128.2, 125.8, 125.1, 20.5, 19.0, 14.6, 12.7; **IR** (neat, ν_{max} , cm⁻¹) 3322, 2914, 1646, 1607, 1513, 1450, 1299, 1273; **LCMS** (LCQ) *R_t* = 0.7 min (method 1), *m/z* (ESI⁺) 337.1 [M+H]⁺; **HRMS** *m/z* (ESI): calcd. for C₂₀H₂₁N₂O₂S [M+H]⁺ 337.1369, found 337.1377.

***N*-(2,3-dimethylphenyl)-4-(6-methyl-2-pyridyl)benzamide (235)**



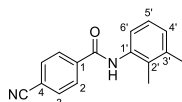
Compound **235** was synthesised according to general procedure V, using the following reagents: *N*-(2,3-dimethylphenyl)-4-(4,4,5,5-tetramethyl-1,3,2-dioxaborolan-2-yl)benzamide (**195**) (120 mg, 0.34 mmol), 2-bromo-6-methylpyridine (39 μL, 0.34 mmol), (1,1'-bis(diphenylphosphino)ferrocene)dichloropalladium(II) (25 mg, 0.03 mmol), sodium carbonate (362 mg, 3.42 mmol), 1,4-dioxane (2 mL) and water (2 mL). The crude was purified by column chromatography (silica 12 g, 0 to 40% ethyl acetate in petroleum ether) to yield the desired product **235** as a white solid (35 mg, 31%).

R_f 0.55 (petroleum ether:ethyl acetate 1:1); **m.p.** 165–167 °C; **¹H-NMR** (500 MHz, DMSO-*d*₆) δ 10.03 (s, 1H), 8.22 (d, *J* 8.4, 2H), 8.09 (d, *J* 8.3, 2H), 7.87 (d, *J* 7.8, 1H), 7.81 (t, *J* 7.7, 1H), 7.28 (d, *J* 7.5, 1H), 7.20 – 7.04 (m, 3H), 2.57 (s, 3H), 2.29 (s, 3H), 2.12 (s, 3H); **¹³C-NMR** (126 MHz, DMSO-*d*₆) δ 158.4, 154.8, 141.9, 138.1, 137.5, 136.7, 135.1, 133.2, 128.5, 128.0, 126.8, 125.7, 125.2, 123.0, 118.3, 25.4, 24.8, 20.6, 14.7; **IR** (neat, ν_{max} , cm⁻¹) 3264, 1641, 1588, 1520, 1473, 1424, 1300; **LCMS** (LCQ) *R_t* = 2.4 min (method 1), *m/z* (ESI⁺) 317.2 [M+H]⁺; **HRMS** *m/z* (ESI): calcd. for C₂₁H₂₁N₂O [M+H]⁺ 317.1648, found 317.1648.

***N*-(2,3-dimethylphenyl)-4-(2-methyloxazol-4-yl)benzamide (236)**

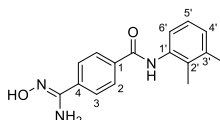
To 4-(2-bromoacetyl)-*N*-(2,3-dimethylphenyl)benzamide (**215**) (70 mg, 0.20 mmol) in *N,N*-dimethylformamide (1 mL) was added acetamide (36 mg, 0.60 mmol) and the reaction mixture stirred at 130 °C for 3 h. The crude product was taken up in water (5 mL) and extracted with ethyl acetate (3 × 5 mL). The combined organic components were then washed with brine (10 mL), dried over MgSO₄, filtered and concentrated under reduced pressure. The crude product was purified by column chromatography (silica 12 g, 0 to 60% ethyl acetate in petroleum ether) and further purified by column chromatography (amino silica 12 g, 0 to 50% ethyl acetate in petroleum ether) to yield the desired compound **236** as a white solid (18 mg, 28%).

R_f 0.50 (petroleum ether:ethyl acetate 3:1); **m.p.** 199–201 °C; **¹H-NMR** (500 MHz, DMSO-*d*₆) δ 9.97 (s, 1H, CONH), 8.62 (s, 1H, H-6), 8.03 (d, *J* 7.3, 2H, H-3), 7.89 (d, *J* 7.3, 2H, H-2), 7.18 – 7.04 (m, 3H, H-3', H-4', H-5'), 2.29 (s, 3H, 2'-CH₃), 2.10 (s, 3H, 2'-CH₃). 8-CH₃ under DMSO peak; **¹³C-NMR** (126 MHz, DMSO-*d*₆) δ 170.8, 165.4, 162.2, 139.4, 137.4, 136.7, 136.3, 134.4, 134.0, 133.2, 128.6, 128.0, 125.7, 125.3, 21.2, 20.6, 14.0; **IR** (neat, ν_{max}, cm⁻¹) 3306, 2918, 1646, 1607, 1512, 1450, 1300, 1274; **LCMS** (LCQ) Rt = 3.5 min (method 1), *m/z* (ESI⁺) 307.1 [M+H]⁺; **HRMS (ESI)**: calcd. for C₁₉H₁₈N₂NaO₂ [M+Na]⁺ 329.1260, found 329.1250.

4-Cyano-*N*-(2,3-dimethylphenyl)benzamide (237)

Compound **237** was synthesised according to general procedure R, using the following reagents: 4-cyanobenzoic acid (1.00 g, 6.8 mmol), HATU (3.10 g, 8.16 mmol), *N,N*-diisopropylethylamine (2.37 mL, 13.6 mmol), 2,3-dimethylaniline (1.00 mL, 8.16 mmol) and *N,N*-dimethylformamide (10 mL). The precipitation formed during the work-up was collected by vacuum filtration and dried under reduced pressure to yield the desired product **237** as a white solid (1.12 g, 63%).

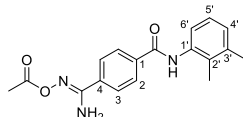
¹H-NMR (500 MHz, DMSO-*d*₆) δ 10.18 (s, 1H, CONH), 8.13 (d, *J* 8.0, 2H, H-3), 8.01 (d, *J* 8.0, 2H, H-2), 7.16 – 7.07 (m, 3H, H-3', H-4', H-5'), 2.28 (s, 3H, 3'-CH₃), 2.10 (s, 3H, 2'-CH₃); **LCMS** (LCQ) Rt = 3.4 min (method 1), *m/z* (ESI⁺) 251.1 [M+H]⁺.

***N*-(2,3-dimethylphenyl)-4-((Z)-*N*'-hydroxycarbamimidoyl)benzamide (238)**

To a solution of 4-cyano-*N*-(2,3-dimethylphenyl)benzamide (**238**) (300 mg, 1.20 mmol) and hydroxylamine hydrochloride (75 μL, 1.80 mmol) in ethanol (3 mL) was added *N,N*-diisopropylethylamine (334 μL, 1.92 mmol) and the reaction mixture heated to 80 °C for 1 h. The crude product was taken up in saturated aq. NaHCO₃ (10 mL) and extracted with ethyl acetate (3 × 10 mL). The combined organic components were then washed with 1 M aq. hydrochloric acid solution (10 mL), 1 M aq. sodium hydroxide solution (10 mL), brine (10 mL), dried over MgSO₄, filtered and concentrated under reduced pressure to yield the desired product **238** as a white solid (102 mg, 24%).

¹H-NMR (500 MHz, DMSO-*d*₆) δ 9.92 (s, 1H), 9.80 (s, 1H), 7.97 (d, *J* 8.1, 2H, H-3), 7.81 (d, *J* 8.1, 2H, H-2), 7.16 – 7.04 (m, 3H, H-3', H-4', H-5'), 5.90 (s, 2H, NH₂), 2.29 (s, 3H, 3'-CH₃), 2.10 (s, 3H, 2'-CH₃); **LCMS** (LCQ) Rt = 0.8 min (method 1), *m/z* (ESI⁺) 284.2 [M+H]⁺.

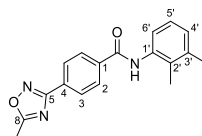
((Z)-(amino-(4-((2,3-dimethylphenyl)carbamoyl)phenyl)methylene)amino) acetate (239)



To a solution of *N*-(2,3-dimethylphenyl)-4-((Z)-*N*'-hydroxycarbamimidoyl)benzamide (**238**) (90 mg, 0.32 mmol) and triethylamine (53 μL, 0.38 mmol) in acetone (1 mL) was added acetyl chloride (27 μL, 0.38 mmol) and the reaction mixture stirred at ambient temperature for 16 h. The reaction mixture was concentrated under reduced pressure. The crude product was taken up in water (5 mL) and the solid collected by filtration to yield the desired product **239** as a white solid (43 mg, 37%).

¹H-NMR (500 MHz, DMSO-*d*₆) δ 10.13 (s, 1H, CONH), 8.14 (m, 4H, H-2, H-3), 7.15 – 7.06 (m, 3H, H-3', H-4', H-5'), 2.69 (s, 3H, OCCH₃), 2.29 (s, 3H, 3'-CH₃), 2.11 (s, 3H, 2'-CH₃); **LCMS** (LCQ) Rt = 0.7 min (method 1), *m/z* (ESI⁺) 325.9 [M+H]⁺.

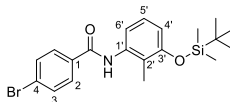
***N*-(2,3-dimethylphenyl)-4-(5-methyl-1,2,4-oxadiazol-3-yl)benzamide (240)**



To a solution of ((Z)-(amino-(4-((2,3-dimethylphenyl)carbamoyl)phenyl)methylene)amino) acetate (**239**) (40 mg, 0.12 mmol) in dimethyl sulfoxide (0.2 mL) was added potassium hydroxide (6.9 mg, 0.12 mmol) and the reaction mixture stirred at ambient temperature for 12 h. Water was added to the reaction mixture and the resulting precipitate was collected by vacuum filtration. The crude was purified by column chromatography (silica 4 g, 0 to 50% ethyl acetate in petroleum ether) to yield the desired compound **240** as a white solid (27 mg, 68%).

R_f 0.39 (petroleum ether:ethyl acetate 1:1); **m.p.** 181–183 °C; **¹H-NMR** (500 MHz, DMSO-*d*₆) δ 10.13 (s, 1H, CONH), 8.20 – 8.09 (m, 4H, H-2, H-3), 7.16 – 7.07 (m, 3H, H-3', H-4', H-5'), 2.69 (s, 3H, 8-CH₃), 2.29 (s, 3H, 3'-CH₃), 2.11 (s, 3H, 2'-CH₃); **¹³C-NMR** (126 MHz, DMSO-*d*₆) δ 178.3 (C-5), 167.6 (C-8 or ArC), 165.2 (C-8 or ArC), 137.5 (ArC), 137.5 (ArC), 136.5 (ArC), 133.2 (ArC), 129.3 (ArC), 129.0 (C-3), 128.2 (ArC), 127.4 (C-2), 125.8 (ArC), 125.1 (ArC), 20.6 (2'-CH₃), 14.7 (3'-CH₃), 12.5 (8-CH₃); **IR** (neat, ν_{max}, cm⁻¹) 3273, 1645, 1587, 1509, 1453, 1300, 1281, 1250; **LCMS** (LCQ) Rt = 3.7 min (method 1), *m/z* (ESI⁺) 308.2 [M+H]⁺; **HRMS (ESI)**: calcd. for C₁₈H₁₈N₃O₂ [M+H]⁺ 308.1394, found 308.1388.

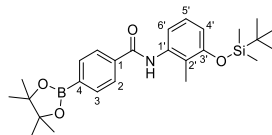
4-Bromo-*N*-(3-(tert-butyl(dimethyl)silyl)oxy-2-methyl-phenyl)benzamide (241)



Compound **241** was synthesised according to general procedure R, using the following reagents: *p*-bromobenzoic acid (500 mg, 2.50 mmol), HATU (1.14 g, 2.98 mmol), *N,N*-diisopropylethylamine (867 μL, 4.97 mmol), 3-(tert-butyl(dimethyl)silyl)oxy-2-methyl-aniline (1.42 g, 2.98 mmol) and *N,N*-dimethylformamide (5 mL). The crude was purified by column chromatography (silica, 0 to 5% ethyl acetate in petroleum ether) to yield the desired compound **241** as a white solid (863 mg, 78%).

¹H-NMR (500 MHz, DMSO-*d*₆) δ 9.99 (s, 1H, CONH), 7.91 (d, *J* 7.5, 2H, H-2), 7.74 (d, *J* 6.8, 2H, H-3), 7.09 (t, *J* 7.6, 1H, H-5'), 6.93 (d, *J* 7.7, 1H, ArH), 6.76 (d, *J* 7.9, 1H, ArH), 2.04 (s, 3H, 2'-CH₃), 1.00 (s, 9H, OSi(CH₃)₂(CH₃)₃), 0.22 (s, 6H, OSi(CH₃)₂(CH₃)₃); **LCMS** (LCQ) Rt = 6.7 min (method 1), no ionisation observed.

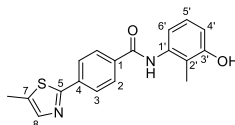
***N*-(3-(tert-butyl(dimethyl)silyl)oxy-2-methyl-phenyl)-4-(4,4,5,5-tetramethyl-1,3,2-dioxaborolan-2-yl)benzamide (242)**



Compound **242** was synthesised according to general procedure U, using the following reagents: 4-bromo-*N*-(3-(tert-butyl(dimethyl)silyl)oxy-2-methyl-phenyl)benzamide (**241**) (300 mg, 0.70 mmol), bis(pinacolato)diboron (217 mg, 0.86 mmol), (1,1'-bis(diphenylphosphino)ferrocene)dichloropalladium(II) (26 mg, 0.04 mmol), potassium acetate (210 mg, 2.14 mmol) and 1,4-dioxane (3 mL) and stirred for 16 h. The crude was purified by column chromatography (silica 12 g, 0 to 15% ethyl acetate in petroleum ether) to yield the desired product **242** as a pale yellow solid (285 mg, 77%).

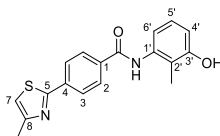
¹H-NMR (500 MHz, DMSO-*d*₆) δ 9.97 (s, 1H, CONH), 7.95 (d, *J* 7.4, 2H, H-2), 7.77 (d, *J* 7.7, 2H, H-3), 7.07 (t, *J* 7.8, 1H, H-5'), 6.92 (d, *J* 7.7, 1H, ArH), 6.73 (d, *J* 7.8, 1H, ArH), 2.02 (s, 3H, 2'-CH₃), 1.30 (s, 12H, B(OC(CH₃)₂)₂), 0.97 (s, 9H, OSi(CH₃)₂(CH₃)₃), 0.20 (s, 6H, OSi(CH₃)₂(CH₃)₃); **LCMS** (LCQ) Rt = 7.0 min (method 1), no ionisation observed.

***N*-(3-hydroxy-2-methyl-phenyl)-4-(4-methylthiazol-2-yl)benzamide (243)**



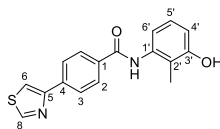
Compound **243** was synthesised according to general procedure V, using the following reagents: *N*-(3-(tert-butyl(dimethyl)silyl)oxy-2-methyl-phenyl)-4-(4,4,5,5-tetramethyl-1,3,2-dioxaborolan-2-yl)benzamide (**242**) (120 mg, 0.26 mmol), 2-bromo-4-methylthiazole (28 μL, 0.26 mmol), (1,1'-bis(diphenylphosphino)ferrocene)dichloropalladium(II) (19 mg, 0.03 mmol), sodium carbonate (272 mg, 2.57 mmol), 1,4-dioxane (2 mL) and water (2 mL). The crude was purified by column chromatography (silica 12 g, 0 to 3% methanol in dichloromethane) to yield the desired product **243** as a brown solid (73 mg, 83%).

R_f 0.77 (ethyl acetate); **m.p.** 210–212 °C; **¹H-NMR** (500 MHz, DMSO-*d*₆) δ 9.97 (s, 1H, CONH), 9.44 (s, 1H, ArOH), 8.10 – 7.99 (m, 4H, H-2, H-3), 7.43 (s, 1H, H-8), 7.00 (t, *J* 7.7, 1H, H-5'), 6.78 (d, *J* 7.8, 1H, ArH), 6.73 (d, *J* 7.9, 1H, ArH), 2.45 (s, 3H, 7-CH₃), 2.02 (s, 3H, 2'-CH₃); **¹³C-NMR** (126 MHz, DMSO-*d*₆) δ 165.7 (C-5 or CO), 165.2 (C-5 or CO), 156.2 (ArC), 154.2 (ArC), 137.6 (ArC), 136.0 (ArC), 129.0 (C-2), 128.0 (ArC), 126.3 (C-3), 126.1 (H-5'), 121.3 (ArC), 118.0 (ArC), 116.2 (C-8), 113.0 (ArC), 17.3 (7-CH₃), 11.4 (2'-CH₃); **IR** (neat, ν_{max}, cm⁻¹) 3216, 1646, 1596, 1490, 1449, 1293, 1267, 1163; **LCMS** (LCQ) Rt = 0.7 min (method 1), *m/z* (ESI⁺) 325.2 [M+H]⁺; **HRMS (ESI)**: calcd. for C₁₈H₁₇N₂O₂S [M+Na]⁺ 325.1005, found 325.1016.

***N*-(3-hydroxy-2-methyl-phenyl)-4-(5-methylthiazol-2-yl)benzamide (244)**

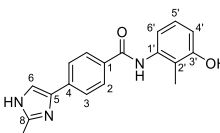
Compound **244** was synthesised according to general procedure V, using the following reagents: *N*-(3-(tert-butyl(dimethyl)silyl)oxy-2-methyl-phenyl)-4-(4,4,5,5-tetramethyl-1,3,2-dioxaborolan-2-yl)benzamide (**242**) (120 mg, 0.26 mmol), 2-bromo-5-methyl-1,3-thiazole (27 μ L, 0.26 mmol), (1,1'-bis(diphenylphosphino)ferrocene)dichloropalladium(II) (19 mg, 0.03 mmol), sodium carbonate (272 mg, 2.57 mmol), 1,4-dioxane (2 mL) and water (2 mL). The crude was purified by column chromatography (silica 12 g, 0 to 45% ethyl acetate in petroleum ether) to yield the desired product **244** as a brown solid (73 mg, 83%).

R_f 0.72 (ethyl acetate); **m.p.** 246–248 °C; **¹H-NMR** (500 MHz, DMSO-*d*₆) δ 9.95 (s, 1H), 9.44 (s, 1H), 8.06 (d, *J* 7.9, 2H), 8.00 (d, *J* 7.8, 2H), 7.68 (s, 1H), 7.00 (t, *J* 7.9, 1H), 6.78 (d, *J* 7.8, 1H), 6.73 (d, *J* 7.9, 1H), 2.52 (s, 3H), 2.02 (s, 3H); **¹³C-NMR** (126 MHz, DMSO-*d*₆) δ 165.1, 164.8, 156.2, 142.6, 137.7, 136.2, 135.9, 129.0, 126.1, 126.1, 121.2, 118.0, 113.0, 12.1, 11.4; **IR** (neat, ν_{max} , cm⁻¹) 3205, 1646, 1596, 1490, 1450, 1293, 1268; **LCMS** (LCQ) *R*_t = 3.0 min (method 1), *m/z* (ESI⁺) 325.2 [M+H]⁺; **HRMS (ESI)**: calcd. for C₁₈H₁₇N₂O₂S [M+H]⁺ 325.1005, found 325.1015.

***N*-(3-hydroxy-2-methyl-phenyl)-4-thiazol-4-yl-benzamide (246)**

Compound **246** was synthesised according to general procedure V, using the following reagents: *N*-(3-(tert-butyl(dimethyl)silyl)oxy-2-methyl-phenyl)-4-(4,4,5,5-tetramethyl-1,3,2-dioxaborolan-2-yl)benzamide (**242**) (80 mg, 0.17 mmol), 4-bromothiazole (28 mg, 0.17 mmol), (1,1'-bis(diphenylphosphino)ferrocene)dichloropalladium(II) (16 mg, 0.02 mmol), sodium carbonate (181 mg, 1.71 mmol), 1,4-dioxane (2 mL) and water (2 mL). The crude was purified by column chromatography (silica 12 g, 0 to 3% methanol in dichloromethane) and purified by column chromatography (silica 12 g, 0 to 3% methanol in dichloromethane) to yield the desired product **246** as a light brown solid (35 mg, 63%).

R_f 0.36 (dichloromethane:methanol 19:1); **m.p.** 248–251 °C; **¹H-NMR** (500 MHz, DMSO-*d*₆) δ 9.89 (s, 1H), 9.41 (s, 1H), 9.25 (s, 1H), 8.36 (s, 1H), 8.14 (d, *J* 8.1, 2H), 8.06 (d, *J* 8.1, 2H), 7.00 (t, *J* 8.0, 1H), 6.79 (d, *J* 7.9, 1H), 6.73 (d, *J* 8.0, 1H), 2.02 (s, 3H); **¹³C-NMR** (126 MHz, DMSO-*d*₆) δ 155.8, 154.3, 137.3, 137.1, 133.9, 128.7, 126.5, 126.4, 121.5, 118.3, 116.7, 11.2. ArC and CO not visible; **IR** (neat, ν_{max} , cm⁻¹) 3215, 1635, 1592, 1492, 1454, 1331, 1269; **LCMS** (LCQ) *R*_t = 1.5 min (method 1), *m/z* (ESI⁺) 311.1 [M+H]⁺; **HRMS (ESI)**: calcd. for C₁₇H₁₄N₂O₂S [M+H]⁺ 309.1239, found 309.1242.

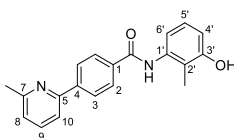
***N*-(3-hydroxy-2-methyl-phenyl)-4-(2-methyl-1H-imidazol-4-yl)benzamide (247)**

Compound **247** was synthesised according to general procedure V, using the following reagents: *N*-(3-(tert-butyl(dimethyl)silyl)oxy-2-methyl-phenyl)-4-(4,4,5,5-tetramethyl-1,3,2-dioxaborolan-2-yl)benzamide (**242**) (100 mg, 0.21 mmol), 4-bromo-2-methyl-1H-imidazole (34 mg, 0.21 mmol), (1,1'-bis(diphenylphosphino)ferrocene)dichloropalladium(II) (16 mg, 0.02 mmol), sodium carbonate (227 mg, 2.14 mmol),

1,4-dioxane (2 mL) and water (2 mL). The crude was purified by column chromatography (silica 12 g, 0 to 10% methanol in dichloromethane) to yield the desired product **247** as a brown solid (13 mg, 19%).

R_f 0.36 (dichloromethane:methanol 19:1); **m.p.** 276–278 °C; **¹H-NMR** (500 MHz, DMSO-*d*₆) δ 11.90 (s, 1H), 9.72 (s, 1H), 9.35 (s, 1H), 8.03 – 7.86 (m, 2H), 7.84 – 7.69 (m, 2H), 7.58 (s, 1H), 6.95 (s, 1H), 6.80 – 6.58 (m, 2H), 2.28 (s, 3H), 1.97 (s, 3H); **IR** (neat, ν_{max} , cm⁻¹) 3205, 1644, 1602, 1535, 1490, 1450, 1434, 1327, 1293; **LCMS** (LCQ) *R*_t = 0.4 min (method 1), *m/z* (ESI⁺) 382.2 [M+H]⁺; Not enough material for ¹³C-NMR and HRMS determination.

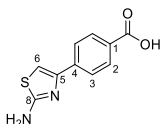
***N*-(3-hydroxy-2-methyl-phenyl)-4-(6-methyl-2-pyridyl)benzamide (248)**



Compound **248** was synthesised according to general procedure V, using the following reagents: *N*-(3-(tert-butyl(dimethyl)silyl)oxy-2-methyl-phenyl)-4-(4,4,5,5-tetramethyl-1,3,2-dioxaborolan-2-yl)benzamide (**242**) (100 mg, 0.21 mmol), 2-bromo-6-methylpyridine (37 mg, 0.21 mmol), (1,1'-bis(diphenylphosphino)ferrocene)dichloropalladium(II) (16 mg, 0.02 mmol), sodium carbonate (227 mg, 2.14 mmol), 1,4-dioxane (2 mL) and water (2 mL). The crude was purified by column chromatography (silica 12 g, 0 to 45% ethyl acetate in petroleum ether) to yield the desired product **248** as a pale yellow solid (25 mg, 35%).

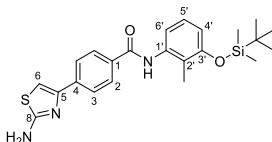
R_f 0.24 (petroleum ether:ethyl acetate 3:1); **m.p.** 198–200 °C; **¹H-NMR** (500 MHz, DMSO-*d*₆) δ 9.93 (s, 1H), 9.43 (s, 1H), 8.21 (d, *J* 8.3, 2H), 8.08 (d, *J* 7.5, 2H), 7.87 (d, *J* 7.8, 1H), 7.81 (t, *J* 6.6, 1H), 7.28 (d, *J* 7.2, 1H), 7.00 (t, *J* 7.9, 1H), 6.79 (d, *J* 7.4, 1H), 6.74 (d, *J* 8.1, 1H), 2.57 (s, 3H), 2.03 (s, 3H); **¹³C-NMR** (126 MHz, DMSO-*d*₆) δ 165.4, 158.4, 156.2, 154.7, 138.2, 137.8, 135.1, 133.6, 128.5, 126.9, 126.1, 123.1, 121.3, 118.4, 118.0, 112.9, 24.7, 11.4; **LCMS** (LCQ) *R*_t = 1.1 min (method 1), *m/z* (ESI⁺) 319.2 [M+H]⁺; **HRMS (ESI)**: calcd. for C₂₀H₁₉N₂O₂ [M+H]⁺ 319.1441, found 319.1450.

4-(2-Aminothiazol-4-yl)benzoic acid (249)



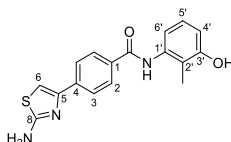
To methyl 4-(2-bromoacetyl)benzoate (195 mg, 0.76 mmol) (**100**) in methanol (5 mL) was added thiourea (58 mg, 0.78 mmol) and the reaction mixture stirred at ambient temperature for 1 h. The reaction mixture was concentrated under reduced pressure. The crude was taken up in methanol (5 mL) and water (2 mL) and to the mixture was added sodium hydroxide (304 mg, 7.60 mmol). The reaction mixture was concentrated under reduced pressure. The crude product was taken up in water (5 mL) and the mixture acidified to pH of 2-3 using 2 M aq. hydrochloric acid solution. The resulting precipitate was collected by vacuum filtration and dried under reduced pressure to afford the desired compound **249** as a pale yellow solid (159 mg, 89%).

¹H-NMR (500 MHz, DMSO-*d*₆) δ 7.98 (d, *J* 8.3, 2H, H-2), 7.89 (d, *J* 8.5, 2H, H-3), 7.34 (s, 1H, H-6); **LCMS** (LCQ) *R*_t = 0.6 min (method 1), *m/z* (ESI⁺) 221.2 [M+H]⁺.

4-(2-Aminothiazol-4-yl)-*N*-(3-hydroxy-2-methyl-phenyl)benzamide (250)

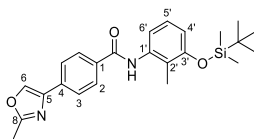
Compound **250** was synthesised according to general procedure R, using the following reagents: 4-(2-aminothiazol-4-yl)benzoic acid (**100**) (85 mg, 0.39 mmol), HATU (161 mg, 0.42 mmol), *N,N*-diisopropylethylamine (134 μ L, 0.77 mmol), 3-(tert-butyl(dimethyl)silyl)oxy-2-methyl-aniline (**120**) (183 mg, 0.39 mmol) and *N,N*-dimethylformamide (1 mL). The crude was purified by column chromatography (amino silica 12 g, 0 to 75% ethyl acetate in petroleum ether) and further purified by column chromatography (silica 12 g, 0 to 50% ethyl acetate in petroleum ether) to yield the desired compound **250** as a white solid (54 mg, 30%).

¹H-NMR (500 MHz, DMSO-*d*₆) δ 7.88 (d, *J* 8.3, 2H), 7.85 (d, *J* 8.2, 2H), 7.79 (s, 1H), 7.49 (d, *J* 7.1, 1H), 7.09 (t, *J* 8.1, 1H), 6.82 (s, 1H), 6.68 (d, *J* 8.1, 1H), 5.39 (s, 2H), 2.18 (s, 3H), 1.02 (s, 9H), 0.22 (s, 6H); **LCMS** (LCQ) Rt = 5.3 min (method 1), *m/z* (ESI⁺) 440.2 [M+H]⁺.

4-(2-Aminothiazol-4-yl)-*N*-(3-hydroxy-2-methyl-phenyl)benzamide (251)

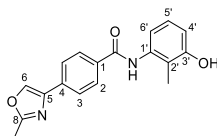
4-(2-Aminothiazol-4-yl)-*N*-(3-hydroxy-2-methyl-phenyl)benzamide (**250**) (53 mg, 0.24 mmol) in tetrahydrofuran (1 mL) and was cooled to 0 °C and to the reaction mixture was added tetrabutylammonium fluoride (241 μ L, 0.31 mmol). The reaction mixture was stirred at 0 °C for 5 min and at ambient temperature for 10 min. The reaction mixture was concentrated under reduced pressure. The crude was purified by column chromatography (silica 12 g, 0 to 8% methanol in dichloromethane) to yield the desired amide (**251**) as a colourless solid (38 mg, 92%).

m.p. 230–232 °C; **¹H-NMR** (500 MHz, DMSO-*d*₆) δ 9.82 (s, 1H), 9.39 (s, 1H), 7.97 (d, *J* 8.2, 2H), 7.92 (d, *J* 8.4, 2H), 7.21 (s, 1H), 7.14 (s, 2H), 6.99 (app t, *J* 8.0, 1H), 6.77 (d, *J* 7.8, 1H), 6.72 (d, *J* 8.1, 1H), 2.01 (s, 3H); **IR** (neat, ν_{max} , cm⁻¹) 3301, 2923, 1610, 1539, 1522, 1289, 1169; **LCMS** (LCQ) Rt = 0.6 min (method 1), *m/z* (ESI⁺) 326.1 [M+H]⁺; **HRMS** (ESI): calcd. for C₁₇H₁₆N₃O₂S [M+Na]⁺ 347.0825, found 347.0827.

***N*-(3-(tert-butyl(dimethyl)silyl)oxy-2-methyl-phenyl)-4-(2-methyloxazol-4-yl)benzamide (252)**

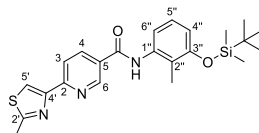
Compound **252** was synthesised according to general procedure M, using the following reagents: 4-(2-methyloxazol-4-yl)benzoic acid (**192**) (100 mg, 0.49 mmol), oxalyl chloride (50 μ L, 0.59 mmol), *N,N*-dimethylformamide (10 μ L) and dichloromethane (3 mL) and stirred for 16 h. Followed 3-(tert-butyl(dimethyl)silyl)oxy-2-methyl-aniline (**120**) (140 mg, 0.59 mmol), *N,N*-diisopropylethylamine (429 μ L, 2.46 mmol) and dichloromethane (1 mL) and stirred for 16 h. The crude was purified by column chromatography (silica 12 g, 0 to 3% methanol in dichloromethane) to yield the desired amide **252** as a white solid (177 mg, 68%).

¹H-NMR (500 MHz, DMSO-*d*₆) δ 9.93 (s, 1H), 8.61 (s, 1H), 8.02 (d, *J* 8.3, 2H), 7.89 (d, *J* 7.9, 2H), 7.10 (t, *J* 8.0, 1H), 6.95 (d, *J* 8.0, 1H), 6.76 (d, *J* 8.1, 1H), 2.06 (s, 3H), 1.00 (s, 9H), 0.25 – 0.20 (s, 6H); **LCMS** (LCQ) Rt = 8.6 min (method 3), *m/z* (ESI⁺) 423.2 [M+H]⁺.

***N*-(3-(hydroxy-2-methyl-phenyl)-4-(2-methyloxazol-4-yl)benzamide (253)**

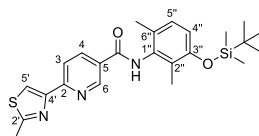
N-(3-(*tert*-butyl(dimethyl)silyl)oxy-2-methyl-phenyl)-4-(2-methyloxazol-4-yl)benzamide (**252**) (177 mg, 0.34 mmol) in tetrahydrofuran (2 mL) and was cooled to 0 °C and to the reaction mixture was added tetrabutylammonium fluoride (67 μ L, 0.67 mmol). The reaction mixture was stirred at 0 °C for 5 min and at ambient temperature for 10 min. The reaction mixture was concentrated under reduced pressure. The crude was purified by column chromatography (silica 12 g, 0 to 5% methanol in dichloromethane) to yield the desired amide **253** as a white solid (54 mg, 50%).

m.p. 252–254 °C; **¹H-NMR** (500 MHz, DMSO-*d*₆) δ 9.86 (s, 1H), 9.40 (s, 1H), 8.61 (s, 1H), 8.02 (d, *J* 7.9, 2H), 7.88 (d, *J* 8.0, 2H), 6.99 (t, *J* 8.0, 1H), 6.77 (d, *J* 7.7, 1H), 6.73 (d, *J* 8.2, 1H), 2.01 (s, 3H). 8-CH₃ under DMSO peak; **IR** (neat, ν_{\max} , cm⁻¹) 3344, 2939, 1698, 1643, 1583, 1531, 1502, 1459, 1376, 1281; **LCMS** (LCQ) *R*_t = 0.6 min (method 1), *m/z* (ESI⁺) 309.1 [M+H]⁺; **HRMS (ESI)**: calcd. for C₁₈H₁₈N₃O₂ [M+Na]⁺ 308.1394, found 308.1394.

***N*-(3-(tert-butyl(dimethyl)silyl)oxy-2-methyl-phenyl)-6-(2-methylthiazol-4-yl)pyridine-3-carboxamide (254)**

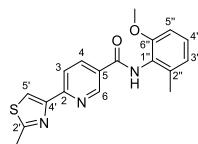
Compound **254** was synthesised according to general procedure Y, using the following reagents: : 6-(2-methylthiazol-4-yl)pyridine-3-carboxylic acid (**183**) (100 mg, 0.46 mmol), oxalyl chloride (58 μ L, 0.68 mmol), *N,N*-dimethylformamide (10 μ L) and dichloromethane (3 mL) and stirred for 16 h. Followed 3-(*tert*-butyl(dimethyl)silyl)oxy-2-methyl-aniline (**120**) (217 mg, 0.91 mmol), triethylamine (190 μ L, 1.37 mmol), 4-(dimethylamino)pyridine (5.6 mg, 0.05 mmol) and dichloromethane (1 mL) and stirred for 2 h. The crude was purified by column chromatography (silica 12 g, 0 to 5% methanol in dichloromethane) to yield the desired amide **254** as a red/brown solid (81 mg, 20%).

¹H-NMR (500 MHz, DMSO-*d*₆) δ 10.14 (s, 1H), 9.14 (s, 1H), 8.41 (d, *J* 7.9, 1H), 8.28 (s, 1H), 8.16 (d, *J* 8.3, 1H), 7.12 (t, *J* 8.0, 1H), 6.98 (d, *J* 7.8, 1H), 6.78 (d, *J* 8.1, 1H), 2.76 (s, 3H), 2.08 (s, 3H), 1.00 (s, 9H), 0.23 (s, 6H).

***N*-(3-(tert-butyl(dimethyl)silyl)oxy-2,6-dimethyl-phenyl)-6-(2-methylthiazol-4-yl)pyridine-3-carboxamide (255)**

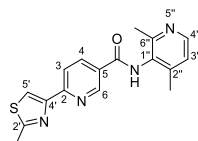
Compound **255** was synthesised according to general procedure Y, using the following reagents: : 6-(2-methylthiazol-4-yl)pyridine-3-carboxylic acid (**183**) (80 mg, 0.36 mmol), oxalyl chloride (77 μ L, 0.91 mmol), *N,N*-dimethylformamide (10 μ L) and dichloromethane (3 mL) and stirred for 16 h. Followed 3-(*tert*-butyl(dimethyl)silyl)oxy-2,6-dimethyl-aniline (**143**) (91 mg, 0.36 mmol), triethylamine (152 μ L, 1.09 mmol), 4-(dimethylamino)pyridine (4.5 mg, 0.04 mmol) and dichloromethane (1 mL) and stirred for 2 h. The crude was purified by column chromatography (silica 12 g, 0 to 5% methanol in dichloromethane) to yield the desired amide **255** as a white solid (20 mg, 11%).

¹H-NMR (500 MHz, Chloroform-*d*) δ 9.12 (s, 1H), 8.29 (dd, *J* 8.2, 1.8, 1H), 8.20 (d, *J* 8.2, 1H), 8.04 (s, 1H), 7.47 (s, 1H), 6.97 (d, *J* 8.3, 1H), 6.73 (d, *J* 8.3, 1H), 2.80 (s, 3H), 2.21 (s, 3H), 2.15 (s, 3H), 1.01 (s, 9H), 0.21 (s, 6H).

***N*-(2-methoxy-6-methyl-phenyl)-6-(2-methylthiazol-4-yl)pyridine-3-carboxamide (256)**

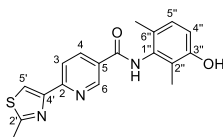
Compound **256** was synthesised according to general procedure Y, using the following reagents: 6-(2-methylthiazol-4-yl)pyridine-3-carboxylic acid (**183**) (100 mg, 0.46 mmol), oxalyl chloride (58 μ L, 0.68 mmol), *N,N*-dimethylformamide (10 μ L) and dichloromethane (3 mL) and stirred for 16 h. Followed 2-methoxy-6-methylaniline (75 mg, 0.55 mmol), triethylamine (190 μ L, 1.37 mmol), 4-(dimethylamino)pyridine (5.6 mg, 0.05 mmol) and dichloromethane (1 mL) and stirred for 2 h. The crude was purified by column chromatography (silica 12 g, 0 to 60% ethyl acetate in petroleum ether) to yield the desired amide **256** as a white solid (45 mg, 81%).

R_f 0.35 (petroleum ether:ethyl acetate 1:1); **m.p.** 188–189 °C; **¹H-NMR** (500 MHz, DMSO-*d*₆) δ 9.84 (s, 1H, CONH), 9.16 (s, 1H, H-6), 8.42 (dd, *J* 8.2, 2.0 Hz, 1H, H-4), 8.27 (s, 1H, H-5'), 8.16 (d, *J* 8.2, 1H, H-3), 7.21 (t, *J* 7.9, 1H, H-4''), 6.94 (d, *J* 8.2, 1H, ArH), 6.89 (d, *J* 7.6, 1H, ArH), 3.75 (s, 3H, OCH₃), 2.76 (s, 3H, 2'-CH₃), 2.18 (s, 3H, 2''-CH₃); **¹³C-NMR** (126 MHz, DMSO-*d*₆) δ 167.0 (2'-C or CO), 163.8 (2'-C or CO), 155.6 (ArC), 153.7 (ArC), 149.4 (C-6), 137.4 (ArC), 137.2 (C-4), 129.0 (ArC), 128.0 (C-4''), 125.1 (ArC), 122.4 (ArC), 120.4 (C-3), 119.8 (C-5'), 109.6 (ArC), 56.0 (OCH₃), 19.4 (2'-CH₃), 18.3 (2''-CH₃); **LCMS** (LCQ) *R_t* = 1.8 min (method 1), *m/z* (ESI⁺) 340.1 [M+H]⁺; **HRMS (ESI)**: calcd. for C₁₈H₁₈N₃O₂S [M+H]⁺ 340.1114, found 340.1131.

***N*-(2,4-dimethyl-3-pyridyl)-6-(2-methylthiazol-4-yl)pyridine-3-carboxamide (257)**

Compound **257** was synthesised according to general procedure O, using the following reagents: 6-(2-methylthiazol-4-yl)pyridine-3-carboxylic acid (**183**) (100 mg, 0.46 mmol), 4,6-dimethyl-3-pyridinamine (139 mg, 1.14 mmol), phosphorus trichloride (40 μ L, 0.45 mmol), tetrahydrofuran (0.75 mL) and acetonitrile (0.25 mL). The crude was purified by column chromatography (silica 12 g, 0 to 2% methanol in ethyl acetate) and further purified by column chromatography (amino silica 12 g, 0 to 75% ethyl acetate in petroleum ether) to yield the desired amide **257** as a light pink solid (38 mg, 25%).

R_f 0.32 (ethyl acetate:methanol 19:1); **m.p.** 150–152 °C; **¹H-NMR** (500 MHz, DMSO-*d*₆) δ 10.20 (s, 1H), 9.18 (s, 1H), 8.44 (d, *J* 9.3, 1H), 8.31–8.25 (m, 2H), 8.19 (d, *J* 8.2, 1H), 7.20 (d, *J* 4.6, 1H), 2.77 (s, 3H), 2.40 (s, 3H), 2.22 (s, 3H); **¹³C-NMR** (126 MHz, DMSO-*d*₆) δ 167.0, 164.0, 156.1, 154.6, 153.7, 149.4, 147.4, 145.2, 137.2, 131.6, 128.6, 123.8, 120.5, 120.0, 21.5, 19.5, 17.9; **IR** (neat, ν_{max} , cm⁻¹) 3198, 1644, 1595, 1505, 1434, 1426, 1372, 1225; **LCMS** (LCQ) *R_t* = 0.6 min (method 1), *m/z* (ESI⁺) 325.2 [M+H]⁺; **HRMS (ESI)**: calcd. for C₁₇H₁₆NaN₄OS [M+H]⁺ 325.1005, found 325.1016.

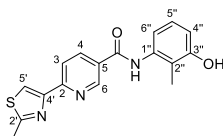
***N*-(3-hydroxy-2,6-dimethyl-phenyl)-6-(2-methylthiazol-4-yl)pyridine-3-carboxamide (258)**

***N*-(3-(tert-butyl(dimethyl)silyl)oxy-2,6-dimethyl-phenyl)-6-(2-methylthiazol-4-yl)pyridine-3-carboxamide (254)** (20 mg, 0.04 mmol) in tetrahydrofuran (1 mL) and was cooled to 0 °C and to the reaction mixture was added tetrabutylammonium fluoride (88 μ L, 0.09 mmol). The reaction mixture was stirred at 0 °C for 5 min and at ambient

temperature for 10 min. The reaction mixture was concentrated under reduced pressure. The crude was purified by column chromatography (silica 12 g, 0 to 5% methanol in dichloromethane) to yield the desired amide **258** as a brown solid (10 mg, 65%).

m.p. 245–247 °C; **¹H-NMR** (500 MHz, DMSO-*d*₆) δ 9.95 (s, 1H), 9.24 (s, 1H), 9.17 (s, 1H), 8.42 (dd, *J* 8.5, 2.4, 1H), 8.27 (s, 1H), 8.16 (d, *J* 8.3, 1H), 6.91 (d, *J* 8.2, 1H), 6.72 (d, *J* 8.2, 1H), 2.76 (s, 3H), 2.08 (s, 3H), 2.00 (s, 3H); **¹³C-NMR** (126 MHz, DMSO-*d*₆) δ 166.4, 165.0, 154.1, 153.3, 137.2, 136.4, 133.9, 128.5, 127.3, 126.2, 126.0, 122.7, 115.9, 113.6, 19.4, 18.0, 11.6; **IR** (neat, *v*_{max}, cm⁻¹) 3211, 1637, 1596, 1498, 1418, 1329, 1294; **LCMS** (LCQ) *R*_t = 2.1 min (method 1), *m/z* (ESI⁺) 340.1 [M+H]⁺; Not enough material for ¹³C-NMR and HRMS determination.

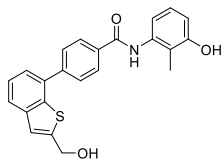
***N*-(3-(hydroxy-2-methyl-phenyl)-6-(2-methylthiazol-4-yl)pyridine-3-carboxamide (259)**



N-(3-(*tert*-butyl(dimethyl)silyloxy-2-methyl-phenyl)-6-(2-methylthiazol-4-yl)pyridine-3-carboxamide (70 mg, 0.16 mmol) in tetrahydrofuran (2 mL) and was cooled to 0 °C and to the reaction mixture was added tetrabutylammonium fluoride (88 μL, 0.09 mmol). The reaction mixture was stirred at 0 °C for 5 min and at ambient temperature for 10 min. The reaction mixture was concentrated under reduced pressure. The crude was purified by column chromatography (silica 12 g, 0 to 5% methanol in dichloromethane) to yield the desired amide **259** as a white solid (40 mg, 73%).

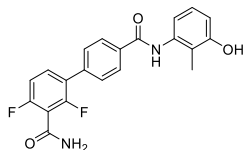
m.p. 226–228 °C; **¹H-NMR** (500 MHz, DMSO-*d*₆) δ 10.07 (s, 1H), 9.45 (s, 1H), 9.14 (s, 1H), 8.41 (d, *J* 7.8 Hz, 1H), 8.27 (s, 1H), 8.15 (d, *J* 8.1, 1H), 7.01 (t, *J* 7.9, 1H), 6.80 (d, *J* 7.3, 1H), 6.74 (d, *J* 8.1, 1H), 2.76 (s, 3H), 2.03 (s, 3H); **¹³C-NMR** (126 MHz, DMSO-*d*₆) δ 166.9, 164.0, 156.3, 154.4, 153.7, 149.3, 137.4, 137.2, 129.3, 126.1, 121.2, 120.4, 119.8, 117.9, 113.1, 19.4, 11.4; **IR** (neat, *v*_{max}, cm⁻¹) 3202, 3043, 1638, 1596, 1540, 1496, 1433, 1327, 1216; **LCMS** (LCQ) *R*_t = 1.5 min (method 1), *m/z* (ESI⁺) 326.2 [M+H]⁺; **HRMS (ESI)**: calcd. for C₁₇H₁₆NaN₃O₂S [M+H]⁺ 326.0958, found 326.0965.

4-(2-(Hydroxymethyl)benzothiophen-7-yl)-*N*-(3-(hydroxy-2-methyl-phenyl)benzamide (260)



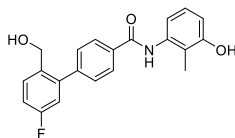
Compound **260** was synthesised according to general procedure V, using the following reagents: *N*-(3-(*tert*-butyl(dimethyl)silyloxy-2-methyl-phenyl)-4-(4,4,5,5-tetramethyl-1,3,2-dioxaborolan-2-yl)benzamide (**242**) (100 mg, 0.21 mmol), (7-bromo-1-benzothiophen-2-yl)methanol (52 mg, 0.21 mmol), (1,1'-bis(diphenylphosphino)ferrocene)dichloropalladium(II) (16 mg, 0.02 mmol), sodium carbonate (227 mg, 2.14 mmol), 1,4-dioxane (2 mL) and water (2 mL). The crude was purified by column chromatography (silica 12 g, 0 to 3% methanol in dichloromethane) to yield the desired product **260** as a yellow solid (28 mg, 32%).

¹H-NMR (500 MHz, DMSO-*d*₆) 9.96 (s, 1H), 9.45 (s, 1H), 8.13 (d, *J* 7.9, 2H), 7.86 (d, *J* 8.3, 2H), 7.83 (d, *J* 8.5, 1H), 7.50 (app t, *J* 7.6, 1H), 7.43 (d, *J* 7.3, 1H), 7.38 (s, 1H), 7.02 (app t, *J* 8.0, 1H), 6.82 (d, *J* 7.9, 1H), 6.75 (d, *J* 8.1, 1H), 5.71 (t, *J* 5.8, 1H), 4.76 (d, *J* 5.4, 2H), 2.05 (s, 3H); **LCMS** (LCQ) *R*_t = 0.6 min (method 2), *m/z* (ESI⁺) 390.1 [M+H]⁺.

2,6-difluoro-3-(4-((3-hydroxy-2-methyl-phenyl)carbamoyl)phenyl)benzamide (261)

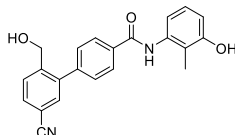
Compound **261** was synthesised according to general procedure V, using the following reagents: *N*-(3-(tert-butyl(dimethyl)silyl)oxy-2-methyl-phenyl)-4-(4,4,5,5-tetramethyl-1,3,2-dioxaborolan-2-yl)benzamide (**242**) (65 mg, 0.15 mmol), 2,6-difluoro-3-(4,4,5,5-tetramethyl-1,3,2-dioxaborolan-2-yl)benzamide (52 mg, 0.13 mmol), (1,1'-bis(diphenylphosphino)ferrocene)dichloropalladium(II) (11 mg, 0.02 mmol), sodium carbonate (164 mg, 1.55 mmol), 1,4-dioxane (1.5 mL) and water (1.5 mL). The crude was purified by column chromatography (silica 12 g, 0 to 5% methanol in dichloromethane) and further purified by column chromatography (amino silica 12 g, 0 to 5% methanol in dichloromethane) to yield the desired product **261** as a pale orange solid (7 mg, 11%).

¹H-NMR (500 MHz, DMSO-*d*₆) 9.94 (s, 1H), 9.43 (s, 1H), 8.23 (s, 1H), 8.08 (d, *J* 8.3, 2H), 7.95 (s, 1H), 7.73 – 7.64 (m, 3H), 7.31 (app t, *J* 8.7, 1H), 7.00 (app t, *J* 7.8, 1H), 6.79 (d, *J* 7.8, 1H), 6.74 (d, *J* 8.1, 1H), 2.03 (s, 3H); LCMS (LCQ) Rt = 1.4 min (method 2), *m/z* (ESI⁺) 383.1 [M+H]⁺.

4-(5-Fluoro-2-(hydroxymethyl)phenyl)-*N*-(3-hydroxy-2-methyl-phenyl)benzamide (262)

Compound **262** was synthesised according to general procedure V, using the following reagents: *N*-(3-(tert-butyl(dimethyl)silyl)oxy-2-methyl-phenyl)-4-(4,4,5,5-tetramethyl-1,3,2-dioxaborolan-2-yl)benzamide (**242**) (100 mg, 0.21 mmol), (2-bromo-4-fluorophenyl)methanol (44 mg, 0.21 mmol), (1,1'-bis(diphenylphosphino)ferrocene)dichloropalladium(II) (16 mg, 0.02 mmol), sodium carbonate (227 mg, 2.14 mmol), 1,4-dioxane (2 mL) and water (2 mL). The crude was purified by column chromatography (silica 12 g, 0 to 5% methanol in dichloromethane) to yield the desired product **262** as an off-white solid (36 mg, 46%).

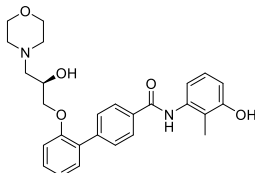
¹H-NMR (500 MHz, DMSO-*d*₆) δ 9.92 (s, 1H), 9.42 (s, 1H), 8.04 (d, *J* 7.9, 2H), 7.61 (dd, *J* 8.6, 6.0, 1H), 7.56 (d, *J* 8.1, 2H), 7.26 (app td, *J* 8.5, 2.9, 1H), 7.13 (dd, *J* 9.8, 2.9, 1H), 7.01 (app t, *J* 8.0, 1H), 6.79 (d, *J* 7.8, 1H), 6.74 (d, *J* 8.0, 1H), 5.26 (t, *J* 5.2, 1H), 4.38 (d, *J* 5.2, 2H), 2.03 (s, 3H); LCMS (LCQ) Rt = 1.5 min (method 2), *m/z* (ESI⁺) 352.1 [M+H]⁺.

4-(5-Cyano-2-(hydroxymethyl)phenyl)-*N*-(3-hydroxy-2-methyl-phenyl)benzamide (263)

Compound **263** was synthesised according to general procedure V, using the following reagents: *N*-(3-(tert-butyl(dimethyl)silyl)oxy-2-methyl-phenyl)-4-(4,4,5,5-tetramethyl-1,3,2-dioxaborolan-2-yl)benzamide (**242**) (100 mg, 0.21 mmol), 3-bromo-4-(hydroxymethyl)benzonitrile (44 mg, 0.21 mmol), (1,1'-bis(diphenylphosphino)ferrocene)dichloropalladium(II) (16 mg, 0.02 mmol), sodium carbonate (227 mg, 2.14 mmol), 1,4-dioxane (2 mL) and water (2 mL). The crude was purified by column chromatography (silica 12 g, 0 to 5% methanol in dichloromethane) and further purified by column chromatography (amino silica 12 g, 0 to 5% methanol in dichloromethane) to yield the desired product **263** as an off-white solid (34 mg, 42%).

¹H-NMR (500 MHz, DMSO-*d*₆) δ 9.94 (s, 1H), 9.42 (s, 1H), 8.05 (d, *J* 7.9, 2H), 7.90 (d, *J* 8.1, 1H), 7.81 (d, *J* 8.1, 1H), 7.74 (s, 1H), 7.55 (d, *J* 7.9, 2H), 7.01 (app t, *J* 8.0, 1H), 6.79 (d, *J* 7.9, 1H), 6.74 (d, *J* 8.1, 1H), 5.49 (t, *J* 5.4, 1H), 4.48 (d, *J* 5.3, 2H), 2.03 (s, 3H); **LCMS** (LCQ) Rt = 1.2 min (method 2), *m/z* (ESI⁺) 359.0 [M+H]⁺.

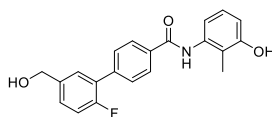
***N*-(3-hydroxy-2-methyl-phenyl)-4-(2-((2R)-2-hydroxy-3-morpholino-propoxy)phenyl)benzamide (264)**



Compound **264** was synthesised according to general procedure V, using the following reagents: *N*-(3-(tert-butyl(dimethyl)silyl)oxy-2-methyl-phenyl)-4-(4,4,5,5-tetramethyl-1,3,2-dioxaborolan-2-yl)benzamide (**242**) (100 mg, 0.21 mmol), (2R)-1-(2-bromophenoxy)-3-morpholino-propan-2-ol (68 mg, 0.21 mmol), (1,1'-bis(diphenylphosphino)ferrocene)dichloropalladium(II) (16 mg, 0.02 mmol), sodium carbonate (227 mg, 2.14 mmol), 1,4-dioxane (2 mL) and water (2 mL). The crude was purified by column chromatography (silica 12 g, 0 to 5% methanol in dichloromethane) to yield the desired product **264** as a pale brown solid (11 mg, 11%).

¹H-NMR (500 MHz, DMSO-*d*₆) 9.84 (s, 1H), 9.40 (s, 1H), 7.98 (d, *J* 7.0, 2H), 7.66 (d, *J* 7.8, 2H), 7.39 – 7.27 (m, 2H), 7.12 (d, *J* 7.8, 1H), 7.04 (app t, *J* 6.4, 1H), 6.98 (app t, *J* 6.9, 1H), 6.76 (d, *J* 7.8, 1H), 6.71 (d, *J* 8.2, 1H), 4.81 (s, 1H), 4.00 – 3.95 (m, 1H), 3.94 – 3.85 (m, 2H), 3.50 (s, 4H), 2.40 – 2.22 (m, 6H), 2.00 (s, 3H); **LCMS** (LCQ) Rt = 0.70 min (method 2), *m/z* (ESI⁺) 463.2 [M+H]⁺.

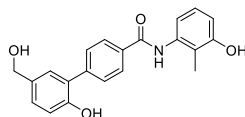
4-(2-Fluoro-5-(hydroxymethyl)phenyl)-*N*-(3-hydroxy-2-methyl-phenyl)benzamide (265)



Compound **265** was synthesised according to general procedure V, using the following reagents: *N*-(3-(tert-butyl(dimethyl)silyl)oxy-2-methyl-phenyl)-4-(4,4,5,5-tetramethyl-1,3,2-dioxaborolan-2-yl)benzamide (**242**) (100 mg, 0.21 mmol), 3-bromo-4-fluorobenzyl alcohol (44 mg, 0.21 mmol), (1,1'-bis(diphenylphosphino)ferrocene)dichloropalladium(II) (16 mg, 0.02 mmol), sodium carbonate (227 mg, 2.14 mmol), 1,4-dioxane (2 mL) and water (2 mL). The crude was purified by column chromatography (silica 12 g, 0 to 5% methanol in dichloromethane) to yield the desired product **265** as an off-white solid (36 mg, 46%).

¹H-NMR (500 MHz, DMSO-*d*₆) δ 9.93 (s, 1H), 9.45 (d, *J* 4.3, 1H), 8.07 (d, *J* 8.0, 2H), 7.69 (d, *J* 7.9, 2H), 7.51 (d, *J* 7.7, 1H), 7.42 – 7.37 (m, 1H), 7.30 (app t, *J* 9.8, 9.3, 1H), 7.00 (app t, *J* 7.9, 1H), 6.79 (d, *J* 7.8, 1H), 6.73 (d, *J* 8.1, 1H), 5.35 – 5.32 (m, 1H), 4.55 (d, *J* 5.7, 2H), 2.03 (s, 3H); **LCMS** (LCQ) Rt = 0.5 min (method 2), *m/z* (ESI⁺) 352.1 [M+H]⁺.

4-(2-Hydroxy-5-(hydroxymethyl)phenyl)-*N*-(3-hydroxy-2-methyl-phenyl)benzamide (266)

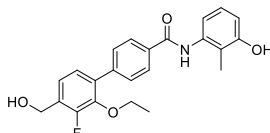


Compound **266** was synthesised according to general procedure Z, using the following reagents: *N*-(3-(tert-butyl(dimethyl)silyl)oxy-2-methyl-phenyl)-4-(4,4,5,5-tetramethyl-1,3,2-dioxaborolan-2-yl)benzamide (**242**) (100 mg, 0.21 mmol), 2-bromo-4-(hydroxymethyl)phenol (43 mg, 0.21 mmol), tris(dibenzylideneacetone)dipalladium(0) (10 mg, 0.02 mmol), tri-*tert*-butylphosphonium tetrafluoroborate (5 mg, 0.02 mmol), potassium fluoride (50 mg,

0.86 mmol), acetonitrile (1.5 mL) and water (0.5 mL). The crude was purified by column chromatography (silica 12 g, 0 to 5% methanol in dichloromethane) to yield the desired product **266** as a yellow solid (28 mg, 36%).

¹H-NMR (500 MHz, DMSO-*d*₆) 9.82 (s, 1H), 9.57 (s, 1H), 9.38 (s, 1H), 7.97 (d, *J* 7.5, 2H), 7.65 (d, *J* 7.8, 2H), 7.24 (s, 1H), 7.12 (d, *J* 8.5, 1H), 6.98 (app t, *J* 7.4, 1H), 6.89 (d, *J* 8.2, 1H), 6.77 (d, *J* 7.8, 1H), 6.71 (d, *J* 8.1, 1H), 5.03 (t, *J* 4.7, 1H), 4.41 (d, *J* 4.8, 2H), 2.00 (s, 3H); **LCMS** (LCQ) *R*_t = 0.5 min (method 2), *m/z* (ESI⁺) 350.1 [M+H]⁺.

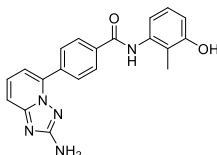
4-(2-Ethoxy-3-fluoro-4-(hydroxymethyl)phenyl)-*N*-(3-hydroxy-2-methyl-phenyl)benzamide (**267**)



Compound **267** was synthesised according to general procedure V, using the following reagents: *N*-(3-(tert-butyl(dimethyl)silyl)oxy-2-methyl-phenyl)-4-(4,4,5,5-tetramethyl-1,3,2-dioxaborolan-2-yl)benzamide (**242**) (27 mg, 0.06 mmol), (3-ethoxy-2-fluoro-4-(4,4,5,5-tetramethyl-1,3,2-dioxaborolan-2-yl)phenyl)methanol (57 mg, 0.06 mmol), (1,1'-bis(diphenylphosphino)ferrocene)dichloropalladium(II) (4 mg, 0.01 mmol), sodium carbonate (67 mg, 0.64 mmol), 1,4-dioxane (1.5 mL) and water (1.5 mL). The crude was purified by column chromatography (silica 12 g, 0 to 5% methanol in dichloromethane), further purified by column chromatography (amino silica 12 g, 0 to 12% methanol in dichloromethane) and triturated in ether to yield the desired product **267** as a white solid (3 mg, 9%).

¹H-NMR (500 MHz, DMSO-*d*₆) 9.85 (s, 1H), 9.38 (s, 1H), 8.01 (d, *J* 7.1, 2H), 7.63 (d, *J* 6.9, 3H), 7.25 (t, *J* 6.9, 1H), 7.20 (d, *J* 7.9, 1H), 6.97 (t, *J* 7.0, 1H), 6.76 (d, *J* 7.5, 1H), 6.70 (d, *J* 8.2, 1H), 5.31 (q, *J* 5.0, 4.5, 1H), 4.56 (d, *J* 5.6, 1H), 3.84 (q, *J* 8.8, 7.9, 2H), 2.00 (s, 3H), 1.09 (t, *J* 7.0, 3H); **LCMS** (LCQ) *R*_t = 2.1 min (method 2), *m/z* (ESI⁺) 379.1 [M+H]⁺.

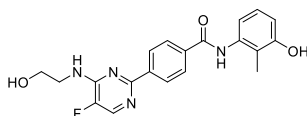
4-(2-Amino-(1,2,4)triazolo(1,5-a)pyridin-5-yl)-*N*-(3-hydroxy-2-methyl-phenyl)benzamide (**268**)



Compound **268** was synthesised according to general procedure V, using the following reagents: *N*-(3-(tert-butyl(dimethyl)silyl)oxy-2-methyl-phenyl)-4-(4,4,5,5-tetramethyl-1,3,2-dioxaborolan-2-yl)benzamide (**242**) (100 mg, 0.21 mmol), 5-Bromo(1,2,4)triazolo(1,5-a)pyridin-2-amine (46 mg, 0.21 mmol), (1,1'-bis(diphenylphosphino)ferrocene)dichloropalladium(II) (16 mg, 0.02 mmol), sodium carbonate (227 mg, 2.14 mmol), 1,4-dioxane (2 mL) and water (2 mL). The crude was purified by column chromatography (silica 12 g, 0 to 3% methanol in dichloromethane) to yield the desired product **268** as a yellow solid (28 mg, 32%).

¹H-NMR (500 MHz, DMSO-*d*₆) 9.95 (s, 1H), 9.40 (s, 1H), 8.08 (s, 4H), 7.53 (app t, *J* 7.8, 1H), 7.40 (d, *J* 8.7, 1H), 7.10 (d, *J* 7.2, 1H), 6.99 (app t, *J* 7.9, 1H), 6.78 (d, *J* 7.8, 1H), 6.72 (d, *J* 8.1, 1H), 6.06 (s, 2H), 2.01 (s, 3H); **LCMS** (LCQ) *R*_t = 0.7 min (method 2), *m/z* (ESI⁺) 360.2 [M+H]⁺.

4-(5-Fluoro-4-(2-hydroxyethylamino)pyrimidin-2-yl)-*N*-(3-hydroxy-2-methyl-phenyl)benzamide (**269**)

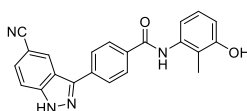


Compound **269** was synthesised according to general procedure V, using the following reagents: *N*-(3-(tert-butyl(dimethyl)silyl)oxy-2-methyl-phenyl)-4-(4,4,5,5-tetramethyl-1,3,2-dioxaborolan-2-yl)benzamide (**242**) (100 mg,

0.21 mmol), 2-((2-chloro-5-fluoropyrimidin-4-yl)amino)ethanol (41 mg, 0.21 mmol), (1,1'-bis(diphenylphosphino)ferrocene)dichloropalladium(II) (16 mg, 0.02 mmol), sodium carbonate (227 mg, 2.14 mmol), 1,4-dioxane (2 mL) and water (2 mL). The crude was purified by column chromatography (silica 12 g, 0 to 5% methanol in dichloromethane) and further purified by column chromatography (amino silica 12 g, 0 to 5% methanol in dichloromethane) to yield the desired product **269** as a white solid (32 mg, 37%).

¹H-NMR (500 MHz, DMSO-*d*₆) 9.92 (s, 1H), 9.43 (s, 1H), 8.38 (d, *J* 8.0, 2H), 8.27 (d, *J* 3.6, 1H), 8.04 (d, *J* 8.0, 2H), 7.74 (app t, *J* 5.2, 1H), 7.00 (app t, *J* 7.9, 1H), 6.79 (d, *J* 7.8, 1H), 6.73 (d, *J* 8.0, 1H), 4.82 (t, *J* 4.3, 1H), 3.63 (t, *J* 5.0, 2H), 3.60 (t, *J* 4.1, 2H), 2.03 (s, 3H); **LCMS** (LCQ) Rt = 0.60 min (method 2), *m/z* (ESI⁺) 383.2 [M+H]⁺.

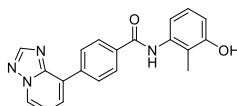
4-(5-Cyano-1H-indazol-3-yl)-*N*-(3-hydroxy-2-methyl-phenyl)benzamide (**270**)



Compound **270** was synthesised according to general procedure V, using the following reagents: *N*-(3-(tert-butyl(dimethyl)silyl)oxy-2-methyl-phenyl)-4-(4,4,5,5-tetramethyl-1,3,2-dioxaborolan-2-yl)benzamide (**242**) (100 mg, 0.21 mmol), 3-bromo-1H-indazole-5-carbonitrile (48 mg, 0.21 mmol), (1,1'-bis(diphenylphosphino)ferrocene)dichloropalladium(II) (16 mg, 0.02 mmol), sodium carbonate (227 mg, 2.14 mmol), 1,4-dioxane (2 mL) and water (2 mL). The crude was purified by column chromatography (silica 12 g, 0 to 5% methanol in dichloromethane) and further purified by column chromatography (amino silica 12 g, 0 to 5% methanol in dichloromethane) to yield the desired product **270** as a yellow solid (7 mg, 8%).

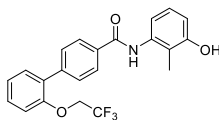
¹H-NMR (500 MHz, DMSO-*d*₆) 13.94 (s, 1H), 9.97 (s, 1H), 9.43 (s, 1H), 8.81 (s, 1H), 8.21 (d, *J* 7.9, 2H), 8.13 (d, *J* 8.0, 2H), 7.81 (d, *J* 9.0, 1H), 7.77 (d, *J* 8.9, 1H), 7.01 (app t, *J* 8.0, 1H), 6.81 (d, *J* 8.0, 1H), 6.74 (d, *J* 8.0, 1H), 2.04 (s, 3H); **LCMS** (LCQ) Rt = 0.7 min (method 2), *m/z* (ESI⁺) 369.1 [M+H]⁺.

N-(3-hydroxy-2-methyl-phenyl)-4-((1,2,4)triazolo(1,5-a)pyridin-8-yl)benzamide (**271**)



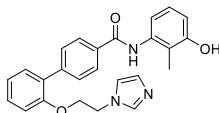
Compound **271** was synthesised according to general procedure V, using the following reagents: *N*-(3-(tert-butyl(dimethyl)silyl)oxy-2-methyl-phenyl)-4-(4,4,5,5-tetramethyl-1,3,2-dioxaborolan-2-yl)benzamide (**242**) (100 mg, 0.21 mmol), 8-bromo(1,2,4)triazolo(1,5-a)pyridine (42 mg, 0.21 mmol), (1,1'-bis(diphenylphosphino)ferrocene)dichloropalladium(II) (16 mg, 0.02 mmol), sodium carbonate (227 mg, 2.14 mmol), 1,4-dioxane (2 mL) and water (2 mL). The crude was purified by column chromatography (silica 12 g, 0 to 5% methanol in dichloromethane) to yield the desired product **271** as a pale orange solid (51 mg, 62%).

¹H-NMR (500 MHz, DMSO-*d*₆) 9.96 (s, 1H), 9.43 (s, 1H), 9.03 (d, *J* 6.7, 1H), 8.62 (s, 1H), 8.33 (d, *J* 8.0, 2H), 8.13 (d, *J* 8.2, 2H), 8.07 (d, *J* 7.3, 1H), 7.36 (app t, *J* 7.1, 1H), 7.01 (app t, *J* 8.0, 1H), 6.81 (d, *J* 7.8, 1H), 6.74 (d, *J* 8.1, 1H), 2.04 (s, 3H); **LCMS** (LCQ) Rt = 1.3 min (method 2), *m/z* (ESI⁺) 345.1 [M+H]⁺.

***N*-(3-hydroxy-2-methyl-phenyl)-4-(2-(2,2,2-trifluoroethoxy)phenyl)benzamide (272)**

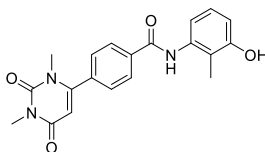
Compound **272** was synthesised according to general procedure V, using the following reagents: *N*-(3-(tert-butyl(dimethyl)silyl)oxy-2-methyl-phenyl)-4-(4,4,5,5-tetramethyl-1,3,2-dioxaborolan-2-yl)benzamide (**242**) (100 mg, 0.21 mmol), 1-bromo-2-(2,2,2-trifluoroethoxy)benzene (55 mg, 0.21 mmol), (1,1'-bis(diphenylphosphino)ferrocene)dichloropalladium(II) (16 mg, 0.02 mmol), sodium carbonate (227 mg, 2.14 mmol), 1,4-dioxane (2 mL) and water (2 mL). The crude was purified by column chromatography (silica 12 g, 0 to 3% methanol in dichloromethane) and further purified by column chromatography (silica 12 g, 0 to 5% methanol in dichloromethane) to yield the desired product **272** as a yellow solid (20 mg, 22%).

¹H-NMR (500 MHz, DMSO-*d*₆) 9.90 (s, 1H), 9.41 (s, 1H), 8.02 (d, *J* 8.0, 2H), 7.64 (d, *J* 7.9, 2H), 7.46 – 7.40 (m, 2H), 7.26 (d, *J* 8.7, 1H), 7.18 (app t, *J* 7.5, 1H), 7.00 (app t, *J* 7.9, 1H), 6.79 (d, *J* 7.9, 1H), 6.73 (d, *J* 8.1, 1H), 4.81 (q, *J* 8.8, 2H), 2.03 (s, 3H); LCMS (LCQ) Rt = 3.1 min (method 2), *m/z* (ESI⁺) 402.1 [M+H]⁺.

***N*-(3-hydroxy-2-methyl-phenyl)-4-(2-(2-imidazol-1-ylethoxy)phenyl)benzamide (273)**

Compound **273** was synthesised according to general procedure V, using the following reagents: *N*-(3-(tert-butyl(dimethyl)silyl)oxy-2-methyl-phenyl)-4-(4,4,5,5-tetramethyl-1,3,2-dioxaborolan-2-yl)benzamide (**242**) (100 mg, 0.21 mmol), 1-(2-(2-bromophenoxy)ethyl)-1H-imidazole (65 mg, 0.21 mmol), (1,1'-bis(diphenylphosphino)ferrocene)dichloropalladium(II) (16 mg, 0.02 mmol), sodium carbonate (227 mg, 2.14 mmol), 1,4-dioxane (2 mL) and water (2 mL). The crude was purified by column chromatography (silica 12 g, 0 to 5% methanol in dichloromethane) to yield the desired product **273** as a white solid (35 mg, 38%).

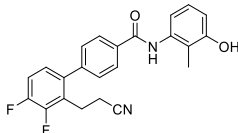
¹H-NMR (500 MHz, DMSO-*d*₆) 9.88 (s, 1H), 9.40 (d, *J* 1.6, 1H), 7.96 (d, *J* 7.5, 2H), 7.52 (s, 1H), 7.42 (d, *J* 7.2, 2H), 7.38 – 7.30 (m, 2H), 7.09 (m, 2H), 7.05 (app t, *J* 7.4, 1H), 6.99 (app t, *J* 7.8, 1H), 6.87 (s, 1H), 6.78 (d, *J* 7.7, 1H), 6.71 (d, *J* 8.0, 1H), 4.34 – 4.25 (m, 4H), 2.02 (s, 3H).

4-(1,3-Dimethyl-2,6-dioxo-pyrimidin-4-yl)-*N*-(3-hydroxy-2-methyl-phenyl)benzamide (274)

Compound **274** was synthesised according to general procedure V, using the following reagents: *N*-(3-(tert-butyl(dimethyl)silyl)oxy-2-methyl-phenyl)-4-(4,4,5,5-tetramethyl-1,3,2-dioxaborolan-2-yl)benzamide (**242**) (100 mg, 0.21 mmol), 6-chloro-1,3-dimethyluracil (37 mg, 0.21 mmol), (1,1'-bis(diphenylphosphino)ferrocene)dichloropalladium(II) (16 mg, 0.02 mmol), sodium carbonate (227 mg, 2.14 mmol), 1,4-dioxane (2 mL) and water (2 mL). The crude was purified by column chromatography (silica 12 g, 0 to 5% methanol in dichloromethane) and further purified by column chromatography (amino silica 12 g, 0 to 5% methanol in dichloromethane) to yield the desired product **274** as a pale yellow solid (7 mg, 8%).

¹H-NMR (500 MHz, DMSO-*d*₆) 9.97 (s, 1H), 9.43 (s, 1H), 8.06 (d, *J* 8.0, 2H), 7.63 (d, *J* 8.0, 2H), 6.98 (app t, *J* 7.9, 1H), 6.76 (d, *J* 7.8, 1H), 6.72 (d, *J* 8.1, 1H), 5.66 (s, 1H), 3.21 (s, 3H), 3.10 (s, 3H), 2.00 (s, 3H); **LCMS** (LCQ) Rt = 0.5 min (method 2), *m/z* (ESI⁺) 366.0 [M+H]⁺.

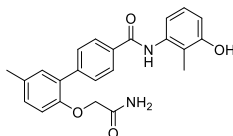
4-(2-(Cyanomethyl)-3,4-difluoro-phenyl)-*N*-(3-hydroxy-2-methyl-phenyl)benzamide (275)



Compound **275** was synthesised according to general procedure V, using the following reagents: *N*-(3-(tert-butyl(dimethyl)silyl)oxy-2-methyl-phenyl)-4-(4,4,5,5-tetramethyl-1,3,2-dioxaborolan-2-yl)benzamide (**242**) (65 mg, 0.15 mmol), 2-(2,3-difluoro-6-(4,4,5,5-tetramethyl-1,3,2-dioxaborolan-2-yl)phenyl)acetonitrile (36 mg, 0.13 mmol), (1,1'-bis(diphenylphosphino)ferrocene)dichloropalladium(II) (11 mg, 0.02 mmol), sodium carbonate (164 mg, 1.55 mmol), 1,4-dioxane (1.5 mL) and water (1.5 mL). The crude was purified by column chromatography (silica 12 g, 0 to 10% methanol in dichloromethane), further purified by column chromatography (amino silica 12 g, 0 to 5% methanol in dichloromethane) and triturated in ether to yield the desired product **275** as a pale yellow solid (7 mg, 11%).

¹H-NMR (500 MHz, DMSO-*d*₆) 9.91 (s, 1H), 9.36 (s, 1H), 8.07 (d, *J* 8.1, 2H), 7.56 (app q, *J* 9.1, 1H), 7.47 (d, *J* 7.9, 2H), 7.22 (dd, *J* 8.1, 5.4, 1H), 6.97 (app t, *J* 7.9, 1H), 6.75 (d, *J* 7.8, 1H), 6.70 (d, *J* 8.1, 1H), 3.90 (s, 2H), 1.99 (s, 3H); **LCMS** (LCQ) Rt = 2.1 min (method 2), *m/z* (ESI⁺) 379.1 [M+H]⁺.

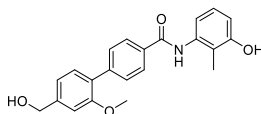
4-(2-(2-Amino-2-oxo-ethoxy)-5-methyl-phenyl)-*N*-(3-hydroxy-2-methyl-phenyl)benzamide (276)



Compound **276** was synthesised according to general procedure V, using the following reagents: *N*-(3-(tert-butyl(dimethyl)silyl)oxy-2-methyl-phenyl)-4-(4,4,5,5-tetramethyl-1,3,2-dioxaborolan-2-yl)benzamide (**242**) (100 mg, 0.21 mmol), 2-(2-bromo-4-methylphenoxy)acetamide (52 mg, 0.21 mmol), (1,1'-bis(diphenylphosphino)ferrocene)dichloropalladium(II) (16 mg, 0.02 mmol), sodium carbonate (227 mg, 2.14 mmol), 1,4-dioxane (2 mL) and water (2 mL). The crude was purified by column chromatography (silica 12 g, 0 to 5% methanol in dichloromethane) and further purified by column chromatography (amino silica 12 g, 0 to 5% methanol in dichloromethane) to yield the desired product **276** as a white solid (36 mg, 41%).

¹H-NMR (500 MHz, DMSO-*d*₆) 9.87 (s, 1H), 9.42 (s, 1H), 8.00 (d, *J* 8.0, 2H), 7.72 (d, *J* 7.9, 2H), 7.41 (s, 1H), 7.25 – 7.11 (m, 3H), 7.00 (app t, *J* 8.0, 1H), 6.92 (d, *J* 8.3, 1H), 6.79 (d, *J* 7.9, 1H), 6.73 (d, *J* 8.1, 1H), 4.42 (s, 2H), 2.30 (s, 3H), 2.03 (s, 3H); **LCMS** (LCQ) Rt = 1.7 min (method 2), *m/z* (ESI⁺) 390.9 [M+H]⁺.

4-(4-(Hydroxymethyl)-2-methoxy-phenyl)-*N*-(3-hydroxy-2-methyl-phenyl)benzamide (277)

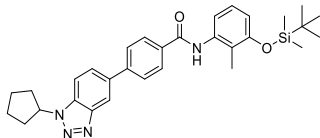


Compound **277** was synthesised according to general procedure V, using the following reagents: *N*-(3-(tert-butyl(dimethyl)silyl)oxy-2-methyl-phenyl)-4-(4,4,5,5-tetramethyl-1,3,2-dioxaborolan-2-yl)benzamide (**242**) (100 mg, 0.21 mmol), (4-bromo-3-methoxyphenyl)methanol (46 mg, 0.21 mmol), (1,1'-bis(diphenylphosphino)ferrocene)dichloropalladium(II) (16 mg, 0.02 mmol), sodium carbonate (227 mg, 2.14 mmol),

1,4-dioxane (2 mL) and water (2 mL). The crude was purified by column chromatography (silica 12 g, 0 to 5% methanol in dichloromethane) to yield the desired product **277** as a off-white solid (18 mg, 22%).

¹H-NMR (500 MHz, DMSO-*d*₆) 9.84 (s, 1H), 9.41 (s, 1H), 7.98 (d, *J* 7.9, 2H), 7.60 (d, *J* 7.9, 2H), 7.30 (d, *J* 7.6, 1H), 7.10 (s, 1H), 7.04 – 6.96 (m, 2H), 6.79 (d, *J* 7.9, 1H), 6.73 (d, *J* 8.0, 1H), 5.29 (t, *J* 5.8, 1H), 4.55 (d, *J* 5.7, 2H), 3.79 (s, 3H), 2.02 (s, 3H); **LCMS** (LCQ) Rt = 1.6 min (method 2), *m/z* (ESI⁺) 364.0 [M+H]⁺.

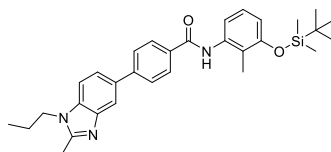
***N*-(3-(tert-butyl(dimethyl)silyl)oxy-2-methyl-phenyl)-1-cyclopentyl-benzotriazole-5-carboxamide (278)**



Compound **278** was synthesised according to general procedure R, using the following reagents: 1-cyclopentyl-1H-benzotriazole-5-carboxylic acid (100 mg, 0.43 mmol), HATU (197 mg, 0.52 mmol), *N,N*-diisopropylethylamine (151 μL, 0.86 mmol), 3-(tert-butyl(dimethyl)silyl)oxy-2-methyl-aniline (**120**) (137 mg, 0.52 mmol) and *N,N*-dimethylformamide (1 mL). The crude was purified by column chromatography (silica 12 g, 0 to 25% ethyl acetate in petroleum ether) to yield the desired compound **278** as a white solid (156 mg, 72%).

¹H-NMR (500 MHz, DMSO-*d*₆) 10.08 (s, 1H), 8.72 (s, 1H), 8.12 (d, *J* 8.7, 1H), 8.01 (d, *J* 8.8, 1H), 7.11 (app t, *J* 7.9, 1H), 6.98 (d, *J* 7.9, 1H), 6.77 (d, *J* 8.0, 1H), 5.42 (app p, *J* 7.4, 1H), 2.30 (m, 2H), 2.15 (m, 2H), 2.08 (s, 3H), 1.94 – 1.88 (m, 2H), 1.78 (m, 2H), 1.00 (s, 9H), 0.23 (s, 6H).

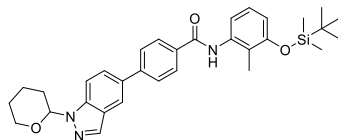
***N*-(3-(tert-butyl(dimethyl)silyl)oxy-2-methyl-phenyl)-2-methyl-1-propyl-benzimidazole-5-carboxamide (279)**



Compound **279** was synthesised according to general procedure R, using the following reagents: 2-methyl-1-propyl-1H-benzimidazole-5-carboxylic acid (100 mg, 0.43 mmol), HATU (94 mg, 0.43 mmol), *N,N*-diisopropylethylamine (150 μL, 0.86 mmol), 3-(tert-butyl(dimethyl)silyl)oxy-2-methyl-aniline (**120**) (137 mg, 0.52 mmol) and *N,N*-dimethylformamide (1 mL). The crude was purified by column chromatography (silica 12 g, 0 to 100% ethyl acetate in petroleum ether) to yield the desired compound **279** as a white solid (134 mg, 64%).

¹H-NMR (500 MHz, DMSO-*d*₆) 8.21 (s, 1H), 7.95 (s, 1H), 7.84 (d, *J* 8.4, 1H), 7.62 (d, *J* 8.5, 1H), 7.09 (app t, *J* 7.9, 1H), 6.96 (d, *J* 7.8, 1H), 6.74 (d, *J* 8.0, 1H), 4.20 (t, *J* 7.2, 2H), 2.58 (s, 3H), 2.07 (s, 3H), 1.75 (app h, *J* 7.0, 2H), 1.00 (s, 9H), 0.88 (t, *J* 7.3, 3H), 0.23 (s, 6H).

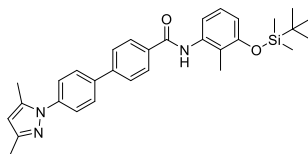
***N*-(3-(tert-butyl(dimethyl)silyl)oxy-2-methyl-phenyl)-1-tetrahydropyran-2-yl-indazole-5-carboxamide (280)**



Compound **280** was synthesised according to general procedure R, using the following reagents: 1-(tetrahydro-pyran-2-yl)-1H-indazole-5-carboxylic acid (100 mg, 0.43 mmol), HATU (94 mg, 0.43 mmol), *N,N*-diisopropylethylamine (150 μL, 0.86 mmol), 3-(tert-butyl(dimethyl)silyl)oxy-2-methyl-aniline (**120**) (137 mg, 0.52 mmol) and *N,N*-dimethylformamide (1 mL). The crude was purified by column chromatography (silica 12 g, 0 to 40% ethyl acetate in petroleum ether) to yield the desired compound **280** as a white solid (175 mg, 78%).

¹H-NMR (500 MHz, DMSO-*d*₆) 9.93 (s, 1H), 8.45 (s, 1H), 8.27 (s, 1H), 7.99 (d, *J* 8.8, 1H), 7.81 (d, *J* 8.8, 1H), 7.08 (app t, *J* 8.0, 1H), 6.95 (d, *J* 7.9, 1H), 6.73 (d, *J* 8.1, 1H), 5.89 (dd, *J* 9.8, 1.9, 2H), 3.88 (app d, *J* 11.4, 1H), 3.78 – 3.71 (m, 1H), 2.40 (app qd, *J* 12.8, 3.6, 1H), 2.05 (s, 3H), 2.02 – 1.91 (m, 2H), 1.81 – 1.68 (m, 1H), 1.57 (app hept, *J* 3.9, 2H), 0.98 (s, 9H), 0.21 (s, 6H).

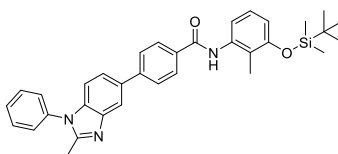
***N*-(3-(tert-butyl(dimethyl)silyl)oxy-2-methyl-phenyl)-4-(3,5-dimethylpyrazol-1-yl)benzamide (281)**



Compound **281** was synthesised according to general procedure R, using the following reagents: 4-(3,5-dimethyl-1H-pyrazol-1-yl)benzoic acid (94 mg, 0.43 mmol), HATU (94 mg, 0.43 mmol), *N,N*-diisopropylethylamine (150 μ L, 0.86 mmol), 3-(tert-butyl(dimethyl)silyl)oxy-2-methyl-aniline (**120**) (137 mg, 0.52 mmol) and *N,N*-dimethylformamide (1 mL). The crude was purified by column chromatography (silica 12 g, 0 to 60% ethyl acetate in petroleum ether) to yield the desired compound **281** as a orange solid (144 mg, 72%).

¹H-NMR (500 MHz, DMSO-*d*₆) 10.01 (s, 1H), 8.08 (d, *J* 8.3, 2H), 7.66 (d, *J* 8.3, 2H), 7.11 (app t, *J* 8.0, 1H), 6.96 (d, *J* 7.9, 1H), 6.77 (d, *J* 8.1, 1H), 6.13 (s, 1H), 2.37 (s, 3H), 2.20 (s, 3H), 2.07 (s, 3H), 1.00 (s, 9H), 0.23 (s, 6H).

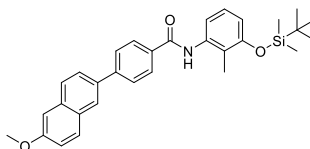
***N*-(3-(tert-butyl(dimethyl)silyl)oxy-2-methyl-phenyl)-2-methyl-1-phenyl-benzimidazole-5-carboxamide (282)**



Compound **282** was synthesised according to general procedure R, using the following reagents: 2-methyl-1-phenyl-1H-benzimidazole-5-carboxylic acid (100 mg, 0.43 mmol), HATU (94 mg, 0.43 mmol), *N,N*-diisopropylethylamine (150 μ L, 0.86 mmol), 3-(tert-butyl(dimethyl)silyl)oxy-2-methyl-aniline (**120**) (137 mg, 0.52 mmol) and *N,N*-dimethylformamide (1 mL). The crude was purified by column chromatography (silica 12 g, 0 to 80% ethyl acetate in petroleum ether) to yield the desired compound **282** as a brown solid (209 mg, 92%).

¹H-NMR (500 MHz, DMSO-*d*₆) 9.91 (s, 1H), 8.33 (s, 1H), 7.86 (d, *J* 8.7, 1H), 7.68 (app t, *J* 7.6, 2H), 7.62 – 7.55 (m, 3H), 7.21 (d, *J* 8.5, 1H), 7.10 (app t, *J* 8.0, 1H), 6.97 (d, *J* 7.9, 1H), 6.75 (d, *J* 8.1, 1H), 2.48 (s, 3H), 2.07 (s, 3H), 1.00 (s, 9H), 0.23 (s, 6H).

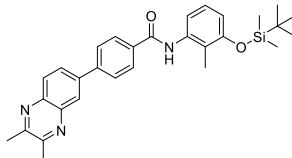
***N*-(3-(tert-butyl(dimethyl)silyl)oxy-2-methyl-phenyl)-6-methoxy-naphthalene-2-carboxamide (283)**



Compound **283** was synthesised according to general procedure R, using the following reagents: 6-methoxy-2-naphthoic acid (87 mg, 0.43 mmol), HATU (94 mg, 0.43 mmol), *N,N*-diisopropylethylamine (150 μ L, 0.86 mmol), 3-(tert-butyl(dimethyl)silyl)oxy-2-methyl-aniline (**120**) (137 mg, 0.52 mmol) and *N,N*-dimethylformamide (1 mL). The crude was purified by column chromatography (silica 12 g, 0 to 80% ethyl acetate in petroleum ether) to yield the desired compound **283** as a white solid (50 mg, 57%).

¹H-NMR (500 MHz, DMSO-*d*₆) 9.97 (s, 1H), 8.50 (s, 1H), 7.96 (app t, *J* 9.4, 2H), 7.90 (d, *J* 8.6, 1H), 7.39 (d, *J* 2.5, 1H), 7.23 (dd, *J* 9.0, 2.5, 1H), 7.09 (app t, *J* 8.0, 1H), 6.96 (d, *J* 7.9, 1H), 6.74 (d, *J* 8.1, 1H), 3.89 (s, 3H), 2.06 (s, 3H), 0.98 (s, 9H), 0.21 (s, 6H).

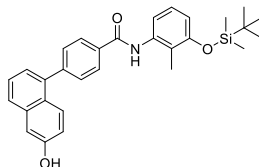
***N*-(3-(tert-butyl(dimethyl)silyl)oxy-2-methyl-phenyl)-2,3-dimethyl-quinoxaline-6-carboxamide (284)**



Compound **284** was synthesised according to general procedure R, using the following reagents: 2,3-dimethyl-6-quinoxalinecarboxylic acid (87 mg, 0.43 mmol), HATU (94 mg, 0.43 mmol), *N,N*-diisopropylethylamine (150 μ L, 0.86 mmol), 3-(tert-butyl(dimethyl)silyl)oxy-2-methyl-aniline (**120**) (137 mg, 0.52 mmol) and *N,N*-dimethylformamide (1 mL). The crude was purified by column chromatography (silica 12 g, 0 to 60% ethyl acetate in petroleum ether) to yield the desired compound **284** as a off-white solid (171 mg, 85%).

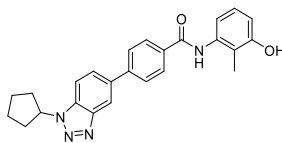
¹H-NMR (500 MHz, DMSO-*d*₆) 10.20 (s, 1H), 8.62 (s, 1H), 8.22 (d, *J* 8.5, 1H), 8.06 (d, *J* 8.6, 1H), 7.12 (app t, *J* 8.0, 1H), 7.00 (d, *J* 7.9, 1H), 6.78 (d, *J* 8.1, 1H), 2.72 (s, 6H), 2.10 (s, 3H), 1.00 (s, 9H), 0.24 (s, 6H).

***N*-(3-(tert-butyl(dimethyl)silyl)oxy-2-methyl-phenyl)-6-hydroxy-naphthalene-1-carboxamide (285)**



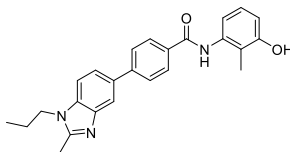
Compound **285** was synthesised according to general procedure R, using the following reagents: 6-hydroxy-1-naphthoic acid (81 mg, 0.43 mmol), HATU (94 mg, 0.43 mmol), *N,N*-diisopropylethylamine (150 μ L, 0.86 mmol), 3-(tert-butyl(dimethyl)silyl)oxy-2-methyl-aniline (**120**) (137 mg, 0.52 mmol) and *N,N*-dimethylformamide (1 mL). The crude was purified by column chromatography (silica 12 g, 0 to 25% ethyl acetate in petroleum ether) to yield the desired compound **285** as a white solid (94 mg, 27%). 50% purity as determined by ¹H-NMR, compound carried forward without further purification.

3-Cyclopentyl-*N*-(3-hydroxy-2-methyl-phenyl)benzotriazole-5-carboxamide (286)



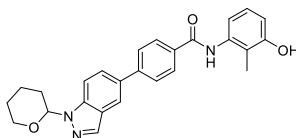
N-(3-(tert-butyl(dimethyl)silyl)oxy-2-methyl-phenyl)-3-cyclopentyl-benzotriazole-5-carboxamide (**278**) (173 mg, 0.35 mmol) in tetrahydrofuran (4 mL) and was cooled to 0 °C and to the reaction mixture was added tetrabutylammonium fluoride (692 μ L, 0.60 mmol). The reaction mixture was stirred at 0 °C for 5 min and at ambient temperature for 10 min. The reaction mixture was concentrated under reduced pressure. The crude was purified by column chromatography (silica 12 g, 0 to 5% methanol in dichloromethane) to yield the desired amide **286** as a white solid (71 mg, 58%).

¹H-NMR (500 MHz, DMSO-*d*₆) 10.02 (s, 1H), 9.45 (s, 1H), 8.71 (s, 1H), 8.12 (d, *J* 8.6, 1H), 8.01 (d, *J* 9.0, 1H), 7.01 (app t, *J* 7.7, 1H), 6.80 (d, *J* 7.8, 1H), 6.74 (d, *J* 8.0, 1H), 5.42 (p, *J* 7.1, 1H), 2.37 – 2.25 (m, 2H), 2.21 – 2.11 (m, 2H), 2.04 (s, 3H), 1.98 – 1.87 (m, 2H), 1.84 – 1.73 (m, 2H); **LCMS** (LCQ) *R*_t = 2.3 min (method 2), *m/z* (ESI⁺) 337.0 [M+H]⁺.

***N*-(3-(tert-butyl(dimethyl)silyl)oxy-2-methyl-phenyl)-2-methyl-1-propyl-benzimidazole-5-carboxamide (287)**

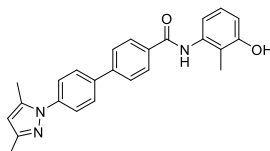
N-(3-(tert-butyl(dimethyl)silyl)oxy-2-methyl-phenyl)-2-methyl-1-propyl-benzimidazole-5-carboxamide (**279**) (134 mg, 0.31 mmol) in tetrahydrofuran (3 mL) and was cooled to 0 °C and to the reaction mixture was added tetrabutylammonium fluoride (612 µL, 0.61 mmol). The reaction mixture was stirred at 0 °C for 5 min and at ambient temperature for 10 min. The reaction mixture was concentrated under reduced pressure. The crude was purified by column chromatography (silica 12 g, 0 to 4% methanol in dichloromethane) to yield the desired amide **287** as a white solid (46 mg, 44%).

¹H-NMR (500 MHz, DMSO-*d*₆) 9.77 (s, 1H), 9.38 (s, 1H), 8.20 (s, 1H), 7.84 (d, *J* 8.4, 1H), 7.62 (d, *J* 8.4, 1H), 6.99 (app t, *J* 7.9, 1H), 6.78 (d, *J* 7.9, 1H), 6.71 (d, *J* 8.1, 1H), 4.19 (t, *J* 7.2, 2H), 2.57 (s, 3H), 2.02 (s, 3H), 1.75 (app h, *J* 7.2, 2H), 0.88 (t, *J* 7.4, 3H); LCMS (LCQ) Rt = 0.6 min (method 2), *m/z* (ESI⁺) 324.2 [M+H]⁺.

***N*-(3-(tert-butyl(dimethyl)silyl)oxy-2-methyl-phenyl)-1-tetrahydropyran-2-yl-indazole-5-carboxamide (288)**

N-(3-(tert-butyl(dimethyl)silyl)oxy-2-methyl-phenyl)-1-tetrahydropyran-2-yl-indazole-5-carboxamide (**280**) (195 mg, 0.38 mmol) in tetrahydrofuran (4 mL) and was cooled to 0 °C and to the reaction mixture was added tetrabutylammonium fluoride (754 µL, 0.75 mmol). The reaction mixture was stirred at 0 °C for 5 min and at ambient temperature for 10 min. The reaction mixture was concentrated under reduced pressure. The crude was purified by column chromatography (silica 12 g, 0 to 5% methanol in dichloromethane) and further purified by column chromatography (amino silica 12 g, 0 to 5% methanol in dichloromethane) to yield the desired amide **288** as a white solid (4 mg, 3%).

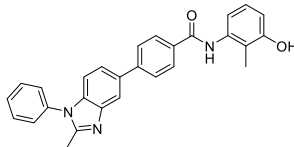
¹H-NMR (500 MHz, DMSO-*d*₆) 9.86 (s, 1H), 9.38 (s, 1H), 8.47 (s, 1H), 8.28 (s, 1H), 8.02 (dd, *J* 8.8, 1.7, 1H), 7.83 (d, *J* 8.8, 1H), 7.00 (app t, *J* 8.0, 1H), 6.80 (d, *J* 7.7, 1H), 6.73 (d, *J* 8.0, 1H), 5.92 (dd, *J* 9.7, 2.6, 1H), 3.93 – 3.87 (m, 1H), 3.77 (ddd, *J* 11.4, 8.3, 6.1, 1H), 2.42 (tdd, *J* 13.3, 9.6, 4.0 Hz, 1H), 2.10 – 1.96 (m, 5H), 1.82 – 1.70 (m, 1H), 1.60 (app tt, *J* 8.4, 4.1, 2H); LCMS (LCQ) Rt = 1.7 min (method 2), *m/z* (ESI⁺) 352.2 [M+H]⁺.

4-(3,5-Dimethylpyrazol-1-yl)-*N*-(3-(tert-butyl(dimethyl)silyl)oxy-2-methyl-phenyl)benzamide (289)

N-(3-(tert-butyl(dimethyl)silyl)oxy-2-methyl-phenyl)-4-(3,5-dimethylpyrazol-1-yl)benzamide (**281**) (144 mg, 0.33 mmol) in tetrahydrofuran (4 mL) and was cooled to 0 °C and to the reaction mixture was added tetrabutylammonium fluoride (661 µL, 0.66 mmol). The reaction mixture was stirred at 0 °C for 5 min and at ambient temperature for 10 min. The reaction mixture was concentrated under reduced pressure. The crude was purified by column chromatography (silica 12 g, 0 to 5% methanol in dichloromethane) to yield the desired amide **289** as a white solid (65 mg, 58%).

¹H-NMR (500 MHz, DMSO-*d*₆) 9.94 (s, 1H), 9.43 (s, 1H), 8.08 (d, *J* 8.5, 2H), 7.66 (d, *J* 8.5, 2H), 7.00 (app t, *J* 7.9, 1H), 6.78 (d, *J* 7.8, 1H), 6.73 (d, *J* 8.0, 1H), 6.13 (s, 1H), 2.37 (s, 3H), 2.20 (s, 3H), 2.02 (s, 3H); **LCMS** (LCQ) Rt = 1.1 min (method 2), *m/z* (ESI⁺) 322.2 [M+H]⁺.

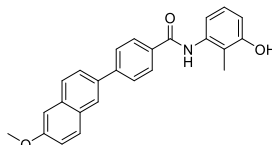
***N*-(3-hydroxy-2-methyl-phenyl)-2-methyl-1-phenyl-benzimidazole-5-carboxamide (290)**



N-(3-(tert-butyl(dimethyl)silyl)oxy-2-methyl-phenyl)-2-methyl-1-phenyl-benzimidazole-5-carboxamide **(282)** (209 mg, 0.44 mmol) in tetrahydrofuran (4 mL) and was cooled to 0 °C and to the reaction mixture was added tetrabutylammonium fluoride (886 μL, 0.89 mmol). The reaction mixture was stirred at 0 °C for 5 min and at ambient temperature for 10 min. The reaction mixture was concentrated under reduced pressure. The crude was purified by column chromatography (silica 12 g, 0 to 5% methanol in dichloromethane) to yield the desired amide **290** as a white solid (47 mg, 47%).

¹H-NMR (500 MHz, DMSO-*d*₆) 9.82 (s, 1H), 9.37 (s, 1H), 8.30 (s, 1H), 7.83 (d, *J* 8.5, 1H), 7.69 – 7.62 (m, 2H), 7.61 – 7.55 (m, 3H), 7.18 (d, *J* 8.4, 1H), 6.97 (app t, *J* 7.9, 1H), 6.77 (d, *J* 7.9, 1H), 6.70 (d, *J* 8.1, 1H), 2.45 (s, 3H), 2.00 (s, 3H); **LCMS** (LCQ) Rt = 1.1 min (method 2), *m/z* (ESI⁺) 358.1 [M+H]⁺.

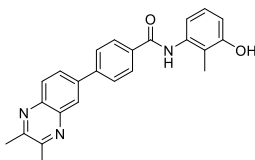
***N*-(3-hydroxy-2-methyl-phenyl)-6-methoxy-naphthalene-2-carboxamide (291)**



N-(3-(tert-butyl(dimethyl)silyl)oxy-2-methyl-phenyl)-6-methoxy-naphthalene-2-carboxamide **(283)** (109 mg, 0.52 mmol) in tetrahydrofuran (4 mL) and was cooled to 0 °C and to the reaction mixture was added tetrabutylammonium fluoride (517 μL, 0.52 mmol). The reaction mixture was stirred at 0 °C for 5 min and at ambient temperature for 10 min. The reaction mixture was concentrated under reduced pressure. The crude was purified by column chromatography (silica 12 g, 100% dichloromethane) and triturated in ether to yield the desired amide **291** as a white solid (49 mg, 59%).

¹H-NMR (500 MHz, DMSO-*d*₆) 9.93 (s, 1H), 9.41 (s, 1H), 8.52 (s, 1H), 8.03 – 7.95 (m, 2H), 7.92 (d, *J* 8.6, 1H), 7.41 (d, *J* 2.6, 1H), 7.25 (dd, *J* 8.9, 2.6, 1H), 7.00 (app t, *J* 8.0, 1H), 6.81 (d, *J* 7.8, 1H), 6.73 (d, *J* 8.1, 1H), 3.91 (s, 3H), 2.04 (s, 3H); **LCMS** (LCQ) Rt = 0.6 min (method 2), *m/z* (ESI⁺) 308.1 [M+H]⁺.

***N*-(3-hydroxy-2-methyl-phenyl)-2,3-dimethyl-quinoxaline-6-carboxamide (292)**

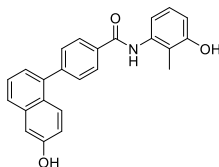


N-(3-(tert-butyl(dimethyl)silyl)oxy-2-methyl-phenyl)-2,3-dimethyl-quinoxaline-6-carboxamide **(284)** (171 mg, 0.41 mmol) in tetrahydrofuran (4 mL) and was cooled to 0 °C and to the reaction mixture was added tetrabutylammonium fluoride (811 μL, 0.81 mmol). The reaction mixture was stirred at 0 °C for 5 min and at ambient temperature for 10 min. The reaction mixture was concentrated under reduced pressure. The crude was purified by

column chromatography (silica 12 g, 0 to 5% methanol in dichloromethane) to yield the desired amide **292** as a white solid (48 mg, 37%).

¹H-NMR (500 MHz, DMSO-*d*₆) 10.13 (s, 1H), 9.44 (s, 1H), 8.61 (s, 1H), 8.22 (d, *J* 8.6, 1H), 8.06 (d, *J* 8.6, 1H), 7.02 (app t, *J* 8.0, 1H), 6.82 (d, *J* 7.9, 1H), 6.75 (d, *J* 8.1, 1H), 2.72 (s, 6H), 2.05 (s, 3H); **LCMS** (LCQ) *R*_t = 0.6 min (method 2), *m/z* (ESI⁺) 308.2 [M+H]⁺.

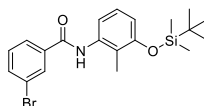
6-Hydroxy-*N*-(3-hydroxy-2-methyl-phenyl)naphthalene-1-carboxamide (293)



N-(3-(tert-butyl(dimethyl)silyl)oxy-2-methyl-phenyl)-6-hydroxy-naphthalene-1-carboxamide (**285**) (94 mg, 0.12 mmol) in tetrahydrofuran (2 mL) and was cooled to 0 °C and to the reaction mixture was added tetrabutylammonium fluoride (230 μL, 0.23 mmol). The reaction mixture was stirred at 0 °C for 5 min and at ambient temperature for 10 min. The reaction mixture was concentrated under reduced pressure. The crude was purified by column chromatography (silica 12 g, 0 to 5% methanol in dichloromethane) and further purified by column chromatography (amino silica 12 g, 0 to 8% methanol in dichloromethane) to yield the desired amide **293** as a white solid (7 mg, 20%).

¹H-NMR (500 MHz, DMSO-*d*₆) 9.90 (s, 2H), 9.42 (s, 1H), 8.12 (d, *J* 9.1, 1H), 7.82 (d, *J* 8.2, 1H), 7.54 (d, *J* 6.8, 1H), 7.47 (d, *J* 7.9, 1H), 7.23 – 7.12 (m, 2H), 7.01 (app t, *J* 7.9, 1H), 6.90 (d, *J* 7.9, 1H), 6.73 (d, *J* 8.0, 1H), 2.10 (s, 3H); **LCMS** (LCQ) *R*_t = 0.6 min (method 2), *m/z* (ESI⁺) 294.0 [M+H]⁺.

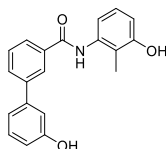
3-Bromo-*N*-(3-(tert-butyl(dimethyl)silyl)oxy-2-methyl-phenyl)benzamide (294)



Compound **294** was synthesised according to general procedure R, using the following reagents: 3-bromobenzoic acid (700 mg, 3.48 mmol), HATU (1.59 g, 4.18 mmol), *N,N*-diisopropylethylamine (1.21 mL, 6.96 mmol), 3-(tert-butyl(dimethyl)silyl)oxy-2-methyl-aniline (1.00 g, 4.21 mmol) and *N,N*-dimethylformamide (7 mL). The crude was purified by column chromatography (silica 30 g, 0 to 5% ethyl acetate in petroleum ether) to yield the desired compound **294** as a white solid (1.07 g, 69%).

¹H-NMR (500 MHz, DMSO-*d*₆) δ 10.04 (s, 1H), 8.14 (s, 1H), 7.96 (d, *J* 7.5, 1H), 7.80 (d, *J* 8.8, 1H), 7.50 (t, *J* 7.9, 1H), 7.10 (t, *J* 8.0, 1H), 6.93 (d, *J* 7.8, 1H), 6.76 (d, *J* 8.1, 1H), 2.04 (s, 3H), 1.00 (s, 9H), 0.22 (s, 6H).

***N*-(3-hydroxy-2-methyl-phenyl)-3-(3-hydroxyphenyl)benzamide (295)**

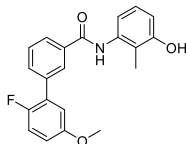


Compound **295** was synthesised according to general procedure V, using the following reagents: 3-bromo-*N*-(3-(tert-butyl(dimethyl)silyl)oxy-2-methyl-phenyl)benzamide (**294**) (80 mg, 0.19 mmol), (3-hydroxyphenyl)boronic acid (26 mg, 0.19 mmol), (1,1'-bis(diphenylphosphino)ferrocene)dichloropalladium(II) (14 mg, 0.02 mmol), sodium carbonate (202 mg, 1.90 mmol), 1,4-dioxane (1.25 mL) and water (1.25 mL). The crude was purified by column

chromatography (silica 12 g, 0 to 40% ethyl acetate in petroleum ether) to yield the desired product **295** as a white solid (20 mg, 31%).

¹H-NMR (500 MHz, DMSO-*d*₆) δ 9.98 (s, 1H), 9.60 (s, 1H), 9.42 (s, 1H), 8.20 (s, 1H), 7.93 (d, *J* 6.7, 1H), 7.81 (d, *J* 7.4, 1H), 7.59 (app t, *J* 6.2, 1H), 7.30 (app t, *J* 7.5, 1H), 7.18 (d, *J* 7.2, 1H), 7.13 (s, 1H), 7.01 (app t, *J* 7.4, 1H), 6.85 – 6.77 (m, 2H), 6.74 (d, *J* 7.8, 1H), 2.03 (s, 3H); **LCMS** (LCQ) Rt = 2.0 min (method 2), *m/z* (ESI⁺) 320.1 [M+H]⁺.

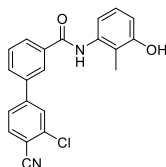
3-(2-Fluoro-5-methoxy-phenyl)-*N*-(3-hydroxy-2-methyl-phenyl)benzamide (**296**)



Compound **296** was synthesised according to general procedure V, using the following reagents: 3-bromo-*N*-(3-(tert-butyl(dimethyl)silyl)oxy-2-methyl-phenyl)benzamide (**294**) (80 mg, 0.19 mmol), (2-fluoro-5-methoxyphenyl)boronic acid (32 mg, 0.19 mmol), (1,1'-bis(diphenylphosphino)ferrocene)dichloropalladium(II) (14 mg, 0.02 mmol), sodium carbonate (202 mg, 1.90 mmol), 1,4-dioxane (1.25 mL) and water (1.25 mL). The crude was purified by column chromatography (silica 12 g, 0 to 60% ethyl acetate in petroleum ether) to yield the desired product **296** as a white solid (41 mg, 58%).

¹H-NMR (500 MHz, DMSO-*d*₆) δ 9.94 (s, 1H), 9.42 (s, 1H), 8.14 (s, 1H), 7.99 (s, 1H), 7.76 (s, 1H), 7.67 – 7.58 (s, 1H), 7.28 (t, *J* 8.7, 1H), 7.15 (s, 1H), 7.00 (s, 2H), 6.78 (d, *J* 7.9, 1H), 6.73 (d, *J* 7.7, 1H), 3.81 (s, 3H), 2.02 (s, 3H); **LCMS** (LCQ) Rt = 2.6 min (method 2), *m/z* (ESI⁺) 352.1 [M+H]⁺.

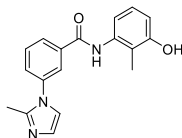
3-(3-Chloro-4-cyano-phenyl)-*N*-(3-hydroxy-2-methyl-phenyl)benzamide (**297**)



Compound **297** was synthesised according to general procedure V, using the following reagents: 3-bromo-*N*-(3-(tert-butyl(dimethyl)silyl)oxy-2-methyl-phenyl)benzamide (**294**) (80 mg, 0.19 mmol), (3-chloro-4-cyanophenyl)boronic acid (34 mg, 0.19 mmol), (1,1'-bis(diphenylphosphino)ferrocene)dichloropalladium(II) (14 mg, 0.02 mmol), sodium carbonate (202 mg, 1.90 mmol), 1,4-dioxane (1.25 mL) and water (1.25 mL). The crude was purified by column chromatography (silica 12 g, 0 to 50% ethyl acetate in petroleum ether) to yield the desired product **297** as a white solid (60 mg, 83%).

¹H-NMR (500 MHz, DMSO-*d*₆) δ 10.02 (s, 1H), 9.45 (s, 1H), 8.37 (s, 1H), 8.22 (s, 1H), 8.12 (d, *J* 8.0, 1H), 8.06 – 8.01 (m, 2H), 7.99 (d, *J* 8.4, 1H), 7.67 (app t, *J* 7.9, 1H), 7.02 (app t, *J* 8.0, 1H), 6.81 – 6.67 (m, 2H), 2.03 (s, 3H); **LCMS** (LCQ) Rt = 2.7 min (method 2), *m/z* (ESI⁺) 363.1 [M(³⁵Cl)+H]⁺.

N-(3-hydroxy-2-methyl-phenyl)-3-(2-methylimidazol-1-yl)benzamide (**298**)

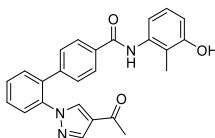


To 3-bromo-*N*-(3-(tert-butyl(dimethyl)silyl)oxy-2-methyl-phenyl)benzamide (**298**) (150 mg, 0.36 mmol) in dimethyl sulfoxide (0.5 mL) was added 2-methylimidazole (29 mg, 0.36 mmol), *N,N*-dimethylglycine, (37 mg, 0.36 mmol) and caesium carbonate (235 mg, 0.71 mmol), and the reaction mixture degassed. Copper(I) oxide (10 mg, 0.36 mmol) was

added to the reaction mixture and stirred for 18 h at 130 °C. The crude product was taken up in ethyl acetate (20 mL) and washed with brine (3 × 10 mL). The organic components were then dried over MgSO₄, filtered and concentrated under reduced pressure. The crude was purified by column chromatography (silica 12 g, 0 to 10% methanol in dichloromethane), further purified by column chromatography (silica 12 g, 0 to 5% methanol in dichloromethane) and triturated in ether to yield the desired product **298** as a pale pink solid (6 mg, 5%).

¹H-NMR (500 MHz, DMSO-*d*₆) δ 9.98 (s, 1H), 9.44 (s, 1H), 8.03 (s, 1H), 8.00 (s, 1H), 7.69 (s, 2H), 7.41 (s, 1H), 7.04 – 6.90 (m, 2H), 6.80 – 6.62 (m, 2H), 2.34 (s, 3H), 2.01 (s, 3H); **LCMS** (LCQ) Rt = 0.3 min (method 2), *m/z* (ESI⁺) 308.3 [M+H]⁺.

4-(2-(4-Acetylpyrazol-1-yl)phenyl)-*N*-(3-hydroxy-2-methyl-phenyl)benzamide (299)



Compound **299** was synthesised according to general procedure V, using the following reagents: *N*-(3-(tert-butyl(dimethyl)silyl)oxy-2-methyl-phenyl)-4-(4,4,5,5-tetramethyl-1,3,2-dioxaborolan-2-yl)benzamide (**294**) (100 mg, 0.21 mmol), 1-(1-(2-chlorophenyl)-1H-pyrazol-4-yl)ethanone (47 mg, 0.21 mmol), (1,1'-bis(diphenylphosphino)ferrocene)dichloropalladium(II) (16 mg, 0.02 mmol), sodium carbonate (227 mg, 2.14 mmol), 1,4-dioxane (2 mL) and water (2 mL). The crude was purified by column chromatography (silica 12 g, 0 to 6% methanol in dichloromethane) to yield the desired product **298** as a pale yellow solid (5 mg, 5%).

¹H-NMR (500 MHz, DMSO-*d*₆) δ 9.84 (s, 1H), 9.39 (s, 1H), 8.47 (s, 1H), 8.01 (s, 1H), 7.87 (d, *J* 7.9, 2H), 7.69 – 7.56 (m, 4H), 7.20 (d, *J* 7.8, 2H), 6.96 (app t, *J* 8.0, 1H), 6.78 – 6.65 (m, 2H), 2.31 (s, 3H), 1.97 (s, 3H).